ISBN: 978-3-95450-210-3 doi:10.18429/JACoW-FEL2019-MOA01

RIDING THE FEL INSTABILITY (DEDICATED TO ALBERTO RENIERI)

G. Dattoli*, ENEA - Frascati Research Center, Frascati, Rome, Italy
C. Pellegrini†, UCLA, Physics & Astronomy, Los Angeles, CA, USA

Abstract

The Free Electron Laser (*FEL*) transforms the kinetic energy of electrons into coherent light. The underlying mechanism occurs through the *FEL* instability, leading to the growth of coherent radiation from noise, characterizing all the generators of coherent radiation from free electrons (Gyrotrons, *CARM* ...). The *FEL* instability shares many features with other instabilities occurring in Plasmas and electron beams, sometimes competing with them. In this paper we give a short description of these analogies, their relevant physical roots and comment on the importance and role of their interplay.

FEL INSTABILITY

The *FEL*, in its modern conception, started in 1976 with the amplification of a CO_2 laser, co-propagating with an electron beam in an undulator magnet [1]. The experiment confirmed what Madey had predicted few years before [2], namely that the electron beam may be induced to lose power, thus enhancing the laser intensity. The FEL small signal gain curve was carefully examined, along with the kinematical conditions under which the laser beam can be amplified or depleted, thus revealing an, albeit inefficient, electron beam acceleration. The following year, an FEL oscillator [3] showed that, under appropriate conditions, the amplification mechanism was sufficient to sustain the laser oscillation in the *IR* and drive the system to complete saturation.

The original conception of *FEL* [2] was a quantum treatment of a process called "stimulated bremsstrahlung" by Madey. The dynamical behavior of *FEL* was successively clarified by Colson [4–6] who showed that all the relevant physics can be described by a classical model based on the use of a pendulum like equation, coupled to those giving the laser field evolution. Many discussions arouse at the time, regarding the nature of the *FEL* itself [7], compared to population inversion devices. However smart the answer was, it could not circumvent the pragmatic observation that the *FEL* is a tool that steels power from a relativistic e-beam, transforming it into coherent "laser-like" power.

The question now becomes what "laser like" means and whether it is true that the *FEL* light is fully coherent. The theoretical treatment developed by Bambini and Renieri [8–12] used means from analytical mechanics to describe the *FEL* problem in terms of a non relativistic Hamiltonian, leading to the pendulum equation and opening the way to the investigation of the *FEL* quantum coherence properties [7, 8]. This is the gross picture before the eighties. It became slowly clear that the *FEL* phenomenology had not to be dissimilar from the Physics of travelling wave tubes. The analogy between *FEL* and other generators of light by other free electron devices (Klystron, Gyrotron, *CARM*, ...) was pointed out in [13] (see also ref. [7] for a more recent discussion. For a comparison with conventional laser sources, see [14]).

The common feature emerging from the relevant theoretical picture was that the optical field growth is associated with a dispersion relation leading to a third (or fourth) order *ODE* [15–17]. The roots of the associated characteristic polynomial fix the condition for the onset and rise of the electromagnetic field. Within this context the field grows as the result of the *FEL* instability, with a rise time or gain length, given by the "fast growing" root.

The breakthrough in this direction came from [18] where a new operating condition for the *FEL* was foreseen, thus paving the way for the fourth generation synchrotron radiation devices, the *X*-Ray *FEL*s, characterized by very high brightness, power and by extremely short pulse duration. A proposal to build an *X*-Ray *FEL* using a 15 *GeV* electron beam from the *SLAC* linac [19] led to the design and construction of *LCLS* and other similar systems in Europe and Asia. *X*-Ray *FEL*s give for the first time the possibility of exploring matter with X-rays at the angstrom-femto-second space and time scale characteristic of atomic systems, thus opening a new window on the exploration of matter and its dynamical processes.

We have pointed out that the *FEL* small signal dynamics is the result of an instability, the further interplay with the e-beam produces a heating, determining the increase of the energy spread, which eventually induces saturation [20]. This is a complex mechanism, associated with Landau damping, and will be further discussed in the next sections of the paper.

STORAGE RING *FEL*, RENIERI LIMIT AND SAW-TOOTH INSTABILITY

In the previous section we have mentioned that the *FEL* growth is the result of an instability, counteracted by the self induced beam energy spread. Many *FEL* oscillators have been proposed and operated in the past [21–28] in an electron storage ring, with the intent of providing

* giuseppe.dattoli@enea.it
† pellegrini@physics.ucla.edu

Content from this work may be used under the terms of the CC BY 3.0 licence (© 2019). Any distribution of this work must maintain attribution to the author(s), title of the work, publisher, and DOI

ISBN: 978-3-95450-210-3 doi:10.18429/JACoW-FEL2019-MOA02

FIRST LASING OF A FREE ELECTRON LASER IN THE SOFT X-RAY SPECTRAL RANGE WITH ECHO ENABLED HARMONIC GENERATION

E. Allaria*, A. Abrami, L. Badano, M. Bossi, F. Capotondi, D. Castronovo, M. Cautero, P. Cinquegrana, I. Cudin, M. B. Danailov, A. Demidovich, S. Di Mitri, B. Diviacco, S. Grulja, W.M. Fawley, M. Ferianis, L. Foglia, G. Gaio, F. Giacuzzo, L. Giannessi, F. Iazzourene, G. Kurdi, M. Lonza, N. Mahne, M. Malvestuto, M. Manfredda, C. Masciovecchio, N.S. Mirian, I. Nikolov, G. Penco, E. Principi, L. Raimondi, P. R. Ribic, R. Sauro, C. Scafuri, P. Sigalotti, S. Spampinati, C. Spezzani, L. Sturari, M. Svandrlik, M. Trovo, M. Veronese, D. Vivoda, M. Zaccaria, D. Zangrando, M. Zangrando, Elettra – Sincrotrone Trieste SCpA, Basovizza
D. Garzella, CEA, Gif-sur-Yvette
P. Miotti, CNR-IFN, Padova
M. Coreno, CNR-ISM, Trieste and Elettra – Sincrotrone Trieste SCpA, Basovizza
V. Grattoni, DESY, Hamburg
G. De Ninno, Elettra – Sincrotrone Trieste SCpA, Basovizza and University of Nova Gorica, Nova Gorica
N. Bruchon, Elettra – Sincrotrone Trieste SCpA, Basovizza and University of Trieste, Trieste
T. Tanikawa, EuXFEL, Schenefeld
G. Penn, LBNL, Berkeley, California
F. Frassetto, L. Poletto, LUXOR, Padova
M.A. Pop, MAX IV Laboratory, Lund
H.H. Braun, E. Ferrari, E. Prat, S. Reiche, PSI, Villigen
E. Roussel, PhLAM/CERCLA, Villeneuve d'Ascq Cedex
C. Feng, SARI-CAS, Pudong, Shanghai
E. Hemsing, SLAC, Menlo Park, California
M.E. Couprie, A. Ghaith, SOLEIL, Gif-sur-Yvette
D. Xiang, Shanghai Jiao Tong University, Shanghai

Abstract

We report on the successful operation of a Free Electron Laser (FEL) in the Echo Enabled Harmonic Generation (EEHG) scheme at the FERMI facility at Sincrotrone Trieste. The experiment required a modification of the FEL-2 undulator line which, in normal operation, uses two stages of high-gain harmonic generation separated by a delay line. In addition to a new seed laser, the dispersion in the delay-line was increased, the second stage modulator changed and a new manipulator installed in the delay-line chicane hosting additional diagnostic components. With this modified setup we have demonstrated the first evidence of strong exponential gain in a free electron laser operated in EEHG mode at wavelengths as short as 5 nm.

INTRODUCTION

With two FEL lines the FERMI user facility [1] is providing powerful radiation in the spectral range from 100 nm to 4 nm characterized by high degree of longitudinal and transverse coherence. Both FEL lines rely on the use of an external seed laser to initialize the coherent emission process. FEL-1 [2], optimized for the long wavelength spectral range (100 nm – 20 nm), is based on a single stage, high gain harmonic generation (HGHG) scheme [3], while FEL-2 [4] operates at a shorter spectral range (20 nm – 4 nm) thanks to a double stage HGHG process employing a fresh bunch scheme(HGHG-FB) [5].

In the recent years, scientists have started exploiting the capability of FERMI of producing fully coherent pulses performing experiments not possible with other sources. Due to FERMI's strong coherence, techniques such as four wave mixing [6], coherent control [7], are now available for scientific users in the EUV- soft x-ray spectral range.

Because longitudinal coherence has become an important distinguishing parameter for FERMI with respect to other FEL sources, studies for possible future upgrades have been driven by the goal of extending its capabilities for coherence control toward even shorter wavelengths [8]. As a first step toward this direction an experiment has been organized at FERMI in 2018 to experimentally validate the benefits predicted by theory for the recently proposed seeding scheme EEHG [9].

We report here on the successful operation of the EEHG FEL at FERMI [10]. We first present the experimental setup pointing out the modifications done to some

* e-mail: enrico.allaria@elettra.eu

Content from this work may be used under the terms of the CC BY 3.0 licence (© 2019). Any distribution of this work must maintain attribution to the author(s), title of the work, publisher, and DOI

ISBN: 978-3-95450-210-3 doi:10.18429/JACoW-FEL2019-MOA03

FIRST LASING AT THE CAEP THz FEL FACILITY*

P. Li, D. Wu†, M. Li, K. Zhou, L. G. Yan, J. X. Wang, Y. Xu, Q. Pan, D. X. Xiao,
X. Luo, H. B. Wang, X. M. Shen, P. Zhang, L. J. Shan, T. H. He, J. Liu, Y. Liu
Institute of Applied Electronics, China Academy of Engineering Physics, Mianyang, China

Abstract

China Academy of Engineering Physics terahertz free electron laser (CAEP THz FEL, CTFEL) is the first THz FEL user facility in China, which was an oscillator type FEL. This THz FEL facility consists of a GaAs photocathode high-voltage DC gun, a superconducting RF linac, a planar undulator and a quasi-concentric optical resonator. The terahertz laser's frequency is continuous adjustable from 0.7 THz to 4.2 THz. The average power is more than 10 W and the micro-pulse power is more than 0.3 MW. In this paper, the specific parameters and operation status of CTFEL are presented. Finally, some user experiments are introduced briefly.

INTRODUCTION

Terahertz (THz) radiation is an electromagnetic wave with a frequency range of 0.1 to 10 THz. It is between microwave and infrared light and has very unique properties such as transient, low energy, penetration, and broadband. It has caused widespread concern in recent years. Free electron laser (FEL) can be the most powerful tool as terahertz power source. It has many advantages, such as monochrome, high-power, linear-polarization, continuously tunable frequency. Many FEL facilities, such as ELBE in Germany [1], FELIX in Holland [2], UCSB in the USA [3] and NovoFEL in Russia [4], have played important roles in the THz sciences. In the near future, of the 20 FEL facilities planned to be built in the whole world, there will be at least 8 ones operating in the THz range [5].

CAEP THz FEL (CTFEL) is the first THz FEL user facility in China [6, 7], which is an oscillator type FEL, see Figure 1. This THz FEL facility consists of a GaAs photocathode high-voltage DC gun, a 1.3 GHz superconducting RF linac [8, 9], a planar undulator and a quasi-concentric optical resonator. The repetition of CTFEL is 54.167 MHz, which means the average current can be up to 5 mA. The effective accelerator field gradient is about 10 MV/m.

CTFEL has achieved the saturation radiation in August, 2017[10] after two year's commissioning. The terahertz wave frequency is now continuously adjustable from 0.7 THz to 4.2 THz. The average power is above 10 W and the micro-pulse power is more than 0.5 MW. In this paper, the components of this facility and some of its applications are introduced. Also an upgrade plan is proposed.

* Work supported by National Natural Science Foundation of China with grant (11575264, 11605190 and 11805192), Innovation Foundation of CAEP with grant (CX2019036, CX2019037)
† wudai04@163.com

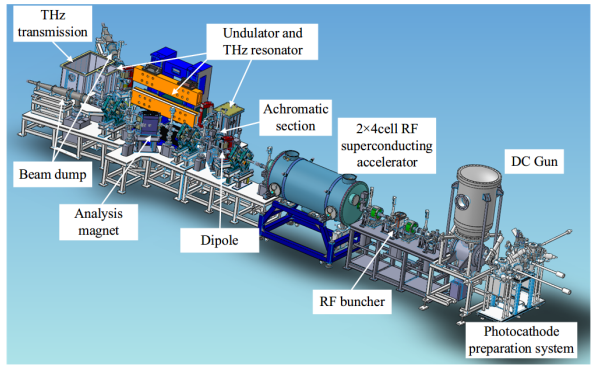


Figure 1: The Layout of the CTFEL Facility.

FACILITY COMPONENTS

Overview

Figure 2 shows the block diagram of the CTFEL facility, in which you can see more details. The 532nm continuous mode-locked driving laser is incident on the photocathode of the gallium arsenide semiconductor. The electrons are laterally focused by a solenoid, longitudinally bunched through the buncher, then enters the superconducting cavity, where electrons are finally accelerated to 7~8 MeV. The accelerated electrons are transported through the achromatic section into the undulator to generate THz spontaneous radiation. The radiation resonates in the THz optical cavity and reaches saturation. Saturated THz light is coupled out through the small hole in downstream mirror, and the output terahertz light is transmitted to the user's laboratory for user experiments.

The electron beam parameters are summarized in Table 1. The accelerator is designed to operate in both CW and macro-pulse mode. It is now working in macro-pulse mode with the duty cycle >10%. In the near future, the CW operation will be reached after the machine fast protection system is installed.

Table 1: Electron Beam Parameters

Parameters	Design goal	Unit
Bunch charge	10~100	pC
Micro-pulse repetition	54.167	MHz
Macro-pulse repetition	1~20	Hz
Duty cycle	10^{-5} ~1	
Average current	1~5	mA
Kinetic energy	6~8	MeV
Normalized emittance	<8	μm
Micropulse length (RMS)	1.5~ 3	ps
Energy spread	~ 0.2	%

Content from this work may be used under the terms of the CC BY 3.0 licence (© 2019). Any distribution of this work must maintain attribution to the author(s), title of the work, publisher, and DOI

ISBN: 978-3-95450-210-3 doi:10.18429/JACoW-FEL2019-MOA07

COMMISSIONING AND FIRST LASING OF THE FELiChEM: A NEW IR AND THz FEL OSCILLATOR IN CHINA*

Heting Li† and Qika Jia on behalf of the FELiChEM team
National Synchrotron Radiation Laboratory (NSRL)
University of Science and Technology of China, Hefei, China

Abstract

A new infrared FEL named FELiChEM aiming at the energy chemistry has been constructed and commissioned at NSRL in Hefei. It consists of two FEL oscillators driven by one normal-conducting S-band linac with maximum beam energy of 60 MeV. The two oscillators generate the mid-infrared and far-infrared lasers covering the spectral range of 2.5-50 μm and 40-200 μm, respectively. First lasing was achieved at a wavelength of 15 μm with an electron energy of 35 MeV. Till now, we have observed the FEL signal from 3.5μm to 30 μm and achieved the maximum micropulse energy up to 27 μJ at 15 μm.

INTRODUCTION OF FELICHEM

Under the financial support of Natural Science Foundation of China, the project "Tunable Infrared Laser for Fundamental of Energy Chemistry" (FELiChEM) was started in 2015. It is a dedicated experimental facility aiming at energy chemistry research [1, 2]. The core device is a free electron laser (FEL) consisting of two oscillators driven by one normal-conducting S-band linac with maximum electron energy of 60 MeV.

Figure 1 shows the schematic layout of FELiChEM. Both the accelerator hall and the experimental hall are existed buildings and we were allowed to design the facility with this constriction. The electron accelerator is located in a 12m×16m semi-underground tunnel, as shown by the photo of Fig. 2. Two branches connected with the linac are the two oscillators. The branch using the electron beam bended from the end of the first accelerating tube is the far-infrared oscillator which generates the 40-200 μm FEL, while another one called the mid-infrared oscillator generates the 2.5-40 μm FEL. The output FEL pulses from the

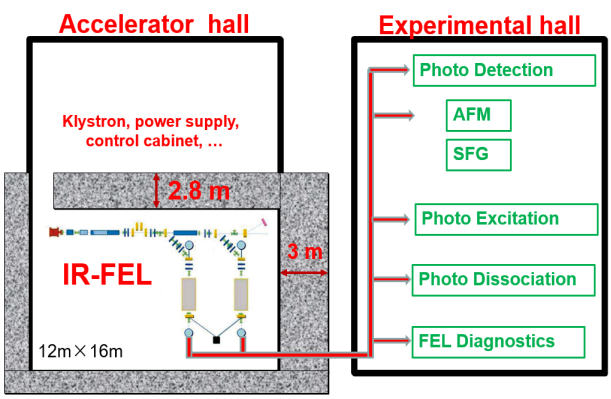


Figure 1: Schematic layout of FELiChEM.

* Work supported by National Natural Science Foundation of China (21327901).
†Email address: liheting@ustc.edu.cn

Table 1: Design Target of FELiChEM

Parameter	Specification
Covering spectrum	2.5 ~ 200 μm
MIR FEL oscillators	2.5 ~ 50 μm
FIR FEL oscillators	40 ~ 200 μm
Macro-pulse length	5~ 10 μs
Repetition of macro-pulse	10/20 Hz
Macro-pulse energy	~100 mJ
Micro-pulse length	1 ~ 5 ps
Micro-pulse energy	~ 50 μJ
Bandwidth	0.3 ~ 3 %

two oscillators share one beam line and are transported to the experimental hall, where the stations for FEL diagnostics, photo dissociation, photo excitation and photo detection are in one line. The total length of the beam line is about 36 m.

The users of these stations have brought out their requirements on the IR-FEL performance, as summarized in Table 1. In addition, some users have extra requirements, for example, the photo excitation and dissociation stations hope that the peak and average power of IR-FEL can be as high as possible. The design of the oscillator and the electron accelerator has been introduced in the Ref. [1-3].

Due to the delay of the civil construction, the installation of the accelerator was delayed by more than one year and was finished in June, 2018. Then in the next month we started the commissioning of the linac. Unfortunately, after two month the high-repetition grid pulser of the electron gun was broken suddenly and we had no choice but to wait it reworking. In May 2019, we restarted the commissioning, and observed the spontaneous radiation at the 15 μm wavelength in 9, June. On the same day, the first lasing up to 1 μJ per micropulse was detected at the same wavelength.

Next, we will briefly introduce the facility and the commissioning status, and then the first lasing results.

ELECTRON ACCELERATOR

The electron accelerator mainly consists of: an 80 kV electron gun, a 476 MHz subharmonic standing wave prebuncher, a 2856 MHz fundamental frequency traveling wave buncher, two 2856 MHz fundamental frequency traveling wave accelerating tubes separated by a magnetic compressor (chicane). Besides, a set of solenoid focusing coils are used from the gun exit to the end of the first accelerating tube.

The triode gun is driven by a grid pulser with the repetition frequency that can be switched in 476/238/119/59.5/29.5 MHz. For the operation safety of the grid pulser, we have turned down the high voltage from 100 kV to 80 kV,

Content from this work may be used under the terms of the CC BY 3.0 licence (© 2019). Any distribution of this work must maintain attribution to the author(s), title of the work, publisher, and DOI

ISBN: 978-3-95450-210-3 doi:10.18429/JACoW-FEL2019-MOC01

REGENERATIVE AMPLIFIER FEL – FROM IR TO X-RAYS

D. C. Nguyen†, P. M. Anisimov, C. E. Buechler, Q. R. Marksteiner, R. L. Sheffield
Los Alamos National Laboratory, Los Alamos, New Mexico, USA

Abstract

The Regenerative Amplifier FEL (RAFEL) feeds back a small fraction of the radiation exiting a high-gain undulator as the seed for the next pass, and achieves narrow linewidth and saturation in a few passes. For the IR RAFEL, we used an optical cavity with annular mirrors to reinject ~10% of the IR radiation back into a two-meter undulator [1]. We theorized the RAFEL output transformed from an annular beam to an on-axis beam due to optical guiding at high power [2]. A number of researchers have proposed RAFEL and XFELO to achieve full temporal coherence in VUV and X-ray FELs [3-8]. For the XFELO, symmetric Bragg backscattering off high-quality diamond crystals can provide very high reflectivity for the XFELO cavity [7-9]. The required reflectivity for a RAFEL feedback cavity is much lower than the XFELO. We show that 6% feedback is sufficient for the X-ray RAFEL at 9.8 keV to saturate and achieve 0.5-eV bandwidth. We discuss options to out-couple more than ~50% of the RAFEL intra-cavity power and discuss challenges associated with X-ray absorption in the out-coupler.

INTRODUCTION

With the successful commissioning of the European XFEL and the on-going construction of the LCLS-II superconducting linac XFEL at SLAC, a fully coherent X-ray free-electron laser delivering transform-limited X-ray pulses with unprecedented brilliance is a real possibility in the near future. Full temporal coherence can be achieved with either an XFELO or an X-ray RAFEL, both of which will require an optical cavity consisting of low-loss, high-quality Bragg mirrors [10]. The XFELO requirements for are more stringent: Bragg crystals with 99% reflectivity forming a long optical cavity with μm dimension accuracy and nanoradian angular stability, in addition to the relatively long and high charge electron bunches at MHz bunch repetition rate. Numerical simulations predict the X-ray pulses inside an XFELO optical cavity will need to recirculate a few hundred passes before they reach steady-state and achieve narrow linewidth [9]. In contrast, the RAFEL requires 2-3 passes in a lower-Q feedback cavity (lower reflectivity) and less stringent angular stability compared to the XFELO. The RAFEL has been demonstrated in the infrared by our group [1] and proposed by a number of researchers for the VUV and X-ray regions as a means to generate fully coherent short-wavelength FELs [3-8].

The RAFEL design shares a number of features of the XFELO such as improved longitudinal coherence and pulse-to-pulse stability over SASE. There are however a few important differences between RAFEL and XFELO. First and foremost is the amount of optical feedback in each pass; in RAFEL, the optical feedback is typically a few percent of radiation power in the previous pass, whereas XFELO requires feedback fraction greater than 90%. Thus, while the intra-cavity power of the XFELO is several times the output power, the RAFEL output power is almost the same as the power exiting the undulator. The small optical feedback in RAFEL significantly relaxes the reflectivity requirements for the cavity mirrors. The second difference is the single-pass gain; the RAFEL single-pass gain is high, on the order of 10^2 to 10^3, compared to the XFELO single-pass gain of ~2X. The higher gains reduce the number of passes for RAFEL to reach saturation and achieve spectral narrowing. The third difference is the output spectral width; the XFELO can achieve a very narrow linewidth (a few meV) whereas the RAFEL output has a spectral width of a single SASE spectral peak, which is approximately the Fourier transform of the X-ray pulse width (about the same as the electron bunch length).

We present experimental results of the IR RAFEL and numerical simulations of a fully coherent RAFEL at 9.8 keV with spectral linewidth of ~0.5 eV (5×10^{-5} relative). We show candidates for the low-loss Bragg reflectors for different X-ray energies, discuss a number of options to out-couple the intra-cavity power and present the results of Genesis FEL simulation for the 9.8-keV RAFEL.

INFRARED RAFEL

The infrared RAFEL was experimentally demonstrated at 16 μm at LANL in 1997. The feedback cavity for this demonstration is shown in Fig. 1. The electron beam entered the cavity from the left through the smaller annular mirror and exit on the right. Approximately two-third of the intra-cavity power was coupled out through the large annular mirror. A summary of the IR RAFEL parameters is shown in Table 1.

Table 1: Summary of IR RAFEL Parameters

Parameter	Symbol	Value
Beam energy	E_b	16.7 MeV
Peak current	I_p	270 A
Bunch length	l_e	5 mm
Undulator period	λ_u	2 cm
Undulator parameter	K_{rms}	0.92
Undulator length	L_u	2 m (1 m taper)
FEL wavelength	λ	16.3 μm
3D gain length	L_G	0.125 m

† dcnguyen@lanl.gov

Content from this work may be used under the terms of the CC BY 3.0 licence (© 2019). Any distribution of this work must maintain attribution to the author(s), title of the work, publisher, and DOI

ISBN: 978-3-95450-210-3 doi:10.18429/JACoW-FEL2019-TUA01

PARALLEL OPERATION OF SASE1 AND SASE3 AT THE EUROPEAN XFEL

S. Liu†, F. Brinker, W. Decking, L. Fröhlich, R. Kammering, D. Nölle, F. Obier, M. Scholz, E. Schneidmiller, T. Wilksen, M. Yurkov, DESY, Hamburg, Germany
R. Boll, N. Gerasimova, T. Mazza, M. Meyer, A. Scherz, H. Sinn, EuXFEL, Schenefeld, Germany

Abstract

At the European XFEL a hard X-Ray SASE FEL (SASE1) and a soft X-Ray SASE FEL (SASE3) share in series the same electron beamline. This configuration couples the operation conditions for both undulators and their subsequent user experiments in terms of SASE intensity and background. We report on our experience in parallel operation and discuss the solutions that enable the operation of both undulators as independently as possible.

INTRODUCTION

The European XFEL is in operation since 2017. It is based on superconducting accelerator technology and serves three undulator beamlines simultaneously [1]. The three beamlines are named as SASE1, SASE2 and SASE3. SASE1 and SASE2 are hard X-Ray beamlines (3-25 keV) and SASE3 is a soft X-Ray beamline (0.25-3 keV). The first lasing of SASE1 beamline was achieved in May 2017 [2], followed by the first lasing of SASE3 in February 2018 and the first lasing of SASE2 in May 2018 [3]. After that the three beamlines are operated in parallel [4, 5].

The layout of the three beamlines is shown in Fig. 1. One can see that SASE1 and SASE3 are located in series in the same electron beamline. This configuration couples the operation conditions for both undulators and their subsequent user experiments in terms of SASE intensity and background.

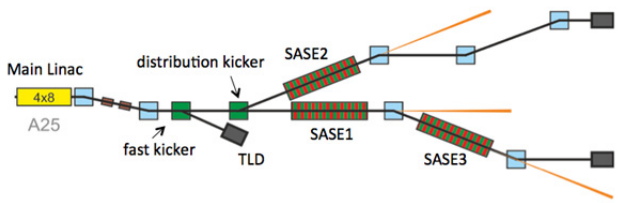


Figure 1: Layout of the three undulator beamlines at the European XFEL starts from the last cryomodule of the main linac.

Coupling Between SASE1 and SASE3 Beamlines

Two different techniques, an afterburner and "fresh bunch", are used to operate SASE1-SASE3 beamline. Spent electron from SASE1 is used to generate radiation in SASE3 in the afterburner configuration [1]. FEL process in SASE1 induces energy spread in the electron beam which is proportional to the radiation pulse energy. As a result, SASE3 and SASE1 performance are coupled such that increase of the radiation pulse energy in SASE1 leads to degradation of SASE3 output. The calculated minimum operational wavelength of SASE3 versus operating wavelength of SASE1 is shown in Fig. 2 (left) (for 14 GeV and 250 pC electron beam case) [6]. Operation of SASE3 in saturation is only possible for the wavelengths above the curves[1]. However, FEL efficiency visibly falls down as it is illustrated with measured pulse energy coupling between SASE1 and SASE3 shown in Fig. 2 (right). Electron energy is 14 GeV and bunch charge is 250 pC in this experiment. SASE1 and SASE3 operate at the wavelength of 0.13 nm and 1.4 nm, respectively.

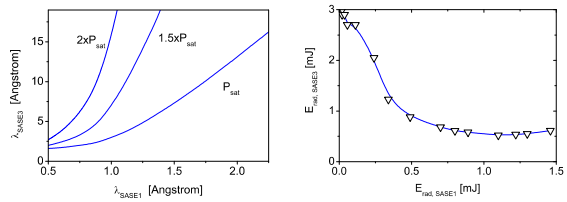


Figure 2: Calculated wavelength coupling (left) and measured pulse energy coupling (right) between SASE1 and SASE3 beamlines when operating SASE3 as a succession of SASE1 for 14 GeV and 250 pC electron beam case.

Mitigate Coupling with Betatron Switcher

In order to mitigate the coupling between SASE1 and SASE3, the betatron switcher technique (also called "fresh bunch" technique) was introduced [7, 8]. Using the fast kicker (4.5 MHz) in front of SASE1 [9], one can give a kick to the SASE3 bunches and generate a betatron oscillation for these bunches in SASE1. This kick is then compensated by a corrector (or a quadrupole kick) in front of SASE3, which also generates a betatron oscillation for the SASE1 bunches in the SASE3 beamline.

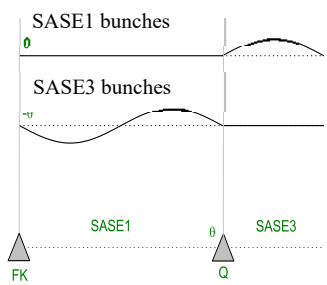


Figure 3: Betatron switcher used to suppress SASE3 bunches lasing in SASE1 and SASE1 bunches lasing in SASE3.

In this way, lasing of SASE3 bunches in SASE1 beamline and SASE1 bunches in SASE3 beamline are suppressed. The scheme of this technique is shown in Fig. 3. Dedicated simulations to study the performance of this

† shan.liu@desy.de

Content from this work may be used under the terms of the CC BY 3.0 licence (© 2019). Any distribution of this work must maintain attribution to the author(s), title of the work, publisher, and DOI

ISBN: 978-3-95450-210-3 doi:10.18429/JACoW-FEL2019-TUA04

HARMONIC LASING EXPERIMENT AT THE EUROPEAN XFEL

E.A. Schneidmiller*, F. Brinker, W. Decking, M. Guetg, S. Liu, D. Noelle,
M. Scholz, M.V. Yurkov, and I. Zagorodnov,
DESY, Hamburg, Germany
N. Gerasimova, G. Geloni, J. Gruenert, J. Laksman, Y. Li, J. Liu, S. Karabekyan, N. Kujala,
Th. Maltezopoulos, I. Petrov, L. Samoylova, S. Serkez, H. Sinn, and F. Wolff-Fabris
European XFEL GmbH, Schenefeld, Germany

Abstract

Harmonic lasing is an opportunity to extend the photon energy range of existing and planned X-ray FEL user facilities. Contrary to nonlinear harmonic generation, harmonic lasing can provide a much more intense, stable, and narrow-band FEL beam. Another interesting application is Harmonic Lasing Self-Seeding (HLSS) that allows to improve the longitudinal coherence and spectral power of a Self-Amplified Spontaneous Emission (SASE) FEL. This concept was successfully tested at FLASH in the range of 4.5 - 15 nm and at PAL XFEL at 1 nm. In this contribution we present recent results from the European XFEL where we successfully demonstrated operation of HLSS FEL at 5.9 Angstrom and 2.8 Angstrom, in the latter case obtaining both 3rd and 5th harmonic lasing.

INTRODUCTION

Successful operation of X-ray free electron lasers (FELs) down to the Angstrom regime opens up new horizons for photon science. Even shorter wavelengths are requested by the scientific community.

One of the most promising ways to extend the photon energy range of high-gain X-ray FELs is to use harmonic lasing, which is the FEL instability at an odd harmonic of the planar undulator [1–5] developing independently from the lasing at the fundamental. Contrary to the nonlinear harmonic generation (which is driven by the fundamental in the vicinity of saturation), harmonic lasing can provide much more intense, stable, and narrow-band radiation.

Another interesting option, proposed in [5], is the possibility to improve spectral brightness of an X-ray FEL by the combined lasing on a harmonic in the first part of the undulator (with an increased undulator parameter K) and on the fundamental in the second part of the undulator. Later this concept was named Harmonic Lasing Self-Seeded FEL (HLSS FEL) [6].

Harmonic lasing was initially proposed for FEL oscillators [7] and was tested experimentally in infrared and visible wavelength ranges. It was, however, not demonstrated in high-gain FELs and at a short wavelength until the successful experiments [8] at the second branch of the soft X-ray FEL user facility FLASH [9,10] where the HLSS FEL operated in the wavelength range between 4.5 nm and 15 nm. Later, the same operation mode was tested at PAL XFEL at 1 nm [11].

* evgeny.schneidmiller@desy.de

In this paper we report on recent results from the European XFEL [12] where we successfully demonstrated operation of HLSS scheme at 5.9 Angstrom and at 2.8 Angstrom. Moreover, we observed for the first time the fifth harmoinc lasing in a high-gain FEL.

HARMONIC LASING

Harmonic lasing in single-pass high-gain FELs [1–5] is the amplification process in a planar undulator of higher odd harmonics developing independently of each other (and of the fundamental) in the exponential gain regime. The most attractive feature of the saturated harmonic lasing is that the spectral brightness (or brilliance) of harmonics is comparable to that of the fundamental [5]. Indeed, a good estimate for the saturation efficiency is $\lambda_w/(hL_{sat,h})$, where λ_w is the undulator period, h is harmonic number, and $L_{sat,h}$ is the saturation length of a harmonic. At the same time, relative rms bandwidth has the same scaling. So, the reduction of power is compensated by the bandwidth reduction and the spectral power remains the same.

Although known theoretically for a long time [1–4], harmonic lasing in high-gain FELs was not considered for practical applications in X-ray FELs. The situation was changed after publication of ref. [5] where it was concluded that the harmonic lasing in X-ray FELs is much more robust than usually thought, and can be effectively used in the existing and future X-ray FELs. In particular, the European XFEL [13] can greatly outperform the specifications in terms of the highest possible photon energy: it can reach 60-100 keV range for the third harmonic lasing. It was also shown [14] that one can keep sub-Angstrom range of operation of the European XFEL after CW upgrade of the accelerator with a reduction of electron energy from 17.5 GeV to 7 GeV. Another application of harmonic lasing is a possible upgrade of FLASH with the aim to increase the photon energy up to 1 keV [15].

HARMONIC LASING SELF-SEEDED FEL

A poor longitudinal coherence of SASE FELs stimulated efforts for its improvement. Since an external seeding seems to be difficult to realize in X-ray regime, a so called self-seeding has been proposed [16, 17]. There are alternative approaches for reducing bandwidth and increasing spectral brightness of X-ray FELs without using optical elements. One of them was proposed in [5], it is based on the combined lasing on a harmonic in the first part of the undulator (with

Content from this work may be used under the terms of the CC BY 3.0 licence (© 2019). Any distribution of this work must maintain attribution to the author(s), title of the work, publisher, and DOI

ISBN: 978-3-95450-210-3 doi:10.18429/JACoW-FEL2019-TUB01

ECHO-ENABLED HARMONIC GENERATION LASING OF THE FERMI FEL IN THE SOFT X-RAY SPECTRAL REGION

P. R. Ribič[†,1], Elettra-Sincrotrone Trieste, Area Science Park, Trieste, Italy
[1]also at University of Nova Gorica, Nova Gorica, Slovenia, on behalf of the EEHG collaboration*

Abstract

The layout of the FERMI FEL-2 undulator line, normally operated in the two-stage high-gain harmonic generation (HGHG) configuration, was temporarily modified to allow running the FEL in the echo-enabled harmonic generation (EEHG) mode. The EEHG setup produced stable, intense, and nearly fully coherent pulses at wavelengths as short as 5.9 nm (~211 eV). Comparing the performance to the two-stage HGHG showed that EEHG gives significantly better spectra in terms of the central wavelength stability and bandwidth, especially at high harmonics, where electron-beam imperfections start to play a significant role. Observation of stable, narrow-band, coherent emission down to 2.6 nm (~474 eV) indicates the possibility to extend the lasing region to even shorter wavelengths.

INTRODUCTION

The FERMI free-electron laser (FEL) in Trieste, Italy is an externally seeded FEL facility consisting of two undulator lines that provide users with laser-like pulses in the entire extreme-ultraviolet (EUV) spectral region. The FEL-1 line is based on a single high-gain harmonic generation (HGHG) stage [1], where an ultraviolet (~264 nm) seed laser is used to trigger the amplification process at a high harmonic h of the seed, producing nearly fully coherent pulses in the range from 100 nm to 20 nm [2]. To reach shorter wavelengths, the FEL-2 line employs a two-stage HGHG cascade based on the fresh-bunch (FB) approach [3], generating output in the range from 20 nm to 4 nm [4]. The high degree of (longitudinal) coherence at FERMI allows performing experiments previously not possible in the EUV, such as, e.g., four wave-mixing [5], and coherent control [6].

Experience has shown, however, that at the shortest wavelengths available at the FEL-2 line, the sensitivity to the shape of the electron-beam (e-beam) phase space becomes critical and may severely affect the FEL radiation in terms of longitudinal coherence, pulse energy, and shot-to-shot stability. In addition, the two-stage HGHG cascade employed at FEL-2 cannot cover the whole harmonic range, as the final harmonic number is a product between the harmonic numbers of the individual stages. Last, but not least, the two-stage setup uses a relatively large portion of the e-beam to accommodate the double seeding process, which makes the implementation of double-pulse operation somewhat difficult.

Recent experiments [7-11] have suggested that the drawbacks of the two-stage HGHG could be overcome by using a seeding technique called echo-enabled harmonic generation (EEHG), where the e-beam phase space is shaped with two seed lasers to enable FEL emission at high harmonics [12]. The method is intrinsically much less sensitive to the initial e-beam imperfections, making it a strong candidate for producing highly stable, nearly fully coherent, and intense FEL pulses, down to soft x-ray wavelengths.

Here, we demonstrate the first EEHG lasing at wavelengths as short as 5.9 nm at the (modified) FEL-2 line at FERMI [13]. We show that EEHG gives significantly better spectra in terms of the central wavelength stability and bandwidth, as compared to the two-stage HGHG cascade. The observation of stable, narrow-band emission down to 2.6 nm indicates the possibility to extend the lasing region to shorter wavelengths.

EXPERIMENT

The implementation of the EEHG seeding scheme at FERMI required modifying the FEL-2 line. The technical details are given in Ref. [14]. In summary, a second seed laser line required by EEHG and delivering up to 50 μJ per pulse at 264 nm was setup; the second stage modulator of FEL-2 was replaced by a new one, allowing resonant interaction at 264 nm; the dispersion of the magnetic chicane normally used for the FB approach was increased to be suitable as the first (strong) chicane for EEHG; new e-beam and laser diagnostics were installed to allow overlapping the e-beam and the second seed laser.

In EEHG, the output wavenumber k_E is given by $k_E = nk_1 + mk_2$, where n and m are non-zero integers and $k_{1,2} = 2\pi/\lambda_{1,2}$ are the wavenumbers of the two seed lasers operating at wavelengths λ_1 and λ_2 [12]. In our experiment, the two seed lasers had the same wavelength, $\lambda_1 = \lambda_2$, so $k_E = (n+m)k_1$, or $\lambda_E = \lambda_1/h$, where $h = n + m$ is the harmonic number and λ_E is the EEHG output wavelength. Most of the measurements were performed in the $n = -1$ configuration to maximize the signal [12], but we have also observed output at $n = -2, -3$, and $n = -4$. The latter option was employed at high harmonics due to the limitations of our setup (limited first dispersion and limited second seed power).

To optimize the EEHG output at a specific harmonic h, the first (strong dispersion) $R_{56}^{(1)}$ was fixed (to typically around 2 mm, depending on the e-beam energy) and the strength of the second dispersion section $R_{56}^{(2)}$ was set according to $R_{56}^{(2)} \approx \frac{|n|}{h} R_{56}^{(1)}$ [12]. All of the parameters (second dispersion and both seed laser intensities) were iteratively tuned to maximize emission.

† primoz.rebernik@elettra.eu

Content from this work may be used under the terms of the CC BY 3.0 licence (© 2019). Any distribution of this work must maintain attribution to the author(s), title of the work, publisher, and DOI

ISBN: 978-3-95450-210-3 doi:10.18429/JACoW-FEL2019-TUP001

Content from this work may be used under the terms of the CC BY 3.0 licence (© 2019). Any distribution of this work must maintain attribution to the author(s), title of the work, publisher, and DOI

EXTENSION OF THE PITZ FACILITY FOR A PROOF-OF-PRINCIPLE EXPERIMENT ON THz SASE FEL

P. Boonpornprasert*, G. Georgiev, G. Koss, M. Krasilnikov, X.K. Li, F. Müller, A. Oppelt, S. Philipp, H. Shaker, F. Stephan, T. Weilbach, DESY, Zeuthen, Germany
Z. Amirkhanyan, CANDLE, Yerevan, Armenia

Abstract

The Photo Injector Test Facility at DESY in Zeuthen (PITZ) has been proposed as a suitable facility for research and development of an accelerator-based THz source prototype for pump-probe experiments at the European XFEL. A proof-of-principle experiment to generate THz SASE FEL radiation by using an LCLS-I undulator driven by an electron bunch from the PITZ accelerator has been planned and studied. The undulator is foreseen to be installed downstream from the current PITZ accelerator, and an extension of the accelerator tunnel is necessary. Radiation shielding for the extended tunnel was designed, and construction works are finished. Design of the extended beamline is ongoing, not only for this experiment but also for other possible experiments. Components for the extended beamline, including magnets for beam transport, a chicane bunch compressor, electron beam diagnostics devices, and THz radiation diagnostics devices have been studied. An overview of these works will be presented in this paper.

INTRODUCTION

The European XFEL has planned to perform pump-probe experiments by using its x-ray pulses and THz pulses. To provide the THz pulses, THz generation using laser-based and accelerator-based sources has been considered and studied [1]. For the accelerator-based sources, an interesting idea is to generate THz pulses using a Self-Amplified Spontaneous Emission (SASE) FEL driven by electron bunches from a "PITZ-like" accelerator. Preliminary simulations in [2] show that the SASE FEL can produce pulse energies up to 1 mJ with a spectrum bandwidth of 2-3 % at a wavelength of 100 µm.

Based on the above idea, PITZ has been considered as an ideal machine for the development of such a THz source. Proof-of-principle experiments to generate THz SASE FEL radiation by using an LCLS-I undulator driven by an electron bunch from the PITZ accelerator has been planned and studied. Preliminary Start-to-End (S2E) simulations based on a model beamline were performed [3, 4], yielding a THz pulse energy of about 0.5 mJ at a wavelength of 100 µm.

In order to demonstrate such SASE FEL generation experimentally, installation of the LCLS-I undulator downstream from the current PITZ accelerator has been planned. Figure 1 shows a schematic layout of the PITZ facility. There are two tunnels, the main tunnel and the tunnel annex, separated by a concrete wall with a thickness of 1.5 m. The undulator is foreseen to be installed in the tunnel annex. Therefore, an extension of the existing beamline to connect with the undulator is required.

This paper describes a proposed configuration of the beamline extension and radiation shielding improvement for the tunnel annex. Note that the configuration has not been fully optimized. Studies towards a final design and construction are ongoing.

TUNNEL EXTENSION AND RADIATION SHIELDING IMPROVEMENT

We plan to transport the electron beam from the main tunnel through an aperture inside the wall to the undulator in the tunnel annex, as shown in Fig. 1. Since the electron beam will be blocked by a beam dump in the tunnel annex, the radiation shielding of this tunnel has to be improved.

The FLUKA simulation package [5] was used to calculate produced radiation dose rates and design appropriate radiation shielding for the tunnel annex. The design goal was to limit the dose rates outside the accelerator area to less than 3 μSv/h during beam operations. The radiation protection wall and the movable door made of barite concrete (density of >3.4 t/m^3) were realized as the appropriate shielding. Construction of the radiation shielding was already finished, as shown in Fig 2.

THE EXTENSION BEAMLINE

The layout of the extension beamline is surrounded by the red dashed box in Fig. 1. Main components of the extended beamline are a chicane bunch compressor, collimators, a switchyard, the LCLS-I undulator, and beam dump sections.

The chicane bunch compressor consists of four magnets (D1-D4) with a negative R56 of -0.17 m. Its total length is 3.56 m and it is designed to deflect the electron beam vertically. Design consideration of the chicane is presented in [6].

Vertical and horizontal collimators are used to remove unwanted parts of the beam. Each collimator is a metal sheet with various apertures. The collimator station is located in the main tunnel before the wall. It consists of horizontal and vertical actuators supplied with the collimators. Each collimator can be used individually or simultaneously with the other one.

The Switchyard is a dipole magnet located directly after the wall in the tunnel annex. It is used as a horizontal steerer magnet in the current configuration. However, there are possible plans to add other beamlines in the tunnel annex

* prach.boonpornprasert@desy.de

ISBN: 978-3-95450-210-3 doi:10.18429/JACoW-FEL2019-TUP002

PROGRESS IN PREPARING A PROOF-OF-PRINCIPLE EXPERIMENT FOR THz SASE FEL AT PITZ*

X.-K. Li†, M. Krasilnikov, P. Boonpornprasert, H. Shaker, Y. Chen, G. Georgiev, J. Good, M. Gross, P. Huang, I. Isaev, C. Koschitzki, S. Lal, O. Lishilin, G. Loisch, D. Melkumyan, R. Niemczyk, A. Oppelt, H. Qian, G. Shu, F. Stephan, G. Vashchenko, DESY, Zeuthen, Germany

Abstract

A proof-of-princle experiment for a THz SASE FEL is undergoing preparation at the Photo Injector Test facility at DESY in Zeuthen (PITZ), as a prototype THz source for pump-probe experiments at the European XFEL, which could potentially provide up to mJ/pulse THz radiation while maintaining the identical pulse train structure as the XFEL pulses. In the proof-of-principle experiment, LCLS-I undulators will be installed to generate SASE radiation in the THz range of 3-5 THz from electron bunches of 16-22 MeV/c. One key design is to obtain the peak current of nearly 200 A from the heavily charged bunches of a few nC. In this paper, we report our simulation results on the optimization of the space charge dominated beam in the photo injector and the following transport line with two cathode laser setups. Experimental results based on a short Gaussian laser will also be discussed.

INTRODUCTION

At the European X-ray free-electron laser facility (EuXFEL) pump-probe experiments play important roles in many research frontiers in biology, chemistry and condensed matters, etc. Among them are the THz-pump X-ray-probe experiments, where a THz pulse is used to excite a sample and the following X-ray pulse is used to detect its reactions [1]. In order to provide the THz pump source, several proposals are under consideration. In one proposal the high-energy electron beam will be re-used to drive a THz undulator [2], as already demonstrated at FLASH [3]. Another idea is to put an independent PITZ-like photo-injector near the user hall to drive a THz undulator [4], which is currently undergoing a proof-of-principle experiment at PITZ. The expected advantages include: 1) Due to the low beam energy, the accelerator needs no big beam dump and can be installed close to user experiments so that no long THz beamline has to be built; 2) The PITZ-like accelerator with identical bunch train structure as the XFEL pulses could support all the EuXFEL end stations with THz pulses, provided that a switchyard for the THz pulses is built. Previous studies [4–7] have showed that milli-joule level THz pulses could be generated from 4 nC electron bunches with 200 A peak current in Apple-II or similar undulators through the SASE process. For the proof-of-principle experiment, the existing PITZ beamline is to be extended with LCLS-I undulators installed in the tunnel annex. In this paper, we will report the current status of this project, including start-to-end simulation studies based on a regularly operating Gaussian cathode laser and on a longitudinally shaped flattop laser. It will be shown that similar peak current can be achieved from both laser setups and the resulting radiation energies are close to 1 mJ. For Gaussian laser pulses, experiments have been carried out to demonstrate the production of a few nC bunch charge and the possibility of matching the heavily charged bunch to the undulator.

* Work supported by the European XFEL GmbH
† xiangkun.li@desy.de

START-TO-END SIMULATIONS

The photo-injector at PITZ consists of an L-band photocathode RF gun, solenoids for emittance compensation, an L-band booster cavity and many correction and focusing magnets, with a total beamline length of 22 m [8]. In the start-to-end simulations, we first optimize the photo-injector and then design the transport line until the proposed undulator entrance. The radiation from the optimized beams is finally evaluated with Genesis 1.3 [9]. At PITZ, two cathode laser setups are available: a short Gaussian laser (FWHM=6~7 ps) which is in stable operation and a long flattop laser (FWHM~22 ps) which can be realized by longitudinal pulse shaping with bi-diffracting crystals before the laser is amplified [8]. Although both lasers are Gaussian transversely, it is also possible to produce approximately uniform transverse distributions by overfilling a tunable beam shaping aperture (BSA). For the THz project, both lasers are under consideration. For the Gaussian laser, relatively small bunch charge of 2.5 nC is employed to avoid emission saturation, as shown later. In the presence of the long flattop laser, the bunch charge of 4 nC is taken.

Optimization of the Injector

In the optimization we took the highest achievable gun gradient of 60 MV/m into account to reduce the space charge effects during emission. With this gradient, the highest beam momentum downstream the booster is about 22 MeV/c, which corresponds to a radiation wavelength of 60 µm in the LCLS-I undulator. In this paper, we consider a nominal wavelength of 100 µm (3 THz in frequency) with a beam momentum of 17 MeV/c.

Since the beam emittance is not critical for FELs in the THz range, the optimization is focused on the peak current and the energy spread [5], as a higher peak current helps to improve the FEL gain and a smaller energy spread simplifies beam transport and also leads to higher FEL gain. With the particle tracking code Astra [10], the laser spot size, the accelerating phases in the gun and in the booster and the solenoid current were searched by the differential-evolution

Content from this work may be used under the terms of the CC BY 3.0 licence (© 2019). Any distribution of this work must maintain attribution to the author(s), title of the work, publisher, and DOI

ISBN: 978-3-95450-210-3 doi:10.18429/JACoW-FEL2019-TUP003

DESIGN OF A MAGNETIC BUNCH COMPRESSOR FOR THE THz SASE FEL PROOF-OF-PRINCIPLE EXPERIMENT AT PITZ*

H. Shaker†, P. Boonpornprasert, G. Georgiev, G. Koss, M. Krasilnikov, X. Li, A. Lueangaramwong, F. Mueller, A. Oppelt, S. Philipp, F. Stephan, G. Vashchenko, T. Weilbach
DESY, Zeuthen, Germany

Abstract

For pump-probe experiments at the European XFEL, a THz source is required to produce intense THz pulses at the same repetition rate as the X-ray pulses from XFEL. Therefore, an accelerator-based THz source with identical electron source as European XFEL was suggested [1] and proof-of-principle experiments utilizing an LCLS I undulator will be performed at the Photo Injector Test Facility at DESY in Zeuthen (PITZ). The main idea is to use a 4nC beam for maximizing the SASE radiation but also to allow different radiation regimes, a magnetic bunch compressor can be used. This helps e.g. to reduce the saturation length inside the undulator and also to study super-radiant THz radiation. In this paper a design of a chicane type magnetic bunch compressor re-using HERA corrector magnets is presented.

INTRODUCTION

To demonstrate an accelerator-based tunable THz source for pump-and-probe experiments at the European XFEL, a proof of principle study is started at the Photo-Injector Test Facility at DESY in Zeuthen site (PITZ) [1-8]. This experiment will be done by using the electron beam produced at PITZ and by using LCLS-I undulators inside the existing accelerator tunnel extension. Since PITZ and European XFEL electron sources are identical, the X-ray and THz radiation can be produced with identical bunch train structure. This means for every X-ray pulse a corresponding THz pulse can be provided for the pump-and-probe experiments.

With nominal 4 nC bunch charge, 200 A peak current and 16-25 MeV, this experiment wants to demonstrate a near one milli-joule pulse energy radiation in the frequency range of 3-15 THz based on the SASE mechanism. To have flexibility to work with lower charges and shorter initial bunches a magnetic bunch compressor is required. By beam compressing, we will have shorter bunch length with higher peak current. This effect reduces the saturation length inside the undulator and also opens the door for coherent or super-radiant radiation studies [9]. In this paper, a design for a chicane-type magnetic bunch compressor will be presented. This bunch compressor will be installed in the main PITZ tunnel and since PITZ is a multi-purpose machine minimum beamline modification is desirable. To take advantages of available components, we will re-use corrector magnets from earlier HERA machine at DESY to assemble the bunch compressor. Figure 1 shows the end-section of the PITZ beamline in the main tunnel. In this figure, you can see the vertical chicane and the rotated beam dump which will be added to the current beamline. We considered both the desired bunch compressing magnitude and available spaces in the beamline to find an optimum design.

R_{56} is a main parameter of the bunch compressor and can be expressed in the first order by $R_{56}=\Delta z/\delta$, where Δz is the difference between output and input bunch lengths and δ is the relative energy spread. Inside a chicane type bunch compressor without any quadrupoles the higher energy particles travels less distance then it has negative R_{56} . This means we need a positive energy chirp for bunch compressing. The positive energy chirp can be produced by changing the booster phase. The acceptable maximum relative energy spread can be calculated based on 1-D FEL theory. Based on this theory the relative energy spread should be less than the Pirece parameter (ρ) [10]:

$$(1)\quad \begin{cases} \rho = \left[\frac{I}{\gamma^3 I_A}\frac{{\lambda_u}^2}{2\pi\sigma_x\sigma_y}\frac{(K\times[JJ])^2}{32\pi}\right]^{1/3} \\ [JJ] = J_0(\xi) - J_1(\xi)\,,\ \xi = \frac{K^2}{2(2+K^2)} \\ I_A \approx 17kA \end{cases}$$

For the LCLS-I undulator, the undulator K parameter is 3.49 and its periodic length (λ_u) is 3 cm. For the rms beam size (σ_x and σ_y) of about 1 mm and peak current (I) of 200 A, the Pierece parameter is equal to 0.015 and 0.01 for the beam energy of 16 MeV and 25 MeV, respectively. To cover the full energy range, the maximum 1% energy chirp is selected for our design. Using equation (1), R_{56} would be about -0.18m for maximum 6ps compression from the bunch center for each side. This means for a relative short bunch we can compress a bunch to sub-picosecond level. R_{56} is only dependent to the first drift length (L_1), dipole length (L_d) and the deflecting angle (θ) and it can be calculated roughly using this equation [11]:

$$(2)\quad R_{56} \approx -\theta^2(2\times L_1 + 4/3\times L_d)$$

To install the bunch compressor, there are two free spaces available at the end of PITZ beamline, one between 1st and 3rd dipole in Second High Energy Dispersive Arm (HEDA2) and another one between the 3rd HEDA2's dipole and the tunnel wall. But both spaces are not enough alone to fit the bunch compressor. Therefore we decided to use a vertical setup which helps us to use both spaces without any need to remove the HEDA2 dipoles. Based on this setup, the minimum acceptable angle for the chicane is 16.77° to not hit the 3rd dipole of HEDA2.

* Work supported by the European XFEL
† hamed.shaker@desy.de

Content from this work may be used under the terms of the CC BY 3.0 licence (© 2019). Any distribution of this work must maintain attribution to the author(s), title of the work, publisher, and DOI

ISBN: 978-3-95450-210-3 doi:10.18429/JACoW-FEL2019-TUP004

A SUPERRADIANT THz UNDULATOR SOURCE FOR XFELS

T. Tanikawa*, S. Karabekyan, S. Serkez, G. Geloni, European XFEL, Schenefeld, Germany
S. Kovalev, Helmholtz-Zentrum Dresden-Rossendorf (HZDR), Dresden, Germany
S. Casalbuoni, Karlsruhe Institute of Technology, Karlsruhe, Germany
V. B. Asgekar, S.P. Pune University, Pune, India
M. Gensch[1], Technische Universität Berlin, Berlin, Germany
[1]also at German Aerospace Center (DRL), Berlin, Germany

Abstract

The European XFEL has successfully achieved first lasing in 2017 and meanwhile three SASE FEL beamlines are in operation. An increasing number of users has great interest in a specific type of two-color pump-probe experiments in which high-field THz pulses are employed to drive nonlinear processes and dynamics in matter selectively. Here, we propose to use a 10-period superconducting THz undulator to provide intense, narrowband light pulses tunable in wide range between 3 and 100 THz. The exploitation of superconducting technology allows us to meet the challenge of generating such low photon energy radiation despite the very high electron beam energy at the European XFEL. In this paper, we will present the latest developments concerning THz undulator design and the expected THz pulse properties for the case of the European XFEL.

CONCEPT AND MOTIVATIONS

X-ray Free-Electron Lasers are currently the extremely bright and tunable sources of ultrashort X-ray pulses available for basic scientific research. Among many possible uses, the ultrahigh brightness and the ultrashort duration of these pulses can be exploited in a "pump-probe" configuration, to probe non-equilibrium states of a matter sample that can be excited by previous interaction with terahertz radiation. Since the latest generation XFELs under early operation stages or construction, such as the European XFEL [1] and the LCLS-II [2] are based on superconducting technology, THz pulses are also required in CW or burst mode with repetition rates of between 100 kHz and 4.5 MHz. The generation of high-field THz pulses at such high duty-cycle by means of femtosecond lasers does not allow achieving the required parameters in terms of pulse energy and narrowbandwidth; therefore, a superradiant THz undulator emerges as one promising solution. In this paper, we describe the technological feasibility for implementing a few-period superradiant THz undulator that fits the particular case of the electron linac of the European XFEL.

THz UNDULATOR PARAMETERS

The main challenge in the construction of a THz undulator for the production of superradiant THz pulses at the European XFEL is the very high-energy of the electron beam, nominally in the range from 8.5 to 17.5 GeV. In fact, the resonance condition on-axis for the first harmonic reads:

$$\lambda = \lambda_U \frac{1 + K^2/2}{2\gamma^2} , \quad (1)$$

and

$$K = 93.66 B[T] \lambda_U[m] \quad (2)$$

with λ the fundamental wavelength, λ_U the undulator period, γ the Lorentz factor, K the undulator parameter, and B the magnetic field. We will limit our considerations to fundamental frequencies higher than 3 THz, corresponding to about $\lambda = 100$ µm, and assuming an electron beam energy fixed throughout the paper of 17.5 GeV. If we now fix $\lambda_U =$ 1 m, we find that in order to reach a minimal frequency of about 3 THz a value K = 685 is needed, corresponding to a maximum field on axis B ≈ 7.3 T, which is feasible to reach using a well-proven NbTi technology.

The total pulse energy generated by a single electron bunch W_{bunch} while passing through any kind of radiator depends on the bunch length and follows the relation

$$W_{bunch} = N_e[1 + (N_e - 1)|\bar{F}(\nu)|^2]W_0 \quad (3)$$

where Ne is the number of electrons in the bunch, W_0 the pulse energy emitted by a single electron and $\bar{F}(\nu)$ the bunch form factor. In order to sustain FEL lasing at X-ray wavelengths, very high peak currents must be achieved (in the order of several kilo amperes for the European XFEL), and hence it is needed to strongly compress the electron bunch in the first place. Therefore, it makes sense to exploit the spent XFEL electron beam for generating superradiant THz pulses, because the form factor until high THz frequency is available. The level of compression depends on the charge, with bunches of lower charge being compressed more to obtain the same peak-current level. In Fig. 1, the nominal electron current profiles, calculated using start-to-end simulation for the European XFEL with different charges [3], are reported. In Fig. 2 we show the pulse energy that can be obtained at different fundamental frequencies (by changing the K parameter of the THz undulator) for several nominal electron bunch charges using 10 % bandpass filter with boxcar line function. From Fig. 2 we can see a competition between the N_e^2 dependence of the pulse energy, which favors high charges, and the form factor dependence on the frequency, which favors low charges (at the same peak current, needed to sustain the previous FEL process). As expected, the highest electron charge considered here, 500 pC, yields the best

* takanori.tanikawa@xfel.eu

Content from this work may be used under the terms of the CC BY 3.0 licence (© 2019). Any distribution of this work must maintain attribution to the author(s), title of the work, publisher, and DOI

ISBN: 978-3-95450-210-3 doi:10.18429/JACoW-FEL2019-TUP006

THE FHI FEL UPGRADE DESIGN

W. Schöllkopf, S. Gewinner, A.M.M. Todd[1], W.B. Colson[1], M. De Pas, D. Dowell[1], S.C. Gottschalk[1], H. Junkes, J.W. Rathke[1], T.J. Schultheiss[1], L.M. Young[1], G. von Helden, and G. Meijer
Fritz-Haber-Institut der Max-Planck-Gesellschaft, Berlin, Germany

Abstract

Since coming on-line in November 2013, the Fritz-Haber-Institut (FHI) der Max-Planck-Gesellschaft (MPG) Free-Electron Laser (FEL) has provided intense, tunable infrared radiation to FHI user groups. It has enabled experiments in diverse fields ranging from bio-molecular spectroscopy to studies of clusters and nanoparticles, nonlinear solid-state spectroscopy, and surface science, resulting in more than 55 peer- reviewed publications so far. A significant upgrade to the original FHI FEL has been funded and is presented here.

A second short Rayleigh range undulator FEL beamline is being added. It will permit lasing from < 5 μm to > 160 μm. Additionally, a 500 MHz kicker cavity will permit simultaneous two-colour operation of the FEL from both FEL beamlines over an optical range of 5 to 50 microns by deflecting alternate 1 GHz pulses into each of the two undulators. We describe the upgraded FHI FEL physics and engineering design and present the plans for two-colour FEL operations by the end of 2020.

FEL LAYOUT & DESIGN PARAMETERS

The layout of the original and proposed FHI FEL Upgrade beamlines is shown in Fig. 1. The existing design consists of the accelerator section, the MIR beamline and a diagnostic beamline. The design performance parameters and physics design [1], the engineering design [2], first lasing [3], and subsequent user performance [4] for the existing FEL have been described.

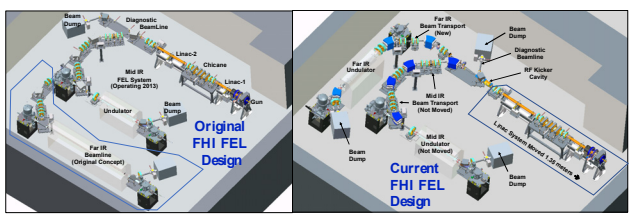


Figure 1: Original (left) and Current (right) FHI MIR and FIR FEL Designs.

The FEL consists of a 50 MeV accelerator driven by a gridded thermionic gun with a beam transport system that feeds two undulators and a diagnostic beamline. The first normal-conducting 2.998 GHz linac accelerates the electron bunches to a nominal energy of 20 MeV, while the second one accelerates or decelerates the electrons to deliver any final energy between 15 and 50 MeV. A chicane between the structures allows for adjustment of the bunch length as required. Originally, the Mid-IR and Far-IR undulators were planned to be parallel to each other directed 180 degrees from the accelerator axis [Refs. 1, 2]. However, we have now selected a single achromat for the Far-IR FEL which is now at 90 degrees to the accelerator axis. The accelerator section has been moved back 1.35 m to allow insertion of an RF kicker cavity, and the diagnostic beamline has been relocated. The principal subject of this paper is the design and fabrication of the Far-IR beamline and FEL, and the changes in configuration from the original design that we have adopted.

MID-IR FEL PERFORMANCE

The generated IR radiation forms ps-long micro-pulses at a pulse repetition rate of 1 GHz. Up to 10,000 consecutive micro-pulses form a pulse train, referred to as the macro-pulse that are repeated at a rate of 10 Hz. Figure 2 shows tuning curves of the macro-pulse energies for 6 different electron energies ranging from 18 to 44 MeV. For any given electron energy, the IR wavelength can be tuned continuously by a factor of 2 to 3 by changing the undulator gap. The data plotted in Fig. 2 has been observed for a relatively narrow FEL line spectrum with $\Delta\lambda / \lambda \sim 0.4$, where λ is the central wavelength and $\Delta\lambda$ denotes the full width at half maximum (FWHM) of the spectral distribution that is monitored with a grating spectrometer. Best performance in terms of macro-pulse energy is found for $\lambda \sim 7.5$ μm. Even more pulse energy (and pulse peak power) can be achieved by fine adjustment of the FEL cavity length (5.4 m nominal length) at the cost of an increased spectral line width. The latter corresponds to shorter mid-IR radiation pulses. This way, pulses as short as 500 fs can be generated.

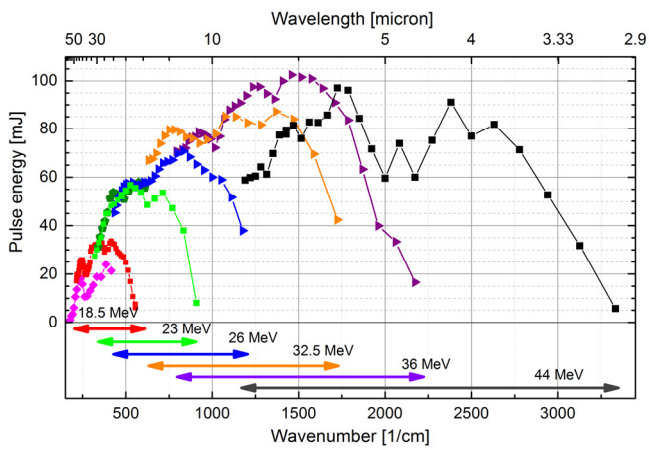


Figure 2: Macro-pulse energy measured at the FHI FEL Mid-IR system which has been in user operation since 2013. Each curve is measured by an undulator gap scan for the electron energies indicated at the bottom.

1 Consultants to the Fritz-Haber-Institut

Content from this work may be used under the terms of the CC BY 3.0 licence (© 2019). Any distribution of this work must maintain attribution to the author(s), title of the work, publisher, and DOI

ISBN: 978-3-95450-210-3 doi:10.18429/JACoW-FEL2019-TUP007

EXPERIENCE WITH THE SUPERRADIANT THz USER FACILITY DRIVEN BY A QUASI-CW SRF ACCELERATOR AT ELBE

M. Bawatna†, Helmholtz-Zentrum Dresden-Rossendorf (HZDR), Dresden, Germany
B. Green, Magnet Science & Technology, Tallahassee, FL, USA

Abstract

Instabilities in beam and bunch parameters, such as bunch charge, beam energy or changes in the phase or amplitude of the accelerating field in the RF cavities can be the source of noise in the various secondary sources driven by the electron beam. Bunch charge fluctuations lead to intensity instabilities in the superradiant THz sources. The primary electron beam driving the light sources has a maximum energy of 40 MeV and a maximum current of 1.6 mA. Depending on the mode of operation required, there are two available injectors in use at ELBE. The first is the thermionic injector, which is used for regular operating modes and supports repetition rates up to 13 MHz and bunch charges up to 100 pC. The second is the SRF photocathode injector, which is used for experiments that may require lower emittance or higher bunch charges of up to 1 nC. It has a maximum repetition rate of 13 MHz, which can be adjusted to lower rates if desired, also including different macro pulse modes of operation. In this contribution, we will present our work in the pulse-resolved intensity measurement that allows for correction of intensity instabilities.

INTRODUCTION

The Electron Linac for beams with high Brilliance and low Emittance (ELBE) superconducting radiofrequency (SRF) accelerator [1] is a facility at the Helmholtz Zentrum Dresden Rossendorf (HZDR). At the ELBE user facility, there are two available electron injectors in use [1,2] as in Fig. 1. The thermionic injector, which supports repetition rates up to 13 MHz and bunch charges up to 100 pC, and the Super Radio Frequency (SRF) photo-cathode injector, which is used for experiments that may require lower emittance or higher bunch charges of up to 1 nC. Moreover, the SRF injector at ELBE also has a maximum repetition rate of 13 MHz with different macro pulse modes of operation. The required properties of the electron bunches (form, charge, position) afford electron beam diagnostics that exceeds presently available solutions at ELBE. Here we discuss ideas of suitable electron bunch diagnostic techniques amongst which novel single-shot electro-optic techniques for online monitoring of electron bunch form and arrival time in a new THz lab, equipped with state of the art spectrometers and laser systems.

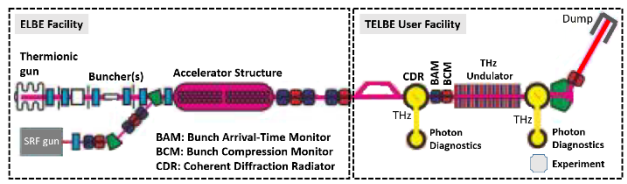


Figure 1: ELBE accelerator beamlines for THz radiation production.

The superradiant THz sources at ELBE accelerator (TELBE) THz facility is performing ultra-fast pump-probe experiments by providing a unique combination of high pulse energies and high repetition rates. In this type of experiment, the electric or magnetic field in the THz pump pulse acts as the excitation of dynamics in the matter. This dynamic in turn is then probed by ultra-short (light) pulses, typically with the sub THz cycle resolution as in [3].

In this paper, we will present the pulse-resolved intensity monitor at TELBE.

The paper is organized as follows: the first section introduces the requirements for the pulse-resolved intensity monitor at TELBE. The second section presents the methods and material used, as well as the intensity instability measurements. After summarizing the results, foreseeable future development and upgrades are discussed.

TERAHERTZ RADIATION DETECTION AT TELBE

Detecting THz radiation can sometimes be problematic because it occupies a position in the electromagnetic spectrum between optical and microwave wavelengths.

There are many different approaches to detecting THz, utilizing a variety of physical phenomena. The ability to detect THz is critical to our work at TELBE user facility, as this is a necessary prerequisite to using it in meaningful experiments and diagnostic setups.

It is crucial to be able to see the intensity of single pulses, to get a reliable measurement of the average power, and to analyze the beam profile. Some experiments require information on the longitudinal (in the time domain) shape of individual pulses or even their actual waveform. The following sections present the pyroelectric THz detection scheme utilized at TELBE to characterize the TELBE THz radiation.

Pyroelectric Detectors

The pyroelectric effect is a phenomenon that occurs when so-called pyroelectric materials change temperature. Changes in temperature cause a change of the electrical polarization, which induces a voltage across the material.

† m.bawatna@hzdr.de

Content from this work may be used under the terms of the CC BY 3.0 licence (© 2019). Any distribution of this work must maintain attribution to the author(s), title of the work, publisher, and DOI

ISBN: 978-3-95450-210-3 doi:10.18429/JACoW-FEL2019-TUP008

CONCEPT OF HIGH-POWER CW IR-THz SOURCE FOR THE RADIATION SOURCE ELBE UPGRADE

P. Evtushenko†, U. Lehnert, P. Michel, T. Cowan,
Helmholtz-Zentrum Dresden-Rossendorf, Dresden, Germany

Abstract

The Radiation Source ELBE at Helmholtz-Zentrum Dresden-Rossendorf (HZDR) is a user facility based on a 1 mA - 40 MeV CW SRF LINAC. Presently HZDR is considering upgrade options for the ELBE or its replacement with a new CW, SRF LINAC-based user facility. A part of the user requirements is the capability to generate IR and THz pulse in the frequency range from 0.1 through 30 THz, with pulse energies in the range from 100 μJ through a few mJ, at the repetition rate between 100 kHz and 1 MHz. This corresponds to the pulse energy increase, dependent on the wavelength, by a factor from 100 through 1000. In this contribution, we outline key aspects of a concept, which would allow to achieve such parameters. These aspects are: 1 - use of a beam with longitudinal density modulation and bunching factor of about 0.5 at the fundamental frequency; 2 - achieving the density modulation through the mechanism similar to the one used in optical klystron (OK); 3 – generating the necessary for the modulation optical beam by an FEL oscillator, and 4 - using two electron injectors. First injector would provide a beam for the FEL oscillator. Second high charge injector would provide the beam for the high pulse energy generation for users. All-in-all the concept of the new radiation source is very similar to an OK, but operating with two beams simultaneously.

INTRODUCTION

To achieve the very high pulse energies of few hundred μJ, at the above-mentioned repetition rates a new configuration of the photon source is proposed. To our knowledge other existing electron beam-based photon generation schemes cannot provide the required combination of the high pulse energy and repetition rate. In the scheme proposed here an electron beam with a longitudinally modulated density will be used to generate coherent undulator radiation. It is suggested to achieve the necessary longitudinal density modulation of the electron beam with the help of a scheme similar to the one used in Optical Klystron FEL OK [1]. Operation of such a photon source will require the seeding, i.e., energy modulating optical beam, tunable, essentially, in the whole frequency range of the source - 0.1 to 30 THz, with sufficiently high peak power. With suggest, that such sources can be realized as an FEL oscillator. Moreover, it is proposed that the intra-cavity optical pulse of the oscillator should be used for the energy modulation of the electron beam. This will allow to significantly relax the requirements on the oscillator and on the electron beam, required to drive it. The required FEL oscillator can be operated with the electron beam with the bunch charge less than 100 pC. To keep the optical resonator length easily manageable, the oscillator can be operated with the bunch frequency of about 10 MHz. The combination of the 100 pC bunch charge and the repetition rate of the 10 MHz would require a CW accelerator system with average current of about 1 mA, which is comfortably within the ELBE's accelerator system capability.

To satisfy the requirements of the high IR-THz pulse energy, the beam with the bunch charge significantly higher, than the 100 pC necessary for the seeding oscillator, will necessary. It is suggested to operate such beam with the bunch charge approximately 10 times higher, i.e., at 1 nC, or higher, when allowed by electron gun technology. For higher reliability, easier tuning and optimization of such a radiation source, it is proposed that the 100 pC beam and 1 nC beam should be generated by two separate electron sources. The repetition rate of high bunch charge beam can be as high as 1 MHz. The minimal repetition frequency of the high charge beam can be arbitrary low, with the only condition that it must be a sub-harmonic of the repetition frequency of the beam in the FEL oscillator-modulator.

The undulator based source will provide a relatively narrowband – multicycle radiation pulses. In parallel to such a source, the new facility would also have a broadband few-cycle THz sources. These sources will be based either on a coherent diffraction radiation CDR, coherent synchrotron radiation (CSR) or coherent edge radiation (CER) from a dipole magnet. To provide high pulse energy this source would be operated by the beam from the high bunch charge electron gun. The continuous pulse train, from the high bunch charge electron gun, can be split into few beams with the help of an RF separator. The different beams, downstream of the RF separator would be used to drive different sources simultaneously.

SUPERRADIANT UNDULATOR WITH STRONGLY COMPRESSED BUNCH

The intensity of coherent undulator radiation, as of any other coherent radiation mechanism, can be expressed as $I_c(\omega) = I_c(\omega)\, N_e^2\, |f_b(\omega)|^2$, where $I_0(\omega)$ is the undulator radiation intensity from a single electron, N_e is the number of the electrons in the bunch, and $f_b(\omega)$ is the Fourier transform of the longitudinal bunch distribution also called bunching factor. Since the coherent radiation intensity dependence on the bunch charge is quadratic, a part of the new facility design direction is to use the bunch charge as high as practical for a CW accelerator system.

To understand the concept proposed here and our design choices, it is helpful to consider, first, the coherent

†P.Evtushenko@hzdr.de

Content from this work may be used under the terms of the CC BY 3.0 licence (© 2019). Any distribution of this work must maintain attribution to the author(s), title of the work, publisher, and DOI

ISBN: 978-3-95450-210-3 doi:10.18429/JACoW-FEL2019-TUP009

Content from this work may be used under the terms of the CC BY 3.0 licence (© 2019). Any distribution of this work must maintain attribution to the author(s), title of the work, publisher, and DOI

INTEGRATION OF AN XFELO AT THE EUROPEAN XFEL FACILITY*

P. Rauer†, I. Bahns, W. Hillert, J. Rossbach, Universität Hamburg , Hamburg, Germany
W. Decking, Deutsches Elektronen Synchrotron (DESY), Hamburg, Germany
Harald Sinn, European XFEL GmbH, Schenefeld, Germany

Abstract

An X-ray free-electron laser oscillator (XFELO) is a fourth generation X-ray source promising radiation with full three dimensional coherence, nearly constant pulse to pulse stability and more than an order of magnitude higher peak brilliance compared to SASE FELs. Proposed by *Kim et al.* in 2008[1] an XFELO follows the concept of circulating the light in an optical cavity - as known from FEL oscillators in longer wavelength regimes - but uses Bragg reflecting crystals instead of classical mirrors. With the new European X-ray free-electron laser (XFEL) facility recently gone into operation, the realization of an XFELO with radiation in the Angstrom regime seems feasible. Though, the high thermal load of the radiation on the cavity crystals, the high sensibility of the Bragg-reflection on reflection angle and crystal temperature as well as the very demanding tolerances of the at least 60 m long optical resonator path pose challenges which need to be considered. In this work these problems shall be summarized and results regarding the possible integration of an XFELO at the European XFEL facility will be presented.

INTRODUCTION

Current hard X-ray free-electron laser (FEL) facilities all use the self-amplified spontaneous emission (SASE) scheme for operation. While these sources produce very brilliant femtosecond X-ray pulses with excellent transverse coherence, they suffer from a lack of longitudinal coherence. A promising approach for reaching full longitudinal coherence in the hard X-ray regime proposed by *Kim et al.* in 2008 [1] is the X-ray free-electron-laser oscillator (XFELO). This scheme is based on using an undulator very short compared to state of the art hard X-ray SASE sources and a highly reflective cavity based on very pure diamond crystals serving as Bragg reflectors. As these Bragg reflectors also act as spectral filters an XFELO promises a spectral bandwidth in the order of the crystals bandwidth ($\Delta\lambda/\lambda_c \approx 10^{-5} - 10^{-7}$) and therefore orders of magnitude better than SASE-FELs. Furthermore, as the radiation field is built up over many cavity round trips, very low shot-to-shot fluctuations can be expected, even making the XFELO a promising candidate for X-ray quantum optics (XQO) [2]. With the recently commissioned European XFEL the realization of an XFELO becomes in reach. This is due to the facility's excellent electron beam properties and especially due to its very high bunch repetition rate of up to 4.5 MHz in pulsed-mode [3] which enables resonator lengths of only 33 m.

* Work supported by BMBF (FKZ 05K16GU4)
† patrick.rauer@desy.de

As will be evident from the following section, given the beam properties of the European XFEL the single pass gain exceeds a simple low gain oscillator, i.e. the case as discussed in the original proposition by *Kim et al.* in 2008. This comes with some advantages such as lower demands on the mechanical tolerances, but also with some disadvantages as will be discussed later.

A major issue one needs to address when dealing with an XFELO is the effect of the light-matter interaction between the X-ray field and the Bragg reflectors. This is due to the high requirements for the angular and spatial stability [4, 5] as well as the necessity of very stable Bragg conditions. In the following simulations excluding and including the effect of heating on the XFELO stability will be shown indicating a high relevance of appropriately handling heating effects.

XFELO WITHOUT HEAT LOAD

The simulations of an X-ray oscillator shown in this paper are all based on a combination of the established FEL code *Genesis1.3*[6] and a self written three dimensional wavefront propagation code which first transforms the radiation from the time into the frequency domain and then propagates each two dimensional frequency slice based on the *Fourier Optics* approach[7, 8]. The reflection of the radiation with the Bragg mirrors (in all three reciprocal dimensions) is currently evaluated based on the approximate two-beam dynamical diffraction theory[1].

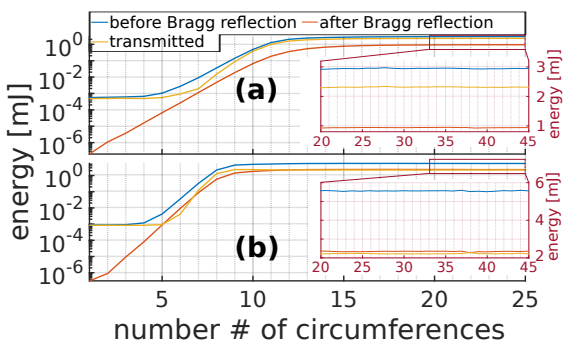


Figure 1: The pulse energy in logscale vs. number of circumferences after the undulator (blue), directly before reentering the undulator (red) and of the forward transmitted pulse (orange) for (a) 250 pC and (b) 500 pC electron bunches. The inset show the saturated energy curve in linear scale and extents the abscissa.

Figure 1 shows the simulation results based on a very simple two diamond mirror XFELO backscattering configuration[2] with one focusing lens. For out-coupling the downstream

[1] It will soon be extended by the more general n-beam diffraction theory.
[2] As such backscattering geometry induces multiple beam diffraction - not included in the simulations - an actually realized XFELO would be based on a more complex mirror setup.

ISBN: 978-3-95450-210-3 doi:10.18429/JACoW-FEL2019-TUP012

SMITH-PURCELL RADIATION EMITTED BY PICO-SECOND ELECTRON BUNCHES FROM A 30 KeV PHOTO-ELECTRON GUN

M. R. Asakawa*, S. Yamaguchi
Department of Pure and Applied Physics, Kansai University, Osaka, Japan

Abstract

A compact radiation source based on the combination of Smith-Purcell radiation and the coherent radiation emitted by the short electron beam is being developed. A photo-electron gun driven by 100 fs laser generated short pulse electron beam with a charge of 300 pC at the space-charge limitation operation. To evaluate the pulsewidth of the photo-electron beam, we developed a method based on the envelope equation. In this method, the pulsewidth was evaluated by the comparison of the measured beam radius and calculated beam radius. The result showed that while the pulsewidth increased with the beam charge, it remained shorter than 3.3 ps even at the maximum charge operation. With this electron beam, experiments to generate Smith-Purcell radiation was performed. Nonlinear dependence of the radiation energy on the charge was observed and this result indicated the occurrence of the collective radiation process.

PULSEWIDTH LENGTHENING OF PHOTO-ELECTRON BEAM

The electron gun consists of a cathode electrode held at -30 keV and a grounded anode electrode. The photo-emission surface of tungsten, 19 mm in diameter, was irradiated by a frequency-tripled Ti:sapphire laser. The pulsewidth of the laser pulse was measured to be 92 fs. The incident angle was set to be 60 degree to the normal and the ellipsoidal laser spot had an area of 1.5×3 mm^2. The irradiation energy onto the cathode was varied from 20 to 260 μJ. Further irradiance led to the unfavorable plasma formation which caused to short-circuit. The spacing between the electrodes were 10 mm. The anode electrode was a metallic disk, 14 mm in diameter, 2 mm in thickness, and had a pinhole with a diameter of 2 mm at the center. The electron passed through this pinhole moved forward to a phosphor screen located at 83 mm from the pinhole. The beam diameter was estimated from the fluorescent image and the beam charge was also measured at the phosphor screen. The pressure of the electron gun was maintained below 5×10^{-7} Pa for all experiments [1].

By irradiating a 220 μJ laser pulse, the photo-electron gun reached to the space-charge limitation [2] and electron beam with a charge of 300 pC emerged from the cathode electrode. Roughly estimated current density at the cathode surface exceeded to 20kA/cm^2, which is 700 times as dense as Child-Langmuir limitation current density. Figure 1 shows the dependence of the beam diameter on the beam charge at the phosphor plate. The maximum charge of the electron beam which passed through the pinhole was measured to be 11.6 pC when the electron gun reached at the space charge limitation operation. It is seen that the diameter increased with the beam charge up to the charge of 4 pC and remained almost constant for larger charge. This result indicates that the electron beam with the charge greater than 5 pC may increase its pulsewidth to relax the repulsive self-field.

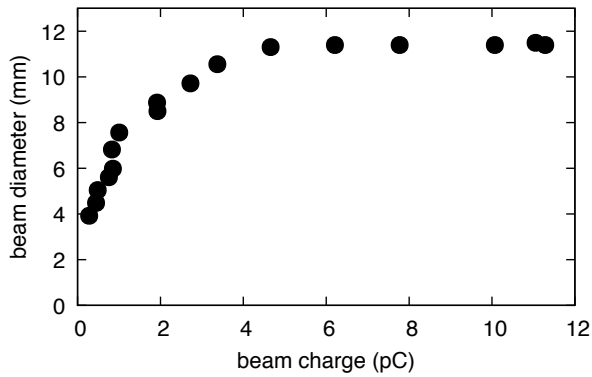


Figure 1: Dependence of the beam diameter on the beam charge.

To estimate the pulsewidth of the beam charge from the dependence of the beam radius on the beam charge shown in Figure 1, we developed a method based on the envelope equation [3]

$$\frac{d^2r}{dz^2} - \frac{K}{r} - \frac{\epsilon}{r^3} = 0, \tag{1}$$

where r denotes the radius of the electron beam moving along $z-$axis with a perviance K and an emittance ϵ. The emittance ϵ of the photo-electron beam emerged from a metallic cathode with a work function ϕ by irradiation of photons with a energy of $h\nu$ is given by

$$\epsilon = \gamma\beta\pi r\sqrt{\frac{2(h\nu - \phi)}{3mc}}, \tag{2}$$

where γ and β are the Lorentz factor and the normalized velocity of the electron beam, respectively. In our case, $\phi = 4.5$ eV and $h\nu = 4.66$ eV. The perviance K for the electron beam with an initial radius r_0, an initial current density j_0 at the pinhole and a normalized pulsewidth τ is defined as

$$K = \alpha(\tau)\frac{ej_0r_0}{2\varepsilon_0 m(\gamma\beta c)^3}, \tag{3}$$

Here $\alpha(\tau)$ is the ratio of the transverse electric field produced by a short-pulse electron beam with a pulsewidth T to that produced by a DC electron beam, and the normalized pulsewidth τ is defined as

$$\tau = \frac{c\beta T}{r} \tag{4}$$

* asakawa@kansai-u.ac.jp

Content from this work may be used under the terms of the CC BY 3.0 licence (© 2019). Any distribution of this work must maintain attribution to the author(s), title of the work, publisher, and DOI

ISBN: 978-3-95450-210-3 doi:10.18429/JACoW-FEL2019-TUP014

CROSSED-UNDULATOR CONFIGURATION FOR VARIABLE POLARIZED THz SOURCE

H. Saito, H. Hama, S. Kashiwagi, T. Muto, K. Nanbu, N. Morita, H. Yamada
Research Center for Electron Photon Science, Tohoku University, Sendai, Japan

Abstract

A variable polarized THz source employing a crossed-undulator configuration has been developed at Research Center for Electron Photon Science (ELPH), Tohoku University. An initial experiment will be demonstrated shortly using newly constructed compact planar undulators at a femtosecond short-bunch facility, t-ACTS, in ELPH. The undulators have equivalent parameters such as the period length of 8 cm and the number of periods is 7, but the field directions are crossed each other perpendicularly. The resonant frequency of 1.94 THz for the beam energy of 22 MeV. Magnetic field measurements have been already performed. The measured field strength distributions of the two undulators were mostly identical to each other. A beam transport line of variable R56 triple bend lattice intersecting the crossed-undulator configuration has been studied for phase control of interference between two radiations (namely the phase shifter). According to a tentative design of the phase shifter beam line, the degree of circular polarization may exceed 0.9 for the fundamental frequency of 1.94 THz in a narrow cone of angular spread of 2 mrad.

INTRODUCTION

Polarization control using the crossed-undulator configuration proposed by M. B. Moiseev et al. and K-J. Kim [1, 2] was firstly demonstrated by J. Bahrdt et al. on a synchrotron radiation source BESSY-1 in 1990 [3]. The crossed-undulator configuration consists with two planar undulators with magnetic fields perpendicular to each other separated by an electromagnetic modulator (we call "the phase shifter line"). The phase shifter had brought variable delay time and then the phase difference between two radiation waves was able to vary from 0 to 2π. Since a monochromator was used the two waves is coherently superposed and then any states of polarization from linear to circular in both helicities can be produced. A great advantage in this method is that first helicity switching is enable owing to small change of beam pass length in the phase shifter line, meanwhile changing magnetic field helicity in the identical helical undulator takes some considerable time even using electromagnetic undulator. In studies for handedness (chirality) in materials, the first helicity switching is pretty important because signal-to-noise ratio of circular dichroism experiment is usually very poor.

Circular dichroism spectroscopy using longer wavelength electromagnetic radiations is valuable for the studies of structural analysis of biomolecules such as proteins, nucleic acids. Since polarization control using optical elements for the solid-state/laser based THz sources is well established yet, it would be worth to consider the first helicity switching of circular polarization for accelerator-based THz source. In this sense, without monochromators, direct superposition of coherent THz radiations from the crossed-undulator configuration is a state-of-the-art solution for the biomolecular circular dichroism.

In this article, a current status of development of the variable polarized THz source at ELPH, Tohoku University.

THz CROSSED-UNDULATOR CONFIGURATION

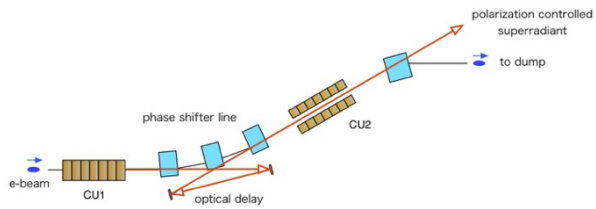


Figure 1: Crossed-undulator configuration. Path length difference between the beam and THz superradiance has to be varied in the phase shifter line. Since the e-beam transport matrix element of R_{56} should be variable for compensation of bunch lengthening due to momentum dispersion, the optical delay is controlled so as to satisfy the radiation phase difference from 0 to 2π.

Conceptual layout of the crossed-undulator configuration is shown in Fig. 1. The lower energy beam causes bunch lengthening in itself because of finite energy spread. In addition, R_{56} inside of the undulator has to be taken into account as well. So careful consideration of the phase shifter line is indispensable. At present, we have a tentative design of triple-bend beam achromat transport with small bending angle, which is better than a chicane type line. The study regarding the phase shifter beam line will be reported elsewhere [4].

Femtosecond Short-Bunch Facility, t-ACTS

At the t-ACTS (test Accelerator as Coherent THz Source) facility [5], Tohoku University, the short-pulse electron beam is stably produced via velocity bunching scheme in a traveling wave accelerating structure [6]. A specially designed independently tunable cells thermionic RF gun (ITC-RF gun) is employed to manipulate the longitudinal phase space of the beam extracted from LaB_6 cathode. The beam filtered in an alpha magnet accelerated in a 3 m S-band linac. The usual bunch length of a micro-pulse deduced from CTR spectrum measured by a Mi-

Content from this work may be used under the terms of the CC BY 3.0 licence (© 2019). Any distribution of this work must maintain attribution to the author(s), title of the work, publisher, and DOI

ISBN: 978-3-95450-210-3 doi:10.18429/JACoW-FEL2019-TUP015

DESIGN OF HIGH-REPETITION TERAHERTZ SUPER-RADIATION BASED ON CAEP THz FEL SUPERCONDUCTING BEAMLINE*

D. Wu, K. Zhou, L. G. Yan, P. Li†, J. X. Wang, L. B. Li, Q. Pan, D. X. Xiao,
X. Luo, H. B. Wang, X. M. Shen, P. Zhang, L. J. Shan, T. H. He, M. Li
Institute of Applied Electronics, China Academy of Engineering Physics, Mianyang, 621900, China

Abstract

China Academy of Engineering Physics terahertz free electron laser (CAEP THz FEL, CTFEL) is the first THz FEL oscillator in China. CTFEL spectrum covers from 0.7 THz to 4.2 THz. However, there are still many applications requiring lower frequency. The super-radiation of the ultra-short electron beam bunches could generate ultra-fast, carrier-envelope-phase-stable, and high-field terahertz. The coherent diffraction/transition radiation (CDR/CTR) and coherent undulator radiation (CUR) can be also synchronized naturally. In this paper, the dynamic and the design of the super-radiation are introduced. The main parameters of the CDR/CTR and CUR are also discussed. A multi-color pump-probe system based on super-radiation is also proposed.

INTRODUCTION

CAEP THz FEL (CTFEL) facility is the first high average THz source based on FEL in China [1, 2], which is driven by a DC gun with a GaAs photocathode [3, 4] and two 4-cell 1.3 GHz super-conducting radio frequency (SRF) accelerator [5, 6]. The repetition rate of CTFEL is 54.167 MHz, one over twenty-four of 1.3 GHz. The effective accelerating field gradient is about 10 MV/m.

CTFEL has achieved the stimulated saturation in August, 2017[7, 8]. The terahertz frequency is continuously adjustable from 0.7 THz to 4.2 THz.

The upgrade of CTFEL is to broaden its spectrum and improve its power. There are many applications on condensed matter physics in the spectrum from 0.1 THz to 1.5 THz, such as control of antiferromagnetic spin waves[9], resonant and nonresonant over matters[10], magnetic order [11], the 2D materials[12], and so on. So, it is important to cover the lower frequency domain, and afford a high-repetition, carrier-envelope-phase-stable THz source.

When the electron beam bunch is compressed to less than 1 ps, et, less than the wavelength of THz wave, the terahertz coherent radiation will be generated as transition radiation, diffraction radiation, synchrotron radiation, or undulator radiation, which are often called as super-radiation. In this paper, a beamline is design based on CTFEL to generate a multi-color THz beams with Coherent Diffraction/Transition Radiation (CDR/CTR) and Coherent Undulator Radiation (CUR). The repetition can reach up to 54 MHz, and the pulse energy is more than 0.1 μJ.

BEAMLINE DESIGN

Figure 1 shows the layout of the CTFEL facility. High average power high-brightness electron beam is emitted from the high-voltage DC gun equipped with a GaAs photocathode. The beam is then energized by a 2×4-cell RF superconducting accelerator and gain kinetic energy from 6 MeV to 8 MeV. Passing through an achromatic section, the beam then goes into the undulator magnet field and generates spontaneous radiation. The radiation resonates in the THz optical cavity and reaches saturations.

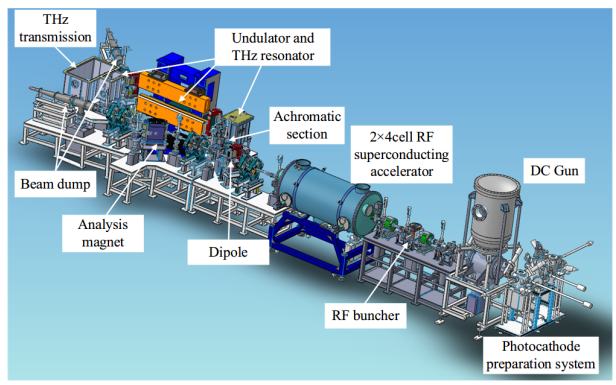


Figure 1: The layout of CTFEL facility.

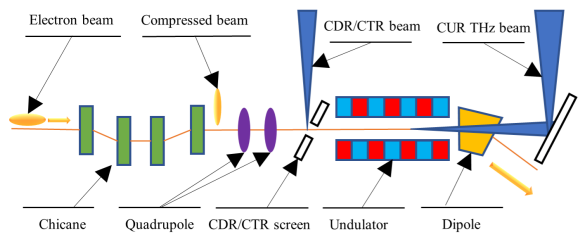


Figure 2: Schematic diagram of the super-radiation beam line.

When the electron pass straight downstream the SRF cavity, it can be used to generate the super-radiation. The schematic is shown on Fig. 2. The chirped bunch firstly passed through a chicane to be compressed, and then a screen with a hole to generate CDR beam (or CTR beam without a hole), then a short undulator to generate CUR beam.

* Work supported by National Natural Science Foundation of China with grant (11575264, 11605190 and 11805192), Innovation Foundation of CAEP with grant (CX2019036, CX2019037)
† burnlife@sina.com

Content from this work may be used under the terms of the CC BY 3.0 licence (© 2019). Any distribution of this work must maintain attribution to the author(s), title of the work, publisher, and DOI

ISBN: 978-3-95450-210-3 doi:10.18429/JACoW-FEL2019-TUP017

TERAHERTZ FEL SIMULATION IN PAL XFEL

J. H. Ko, H.-S. Kang, Pohang Accelerator Laboratory, Pohang, Republic of Korea

Abstract

Terahertz radiation is being used in various fields such as imaging, diagnosis, inspection, etc. For the Terahertz research, the Pohang accelerator laboratory (PAL) is planning to make a terahertz free electron laser based on self-amplified spontaneous emission (SASE). Using free electron laser method, we will be able to conduct the THz-pump x-ray probe experiment. For the terahertz free electron laser, we conducted the simulation study on the accelerator with e-beam energy below 40 MeV, using a photo-cathode RF gun, one s-band accelerator and one undulator shorter than 4 meters.

INTRODUCTION

In Pohang accelerator laboratory, we have a plan to make a THz FEL facility to conduct the THz pump X-ray probe experiment and other experiments of using THz radiation. For this purpose, a demanded condition of THz radiation is an intensity over 100 μJ, a various frequency range (5 to 20 THz) and a spectrum under 5%. To make a THz FEL facility which is satisfied with these conditions, we conduct the Accelerator simulation and FEL simulation using ASTRA and SIMPLEX [1, 2]. We conduct the ASTRA simulation for designing a photo-cathode RF gun, an S-band accelerator, accelerator solenoids, and two quadrupole magnet triplets. We conduct the SIMPLEX simulation using the result of ASTRA simulation. The simulation parameters are listed in Table 1 and 2, and the structure of the THz FEL accelerator is shown in Figure 1.

Table 1: Electron Beam Parameter

Electron beam	
Electron beam energy	25 MeV to 35 MeV
Electron beam charge	4 nC
RMS electron bunch length	1.8 mm
Peak current	265 A
Horizontal Emittance	4 mm-mrad
Vertical Emittance	5 mm-mrad
Energy spread	0.001

Table 2: Undulator Parameter

Undulator	
Type	Planar
Period	3.5 cm
K	1.6 to 3.321
Magnetic field	0.7 T to 1.016 T
Length	4 m
Gap	9 mm

ACCELERATOR SIMULATION

The wavelength of terahertz radiation is much longer than the wavelength of x-ray or UV radiation. Accordingly, the electron bunch length of the THz FEL is allowed to be as long as 1.8 mm. To make a THz FEL radiation, we need high peak current. To satisfy these conditions, we need a high electron charge over 4 nC.

The wavelength of the FEL radiation is calculated by the below equation.

$$\lambda = \frac{\lambda_u}{2\gamma^2}\left(1 + \frac{K^2}{2}\right)$$

λ is an FEL wavelength, λ_u is a period length of the undulator, $K=93.4*\lambda_u B_{peak}$. Using this equation, we can get the electron beam energy when the radiation frequency is in the THz range. When the undulator period length is 3.5 cm, the magnetic field of the undulator is under 1.016 T, undulator gap is 9 mm, and electron beam energy in 25 MeV to 35 MeV, the available range of the THz radiation wavelength is 5 THz to 30 THz. We make a specific electron beam condition using the ASTRA, which satisfies the electron beam parameter. The ASTRA simulation results are shown in Figure 2, 3, 4, and 5.

To generate a high charge electron beam, we should use a larger laser beam size in the input condition and control the gun solenoid condition. Using quadrupole triplets, we can match the electron beam between accelerator and undulator.

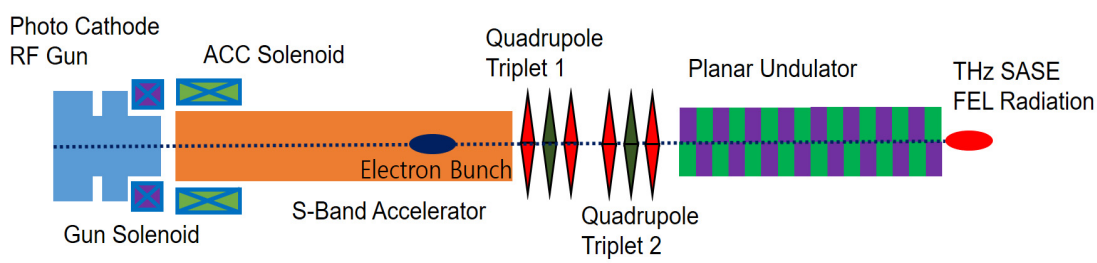


Figure 1: Schematic structure of THz FEL facility in PAL XFEL.

Content from this work may be used under the terms of the CC BY 3.0 licence (© 2019). Any distribution of this work must maintain attribution to the author(s), title of the work, publisher, and DOI

ISBN: 978-3-95450-210-3 doi:10.18429/JACoW-FEL2019-TUP018

Content from this work may be used under the terms of the CC BY 3.0 licence (© 2019). Any distribution of this work must maintain attribution to the author(s), title of the work, publisher, and DOI

SUPERRADIANT EMISSION OF ELECTRON BUNCHES BASED ON CHERENKOV EXCITATION OF SURFACE WAVES IN 1D AND 2D PERIODICAL LATTICES: THEORY AND EXPERIMENTS*

A.M. Malkin†, N.S. Ginzburg[1], I.V. Zheleznov, V.Yu. Zaslavsky[1], A.S. Sergeev, I.V. Zotova,
Institute of Applied Physics RAS, Nizhny Novgorod, Russia
M.I. Yalandin, Institute of Electrophysics, Ekaterinburg, Russia
[1]also at Nizhny Novgorod State University, Nizhny Novgorod, Russia

Abstract

We report of the experiments on Cherenkov generation of 150 ps superradiance pulses with a central frequency of 0.14 THz, and an extremely high peak power up to 70 MW. In order to generate spatially coherent radiation in shorter wavelength ranges (including THz band) in strongly oversized waveguiding systems, we propose a slow wave structure with double periodic corrugation (2D SWS). Using quasi-optical theory and PIC simulations, we demonstrate the applicability of such 2D SWS and its advantages against traditional 1D SWS. Proof-of-principle experiments on observation G-band Cherenkov superradiance in 2D SWS are currently in progress.

INTRODUCTION

In recent years, significant progress was achieved in generation of high-power ultrashort microwave pulses based on superradiance (SR) of electron bunches extended in the wavelength scale. In this process, coherent emission from the entire volume of the bunch occurs due to the development of microbunching and slippage of the wave with respect to electrons.

The SR pulses with the highest peak power were obtained for the Cherenkov mechanism when electrons interact with the backward wave propagating in slow-wave structures (SWS). In the Ka-band, peak power exceeding 1 GW was obtained [1, 2]. In these experiments, an electron bunch interacts with a synchronous spatial harmonic of the lowest TM-polarized volume mode of periodically corrugated waveguide with an oversize factor $D/\lambda \approx 1$ (D is the mean diameter and λ is the radiation wavelength). However, in the shorter wavelength bands, the use of single-mode SWS is becoming more complicated due to strict requirements for transportation of the high-current electron beams and increase of the Ohmic losses.

Advancement of vacuum electronic devices into sub-THz and THz frequency ranges calls for oversized beam-wave interaction space due to the fact that that the dimensions of the beam guiding systems can not be reduced lower than the millimeter scale. Thus, in order to provide coherent THz radiation from the spatially extended beams, excitation of surface modes existing in 1D and 2D corrugated systems appears to be attractive [3-6].

* Work supported by RFBR grant No. 17-08-01072 and the Program of Presidium RAS No.10 (0035-2018-0022).
† malkin@appl.sci-nnov.ru

In this paper, we present recent results of theoretical and experimental studies of SR emission based on excitation of surface waves by extended bunches. Using oversized 1D slow-wave structures allows for a significant increase of total current and, correspondingly, the output radiation power. Based on SR of electron bunches in a cylindrical corrugated waveguide, 150 ps short-pulse SR emission with a central frequency of 0.14 THz, and an extremely high peak power reaching 50-70 MW were obtained in the joint effort by the Institute of Electrophysics RAS and IAP RAS.

Further increase of the frequency or of the aimed radiation power requires the increase of the transverse dimensions of the interaction space, which, in turn, leads to the loss of the mode control over the azimuthal coordinate. The problem of mode synchronization over this coordinate can be solved by using the SWS with 2D corrugation. Proof-of-principle experiments are in progress based on the RADAN accelerator. We present here the results of 3D numerical simulation of Cherenkov SR emission in the 3mm wavelength range in an oversized cylindrical waveguide with 2D corrugation of the wall. A SR pulse with a duration of 0.5 ns and an output power of ~ 70 MW was obtained.

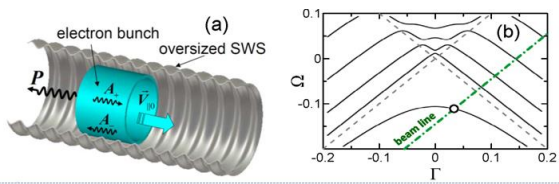


Figure 1: a) Scheme of SR pulse generation with excitation of a surface wave in an oversized periodically corrugated waveguide. b) Dispersion characteristics of the corrugated waveguide and an electron beam.

SIMULATION AND EXPERIMENTS ON GENERATION OF SURFACE-WAVE SR PULSES IN 1D LATTICES

Cherenkov SR of electron bunch exciting the surface wave in an oversized 1D corrugated cylindrical waveguide (Fig. 1a) can be considered within quasi-optical approach [3]. In this case the radiation field near a shallow corrugation is presented as a sum of two counter-propagating TM polarized wavebeams:

$$H_\varphi = \mathrm{Re}(A_+(z,r,t)e^{i\bar{\omega}t-ikz} + A_-(z,r,t)e^{i\bar{\omega}t+ikz}), \quad (1)$$

ISBN: 978-3-95450-210-3 doi:10.18429/JACoW-FEL2019-TUP019

REGIME OF MULTI-STAGE NON-RESONANT TRAPPING IN FREE ELECTRON LASERS*

A. V. Savilov†, I.V. Bandurkin, Yu. S. Oparina, N. Yu. Peskov, Institute of Applied Physics, Nizhny Novgorod, Russian Federation

Abstract

We describe three works united by the idea of the non-resonant regime providing an effective trapping in a beam with a great energy spread. (I) Operability of this regime was demonstrated in the high-efficient 0.8 MeV Ka-band FEM-amplifier. (II) In short-wavelength FELs the multi-stage trapping in several consecutive sections can be organized. We describe efficiency enhancement and improving the frequency wave spectrum in multi-stage SASE and super-radiant FELs. (III) The multi-stage amplification of a single-frequency wave signal can provide cooling of the electron bunch.

NON-RESONANT AND MULTI-STAGE TRAPPING

A key problem in realization of free-electron lasers (FELs) is a small efficiency at the saturated stage of the electron-wave interaction. The averaged radiation loss in the relativistic Lorentz-factor is determined by the so-called FEL parameter, $\Delta\gamma_{rad}/\gamma_0 \sim \rho$, which is typically $\rho \sim 10^{-3}$ for X-ray FELs [1]. A similar condition limits the admissible energy spread in the electron bunch, $\Delta\gamma_{spread}/\gamma_0 \sim \rho$. A known way to increase the efficiency is the use of trapping and adiabatic deceleration of electrons in a tapered undulator. Due to tapering, the energy $\gamma_{res}(z)$ corresponding to the exact electron-wave resonance decreases slowly with the axial coordinate (Fig. 1 a). A fraction of electrons is trapped by the radiated wave, end energies of these particles decrease together with γ_{res}. In principle, it is possible to exceed limitation $\Delta\gamma_{rad}/\gamma_0 \sim \rho$ in this scheme, but it is difficult to provide trapping of a significant fraction of the beam, if the limitation $\Delta\gamma_{spread}/\gamma_0 \sim \rho$ is not fulfilled. This is because only electrons being close to the resonance with the wave at the beginning of the interaction can be trapped.

The regime of non-resonant trapping [2, 3] can provide an effective trapping in a beam with a great energy spread. In this regime, the wiggler is profiled in such a way that the electron beam is out of resonance with the operating wave at the beginning of the wiggler, and different electron fractions gradually get into synchronism as the wiggler's period decreases (Fig. 1 b).

Recently, the regime of multi-stage trapping was proposed for FELs and for other types of electron devices [4].

* Work supported by the RFBR (grants 18-02-40009, 18-02-00765) and by the IAP RAS Project 0035-2019-0001
† savilov@appl.sci-nnov.ru.

In the multi-stage system, the non-resonant trapping is provided several times in several consecutive sections (Fig. 1 c). In each section only a relatively small fraction of the beam is trapped and pass their energy to the wave. However, repetition of this process from section to section involves in the electron-wave interaction almost all particles of the electron beam.

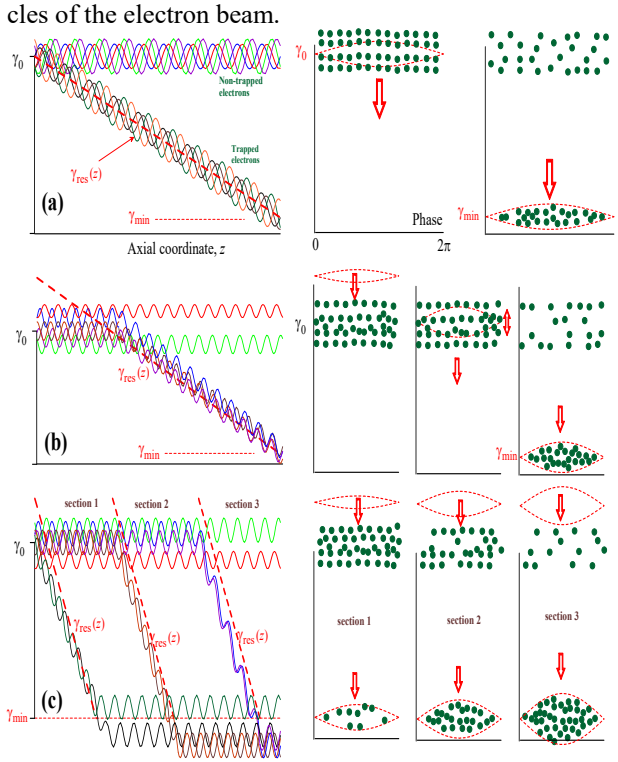


Figure 1: (a) Traditional regime of trapping. (b) Regime of non-resonant trapping. (c) Regime of the multi-stage non-resonant trapping.

KA-BAND FEM-AMPLIFIERF

The regime of non-resonant trapping has been developed and experimentally demonstrated in Ka-band. In this regime, the wiggler is profiled in such a way that the electron beam is out of resonance with the operating wave at the beginning of the wiggler, and different electron fractions gradually get into synchronism as the wiggler's period decreases.

Examination of this regime in the FEM-amplifier was performed in collaboration between JINR (Dubna) and IAP RAS (N. Novgorod) at the experimental facilities of the linear induction accelerator LIU-3000 [5, 6]. Simulation of the FEM was carried out for the parameters close to the experimental conditions. The regime of a reversed guide magnetic field [7, 8] was chosen; this regime provides a high quality of formation of the helical electron beam in the smoothly up-tapered wiggler.

Content from this work may be used under the terms of the CC BY 3.0 licence (© 2019). Any distribution of this work must maintain attribution to the author(s), title of the work, publisher, and DOI

ISBN: 978-3-95450-210-3 doi:10.18429/JACoW-FEL2019-TUP020

TERAHERTZ FREE ELECTRON MASER BASED ON EXCITATION OF A TALBOT-TYPE SUPER-MODE IN AN OVERSIZED MICROWAVE SYSTEM *

A. V. Savilov†, Yu.S. Oparina, N.Yu. Peskov,
Institute of Applied Physics, Nizhny Novgorod, Russian Federation

Abstract

We propose an electron maser operating in the THz frequency range and based on the excitation of not a fixed transverse mode of the operating cavity but of a supermode formed by a fixed set of the transverse modes. This allows selective excitation of a THz operating wave in an oversized microwave system fed by a high-current relativistic electron beam.

INTRODUCTION

A natural problem arising in the case of realization of a THz electron oscillator with a high-current relativistic electron beam is an inevitable use of an oversized microwave system, which characteristic transverse size significantly exceeds the wavelength of the operating wave [1,2]. In this situation, it becomes difficult (and even just impossible starting from a certain limit) to provide selective excitation of a chosen transverse mode of the operating cavity. First of all, the selectivity of the feedback is a serious problem. A typical configuration of the electron-wave interaction region in an auto-oscillator is a piece of a waveguide terminated at the input/output ends by two mirrors providing the feedback; for instance, Bragg-type mirrors can be used to provide effective reflection of far-from-cut-off waves (Fig. 1a). Naturally, in the case of a far-from-cut-off wave excited in an oversized waveguide, it is difficult to create a reflector providing reflection of only one transverse mode [2]. Second, it is difficult to ensure the single-mode electron-wave interaction in an oversized system, as in these situations many transverse modes are close to resonance with electrons [3].

In this work, we propose a different concept of selective excitation of a THz operating wave in a high-power relativistic electron maser with an oversized microwave system fed by a high-current relativistic electron beam. Our basic idea is to give up working in a fixed transverse mode. Instead, we propose to work in a supermode, which is formed by a fixed spectrum of several transverse modes of an oversized waveguide (Fig. 1 b). The spectrum of the partial transverse modes is determined by both electronic and electrodynamic factors. First, effective interaction between the supermode formed by these partial modes and the electron beam should be provided. This means that in the middle part of the waveguide the supermode field should have a maximum at the point of injection of the electron beam into the transverse cross-section of the waveguide. Second, the supermode should possess a high Q-factor. Therefore, at the input/output ends of the waveguide, the transverse structure of the supermode should be very specific; namely, the field should be present only close to the mirrors to provide almost complete reflection of the supermode back to the cavity (Fig. 1b).

To organize such a super-mode, we propose a simple approach, which is based on the use of Talbot's effect [1,4,5], namely, periodic reproduction of the transverse structure of a multi-mode wave field in an oversized waveguide. We propose to use this approach to fix a high-Q operating supermode in a simple microwave system consisting of a waveguide terminated by two simple mirrors (Fig. 1 b). On the basis of a multi-mode set of self-consistent equations of the electron-wave interaction we demonstrate the possibility of selective self-excitation of the supermode. The "proper" transverse-axial structure of the high-Q supermode is formed at the small-signal stage of the gain guiding during several trips of the wave over the cavity. In fact, this effect (formation of a high-Q supermode by a set of several partial transverse modes) is analogous to the effect of mode locking known in the physics of quantum lasers [6].

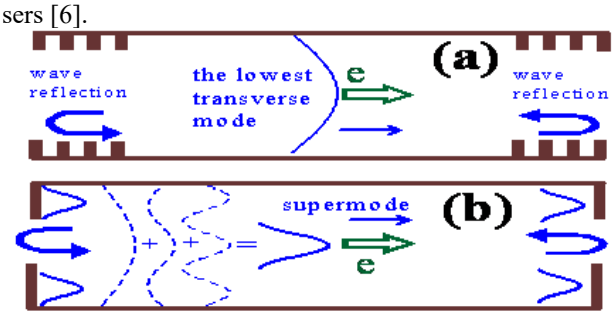


Figure 1: (a) Traditional scheme of excitation of a far-from-cutoff travelling wave in the cavity formed by a piece of waveguide with two input/output mirrors (Bragg-type mirrors are shown as an example). (b) Excitation of a supermode formed by a set of several transverse modes.

THE SIMPLEST 2-D MODEL: DEMONSTRATION OF THE BASIC IDEA

Let us consider a waveguide with a characteristic transverse size much bigger than the wavelength of the operating wave, $D>>\lambda$ (Fig. 2). Any symmetrical transverse distribution of the wave field in this waveguide is reproduced $E(x,z+L)=E(x,z)$ with the period $L=D^2/\lambda$. This phenomenon of repetition of the transverse wave structure is well known in the literature as the Talbot effect [4] and widely used for designing various microwave systems [1,5].

* Work supported by supported by the Russian Science Foundation, Project # 19-12-00212.
† email address savilov@appl.sci-nnov.ru.

Content from this work may be used under the terms of the CC BY 3.0 licence (© 2019). Any distribution of this work must maintain attribution to the author(s), title of the work, publisher, and DOI

ISBN: 978-3-95450-210-3 doi:10.18429/JACoW-FEL2019-TUP021

DEVELOPMENT OF POWERFUL LONG-PULSE TERAHERTZ BAND FELS BASED ON LINEAR INDUCTION ACCELERATORS*

V.Yu. Zaslavsky†, N.S. Ginzburg[1], A.M. Malkin, N.Yu. Peskov[1], A.S. Sergeev,
Institute of Applied Physics RAS, Nizhny Novgorod, Russia
A.V. Arzhannikov, E.S. Sandalov, S.L. Sinitsky, D.I. Skovorodin, A.A. Starostenko,
Budker Institute of Nuclear Physics, Novosibirsk, Russia
[1]also at Nizhny Novgorod State University, Nizhny Novgorod, Russia

Abstract

The paper is devoted to development of high-power long-pulse THz-band FELs based on the new generation of linear induction accelerators elaborated recently at Budker Institute (Novosibirsk). These accelerators generate microsecond electron beams with a current at kA-level and an energy of 2 to 5 MeV (with a possibility to increase the electrons energy up to 20 MeV). Based on this beam, we initiated a new project of multi-MW long-pulse FEL operating in the frequency range of 1 to 10 THz using a wiggler period of 3 to 6 cm. For this FEL oscillator, we propose a planar two-mirror resonator comprising highly selective advanced Bragg reflectors. Alternately, electrodynamic system for oscillators of this type can use hybrid two-mirror resonator consisting of an upstream advanced Bragg reflector and a downstream weakly reflecting conventional Bragg reflector. Simulations demonstrate that the advanced Bragg reflector based on coupling of propagating and quasi-cutoff waves ensures the mode control at the values of the gap between the corrugated plates forming such a resonator of up to 20 wavelengths. Simulations of the FEL driven by electron beam generated by the LIA-2 in the frame of both averaged approach and 3D PIC code demonstrate that the THz radiation power can reach the level of 10 to 20 MW.

INTRODUCTION

Distributed feedback based on periodic Bragg structures is widely used in classical and quantum generators of coherent radiation. Correspondingly, the frequency band of oscillators with this feedback mechanism covers the millimeter and optical (infrared) bands [1–3]. Use of Bragg mirrors in X-ray lasers was discussed in multiple works (for example, [4]). In the present paper, we show that the advanced Bragg structures can be efficiently used in terahertz free-electron lasers. In addition to the compatibility with the transport channels of intense electron beams, the advantage of the proposed structures is the spatial coherence of radiation at large values of the oversize factor of the interaction region with respect to both transverse coordinates.

Scheme of a planar FEL under consideration is shown in Fig. 1. A feature of this scheme is the use of Bragg mirrors coupling the longitudinal and transverse (with respect to the velocity of the particles) wavebeams.

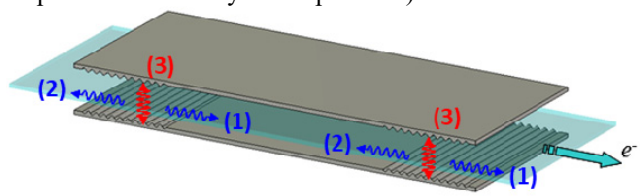


Figure 1: Scheme of FEL with two-mirror advanced Bragg resonator. Arrows (1), (2) indicate propagating of paraxial waves, (3) – quasi-cutoff feedback wave.

TUNABLE TERAHERTZ BRAGG REFLECTORS BASED ON COUPLING OF PROPAGATING AND CUTOFF WAVES

Bragg reflectors in the form of corrugated waveguide sections were proposed in [2] and are widely used currently as elements of electrodynamical systems in relativistic masers [3]. An obvious advantage of such systems is the compatibility with transportation of a high-current relativistic electron beam. Similarly to their optical prototypes, conventional variants of Bragg structures provide coupling and mutual scattering of the two counter-propagating paraxial waves. In the experiments on generation of radiation in the long wavelength part of the millimeter wavelength band, usual diameter of such cavities is restricted by size of several wavelengths.

In order to advance the relativistic masers into the sub-millimeter wavelength band, an increase in the oversize parameter of the cavities is required. However, this leads to a dramatic reduction in selectivity of the resonators composed from conventional Bragg structures due to overlapping of the reflection zones for different waveguide modes. Besides, a significant drop of the absolute values of the reflection coefficient of such structures takes place.

This problem can be solved using advanced Bragg structures based on coupling of propagating and quasi-cutoff waves. Similarly to sub-millimeter wave gyrotrons, the inclusion of the cutoff wave into the feedback loop leads to mode spectrum purification because the frequency interval between the cutoff waveguide modes is much higher than that between the paraxial waves. As a result, an advanced Bragg structures can be efficiently used as a narrow band reflector in the long-pulse THz-band FELs.

*This work was supported by the Russian Scientific Foundation (RSCF), grant No. 19-12-00212 and the Program of Presidium RAS No.10 (0035-2018-0022).
† zas-vladislav@appl.sci-nnov.ru

Content from this work may be used under the terms of the CC BY 3.0 licence (© 2019). Any distribution of this work must maintain attribution to the author(s), title of the work, publisher, and DOI

ISBN: 978-3-95450-210-3 doi:10.18429/JACoW-FEL2019-TUP023

Content from this work may be used under the terms of the CC BY 3.0 licence (© 2019). Any distribution of this work must maintain attribution to the author(s), title of the work, publisher, and DOI

ANALYTICAL AND NUMERICAL COMPARISON OF DIFFERENT APPROACHES TO THE DESCRIPTION OF SASE IN HIGH GAIN FELs

O.A. Shevchenko†, N.A. Vinokurov[1], Budker Institute of Nuclear Physics, Novosibirsk, Russia
[1]also at Novosibirsk State University Novosibirsk, Russia

Abstract

Correlation function theory which has been developed recently gives rigorous statistical description of the SASE FEL operation. It directly deals with the values averaged over many shots. There are two other approaches which are based either on Vlasov equation or on direct solution of particle motion equations. Both of them perform calculations for some particular initial conditions. After that one can either consider the result as a "typical" sample, or repeat calculations for other initial conditions and then average the results. To check the validity of these three approaches it might be interesting to compare them with each other. In this paper we present the results of such comparison obtained for the 1-D FEL model. We show that two-particle correlation function approximation is equivalent to the quasilinear approximation for the Vlasov equation approach. These two approximations are in a good agreement with the results of direct solution of particle motion equations at linear and early saturation stages. To obtain this agreement at strong saturation, high order harmonics in Vlasov equation have to be taken into account, which corresponds to taking into account of three and more particle correlations in the correlation function approach.

INTRODUCTION

SASE FELs are widely used now as bright sources of coherent radiation in X-ray region [1]. Radiation of such FELs is a result of initial inhomogeneity of particle density, and therefore its parameters fluctuate significantly from shot to shot and within one pulse. To determine these parameters in a single shot one has to solve particle motion equations together with Maxwell equations. For a real shot it is not possible not only because of large number of particles but also because of unknown initial conditions. However, parameters averaged over many shots can be found by standard methods of statistical mechanics. Recently the correlation function theory, which deals with such parameters, was developed based on BBGKY chain of equations. Detailed description of this theory for general case is given elsewhere [2]. In this paper we shell consider simple 1-D case where the theory can be verified by comparing with other approaches based on direct solution of motion equations and solution of Vlasov equation for random smoothed density distribution in one-particle phase space.

BASIC EQUATIONS AND NUMERICAL SOLUTION ALGORITHM

The 1-D approximation is widely used in the FEL theory [3]. Despite the fact that it does not have rigorous foundation, it gives a good qualitative description of the physical processes taking place in single pass FEL.

Equations of Motion

Interaction of two particles in FEL occurs mainly through radiation. Knowing the particle trajectory one can calculate its radiation field and formally substitute it to the motion equations. But, unlike the case of the Coulomb interaction, the resulting set of equations will contain retardation. Fortunately some approximations relevant to FEL radiation field allow to eliminate retardation by special choice of independent variable and to obtain a set of ordinary differential equations. In 1-D case the resulting set of equations can be written in the following simple form:

$$\frac{dz^{(k)}}{d\theta} = 1 + 2\Delta^{(k)}; \quad \frac{d\Delta^{(k)}}{d\theta} = \frac{1}{N_\lambda} \sum_{z^{(l)} < z^{(k)}} \Phi\left(z^{(k)}, z^{(l)}\right). \quad (1)$$

where $z^{(k)}$ and $\Delta^{(k)}$ - longitudinal coordinate and relative energy deviation of the *k*-th particle, N_λ - number of particles per radiation wavelength, $\theta = 2\gamma_\parallel^2 (t - z)$ - special "time" variable (see [2] for details) . Particular form of interaction "force" $\Phi\left(z^{(k)}, z^{(l)}\right)$ depends on the used approximation. Further we shell restrict our consideration to the model of charged sheets. In this model $\Phi\left(z^{(k)}, z^{(l)}\right) = -8\rho^3 \cos\left(z^{(k)} - z^{(l)}\right)$, ρ - Pierce parameter. For the numerical solution of (1) it is also convenient to make substitution $z^{(k)} = \theta + \tilde{z}^{(k)}$ .The resulting set of equations is given bellow:

$$\frac{d\tilde{z}^{(k)}}{d\theta} = 2\Delta^{(k)}; \quad \frac{d\Delta^{(k)}}{d\theta} = -\frac{1}{N_\lambda} 8\rho^3 \,\mathrm{Re}\left(e^{i\tilde{z}^{(k)}} S^{(k)}\right). \quad (2)$$

where $S^{(k)} = \sum_{z^{(l)} < z^{(k)}} e^{-i\tilde{z}^{(l)}}$. The set of equations (2) can be easily solved numerically using any simple difference scheme. The only difficulty is the large number of particles. One also needs to remember that to obtain averaged values the system has to be solved many times with "random" initial conditions. Calculation of the value $S^{(k)}$ can be simplified substantially if one sorts particles at each integration step so, that $\tilde{z}^{(l)} < \tilde{z}^{(k)}$ if $i < k$. In this case $S^{(k)} = S^{(k-1)} + e^{-i\tilde{z}^{(k-1)}}$. The order of particle arrangement

† O.A.Shevchenko@inp.nsk.su

ISBN: 978-3-95450-210-3 doi:10.18429/JACoW-FEL2019-TUP024

ELECTRONIC MODULATION OF THE FEL-OSCILLATOR RADIATION POWER DRIVEN BY ERL

O. A. Shevchenko†, S. V. Tararyshkin, Ya. V. Getmanov[1], S. S. Serednyakov[1], E. V. Bykov, Budker Institute of Nuclear Physics, Novosibirsk, Russia,
A. Melnikov[1], M. Fedin, S. Veber[1], International Tomography Center SB RAS, Novosibirsk, Russia,
[1]also at Novosibirsk State University, Novosibirsk, Russia

Abstract

FEL oscillators usually operate in CW mode and produce periodic train of radiation pulses but some user experiments require modulation of radiation power. Conventional way to obtain this modulation is using of mechanical shutters but it cannot provide very short switching time and may lead to decreasing of the radiation beam quality. Another way could be based on the electron beam current modulation but it cannot be used in the ERL. We propose a simple way of fast control of the FEL lasing which is based on periodic phase shift of electron bunches with respect to radiation stored in optical cavity. The phase shift required to suppress lasing is relatively small and it does not change significantly repetition rate. This approach has been realized at NovoFEL facility. It allows to generate radiation macropulses of desirable length down to several microseconds (limited by quality factor of optical cavity and FEL gain) which can be synchronized with external trigger. We present detailed description of electronic power modulation scheme and discuss the results of experiments.

INTRODUCTION

Novosibirsk Free Electron Laser (NovoFEL) facility comprises three FELs, which use energy recovery linac (ERL) as a source of electrons [1]. All three FELs are FEL oscillators. They operate in CW mode and produce periodic train of radiation pulses. Energy recovery allows to achieve very high averaged current of the electron beam which results in high average power of radiation. There are applications where this power is really needed [2] but most often it has to be attenuated. In some experiments users want to have large peak power and to avoid overheating of their samples at that [3]. This demand can be fulfilled by modulation of FEL radiation. For this purpose one can think of mechanical shutter but this shutter cannot be done to be fast enough and it also disturbs transverse profile of radiation.

Ideal solution of this problem would be to instantly turn on and off the FEL lasing process. For the single pass FEL based on linear accelerator the lasing can be controlled by the beam injection [4]. In ERL, injection is required to operate in CW mode; it is not possible to switch it on and off instantly. Particularly, for the case of NovoFEL accelerator, beam loading effects in the accelerating structure are very significant because of high average current: fast switching of the current leads to transient effects resulting in beam loss. Instead of that, more "delicate" approach should be developed that keeps the electron beam current almost constant, but efficiently suppresses the lasing in FEL. In this work we developed and implemented at NovoFEL the approach that allows to generate the THz macropulses at any repetition rate and almost any individual length from several seconds and down to several microseconds (the minimal pulse duration is determined by growing up and decay time of lasting which depends on the FEL gain and the quality factor of the optical cavity). This regime has been examined at all three FELs by generation of macropulses with tens of microseconds duration. Possible applications of the electronic modulation of THz radiation are discussed in this paper.

IMPLEMENTATION OF ELECTRONIC POWER MODULATION

In FEL oscillator lasing is possible only when radiation and electron bunches come to undulator simultaneously. In other words electron bunch repetition rate has to be almost equal to the round-trip frequency of the optical cavity (usually acceptable detuning does not exceed 10^{-4}). Changing repetition rate by about 1% will certainly stop lasing, at the same time corresponding variation of the average beam current is not significant and can be easily tolerated by the accelerating structure of ERL. Bunch repetition rate is determined by the frequency of the master oscillator which signal is also used as an input for RF generators. This frequency cannot be changed very fast. Fortunately there is another approach which results in the change of repetition rate and in the termination of lasing.

If injection of one electron bunch is delayed by, e.g., one period of the RF accelerating field it almost does not influence on beam dynamics in accelerator but this bunch comes to undulator in wrong time and does not interact with THz wave, which stops its amplification and leads to fast decay of radiation power. To prevent the formation of new THz wave, injection phase has to be shifted periodically, which actually leads to the small decreasing of the repetition rate.

Implementation Scheme

The scheme of practical implementation of the injection phase shifting is shown in Fig. 1. Injection is triggered by trigger signal modulator, which counts the pulses coming from the master clock. Pulses come with the repetition rate equal to RF accelerating field frequency 180.4 MHz. The simplest algorithm of the trigger signal modulator operation is the following: it bites N-1 successive pulses out of the 180.4 MHz pulse sequence and then triggers injection with the next N^{th} pulse (for the 1st FEL N = 32, for the 2nd FEL N = 24 and for the 3d FEL N = 48). In normal regime

† email address O.A.Shevchenko@inp.nsk.su

Content from this work may be used under the terms of the CC BY 3.0 licence (© 2019). Any distribution of this work must maintain attribution to the author(s), title of the work, publisher, and DOI

ISBN: 978-3-95450-210-3 doi:10.18429/JACoW-FEL2019-TUP025

CURRENT STATUS OF FREE ELECTRON LASER @ TARLA *

A. Aksoy†, Ç. Kaya, Ö. Karslı, B. Koç, Ö. F. Elçim
Institute of Accelerator Technologies, Ankara University, Ankara, Turkey

Abstract

Turkish Accelerator and Radiation Laboratory (TARLA), which is supported by the Presidency Strategy and Budget Directorate of Turkey, aims to be a state-of-art research instrument for light source users in Turkey. Two superconducting accelerating modules of TARLA will drive two different planar undulator magnets with periods of 110 mm (U110) and 35 mm (U35) in order to generate high brightness Continuous Wave (CW) Free Electron Laser (FEL) tunable in between 5-350 μm. Additionally, the linacs will drive a Bremstrahlung radiation station to generate polarized gamma radiation. Main components of TARLA, such as injector, superconducting accelerating modules and cryoplant are under commissioning, currently. In this study, we present the current status of the facility as well as expected FEL performance.

INTRODUCTION

TARLA has been proposed as the first accelerator based FEL user facility in Turkey. The facility which has been commissioning is located at Institute of Accelerator Technologies in Golbasi Campus of Ankara University, which is about 15 km south of the capital city of Turkey, Ankara. The first priority of the facility is to make the country understood that the accelerator technology is the only tool for the solution of challenges of the new science. High brightness, tunable and powerful FEL beam will be generated between 5-350 μm by two planar undulators in a period of 35 mm and 110 mm, respectively. Furthermore, 5-30 MeV Bremsstrahlung radiation will be produced for fixed target and astro-physics experiments [1, 2]. The schematic view of the facility is given in Fig. 1.

FACILITY DESCRIPTION

TARLA accelerator design consists of two sections called injector and main accelerating section. Main accelerating section consists of two superconducting RF (SRF) modules will be installed following the high power low energy injector section. Each module has two superconducting Nb cavities operating at frequency of 1.3 GHz and temperature of 1.8 K (super-liquid helium). The cavities that have maximum accelerating gradient of up to 15 MV/m at continuous wave (CW) mode will allow beam to be accelerated up to 50 MeV. The high power beam operating at quasi-CW mode will be employed to generate radiation and secondary particles in a wide energy range to a diverse user community. Main electron beam parameters of TARLA are given in Table 1.

Table 1: TARLA Main Electron Beam Parameters

Parameter	Unit	Value
Beam Energy	MeV	15 - 40
Max. Average Beam Current	mA	1.5
Max. Bunch Charge	pC	120
Horizontal Emittance	mm.mrad	<15
Vertical Emittance	mm.mrad	<12
Longitudinal Emittance	keV.ps	<85
Bunch Length	ps	0.4 - 6
Bunch Repetition Rate	MHz	0.001-104
Macro Pulse Duration	μs	50 - CW
Macro Pulse Repetition Rate	Hz	1 - CW

Injector

The injector fed by a grid modulated thermionic triode DC electron gun, consists of two buncher cavities operating at 260 MHz and 1.3 GHz, several focusing magnets and diagnostic tools. The electron current is extracted from a tungsten dispenser cathode with a modulated grid voltage yielding bunches with 600 ps inital FWHM length. The bunches will first be compressed in the drift following the energy modulation obtained in the subharmonic buncher (SHB) in order to get into the linear phase range of the second buncher. The following 1.3 GHz fundamental buncher (FB) then introduces enough energy chirp to generate longitudinal (temporal) waist inside the first cell of the first SC cavity via ballistic bunching. Following successful commissioning of electron gun, the injector section has been tested at present.

Accelerator

TARLA main acceleration unit is composed of two similar superconducting linear accelerator modules mounted in a common vessel and constitute so called cryomodules [3], and a bunch compressor section between them. A cryomodule has two TESLA RF cavities [4] with an accelerating gradient of 10 MV/m at CW mode, for each cavity. The beam will further be accelerated to 40 MeV by main accelerating section. The (fixed R_{56}) bunch compressor between the cryomodules will allow highly stable beam by magnetic insertions. The electron beam will reach the required energy by the second cryomodule while reducing the energy spread [5]. Once the electron beam will arrive to the expected energy, it will send either to FEL hall or Bremsstrahlung hall. The parameters of TARLA cryomodule is given with Table 2.

The cryostat and mechanical tuning systems of cryomodules are originated by ELBE project [6]. The tunning system of the cryomodules has been modified slightly by mounting piezo-actuators on lever arms to have better RF performance for pulsed RF operations. The resolution and the speed of

* Work supported by Strategy and Budget Department of Turkey with Grand No: 2006K-120470
† avniaksoy@ankara.edu.tr

Content from this work may be used under the terms of the CC BY 3.0 licence (© 2019). Any distribution of this work must maintain attribution to the author(s), title of the work, publisher, and DOI

ISBN: 978-3-95450-210-3 doi:10.18429/JACoW-FEL2019-TUP026

Content from this work may be used under the terms of the CC BY 3.0 licence (© 2019). Any distribution of this work must maintain attribution to the author(s), title of the work, publisher, and DOI

UNAVERAGED SIMULATION OF A REGENERATIVE AMPLIFIER FREE ELECTRON LASER

P. Pongchalee, B.W.J. McNeil
SUPA, Department of Physics, University of Strathclyde, Glasgow, UK
also at Cockcroft Institute, Warrington, WA4 4AD, UK

Abstract

A regenerative amplifier free-electron laser (RAFEL) design and simulation requires the modelling of both the electron-light interaction in the FEL undulator and the optical propagation within the cavity. An unaveraged 3D simulation was used to model the FEL interaction within the undulator using the Puffin code. This allows a broadband, high temporal-resolution of the FEL interaction. The Optical Propagation Code (OPC) was used to model the optical beam propagation within the cavity and diagnostics at the cavity mirrors. This paper presents the optical field conversion method between Puffin and the OPC codes and demonstrates the full model via a VUV-RAFEL simulation.

INTRODUCTION

When using an oscillator FEL at shorter wavelengths, such as UV and X-ray, the optical components used to create the cavity will be a limiting factor due to the absorption of the optical materials at shorter wavelengths, or due to a lack of tunability via e.g. Bragg reflections. The RAFEL uses the high-gain undulator and a *small* amount of feedback to obtain the system saturation. Hence, the RAFEL can use low reflectivity mirrors for the optical cavity and operate into the short wavelength regime [1]. An overview of RAFEL operation over a wide range of parameters in the 1D limit is given in [2].

Several 3D FEL codes, such as Genesis 1.3 [3], are used to model the FEL interaction based on the Slowly Varying Envelope Approximation (SVEA). However, Puffin [4] is an unaveraged FEL code without the SVEA approximation and does not use undulator period averaging of the electron trajectories. The resultant radiation field retains the fast-oscillating term and allows the modelling of broadband (few cycle radiation field) and more complex electron dynamics. This paper describes how the modelling of such behaviour can be achieved in a RAFEL.

Previously, Genesis 1.3 was used with the Optical Propagation Code (OPC) [5], to simulate a RAFEL in the VUV-FEL by running both codes sequentially [6]. OPC includes 3D mirror reflection and free-space propagation through the optical path of the cavity. OPC is used here to model the optical propagation inside the RAFEL cavity while the FEL interaction inside the undulator is modelled using Puffin.

This paper first describes the translation of the input/output optical field files between Puffin and OPC necessary for linking the two codes. A RAFEL design operating in the VUV at 100 nm is then described. The optical cavity was designed to satisfy the cavity stability condition and match the undulator length and the electron beam repetition rate.

FORMAT CONVERSION

The Puffin field data consists of 4D array data set in the HDF5 format with the dimension of (2, n_z, n_y, n_x), which is the two sets of 3D field data in space separated by the polarised orientation (x-polarized and y-polarized field). The n_z represents the data in the direction corresponding to the propagation of the field. For one-wavelength long data simulation, the output field from Puffin is a single period oscillation, as shown the example of the transverse Gaussian field in Figure 1.

The OPC field is described in two files. The first is the field data in the format of binary data in the Genesis '.dfl' field file format. Each point of data contains 8 bytes (64-bit) of binary data that represents the floating number, which can be dumped into a 1D array. The size of the product of the number of grid points in *x* and *y* etc, is contained in the second OPC parameter file containing the gridpoint parameters, number of slices in z etc. The transverse optical field profile data consists of two components of the complex number – real and imaginary parts, which interleave in the array by odd and even indices of the 1D data array. For the temporal information in the OPC data, the number of slices sets as the additional axis of the array corresponding to the z-direction of the optical propagation.

The Python conversion script starts by considering the envelope of the optical field from the analytical function, which includes real and imaginary parts of the sinusoidal function. For a simple plane wave, the real-valued radiation field that would be obtained from Puffin is written in Eq. (1)

$$A_{puffin}(\mathbf{r},t) = A_0(\mathbf{r},t)\cos\left(kz - \omega t + \phi(\mathbf{r},t)\right) \quad (1)$$

where A_{puffin} is the scaled radiation field with the amplitude of A_0, k is the radiation wave number, ω is the angular frequency of the radiation wave, and $\phi(\mathbf{r},t)$ is the phase of the field. The analytic signal will be used to translate the real-value field from Puffin into the complex representation of OPC field format using the Hilbert transform [7], which has the effect of shifting the phase of the original signal by $-\pi/2$. The Hilbert transform (denoted by a 'hat') of the original Puffin field can then be written in Eq. (2) as:

$$\hat{A}_{puffin}(\mathbf{r},t) = A_0(\mathbf{r},t)\sin\left(kz - \omega t + \phi(\mathbf{r},t)\right) \quad (2)$$

ISBN: 978-3-95450-210-3 doi:10.18429/JACoW-FEL2019-TUP027

MODELLING CRYSTAL MISALIGNMENTS FOR THE X-RAY FEL OSCILLATOR*

R. R. Lindberg†, Argonne National Laboratory, Lemont, IL 60439 USA

Abstract

The X-ray FEL oscillator has the potential to be a revolutionary new light source providing unprecedented stability in a narrow bandwidth [1]. However, a detailed understanding of cavity tolerance and stability has only begun, and there are presently no suitable simulation tools. To address this issue, we have developed a fast FEL oscillator code that discretizes the field using a Gauss-Hermite mode expansion of the oscillator cavity. Errors in crystal alignment result in a mixing of the modes that is easily modeled with a loss and coupling matrix. We show first results from our code, including the effects of static and time-varying crystal misalignments.

INTRODUCTION

The x-ray FEL oscillator [1, 2], in which the output from a low-gain FEL is returned to interact with subsequent electron bunches by an x-ray cavity built of Bragg crystals and focusing elements, has garnered much interest over the past decade. In this paper we will focus on how the output of a single frequency component can be affected by crystal tilts, as this will provide the first look into what tolerances we require for the crystal optics.

XFELO CAVITY MODES

We expand the transverse profile using the Gauss-Hermite modes defined by the optical cavity. Along x we write

$$E(x;z) = \sum_\ell \frac{\mathcal{E}_\ell(z)\exp\left[-\frac{x^2(1+iz/z_R)}{4\sigma_x^2(1+z^2/z_R^2)}\right]}{\sqrt{2^\ell \ell!\,\sigma_x(1+z^2/z_R^2)^{1/2}}} \times H_\ell\left[\frac{x/\sigma_x}{\sqrt{2(1+z^2/z_R^2)}}\right] e^{-i(\ell+1/2)\mathrm{atan}(z/z_R)} \quad (1)$$

$$= \sum_\ell \mathcal{E}_\ell(z) M_\ell(x;z), \quad (2)$$

where M_ℓ is the mode shape of the ℓth Gauss-Hermite mode that is defined in terms of the rms width σ_x and the Rayleigh range $z_R = \sigma_x/\sigma_{x'} = 2k_1\sigma_x^2$ for a paraxial field with carrier wavevector $k_1 = 2\pi/\lambda_1$; a similar expansion holds in y. Ignoring slippage, the FEL field equation is then

$$\frac{d}{dz}\mathcal{E}_{\ell,m} = -\frac{ek_1K[\mathrm{JJ}]}{4\gamma_0\epsilon_0}\sum_j e^{-i\theta_j} M_\ell(x_j)M_m(y_j), \quad (3)$$

where the sum is over all particles in the FEL slice, γ_0 is the reference energy, the ponderomotive phase $\theta_j(z) = (k_1 + k_u)z - ck_1t_j(z)$ for a particle with time t_j moving in an electromagnetic wave with wavenumber $k_1 = 2\pi/\lambda_1$ and undulator wavenumber $k_u = 2\pi/\lambda_u$, e and ε_0 are the electric charge and permittivity of free space, and [JJ] is the Bessel function factor for an undulator with deflection parameter K. The equations of motion for the phase θ_j and the scaled particle energy difference $\eta_j = (\gamma_j - \gamma_0)/\gamma_0$ are

$$\frac{d\theta_j}{dz} = 2k_u\eta_j - \frac{k_1}{2}(\boldsymbol{p}_j^2 + K^2k_u^2\boldsymbol{x}_j^2/2\gamma^2) \quad (4)$$

$$\frac{d\eta_j}{dz} = \frac{eK[\mathrm{JJ}]}{2mc^2\gamma_0^2}\sum_{\ell,m}\mathcal{E}_{\ell,m}e^{i\theta_j}M_\ell(x_j)M_m(y_j) + c.c., \quad (5)$$

where transverse position and angle are $\boldsymbol{x}_j$ and $\boldsymbol{x}'_j$.

Upon exiting the undulator, the field is returned to the undulator beginning by the x-ray cavity. For a perfectly aligned cavity this results in some loss for each mode $\mathcal{E}_\ell$, but imperfections and misalignments result in mode coupling and effective loss in the fundamental Gaussian mode.

At lowest order misalignments act to shift the optical axis by a position and angle at each pass that can be found by tracking a ray through the system. The result is that the optical axis becomes offset in position by $\boldsymbol{X}_d = (X_d, Y_d)$, and in angle by $\boldsymbol{\Theta}_d = (\theta, \psi)$. Then, the displaced field at the beginning of the undulator for pass $n+1$ is related to the field at the end of the undulator from pass n via

$$E^{(n+1)}(\boldsymbol{x};0) = (1-\alpha)e^{ik(\boldsymbol{x}-\boldsymbol{X}_d)\cdot\boldsymbol{\Theta}_d} \times E^{(n)}(\boldsymbol{x}-\boldsymbol{X}_d;L_u), \quad (6)$$

where α is the amplitude loss due to imperfect reflectivity. To transform this into a relationship between mode expansion coefficients, we need to project the displaced field onto the Gauss-Hermite basis. We will do this explicitly for the x-direction only, as expressions for y are essentially the same. We insert the expansion (1)-(2), multiply by the mode $M_\ell(x)$, and integrate over x to obtain

$$\mathcal{E}_\ell^{(n+1)}(0) = (1-\alpha)\int dx\, e^{ik\theta(x-X_d)}M_\ell(x) \times \sum_{\ell'} M_{\ell'}(x-X_d)\mathcal{E}_{\ell'}^{(n)}(L_u). \quad (7)$$

$$= (1-\alpha)\sum_{\ell'}\mathcal{P}_{\ell,\ell'}(\theta,X_d)\mathcal{E}_{\ell'}^{(n)}(L_u), \quad (8)$$

where we have defined the projection operator $\mathcal{P}$ as shown. It turns out that this integral can be done in terms of the associated Laguerre polynominal $L_n^m(x)$; if $\ell \geq \ell'$ we have

$$\mathcal{P}_{\ell,\ell'} = \sqrt{\ell'!/\ell!}e^{-ik_1X_d\theta/2}e^{-[(X_d/\sigma_x)^2+(\theta/\sigma_{x'})^2]/8} \times \left(\frac{X_d + iz_R\theta}{\sqrt{2}\sigma_x}\right)^{\ell-\ell'} L_{\ell'}^{\ell-\ell'}\left(\frac{X_d^2+z_R^2\theta^2}{4\sigma_x^2}\right), \quad (9)$$

* Work supported by U.S. Dept. of Energy Office of Sciences under Contract No. DE-AC02-06CH11357.
† lindberg@anl.gov

Content from this work may be used under the terms of the CC BY 3.0 licence (© 2019). Any distribution of this work must maintain attribution to the author(s), title of the work, publisher, and DOI

ISBN: 978-3-95450-210-3 doi:10.18429/JACoW-FEL2019-TUP028

POWER VARIATIONS OF AN X-RAY FEL OSCILLATOR IN SATURATION*

R. R. Lindberg† and K.-J. Kim[1], Argonne National Laboratory, Lemont, IL, USA
[1]also at University of Chicago, Chicago, IL, USA

Abstract

Basic FEL theory predicts that the fractional power fluctuations of an ideal oscillator in steady state should be given by the ratio of the spontaneous power in the oscillator bandwidth to that stored in the cavity at saturation. For the X-ray FEL oscillator with its narrow bandwidth Bragg crystal mirrors, this ratio is typically a few parts per million, but some simulations have shown evidence of power oscillations on the percent level. We show that this is not related to the well-known sideband instability, but rather is purely numerical and can be eliminated by changing the particle loading. We then briefly discuss to what extent variations in electron beam arrival time may degrade the power stability.

INTRODUCTION

The x-ray FEL oscillation (XFELO) has the potential to be an intense source of narrow-bandwidth x-rays that is also incredibly stable [1, 2]; theory predicts that the fractional pulse-to-pulse energy stability could approach the 10^{-5} to 10^{-6} level. We investigate ways in which this stability might be disturbed, showing that the sideband instability will not be an issue, that certain power fluctuations observed in simulation are purely numerical, and the extent to which electron arrival time jitter affects FEL output.

SIDEBAND INSTABILITY

Ideally, an FEL oscillator at saturation should operate like standard atomic lasers, outputting steady-state pulses of radiation whose energy is approximately constant and whose spectral content can approach the Fourier limit. On the other hand, there are many potential causes for variations in the saturated output power of an FEL oscillator. These include fluctuations in the cavity and/or electron beam properties, short-pulse effects that arise when the distance that the radiation of central wavelength λ_1 slips ahead of an electron after N_u undulator periods becomes comparable to the electron beam duration σ_e, and instabilities. Perhaps the best-known instability is the sideband or trapped particle instablity, in which particle motion in the ponderomotive bucket during a single pass can lead to large variations in output power and multi-modal spectral output.

We can understand the physics of the sideband instability using the arguments of [3]: we consider a perturbation of the radiation power like that shown in Fig. 1(a), where the power $P_1 \sim P_{\rm sat} = (I/e)\gamma mc^2/2N_u$, with I the electron beam current, γ the Lorentz factor, and e, m, and c the electron charge, mass, and the speed of light. If the width of region 1 equals the synchrotron period in region 1 $\sim \lambda_1(P_{\rm sat}/P_1)^{1/4} \sim N_u\lambda_1$, then in the first half of the undulator the particles in region 1 make one-half a synchrotron oscillation and lose the energy $\sim \gamma mc^2(P_1/P_{\rm sat})^{1/4}/2N_u$ to the field. In the second half of the undulator where these particles are in the absorptive phase, the field has slipped ahead by a distance $N_u\lambda_1/2$ and the particles extract energy from the wave in region 2. On the other hand, if we consider the particles initially in region 2 we find that since the power and hence the synchrotron frequency is initially smaller, they do not make a full half-rotation in the bucket after half the undulator length. Thus, they lose less energy to region 2 than is given to region 1, and extract less energy from region 3 than particles initially in region 1 take from region 2. The net effect is that the perturbation is amplified, so that in general the FEL oscillator in saturation is unstable to the growth of sidebands at frequencies $\omega_1 \pm \omega_s \sim (2\pi c/\lambda_1)(1 \pm 1/N_u)$.

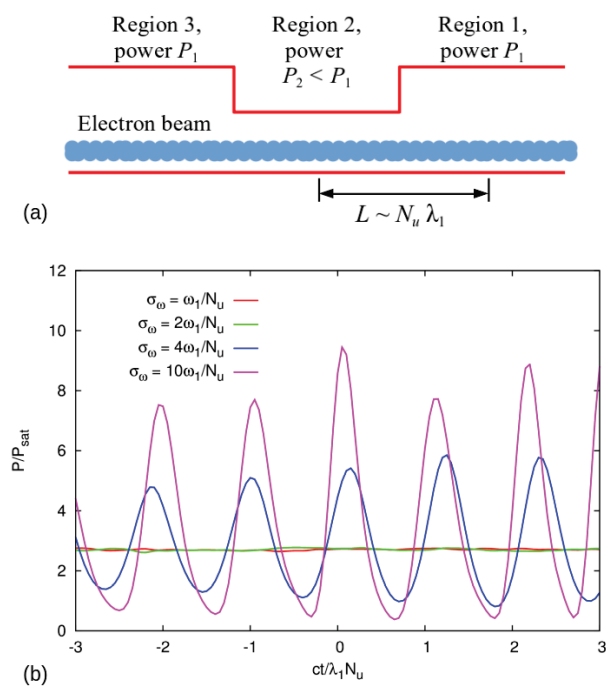


Figure 1: (a) Illustration of a perturbation that would be amplified by the sideband instability. (b) Saturated output power for various mirror bandwidths σ_ω that are of order the synchrotron frequency at saturation ω_1/N_u.

Since the instability amplifies the sidebands at normalized frequency difference $\pm 1/N_u$, we expect that it can be suppressed in oscillators that have narrow-bandwidth reflective mirrors. For example, the x-ray FEL oscillator [1, 2]

* Supported by U.S. Dept. of Energy Office of Sciences under Contract No. DE-AC02-06CH11357 and from the DOE ADRP grant #29545.
† lindberg@anl.gov

Content from this work may be used under the terms of the CC BY 3.0 licence (© 2019). Any distribution of this work must maintain attribution to the author(s), title of the work, publisher, and DOI

ISBN: 978-3-95450-210-3 doi:10.18429/JACoW-FEL2019-TUP032

REGENERATIVE AMPLIFICATION FOR A HARD X-RAY FREE-ELECTRON LASER

G. Marcus, Y. Ding, Y. Feng, A. Halavanau, Z. Huang, J. Krzywinski, J. MacArthur, R. Margraf, T. Raubenheimer, D. Zhu, SLAC National Accelerator Laboratory, Menlo Park, CA 94025, USA
V. Fiadonu, Santa Clara University, Santa Clara, CA 95053, USA

Abstract

An X-ray regenerative amplifier FEL (XRAFEL) utilizes an X-ray crystal cavity to provide optical feedback to the entrance of a high-gain undulator. An XRAFEL system leverages gain-guiding in the undulator to reduce the cavity alignment tolerances and targets the production of longitudinally coherent and high peak power and brightness X-ray pulses that could significantly enhance the performance of a standard single-pass SASE amplifier. The successful implementation of an X-ray cavity in the XRAFEL scheme requires the demonstration of X-ray optical components that can either satisfy large output coupling constraints or passively output a large fraction of the amplified coherent radiation. Here, we present new schemes to either actively Q-switch a diamond Bragg crystal through lattice constant manipulation or passively output couple a large fraction of the stored cavity radiation through controlled FEL microbunch rotation. A beamline design study, cavity stability analysis, and optimization will be presented illustrating the performance of potential XRAFEL configurations at LCLS-II/-HE using high-fidelity simulations.

INTRODUCTION

The production of longitudinally coherent radiation from single-pass self-amplified spontaneous emission (SASE) FEL amplifiers has been the subject of continued interest. Cavity-based X-ray FELs (CBXFELs) [1] such as the X-ray free-electron laser oscillator (XFELO) [2] and the X-ray regenerative amplifier free-electron laser (XRAFEL) [3, 4] have seen renewed interest as a means of producing and preserving longitudinally coherent hard X-ray (HXR) FEL pulses. While the XFELO and XRAFEL schemes share a common infrastructure (a high-brightness, high repetition rate electron beam, an undulator, and an X-ray cavity) they target very different but complementary FEL performance characteristics (see, for example, [1] and references therein). The XFELO relies on a low-loss cavity supporting a low-gain FEL while the XRAFEL leverages a high-gain FEL interaction. Consequently, the requirements on the cavity for a XRAFEL are relatively relaxed. The science that is enhanced and/or enabled by these two concepts are therefore very different. Here, we focus on the practical elements and performance characteristics of an XRAFEL implementation of a CBXFEL at the LCLS-II facility.

The LCLS-II [5, 6] and the LCLS-II-HE upgrade [7, 8] will be capable of delivering high-brightness electron beams to the HXR undulator at repetition rates as high as ∼ 1 MHz, making realistic X-ray cavity geometries and footprints feasible. Significant cavity component development and evaluation has been undertaken by the team at Argonne National Lab in the context of the XFELO. They have shown that high quality diamond Bragg crystals have record-high reflectivities [9], ultra-low thermal expansion and high thermal diffusivity [10], and high mechanical and radiation hardness [11]. These properties make diamond an excellent candidate for the XRAFEL.

The flexibility of the high-gain XRAFEL system, however, allows for the investigation of strongly tapered undulators for high conversion efficiency of electrical to optical power. Efficient undulator tapering relies on stable, high power, and longitudinally coherent seed pulses [12, 13], which a RAFEL would excel at delivering. In this regard, diamond optics present a challenge because of their ultra-high reflectivities, making it difficult to extract a large fraction of the stored X-ray pusle energy. Here, we briefly present two methods that may be used to output couple a significant fraction of the stored cavity X-ray power. One method, cavity Q-switching, relies on a manipulation of the cavity optics while the second method, microbunch rotation and off-axis lasing, manipulates the gain medium itself (the electron bunch). We also explore the consequence of the Q-switching concept on the design of the cavity and the performance of the scheme.

RADIATION OUTPUT COUPLING METHODS

Various output coupling methods have been explored within the context of an XRAFEL implementation at the LCLS-II facility. These include both active and passive methods that require manipulation of either the cavity optical components or the gain medium iteslf. We briefly present two concepts below.

Transient Thermal Expansion of Diamond Lattice Constant

Transient thermal expansion of the diamond lattice constant can be achieved through short-pulsed optical laser excitation. The lattice spacing, therefore, can be manipulated to satisfy or not satisfy the Bragg reflection condition on demand - the cavity can be actively 'Q-switched'. The thermal transport time scale of absorbed energy out of the primary absorbed region on the crystal is 10's of ns due to the high thermal conductivity of diamond, which is sufficiently short compared to a typical roundtrip time in the cavity (∼ 1μs for LCLS-II). Since all of the cavity power is dumped through this process, the effective repetition rate of the XRAFEL is lowered from ∼ 1 MHz to ∼ 10 − 50 kHz, and depends on

Content from this work may be used under the terms of the CC BY 3.0 licence (© 2019). Any distribution of this work must maintain attribution to the author(s), title of the work, publisher, and DOI

ISBN: 978-3-95450-210-3 doi:10.18429/JACoW-FEL2019-TUP033

Q-SWITCHING OF X-RAY OPTICAL CAVITIES BY USING BORON DOPED BURIED LAYER UNDER A SURFACE OF A DIAMOND CRYSTAL

J. Krzywinski, D. Zhu, G. Marcus, Y. Feng, A. Halavanau, J. MacArthur, Z. Huang
SLAC National Accelerator Laboratory, Stanford University, Menlo Park CA, USA
A. Kissas, Santa Clara University, Santa Clara CA, USA

Abstract

Improvement of the longitudinal coherence of X-ray Free Electron Lasers has been the subject of many recent investigations. The XFEL oscillator (XFELO) and Regenerative Amplifier Free-Electron Laser (RAFEL) schemes offer pathways to fully coherent, high brightness X-ray radiations. The XFELO and RAFEL both consist of a high repetition rate electron beam, an undulator, and an X-ray crystal cavity to provide optical feedback. The X-ray cavity will be based on diamond crystals in order to manage a high thermal load. We are investigating a 'Q switching' mechanism that involves the use of a 'Bragg switch' to control the X-ray pulse energy built-up and outcoupling inside the X-ray cavity. In particular, one can use an optical laser to manipulate the diamond crystal lattice constant to control the crystal reflectivity and transmission. It has been shown that a 9 MeV focused boron beam can create a buried layer, approximately 5 microns below surface, with a boron concentration up to 10^{21} atoms/cm^3, with localized and enhanced optical absorption. Here, we present simulations showing that absorbing laser pulses by a buried layer under the crystal surface would allow creating a transient temperature profile which would be well suited for the 'Q switching' scheme.

INTRODUCTION

The brightness of x-ray sources has been increased one to ten billion times by x-ray free-electron lasers (XFELs) that generate high intensity coherent photon pulses at wavelengths from nanometers to less than one angstrom and a duration of a few to 100 femtoseconds [1]. For the first time XFELs allow for experimental exploration of the structure and dynamics of atomic and molecular systems at the angstrom-femtosecond space and time scale. This have created a plethora of new opportunities for scientific research in physics, chemistry, biology, material science and high energy density physics [1, 2]. A characteristic feature of single-pass SASE FELs, however, is the poor longitudinal coherence, which results from the initial amplification of incoherent radiation shot-noise [1]. Improvement of the longitudinal coherence is of great practical importance and has been the subject of many recent investigations. With high repetition rate machines, such as European XFEL [3], and LCLS-II [4] coming online soon, an XFEL oscillator (XFELO) [5, 6] or Regenerative Amplifier Free-Electron Laser (RAFEL) [7, 8] offers a pathway to the production of stable, fully coherent, high brightness, and high average power X-ray radiation. These so-called cavity-based X-ray free-electron lasers (CBXFELs) consist of a high repetition rate electron beam, a short undulator, and an x-ray crystal cavity (in the case of hard X-rays) to provide optical feedback (Fig. 1).

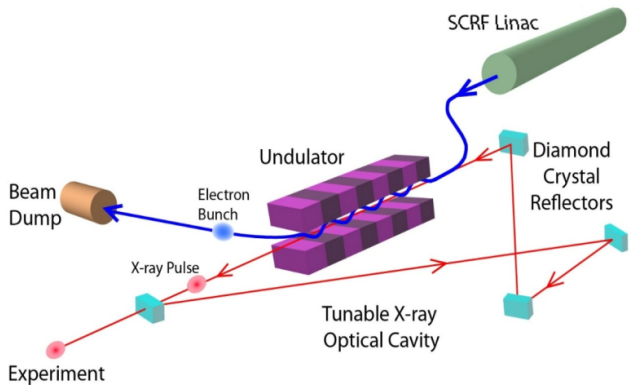


Figure 1: Schematic illustration of an X-ray cavity for XFELO or RAFEL. Four crystals form a closed X-ray cavity via Bragg reflection [9].

Q-SWITCHING OF X-RAY OPTICAL CAVITIES

Like optical laser cavities, outcoupling optics and mechanisms is one of the essential components, which can come in the form of a partial reflector or cavity 'dumper'. We are investigating the viability of a 'Q switching' mechanism that involves the use of a 'Bragg switch' to dump the x-ray pulse energy built-up inside an x-ray cavity [10, 11]. The idea of Bragg switching by a controlled lattice deformation using piezoelectric excitation, generation of optical and acoustic phonons or picosecond thermal excitations has been proposed and demonstrated at synchrotron sources by several authors [10–18]. However, the construction of an x-ray cavity around a high repetition rate XFEL will require using materials that can manage high thermal load. Single crystal diamond is a good candidate as it has superb thermal and mechanical properties and, because it is a low Z material, X-ray energy deposition per volume is much less than other candidates such as silicon crystal [19]. Therefore techniques that have been already proposed cannot be applied directly here as our choice of materials is limited to low Z materials and the XRAFEL cavity output-coupling techniques needs further studies.

In this work we investigate the use of optical laser to manipulate the crystal lattice constant in such a way that the crystal reflectivity/transmission can be controlled by the relative timing of the optical laser excitation and the

Content from this work may be used under the terms of the CC BY 3.0 licence (© 2019). Any distribution of this work must maintain attribution to the author(s), title of the work, publisher, and DOI

ISBN: 978-3-95450-210-3 doi:10.18429/JACoW-FEL2019-TUP035

SENSITIVITY OF LCLS SELF-SEEDED PEDESTAL EMISSION TO LASER HEATER STRENGTH

G. Marcus, D. Bohler, Y. Ding, W. M. Fawley, Y. Feng, E. Hemsing,
Z. Huang, J. Krzywinski, A. Lutman, D. Ratner
Menlo Park, CA 94025, USA

Abstract

Measurements of the soft X-ray, self-seeding spectrum at the LCLS free-electron laser generally display a pedestal-like distribution around the central seeded wavelength that degrades the spectral purity. We have investigated the detailed experimental characteristics of this pedestal and found that it is comprised of two separate components: (1) normal SASE whose total strength is nominally insensitive to energy detuning and laser heater (LH) strength; (2) sideband-like emission whose strength positively correlates with that of the amplified seed and negatively with energy detuning and LH strength. We believe this latter, non-SASE component arises from comparatively long wavelength amplitude and phase modulations of the main seeded radiation line. Its shot-to-shot variability and LH sensitivity suggests an origin connected to growth of the longitudinal microbunching instability on the electron beam. Here, we present experimental results taken over a number of shifts that illustrate the above mentioned characteristics.

INTRODUCTION

This work was recently accepted for publication in Physical Review Accelerator and Beams [1].

REFERENCES

[1] G. Marcus *et al.*, "Experimental observations of seed growth and accompanying pedestal contamination in a self-seeded, soft x-ray free-electron laser," *Phys. Rev. Accel. and Beams*, vol. 22, pp. 080702, 2019. doi:10.1103/PhysRevAccelBeams.22.080702

Content from this work may be used under the terms of the CC BY 3.0 licence (© 2019). Any distribution of this work must maintain attribution to the author(s), title of the work, publisher, and DOI

ISBN: 978-3-95450-210-3 doi:10.18429/JACoW-FEL2019-TUP036

A WAVEGUIDE-BASED HIGH EFFICIENCY SUPERRADIANT FEL OPERATING IN THE THz REGIME *

P. Musumeci†, A. Fisher, UCLA Department of Physics and Astronomy, Los Angeles, CA, USA
B. Van Der Geer, Pulsar Physics
E. A. Nanni, E. C. Snively, SLAC National Accelerator Laboratory, Menlo Park, CA, USA
A. Gover, Tel Aviv University, Tel Aviv, Israel

Abstract

In this paper we describe a novel self-consistent 3D simulation approach for a waveguide FEL operating in the zero-slippage regime to generate high power THz radiation. In this interaction regime, the phase and group velocity of the radiation are matched to the relativistic beam traveling in the undulator achieving long interaction lengths. Our numerical approach is based on expanding the existing 3D particle tracking code GPT (General Particle Tracer) to follow the interaction of the particles in the beam with the electromagnetic field modes of the waveguide. We present two separate studies: one for a case which was benchmarked with experimental results and another one for a test case where, using a longer undulator and larger bunch charge, a sizable fraction of the input beam energy can be extracted and converted to THz radiation. The model presented here is an important step in the development of the zero-slippage FEL scheme as a source for high average and peak power THz radiation.

INTRODUCTION

Free-Electron Laser radiation sources have long been an attractive solution to generate large amounts of electromagnetic radiation in spectral ranges where solid-state based devices are less effective including THz, extreme UV, soft and hard X-rays[1]. The THz range is particularly interesting for an FEL due to the fact that only relatively modest energy (~ few up to tens of MeV) electron beams are required in order to match the resonance condition for efficient interaction in an undulator magnet.

In the THz range, fueled by the recent developments in laser-based generation of nearly single-cycle radiation pulses[2], much interest has been diverted towards broad bandwidth THz applications, for example in the study of non-linear response in materials. On the other hand, most THz FEL operate with fairly long electron beams and target the generation of narrowband THz radiation [3,4]. This is due to the intrinsic bandwidth of the FEL associated with the slippage effects which limits the number of undulator periods over which a strong interaction can be maintained.

Following earlier work on wave-guided FEL[5,6], we recently revisited a strong coupling scheme for electrons and electromagnetic wave co-propagating in an undulator, based on the zero-slippage interaction where the group velocity of the radiation in a waveguide is matched to the electron beam axial velocity [7]. This scheme has the potential for broadband interaction (see Fig. 1), extended interaction lengths and high efficiency energy conversion.

Two sets of experiments where completed using the same setup at UCLA Pegasus Laboratory. In the first one, we used a laser-generated THz pulse to impart energy modulation on an electron beam to show THz-based beam compression. In the second one, raising the charge of the e-beam we showed THz amplification and generation. [8,9]. In the design and analysis of the results for these experiments, an interesting issue we had to face was the lack of adequate simulation tools to model this interaction. Standard wide-spread use FEL codes such as GENESIS or GINGER typically employ the slice-model and suffer from limitations related to period-averaging and slowly varying envelope approximation which fail to capture the dispersion dominated radiation evolution and the broad bandwidth of the interaction in a waveguide FEL.

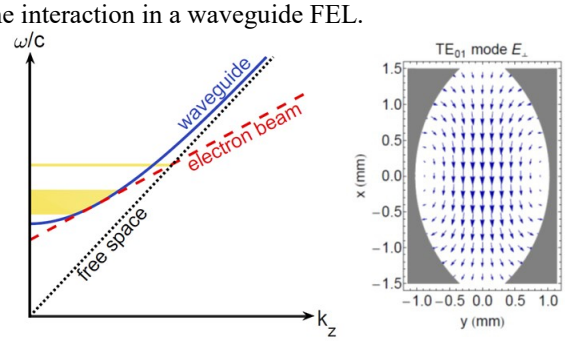


Figure 1: Left) Schematics of the waveguide coupling scheme. Strong interaction occurs where phase synchronicity between the radiation and the electron occurs. In the free space case, this intersection is limited to a single point. In the waveguide an entire range of frequencies can interact with the beam (due to the tangential crossing). Right) Spatial profile of the TE_{01} fundamental curved parallel plate waveguide mode which dominates the interaction.

In order to understand our experiments we used a mixture of a GPT module [10] to follow the particle evolution assuming a frozen-field approximation (radiation fields propagating unperturbed by the presence of the e-beam), and a 1D self-consistent modal-decomposition based FEL simulation wafFEL [9] where the full dispersion relation for the waveguide was used. In this paper we combine the two approaches and use GPT to calculate the spectrum of the radiation along the undulator. We will first describe the

* Work mainly supported by DOE grant DE-SC0009914 and NSF grant PHY-1734215.
† musumeci@physics.ucla.edu

Content from this work may be used under the terms of the CC BY 3.0 licence (© 2019). Any distribution of this work must maintain attribution to the author(s), title of the work, publisher, and DOI

ISBN: 978-3-95450-210-3 doi:10.18429/JACoW-FEL2019-TUP037

OPTIMIZATION OF THE TRANSVERSE GRADIENT UNDULATOR (TGU) FOR APPLICATION IN A STORAGE RING BASED XFELO*

Y. S. Li†, University of Chicago, IL, USA
R. R. Lindberg and K.-J. Kim, Argonne National Laboratory, IL, USA

Abstract

The stringent energy spread requirement of the XFELO poses a challenge for its application in storage rings. One way to overcome this is by using a transverse gradient undulator (TGU) [1]. The TGU gain formula was discussed previously [2,3]. In this paper, we begin by reviewing the analytical 3D gain formula derived from the gain convolution formula. Following that, we apply numerical optimization to investigate the optimal beam and field parameters for maximal TGU gain. We found that a small emittance ratio (i.e. "flat beam" configuration) has a strong positive impact on TGU gain, as well as other patterns in the optimal parameters.

THEORY

An in-depth exploration of TGU physics can be found in [2]. Here, we provide an essential summary. A TGU scheme has two key ingredients. First, we introduce dispersion upstream of the TGU that correlates electron position and energy, i.e.

$$y = y_0 + D\eta, \tag{1}$$

where D is the dispersion strength and y_0, η are the initial vertical electron position and relative energy deviation respectively. (We assume here that the TGU acts in the y-direction.) Secondly, the TGU introduces a linear dependence in K on transverse displacement, i.e. $K(y) \approx (1 + \alpha y)K_0$, where K_0 is the on-resonance undulator parameter and α is the TGU magnetic gradient. Then, we can cancel out the energy spread by requiring

$$\alpha D = (2 + K_0^2)/K_0^2 \tag{2}$$

The TGU is only effective if $D\sigma_\eta \gg \sigma_y$, i.e. if beam size is primarily dominated by dispersion.

The 3D gain formula in this scenario is derived to be

$$G = \frac{G_0}{4\pi}\int_{-1/2}^{1/2} dz\, ds\, \frac{i(z-s)}{\sqrt{\mathfrak{D}_x \mathfrak{D}_y}} \exp\left[-2ix(z-s) - \frac{2\tilde{\sigma}_\eta^2 (z-s)^2}{1+\Gamma^2} - \left(\frac{\Gamma}{1+\Gamma^2}\frac{\tilde{\sigma}_\eta}{\tilde{\beta}_y}\right)^2 \frac{(z^2-s^2)^2}{2}\frac{\mathfrak{d}_y}{\mathfrak{D}_y}\right], \tag{3}$$

where

$$\Gamma = \frac{D\sigma_\eta}{\sigma_y}, \quad x = \pi N_u \Delta\nu, \tag{4}$$

$$\tilde{\sigma}_\eta = 2\pi N_u \sigma_\eta, \quad \tilde{\beta}_y = \beta_y / L_u, \tag{5}$$

$$\frac{G_0}{4\pi} = 4\pi\gamma_r \frac{I}{I_A}\frac{K_0^2 [JJ]^2}{(1+K_0^2/2)^2} N_u^3 \lambda_1^2, \tag{6}$$

and $\sigma_{x,y}$ are the RMS electron beam sizes, L_u, N_u are the undulator length and number of undulator periods respectively, $\Delta\nu \equiv (1 - \lambda/\lambda_1)$ is the detuning factor based on resonant FEL wavelength λ_1, σ_η is the relative energy spread, $\beta_{x,y}$ is the respective betatron function, γ_r is the resonant Lorentz factor, I is the beam current, $I_A \approx 17\,\mathrm{kA}$ is the Alfvén current, $[JJ] \equiv J_0[K_0^2/(4+2K_0^2)] - J_1[K_0^2/(4+2K_0^2)]$ is the Bessel factor, and

$$\mathfrak{D}_{x,y} = \Sigma_{x,y}^2 + sz\, L_u^2 \Sigma_{\phi x,y}^2 - iL_u(z-s)\left[\frac{1}{4k} + k\Sigma_{\phi x,y}^2 \Sigma_{x,y}^2\right], \tag{7}$$

$$\mathfrak{d}_y = \Sigma_y^2 + sz\, L_u^2 \sigma_{\phi y}^2 - iL_u(z-s)\left[\frac{1}{4k} + k\sigma_{\phi y}^2 \Sigma_y^2\right], \tag{8}$$

$$\Sigma_y^2 = \sigma_y^2 + \sigma_{ry}^2 + D^2\sigma_\eta^2, \tag{9}$$

$$\Sigma_x^2 = \sigma_x^2 + \sigma_{rx}^2, \tag{10}$$

$$\Sigma_{\phi x,y}^2 = \sigma_{px,y}^2 + \sigma_{\phi x,y}^2. \tag{11}$$

Here, $\sigma_{px,py}$ are the RMS electron beam divergences, $\sigma_{rx,ry}$ are the RMS radiation beam sizes, and $\sigma_{\phi x,\phi y}$ are the RMS radiation beam divergences.

In the context of a storage ring, there is a further constraint on the transverse emittances, namely $\epsilon_x + \epsilon_y = \epsilon_{x,0}$, with $\epsilon_{x,0}$ being the natural electron beam emittance [4]. We define the coupling constant k_c such that

$$\epsilon_x = \frac{\epsilon_{x,0}}{1+k_c}, \quad \epsilon_y = \frac{k_c \epsilon_{x,0}}{1+k_c}. \tag{12}$$

Modern storage rings are capable of operating in both round ($k_c = 1$) and flat ($k_c \ll 1$) beam configurations. Therefore, the coupling constant will be an important parameter in our investigation.

NUMERICAL OPTIMIZATION

We wish to optimize gain, as given by Eq. 3, with respect to electron and radiation beam parameters.In each optimization run, we fixed $\{\epsilon_{x,0}, \sigma_\eta\}$ and scan over k_c ranging from 0.001 to 1. At each value of k_c, the optimal parameters

* This work is supported by U.S. Dept. of Energy, Office of Science, Office of Basic Energy Sciences, under Contract No. DE-AC02-06CH11357, and U.S. National Science Foundation under Award No. PHY-1549132, the Center for Bright Beams.
† ysli@uchicago.edu

Content from this work may be used under the terms of the CC BY 3.0 licence (© 2019). Any distribution of this work must maintain attribution to the author(s), title of the work, publisher, and DOI

ISBN: 978-3-95450-210-3 doi:10.18429/JACoW-FEL2019-TUP038

Content from this work may be used under the terms of the CC BY 3.0 licence (© 2019). Any distribution of this work must maintain attribution to the author(s), title of the work, publisher, and DOI

AXIAL SYMMETRY IN SPONTANEOUS UNDULATOR RADIATION FOR XFELO TWO-BUNCH EXPERIMENT*

Y. S. Li†, University of Chicago, IL, USA
R. R. Lindberg and K.-J. Kim, Argonne National Laboratory, IL, USA

Abstract

A well known discrepancy exists between 2D and 3D FEL simulation codes with respect to the radiation field intensity prior to the exponential gain regime [1]. This can be qualitatively explained by the fact that the 3D field representation preserves many more modes than does the axisymmetric field solved for by a 2D code. In this paper, we seek to develop an analytical model that quantifies this difference. We begin by expanding the spontaneous undulator radiation field as a multipole series, whose lowest order mode is axisymmetric. This allows us to calculate the difference in predicted intensity. Next, we confirm these results with numerical calculation and existing FEL codes GINGER and GENESIS. Finally, we discuss the implications of this study with respect to the XFELO two-bunch experiment to be conducted at LCLS-II.

INTRODUCTION

The x-ray FEL oscillator (XFELO) has the potential to be a new source of bright x-rays with unprecendented spectral purity [2–4]. Over the last decade, there have been separate experiments demonstrating the necessary technologies to meet the stringent operational demands of the XFELO: diamond Bragg crystal reflectors with high reflectivity [5], low thermal conductivity [6], and sufficient resilience to high-intensity x-rays [7]; availability of suitable compound refractive mirrors [8]; feedback system for the stabilization of x-ray components [9]. The next logical step is a holistic experiment integrating these technologies together into a proof-of-concept for the XFELO.

To this end, a collaboration between Argonne and SLAC has recently proposed a cavity-based XFELO (CBXFELO) experiment to be performed at the hard x-ray line at LCLS-II [10, 11]. The goal is to test whether we can sufficiently stabilize a large-scale x-ray cavity so as to observe FEL gain. Specifically, we plan to send two electron bunches separated longitudinally by about 2 ns into an undulator, such that the first bunch generates spontaneous undulator radiation (SUR) that is then returned by the x-ray cavity to be amplified by the second bunch. Doing this requires coordinating a number of engineering and physics efforts.

This paper is focused on one aspect of the physics – the symmetry of SUR and its impact on subsequent gain. This is important to our numerical modelling process, specifically in comparing 2D vs 3D FEL codes. To clarify, 2D codes, such as GINGER [12], assumes cylindrical symmetry in the electric field, such that there is only one transverse dimension. 3D codes, such as GENESIS [13], preserve the full two dimensional transverse space, but at the cost of significantly larger computational complexity. Previous literature [14] have shown that 2D and 3D codes agree well in the exponential gain and nonlinear saturation regime, for both high-gain FELs and low-gain oscillators. This is because axisymmetric modes typically experience the largest FEL gain, so that they eventually overwhelm all other transverse modes.

On the other hand, this situation does not apply early in the gain process, where the two-bunch CBXFEL experiment is expected to operate. In this case, we expect significantly lower field intensity predicted from a 2D code vs the 3D version. Understanding and quantifying this difference is an important step in the numerical modeling process, which in the bigger picture, will allow us to better predict and optimize the number of photons measurable in the experimental setup.

THEORY

We begin by investigating the degree to which SUR can be described by an axisymmetric mode most suitable for amplification. Consider the SUR from a collection of electrons: any single electron j with 6D coordinates $(t_j, \eta_j, \mathbf{x}_j, \mathbf{x}'_j)$ contributes the field [14]

$$\mathcal{E}_{\nu,j}(\vec{\phi}) = e^{i\omega t_j} e^{-ik\vec{\phi}\cdot\vec{\mathbf{x}}_j} \int_0^{L_u} dz\, e^{i(\Delta\nu - 2\eta_j)k_u z} \times e^{\frac{1}{2}ik(\vec{\phi}-\vec{\mathbf{x}}'_j)^2(z-L_u/2)}, \tag{1}$$

where for simplicity we neglect constant prefactors in this discussion. The field in (1) is in frequency-angular representation, with $\nu \equiv \omega/\omega_1$ being the scaled frequency relative to the resonant FEL frequency $\omega_1 = 2\pi c/\lambda_1$, and $\vec{\boldsymbol{\phi}}$ being the 2D angular coordinate. Furthermore, let $\Delta\nu \equiv \nu - 1$ be the detuning and L_u be the undulator length.

Next, we write in polar coordinates $\vec{\boldsymbol{\phi}} \equiv (\phi, \psi)$, where ϕ, ψ are the magnitude and phase of the angle vector respectively. Using the Jacobi-Anger identity, we perform a multipole expansion to obtain

$$\mathcal{E}_{\nu,j}(\phi,\psi) = e^{i\omega t_j} \sum_{n=-\infty}^{\infty} \int_{-L_u/2}^{L_u/2} dz\, i^n e^{in(\psi-\theta(z))} \times J_n(k\phi|\vec{\mathbf{x}}_j + z\vec{\mathbf{x}}'_j|) e^{ik(\phi^2+\vec{\mathbf{x}}'^2_j)z/2} \times e^{ik_u(\Delta\nu - 2\eta_j)(z-L_u/2)}. \tag{2}$$

* This work is supported by U.S. Dept. of Energy, Office of Science, Office of Basic Energy Sciences, under Contract No. DE-AC02-06CH11357, and U.S. National Science Foundation under Award No. PHY-1549132, the Center for Bright Beams.
† ysli@uchicago.edu

ISBN: 978-3-95450-210-3 doi:10.18429/JACoW-FEL2019-TUP041

Content from this work may be used under the terms of the CC BY 3.0 licence (© 2019). Any distribution of this work must maintain attribution to the author(s), title of the work, publisher, and DOI

XCOS SCILAB MODEL FOR SIMULATION OF INTENSITY AND GAIN OF PLANAR UNDULATOR RADIATION

H. Jeevakhan, National Institute of Technical Teachers' Training and Research, Bhopal, India
G. Mishra, Physics Department, Devi Ahilya University, Indore, India

Abstract

Scilab Xcos based model has been designed to simulate the intensity and gain of planar undulator radiation. Numerical approach has been used to determine the trajectories of an electron along 'x' and 'z' directions, traversing through a planar undulator. The present paper describes the technical details of the different blocks, parameters and possibility of combined model used for trajectories and intensity. Simulation results are compared with the previous conventional syntax based codes.

INTRODUCTION

Free electron laser (FEL), attosecond pulses can be used in attosecond interferometry to explain the nature of materials [1-2], design of Q-bits [3] and in other cutting age multidisciplinary researches. FEL is coherent light source generated due to passage of relativistic electron beam through a periodic magnetic structure in presence of resonating electromagnetic radiation. Trajectory of electron beam in undulator, Intensity of out coming radiation and the transfer of energy from electron beam to radiation i.e. overall gain in FEL system are the parameters of interest in FEL technology and applications. Simulation software's are used to calculate the intensity and gain of real FEL system before actual experimentation.

Scilab is an open source software with numerous applications in engineering and research[4]. Scilab Xcos based simulation models for analytical solutions of electron trajectory equations have been presented with some limitations by H Jeevakhan *et al*. [5]. An improved analytical Xcos Model has been used to find the trajectory of the electron moving in the Harmonic undulator and variation of magnetic field along the axis of undulator [6]. This paper has also presented a model to find trajectory by second integral of the undulator magnetic field profile given by real measurements.

In the present paper, Scilab Xcos model has been presented based on numerical approach for trajectory of electron along undulator along 'x' and 'z' direction. The intensity of the out coming spontaneous radiation can also be simultaneously calculated by numerical method, by using this same model. The gain can further be simulated by employing Madey's Theorem for a given FEL system. The results are also compared with the previous program results based on Fortran.

PLANAR UNDULATOR FIELD

For present simulation, planar undulator magnetic field is considered and is given by [7-8]:

$$B = [0, a_0 B_0(sink_u z), 0] \quad (1)$$

Where, $k_u = \frac{2\pi}{\lambda_u}$ and where k_u is undulator wave number, λ_u is undulator wave length, B_0 is peak magnetic field.

The equation of motion of relativistic free electron moving in undulator field is given by

$$ma = -\frac{e}{c}[\vec{v} \times \vec{B}] \quad (2)$$

For numerical calculation, the acceleration along 'x' and 'z' direction can be written as

$$m\ddot{x} = \frac{K}{\gamma}\Omega_u v_z \, sin(\Omega_u \beta_*)t \quad (3)$$

$$m\ddot{z} = \frac{K}{\gamma}\Omega_u v_x \, sin(\Omega_u \beta_*)t \quad (4)$$

The component of β along x' and 'z' direction can be evaluated analytically as,

$$\beta_x = -\frac{K}{\gamma}[\cos(\Omega_u)t] \quad (5)$$

$$\beta_z = \beta_* - \frac{K^2}{4\gamma^2}[\cos(2\Omega_u)t] \quad (6)$$

corresponding initial values read as,

$$\beta_{x=0} = -\frac{K}{\gamma} \quad (7)$$

$$\beta_{z=0} = -\frac{K^2}{4\gamma^2} \quad (8)$$

Where $\beta_* = 1 - \frac{1}{2\gamma^2}\left(1 + \frac{K^2}{2}\right)$, γ is relativistic parameter, $K = \frac{a_0 e B_0}{\Omega_u m_0 c}$ is the undulator parameter, m_0 is rest mass of electron, and $\Omega_u = k_u c$

The Intensity of radiation can be evaluated from Lienard - Wiechart integral [9],

$$\frac{d^2I}{d\omega d\Omega} = \frac{e^2\omega^2}{4\pi^2 c}\left|\int_{-\infty}^{\infty}\{\hat{n} \times (\hat{n} \times \hat{\beta}\}exp\left[i\omega(t - \frac{z}{c})\right]dt\right|^2 \quad (9)$$

For Numerical simulation of Intensity along the axis the Eq. (9) can be re written as

$$\frac{d^2I}{d\omega d\Omega} = \frac{e^2\omega^2}{4\pi^2 c}\left|\int_0^T\{\widehat{\beta_x}\}exp\left[i\omega(t - \frac{z}{c})\right]dt\right|^2 \quad (10)$$

SIMULATION MODEL AND RESULTS

The model design based on numerical analysis is given in Fig. 1. It is based on execution of equations. Single execution of this model in Xcos window gives the numerical simulation of trajectory along 'x' and 'z' direction for a particular value of 'ω'. Intensity and gain can be calculated by running the model on console for various values of 'ω'. The present model comprises of three sections.

ISBN: 978-3-95450-210-3 doi:10.18429/JACoW-FEL2019-TUP042

ANALYSIS OF UNDULATOR RADIATIONS WITH ASYMMETRIC BEAM AND NON-PERIODIC MAGNETIC FIELD

H. Jeevakhan, National Institute of Technical Teachers' Training and Research, Bhopal, India
G. Mishra, Physics Department, Devi Ahilya University, Indore, India

Abstract

Harmonic Undulator radiations at third harmonics with non periodic constant magnetic field has been analysed. Symmetric and asymmetric electron beam with homogeneous spread has been used to present viable solution for the resonance shift inherited in undulator with constant magnetic field. The out coming radiation, recovers shifts in resonance and regain its intensity with asymmetric electron beam and harmonic field.

INTRODUCTION

Free electron lasers [FEL] generation is a cutting edge technology and has large numbers of research applications [1]. Tunablity and brilliance at lasing wave length in FEL are key parameters for number of applications. Lasing wavelength of FEL depends upon the value of undulator parameter, undulator wavelength and relativistic parameter of electron beam used. Recent works in FEL theory has emphasised the effect on non periodic magnetic field i.e. constant magnetic field component along or perpendicular or in both directions of the periodic magnetic field of planar undulator on the out coming undulator radiations. Quality of electron beam is also major concern in analysis of output undulator radiation. Partial compensation on the divergence of undulator radiation has been demonstrated by imposing weak constant magnetic component in the analytical form and all the major sources of homogeneous and inhomogeneous broadening have been accounted for the characteristics of the electrons beam by K. Zhukovsky [2]. The constant non-periodic magnetic constituents are studied to compensate the divergence of the electronic beam [3]. Dattoli *et al* has initially reported the effect on undulator radiation given by planar undulator with constant magnetic field component [4]. The later studies focus on higher harmonics generation by addition of additional harmonic field [5].

Harmonic planar undulator consists additional harmonic field along with sinusoidal planar magnetic field, uses modest electron beam energy and to increase the efficiency of FELs [6-9]. H jeevakhan et al have presented semi analytical results for the effect of perpendicular constant magnetic field on the gain of harmonic undulator at higher harmonics [10]. In the present paper we have analysed harmonic undulator with perpendicular non periodic magnetic field with asymmetric electron beam with energy spread and having shifted mean energy. The Harmonic field compensate the intensity loss and the asymmetric electron beam brings the undulator radiation back to resonance.

UNDULATOR FIELD

Planar undulator sinusoidal magnetic field encompass with a perpendicular constant magnetic field in present analysis and is given by

$$H = \left[H_0\kappa, b_0 H_0(sink_p + \Delta sink_l)z, 0\right] \quad (1)$$

Where, $k_p = \frac{2\pi}{\lambda_p}$ and $\mathrm{k_l} = \frac{2\pi}{\lambda_l}$ where k_p and k_l are undulator and harmonic undulator wave number respectively, λ_p is undulator wave length and $\lambda_l = l\lambda_p$, l is harmonic integer , H_0 is peak magnetic field, $\Delta = \frac{b_1}{b_0}$, b_0 and b_1 controls the amplitude of main undulator field and additional harmonic field and κ is the magnitude of constant non periodic magnetic field. The harmonic undulator can be designed by introducing shims in regular interval as per the design of harmonic undulator as shown in Fig. 1. The spacing between shims decides it, as 3rd or 5th harmonic undulator similarly as the harmonic number 'l' decides in Eq. (1).

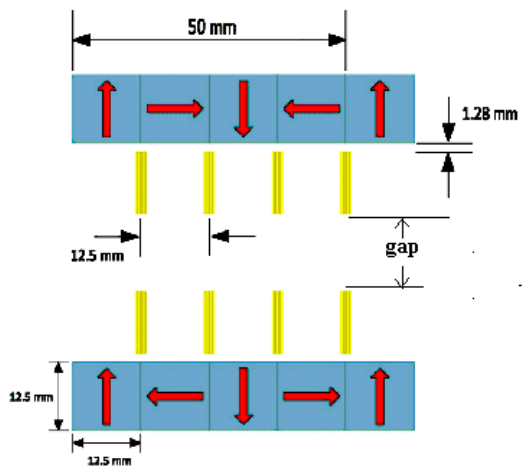


Figure 1: Schematic of one Period of harmonic Undulator*(l=3)*.

The velocity of electron traversing through undulator is derived by using Lorentz force equation:

$$\frac{dv}{dt} = -\frac{e}{\gamma mc}\left(\vec{v} \times \vec{H}\right) \quad (2)$$

This gives

$$\beta_x = -\frac{K}{\gamma}\left[\cos(\Omega_p) + \Delta\frac{\cos(l\Omega_p)}{l}\right]t$$

$$\beta_y = -\frac{K}{\gamma}\kappa\Omega_p t \quad (3)$$

Content from this work may be used under the terms of the CC BY 3.0 licence (© 2019). Any distribution of this work must maintain attribution to the author(s), title of the work, publisher, and DOI

ISBN: 978-3-95450-210-3 doi:10.18429/JACoW-FEL2019-TUP047

AN ANALYSIS OF OPTIMAL INITIAL DETUNING FOR MAXIMUM ENERGY-EXTRACTION EFFICIENCY*

Qika Jia†, National Synchrotron Radiation Laboratory,
University of Science and Technology of China, Hefei, Anhui, China

Abstract

For low gain free electron laser (FEL), the phase space evolutions of trapped electrons in the phase bucket are analyzed through calculating their synchrotron oscillation periods, which vary with the initial detuning and initial phase. The optimal initial detuning for the maximum energy-extraction efficiency and the corresponding saturation length are given. The analysis demonstrated that for the low gain case the gain of the strong optical field is about a quarter of that of the weak optical field (small signal gain), and the saturation power larger than that of high gain FEL can be achieved in the resonator of oscillator FEL.

INTRODUCTION

In free-electron laser (FEL), the phase of the electron in the combined radiation optical field and the undulator magnetic field plays a crucial role in the interaction between the optical field and the electron. The evolution of electron distribution in the phase space strongly affects the FEL performance [1, 2].

Usually, the electron phase space evolution has been studied with numerical simulations (e.g. [3-5]), an analytical solution for the phase space evolution of electrons in a self-amplified spontaneous emission (SASE) FEL was given in [6]. In this paper, I present an analysis of electron phase space evolution for low gain FEL based on calculation of the synchrotron oscillation period for different electrons, and study the relations of initial detuning with the energy-extraction efficiency and saturation power.

THE EQUATIONS OF PHASE SPACE EVOLUTION

The energy exchange between the optical field and the electron beam depends on the phase of the electron in the optical field plus the undulator magnetic field: $\phi=(k_s+k_u)\,z-\omega t$, where k_s, k_u are the corresponding wave numbers of the optical field and the undulator magnetic field. For the resonant electron its phase is fixed, namely it has $\phi'=0$. Therefore the phase velocity of the electron ϕ' describe the resonance offset of the electron, so it is called the detuning parameter. The detuning parameter can be expressed as the relative energy deviation from the resonant energy

$$\phi' = 2k_u(\gamma-\gamma_r)/\gamma_r \tag{1}$$

where γ is the normalized energy of the electrons, γ_r is the resonant energy. From above phase equation and the energy equation of the electron, the FEL pendulum equation can be obtained (for convenience, denoting $\psi=\phi+\varphi_s+\pi/2$, φ_s is the phase of the radiation field) [2]:

$$\psi'' = -\Omega^2 \sin\psi \tag{2}$$

where $\Omega=\sqrt{2k_u k_s a_u a_s f_c}/\gamma$, $a_s=eE_s/(mc^2k_s)$ and $a_u=eB_u/(mc^2k_u)$ are dimensionless vector potential of the *rms* radiation optical field E_s and undulator magnetic field B_u, respectively; f_c is the undulator coupling factor: for circularly polarized helical undulator $f_c=1$; for linearly polarized planar undulator it is a difference of the two Bessel function $f_c=J_0(\xi)-J_1(\xi)$, $\xi=a_u^2/2(1+a_u^2)$.

The evolution of electron longitudinal dynamics can be described with the motion of electrons in the phase space (ψ, ψ'). There are two classes of electron trajectory in the phase space: the bounded and the unbounded. The separatrix is the boundary separating the two of them. The region enclosed by the separatrix is called the ponderomotive bucket. The maximum value of ψ' along the separatrix gives the half-height of the bucket : $\psi'_m=2\Omega$. As the optical field intensity increase, the bucket separatrix expands, more electrons can be trapped.

For low gain case, such as amplification of the light at each pass through the undulator in oscillator FEL, the Ω can be regarded as a constant, and the change of φ_s can be neglected, (thus the bucket can be regarded as invariant), then from the pendulum equation, one can get the first integral

$$\psi'^2/2-\Omega^2\cos\psi = U \tag{3}$$

where U is a constant determined by the initial conditions.

As a trapped electron undergoes one complete orbit in the ponderomotive bucket, it travels down the undulator by a distance called synchrotron oscillation period L_{sy}. To extract the energy from the electrons to the optical field, the electrons initially are injected in the top of the bucket, i.e. the initial energy of electron beam is larger than the resonant energy. The interaction saturates after the electrons have executed approximately half of an oscillation in the ponderomotive well. At this point, the most of electrons are located in the bottom of the ponderomotive bucket.

For the phase near zero $\psi\approx0$, the pendulum equation (Eq. (2)) can be approximately written as

$$\psi'' \approx -\Omega^2\psi$$

So the electrons near the $\psi=0$ make a simple harmonic vibration in the phase space, the corresponding period of the synchrotron oscillation is $L_{sy0}=2\pi/\Omega$. Therefore Ω is the wave number of the synchrotron oscillation for the zero

* Work supported by the National Nature Science Foundation of China under Grant No. 11675178, and National Key Research and Development Program of China No. 2016YFA0401901.
† jiaqk@ustc.edu.cn

Content from this work may be used under the terms of the CC BY 3.0 licence (© 2019). Any distribution of this work must maintain attribution to the author(s), title of the work, publisher, and DOI

ISBN: 978-3-95450-210-3 doi:10.18429/JACoW-FEL2019-TUP049

SIMULATING SHOT-NOISE OF 'REAL' ELECTRON BUNCHES

P. Traczykowski[1,2,3], L.T. Campbell[1,2,3], B.W.J. McNeil[1,2]
[1]SUPA, Department of Physics, University of Strathclyde, Glasgow, G4 0NG
[2]Cockcroft Institute, Warrington, WA4 4AD, UK
[3]ASTeC, STFC Daresbury Laboratory, Warrington, WA4 4AD, UK

Abstract

An algorithm and numerical code for the up-sampling of a system of particles, from a smaller to a larger number, is described. The method introduces a Poissonian 'shot-noise' to the up-sampled distribution, typical of the noise statistics arising in a bunch of particles generated by a particle accelerator. The algorithm is applied on a phase-space distribution of relatively few simulation particles representing an electron beam generated by particle accelerator modelling software, for subsequent injection into an Free Electron Laser (FEL) amplifier which is used here to describe the model. A much larger number of particles is usually required to model the FEL lasing process than is required in the simulation models of the electron beam accelerators that drive it. A numerical code developed from the algorithm was then used to generate electron bunches for injection into to the unaveraged 3D FEL simulation code, Puffin. Results show good qualitative and quantitative agreement with analytical theory. The program and user manual are available at [1].

INTRODUCTION

When modelling a Free Electron Laser (FEL) [2], the number of simulation particles used to model the acceleration stages often needs to be increased before simulation of the FEL itself. This is mainly due to the fine longitudinal electron bunching structures at the FEL radiation wavelength that need to be modelled. Such fine detail is unlikely to be required when modelling the accelerator stages before the FEL. The data from the accelerator stages usually have a relatively sparse '*macroparticle*' distribution in phase space, and do not model the Poissonian noise statistics of a real electron distribution. Here, a method is described which breaks up this sparse phase–space distribution of macroparticles into a greater number of '*microparticles*', each representing fewer electrons, to give a more dense phase–space distribution that is suitable for injection into an FEL simulation code such as Puffin [3], used here as the target code to demonstrate the methods used. The method ensures that the microparticle distribution has the correct Poissonian shot–noise statistics of a real electron beam [4]. This is necessary to simulate the spontaneous light generation which arises from the shot-noise and acts as the seed field from which shorter wavelength amplifier FELs start up in the Self Amplified Spontaneous Emission mode of operation [2].

DENSITY DISTRIBUTION FUNCTIONS

The method first uses the macroparticles of the accelerator modelling stage to create a discrete charge histogram of bin width Δz_h along the longitudinal z-axis of beam propagation at a given time (e.g. on entering the FEL). A continuous, optionally smoothed, longitudinal charge distribution function $f_z(z)$, so the beam current $I(z) \approx c f_z(z)$ for the relativistic beams assumed here, is then created by interpolating from this histogram. This charge density function is then used to apply the correct charge $f_z(z)\Delta z_s$, to each longitudinal slice of microparticles of width Δz_s, where usually $\Delta z_h > \Delta z_s$. A transverse, optionally smoothed, charge density function $f_\perp(x, y, z)$ is then created for each longitudinal slice using a similar 2-D histogram-interpolation method. Here the z-dependence of $f_\perp(x, y, z)$ will be in integer units of the slice width Δ_s. The longitudinal density function and the transverse density function can then be interpolated to create a continuous 3-D charge density function, $f(x, y, z) = f_z(z) f_\perp(x, y, z)$. This function is significantly smoother than a discrete charge distribution of the initial, often relatively sparse, macroparticle distribution and allows for a less noisy, more realistic, distribution of microparticles for input into the FEL modelling software. The new set of microparticles is created in each longitudinal slice via a 2-D Cumulative Distribution Function (CDF) approach in the transverse plane – in this case we will call it Joint Distribution Function (JDF) [6]. The effects of Poissonian shot-noise are then added to each microparticle using the method of [4]. The microparticle distributions so generated can then model complex electron beam phase spaces. The longitudinal charge histogram and the corresponding current

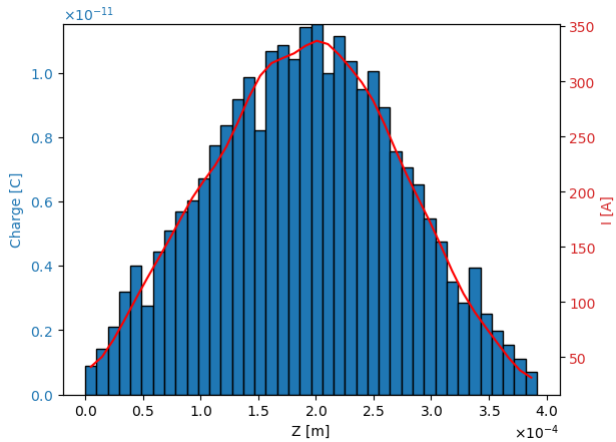


Figure 1: Sample electron density profile along the z–axis. The plot shows the original binned histogram of the macroparticle charge and the interpolated data. The original beam is sampled over 50 bins and then smoothed using the *Python SciPy scipy.ndimage.gaussian* filter [5].

Content from this work may be used under the terms of the CC BY 3.0 licence (© 2019). Any distribution of this work must maintain attribution to the author(s), title of the work, publisher, and DOI

ISBN: 978-3-95450-210-3 doi:10.18429/JACoW-FEL2019-TUP050

COMPARISON BETWEEN, AND VALIDATION AGAINST AN EXPERIMENT OF, A SLOWLY-VARYING ENVELOPE APPROXIMATION CODE AND A PARTICLE-IN-CELL SIMULATION CODE FOR FREE-ELECTRON LASERS

L.T. Campbell[1,3], H.P. Freund[4], J.R. Henderson[1,3], B.W.J. McNeil[1,2], P. Traczykowski[1,2,3] and P. J. M. van der Slot [5]
[1]SUPA, Department of Physics, University of Strathclyde, Glasgow, G4 0NG
[2]Cockcroft Institute, Warrington, WA4 4AD, UK
[3]ASTeC, STFC Daresbury Laboratory, Warrington, WA4 4AD, UK
[4]University of New Mexico, Albuquerque, New Mexico, 87131 United States of America
[5]Mesa+ Institute for Nanotechnology, University of Twente, Enschede, The Netherlands

Abstract

Free-electron lasers (FELs) operate at wavelengths down to hard x-rays, and are either seeded or start from noise. There is increasing interest in x-ray FELs that rely on Self-Amplified Spontaneous Emission (SASE), and this involves increasing simulation activity in the design, optimization, and characterization of these x-ray FELs. Most of the simulation codes in use rely on the Slowly-Varying Envelope Approximation (SVEA) in which Maxwell's equations are averaged over the fast time scale resulting in relatively small computational requirements. While the SVEA codes are generally successful, the predictions of these codes sometimes differ in various aspects of the FEL interaction. In contrast, Particle-in-Cell (PiC) simulation codes do not average Maxwell's equations and are considered to be a more complete model of the underlying physics. Unfortunately, they require much longer run times than SVEA codes and have not been validated by comparison with experiment as often as the SVEA codes. In order to remedy this, and to resolve issues that arise due to different predictions between the SVEA codes, we present a comparison between one SVEA code (MINERVA) and a PiC simulation code (PUFFIN) with the experimental measurements obtained at the SPARC SASE FEL experiment at ENEA Frascati. The results show good agreement between the two codes and between the codes and the experiment. Since the formulations of the two codes share no common elements, this validates both formulations and demonstrates the capability to model the FEL interaction from the start of the undulator through the undulator and into deep saturation.

INTRODUCTION

While free-electron lasers (FELs) have been intensively studied since the 1970s, new developments and concepts keep the field fresh. Intensive work is ongoing into new FEL-based light sources that probe ever shorter wavelengths with a variety of configurations. There presently exists a large variety of FELs ranging from long-wavelength oscillators using partial wave guiding to ultraviolet and hard x-ray FELs that are either seeded or starting from noise (SASE). As these new light sources come on-line, interest will grow in shorter pulses, new spectral ranges and higher photon fluxes. The increasing activity in the design and construction of FEL light sources is associated with increasing simulation activity to design, optimize, and characterize these FELs. Most of the FEL simulation codes in use at the present time can be categorized as either SVEA or PiC simulations. In the SVEA, the optical field is represented by a slowly-varying amplitude and phase in addition to a rapid sinusoidal oscillation. The field equations are then averaged over the rapid sinusoidal time scale and, thereby, reduced to equations describing the evolution of the slowly-varying amplitude and phase. Within the context of the SVEA, FEL simulation codes fall into two main categories where the particle trajectories are found by first averaging the trajectories over an undulator period (the so-called wiggler-averaged-orbit approximation), or by the direct integration of the Newton-Lorentz equations. There is a further distinction between the SVEA codes based upon the optical field representation, and codes have been written using either a grid-based field solver or a superposition of optical modes. Simulation codes using the wiggler-averaged-orbit analysis in conjunction with a grid-based field solver include (but are not limited to) GINGER [1], GENESIS [2], and FAST [3]. In contrast, SVEA codes that integrate the Newton-Lorentz equations in conjunction with a Gaussian mode superposition for the optical fields include MEDUSA [4] and MINERVA [5]. One common feature of all the SVEA codes, however, is the way in which time-dependence is treated. The fast time scale average results in a breakdown of the optical pulse into temporal slices each of which is a single wave period in duration. The optical slices slip ahead of the electron slices at the rate of one wavelength per undulator period. As a result, the SVEA codes integrate each electron and optical slice from $z \rightarrow z + \Delta z$ and then allow the optical slice to slip ahead of the electron slices. These codes have been extremely successful in modeling FELs; however, their predictions are not always identical for all aspects of the FEL interaction. In contrast, PiC codes do not average Maxwell's equations and are considered to represent a more fundamental model of the physics of FELs.

Content from this work may be used under the terms of the CC BY 3.0 licence (© 2019). Any distribution of this work must maintain attribution to the author(s), title of the work, publisher, and DOI

ISBN: 978-3-95450-210-3 doi:10.18429/JACoW-FEL2019-TUP051

PLASMA ACCELERATOR DRIVEN COHERENT SPONTANEOUS EMISSION

B.M. Alotaibi[1,2], R. Altuijri[1,2], A. F. Habib[2,3], B. Hidding[2,3], B.W.J. M[c]Neil[2,3], P. Traczykowski[2,3]
[1]Physics Department, Faculty of Science,
Princess Nourah Bint Abdulrahman University, Riyadh, KSA
[2]SUPA, Department of Physics, University of Strathclyde, Glasgow, UK
[3]Cockcroft Institute, Warrington, UK

Abstract

Plasma accelerators [1] are a potentially important source of high energy, low emittance electron beams with high peak currents and generated within a relatively short distance. While novel plasma photocathodes [2] may offer improvement to the normalised emittance and brightness of electron beams compared to Radio Frequency-driven accelerators, a challenge is the energy spread and chirp of the beams, which can make FEL operation impossible. In this paper it is shown that such an energy-chirped beam, with a dynamically evolving current profile due to ballistic bunching, can generate significant coherent radiation output via the process of Coherent Spontaneous Emission (CSE) [3]. While this CSE is seen to cause some FEL-induced electron bunching at the radiation wavelength, the dynamic evolution of the energy chirped pulse dampens out any high-gain FEL interaction.

INTRODUCTION

Significant effort have been dedicated to demonstrating a plasma-based accelerator driven FEL [4–6]. However, next to stability challenges, the inherent by-product of plasma-based accelerators is a relatively large slice energy spread ($\sigma_\gamma/\gamma > \rho$) and a correlated energy spread ('chirp') when compared with RF linacs. In this paper, the dynamics of the electron bunch from a plasma photocathode [2], which can have an inherent negative energy chirp, is explored. One effect, which to the authors knowledge has not been modelled before with such a PWFA plasma photocathode-generated energy chirped beam, is to induce the generation of Coherent Spontaneous Emission (CSE) [3, 7]. CSE arises when the electron pulse has significant *current* gradients over a resonant radiation wavelength. It is shown that for the electron beam parameters used here, such current gradients can be realised when the energy chirped beam undergoes spatial dispersive compression in its propagation direction due to the correlated energy spread [3, 7]. By dominating any normal spontaneous emission, it has been shown in 1D simulations that CSE can also self-seed the FEL interaction in a process called Self Amplified Coherent Spontaneous Emission (SACSE) [8]. The CSE was also shown in 1D to help mitigate the effects of a homogeneous electron energy spread in beams without an energy chirp, significantly reducing the start-up time and enhancing the generation of high intensity, short, superradiant radiation pulses from a poor-quality electron pulse [9].

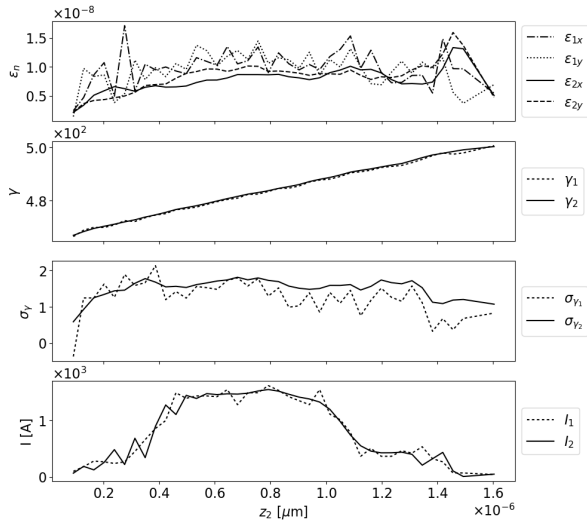


Figure 1: From top, the electron beam normalised emittance ϵ_n, localised Lorentz factor γ, RMS energy spread σ_γ and current I, as a function of window position $z_2 = (ct - z)$ of the beam. In this window, travelling at speed c along the z-axis of the undulator, the head of the electron bunch is on the left, the tail on the right, and the beam will propagate to larger values of z_2 as the beam propagates through the undulator. The dashed plots (index 1) show the original macroparticle beam from the VSim simulation and the solid plots (index 2) show the beam following smoothing and up-sampling to a greater number of microparticles with the correct shot-noise statistics.

ELECTRON BUNCH SIMULATION

A macroparticle distribution is taken from a VSim simulation of a PWFA. These macroparticles have too sparse a phase-space distribution for an accurate FEL simulation as there are too few macroparticles per resonant wavelength and they have unrealistic shot-noise statistics. These macroparticles are converted into a suitable distribution of *microparticles* using the scripts [10] and [11]. The relevant bunch parameters of a microparticle beam are compared to the original beam of macroparticles in Fig. 1. The microparticle distribution has had the correct shot-noise statistics applied as described in [12]. It is seen that the electron beam has a negative longitudinal energy chirp, which is the result of the beam acceleration in the electric field of the nonlinear plasma wave.

Content from this work may be used under the terms of the CC BY 3.0 licence (© 2019). Any distribution of this work must maintain attribution to the author(s), title of the work, publisher, and DOI

ISBN: 978-3-95450-210-3 doi:10.18429/JACoW-FEL2019-TUP053

AN INVESTIGATION OF POSSIBLE NON-STANDARD PHOTON STATISTICS IN A FREE-ELECTRON LASER I: EXPERIMENT

Jeong-Wan Park*, University of Hawaii at Manoa, Honolulu, U.S.
Kwang-Je Kim[1], Ryan Lindberg, Argonne National Laboratory, Lemont, U.S.
[1]also at University of Chicago, Chicago, U.S.

Abstract

It was reported that the photon statistics of the seventh coherent spontaneous harmonic radiation of the MARK III FEL was sub-Poissonian [1], which concludes that Fano factor F (the ratio of photon number variance to the average photon number) is less than unity. Whether FEL light exhibits such non-standard behavior is an important issue; if it does, our understanding of the FEL needs to be radically modified. In this paper, we re-examine the analyses of experimental data in Ref. [1]. We find that the observed value of F could be explained within the standard FEL theory if one combines the detector dead time effect with photon clustering arising from the FEL gain. We propose an improved experiment for a more definitive measurement of the FEL photon statistics.

INTRODUCTION

In an experiment performed some time ago by Chen and Madey [1], it was reported that the photon statistics of the seventh coherent spontaneous harmonic radiation (CSHR) of the MARK III infrared (IR) free-electron laser (FEL) was sub-Poissonian–neither Poissonian as expected from a coherent FEL output nor chaotic as expected from an incoherent radiation source. If FEL light exhibits such non-standard behavior, our understanding of the FEL needs to be radically modified. In this paper we present a re-examination of the data analysis by Chen and Madey. In the companion paper [2], we study theoretical basis for the non-standard FEL photon statistics.

SET-UP OF THE EXPERIMENT

The Chen-Madey experiment was made at the MARK III FEL [3] operating at a fundamental IR wavelength of 2.68 μm; further parameters are presented in Table 1. The photon counting measurements used the seventh harmonic at 382 nm where high efficiency photo-multiplier tubes (PMTs) are available, since a poor efficiency PMT typically emphasizes the statistics of the measurement itself, resulting in a Possion distribution irrespective of the statistics of the source [1, 4]. In classical terms, the coherent spontaneous harmonic radiation (CSHR) is produced by the nonlinear components of the wiggle motion in the undulator, and enhanced by the seventh harmonic component of the electron current that occurs as the fundamental mode approaches the oscillator saturation [1].

* jwpark@hawaii.edu

Table 1: MARK III FEL Specification

Parameters	Value	Unit
K (undulator parameter)	1.13	
λ_u (undulator period)	2.3	cm
λ_1 (fundamental mode wavelength)	2.68	μm
Macropulse length	2	μs
Macropulse repetition rate	15	Hz
Micropulse length	2	ps
Micropulse repetition rate	2.856	GHz
Average electron beam energy	43.5	MeV
Energy spread (FWHM)	0.4%	
Peak micropulse current	30	A

The set-up of Chen-Madey experiment is shown in Fig. 1. The output FEL light from the cavity passed through an aperture and then a lens before it reached a dichroic beam splitter that transmitted the fundamental mode and reflected the CSHR. The beam line for the CSHR consisted of a monochrometer, an adjustable slit, a fast, high quantum efficiency PMT, and an amplifier. The CSHR was brought to a focus at the adjustable slit and monochromator combination; the former was used to adjust the count rate, while the latter selected the 7th harmonic. Since the slit was at the focal plane of the lens, its size defined the effective optical mode waist of the measured seventh CSHR photons.

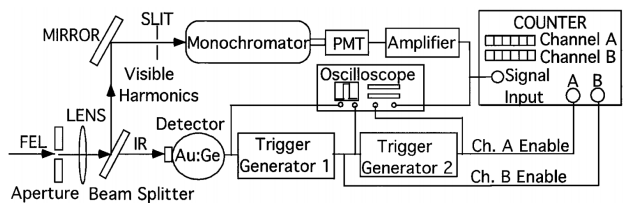


Figure 1: Diagram of photon counting experiment of the seventh CSHR from Mark III FEL [1].

Measurements of the CSHR were triggered by the signal of the IR fundamental which is measured by a fast Au:Ge IR detector. A start signal was sent to the counter by trigger generator 1 when the amplitude of the IR detector reaches a pre-set voltage, followed by an end signal after 80 ns. During the 80 ns time window the counter records the number of 7th harmonic pulses from the PMT along channel B. In addition, trigger generator 2 enables channel A of the counter to record the number of background photons.

The linac delivered about 230 electron bunches within each 80 ns observation window which corresponds to about 6

Content from this work may be used under the terms of the CC BY 3.0 licence (© 2019). Any distribution of this work must maintain attribution to the author(s), title of the work, publisher, and DOI

ISBN: 978-3-95450-210-3 doi:10.18429/JACoW-FEL2019-TUP054

AN INVESTIGATION OF POSSIBLE NON-STANDARD PHOTON STATISTICS IN A FREE-ELECTRON LASER II: THEORY

Jeong-Wan Park*, University of Hawaii at Manoa, Honolulu, U.S.
Kwang-Je Kim[1], Ryan Lindberg, Argonne National Laboratory, Lemont, U.S.
[1]also at University of Chicago, Chicago, U.S.

Abstract

In this paper we explore whether we can at present find a theoretical basis for non-standard, sub-Poissonian photon statistics in the coherent spontaneous harmonic radiation of an FEL as was claimed to have been measured with the Mark III FEL [1]. We develop a one dimensional quantum FEL oscillator model of the harmonic radiation in the linear gain regime to calculate the photon statistics. According to our study, it seems unlikely that the photon statistics for an FEL oscillator starting from the noise could be sub-Poissonian.

INTRODUCTION

This is the second, theoretical part of our study into possible non-standard, sub-Poissonian photon statistics for harmonic emission from an FEL. The motivation is an experiment by Chen and Madey [1], which claimed to have observed sub-Poissoinian statistics at the seventh harmonic during the linear gain regime of the MARK III FEL oscillator. In our first paper we take a critical look at the experiment [2]; here, we revisit the standard theory of FEL photon statistics of the fundamental mode starting from the noise, and then develop the simplest quantum extension of the classical theory of harmonic radiation production as driven by the fundamental mode. We include the cavity loss with a beam splitter model, and compute the photon statistics of the harmonic modes. We show that the statistics cannot be sub-Poissonian for any initial state of the electrons.

A MODEL OF LIGHT EMITTED BY RANDOMLY DISTRIBUTED ELECTRONS

First, we revisit the photon statistics of undulator radiation when there is no significant bunching in the electron beam. The variance of the number of photons for coherent wave trains emitted by randomly distributed electrons (Fig. 1) is given by [3, 4]:

$$\langle(\delta n)^2\rangle = \langle(\delta n)^2\rangle_Q + \langle(\delta n)^2\rangle_C; \tag{1}$$

$\langle(\delta n)^2\rangle_Q$ is the portion of variance originating from quantum mechanics, whereas $\langle(\delta n)^2\rangle_C$ arises from classical fluctuation of the electrons [5]. Consequently, the Fano factor $F = \frac{\langle(\delta n)^2\rangle}{\langle n\rangle}$ of the photon statistics can also be decomposed into the quantum and classical portions:

$$F = F_Q + F_C. \tag{2}$$

* jwpark@hawaii.edu

When the mode number $M = t_p/\tau_{coh} \gg 1$ (t_p is the pulse length and τ_{coh} is the coherence time) one can write [4, 5]

$$F_Q = \frac{\langle(\delta n)^2\rangle_Q}{\langle n\rangle} = 1,\ F_C = \frac{\langle n\rangle}{M}. \tag{3}$$

Thus, in this case $F > 1$ and the photon statistics is super-Poissonian.

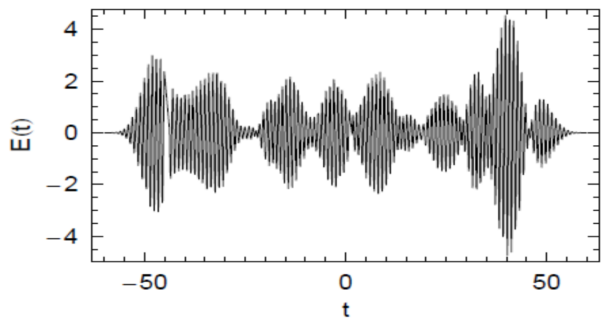


Figure 1: A sum of coherent wave trains emitted by randomly distributed electrons [5].

PHOTON STATISTICS OF THE FUNDAMENTAL MODE

A one Dimensional Quantum FEL Model

To investigate the photon statistics, we shall develop a quantum model of the FEL oscillator starting from the noise. In this model we will only consider one frequency mode of the field, since in the linear gain regime the FEL acts as a linear amplifier and all frequency components are independent [6]. When energy spread can be neglected the evolution of the electric field operator as the pass number n increases becomes [5, 7]

$$\mathfrak{a}_{1,n+1} = g\mathfrak{a}_{1,n} + \mathcal{F}_n; \tag{4}$$

the first subscript of field operator $\mathfrak{a}$ represents the harmonic number, the second denotes the cavity round-trip number, and $|g|^2$ is the gain per cavity round-trip. An explicit expression for g is:

$$g \equiv \frac{1}{3}\sum_{\alpha} e^{-i\mu_\alpha 2k_u\rho L_u}, \tag{5}$$

where μ_α are the three roots of $\left(\mu - \frac{\Delta\nu}{2\rho}\right)\left(\mu^2 - \frac{q^2}{4}\right) = 1$, $\Delta\nu = \frac{\omega-\omega_1}{\omega_1}$, ω_1 is the fundamental mode's angular frequency, $q = \frac{\hbar\omega_1}{\rho\gamma_r mc^2}$ is the ratio of the characteristic photon energy to

Content from this work may be used under the terms of the CC BY 3.0 licence (© 2019). Any distribution of this work must maintain attribution to the author(s), title of the work, publisher, and DOI

ISBN: 978-3-95450-210-3 doi:10.18429/JACoW-FEL2019-TUP055

TWO-COLOR OPERATION OF FLASH2 UNDULATOR

E.A. Schneidmiller*, M. Braune, B. Faatz, F. Jastrow, M. Kuhlmann,
A. Sorokin, K. Tiedtke, and M.V. Yurkov
DESY, Hamburg, Germany

Abstract

FLASH is the first soft X-ray FEL user facility, routinely providing brilliant photon beams for users since 2005. The second undulator branch of this facility, FLASH2, is gap-tunable which allows to test and use advanced lasing concepts. In particular, we tested recently a two-color mode of operation based on the alternation of tunes of the undulator segments (every other segment is tuned to the second wavelength). This scheme is advantageous in comparison with a subsequent generation of two colors in two consecutive sections of the undulator line. First, source positions of the two FEL beams are close to each other which makes it easier to handle them. Second, the amplification is more efficient in this configuration since the segments with respectively "wrong" wavelength still act as bunchers. We developed methods for online intensity measurements of the two colors simultaneously that require a combination of two detectors. We present some examples of such measurements in the XUV and soft X-ray regimes.

INTRODUCTION

Two-color lasing is a popular operation mode of X-ray FEL user facilities. A possible way to generate two colors in a gap-tunable undulator, operating in SASE regime, is to split the undulator into two sections, and set different K-values in each of these sections. An additional useful element for X-ray pump, X-ray probe experiments could be a chicane between the two sections to control a time delay between the pulses of two different colors. One can use the same electron bunch (parts of the same bunch) for lasing in the two sections of the undulator [1]. In this case the beam quality is partially spoiled in the first section (that typically operates at the onset of saturation), and one has to compromise intensities of two colors. As an alternative, one can use fresh-bunch technique based on the principle of the betatron switcher [2]. A practical realization of this principle was done in a way that the head and the tail of the bunch lase in two different sections of the undulator [3, 4].

One of the issues with these sectioned-undulators schemes (or, split undulators) is a significant spatial separation of effective source positions of the two X-ray beams. This separation can make it difficult to efficiently focus both beams on a sample. As an alternative, one can consider two-color lasing in the undulator with the alternation of tunes of single undulator segments enabling close positions of source points. This scheme was realized at LCLS for small separation of tunes (about 1%) and was described in [5] as the gain-modulated FEL.

* evgeny.schneidmiller@desy.de

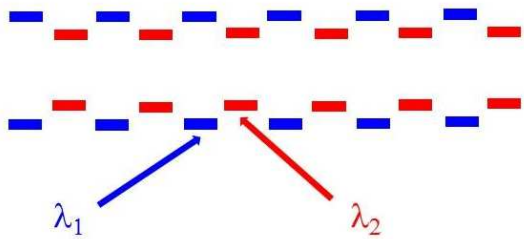


Figure 1: Conceptual scheme of two-color lasing with the alternation of undulator tunes.

We tested the two-color mode with the alternation of undulator tunes at FLASH [6,7] in the regime of a large separation of tunes (several tens percents), and present the main results in this paper.

TWO-COLOR LASING WITH THE ALTERNATION OF UNDULATOR TUNES

The principle of operation of the described two-color scheme is simple. Let us consider the gap-tunable undulator of the FLASH2 branch of the soft X-ray free electron laser facility FLASH [7]. The undulator consists of twelve 2.5 m long segments, maximum K-value is 2.7. For generation of two colors, all odd segments are tuned to wavelength λ_1, and even segments to λ_2 (see Fig. 1). With respect to the amplification of the electromagnetic wave with the wavelength λ_1, the FEL process is disrupted as soon as the electron beam leaves λ_1 segment and enters a "wrong" segment tuned to λ_2. However, energy modulations in the electron bunch, accumulated due to the interaction with the electromagnetic field in the λ_1 segment, continue to get converted into density modulations (bunching) in the λ_2 segment due to its longitudinal dispersion. Thus, in the next λ_1 segment the beam with an enhanced bunching quickly radiates a stronger field than the one coming from the previous λ_1 segment (which in addition is diffracted), and the FEL process continues with higher amplitudes. In some sense the mechanism is similar to that of the multi-stage (or distributed) optical klystron [8–11]. In this qualitative description we do not consider effects of longitudinal velocity spread due to the energy spread and emittance of the electron beam. According to our estimates, these effects were practically negligible in our experiments.

The longitudinal dispersion of an undulator segment is characterized by a transfer matrix element $R_{56} = 2N_w\lambda$, where N_w is the number of undulator periods per segment and λ is the resonance wavelength. If $\lambda_1 < \lambda_2$, the FEL gain is, obviously, weaker for λ_1 in the corresponding λ_1

Content from this work may be used under the terms of the CC BY 3.0 licence (© 2019). Any distribution of this work must maintain attribution to the author(s), title of the work, publisher, and DOI

ISBN: 978-3-95450-210-3 doi:10.18429/JACoW-FEL2019-TUP056

Content from this work may be used under the terms of the CC BY 3.0 licence (© 2019). Any distribution of this work must maintain attribution to the author(s), title of the work, publisher, and DOI

FEASIBILITY STUDIES OF THE 100 keV UNDULATOR LINE OF THE EUROPEAN XFEL

E.A. Schneidmiller*, V. Balandin, W. Decking, M. Dohlus, N. Golubeva,
D. Noelle, M.V. Yurkov, I. Zagorodnov
DESY, Hamburg, Germany
G. Geloni, Y. Li, S. Molodtsov, J. Pflueger, S. Serkez, H. Sinn, T. Tanikawa, S. Tomin
European XFEL GmbH, Schenefeld, Germany

Abstract

The European XFEL is a multi-user X-ray FEL facility based on superconducting linear accelerator. Presently, three undulators (SASE1, SASE2, SASE3) deliver high-brightness soft- and hard- X-ray beams for users. There are two empty undulator tunnels that were originally designed to operate with spontaneous radiators. We consider instead a possible installation of two FEL undulators. One of them (SASE4) is proposed for the operation in ultrahard X-ray regime, up to the photon energy of 100 keV. In this contribution we present the results of the first feasibility studies of this option.

INTRODUCTION

The European XFEL is a X-ray FEL user facility, based on superconducting accelerator [1]. It provides ultimately bright photon beams for user experiments since 2017. Two hard X-ray undulators (SASE1 and SASE2) and one soft X-ray undulator (SASE3) are presently in operation [2], see Fig. 1. There are two empty undulator tunnels that were originally designed [3] to host the undulators U1 and U2 (see Fig. 1) to be used for generation of spontaneous undulator radiation in the range 20-90 keV.

Recently, design studies have been initiated aiming at conceptual and technical designs of FEL undulator lines instead of spontaneous radiators in the empty tunnels. One of the options, requested by the user community, is an undulator capable of generation of powerful X-ray radiation in the ultrahard photon energy range, up to 100 keV. Realization of such an option would rely on the unique features of the European XFEL among other facilities of such kind, namely the highest electron energy (17.5 GeV) and the longest tunnels. Note that the idea of using a SASE undulator for lasing up to 90 keV instead of spontaneous radiators in one of the empty tunnels was suggested and illustrated with numerical simulations in [4]. In this paper we perform extended considerations of this option.

UNDULATOR LENGTH AND LOCATION

The hard and ultrahard X-ray undulator can be located in the tunnel XTD3 (place for U1 in Fig. 1) or in XTD5 (place for U2). The planned lengths for the installation of the spontaneous radiators is 120 m in XTD3 and 140 m in XTD5. It would be desirable to have a larger length for

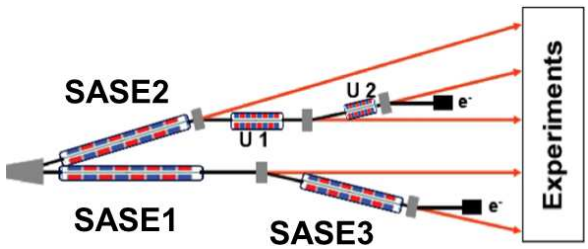


Figure 1: Layout of undulator tunnels of the European XFEL

SASE4 if it is supposed to lase up to 100 keV, and one can consider alterations to the tunnel infrastructure and electron lattice. In particular, a more aggressive bending can be considered at the end of XTD3, thus making about 200 m in this tunnel available for the installation of the SASE4 undulator. Also, we discuss an installation of a bypass line (as an alternative to the fresh bunch technique [4]) to avoid beam quality deterioration in SASE2 undulator (see below).

EXPECTED PROPERTIES OF THE ELECTRON BEAM

Electron beams with a high peak current, low emittance and energy spread are required for operation of short-wavelength FELs. This is especially important when we discuss a challenging range of photon energies, up to 100 keV. We performed start-to-end simulations of the beam dynamics in the European XFEL accelerator (tools and methods are described in [5]), and present here the results for 100 pC bunches, accelerated to 17.5 GeV and transported to the SASE2 undulator. The current, emittance, uncorrelated energy spread are presented in Fig. 2 as functions of a position along the bunch length. One can see that slice parameters in the bunch core are good: peak current is 5 kA, slice emittance is below 0.3 mm mrad, and uncorrelated energy spread is below 1 MeV. The latter parameter can degrade if the bunches are transported through SASE2 undulator, it can increase up to 3 MeV due to the quantum diffusion [6] if SASE2 operates with fully closed gap. To fully decouple operation of SASE2 and SASE4, it would be desirable to consider a bypass line (also wakefield effects would be strongly reduced then).

We also consider an advanced compression, namely eSASE [7]. In that case, we compress the beam relatively weakly in bunch compressors (to 1-2 kA) thus avoiding strong CSR effects during compression and transport. Then

* evgeny.schneidmiller@desy.de

ISBN: 978-3-95450-210-3 doi:10.18429/JACoW-FEL2019-TUP057

Content from this work may be used under the terms of the CC BY 3.0 licence (© 2019). Any distribution of this work must maintain attribution to the author(s), title of the work, publisher, and DOI

ANALYSIS OF PARAMETER SPACE OF SOFT X-RAY FREE ELECTRON LASER AT THE EUROPEAN XFEL DRIVEN BY HIGH AND LOW ENERGY ELECTRON BEAM

E.A. Schneidmiller, M.V. Yurkov, DESY, Hamburg, Germany

Abstract

Three undulator beamlines: SASE1 and SASE2 (hard X-ray), and SASE3 (soft X-ray) are in operation at the European XFEL serving six user instruments. Next stages of the facility development are installation of two undulator beamlines in empty tunnels SASE4 and SASE5 as middle term upgrade, and extension of the facility with the second fan of undulators as long term upgrade. Construction of soft X-ray beamlines is considered in both upgrade scenario. In the case of SASE4/SASE5 electron beam with energies 8.5 GeV - 17.5 GeV will be used in order to provide simultaneous operation of new undulator beamlines with existing SASE1-SASE3. One of the scenarios for a second fan of undulators involves using of low energy (2.5 GeV) electron beam. In this paper we analyze parameter space of soft X-ray SASE FELs driven by high energy and low energy electron beam, compare output characteristics, and discuss potential advantages and disadvantages.

INTRODUCTION

Start-up configuration of the European XFEL includes two hard X-ray SASE FELs, SASE1 and SASE2, and one soft X-ray SASE FEL, SASE3 serving six user instruments [1]. All undulators are planar, variable gap devices. SASE1 and SASE2 are equipped with identical undulators with 4 cm period length. SASE3 undulator has similar mechanical design, but the period length is 6.8 cm. Radiation wavelength at fixed electron energy is changed by means of changing the undulator gap. Trusted tunability ranges of undulators are limited to $\lambda_{max}/\lambda_{min} = 3.6$ for SASE1/SASE2 and 4.5 for SASE3 which is not sufficient for covering all user experiments at one fixed electron energy. By the time, five operating points of the electron beam energy have been fixed (8.5, 11.5, 14, 16.5, and 17.5 GeV) providing most flexible way for simultaneous operation of users at all three beamlines. Full wavelength range covered by start-up configuration spans from 0.05 nm to 5.1 nm.

Start-up of the facility operation proceeded smoothly: all three SASE radiators produce x-ray radiation with parameters close to design values, and all six user stations serve user experiments [2, 3]. Middle term plans of the facility development assume installation of two more SASE FEL beamlines in empty tunnels and construction of four user instruments [1]. Strategic extension of the facility assumes installation of new undulator beamlines and user stations doubling user capacity. Here an option of low energy beamline has been considered when electron beam at the energy of 2.5 GeV is extracted from accelerator and is transported via bypass electron beamline to the undulator for generation of soft X-ray radiation. Upgrade of the the accelerator to CW mode of operation is also included in a long term R&D program [4].

Next generation X-ray FELs should provide wide capabilities for performing user experiments:

- wide tunability range;
- control of the radiation pulse duration;
- coherence control: temporal and spatial;
- polarization control: linear, circular, elliptical;
- wide capabilities for pump-probe experiments involving FEL radiation (fundamental harmonic, higher harmonics, independent colors), laser and accelerator based radiation sources;
- control of the photon flux up to ultimate level.

Not all of these features are implemented in the start-up configuration of the European XFEL. In this paper we discuss possible potential development of soft-Xray/VUV FEL beamline with extended wavelength range and extended user capabilities. We consider two options: high energy option, 8.5 GeV - 17.5 GeV, and low energy, 2.5 GeV option. Our study shows that high energy option has evident advantages in terms of peak radiation power, pulse energy, photon flux, and transverse coherence. Additionally, operation at higher charges and higher electron energies holds potential for generation of the radiation pulse energies on a sub-Joule level [5]. High energy option can be realized on a middle term time scale using present infrastructure of the European XFEL which foreseens installation of two more undulators and four user instruments.

HIGH ELECTRON ENERGY: 8.5 - 17.5 GeV

First step of our study is an overview of parameter space aiming extension of the operating range in the direction of longer wavelengths. The only mean to do this is to increase the undulator period. Figure 1 shows contour plot of the maximum wavelength as function of the undulator period and electron beam energy. We find that undulator with period length 10 to 12 cm provides maximum wavelength of 25 - 45 nm at the electron energy of 8.5 GeV. Operation at the electron energy of 17.5 GeV with an open undulator gap will allow to reach radiation wavelengths below 1 nm.

Plot in Fig. 2 illustrates main parameters of SASE FEL for the case of 11 cm undulator period length. Numerical example is calculated for electron bunch with baseline parameters: bunch charge 250 pC, peak current 5 kA, rms normalized emittance 0.6 mm-mrad, rms energy spread 2.5 MeV [6]. Blue, black and red colors refer to the radiation wavelength, saturation length, and radiation pulse energy in the saturation regime. Solid lines show values of the parameters for closed

ISBN: 978-3-95450-210-3 doi:10.18429/JACoW-FEL2019-TUP058

Content from this work may be used under the terms of the CC BY 3.0 licence (© 2019). Any distribution of this work must maintain attribution to the author(s), title of the work, publisher, and DOI

FIRST CHARACTERIZATION OF THE PHOTON BEAM AT THE EUROPEAN XFEL IN JULY, 2017

V. Balandin, B. Beutner, F. Brinker, W. Decking, M. Dohlus, L. Fröhlich, U. Jastrow, R. Kammering, T. Limberg, D. Noelle, M. Scholz, A. Sorokin, K. Tiedtke, M.V. Yurkov, I. Zagorodnov, DESY, Hamburg, Germany
U. Boesenberg, W. Freund, J. Grünert, A. Koch, N. Kujala, J. Liu, T. Maltezopoulos, M. Messerschmidt, I. Petrov, L. Samoylova, H. Sinn, European XFEL, Germany

Abstract

This report present the first characterization of the photon beam properties from SASE1 FEL at the European XFEL. Development of the amplification process has been traced from the level of the radiation pulse energy in sub-μJ level (beginning of high gain linear regime) up to mJ level (saturation regime). Experimental method is based on the analysis of single shot photon beam images allowing to derive spatial properties of the FEL radiation mode. An important conclusion is that experimental results demonstrate reasonable agreement with baseline parameters. Developed techniques of the photon beam characterization also provided solid base for identification of the problems and means for improving SASE FEL tuning and operation.

INTRODUCTION

First light from the European XFEL [1] has been detected on May 3rd, 2017 at the photon energy of 1.3 keV and electron beam energy of 6.4 GeV [2]. Start-up phase of the European XFEL included a lot of tasks performed in parallel such as gradual increase of electron energy, tests of hardware, electron beam diagnostics, electron beam formation system, electron beam optics, test and tuning of the undulator, commissioning of photon beam diagnostics and photon beam transport system. Two months after the event of the "first light", operation of all systems improved significantly, and detected radiation pulse energies reached design values in a mJ range. First characterization of the photon beam has been performed in July 2017, a month before an official starting date of user experiments (September 1st, 2017). Energy of the electron beam was 13.5 GeV, bunch charge was 500 pC, radiation wavelength 0.15 nm. Two photon diagnostic systems (FEL imager and X-ray gas monitor (XGM) detector) were available at that time which was sufficient for basic characterization of the radiation. This allowed us to measure the gain curve and trace evolution of the FEL radiation mode along significant part of the amplification regime, from almost beginning of the high gain exponential regime to saturation. Analysis of the FEL radiation modes have shown that in the whole range of the radiation pulse energies (from μJ to mJ level) they are surprisingly close to those predicted ten years ago at the design stage of the project [3]. Measured properties of the electron beam in the accelerator were also in agreement with design parameters [2, 4]. Thus, both results of the electron beam and photon beam measurements provide strong argument in favor of conclusion that physical parameters of the machine are close to design values.

It turned out that analysis of the spatial properties of FEL radiation modes demonstrated to be a powerful tool for characterization physical parameters of SASE FEL process. As an extension of this experimental method we plan to implement correlations of FEL images with machine parameters which will allow to apply statistical techniques for determination of important parameters of SASE FEL such as gain length, saturation length, coherence time, radiation pulse duration, number of radiation modes in the pulse (longitudinal and transverse), degree of transverse coherence [5–8].

EXPERIMENTAL RESULTS

Measurements have been performed at the North branch of the European XFEL, SASE1 FEL. It is equipped with planar, variable gap undulator with 4 cm period length. It consists of 35 modules, each of 5 meter long. Machine operated at the energy of 13.5 GeV, bunch charge 500 pC, and the radiation wavelength was 0.15 nm. Special efforts have been taken for tuning machine to design parameters of the electron beam [2, 4].

By the time of described experiment only two photon diagnostics tools were in operation: FEL imager and XGM detector [9–13]. FEL imager is equipped with scintillating Ce:YaG screen and a scientific CMOS camera, and is located at a distance of 230 meters downstream the undulator end. XGM detector, located at 185 m behind the undulator, is cal-

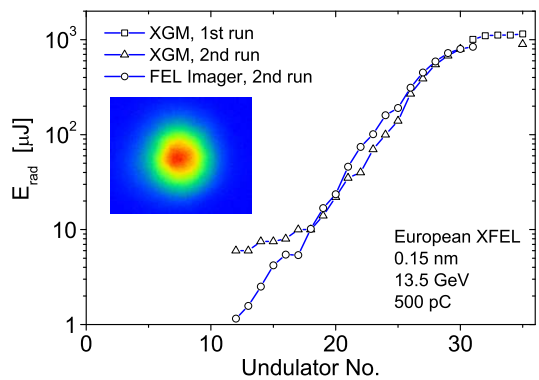


Figure 1: Gain curve of the European XFEL. The inset shows a single photon beam image. Electron energy is 13.5 GeV, bunch charge is 500 pC, radiation wavelength is 0.15 nm.

ISBN: 978-3-95450-210-3 doi:10.18429/JACoW-FEL2019-TUP059

INFLUENCE OF ENERGY CHIRP IN THE ELECTRON BEAM AND UNDULATOR TAPERING ON SPATIAL PROPERTIES OF THE RADIATION FROM SEEDED AND SASE FEL

E.A. Schneidmiller, M.V. Yurkov, DESY, Hamburg, Germany

Abstract

In this report we present analysis of the spatial properties of the radiation from an FEL amplifier for the case of energy chirp in the electron beam and undulator tapering. Two configurations, seeded FEL amplifier, and SASE FEL are under consideration. Studies are performed with numerical simulations using time-dependent FEL simulation code FAST. Evolution of the amplification process is traced along the undulator. It is shown that spatial properties of the radiation may be significantly distorted by the effect of energy chirp in the electron beam and undulator tapering.

INTRODUCTION

FEL amplification process is sensitive to the detuning from the FEL resonance. Energy chirp in the electron beam and undulator tapering are responsible for the change of the resonance condition. Undulator tapering is widely used in practical devices. Well known examples are post-saturation undulator tapering for radiation power increase, reverse undulator tapering for effective operation of afterburners, and application of linear undulator tapering for compensation of energy chirp effect [1–3]. These are essentially one dimensional effects [3–5]. Detuning effects significantly influence on the spatial properties of the radiation from FEL amplifier [6]. It has been shown in [7] in the framework of 3D FEL theory that effects of energy chirp and undulator tapering will result in an increase of the angular divergence and decrease of the degree of transverse coherence of the radiation from SASE FEL.

In this paper we trace evolution of amplification process in an FEL amplifier from start-up to the deep nonlinear regime. The case of linear frequency detuning (along undulator or along electron bunch) is under study. We compare two configurations: seeded FEL amplifier, and SASE FEL. We found that for positive linear detuning there is optimum value of chirp (tapering rate) when maximum output radiation power is achieved. Increase of the detuning in the positive direction leads to significant increase of the angular divergence of the radiation. On the other hand, radiation power significantly drop when increasing strength of the detuning in th negative direction (the power of the effect is similar to that given by 1D approximation). Stronger negative tapering results in shrinking of the angular divergence of the radiation.

BASIC DEFINITIONS

Detuning from the FEL resonance is defined as:

$$C = \frac{2\pi}{\lambda_w} - \frac{\pi(1+K^2)}{\lambda\gamma^2} ,$$

where λ_w is undulator period, λ is radiation wavelength, K is rms value of th undulator parameter, γ is Lorentz factor. Figure of merit of the detuning effect on the FEL performance is detuning parameter $\hat{C} = C/\Gamma$ with the gain parameter Γ given by [6]:

$$\Gamma = \left[\frac{I}{I_A}\frac{16\pi^2 K^2 A_{JJ}^2}{(1+K^2)\lambda_w^2\gamma}\right]^{1/2} .$$

3D FEL parameter relates to the FEL gain parameter as $\bar{\rho} = \lambda_w\Gamma/(4\pi)$.

For the linear law of the undulator tapering the detuning parameter is

$$\hat{C}(\hat{z}) = \beta\hat{z} , \qquad \beta = -\frac{\lambda_w}{4\pi\bar{\rho}^2}\frac{K_0}{1+K_0^2}\frac{dK}{dz} .$$

Here longitudinal coordinate is normalized as $\hat{z} = \Gamma z$, and K_0 refers to the initial value of the undulator parameter.

The chirp parameter α is the figure of merit for an effect on FEL amplification process of the energy chirp along the electron bunch:

$$\alpha = -\frac{d\gamma}{dt}\frac{1}{\gamma\omega\bar{\rho}^2} ,$$

where $\omega = 2\pi c/\lambda$.

There is a symmetry between the linear energy chirp and the undulator tapering [3]. Indeed, if we look at the radiation field acting on some test electron from an electron behind it, this field was emitted at a retarded time. In the first case a radiating electron has a detuning due to an energy offset, in the second case it has the same detuning because undulator parameters were different at a retarded time. The effect of the energy chirp is compensated by the undulator tapering when

$$\frac{1}{H_{w0}}\frac{dH_w}{dz} = -\frac{1}{2}\frac{(1+K_0^2)^2}{K_0^2}\frac{1}{\gamma_0^3}\frac{d\gamma}{cdt} .$$

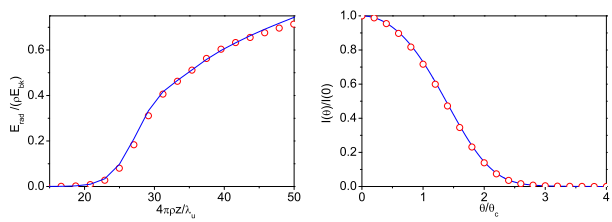


Figure 1: Equivalence of energy chirp and undulator tapering. Left: Average radiation pulse energy along undulator. Right: Average angular divergence in the far zone in the saturation. Solid curve: $\alpha = 0.07$, $\beta = 0$. Circles: $\alpha = 0$, $\beta = 0.035$.

Content from this work may be used under the terms of the CC BY 3.0 licence (© 2019). Any distribution of this work must maintain attribution to the author(s), title of the work, publisher, and DOI

ISBN: 978-3-95450-210-3 doi:10.18429/JACoW-FEL2019-TUP060

AN ADVANCED COMPRESSION OPTION FOR THE EUROPEAN XFEL

I. Zagorodnov, M. Dohlus, E.A. Schneidmiller, M.V. Yurkov
Deutsches Elektronen-Synchrotron, Hamburg, Germany

Abstract

An advanced compression scheme which allows to obtain a high peak current while preserving the low slice emittance is considered. The beam is compressed weakly in the bunch compressors and the current is increased by ESASE setup at the entrance of the undulator line. It is shown by numerical studies that such approach allows to reduce harmful collective effects in the bunch compressors and in the transport line. Simulations of FEL physics confirm the possibility to obtain a high level of SASE radiation at the ultra-hard photon energy level of 100 keV.

INTRODUCTION

The European XFEL provides SASE photon beams for user operation since 2017 [1]. Currently it has three photon lines (SASE1, SASE2, SASE3, see Fig. 1) and should reach the photon energy of 25 keV [2].

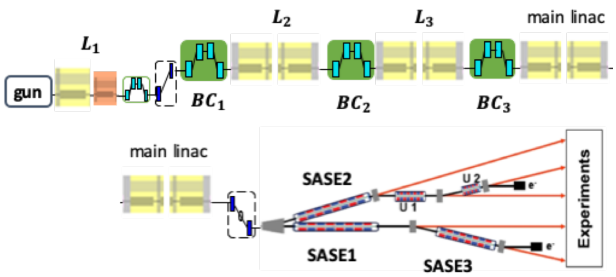


Figure 1: The European XFEL layout.

There is a possibility to use one of free tunels (U1 or U2, see Fig. 1) for the ultrahard x-ray undulator line to produce the SASE photons with energy of 100 keV [3].We study two possible scenarios: standard compression to 5 kA and an advanced compression with ESASE setup [4] up to 10 kA. The latter compression scheme allows to reduce the collective effects and to obtain a better electron slice parameters and to reach a higher level of SASE energy per electron bunch.

ACCELERATOR BEAM DYNAMICS

We have done numerical modeling of the accelerator beam dynamics up to the entrance of SASE2 undulator line. We have not included the effect of the last arc from SASE2 to U1 tunnel. The electron bunch with charge of 100 pC has been compressed to 2 and 5 kA. In the choice of the working points we have followed the approach of paper [5] and have used two codes: Ocelot [6] and Krack3 [7].

The tracking of particles in Ocelot is done in the same way as, for example, in Elegant [8]. Quadrupoles, dipoles, sextupoles, RF cavities and other lattice elements are modeled by linear and second order maps. The focusing effect of RF cavities is taken into account according to the Rosenzweig-Serafini model. The space charge forces are calculated by solving the three-dimensional Poisson equation in the bunch frame. The CSR module uses a fast 'projected' one-dimensional method [9]. The wakefields and the incoherent synchrotron radiation (ISR) effects are included.

Beam Dynamics in Linac

Table 1: Compression Parameters

Parameter	5 kA	2 kA
energies $E_1/E_2/E_3$, MeV	130 / 700 / 2400	
R^1_{56}/R^2_{56}, mm	56 / 52	
compression factors C_1/C_2	3.5 / 28	
R^3_{56}, mm	55	37
total compression C_3	862	340
Z'_3, 1/m	0	
Z''_3, 1/m/m	600	300

In standard operation we compress the electron bunch to the peak current of 5 kA and accelerate it to 17.5 GeV. The parameters of the longitudinal beam dynamics are listed in Table 1. The positive value of the second derivative of the inverse compression function Z_3 allows to reduce the compression strength in the bunch head [5]. To suppress the microbunching instability the energy spread in the bunch was increased in the laser heater, which is installed before the injector dogleg. The power of the laser is choosen to have at the linac end the rms slice energy spread of 1 MeV. The results of the simulation are shown in Fig. 2. The bunch has relatively small slice emittance: 0.2 µm in the horizontal plane and 0.3 µm in the vertical plane. The projected emittances are listed in Fig. 2 as well. The larger slice emittance in the y-plane is due to CSR effects in the vertically oriented bunch compressors. The larger horizontal projected emittance and the "banana" shape of the bunch in x-plane are due to not compensated CSR effects in the switchyard arc before SASE2 undulator line.

In order to suppress the self-fields and to improve the bunch properties we consider an another compression scenario: to compress the same bunch to 2 kA current in the linac and to 10 kA current in ESASE setup in the vicinity of the undulator line. The main parameters are listed in Table 1. The power of the heater is chosen to have after main linac the rms slice energy spread of 0.65 MeV. The results of the simulation for the bunch before ESASE setup are shown in Fig. 3. The bunch has slice emittance of 0.2 µm in both planes. The projected emittances in both planes are by factor 2 smaller than in the former case. Nevertheless, we see a larger projected emittance in the horizontal plane due to CSR impact in the arc before SASE2 undulator line.

Content from this work may be used under the terms of the CC BY 3.0 licence (© 2019). Any distribution of this work must maintain attribution to the author(s), title of the work, publisher, and DOI

ISBN: 978-3-95450-210-3 doi:10.18429/JACoW-FEL2019-TUP061

SUPER-X: SIMULATIONS FOR EXTREMELY HARD X-RAY GENERATION WITH SHORT PERIOD SUPERCONDUCTING UNDULATORS FOR THE EUROPEAN XFEL

S. Serkez*, G. Geloni, S. Karabekyan, Y. Li, T. Tanikawa,
S. Tomin, F. Wolff-Fabris, European XFEL, Schenefeld, Germany
S. Casalbuoni, KIT, Karlsrhue, Germany
C. Boffo†, Bilfinger Noell, Würzburg, Germany
M. Dohlus, E. Schneidmiller, M. Yurkov, I. Zagorodnov, DESY, Hamburg, Germany
A. Trebushinin, BINP, Novosibirsk, Russia

Abstract

The European XFEL is a high-repetition multi-user facility with nominal photon energy range covering almost 3 orders of magnitude: 250 eV - 25 keV. In this work we explore the possibility to extend the photon energy range of the facility up to 100 keV via combination of superconducting undulator technology, period doubling and harmonic lasing, thus allowing for excellent tunability. To this purpose, we propose a dedicated FEL line, discuss its overall concept and provide analytical and numerical estimations of its expected performance.

INTRODUCTION

The European XFEL first lased in 2017 [1] and can currently sustain simultaneous operation of three separate FEL lines, SASE1, SASE2 and SASE3 [2]. One distinctive trait of the facility is its high-energy, supercounducting linear accelerator reaching up to 17.5 GeV and up to 27000 pulses per second distributed in 10 macrotrains with an intra-train repetition rate up to 4.5 MHz. In the mid-term, two novel FEL lines will be installed in two already available empty tunnels [3] and possibly, in the longer term, a second fan of FEL tunnels will be excavated [4]. The high electron energy strongly hints at the possibility of generating extremely hard X-ray pulses well beyond the nominal 25 keV with an ad-hoc superconducting FEL undulator line that we call Super-X. In this paper we explore Super-X up to the 100 keV range. We assume -from the very beginning- the use of a nominal electron beam as is, from start-to-end simulations, at the entrance of the SASE1 undulator, i.e. not spoiled by collective interactions or wakes during the transport to different undulator lines. Superconducting undulators (SCU) can produce, with respect to permanet magnet ones, for the same period length and vacuum gap a higher peak field on axis. This allows to increase the photon energy range as well as the flux. Superconducting technology allows period doubling using a single magnetic structure. Period doubling further increases the photon energy tunability [5–8]. Although other technical realizations of super-hard X-ray FEL lines have been positively assessed [9], Super-X is an appealing option for reaching lasing at ultra-high photon energies with a large tunability range considering SASE and additional advanced FEL schemes discussed in this contribution.

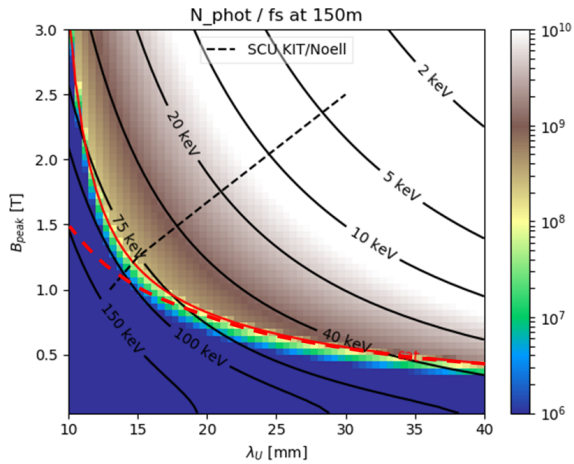


Figure 1: Estimated performance of a SCU XFEL line. The black dotted line shows the state-of-the-art magnetic field achievable for a 5 mm vacuum gap. The red solid and dashed lines refer to FEL saturation, the dashed line excluding quantum fluctuations effects.

ANALYTICAL ESTIMATIONS

We envision a SCU system with a geometrical length of 150 m, which fits conservatively the empty tunnels currently available at the European XFEL [3], and a filling factor of about 80%. In order to study the relevant parameter space we parametrized the 3D gain length according to [10, 11], which provide two alternative methods to estimate the FEL performance. We fixed, as just described, a total setup length of 150 m, assumed a flat-top electron beam with a current of 5 kA, an energy of 17.5 GeV, a normalized slice emittance of 0.4 mm mrad, an rms energy spread of 1 MeV and average betatron functions around 30 m. Using [10,11] we estimated the number of photons per femtosecond duration of the electron bunch as a function of on-axis peak magnetic field and undulator period, for different photon energies. We validated our estimations with time-dependent FEL simulations performed with Genesis [12] and Simplex [13]. Results are shown in Fig. 1. The black dotted line refers to the maximum magnetic field in reach of state-of-the-art SCU assuming a

* svitozar.serkez@xfel.eu
† Current address: Fermilab, Battavia, Illinois, USA

Content from this work may be used under the terms of the CC BY 3.0 licence (© 2019). Any distribution of this work must maintain attribution to the author(s), title of the work, publisher, and DOI

ISBN: 978-3-95450-210-3 doi:10.18429/JACoW-FEL2019-TUP062

TWO COLORS AT THE SASE3 LINE OF THE EUROPEAN XFEL: PROJECT SCOPE AND FIRST MEASUREMENTS

S. Serkez*, G. Geloni, N. Gerasimova, J. Grünert, S. Karabekyan, A. Koch, J. Laksman, Th. Maltezopoulos, T. Mazza, M. Meyer, S. Tomin, European XFEL, Schenefeld, Germany
W. Decking, L. Froehlich, V. Kocharyan, Y. Kot, E. Saldin, E. Schneidmiller, M. Scholz, M. Yurkov, I. Zagorodnov, DESY, Hamburg, Germany
M. Huttula, University of Oulu, Finland
E. Kukk, University of Turku, Turku, Finland

Abstract

The European XFEL is a high-repetition rate facility that generates high-power SASE radiation pulses in three beamlines. A joint upgrade project, with Finnish universities, to equip the SASE3 beamline with a chicane has been recently approved to generate two SASE pulses with different photon energies and temporal separation. In this work we report the status of the project, its expected performance, and recent experimental results. Additionally, we discuss methods to diagnose the properties of the generated radiation.

INTRODUCTION AND PROJECT SCOPE

Funding has been recently granted by the Academy of Finland, with co-funding by the European XFEL, for constructing a device at the SASE3 undulator of the European XFEL. This will add two-color capability with tunable delay, and enable pump-probe experiments at the SASE3 endstations. A similar scheme is already enabled at SASE2, owing to the presence of the Hard X-ray Self-Seeding chicanes. The proposed setup relies on the simplest method available at date for generating two closely separated pulses of different colors at XFELs as suggested in [1] and experimentally proven in [2, 3]. The scheme is illustrated in Fig. 1, where the baseline SASE3 soft X-ray undulator is split into two independently radiating parts, *U1* and *U2*, by a magnetic chicane. The chicane introduces a tunable delay and washes out the electron microbunching from *U1*, which is important if the color separation, in energy, is smaller than the FEL amplification bandwidth. One must ensure that the electron beam quality at the entrance of *U2* is still good enough to sustain the FEL process, which limits the power that can be extracted below the saturation level. The photon energy separation between the two pulses can theoretically span across the entire range made available by the undulator system. In the case of SASE3 at the electron energy of 8.5 GeV, this range roughly spans between 240 eV and 1 keV. At 14 GeV – between 650 eV and 2.9 keV. For 17.5 GeV – between 1.02 keV and 3 keV. However, the impact of the FEL process on the electron beam quality depends on the photon energy, so that the first pulse to be produced should be at the highest energy.

A dedicated chicane will allow for a maximum delay of about 2.3 ps, see [4]. The minimum delay between pump and probe radiation pulses is not zero. The electron beam is naturally overtaken by the radiation emitted in *U1*, as it moves slower than the speed of light in *U2*. The delay between pump and probe FEL pulses is thus larger than zero even when chicane is switched off and is in the order of 1 µm (3fs).

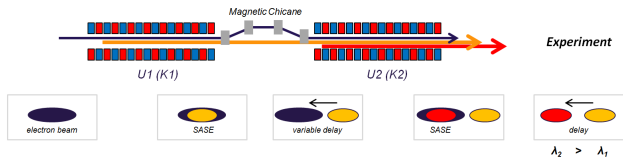


Figure 1: Simplest 2-color scheme relying on a single magnetic chicane.

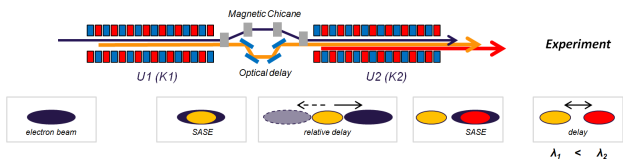


Figure 2: Solving the zero-crossing problem by implementing an optical delay line.

Optical Chicane and Possible Further Upgrades

The magnetic chicane can only increase the delay between the FEL pulses, and its construction and commissioning constitutes only the first phase of the two-color project at SASE3. In fact, in order to enable a zero-delay and even a negative one, two possible solutions can be considered. The first, which constitutes the second phase of the project, consists in the introduction of an optical delay line to retard the radiation emitted in the first undulator with respect to the electron beam and, therefore, to compensate or overcompensate the radiation slippage, Fig. 2. A more detailed concept for the chicane with an optical delay line was developed in [4], see Fig. 3. It will allow for a negative delay of up to 100 fs, thus enabling zero-crossing and subsequent scan until 2.3 ps. Further investigation on the actual implementation of the scheme is being conducted.

An alternative solution can be found in electron beam manipulations enabling fresh slice lasing, which may be achieved by means of a “dechirper module”, or other techniques inducing a kick in part of the electron beam [5]. In this way, the trajectory of electrons vary as a function of the

* svitozar.serkez@xfel.eu

Content from this work may be used under the terms of the CC BY 3.0 licence (© 2019). Any distribution of this work must maintain attribution to the author(s), title of the work, publisher, and DOI

ISBN: 978-3-95450-210-3 doi:10.18429/JACoW-FEL2019-TUP063

PHYSICAL DESIGN AND FEL PERFORMANCE STUDY FOR FEL-III BEAMLINE OF SHINE

N.S. Huang *, Shanghai Institute of Applied Physics, Chinese Academy of Sciences, Shanghai, China
also at University of Chinese Academy of Sciences, Beijing, China
H.X. Deng †, B. Liu, D. Wang,
Shanghai Advanced Research Institute, Chinese Academy of Sciences, Shanghai, China

Abstract

The first hard X-ray free electron laser (XFEL) facility in China, the Shanghai High-Repetition-Rate XFEL and Extreme Light Facility (SHINE), is under construction, which allows for generating X-ray pulses in the photon energy range from 3 keV to 25 keV. To produce X-ray pulses with photon energy up to 25 keV, FEL-III undulator line of SHINE employs superconducting undulators. However, the smaller gap of the superconducting undulator poses serious wakefield effect reducing the FEL power, compared to the normal planar undulator. For a setup design optimization, the design and performance of the FEL-III undulator line are presented using start-to-end beam simulations at self-amplified spontaneous emission (SASE) and self-seeding mode. The wakefield impact on FEL performance is then investigated. A linear undulator tapering technique is adopted for recovering the FEL power to the non-wakefield level.

INTRODUCTION

Advanced high brightness X-ray light sources, X-ray free electron lasers (XFELs), bring significant opportunities to many fields for scientific exploring. The Shanghai High-Repetition-Rate XFEL and Extreme Light Facility (SHINE) is the first hard X-ray FEL facility in China [1], that will be fed by a superconducting linac at a high repetition rate, up to 1 MHz, and is being designed under a multi undulator line collaboration to generate X-ray of photon energy range from 3 keV to 25 keV. One of the undulator lines, FEL-III, will cover the spectral range between 10 keV and 25 keV. Reaching such wide spectral range requires high tunability of undulator parameter owing to the resonance condition of the FEL process. Superconducting undulator with a short period length is probably a better choice. However, the designed FEL performance is degrading due to resistive wall wakefield effects along the superconducting undulator line, which is more serious compared to normal conducting one.

Thus, it is necessary to investigate the wakefield impact on FEL performance of FEL-III, e.g., the pulse energy and FEL bandwidth. While various advanced FEL concepts are being explored for SHINE, this paper presents the detailed FEL simulations in only the self-amplified spontaneous emission (SASE) and self-seeding case for start-to-end electron beam coming from the superconducting linac. The basic parameters are listed in Table 1. The slice parameters of the start-to-end electron beam are illustrated in Fig. 1. The core of the bunch has relatively flat energy with a current of 1500 A, slice energy spread 0.8 MeV and slice emittance of 0.2 mm-mrad. The generations of 15 keV X-ray pulse based on a 8 GeV electron beam are performed. The FEL simulations were carried out by the time-dependent mode of GENESIS [2]. The interaction between X-ray pulse and crystal is calculated by BRIGHT [3].

Table 1: Normal Electron Beam and Undulator Parameters

Parameter	Value	Unit
Electron beam energy	8	GeV
Slice energy spread	0.8	MeV
Total charge	100	pC
Photon energy	15	keV
Undulator period length	16	mm
Undulator segment length	4	m
Break length	1	m
Total length	200	m

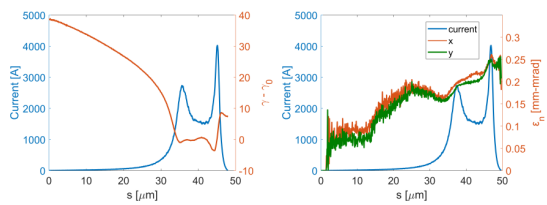


Figure 1: Slice energy (left), x (red) and y (green) slice emittance (right) of the start-to-end electron beam.

FEL PERFORMANCE

According to the project targets, several different operating modes have been explored for the different undulator line of SHINE. These modes include, but are not limited to, SASE, self-seeding [4], echo-enabled harmonic generation (EEHG) [5] and cascading schemes. FEL-III beamline is envisioned to operate from 10-25 keV in the SASE and self-seeding mode using the superconducting undulator. To estimate the capacity of FEL-III, we begin with the start-to-end simulation results without wakefield effects at 15 keV photon energy for SASE and self-seeding mode.

Fig. 2 illustrates the SASE performance of 15 keV output. The final pulse energy is about 380 μJ, corresponding to

* huangnanshun@sinap.ac.cn
† denghaixiao@zjlab.org.cn

Content from this work may be used under the terms of the CC BY 3.0 licence (© 2019). Any distribution of this work must maintain attribution to the author(s), title of the work, publisher, and DOI

ISBN: 978-3-95450-210-3 doi:10.18429/JACoW-FEL2019-TUP064

EFFECT ON FEL GAIN CURVE USING PHASE SHIFTERS

Myung-Hoon Cho *, Chi-Hyung Shim, Gyu-Jin Kim, H. Yang, and Heung-Sik Kang
PAL, Pohang, Korea

Abstract

Phase matching between FEL and electron beam should be precisely controlled for FEL amplification. Phase shifters located between undulators performs the phase matching. An electron beam can be controlled to be in the in- or out-phase by setting the phase shifters from the phase shifter scan. In this article, we show effects of FEL gain curve by setting the in- and out-phase of electron beam. We address reasons of the reduction of FEL intensity in the out-phase condition dividing the linear and saturation FEL amplification regimes. In the linear regime the gain curve is shifted, and in the saturation regime the electron loss occurs during the undulator tapering. Our results show agreements with experiments performed at PAL-XFEL.

INTRODUCTION

Most x-ray free-electron laser (XFEL) facility requires segmented undulators with drift sections. Drift sections include quadrupoles for beam focus, beam path correctors, diagnostics, and beam phase shifters [1,2]. While an electron beam travels drift sections, the electron beam phase can be mismatched to the generated X-ray. This phase mismatch can lead to a reduction of XFEL intensity, therefore the phase matching can be an import optimization process.

Enhancement of FEL efficiency by matching phase can be understood by so-called 'phase jump' at the saturation region [3,4]. The key idea is setting a dominant electron beam phase zero so called 'synchronous phase' before entering the next undulator. To investigate effects on the FEL gain curve, two cases of the phase-matched condition (the in-phase) and 180^0 off-set condition from the in-phase condition (the out-phase) are considered.

THEORY AND SIMULATION

We show optimization of FEL and FEL gain curve by the phase shifters. To understand the changes of FEL gain curve, we develop a linear theory for the linear region and use KMR analysis [4,5] for the saturation region, those are compared with FEL simulations.

Linear Regime

If we ignore the time dependent terms, 1D FEL equations are given as [6]

$$\frac{d\theta}{d\hat{z}} = \hat{\eta} \tag{1.a}$$

$$\frac{d\hat{\eta}}{d\hat{z}} = ae^{i\theta} + a^* e^{-i\theta} \tag{1.b}$$

$$\frac{da}{d\hat{z}} = -\left\langle e^{-i\theta} \right\rangle_{slice} \tag{1.c}$$

Here, $\theta \equiv (k + k_u)z - \omega t$ is the electron phase, $\eta \equiv (\gamma - \gamma_0)/\gamma_0$ is the energy deviation ratio to γ_0, and a is the slowly varying electric field envelope. The equations are normalized by $\hat{z} = 2\mathrm{k_u}\rho z$, $\hat{\eta} = \eta/\rho$, and $a = \mathrm{eK}[JJ]\mathrm{E}/4\gamma_0^2 k_u mc^2\rho^2$, where $[JJ]$ is the harmonic factor, and ρ is the FEL parameter. Introducing the collective variables : the bunching factor $b = \left\langle e^{-i\theta} \right\rangle_{slice}$ and the collective momentum $P = \left\langle \hat{\eta} e^{-i\theta} \right\rangle_{slice}$, Eq. (1) is rewritten by ignoring the non-linear terms : $\mathrm{dP/d}\hat{z} = \mathrm{a} + \mathrm{a}^* \langle e^{-i2\theta} \rangle - \mathrm{i}\langle \hat{\eta}^2 e^{-i\theta} \rangle \approx \mathrm{a}$

$$\frac{da}{d\hat{z}} = -b \tag{2.a}$$

$$\frac{db}{d\hat{z}} = -iP \tag{2.b}$$

$$\frac{dP}{d\hat{z}} = a \tag{2.c}$$

Eq. (2) is the linearized FEL equation, which can be summarized to be an third-order differential equation

$$\frac{d^3 a}{d\hat{z}^3} = ia \tag{3}$$

The general solution of Eq.(3) can be obtained as

$$a(\hat{z}) = \frac{1}{3}\sum_{l=1}^{3}\left[a(\hat{z}_0) - i\frac{b(\hat{z}_0)}{\mu_l} - i\mu_l P(\hat{z}_0)\right] e^{-i\mu_l \hat{z}} \tag{4}$$

, where μ_l indicates three radiation modes : a simple propagator $\mu_1 = 1$, a damper $\mu_2 = -\left(1 + \sqrt{3}i\right)/2$, and a grower $\mu_3 = \left(-1 + \sqrt{3}i\right)/2$. Assuming the electron beam in the in-phase, the initial conditions at $\hat{z}_0 = 0$ are $a(0) = C_1 + C_2 + C_3$, $b(0) = \mu_1 C_1 + \mu_2 C_2 + \mu_3 C_3$, and $P(0) = i(\mu_1^2 C_1 + \mu_2^2 C_2 + \mu_3^2 C_3)$. Considering a SASE condition of $a(0) = P(0) = 0$ with initial bunching factor of $b(0) = b_0$, a grower mode becomes dominant, then Eq.(4) is simplified to be

$$a_{in}(\hat{z}) \cong \frac{i-\sqrt{3}}{6} b_0 e^{\frac{\sqrt{3}+i}{2}\hat{z}} \tag{5}$$

To calculate the changed gain curve at the out-phase, we simply set the phase replacing θ by θ + π. Eq. (1) is then reformulated to be the linearized equations which is reduced to a single third-order differential equation same as Eq. (3). Therefore, the expression of the solution is identical to the in-phase solution of Eq. (4) except of the initial conditions. according to the phase shifter position $\hat{z}_0 \neq 0$. The initial conditions at $\hat{z} = \hat{z}_0$ can be defined obtained using Eq. (5):

$$a(\hat{z}_0) = -\frac{1}{3} b_0 e^{i\left(\frac{\hat{z}_0}{2} - \frac{\pi}{6}\right)} e^{\frac{\sqrt{3}}{2}\hat{z}_0} \tag{6.a}$$

* mh0309@postech.ac.kr

Content from this work may be used under the terms of the CC BY 3.0 licence (© 2019). Any distribution of this work must maintain attribution to the author(s), title of the work, publisher, and DOI

ISBN: 978-3-95450-210-3 doi:10.18429/JACoW-FEL2019-TUP065

OPTIMIZATION OF A COHERENT UNDULATOR BEAMLINE FOR NEW ADVANCED SYNCHROTRON LIGHT SOURCE IN KOREA

Ingyo Jeong[1,2,*], Yujong Kim[1,2,†], Seunghyun Lee[2], Jaeyong Lee[2], Pikad Buaphad[1,2], Youngwoo Joo[1,2], Hyeri Lee[1,2], and Moonyoung Han[2]
[1]Dept. of Accelerator and Nuclear Fusion Physical Engineering, UST, Daejeon, 34113, Korea
[2]Future Accelerator R&D Team, Nuclear Data Center, KAERI, Daejeon, 34057, Korea

Abstract

Recently, the demand for a new advanced synchrotron light source in Korea is rapidly growing. Six local governments in Korea would like to host the new synchrotron light source project in their own provinces. The new advanced synchrotron light source will be the Diffraction-Limited Storage Ring (DLSR), which is based on the Multi-Bend Achromat (MBA) lattice. For the new synchrotron light source, we would like to build a special 60-m long coherent undulator beamline, which can deliver high-intensity coherent radiation at the hard X-ray region. To design the coherent undulator beamline, we have performed numerous beam dynamics simulations with GENESIS and SIMPLEX codes. In this paper, we report design concepts and those simulation results for the coherent undulator beamline.

INTRODUCTION

PLS-II, the third generation light source at Pohang in Korea, has been well utilized so far. Since the recent annual growth of PLS-II users is about 600, and its total users are about 7,000 in 2018, PLS-II is close to facility saturation, and the demand for a new advanced synchrotron light source is growing. In addition, due to the suddenly changing international situation between Korea and Japan, Korean government is planning to develop and produce advanced materials in Korea. To do this, the Korean government is also considering to build new advanced synchrotron light sources and has already allocated $1.2M budget to design a new advanced synchrotron light source in 2020.

Currently, several studies have been conducted for a new advanced synchrotron light source in Korea, and one of them is ongoing by Future Accelerator R&D Team in Korea Atomic Energy Research Institute (KAERI). The blueprint of the new advanced synchrotron light source in Korea is shown in Fig. 1, which consists of three parts; a CW SRF injection linac, a small UV & soft X-ray storage ring [1], and a main Diffraction-Limited Storage Ring (DLSR) with a Multi-Bend Achromat (MBA) lattice [2]. As shown in Fig. 2, we would like to use long drift spaces between the superperiods for coherent beamlines with many undulators. By injecting high quality electron beam from the injector linac continuously, the 60-m undulator beamline in the main storage ring can generate coherent high-brightness X-rays during the tens-of-turn operation mode. In this study, we present the design concepts and the simulation results of the coherent undulator beamline to generate hard X-ray at a wavelength of 0.1 nm with the Self-Amplified Spontaneous Emission Free Electron Laser (SASE FEL) concept [3, 4]. The beam dynamics and the radiation along the beamline are simulated with GENESIS and SIMPLEX codes [5, 6].

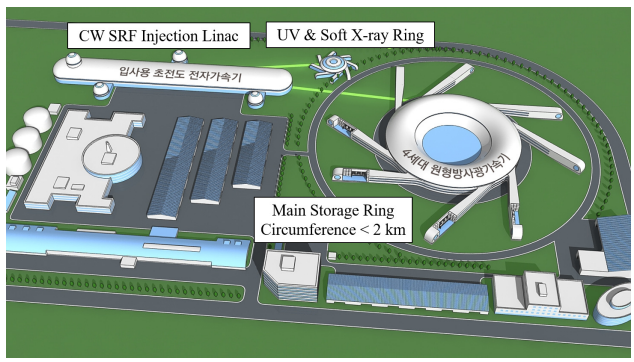


Figure 1: The blueprint of a new advanced synchrotron light source in Korea. The large round building on the right is the MBA-based main storage ring [2].

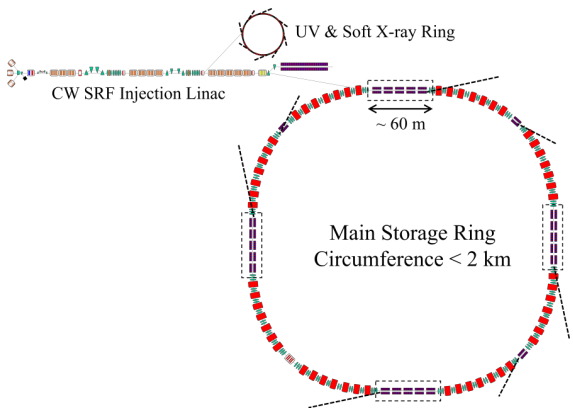


Figure 2: The layout of the new advanced synchrotron light source in Korea. Boxed sections are the coherent undulator beamlines [2].

DESIGN OF UNDULATOR BEAMLINE

Design Parameters

Although the design of the accelerator is ongoing, several key properties of the accelerator are already determined. The energy of the electron beam under consideration is 6 GeV for

* jungingyo@gmail.com
† yjkim@kaeri.re.kr

Content from this work may be used under the terms of the CC BY 3.0 licence (© 2019). Any distribution of this work must maintain attribution to the author(s), title of the work, publisher, and DOI

ISBN: 978-3-95450-210-3 doi:10.18429/JACoW-FEL2019-TUP066

START-TO-END SIMULATIONS FOR THE SOFT X-RAY FEL AT THE MAX IV LABORATORY

W. Qin*, F. Curbis, M. Pop, S. Werin, Lund University and MAX IV Laboratory, Lund, Sweden
J. Andersson, L. Isaksson, M. Kotur, E. Mansten, S. Thorin, MAX IV Laboratory, Lund, Sweden

Abstract

A Soft X-ray FEL (the SXL) using the existing 3 GeV linac at the MAX IV Laboratory is currently in the design phase. In this contribution, start-to-end simulations, including the photo-injector simulations using ASTRA, the linac simulations using ELEGANT and the FEL simulations using GENESIS, are presented for 100 pC and 10 pC operation modes. The features of the electron beam from the MAX IV linac and their impact on the FEL performance are discussed.

INTRODUCTION

A Soft X-ray FEL (the SXL) [1] at the MAX IV Laboratory is currently in conceptual design phase. The SXL utilizes the existing 100 Hz, 3 GeV linac [2] and the photocathode injector [3,4] at MAX IV to generate high brightness electron beams to drive radiation ranging from 1 nm to 5 nm. Considering the features of the 3 GeV beam from the existing linac, phase I of the SXL would be mostly operating in SASE mode using beam parameters that do not require major modification of the existing linac. With improvement of the beam quality, especially removal of the beam chirp, more advanced schemes are foreseen in phase II.

The layout of the SXL FEL is sketched in Figure 1. There are two injectors, one based on a thermionic RF gun to produce beams for the 1.5 GeV and 3 GeV ring injection, the other based on a photocathode RF gun to produce high brightness beams for the Short Pulse Facility (SPF) [5] and the SXL. After the injector, the electron beam is accelerated in the S-band linac and compressed by two double-achromat bunch compressors. The 3 GeV electron beam is then matched and sent into the undulator line, which consists of 3 m long, 40 mm period, APPLE-X undulator modules. The overall undulator line length is not fully defined yet. Empty sections before the main undulator and in the middle of the undulator are reserved for possible advanced schemes such as external seeding or self-seeding. Small chicanes could be added in the undulator break sections to delay the electron beam for possible coherence improvement schemes and high power schemes. The X-ray pulses are transported through the photon diagnostic section and then to the experimental stations.

In this paper, we present start-to-end particle tracking results from the photocathode gun to the end of the undulator line. The particle tracking is conducted in three stages. The injector is simulated with ASTRA [6] from the cathode to approximately 100 MeV. At the end of the first linac, ELEGANT [7] is used to model the downstream acceleration to 3 GeV and two-stage bunch compressions, including wakefields and CSR effect. The ELEGANT output distribution is sent into GENESIS [8] to simulate the generation of FEL pulses. 2M macro-particles are used in the simulations. Simulation details for the three stages are described in the following sections.

INJECTOR SIMULATION

The designed SXL injector is optimized based on the currently operating 10 Hz MAX IV injector, consisting of a 1.6 cell S-band BNL/SLAC type RF gun with a copper cathode, an emittance compensation solenoid, a 5.2 m long S-band linac, a drive laser system and relevant diagnostics. Standard operation of the designed injector generates 100 pC electron beam with 100 Hz repetition rate. Another operation mode aims at generating 10 pC electron beams with lower emittance and shorter pulse duration. To generate 100 pC charge, a 263 nm laser pulse with plateau temporal distribution and cut-gaussian transverse distribution is illuminated on the copper cathode, with 7.6 ps temporal duration and 0.24 mm transverse rms size. The maximum field is 100 MV/m and the gun phase is 25 degrees. Figure 2 shows the electron beam slice parameters and longitudinal phase space at the injector exit for the 100 pC case. An electron beam with about 18 A current, 6 ps FWHM duration and slice emittance lower than 0.4 μm is obtained. By adjusting the laser diameter and gun settings, a 10 pC electron beam with 11 A current, 1 ps FWHM duration and 0.2 μm slice emittance is obtained.

Further optimization of the gun and injector setup is ongoing. More parameters are included and advanced algorithm like MOGA is deployed in the optimization procedure. Comparing ASTRA results with full space charge code Impact-T [9] is also ongoing. A gun test stand has been setup at MAX IV as a useful platform to test the performance of the SXL gun.

LINAC SIMULATION

The MAX IV linac consists of 39 normal conducting S-band accelerating sections. Bunch compression is accomplished with two double-achromat type bunch compressors at 260 MeV and 3 GeV. The bunch compressors have positive R56 and positive T566, thus linearizing the longitudinal phase space without the help of a prior harmonic cavity. The linearization effect can also be tweaked using sextupoles in the bunch compressors. The second bunch compressor is also used as a beam distributor for the SPF and a diagnostic beamline. Figure 3 shows the electron beam slice parameters and longitudinal phase space at the exit of the linac for the 100 pC case. After the two-stage compression, the

* weilun.qin@sljus.lu.se

Content from this work may be used under the terms of the CC BY 3.0 licence (© 2019). Any distribution of this work must maintain attribution to the author(s), title of the work, publisher, and DOI

ISBN: 978-3-95450-210-3 doi:10.18429/JACoW-FEL2019-TUP067

ADVANCED CONCEPTS IN THE DESIGN FOR THE SOFT X-RAY FEL AT MAX IV

W. Qin*, F. Curbis, M. Pop, S. Werin
Lund University and MAX IV Laboratory, Lund, Sweden

Abstract

A Soft X-ray FEL (the SXL) is currently being designed at the MAX IV Laboratory. In the work to adapt the FEL to the scientific cases several advanced options are being studied for coherence enhancement, generation of short pulses and two-color pulses. We will discuss the current status and initial results of the schemes studied, especially regarding the FEL performance with the features of the MAX IV linac, including a positive energy chirp.

INTRODUCTION

A Soft X-ray FEL (the SXL) [1] at the MAX IV Laboratory is currently in conceptual design phase. Phase I of the SXL will be based on realistic chirped electron beam from the existing 3 GeV linac [2]. The baseline is SASE FEL operating with 100 pC and 10 pC charge. To meet the increasing demand of various features of the FEL pulses, such as ultra-short pulses, two-color pulses, coherence improvement as well as high flux pulses, advanced FEL schemes need to be employed. The SXL is based on 3 m long, 40 mm period APPLE-X undulator with strength K tuning range from 1.2 to 3.9. The length of the whole undulator line is not yet fully defined but should be enough to bring the shortest wavelength to saturation. To allow possible implementation of advanced schemes, a few sections are reserved, as sketched in Figure 1. Prior to the undulator line, one section is reserved for modulator and chicane modules for external seeding methods such as the Echo-Enabled Harmonic Generation (EEHG) [3, 4], or attosecond pulse generation methods such as the XLEAP [5]. In the middle of the undulator line one section is reserved for split undulator based two-color FEL pulse generation as well as monochromator based self-seeding [6]. Space for small delay chicanes in each undulator break section is reserved for schemes such as high-brightness SASE [7] and high power short pulse generation. In this paper we present preliminary advanced concepts for the design of the SXL as well as example simulations for the schemes that are relatively straightforward to implement. FEL simulations are conducted using 3D FEL code GENESIS [8].

SHORT PULSE GENERATION

Ultra-short pulse is crucial for probing ultra-fast dynamics as it defines the resolution in time. Typical operation of FELs provides pulses with a few tens of femtosecond duration, close to the length of the electron beam. While for ultra-fast applications, FEL pulses down to a few femtosecond or even subfemtosecond are required. To generate ultra-short FEL pulses, common methods are selecting an ultra-short region of the electron beam to lase or shortening the electron beam itself. To select an ultra-short region, one can use a slotted foil [9] or a modulation laser [10] in the laser heater section, one can also enhance the beam current of a local region using a few-cycle laser [11], another method is transversely tilting the electron beam [12] to create good interaction region in the beam. One way to shorten the electron beam is to start with lower bunch charge, which produces a shorter beam with lower emittance from the beginning and allows higher compression factor [13]. Selecting an ultra-short region usually requires additional hardware, while low charge method is straightforward to implement, despite it produces less pulse energy. In the current design of the SXL, the low charge method is considered as a standard way to produce ultra-short pulses and thus one of the two baseline operation modes.

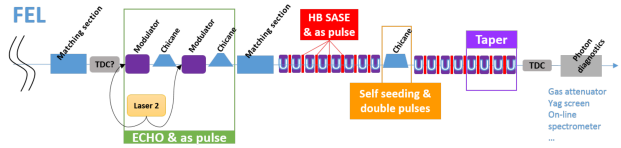


Figure 1: Schematic layout showing the implementation of various FEL schemes.

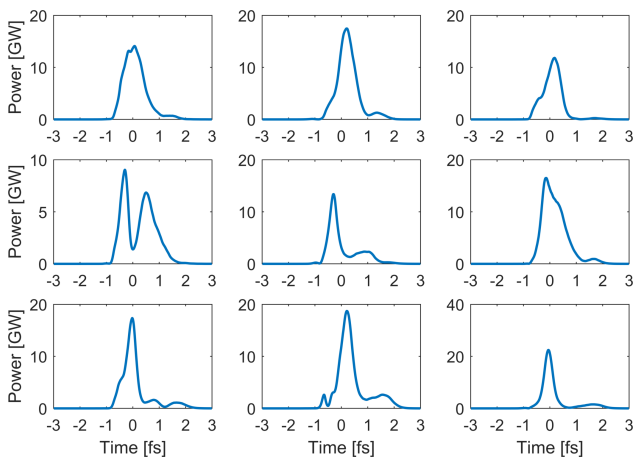


Figure 2: 9-shot simulated temporal profiles for the 10 pC mode of the SXL. The resonant wavelength is 1 nm.

Start-to-end simulations have been conducted for the low charge operation mode of the SXL. Beam parameters and phase space before the undulator can be found in Ref. [14]. The 10 pC electron beam is compressed to about 3.5 kA after two double-achromat compressions. Figure 2 shows

* weilun.qin@sljus.lu.se

Content from this work may be used under the terms of the CC BY 3.0 licence (© 2019). Any distribution of this work must maintain attribution to the author(s), title of the work, publisher, and DOI

ISBN: 978-3-95450-210-3 doi:10.18429/JACoW-FEL2019-TUP072

ORBITAL ANGULAR MOMENTUM FROM SASE

J. Morgan[1,2], B.W.J. McNeil[1,2], B.D. Muratori[2,3], P. Williams[2,3], A. Wolski[2,4]
[1]SUPA, Department of Physics, University of Strathclyde, Glasgow
[2]Cockcroft Institute, Warrington, UK
[3]ASTeC, STFC Daresbury Laboratory, Warrington, UK
[4]University of Liverpool, Liverpool, UK

Abstract

To reach very short wavelengths and high intensities of light, free-electron lasers, FELs, are used which produce radiation from amplified noise in an electron beam. In this SASE regime, mode competition dictates that the dominant transverse mode of the radiation will be Gaussian. A method is proposed to suppress the Gaussian mode via phase shifts which allows higher order Laguerre-Gaussian modes to be amplified. These modes are of interest as they carry orbital angular momentum, OAM. Techniques for generating OAM radiation with a FEL have been proposed previously, however, this is the first look at altering mode competition in order to get a dominant OAM mode starting from the initial shot noise in the electron beam.

INTRODUCTION

Recently, much attention has been paid to light which carries OAM. This light has helical phase-fronts characterized by $e^{il\phi}$, where ϕ is the azimuthal coordinate and l is an integer number named the topical charge. The magnitude of l gives the number of intertwined helices in the phase front and the sign of l gives the handedness of these helices. Conventional methods for generating OAM light require downstream optics which convert the radiation from a standard laser [1]. This has its limitations. The optical elements' damage threshold limits the brightness and wavelength of light which is transmitted and constraints arise from the lasers themselves. In contrast, in the FEL, the phase structure of light can be controlled through the manipulation of the electrons themselves and offers the benefit of having a wide range of wavelengths accessible.

Previous work has shown that OAM can be produced in a FEL through a variety of methods. Recently, OAM radiation has been produced at FERMI through harmonic lasing schemes involving helical undulators as well as using a spiral zone plate to convert the radiation downstream from normal FEL output [2]. Another method from Hemsing and colleges creates OAM radiation by first bunching electrons into a helix through second harmonic interaction with a helical undulator. [3].

The current methods for producing OAM radiation in a FEL have their limitations. The intensity of light from harmonic lasing schemes is less than that at the fundamental frequency [2]. Other methods rely on seeding the FEL either with an OAM seed laser for amplification or with a pre-bunched electron beam. When a FEL is seeded in this way, the output is restricted by the quality of seeds available. This causes difficulty at very short wavelengths as a seed may not be available at the required wavelength and the intensity of the seed must be large to overcome the initial shot noise in the beam. It would be useful, instead, for the initial seed for amplification to come from the shot noise in the electron beam itself. This work looks at the feasibility of just this, generating OAM through suppression of the Gaussian mode.

THEORY

Electrons enter the undulator with random phases due to shot noise in the electron gun. In the self-amplified-spontaneous emission (SASE) mode of operation, the initial amplitude due to the noise acts as a seed for the FEL interaction and is amplified. The incoherence of the electrons is mimicked by the radiation they produce. This radiation can be described by a superposition of the orthogonal Laguerre-Gaussian beams, $LG_{pl}(\phi, \hat{r})$,

$$E(\phi, \hat{r}) = \sum_{l=-\infty}^{\infty} \sum_{p=0}^{\infty} a_{pl} LG_{pl}(\phi, \hat{r}), \tag{1}$$

where a_{pl} is the initial mode amplitude. The Laguerre-Gaussian, LG, modes are chosen as they provide a convenient mode basis and are often used in the study of OAM beams. These modes are written in terms of their OAM index l and the radial mode index p. The fundamental Gaussian mode is found when $p = l = 0$.

All of the modes will have a contribution from the initial electron density. However, due to their transverse profile, the higher order modes have longer gain lengths [4] with the shortest gain length belonging to the Gaussian mode. The Gaussian mode, therefore, dominates FEL interaction, suppressing the higher order modes, leading to the Gaussian mode of operation typical of a FEL. Here we demonstrate that suppressing the Gaussian mode will lead to the amplification of the higher order modes.

Suppression of the Gaussian Mode

It is possible to disrupt the interaction between electrons and radiation through a relative phase shift. A longitudinal delay of the electrons which shifts the electron phase relative to the fundamental wavelength by $\Delta\theta$ will shift the electrons relative to the nth harmonic by $n\Delta\theta$. It has been demonstrated that the exponential gain of the fundamental wavelength can be suppressed when $\Delta\theta$ is a non-integer multiple of 2π and can increase the power in higher harmonics [5]. Instead of considering the higher harmonics of

Content from this work may be used under the terms of the CC BY 3.0 licence (© 2019). Any distribution of this work must maintain attribution to the author(s), title of the work, publisher, and DOI

ISBN: 978-3-95450-210-3 doi:10.18429/JACoW-FEL2019-TUP073

HIGH-REPETITION-RATE SEEDING SCHEMES USING A RESONATOR-AMPLIFIER SETUP

S. Ackermann*, B. Faatz, V. Grattoni, C. Lechner, G. Paraskaki, DESY, Hamburg, Germany
G. Geloni, S. Serkez, T. Tanikawa, EuXFEL, Schenefeld, Germany
W. Hillert, University of Hamburg, Hamburg, Germany

Abstract

The spectral and temporal properties of Free-Electron Lasers (FEL) operating on the basis of self-amplified spontaneous emission (SASE) suffer from the stochastic behavior of the start-up process that fluctuates on a bunch-to-bunch basis. Several so-called "seeding"-techniques using external radiation fields to overcome this limitation have been proposed and demonstrated. The external seed is usually generated by high-power laser systems, which are not yet available with a sufficient laser pulse energy at the high repetition rates of superconducting FEL facilities. In this contribution we discuss several seeding schemes that lower the requirements for the used laser systems, enabling seeded operation at high repetition rates by the means of a resonator-amplifier setup.

INTRODUCTION

Recently, more and more FEL facilities worldwide have been built to meet the risen number of photon scientists' experiments. The first of those facilities is FLASH, the Free-Electron Laser in Hamburg [1, 2]. Many facilities use the self-amplification by stimulated emission of radiation (SASE) principle, which suffers from poor temporal and spectral properties due to the stochastic behavior of the start-up process.

Several seeding techniques [3] have been experimentally studied, from the direct-seeding approach, e.g. using High-Harmonic Generation (HHG) [4] to phase-space manipulation techniques like High-Gain Harmonic Generation (HGHG) [5–7] or Echo-Enabled Harmonic Generation (EEHG) [8, 9] using external laser fields, which are currently limited in target wavelength and repetition rate. For FLASH, the future use of these techniques is currently under study [10, 11] as well as for the European X-Ray Free-Electron Laser (EuXFEL) [12].

In contrast to the aforementioned laser-based seeding chemes, methods like active spectral filtering of SASE radiation allow for amplification of radiation without the need of an external seed laser, thus they are working at any wavelength or repetition rate and are not in the scope of this contribution.

Motivation

Most of the seeding techniques rely on the availability of laser systems with high power, short wavelengths, and high peak intensities. For the typical burst repetition rates of free-electron lasers driven by superconducting linear accelerators - 4.5 MHz at EuXFEL or 1.003 MHz at FLASH - and depending on the power needed, such laser systems are not easily available. A reduction in the repetition rate of the photon burst is sometimes not desired, as for the usual diluted samples a large number of FEL pulses is needed to get sufficient statistics. Some photon science experiments however only use a fraction of this repetition rate like time-of-flight measurements with typical timescales of several µs.

In the past, resonators at low-gain FELs have been investigated using time-independent simulation codes [13–16]. Recently, also some studies taking advantage of time-dependent and three-dimensional simulation codes have been performed [17]. The idea of building an optical cavity around an undulator at FLASH has also already been studied [18].

The usage of a resonator-amplifier setup for a seeded FEL is a promising approach to reach short wavelengths at the high repetition-rates of superconducting linear accelerators - reaching the water window at around 4 nm using HGHG seeding and 1 nm using EEHG.

First simulations relying upon a resonator setup to drive an High-Gain Harmonic-Generation seeded FEL operating at the 10th harmonic for operating parameters in the FLASH parameter range are currently being conducted, showing promising results [19].

BASIC SETUP

An electron bunch generates radiation, either directly seeded or by the spontaneous undulator radiation, in an undulator called modulator. This modulator can consist of several undulator modules. Its main purpose is to imprint an energy modulation onto the electron bunch. The radiation is reflected by mirrors, then stretched and slightly monochromatized by a grating, and focused in the modulator again where it is overlapped with the next electron bunch. This set of hardware components is called resonator and can be seen in Fig.1. Eventually, after several fresh bunches, an equilibrium state will be reached where the radiation losses over a round trip are compensated by the generation of radiation in the modulator. The electron bunches can then be used in the different seeding schemes exploiting their beneficial longitudinal electron density distribution.

* sven.ackermann@desy.de

Content from this work may be used under the terms of the CC BY 3.0 licence (© 2019). Any distribution of this work must maintain attribution to the author(s), title of the work, publisher, and DOI

ISBN: 978-3-95450-210-3 doi:10.18429/JACoW-FEL2019-TUP074

FLASH UPGRADE FOR SEEDING *

V. Grattoni†, B. Faatz, G. Paraskaki, S. Ackermann, C. Lechner, J. Zemella,
M. M. Kazemi, T. Lang, DESY, Hamburg, Germany
W. Hillert, University of Hamburg, Hamburg, Germany

Abstract

An upgrade for FLASH, the SASE FEL in Hamburg, is planned after 2020 aiming at fulfilling user requirements like fully coherent, variable polarization, and multi-colour pulses. In this proceeding, we focus on the FLASH1 beamline that will be operated in seeded mode at a high repetition rate. In particular, we will present and discuss the proposed seeding schemes for delivering FEL radiation with wavelengths from 60 down to 4 nm.

INTRODUCTION

FLASH is the free-electron laser in DESY, Hamburg [1]. It has three beamlines: FLASH1, FLASH2 and FLASH-Forward, and the maximum number of bunches per second for user experiments is 5000 shared amongst the beamlines thanks to the long flat top of the RF-Voltages enabled by the TESLA cavities. The various beamlines can share the produced bunches, in fact, simultaneous operation between FLASH1 and either FLASH2 or FLASHForward is possible [2] thanks to a kicker septum placed in front of the FLASH2 beamline. Also, seeding techniques are studied at sFLASH that is placed upstream of the FLASH1 undulator. The current status of the sFLASH project is discussed in [3]. At the moment the HGHG seeded radiation is operated at 10 Hz, which corresponds to the repetition rate of the current seed laser so that the potential of FLASH is only partially exploited. In addition, the radiation is not accessible by the users of the FLASH1 experimental hall. But, using the FLASH1 undulator as radiator for seeding is not a solution, because the transport of the bunched electron beam from the second sFLASH chicane to the undulator is challenging and saturation is reached before the end of the undulator [4]. The foreseen FLASH upgrade [5] is going to dedicate FLASH1 as a seeding beamline for user delivery at wavelengths spanning from 60 down to 4 nm and increase the repetition rate for seeding operation to 100 kHz in a first stage, and then to 1 MHz by the implementation of an innovative seed laser scheme.
In this contribution, the main details of the seeding upgrade and preliminary start-to-end simulation results are presented.

FLASH UPGRADE OVERVIEW

The upgrade plans of the FLASH facility are described in Ref. [5]. It includes a laser heater, an energy increase from 1.25 to 1.35 GeV and a redesign of the bunch compressors [6]. A modification of FLASH2 is planned to allow for more advanced FEL schemes like multi-colour and attosecond pulses [7]. As mentioned in the introduction, FLASH1 will be devoted to seeding, delivering FEL radiation with a wavelengths between 60 and 4 nm. Figure 1 shows a scheme of the designed FLASH1 beamline. It consists of two modulators and one radiator, the first modulator is followed by a magnetic chicane with maximum longitudinal dispersion of 25 mm, enabling EEHG operation at the n=-1 working point even at the shortest wavelength (4 nm). A second chicane is installed before the radiator, with a foreseen maximum dispersion of 300 µm and it will be used as bunching chicane for both EEHG and HGHG. The current FLASH1 fixed gap undulators are going to be replaced by variable gap helical undulators. The detailed undulator parameter are going to be presented in the next section. So far, fixed gap undulators in FLASH1 has limited FLASH2 operation, as for every wavelength change it is also necessary to change the electron beam energy. With this upgrade, the machine will be operated at two fixed electron beam energies: 750 MeV and 1.35 GeV to reach all design wavelengths. This will significantly ease wavelength changes. Three seed laser options are under study for FLASH1: two are in the ultra-violet (UV) range and one in the visible in the range 413-480 nm. The UV seed laser in one case is the result of a cascaded process with final wavelength range 294-327 nm, in the other case it is the third harmonic of the seed source resulting in the range 230-300 nm, but it has a much lower energy. For this reason, in this and previous studies (see [8]) only the VIS option and the UV option in the range 294-327 nm are studied.

UNDULATOR PARAMETERS AND TUNABILITY

The undulators foreseen for the radiator section are APPLE III type with variable polarization and gap (with minimum gap 8 mm). The undulator has a period λ_u of 33 mm, and a total length of 2.5 m. This undulator enables wavelengths from 60 to 20 nm within the e-beam energy of 750 MeV and wavelengths from 20 to 4 nm at 1.35 GeV.
For the external seeding schemes, also seed laser tunability should be considered. The UV seed laser gives a continuous tunability starting from FEL wavelengths of 36.4 nm and shorter, but for longer wavelengths there are gaps as shown in fig. 2. While the VIS seed gives a continuous tunability for the whole FEL wavelength range of interest. Up to the 12th harmonic FEL radiation will be generated using the HGHG scheme by enabling only one of the two modulators and seed lasers. In fact, this harmonic is the lowest one rou-

* Work supported by the Federal Ministry of Education and Research of Germany within FSP-302 under FKZ 05K13GU4, 05K13PE3, and 05K16PEA and the German Research Foundation within GrK 1355.
† vanessa.grattoni@desy.de

Content from this work may be used under the terms of the CC BY 3.0 licence (© 2019). Any distribution of this work must maintain attribution to the author(s), title of the work, publisher, and DOI

ISBN: 978-3-95450-210-3 doi:10.18429/JACoW-FEL2019-TUP076

Content from this work may be used under the terms of the CC BY 3.0 licence (© 2019). Any distribution of this work must maintain attribution to the author(s), title of the work, publisher, and DOI

SEEDING R&D AT sFLASH*

C. Lechner†, S. Ackermann, R. W. Assmann, B. Faatz, V. Grattoni,
I. Hartl, S. D. Hartwell, R. Ivanov, M. M. Kazemi, T. Laarmann, T. Lang, G. Paraskaki,
A. Przystawik, J. Zheng, DESY, Hamburg, Germany
S. Khan, DELTA, TU Dortmund University, Dortmund, Germany
A. Azima, H. Biss, M. Drescher, W. Hillert,
V. Miltchev, J. Rossbach, University of Hamburg, Hamburg, Germany

Abstract

Free-electron lasers (FELs) based on the self-amplified spontaneous emission (SASE) principle generate photon pulses with typically poor longitudinal coherence. FEL seeding techniques greatly improve longitudinal coherence by initiating FEL amplification in a controlled way using coherent light pulses. The sFLASH experiment installed at the FEL user facility FLASH at DESY in Hamburg is dedicated to the study of external seeding techniques. In this paper, the layout of the sFLASH seeding experiment is presented and an overview of recent developments is given.

INTRODUCTION

The exponential amplification process in soft and hard x-ray free-electron lasers (FELs) is typically initiated by spontaneous undulator radiation generated by the high-brightness electron bunches at the beginning of the undulator. This stochastic start-up of FELs based on the self-amplified spontaneous emission (SASE) principle results in poor longitudinal coherence.

In the seeded mode of operation, the FEL amplification process is initiated by coherent light pulses generated in an external source. At sFLASH, the high-gain harmonic generation (HGHG) [1] seeding scheme is employed.

The seeding experiment sFLASH is installed in the FLASH1 beamline of the FEL user facility FLASH [2], which has been in user operation since 2005 [3], now delivering SASE FEL radiation down to 4.1 nm [4]. The superconducting linear accelerator of the FLASH facility can generate a maximum of 5000 electron bunches per second for user experiments, which can be distributed between the beamlines FLASH1 and FLASH2 or the plasma wakefield acceleration experiment FLASHForward [5] using a flat-top kicker and a Lambertson DC septum [2], enabling flexible parallel operation of the beamlines [6–8].

THE sFLASH EXPERIMENT

The essential components of the seeding experiment sFLASH are shown in Fig. 1, their parameters are listed in Tab. 1. The electron bunches arriving from the energy collimation section of the FLASH1 electron beamline can interact with ultraviolet seed pulses in two electromagnetic wigglers [9] (M_1 and M_2 in Fig. 1). After each of these so-called modulators, a four-dipole chicane is installed (C_1 and C_2). For HGHG-seeded FEL operation, modulator M_2 and chicane C_2 are used. The seeded electron bunches then enter the 10-meter-long variable-gap radiator system [10] where FEL emission at the desired harmonic takes place. After extraction from the electron beamline, the generated light pulses are either transported to the in-tunnel photon diagnostics (photon energy detectors; Ce:YAG fluorescence screens; spectrometer with $\lambda/\Delta\lambda \approx 500$) or to a photon diagnostics laboratory outside of the accelerator tunnel. There, the seeded FEL pulses can be analyzed in a THz streaking [11] setup by overlapping them with the THz field from a source driven by the seed laser system. At a second beamline in the photon diagnostics laboratory, a reflective extreme ultraviolet (XUV) pulse shaper [12] is currently being set up.

The longitudinal phase-space distribution of the electron bunches is diagnosed by virtue of a transverse-deflecting

Table 1: Experimental Parameters

parameter	value
modulators	
period length	200 mm
number of periods	5
maximum K value	10.8
radiator	
number of modules	3 / 1
length of module	2 m / 4 m
period length	31.4 mm / 33 mm
maximum K value	2.72 / 3.03
chicanes	
R_{56} of C_1 (for HGHG)	0 µm
R_{56} of C_2 (for HGHG)	<150 µm
electron bunches	
beam energy	680 – 700 MeV
typ. peak current	0.6 kA
bunch charge	0.4 nC
bunch duration	>500 fs (fwhm)
seed laser pulses	
UV wavelength (seed 1/2)	269 nm/270 nm
UV pulse energy	0.40 – 0.50 mJ
approx. UV pulse duration	100 – 400 fs (fwhm)
approx. NIR pulse duration	40 – 50 fs (fwhm)

* Work supported by Federal Ministry of Education and Research of Germany under contract No. 05K13GU4, 05K13PE3, and 05K16PEA.
† christoph.lechner@desy.de

ISBN: 978-3-95450-210-3 doi:10.18429/JACoW-FEL2019-TUP077

STUDY OF A SEEDED OSCILLATOR-AMPLIFIER

G. Paraskaki*, S. Ackermann, B. Faatz, V. Grattoni, C. Lechner, M. Mehrjoo, DESY, Hamburg
G. Geloni, S. Serkez, T. Tanikawa, EuXFEL, Schenefeld
W. Hillert, University of Hamburg, Hamburg

Abstract

In recent years, there is interest of the Free-Electron Laser (FEL) community in external-seeding techniques such as the Echo-Enabled Harmonic Generation (EEHG) and the High-Gain Harmonic Generation (HGHG). With these techniques, pulses of an improved temporal coherence are generated, but at the same time, they are limited by the repetition rates that seed lasers can currently offer with the required pulse energies. A big challenge is to combine the advantages of seeding schemes with high repetition rates. For this purpose, we study a combination of an oscillator-amplifier. The modulator in the oscillator is used at a long wavelength to modulate the electron beam and an amplifier is operated to extract the FEL radiation of the desired harmonic. This way we can use a seed laser of 10 Hz in a burst mode and a resonator to feedback the radiation at repetition rates of superconducting accelerators instead of using an external seed at these high-repetition rates. In this contribution, we present simulation results of a seeded oscillator-amplifier FEL in an HGHG scheme.

INTRODUCTION

For over ten years, SASE FELs have been delivering radiation to users in XUV and X-ray wavelength range [1]. Wavelengths from 100 nm down to below 0.1 nm have been achieved with 100 to several thousand pulses per second. In more recent years, several user facilities have improved the radiation properties by using different seeding schemes, mostly external seeding [2–4] and self-seeding at shorter wavelengths [5]. The next development that is planned is to go towards continuous wave (CW)-operation with superconducting accelerator technology, thus increasing the number of pulses per second to a million [6, 7]. A big challenge is to improve the radiation properties at high repetition rates and at short wavelengths simultaneously. Present schemes that use an external laser are investigating the possibility to work with superconducting machines such as FLASH and XFEL which could reach repetition rates of 1 MHz and 4.5 MHz respectively.

A system of an oscillator-amplifier has been studied in the past [8–11] and more recently as a high-gain oscillator with time-dependent three-dimensional simulations [12, 13]. The system was successfully studied up to the third harmonic of the initial frequency and, in all cases, the process was starting by amplifying the initial shot noise. It should be noted that since the initial studies the mirror and laser technology have been improved and at the same time, the simulation codes have been further developed allowing a more systematic and detailed study.

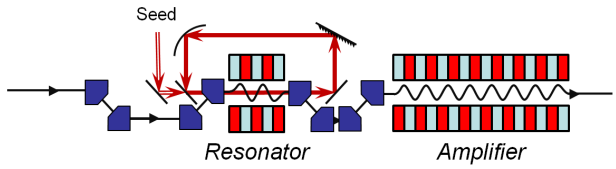


Figure 1: A possible design for the implementation of an HGHG seeded Oscillator-Amplifier.

THE LAYOUT

High-Gain Harmonic Generation [14] is a seeding scheme that is normally realized in a single-stage. In this process, the electron beam energy is modulated with a seed laser in the modulator, which is an undulator tuned to be resonant with the frequency of the seed laser. The energy modulation is converted into a density modulation in a dispersive section of a longitudinal dispersion R_{56}. After achieving the required density modulation for the desired harmonic of the seed laser, the electrons enter the radiator which is tuned to be resonant with the chosen harmonic of the seed laser. This scheme is aiming at fully coherent FEL radiation.

The layout under study is shown in Fig. 1. The process of a seeded oscillator-based HGHG, which will be referred to as a "multi-pass HGHG" in this contribution, is following the same principles of a "single-pass HGHG". The electron and the laser beam interact along the modulator to achieve energy modulation. Even though the energy modulation required can be achieved in a short distance, such as 2 gain lengths [14], in this case we use a longer undulator to achieve higher gain and compensate for the cavity losses. The radiation generated in one pass along the modulator is following the optical elements of the cavity and is redirected back to the beginning of the modulator for the next pass. The length of the cavity must be such that the roundtrip time of the radiation after travelling one time within the cavity is synchronised with the bunch separation. The cavity can in principle consist of simple transportation mirrors. Additionally, a monochromator (grating) and a focusing mirror can be added. Diagnostics could also be installed along this photon beamline for further control. The electron beam, after leaving the modulator, is guided to the next section through the bunching chicane. Finally, it generates radiation at a harmonic of the modulator wavelength in the amplifier.

In our studied cases, the FEL process starts with a seed laser of 300 nm or 50 nm. For the ultraviolet (UV) seed laser, a regular seed laser could be used to initiate the process,

* georgia.paraskaki@desy.de

Content from this work may be used under the terms of the CC BY 3.0 licence (© 2019). Any distribution of this work must maintain attribution to the author(s), title of the work, publisher, and DOI

ISBN: 978-3-95450-210-3 doi:10.18429/JACoW-FEL2019-TUP078

Content from this work may be used under the terms of the CC BY 3.0 licence (© 2019). Any distribution of this work must maintain attribution to the author(s), title of the work, publisher, and DOI

IMPACT OF ELECTRON BEAM ENERGY CHIRP ON SEEDED FELS

G. Paraskaki*, S. Ackermann, B. Faatz, V. Grattoni,
C. Lechner, J. Zemella, DESY, Hamburg, Germany
W. Hillert, University of Hamburg, Hamburg, Germany

Abstract

Seeded FELs enable the generation of fully coherent, transform-limited and high brightness FEL pulses, as the start-up process is driven by an external coherent light pulse. During the design process of such FELs, it is important to choose carefully the electron beam parameters to guarantee high performance. One of those parameters is the electron beam energy chirp. In this contribution, we show simulation results and we discuss how the electron beam energy chirp affects the final spectrum.

INTRODUCTION

It is a quite common choice to study seeding techniques with an electron beam that has a relatively constant current, as far as this can be realistic, and is unchirped with a temporally constant energy. An energy chirp would possibly degrade the performance of the FEL since it might affect the density modulation efficiency and in addition, it shifts the central wavelength of the output radiation [1]. At the same time, in SASE FELs, it has been shown that a slightly positive chirp may be beneficial [2]. In seeded FELs, the energy chirp has already been proposed as a method to distinguish the signal of Echo-Enabled Harmonic Generation (EEHG) from High-gain Harmonic Generation (HGHG) for low harmonics [3], and as a method to produce two-color lasing as well [4]. In addition, it can be used as an FEL-chirp control technique [5, 6], since there is a correlation between the energy of the electron beam and the frequency of the FEL pulse that is defined through the resonance condition. Finally, the performance of EEHG with a chirped electron beam has been evaluated [7] for future designs.

In this contribution, we study the impact of a linear electron beam energy chirp of variable amplitude and sign on the HGHG-seeded FEL. More specifically, the wavelength shift and the impact on intensity and bandwidth are discussed and presented with simulation results. The optimum working points are determined and their stability is compared under an electron beam energy jitter and timing jitter study.

IMPACT ON HGHG

Wavelength Shift

The essential components for HGHG are a modulator in which the seed laser interacts with the electron beam and induces electron beam energy modulation, a dispersive section in which the energy modulation is converted into density modulation and a radiator that is resonant with the wavelength of the wanted harmonic of the seed laser [8]. For a better understanding of the effect of an energy chirp on the dispersive section that is used for the creation of density modulation in HGHG, it is useful to recall the process of bunch compressors. Bunch compressors (BCs) are sections with longitudinal dispersion R_{56} that are used to compress an electron beam temporally, usually to achieve a higher peak current and shorter FEL pulses. For an effective compression, the electron beam needs to travel in the dispersive section with, for instance, a linear energy chirp $h = \frac{dE}{ds}\frac{1}{E}$. This can be expressed mathematically as:

$$\delta = \delta_0 + hs_i + h's_i^2 + O(s^3),$$

where δ the is the relative energy offset, δ_0 represents the uncorrelated energy offset, s_i is the initial longitudinal intrabunch coordinate within the bunch and $h' = \frac{d^2E}{ds^2}\frac{1}{E}$. A chirp with a positive sign represents an electron bunch with a head of higher energy and a tail of lower energy. In this contribution, we restrict ourselves to a linear energy chirp h. An electron of an energy offset δ would exit a BC of a longitudinal dispersion R_{56} with a new longitudinal coordinate [9]:

$$s_f = s_i + R_{56}\delta = s_i(1 + hR_{56}) + R_{56}\delta_0.$$

Therefore, after differentiating, we get the linear compression factor:

$$C_{BC} = \frac{ds_i}{ds_f} = (1 + h \cdot R_{56})^{-1}. \quad (1)$$

In the case of HGHG, the dispersive section converts the energy modulation to density modulation by forming microbunches with a longitudinal periodicity that is equal to the wavelength of the seed laser. However, if the electron beam is chirped, the periodicity will be affected by the compression/decompression that takes place due to Eq. (1). This is illustrated schematically in Fig. 1. The compression factor of the wavelength of the FEL radiation would be [10]:

$$C_{HGHG} = \frac{\lambda_{HGHG}}{\lambda'_{HGHG}} = (1 + H \cdot B)^{-1}, \quad (2)$$

where $H \cdot B \propto h \cdot R_{56}$ [10]. This result is analogous to the derived formula of Eq. (1) for bunch compression.

* georgia.paraskaki@desy.de

ISBN: 978-3-95450-210-3 doi:10.18429/JACoW-FEL2019-TUP079

STATUS OF THE HARD X-RAY SELF-SEEDING SETUP AT THE EUROPEAN XFEL

G. Geloni, X. Dong, S. Karabekyan, D. La Civita, L. Samoylova, S. Serkez, R. Shayduk, H. Sinn, V. Sleziona, M. Vannoni, M. Yakopov, European XFEL, Schenefeld, Germany
J. Anton, S. Kearney and D. Shu, ANL, Argonne, Illinois, United States
W. Decking, V. Kocharyan, S. Liu, E. Negodin, E. Saldin, T. Wohlenberg, DESY, Hamburg, Germany
V. D. Blank, S. Terentiev, TISNCM, Troitsk, Russia

Abstract

A Hard X-Ray Self-Seeding (HXRSS) setup will be soon commissioned at the European XFEL. It relies on a two-chicanes scheme to deal, in particular, with the high pulse repetition rate of the facility. In this contribution we review the physics choices made at the design stage and the expected performance of the setup. We will also focus on the description of the hardware installations made at the SASE2 line of the European XFEL.

INTRODUCTION AND SETUP

Single crystal monochromator Hard X-ray Self-Seeding (HXRSS) [1, 2] allows for an increased spectral density and longitudinal coherence at hard X-ray SASE FELs by means of active spectral filtering. This capability is now being enabled at the European XFEL, where the compatibility with the high-repetition rate in burst mode is important and heat-loading of the crystals needs to be dealt with. This issue can be mitigated with the introduction of a two-chicane HXRSS setup, Fig. 1. As shown in [3], and reviewed here, a two-chicane solution allows for an increased Signal-to-Noise Ratio (SNR), the signal being the seeded FEL pulse, and the noise being, in this case, the underlying shot-noise amplification. The natural exploitation of this increased ratio is for decreasing the crystals heat loading, while keeping the seed signal large enough for the setup to work. One should consider that there are two sources of heat-load on the crystals: one is related to radiation around the undulator resonant frequency (both SASE and seeded signals), which tends to heat-up the crystal as illustrated in Fig. 2, while the second one is related to the broadband spontaneous emission. One always needs to confront with the spontaneous radiation (SR) heat-load, which is always present and is nearly independent of the fundamental tune. However, a higher SNR of the 2-stage self-seeding can be used to decrease the FEL power level needed at the crystal position, and therefore the crystal heat-load caused by FEL radiation. Since the heat-load due to both FEL and SR heavily depends on the wavelength, the relative importance of the two contributions also depends on the wavelength.

In this paper we will first discuss simulation results relying on start-to-end simulations of the electron beam that drives the FEL process. We stress that a comparison between the simulated electron beam properties and those achieved in reality is important. First, to precisely foresee the actual performance of the HXRSS setup at the European XFEL and, second, to optimize performance by changing the electron beam properties. This, however, will require an ad-hoc experimental measurements campaign and is beyond the scope of this work.

Furter on, based on simulations we will show the nominal performance of the HXRSS setup designed for the European XFEL, which is expected to operate from below 5 keV (theoretically down to 3 keV, with probable limitations due to heat-loading) up to 14.4 keV (and above, if one considers the option of tuning part of the radiator to a harmonic of the fundamental [4]). Finally, we will discuss the hardware implementation of the setup at the European XFEL.

SIMULATIONS

We first consider an upper target for seeding of a photon energy of 14.4 keV, to be generated at the SASE2 undulator at the European XFEL. SASE2 consists of 35 segments of 5 m magnetic length each, with a period of 40 mm, and we assume a 100 pC beam optimized for seeding, as described in [3]. The 14.4 keV energy point is the most demanding in terms of electron beam quality and necessary undulator length, and its analysis allows to optimize the chicane

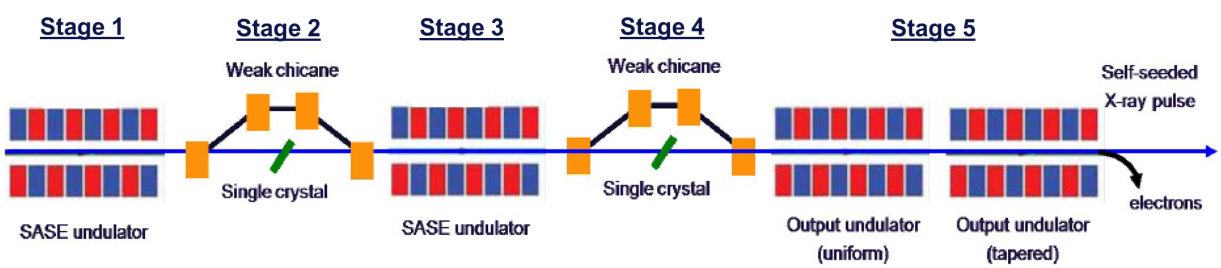


Figure 1: Sketch of the two-chicane HXRSS at the European XFEL.

Content from this work may be used under the terms of the CC BY 3.0 licence (© 2019). Any distribution of this work must maintain attribution to the author(s), title of the work, publisher, and DOI

ISBN: 978-3-95450-210-3 doi:10.18429/JACoW-FEL2019-TUP080

HARMONIC OFF-AXIS SEEDING AT THE DELTA SHORT-PULSE SOURCE*

A. Meyer auf der Heide†, B. Büsing, S. Khan, D. Krieg, C. Mai
Center for Synchrotron Radiation (DELTA), TU Dortmund, Dortmund, Germany

Abstract

At the 1.5-GeV synchrotron light source DELTA operated by the TU Dortmund University, a short-pulse source employs the coherent harmonic generation (CHG) scheme. Here, a laser pulse interacts with a stored electron bunch forming a microbunching structure to generate ultrashort synchrotron light pulses at harmonics of the laser wavelength. As an upgrade of the short-pulse facility, the echo-enabled harmonic generation (EEHG) scheme will be implemented, which requires a second laser-electron interaction to yield much higher harmonics compared to CHG. In a study towards twofold laser seeding, the possibility of seeding at undulator harmonics with a crossing angle between laser and electron beam was investigated.

THE DELTA SHORT-PULSE SOURCE

At DELTA, a 1.5-GeV synchrotron light source operated by the TU Dortmund University, a short-pulse source employs the coherent harmonic generation (CHG) scheme to generate ultrashort pulses in the vacuum ultraviolet (VUV) regime [1]. As depicted in Fig. 1 (top), the concept [2] is based on an interaction between an electron bunch and a co-propagating external ultrashort laser pulse in an undulator (modulator) which results in a sinusoidal modulation of the electron energy. In a following magnetic chicane, the energy modulation leads to a density distribution with the periodicity of the laser wavelength. While preserving the duration of the laser pulse, this microbunching structure gives rise to coherent emission in a second undulator (radiator) tuned to a harmonic of the laser wavelength.

In a planned upgrade, a more sophisticated seeding scheme known as echo-enabled harmonic generation (EEHG) [3] will be implemented at the DELTA short-pulse source [4]. This scheme comprises two laser-electron interactions in undulators (modulators), each followed by a magnetic chicane, as well as a third undulator (radiator). As shown in Fig. 1 (bottom), the strong chicane after the first energy modulation leads to stripes of small energy spread in longitudinal phase space. The second modulation and chicane converts the stripes to a density distribution with narrow structures resulting in the coherent emission of higher laser harmonics compared to the CHG scheme.

In addition to coherently emitted VUV pulses, the energy-dependent path length along the storage ring causes a longitudinal displacement of the modulated electrons leaving a sub-ps dip in the temporal charge distribution. Like an equally short bunch, the dip gives rise to coherent emission of THz radiation, which is detected at a dedicated beamline [5] and provides information on the quality of the laser-electron interaction. Temporal modulation of the seed pulse allows to control the THz spectrum, e.g., a periodically modulated laser pulse leads to narrowband emission [6, 7]. Currently, CHG is performed by seeding with 50-fs pulses from a Ti:sapphire laser system at a wavelength of either 800 or 400 nm and a repetition rate of 1 kHz. Experiments are usually performed with a single bunch in the storage ring at a maximum current of 20 mA and a revolution frequency of 2.6 MHz. Modulator and radiator are parts of an electromagnetic undulator with 250 mm period length and 7 periods each. Three rewired undulator periods between them are used as a chicane.

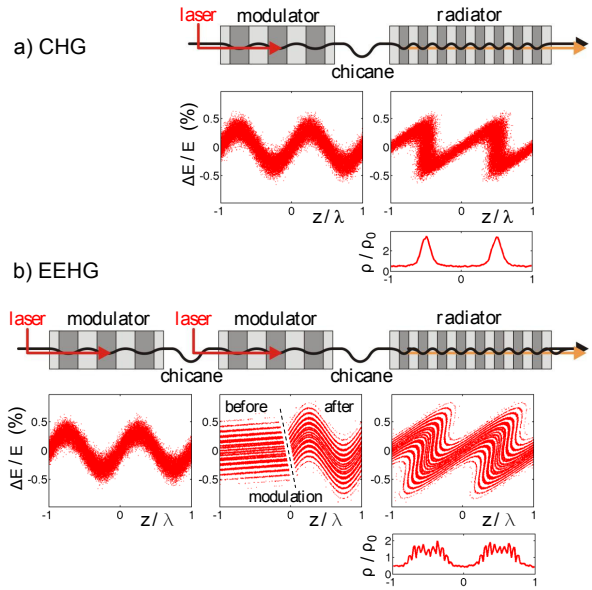


Figure 1: Top: Setup for CHG, corresponding longitudinal phase space distributions (energy deviation vs. longitudinal position) and final longitudinal electron density. Bottom: Setup for EEHG and corresponding distributions.

LASER ELECTRON INTERACTION

The change ΔE of the electron energy in the electric field $\vec{\mathcal{E}}_\mathrm{L} = (\mathcal{E}_\mathrm{L}, 0, 0)$ of the laser pulse with horizontal polarization is given by

$$\Delta E = -e \int \vec{\mathcal{E}}_\mathrm{L} \cdot \vec{v}\, dt = -e \int \mathcal{E}_\mathrm{L} \cdot v_x\, dt\,, \qquad (1)$$

where v_x is the horizontal component of the electron velocity $\vec{v}$ in a planar undulator. The key for an optimum energy

* Work supported by the BMBF (05K16PEA, 05K16PEB), MERCUR (Pr-2014-0047), DFG (INST 212/236-1 FUGG) and the state of NRW.
† arne.meyeraufderheide@tu-dortmund.de

Content from this work may be used under the terms of the CC BY 3.0 licence (© 2019). Any distribution of this work must maintain attribution to the author(s), title of the work, publisher, and DOI

ISBN: 978-3-95450-210-3 doi:10.18429/JACoW-FEL2019-TUP083

ENERGY SPREAD IMPACT ON HGHG AND EEHG FEL PULSE ENERGY

S. Spampinati†, E. Allaria, L. Giannessi[1], P. Rebernik Ribic[2],
Elettra - Sincrotrone Trieste S.C.p.A., Basovizza, Trieste
[1]also at ENEA C.R. Frascati, Rome, Italy
[2]also at University of Nova Gorica, Nova Gorica, Slovenia

Abstract

VUV and X-ray free electron lasers (FELs) require a very bright electron beam. Seeded FEL harmonic generation is particularly sensible to energy spread and slice energy spread can limit the highest harmonic conversion factor at which coherent radiation can be produced. Different cascade schemes can have different sensibility to the slice energy spread. At FERMI we have evaluated the impact of the slice energy spread on the performance of high gain harmonic generation (HGHG) and of echo enable harmonic generation (EEHG) by measuring the FEL pulse energy as function of the electron beam slice energy spread. The measurements were done at different harmonics. The slice energy spread was varied trough the laser heater located in the linac that drives FERMI.

INTRODUCTION

Facility based on X-ray and VUV free electron lasers (FELs) [1-7] permits to perform a wide class of experiments in physics and chemistry with implications in other fields such as biology.

Most of the existing FEL facilities [1, 2, 4-7] rely on the Self Amplified Spontanous Emission requiring a very bright electron beam characterized by high density in the 6-dimensional phase space implying high current, low transverse emittance and low energy spread [8]. Sensitivity to the energy spread is enhanced for seeded FELs [3]. The high current required by the FEL is obtained compressing the beam in one or more magnetic chicanes. Several collective effects can develop in the linac and in the bunch compressors spoiling the final beam quality and particular techniques have to be used to counteract these effects. Longitudinal microbunching instabilities MBI is one of the most relevant collective effect that can spoil the electron beam quality and the FEL performance [9].

To counteract MBI, linacs used to drive FELs are usually equipped with a laser heater located in the injector [10-12]. The laser heater consists of a short undulator located in a magnetic chicane where an external infrared laser pulse interacts with the electron beam. The increased energy spread can be adjusted to the right level to smear the density modulation in the bunch compressor and then dumping the MBI. Control of MBI and energy spread is particularly important for those seeded schemes based on frequency up conversion mechanisms used to produce highly coherent radiation at an harmonic of the seed.

In High gain harmonic generation (HGHG) [13, 14] an external laser is used to modulate the electron beam energy in a first undulator. This periodic energy modulation at the seed laser wavelength is then converted to current modulation, containing components at the harmonics of the seed. The bunched beam is then injected in a second undulator, tuned at one of the harmonics of the seed, where the coherent emission starts and is amplified by the FEL process. In order to produce a significant bunching the induced energy modulation has to overcome the natural slice energy spread of the beam, at the same time the final energy spread has to be small enough to allow FEL amplification. This makes the scheme very sensitive to energy spread and limit the maximum number of harmonic conversion to slightly more than 10.

A new seeded mechanism call echo enable harmonic generation (EEHG) was proposed [15, 16] and demonstrated on test facilities [17-19]. Recently EEHG has been extended in the soft x-ray down to 5nm in a series of tests done at FERMI [20].

In this work we report measurements performed during the EEHG experiment at FERMI aimed at evaluating the impact of the slice energy spread on the performance of EEHG. The experiment rely on measurements of the FEL pulse energy as function of the electron beam slice energy spread. The measurements were done at different harmonics. In several cases the behaviour of EEHG as a function of the slice energy spread has been compared with similar measurements done with the same beam using the HGHG scheme. The slice energy spread was varied trough the laser heater and the FEL properties were characterized using few different kind of detectors.

HGHG AND EEHG AT FERMI

The FERMI user facility is based upon two externally seeded FELs and covers the extreme ultraviolet (FEL-1) [3] and soft x-ray (FEL-2) [17]. Figure 1a shows the layout of FEL-2 line. FEL-2 is composed of two stage each one working according to the HGHG scheme described above. The seed of the first stage is provided by an external seed while the output of the first stage is used as seed for the second stage. The electron beam coming from the first stage is delayed by a magnetic chicane before entering in the second stage. The electron beam modulation in the second modulator and the FEL emission in the second stage occur now in a fresh part of the electron beam. Figure 1b shows EEHG scheme implemented in FEL-2 line [20]. The first dispersive section is switched off and the undulator segments of the first radiator are opened at a large gap to provide an almost null field on the axis. In the first modulator, the e-beam energy is modulated by the interaction with the first seed laser, as in HGHG. The

† simone.spampinati@elettra.eu

Content from this work may be used under the terms of the CC BY 3.0 licence (© 2019). Any distribution of this work must maintain attribution to the author(s), title of the work, publisher, and DOI

ISBN: 978-3-95450-210-3 doi:10.18429/JACoW-FEL2019-TUP087

START-TO-END SIMULATIONS OF THE REFLECTION HARD X-RAY SELF-SEEDING AT THE SHINE PROJECT *

Tao Liu†, Chao Feng, Xiaohao Dong
Shanghai Advanced Research Institute, Chinese Academy of Sciences, Shanghai 201210, China

Abstract

The Shanghai high repetition rate XFEL and extreme light Facility (SHINE) project is designed to produce fully coherent X-ray photons covering the photon energy from 3 keV to 25 keV. We have reported our FEL proposal and schemes in the hard X-ray regime which is self-seeding based on the crystal monochromator previously. Comparing to the transmission self-seeding scheme, the reflection one has several advantages and might be the base proposal. Start-to-end (S2E) simulations from the beam generation by Astra, the linac accelerating by Elegant to the FEL simulation by Genesis are performed. In this manuscript, the FEL simulations based on the S2E beam will be presented mainly. The results demonstrate the feasibility of the reflection hard X-ray self-seeding at the SHINE project.

INTRODUCTION

Hard X-ray self-seeding FEL scheme based on a crystal monochromator was proposed and has been demonstrated that it is a practicable method to generate a fully coherent hard X-ray pulse. Currently, transmission and reflection modes are considered each FEL facility worldwide. The transmission mode [1] has been adopted more popular, such as LCLS [2], PAL-XFEL and European XFEL. The reflection mode is also feasible which has been used and demonstrated successfully at SACLA [3].

Both of the line FEL-1 and FEL-3 at SHINE will work on hard X-ray self-seeding FEL schemes for covering 5-15 keV (nominal 3-25 keV). In the previous papers [4, 5], the transmission case and the reflection case have been proposed and discussed, where both of the advantages and disadvantages were presented and compared. In some degree, the reflection case shows a higher monochromatic efficiency, a lower heat-loading, better signal-to-noise ratio and higher pulse energy.

In this manuscript, we will present a start-to-end simulation results. The tracked electron beam generated by Astra [6], and accelerated and transported by Elegant [7], is used for generation of hard X-ray FEL by Genesis [8] with typical photon energy of 12.4 keV at the line FEL-1, where SASE, single-stage self-seeding and two-stage self-seeding configurations are carried out.

REFLECTION SELF-SEEDING

As shown in Fig. 1, the layout of a two-stage reflection self-seeding scheme is presented here. Adopting two-stage scheme, one can decrease the heat-loading on the crystal, enhance the monochromaticity, and correct the beam offset of the s-polarized reflection.

The magnetic field centre of the second undulator section will be adjusted according to the beam offset. The second monochromator with opposite direction can make the trajectory back to the initial one. However, this method does not work on the gap-fixed undulator.



Figure 1: Layout of the two-stage reflection hard X-ray self-seeding scheme at the SHINE.

The basic double-crystal monochromator is shown in Fig. 2, where the layout consists of a channel-cut crystal and a beam stopper. The beam stopper is pressed against the right edge of the forward crystal which is used to block the SASE pulse transmitting the crystal. Refer to the normal monochromator of the beam line, smaller Bragg angle is used for higher energy photon. Typically, the C111 symmetric diamond crystal can cover 5-15 keV energy photons in the range of 11.6-37 degree Bragg angles. The channel-cut gap D is assumed as 100 μm. For the 12.4 keV photon, the Bragg angle of C111 is 14.1 degree and then the induced time delay is 162 fs and the transverse offset is 194 μm.

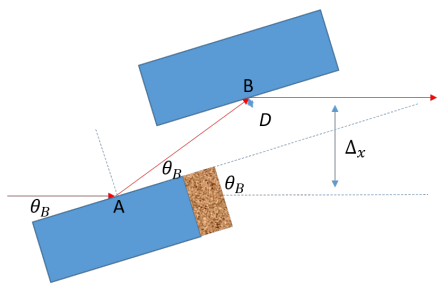


Figure 2: Reflection monochromator with double-crystal for self-seeding.

LINAC AND BEAM PARAMETERS

The schematic layout of the SHINE is shown in Fig. 3, which includes a 8 GeV accelerator and three FEL lines. In the baseline of the SHINE, an 100 MeV electron beam with 100 pC charge is generated in the photon-injector section and accelerated to 8 GeV at the exit of the linac. The peak current is more than 1500 A, the rms normalized slice emittance is less than 0.5 mm·mrad and the rms slice energy spread is less than 0.01%.

* Work supported by the National Natural Science Foundation of China Grant No. 11605277
† liutao@sinap.ac.cn;liutao@zjlab.org.cn

Content from this work may be used under the terms of the CC BY 3.0 licence (© 2019). Any distribution of this work must maintain attribution to the author(s), title of the work, publisher, and DOI

ISBN: 978-3-95450-210-3 doi:10.18429/JACoW-FEL2019-TUP088

NUMERICAL SIMULATIONS FOR GENERATING FULLY COHERENT SOFT X-RAY FREE ELECTRON LASERS WITH ULTRA-SHORT WAVELENGTH

K. S. Zhou†, H. X. Deng, B. Liu, D. Wang,
Shanghai Advanced Research Institute, Chinese Academy of Sciences, Shanghai, China

Abstract

For the fully coherent, ultra-short and high power soft x-rays are becoming key instruments in many different research fields, such as biology, chemistry or physics. However, it's hard to generate this kind of advanced light source by the conventional lasers, especially for the soft x-rays with ultra-short wavelength because of no suitable reflectors. The external seeded free electron laser (FEL) is considered as one feasible method. Here, we give an example to generate highly temporal coherent soft x-rays with the wavelength 1nm by the two-stage cascaded schemes. The external seeded scheme EEHG is used as the first-stage while the HGHG scheme is used as the second-stage.

INTRODUCTION

The SASE scheme, external seeded scheme and self-seeding scheme are three important methods for the high-gain free electron lasers (FEL). The SASE scheme is now the main method to generate X-ray FEL which has been successfully used in many facilities [1, 2, 3], however, the SASE scheme use the local shot noise of the electron beam which will cause a few spikes in the output spectrum. The external seeded scheme use the fully coherent conventional laser as the seed to modulate the electron beam, if the power of the seed laser are large enough to suppress the shot noise of the electron beam, the output radiation pulse will be fully coherent in principle [4, 5]. Self-seeding scheme is another way to generate the fully coherent radiation pulse, this scheme uses crystals to filter the radiation pulse from the upstream sections to get monochromatic seeding pulse for the downstream sections, however, the output radiation power and central wavelength may have larger shot-to-shot fluctuations than SASE scheme according to the experiment [6].

China will build a high-repetition rate of 1MHz FEL facility (SHINE) based on superconducting LINAC technology. According to the requirements of the users, three beam lines will be built at the first time (FEL-I, FEL-II and FEL-III), one of them (FEL-II) is designed to generate highly temporal coherent soft x-rays with the central wavelength 1nm.

To generate this kind of advanced light source, the two-stage cascaded EEHG/HGHG scheme with fresh bunch technology is chosen as the baseline for FEL-II, it is comprised of two stages while the First-stage is EEHG and the second stage is HGHG. The principle of HGHG was proved in 1990s [7] and it is currently adopted in FERMI FEL user facility. EEHG scheme can work at high harmonics of seeding lasers which is successfully demonstrated by NLCTA, SDUV and FERMI recently [8, 9, 10, 11].

LAYOUT AND DESCRIPTION

The layout of the two-stage cascaded EEHG/HGHG scheme for FEL-II is shown in Figure 1.

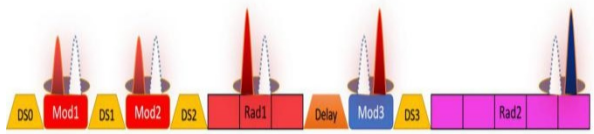


Figure 1: The layout of the two-stage cascaded scheme.

The first-stage EEHG is designed to generate 5nm fully coherent soft x-rays, the up-conversion harmonic number is 54 of 270nm seeding lasers, it has two modulators, two dispersion sections, and a long radiator. Then, the electron beam is delayed to interact with the radiation pulse from the first-stage, and the up-conversion harmonic number for the second-stage HGHG is 5, the second stage HGHG is comprised of one modulator, one dispersion section and a lone radiator. Finally, the highly temporal coherent 1nm soft x-ray is generated by the second long radiator.

The parameters of electron bunch from the output of LINAC for start-to-end simulations are given in Figure 2.

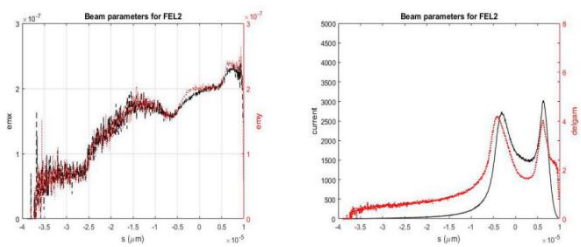


Figure 2: The emittance of x/y (left). The current and energy spread of electron bunch (right).

From Figure 2, one can find that the emittance for both sides x and y is lower than 0.3mm*mrad of the electron beam according to the first version from LINAC, and the peak current of the electron beam is larger than 1500A, besides , the energy of the electron beam is about 8GeV.

The lattice of the two-stage cascaded EEHG/HGHG scheme is given in Figure 3 based on the particle tracing program Elegant.

† zhoukaishang@sinap.ac.cn

Content from this work may be used under the terms of the CC BY 3.0 licence (© 2019). Any distribution of this work must maintain attribution to the author(s), title of the work, publisher, and DOI

ISBN: 978-3-95450-210-3 doi:10.18429/JACoW-FEL2019-TUP090

CONSIDERATIONS ON IMPLEMENTING EEHG WITH A STRONG LINEAR CHIRP

Mihai Pop*, Sverker Werin, Francesca Curbis,Weilun Quin
Physics department, Lund University, Lund, Sweden

ABSTRACT

Due to the stochastic nature of SASE radiation its longitudinal coherence is limited to a small fraction of the electron bunch. By pre-bunching the electrons before entering a radiator, the FEL radiation is ensured to have the same initial phase all through the bunch. Echo enabled harmonic generation (EEHG) is a technique that, by cleverly using two modulators and two dispersive sections, creates microbunches of electrons at a high harmonic of the seed laser used in the modulators. In this paper we will present some of the challenges of using this technique in combination with a strongly chirped beam and indicate a few ways to overcome said challenges.

INTRODUCTION

In a recent experiment [1], EEHG has been shown to be suitable as a high harmonic generation scheme with evidence of coherent radiation up to the 100th harmonic of a 260 nm UV laser.

The motivation for this work partly emerges in the wake of a bigger project to build a soft X-Ray FEL laser at MAX-IV the design would have account a large energy chirp of the electron beam at the Linac exit.

The scope of this paper is to have a better understanding of the effects of a strong linear chirp on the EEHG concept, not to give a definitive answer on using EEHG as a seeding method for SXL. For starters it is worth going through the classic EEHG process as proposed in [2].

The electron beam is modulated by having it co-propagate with a high intensity laser (Seed 1), in what is usually a strong insertion device Figure 1 Modulator 1. For long undulators with narrow gain bandwidth it is possible to have different modulation levels for different parts of the electron beam as electrons get off-resonance energies.

A strong dispersive section(in our case Chicane 1) folds the energy modulation of the electron bunch creating a fine structure of equally spaced energy slices. If the electron beam has a chirp, this element will either compress or de-compress the electron bunch depending on the combination of the chirp and dispersion sign.

To convert the fine energy separation into longitudinal bunching, a classic scheme involving a modulator (Figure 1 Modulator 2) and a weak dispersive section is used (Figure 1 Chicane 2).

In our analysis we use scaled notations as in [3] to have a feeling for the general phenomena rather than particular cases.

- **Scaled chirp** $Ch = \frac{\lambda_{mod1} Chirp[eV/m]}{2\pi\sigma_e}$. We can think of it as how many σ_e will the energy increase in one wavelength along the bunch.
- **Scaled Amplitude** $A_i = \frac{E-E_0}{\sigma_e}$. This parameter may be understood as the beam energy modulation amplitude in units of energy spread.
- **Scaled dispersion strength** $B_i = \frac{2\pi R56_i \cdot \sigma_e}{\lambda_{mod1} E_0}$. where $R56[m]$, is the normal momentum compaction factor. It is useful to think about B_i as the number of λ_{mod1} a particle with energy deviation of 1 σ_e is shifted w.r.t. a particle with reference energy.

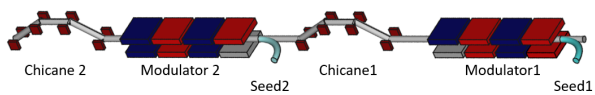


Figure 1: Layout of the EEHG scheme depicting the first modulator Modulator 1, the first dispersive section , in our case a chicane (Chicane 1), the second modulator Modulator 2, the second dispersive section, Chicane 2.

FEL SIMULATIONS

Common Settings

Simulations were carried out on LUNARC [4] using the FEL simulation code Genesis1.3 V4.3.1 with the *one4one* control parameter on, meaning that each electron is simulated as an individual particle. The layout used in simulations is similar to the one depicted in Figure 1. And it comprises of two identical modulators and two chicanes with positive momentum compaction $R_{56} > 0$. A summary of the electron beam and lattice parameters is show in Table 1.

All the simulations are based on the matching presented in Figure 2. The radiator is tuned to 5 nm and for the EEHG simulations the seed has the wavelength of 260 nm or 248 eV. As a test case we use a SASE run with 0.23 scaled (0.5 MeV/fs) energy chirp using the same radiator.

*mihai.pop@maxiv.lu.se

Content from this work may be used under the terms of the CC BY 3.0 licence (© 2019). Any distribution of this work must maintain attribution to the author(s), title of the work, publisher, and DOI

ISBN: 978-3-95450-210-3 doi:10.18429/JACoW-FEL2019-TUP091

START-TO-END SIMULATION OF THE NSRRC SEEDED VUV FEL

S. Y. Teng[1], C. H. Chen[2], W. K. Lau[2], A. P. Lee[2]
[1] Department of Physics, NTHU, Hsinchu, Taiwan
[2] NSRRC, Hsinchu, Taiwan

Abstract

A free electron laser (FEL) driven by a high brightness electron linac system has been proposed to generate ultrashort intense coherent radiation in the vacuum ultraviolet region. It is a third harmonic high-gain high harmonic generation (HGHG) FEL for generation of VUV radiation with wavelength at 66.7 nm from a 20 mm period length helical undulator. A 200 nm seed laser is used for beam energy modulation in a 10-periods helical undulator of 24 mm period length. A small chicane is placed between the two undulators to optimize power growth in the radiator. In this study, we perform start-to-end simulation to foresee the operational performance of the test facility and preliminary results are presented.

INTRODUCTION

The VUV FEL is a third harmonic HGHG FEL seeded by a 200 nm laser. The beam energy modulator is a 10-periods helical undulator with 24 mm period length. The radiator is also a helical undulator but of 20 mm period length which allows generation of high power coherent radiation at 66.7 nm wavelength [1]. Schematics of the NSRRC seeded VUV FEL is shown in Fig.1. The FEL is driven by a linac system that delivers a 100 pC, ~250 MeV high brightness electron beam. It is worth noting that a dogleg bunch compressor with linearization optics is used [2]. In this study, we perform simulation of beam dynamics in the proposed system starting from photoinjector cathode to FEL output. Space charge tracking in the photoinjector is done by GPT code [3], tracking of particles in the bunch compressor and linac systems is done by ELEGANT [4] and 3D time-dependent simulation of high gain FEL using GENESIS [5]. Data transfer between these two codes is done with SDDS [4].

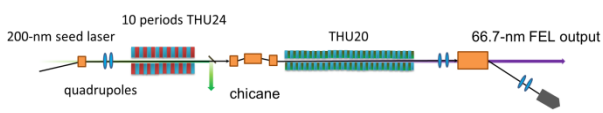


Figure 1: Schematics of the NSRRC third harmonic HGHG FEL.

Simulated drive beam properties by GPT and ELEGANT such as electron distribution in longitudinal phase space and beam current profile are summarized in the next section. The third section shows preliminary GENESIS simulation results of FEL interactions in modulator and radiator. The last section is the conclusions and summarized the direction for future study.

DRIVE BEAM

The bunch compressor designed for the driver is a double dog-leg configuration that provides a first order longitudinal dispersion function (i.e. R_{56}) and linearization optics for correction of nonlinearity introduced into the beam due to rf curvature. Bunch length or the peak current under various operation conditions can be adjusted by tuning R_{56}. It can be realized by changing the longitudinal positions of the outside dipoles of the dogleg compressor and by adjusting the quadrupoles and sextupoles. After bunch compression, the beam is accelerated to designed energy by two rf linac sections. In this simulation study, beam energy is at 263 MeV.

Electron Distribution in Longitudinal Phase Space

There is a residual energy chirp left after bunch compression. The beam is actually slightly over-compressed and the chirp is of ~42 keV/□m. This is tentatively corrected by a 1 m corrugated pipe dechirper structure [2]. Electron distribution of the dechirpered beam in longitudinal phase space at linac system exit is showed in Figure 2. Sliced energy spread in this case can be as low as 0.05%. In order to save tunnel space, dechirper using rectangular dielectric-lined waveguide is recently under study.

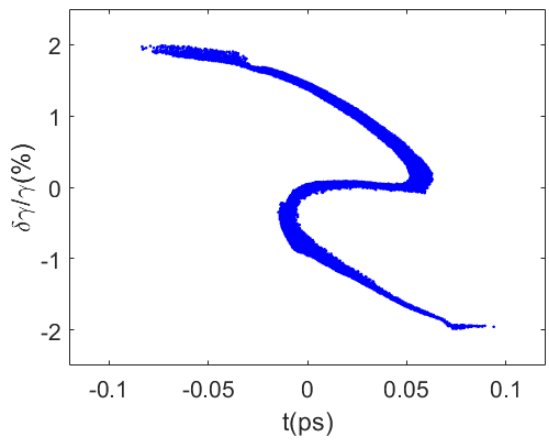


Figure 2: Electron distribution of the compressed beam in longitudinal phase space at linac system exit. Residual beam energy chirp is compensated by a 1 m corrugated pipe dechirper.

Beam Current Profile

After the dogleg bunch compressor, the 100 pC beam is compressed into 51 fs in duration so that the beam current profile is roughly uniform in the middle part. Fig. 3 shows

Content from this work may be used under the terms of the CC BY 3.0 licence (© 2019). Any distribution of this work must maintain attribution to the author(s), title of the work, publisher, and DOI

ISBN: 978-3-95450-210-3 doi:10.18429/JACoW-FEL2019-TUP092

XFEL THIRD HARMONIC STATISTICS MEASUREMENT AT LCLS

A. Halavanau, E. Hemsing, A. Lutman, C. Emma, G. Marcus, C. Pellegrini,
SLAC National Accelerator Laboratory, Stanford University, Menlo Park, USA

Abstract

We investigate the statistical properties of the 6 keV third harmonic XFEL radiation at 2 keV fundamental photon energy at LCLS. We performed third harmonic self-seeding in the hard X-ray self-seeding chicane and characterized the attained non-linear third harmonic spectrum. We compare theoretical predictions with experimental results.

INTRODUCTION

Third harmonic XFEL generation is often considered to be very useful for tripling the photon frequency in planar undulators. The odd harmonic wavelength on axis is given by

$$\lambda = \frac{\lambda_u}{2h\gamma^2}(1 + K^2/2). \quad (1)$$

where λ is the fundamental FEL radiation wavelength, λ_u is the undulator period with magnetic parameter K, $h = 3, 5, 7$ is the odd harmonic number. Initially, harmonics are evolving independently from the fundamental in the linear regime [1,2]. Very quickly, the linear regime is altered by the nonlinear bunching at the fundamental frequency, entering the nonlinear harmonic generation (NHG) regime [1–4]. Thus, most of the XFEL third harmonic power is generated in NHG regime, and is estimated to be a few percent level of the fundamental XFEL power [5].

It was shown, however, that harmonic power can be drastically increased by disrupting the fundamental, but letting third harmonic bunching continue to develop linearly. It can be done in numerous ways, e.g. introducing phase shifters to disrupt the fundamental, and/or by using frequency filters [2,3]. This process, known as "harmonic lasing", allows accessing high photon energies at much higher power level at existing XFEL facilities. It has been previously considered for LCLS-II operations in detail in [6]. Recently, harmonic lasing has been performed at DESY [3] and at Pohang Accelerator Laboratory [7] in EUV regime.

EXPERIMENTAL SETUP

In this proceeding, we study the possibility of using the LCLS hard X-ray self-seeding (HXRSS) chicane Diamond crystal as a frequency filter in an HXR harmonic lasing setup. The first experimental results were reported in [8]. Since the original LCLS HXR beamline did not have variable gap and phase-shifters, experimental demonstration of the harmonic lasing was challenging and it will be done when the new LCLS-II HXR undulator is available. Here we focus on analyzing recorded data for the NHG and third harmonic self-seeding processes.

Our experimental setup, presented in Fig. 1, generated 2 keV photons at fundamental in U1-U15 undulator section, and thereby produced 6 keV photons at the third harmonic. The LCLS pulse intensity was reduced by retracting first 3 undulators, to ensure a safe level of X-ray pulse energy absorbed by the diamond crystal. The generated non-linear third harmonic field was overlapped with the electron beam downstream of the HXRSS chicane, where the bunching at fundamental was removed. The Diamond crystal, while strongly absorbing the fundamental photon energy, propagated 6 keV photons with about 60 % attenuation. The LCLS HXR beamline experimental parameters are grouped in Table 1.

Table 1: LCLS HXR Beamline Parameters During the Measurements

Parameter	Units	Value
Pulse duration	fs	80
Pulse energy (xtal)	μJ	80
Fundamental	keV	2
Third harmonic	keV	6
Gain length	m	4.1
Beam current	kA	1800
Energy spread	MeV	2.0
Emittance (proj.)	μm	0.8

We registered the fundamental pulse energy with the gas intensity monitor and third harmonic spectra with a spectrometer. The data was then accumulated to provide spectral sums for the statistical analysis.

STATISTICAL PROPERTIES OF THE THIRD HARMONIC RADIATION

To derive the statistical properties of XFEL radiation at the fundamental frequency, we consider a chaotic ensemble of fully polarized sources [9]. It can be shown that a single mode probability density obeys negative exponential law:

$$p_1(I) = \frac{1}{\langle I \rangle} \exp\left(-\frac{I}{\langle I \rangle}\right). \quad (2)$$

Here I is the instantaneous single mode radiation intensity and $\langle I \rangle$ is its time average. Iteratively integrating using a convolution rule $p_2(W) = \int_0^W p_1(W - x)p_1(x)dx$, one



Figure 1: Experimental layout of XFEL third harmonic studies at LCLS.

Content from this work may be used under the terms of the CC BY 3.0 licence (© 2019). Any distribution of this work must maintain attribution to the author(s), title of the work, publisher, and DOI

ISBN: 978-3-95450-210-3 doi:10.18429/JACoW-FEL2019-TUD02

APPLICATION OF INFRARED FEL OSCILLATORS FOR PRODUCING ISOLATED ATTOSECOND X-RAY PULSES VIA HIGH-HARMONIC GENERATION IN RARE GASES

R. Hajima*, R. Nagai, K. Kawase,
National Institutes for Quantum and Radiological Science and Technology, Tokai, Ibaraki, Japan
H. Ohgaki, H. Zen,
Kyoto University, Uji, Kyoto, Japan
Y. Hayakawa, T. Sakai, Y. Sumitomo,
Nihon University, Funabashi, Chiba, Japan
M. Shimada, T. Miyajima,
High Energy Accelerator Research Organization, Tsukuba, Ibaraki, Japan

Abstract

High harmonic generation (HHG) in rare gases is now becoming a common technology to produce attosecond pulses in VUV wavelengths. So far HHG sources have been realized by femtosecond solid-state lasers, not FELs. We propose a FEL-driven HHG source to explore attosecond pulses at photon energies above 1 keV with a MHz-repetition, which is difficult with solid-state lasers. A research program has been funded to establish technologies for the FEL-HHG, which covers generation and characterization of few-cycle IR pulses in a FEL oscillator, stacking of FEL pulses in an external cavity, and a seed laser for stabilization of carrier-envelope phase in a FEL oscillator. In this paper, we present the scheme of FEL-HHG and the status of the research program.

INTRODUCTION

Recent development of solid-state laser technologies has realized a generation of isolated attosecond pulses in ultraviolet and X-ray wavelengths via high harmonic generation (HHG) in rare gas and solid-state targets [1]. As such attosecond photon sources are routinely available in laboratories, attosecond science is becoming an active research field, in which ultrafast dynamics in atoms and molecules is investigated in detail.

Combination of HHG and a free-electron laser (FEL) was examined at a SASE FEL, where a UV pulse from HHG was used as a seed laser to stabilize the shot-to-shot variation in spectrum and energy of the FEL pulses [2]. The experiment can be called HHG-seeded FEL or HHG-FEL. To the contrary, an optical pulse generated from an infrared FEL can be used, in principle, to drive HHG, that is FEL-HHG [3]. However, such an experiment has never been considered seriously.

In the present paper, we describe a research project towards the FEL-HHG to generate attosecond VUV and X-ray pulses from an infrared FEL oscillator.

* hajima.ryoichi@qst.go.jp

FEL-HHG

Advantage of FEL-HHG

There are several trends in the development of HHG photon sources. One of the major trends is increasing the photon energy (or decreasing the photon wavelength) available in HHG photon sources. The highest photon energy so far demonstrated is a generation of a bright supercontinuum that spans from the ultraviolet to more than 1.6 keV [4]. The experiment utilized a mid-infrared laser pulse, a wavelength of $\lambda = 3.9\ \mu m$, as a driver of HHG. Theoretical and experimental studies revealed that the HHG cut-off energy scales as $\lambda^{1.7}$ in the phase-matched condition [4]. Pushing the cut-off energy above 1.6 keV has not realized mainly due to the lack of mid-infrared laser pulses satisfying conditions for HHG, wavelength, pulse energy, pulse duration, and repetition. Thanks to wavelength tunability and high-repetition availability, a FEL oscillator is a potential driver of HHG photon sources complementary to conventional solid-state femtosecond lasers.

Few-Cycle Pulse Generation

Generation of isolated attosecond pulses from HHG is available in several schemes [5]. The simplest one is utilizing carrier-envelope-phase-stable (CEP-stable) few-cycle pulses as a driver of HHG.

In a FEL oscillator, few-cycle lasing has been studied experimentally and theoretically. In normal conducting linac FELs, few-cycle lasing was observed in a transient regime before the onset of saturation, when the FEL oscillator was operated at a small negative detuning of the cavity length [6]. This lasing behavior was analytically studied in the context of supermode theory and recognized as a multisupermode regime that occurs in the limit where all the supermodes converge toward a unique degenerate supermode [7]. After the onset of saturation, the lasing shifts to a chaotic regime and a few-cycle solitary pulse is no longer available.

Another type of few-cycle lasing appears in a FEL oscillator operated with a long macro pulse from a superconducting linac [8]. This steady-state few-cycle lasing is accompanied by high extraction efficiency and occurs at the condition of a

Content from this work may be used under the terms of the CC BY 3.0 licence (© 2019). Any distribution of this work must maintain attribution to the author(s), title of the work, publisher, and DOI

ISBN: 978-3-95450-210-3 doi:10.18429/JACoW-FEL2019-TUD03

FINE AND HYPERFINE STRUCTURE OF FEL EMISSION SPECTRA

V.V. Kubarev†, Ya.V. Getmanov, O.A. Shevchenko
Budker Institute of Nuclear Physics, Novosibirsk, Russian Federation
Y.U. Jeong, S.Y. Bae, Korea Atomic Energy Research Institute, Daejon, Republic of Korea

Abstract

This paper presents the results of experimental investigations of the fine and hyperfine spectral structures of the Novosibirsk free-electron laser (NovoFEL) and the compact free-electron laser of the Korea Atomic Energy Research Institute (KAERI FEL) by means of the optimal instruments, resonance Fabry-Perot interferometers. The very high coherence of the NovoFEL spectrum was measured in regimes with one pulse circulating inside its optical resonator (the coherence length is 7 km, and the relative width of the hyperfine structure lines is $2 \cdot 10^{-8}$) and with total absence of coherence between two circulating pulses, i.e. the fine structure.

Sixty pulses circulate simultaneously inside the KAERI FEL optical resonator, and the measured coherence length on average covers ten pulses (the coherence length is 1 m; the relative width of the fine structure lines is 10^{-4}).

INTRODUCTION

The spectrum of FEL radiation depends on its coherence. Practically all FELs radiate some sequence of short pulses, which are produced by pulse/pulses circulating inside the optical resonator and periodically fed by the electron beam. The spectral contour of the FEL radiation is determined by the intra-pulse coherence, which depends on fast radiation instabilities and their suppression. For example, two different types of fast side-band instabilities were observed in the terahertz NovoFEL. The instabilities, studied in works [1-3], can be fully suppressed due to detuning between the electron and light repetition frequencies. In such a stabilized regime, the contour of the NovoFEL laser line has a Gaussian form with a width equal to the Fourier-transform limit.

A fine structure of FEL radiation can appear in systems with many pulses inside an optical resonator due to certain coherence between the pulses, which is usually some technical feature of the FEL facility. It is clear that in common case, intra-cavity light pulses are physically independent because they neither overlap nor interfere with one another. However, on the other hand, the main feature of any laser is the tendency to generate coherent radiation. Such tendency can be realized if intra-cavity light pulses are linked with one another by means of electron beam, when the electron pulse density has a spike or front shorter than the radiation half wavelength. A fine structure of FEL radiation caused by coherency of intra-cavity pulses was observed earlier on the INEA [4], FELIX [5], and FLARE [6] FELs. In the paper we describe such effect on the KAERI FEL and its absence on the NovoFEL.

† V.V.Kubarev@inp.nsk.su

Finally, a hyperfine structure of FEL emission spectrum (optical resonator modes) is *a priory* present in all FELs with an optical resonator. In the simplest case of one radiation pulse inside an optical resonator, the output train of FEL light pulses is radiation of one and the same intra-cavity pulse, which is periodically partly outcoupled and coherently refreshed by the electron beam. It is clear that coherency of output pulses can be very high as coherency of radiation of any stationary laser. It depends on slow fluctuations in the active medium because the physical limit of quantum fluctuations, determined by the ratio of spontaneous and stimulated emissions (Schawlow-Townes limit), is very high. Thus, the subject of this investigation is the real value of hyperfine coherency or the average number of output coherent pulses. In the work, the value was exactly measured for the terahertz NovoFEL.

FEL FACILITIES

Compact KAERI FEL

A detailed description of the KAERI FEL is presented in papers [7-9]. The acceleration system of the installation includes the 6- to 7-MeV microtron with a current of 40 to 50 mA in a macropulse 5 to 6 μs long consisting of 2.8-GHz micropulses, as well as the electron-optical beam-line with bending magnets and quadrupole lenses. This beam-line connects the acceleration system with the radiation-source one. The radiation-source system includes the 2-m 80-pole planar electromagnetic undulator with a magnetic field of 4.5 to 6.8 kG and the optical resonator. A detailed description of the optical resonator and its optimization is given in [9].

The laser generation by the KAERI FEL takes place in the wavelength range of 110 to 160 μm. The macropulse and micropulse radiation power is 50 to 100 W and ~ 0.5 to 1 kW, respectively. The micropulse duration is about of 30 ps. The repetition frequency of macropulses is 1 Hz in the typical operation regime. The contour spectrum of the laser radiation is the main fundamental mode with FWHM = 1-2 % and a moderate admixture of two side-band modes with a total spectrum base width of 2-3 % [8].

The optical resonator of the KAERI FEL is a hybrid resonator open in the horizontal x direction. It has a Gauss-beam field distribution, set by the horizontal curvature of its mirrors. In the transverse vertical y direction, it is a planar waveguide resonator with an operational TE_1 mode formed by the waveguide parallel metallic surfaces, slid apart to a distance of 2 mm. In the KAERI FEL, the repetition frequency of electron bunches is fixed equal to the magnetron frequency of the microtron RF system (2.8 GHz). The radiation of the optical resonator is output through a circular hole with a diameter 0.75 mm in one of

Content from this work may be used under the terms of the CC BY 3.0 licence (© 2019). Any distribution of this work must maintain attribution to the author(s), title of the work, publisher, and DOI

ISBN: 978-3-95450-210-3 doi:10.18429/JACoW-FEL2019-TUD04

CAVITY-BASED FREE-ELECTRON LASER RESEARCH AND DEVELOPMENT: A JOINT ARGONNE NATIONAL LABORATORY AND SLAC NATIONAL LABORATORY COLLABORATION

G. Marcus, F.-J. Decker, G. L. Gassner, A. Halavanau, J. Hastings, Z. Huang, Y. Liu, J. MacArthur, R. Margraf, T. Raubenheimer, A Sakdinawat, T. Tan, D. Zhu, SLAC National Accelerator Laboratory, Menlo Park, CA 94025, USA
J. W. J. Anton, L. Assoufid, K. Goetze, W. Jansma, S. Kearney, K.-J. Kim, R. Lindberg, A. Miceli, X. Shi, D. Shu, Y. Shvyd'ko, J. P. Sullivan, M. White, Argonne National Laboratory, Argonne, IL 60439, USA
B. Lantz, Stanford University, Stanford, CA 94305, USA

Abstract

One solution for producing longitudinally coherent FEL pulses is to store and recirculate the output of an amplifier in an X-ray cavity so that the X-ray pulse can interact with following fresh electron bunches over many passes. The X-ray FEL oscillator (XFELO) and the X-ray regenerative amplifier FEL (XRAFEL) concepts use this technique and rely on the same fundamental ingredients to realize their full capability. Both schemes require a high repetition rate electron beam, an undulator to provide FEL gain, and an X-ray cavity to recirculate and monochromatize the radiation. The shared infrastructure, complementary performance characteristics, and potentially transformative FEL properties of the XFELO and XRAFEL have brought together a joint Argonne National Laboratory (ANL) and SLAC National Laboratory (SLAC) collaboration aimed at enabling these schemes at LCLS-II. We present plans to install a rectangular X-ray cavity in the LCLS-II undulator hall and perform experiments employing 2-bunch copper RF linac accelerated electron beams. This includes performing cavity ring-down measurements and 2-pass gain measurements for both the low-gain XFELO and the high-gain XRAFEL schemes.

INTRODUCTION

The incontrovertible success of the world's first hard X-ray free-electron laser (XFEL), LCLS [1], has led to a significant increase in the global FEL capacity. Additional facilities in Japan, Germany, Switzerland, Korea and China are either planned or are currently operating. These light sources, based primarily on Self-Amplified Spontaneous Emission (SASE) [2], are capable of producing extremely bright, transversely coherent, ultra-short X-ray pulses that have opened the door to new regimes of photon science [3, 4]. They have revolutionized the study of chemistry, physics, biology, and many other related fields of science and technology. Single-pass SASE FEL amplifiers, however, suffer from poor longitudinal coherence due to the stochastic nature of the start-up process. The improvement of the FEL longitudinal coherence and the ability to trade off peak power, average power, pulse duration, and bandwidth is of great practical importance [5].

Longitudinal coherence can be obtained by seeding an FEL amplifier with narrow bandwidth radiation well above the effective shot noise power in the electron beam. Examples of this include self-seeding [6, 7], which has been successfully implemented at LCLS in both the hard [8] and soft [9] X-ray spectral regions. Variations on this concept are also being studied [10, 11]. Self-seeding, however, nominally suffers from low seed power in an attempt to preserve the electron beam properties important for lasing and is fundamentally still dependent on the noisy SASE process leading to large (potentially 100%) seed power fluctuations.

Another leading candidate for obtaining longitudinal coherence leverages an X-ray cavity to monochromatize and store a fraction of a recirculating X-ray pulse so that it can interact with following fresh electron bunches over many passes. These so-called cavity-based X-ray free-electron lasers (CBXFELs) include the X-ray free-electron laser oscillator (XFELO) [12] and the X-ray regenerative amplifier free-electron laser (XRAFEL) [13]. In the past, these concepts were not feasible at X-ray FEL facilities because of the lack of high-reflectivity X-ray cavity mirrors and because of the limited repetition rate of the normal conducting technologies responsible for the production and acceleration of the electron bunches delivered to the undulator. The progress in achieving high-reflectivity diamond crystal mirrors in the hard x-ray regime [14–16] and in superconducting technology adopted by LCLS-II [17, 18] and LCLS-II-HE [19], however, will be capable of supporting steady-state repetition rates up to ~ 1 MHz, making the footprint of the recirculating optical cavity reasonable.

The XFELO and XRAFEL concepts rely on the same fundamental ingredients to realize their full capability. Each scheme requires a high repetition rate electron beam, an undulator to provide FEL gain, and an X-ray optical cavity to recirculate and monochromatize the X-ray radiation. While the XFELO and XRAFEL schemes share a common infrastructure, they target different but complementary FEL performance characteristics. The XFELO relies on a low-loss cavity supporting a low-gain FEL for ultra-narrow bandwidth while the XRAFEL leverages a high-gain FEL interaction that can support much larger radiation output coupling.

As an example of the difference between the two CBXFEL schemes, Table 1 shows a semi-qualitative comparison of operational characteristics while Table 2 shows the typical hard X-ray (HXR) performance characteristics that are ex-

Content from this work may be used under the terms of the CC BY 3.0 licence (© 2019). Any distribution of this work must maintain attribution to the author(s), title of the work, publisher, and DOI

ISBN: 978-3-95450-210-3 doi:10.18429/JACoW-FEL2019-TUT01

SUPERRADIANT AND STIMULATED-SUPERRADIANT EMISSION OF BUNCHED ELECTRON BEAMS

A. Gover, Tel-Aviv University, Tel-Aviv, Israel
R. Ianconescu, Tel-Aviv University, Tel-Aviv and Shenkar College, Ramat-Gan, Israel
Friedman, Ariel University, Ariel, Israel
C. Emma, N. Sudar, P. Musumeci and C. Pellegrini, UCLA, Los Angeles, CA, USA

Content from this work may be used under the terms of the CC BY 3.0 licence (© 2019). Any distribution of this work must maintain attribution to the author(s), title of the work, publisher, and DOI

Abstract

We outline the fundamental processes of coherent radiation emission from a bunched charged particles beam [1]. In contrast to spontaneous emission of radiation from a random electron beam that is proportional to the number of particles N, a pre-bunched electron beam emits spontaneously coherent radiation proportional to N^2 through the process of (spontaneous) superradiance (SP-SR) (in the sense of Dicke's [2]). The SP-SR emission of a bunched electron beam can be even further enhanced by a process of stimulated-superradiance (ST-SR) in the presence of a seed injected radiation field. These coherent radiation emission processes are presented in term of a radiation mode expansion model, applied to general free electron radiation schemes: Optical-Klystron, HGHG, EEHG, and coherent THz sources based on synchrotron radiation, undulator radiation or Smith-Purcell radiation. The general model of coherent spontaneous emission is also extended to the nonlinear regime - Tapering Enhanced Stimulated Superradiance (TESSA) [3], and related to the tapered wiggler section of seed-injected FELs. In X-Ray FELs, these processes are convoluted with other effects, but they are guidelines for strategies of wiggler tapering efficiency enhancement.

MANUSCRIPTS

This tutorial lecture is based on a recently published review article [1] that details the physics and state of the art of research on the subject of superradiant emission of bunched electron beams, and particularly pre-bunched beam FEL. The readers are referred to this article for detailed presentation. Here is a short summary of the contents and conclusions of the tutorial lecture.

The fundamental coherent radiation emission processes from a bunched charged particles beam were outlined. In contrast to spontaneous emission of radiation from a random electron beam that is proportional to the number of particles, a prebunched electron beam can emit spontaneously coherent radiation proportional to the number of particles—squared, through the process of (spontaneous) superradiance (SP-SR) (in the sense of Dicke's [2]), as shown in Fig. 1.

In the presence of a seed-injected radiation field, the coherent SP-SR emission of a bunched electron beam can be even further enhanced by a process of stimulated superradiance – ST-SR.

In this review, these fundamental coherent radiation emission processes were considered for both single bunch and periodically bunched beams in a model of radiation mode expansion. The general model of coherent spontaneous emission was extended to the nonlinear regime, particularly for undulator (wiggler) interaction, where an exceedingly efficient radiative energy extraction process has been identified [3]: "Tapering-Enhanced Stimulated-Superradiant Amplification" (TESSA) (see Fig. 2).

Processes of SP-SR and TESSA take place also in tapered wiggler seed-injected free-electron lasers (FELs). In such FELs, operating in the x-ray regime, these processes are convoluted with other effects. However, these fundamental emission concepts are still useful guidelines for the strategy of wiggler tapering efficiency and power enhancement.

Based on this model, previous theories and experiments were reviewed on coherent radiation sources based on SP-SR (coherent undulator radiation, synchrotron radiation, Smith-Purcell radiation, transition radiation etc.) in the THz regime, and other on-going works on tapered wiggler efficiency-enhancement concepts in all optical frequency regimes up to UV and x rays.

Spontaneous Emission	Spontaneous Superradiance
(Shot-Noise Radiation)	P-SR

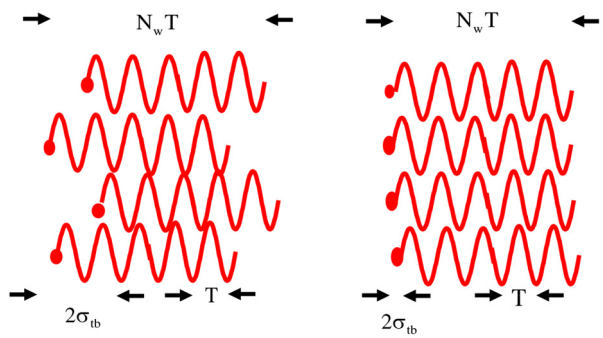


Figure 1: Coherent (right) vs. Random (left) superposition of radiation wavepackets.

ISBN: 978-3-95450-210-3 doi:10.18429/JACoW-FEL2019-WEA01

Content from this work may be used under the terms of the CC BY 3.0 licence (© 2019). Any distribution of this work must maintain attribution to the author(s), title of the work, publisher, and DOI

OVERVIEW OF CW RF GUNS FOR SHORT WAVELENGTH FELs

H. Qian*, Deutsches Elektronen Synchrotron, Zeuthen, Germany
E. Vogel†, Deutsches Elektronen Synchrotron, Hamburg, Germany

Abstract

Hard X-ray FELs (XFELs) operating with pulsed RF provides unprecedented peak brilliance for scientific research. Operating the accelerators with CW RF improves the flexibility w.r.t. the available time structure for experiments and opens the next frontier of average brilliance. One of the challenges of CW XFELs is the electron source, which requires both the CW operation and the highest possible beam quality allowing lasing at shortest wavelengths. With a given linac energy, higher beam brightness results in shorter X-ray wavelength. As the injector defines the lower limit of the electron beam brightness of the complete accelerator, R&D is devoted to CW photoinjector improvements since decades. In this contribution, the worldwide development status of CW RF guns, both normal conducting and superconducting, is reviewed.

INTRODUCTION

Short wavelength free electron lasers (FEL) in the X-ray regime have seen great success in the last decades, such as FLASH, LCLS, the European XFEL and so on [1–3]. These X-ray FEL light sources provide much shorter (sub 100 fs) and much brighter pulses than storage rings [4]. Current X-ray FEL facilities are based on pulsed RF linacs with duty factors lower than 1%, which reduces the average electron beam pulse rate (<27000/second) and thus the average X-ray brightness. Operating the superconducting (SC) linacs in CW mode enables both higher average brightness and more flexible timing patterns for X-rays. Two CW X-ray FELs are under construction, one is LCLS-II in the US, and the other is SHINE in China [5,6]. Compared to the pulsed X-ray FEL, the linac energy of CW X-ray FEL is roughly a factor of 2 lower. According to LCLS-II high energy upgrade (LCLS-II-HE) studies, an even brighter electron source (0.1 µm at 100 pC) is needed to extend the lasing energy from 13 keV to 20 keV [7].

Due to the common needs of high brightness CW injectors, both the energy recovery linac (ERL) community and the FEL community are pushing the R&Ds of CW guns. The ERL guns focuse more on high average current (~100 mA), while the FEL guns focuse more on low emittance beams. Both communities emphasize the developments of high QE cathodes and high gradient guns. R&D is performed on DC guns, normal conducting (NC) RF guns, SC RF gun and hybrid guns [8–11]. Due to the relatively low cathode gradient (<5 MV/m) and low gun voltage (<500 kV), DC guns are mainly developed for the ERL applications to achieve a high average current. The Cornell DC gun also demonstrated the baseline emittance required by LCLS-II, but the linac bunch compression is compromized according to LCLS-II studies [12, 13]. Therefore in this paper, overview on CW guns is focused on photocathode RF guns for applications in short wavelength FELs.

HIGH BRIGHTNESS INJECTORS FOR FELs

There are two types of photoinjectors for X-ray FELs, one is based on a high gradient RF gun, and the other is based on a medium to low gradient gun. A high gradient gun enables photoemission of both high peak current and low thermal emittance, i.e. 'pancake' emission, and the beam is then matched into a booster linac by a gun solenoid for emittance compensation. This type of injector uses high frequency (>1 GHz) pulsed NC guns, and the emission gradient is about 40 to 60 MV/m, which is roughly 50% to 70% of the peak cathode field due to the phase slippage. Such pulsed gun performances cannot be scaled to the CW mode for NC guns due to a few megawatt average RF heating. SC CW guns have the potential to reach similar fields. SC L-band guns are under development at HZDR, HZB, DESY, KEK and PKU. VHF-band quarter wave resonator (QWR) guns are under development at BNL and Wisconsin/SLAC/ANL.

To reach similarly low emittance as achieved in high gradient guns, photoemission in medium to low gradient guns has to start with a longer laser pulse to keep the low thermal emittance, i.e. 'cigar' emission. The long beam is compressed by a buncher cavity following the gun to restore the high peak current, and then matched into the booster linac by solenoid focusing for emittance compensation. To host the long beam, the gun cavity should be low frequency, which makes the beam dynamics like DC gun. The phase slippage is negligible in the low frequency gun, hence the emission field is almost equal to the peak cathode field. This type of injector was originally optimized for a DC gun based ERL injector, and was later adapted for the VHF-band NC CW gun developped at LBNL. The NC VHF gun is also under study at SLAC, DESY and SHINE.

APEX Gun and APEX2 Gun at LBNL

Inspired by the Cornell DC gun, a VHF band (185.7 MHz) gun was developed at the Advanced Photoinjector EXperiment (APEX) for CW soft X-ray FEL project NGLS. The low frequency and large cavity is good for both the cavity cooling and the vacuum. The reentrant cavity shape not only enhances the cathode field and shunt impedance, but also makes the cavity size compact as compared to a pillbox cavity. The APEX gun concept was demonstrated in three phases. In phase 0, the designed CW RF power and ultra high vacuum was demonstrated [14]. In phase I, the

* h.qian@desy.de
† e.vogel@desy.de

ISBN: 978-3-95450-210-3 doi:10.18429/JACoW-FEL2019-WEA04

GROWING AND CHARACTERIZATION OF Cs_2Te PHOTOCATODES WITH DIFFERENT THICKNESSES AT INFN LASA

L. Monaco*, P. Michelato, D. Sertore, INFN LASA, Segrate, Italy
C. Pagani, G. Guerini Rocco, Università degli Studi di Milano e INFN LASA, Segrate, Italy

Abstract

The INFN LASA group has a long standing experience in the production of cesium telluride photocathodes for high brightness photoinjectors. The well-established recipe relies on the deposition of a typical amount of 10 nm of Te, followed by the Cs deposition until reaching the maximum QE. Nevertheless, for improving the understanding of photocathode properties, we are investigating the effect of Te thickness on the growing process, evaluating photocathode optical properties and quantum efficiency during the growing process and on the final film. These photocathodes will be then operated and analyzed in the real environment of the RF Gun at the PITZ facility in DESY Zeuthen, to estimate their impact on the electron beam properties.

INTRODUCTION

The INFN LASA activities on photocathodes to be used in high brightness photoinjectors started in the '90s in the framework of the TESLA collaboration. After a first phase mainly dedicated to R&D studies, we started the production of Cs_2Te photocathodes and we delivered the first photocathodes in 1998 to the TTF RF Gun at DESY-Hamburg. Since then, we continuously produced photocathodes, reaching now a total delivery of about 150 Cs_2Te films, distributed to several laboratories such DESY-Hamburg for FLASH, DESY-Zeuthen for PITZ, LBNL for APEX and, SLAC for the commissioning of LCLS-II photoinjector.

The need to satisfy requests for usage of our photocathodes in RF guns of accelerators and user facilities guided our activity to develop reproducible and robust recipe, able to furnish the needed Quantum Efficiency (QE) for the operation, a good QE spatial uniformity, a long operative lifetime and a low dark current (DC). All these issues were reached [1] and, as an example, the operative lifetime was increased from few months to few years (24/7) [2]. The development of a multi-wavelength technique for monitoring QE and reflectivity during cathode formation improved further the reproducibility of the final photocathodes [3].

In this paper, we present the results obtained on photocathodes produced with different Te layer thicknesses and we compared them with the properties of our well known standard cathodes. Moreover, these photocathodes have then been used at PITZ for their characterization in the RF Gun, in the framework of the INFN LASA and DESY PITZ collaboration and the results are presented at this conference [4].

* laura.monaco@mi.infn.it

CATHODE DEPOSITION AND DIAGNOSTIC

Photoemissive films are evaporated sequentially on high purity Mo plugs (99.95 %), optically polished (typical roughness R_a = 10 nm). The deposition is done in the preparation chamber (base pressure 1×10^{-10} mbar) with a diameter of 5 mm realized with a Mo masking system. After an heating cycle up to 450 °C, the plug is cooled to 120 °C and the Te deposition starts (1 nm/min). When 10 nm of Te are deposited, the Cs deposition starts at 1 nm/min and ends when the QE reaches the typical maximum [5]. For the purpose of this work, we have grown photocathodes with 5 nm and 15 nm of Te besides a standard "10 nm". In all cases, the Cs deposition stopped when the QE reached its maximum.

Reflectivity

During the film growth, the plug is illuminated at different wavelengths, with a spot of approximately 5 mm (corresponding to the active area) to ensure a uniform reaction of the entire film area. The reflected power is extremely useful especially for the control of the real amount of Te deposited on the plug surface. Figure 1 reports the reflectivity variation for three different Te thicknesses and the theoretical predictions based on tabulated values for Mo and Te [6], in the assumption of a formation of a uniform Te layer on top of Mo substrate. The deviation from theory at thicker layers is possibly due to formation of islands of Te on Mo that our model does not take into account.

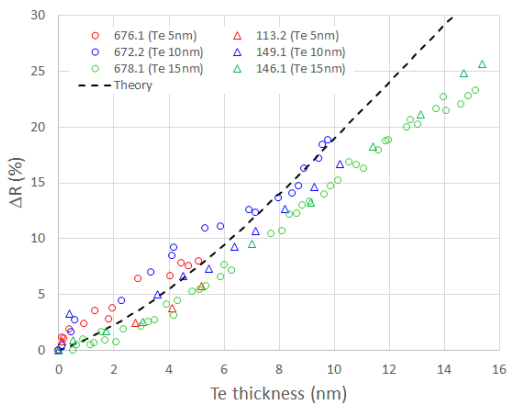


Figure 1: Te reflectivity decrease (ΔR) for three different film thickness and the expectation from tabulated values.

Table 1 reports the average reflectivity variation for the three different types of photocathodes based on all measurements so far available (26 films for "10 nm", 3 films for "5 nm" and "15 nm").

Content from this work may be used under the terms of the CC BY 3.0 licence (© 2019). Any distribution of this work must maintain attribution to the author(s), title of the work, publisher, and DOI

ISBN: 978-3-95450-210-3 doi:10.18429/JACoW-FEL2019-WEB01

IDENTIFICATION AND MITIGATION OF SMOKE-RING EFFECTS IN SCINTILLATOR-BASED ELECTRON BEAM IMAGES AT THE EUROPEAN XFEL

G. Kube, A. Novokshonov, S. Liu, M. Scholz, DESY, Hamburg, Germany

Abstract

Standard transverse beam profile measurements at the European XFEL are based on scintillating screen monitors using LYSO:Ce as scintillator material. While it is possible to resolve beam sizes down to a few micrometers with this material, the experience during the XFEL commissioning showed that the measured emittance values were significantly larger than the expected ones. In addition, beam profiles measured at bunch charges of a few hundred pC showed a 'smoke ring' structure. While coherent OTR emission and beam dynamical influence could be excluded, it is assumed that the profile distortions are caused by effects from the scintillator material itself. Following the experience in high energy physics, a simple model was developed which takes into account quenching effects of excitonic carriers inside the scintillator in a heuristic way. Based on this model, the observed beam profiles can be understood qualitatively. Possible new scintillator materials suitable for beam profile diagnostics are discussed and preliminary test results from beam measurements at the European XFEL are presented.

INTRODUCTION

Transverse beam profile diagnostics in electron linacs is widely based on optical transition radiation (OTR) as standard technique which is observed in backward direction when a charged particle beam crosses the boundary between two media with different dielectric properties. Unfortunately, microbunching instabilities in high-brightness electron beams of modern linac-driven free-electron lasers (FELs) can lead to coherence effects in the emission of OTR, thus rendering it impossible to obtain a direct image of the particle beam and compromising the use of OTR monitors as reliable diagnostics for transverse beam profiles. The observation of coherent OTR (COTR) has been reported by several facilities (see e.g. Ref. [1]), and in the meantime the effect of the microbunching instability is well understood [2].

For the European XFEL it was therefore decided to use scintillation screen monitors because the light emission in a scintillator is a multistage stochastic process from many atoms which is completely insensitive to the longitudinal bunch structure. In a series of test measurements performed in the past few years, the applicability of inorganic scintillators for high resolution electron beam profile measurements was investigated [3, 4]. Most notably, the dependency of the resolution on the scintillator material and on the observation geometry was studied with respect to resolve beam profiles in the order of several tens of micrometers, and it was concluded that LYSO ($Lu_{2(1-x)}Y_{2x}SiO_5$:Ce) is a suitable material because it gives the best spatial resolution. Based on these measurements, screen monitor stations were designed for the European XFEL using 200 µm thick LYSO screens [5]. In a high resolution beam profile measurement using an XFEL-type screen it was demonstrated that it is possible to resolve a vertical beam size of $\sigma_y = 1.44$ µm [6].

However, the experience during the commissioning of the XFEL showed that the measured emittance values were significantly larger than the expected ones [7, 8]. In addition, beam profiles measured at bunch charges of a few hundreds of pico-Coulomb show a 'smoke ring' shaped structure, see e.g. Fig. 1.

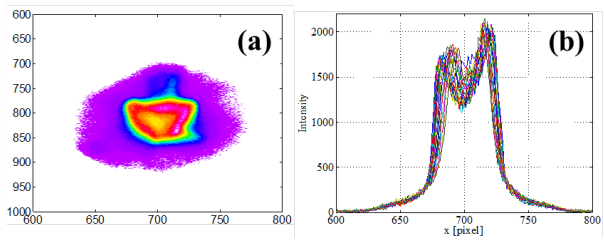


Figure 1: (a) Typical smoke ring shaped beam profile as measured with an XFEL screen monitor based on a 200 µm thick LYSO screen. (b) Various horizontal cuts through the 2D-profile demonstrate the intensity drop in the central part of the beam spot.

While the contribution of COTR emission from the scintillator surface, beam dynamical influence, and camera effects could be excluded to explain this observation, it is assumed that the beam profile distortions are caused by effects from the scintillator material.

In Ref. [9], a simple model was presented which takes into account quenching effects of excitonic carriers inside a scintillator in a heuristic way. Based on this model, the observed beam profiles could be understood qualitatively. In the following, the underlying ideas are briefly summarized with the emphasis on first results from beam measurements at the European XFEL with new scintillator materials suitable for beam profile diagnostics.

SCINTILLATOR MODEL

Degradation effects in scintillator based beam profile measurements are reported in a number of publications, see e.g. Refs. [10–15]. The scintillator influence is mainly interpreted as saturation of the measured profiles, caused e.g. by full excitation of the luminescent centers in some regions inside the scintillator. While inspecting Fig. 1 it is obvious that the XFEL observations cannot simply be described by a saturation effect which would result in a flattening of the

Content from this work may be used under the terms of the CC BY 3.0 licence (© 2019). Any distribution of this work must maintain attribution to the author(s), title of the work, publisher, and DOI

ISBN: 978-3-95450-210-3 doi:10.18429/JACoW-FEL2019-WEB02

WIRE-SCANNERS WITH SUB-MICROMETER RESOLUTION: DEVELOPMENTS AND MEASUREMENTS

G.L. Orlandi*, S. Borrelli, C. David, E. Ferrari, V. Guzenko,
B. Hermann, O. Huerzeler, R. Ischebeck, C. Lombosi, C. Ozkan-Loch, E. Prat,
Paul Scherrer Institut, Villigen PSI, Switzerland
M. Ferianis, G. Penco, M. Veronese,
Elettra-Sincrotrone Trieste S.C.p.A, Basovizza, Trieste Italy
N. Cefarin, S. Dal Zilio, M. Lazzarino,
IOM-CNR Laboratorio TASC, c/o Area Science Park - Basovizza, Trieste, Italy

Abstract

Monitors of the beam transverse profile with ever more demanding spatial resolution and minimal invasivity are required by the FEL community. In order to improve the spatial resolution towards the sub-micrometer limit as well as to decrease the impact on the lasing process, nano-fabricated wire-scanners have been manufactured independently at PSI and FERMI by means of a lithographic technique. Experimental tests carried out at SwissFEL at a low emittance demonstrated the capability of such innovative wire-scanner solutions to resolve beam transverse profiles with a size of 400-500 nm without being affected by any resolution limit. Status and outlook of nano-fabricated wire-scanners (WS) will be presented.

PREMISE

The present proceeding briefly reports on the recent experimental results obtained in the nano-fabrication and electron beam characterization of free-standing WS with sub-micrometer resolution. The free-standing WS prototypes - independently nano-fabricated at PSI and FERMI by means of lithographic techniques - can measure the transverse profile of an electron beam with a rms geometrical resolution of about 250 nm. The experimental test of the PSI and FERMI WS prototype have been performed at SwissFEL, where electron beams with a vertical size smaller than 500 nm have been successfully and consistently resolved. All information and technical details on the nano-fabrication and experimental tests - carried out at SwissFEL - of the PSI and FERMI free-standing WS with sub-micrometer resolution are reported in a manuscript submitted to a peer-reviewed journal for a publication. For more details on the WS nano-fabrication and characterization, the reader is hence addressed to the archived version of the manuscript, to the paper submitted to the journal and to the slides of the conference talk [1, 2]. In the present proceeding, the authors will summarize the main highlights, achievements and perspectives of the experimental work on free-standing WS with sub-micrometer resolution. In addition, the authors will briefly summarize the background experience of PSI and FERMI on nano-fabrication and test of WS. Results of satellite tests carried out at SwissFEL in parallel with the characterization of the free-standing WS will be reported as well. The introduction and the conclusion sections are directly derived from [1, 2].

* gianluca.orlandi@psi.ch

INTRODUCTION

Wire-scanners (WS) constitutes a precious complement to view-screens for monitoring the transverse profile of the electron beam in a linac [3–12]. Because of the multi-shot and mono-dimensional reconstruction of the beam transverse profile, WS are not timewise competitive with view-screens for beam finding and for matching the magnetic optics in an electron linac. WS are inappropriate for slice emittance measurements as well. Nevertheless, WS are a unique and essential diagnostics whenever the beam characterization requires a high spatial resolution along with a minimal invasivity to the beam operation. The spatial resolution of a WS depends on the measurement resolution of the wire positioning, on the possible wire vibrations and, finally, on the geometry of the wire. The geometrical resolution of a WS is inversely proportional to the wire width. This also determines the surface of impact of the wire with the electron beam and hence the wire transparency to the beam (also depending on the wire thickness for non-cylindrical wires). Conventional WS solutions - as normally in operation in several free-electron lasers (FELs) - are realized according to the standard technique to fix and stretch a metallic wire (beam-probe) onto a metallic frame (fork). They are able to attain a spatial resolution at the micrometer scale [12] which is at least an order of magnitude higher than the spatial resolution of a typical view-screen operating in a FEL [13, 14]. Low charge and low emitance machine operation modes - presently under investigation in several FEL facilities - requires the characterization of ever smaller beam profiles. This triggers the community of the electron-beam diagnostics to push forward the resolution limit of the conventional WS beyond the micrometer limit. In order to improve the WS spatial resolution, new fabrication techniques are under investigation at PSI and FERMI. At PSI, a WS prototype with a sub-micrometer resolution nano-fabricated on-a-membrane (250 nm thick Silicon Nitride membrane) was successfully tested [15]; while at FERMI a free-standing nanofabricated WS with a resolution of about 2.9 μm has been successfully tested [16]. These experiences paved the way to use the

Content from this work may be used under the terms of the CC BY 3.0 licence (© 2019). Any distribution of this work must maintain attribution to the author(s), title of the work, publisher, and DOI

ISBN: 978-3-95450-210-3 doi:10.18429/JACoW-FEL2019-WEB03

APPLICATION OF MACHINE LEARNING TO BEAM DIAGNOSTICS

E. Fol*[1,2], R. Tomás[1], G. Franchetti[2,3], J. Coello de Portugal[4], [1]CERN, 1211 Geneva 23, Switzerland
[2]Johann-Wolfgang Goethe University, 60438 Frankfurt am Main, Germany
[3] GSI Helmholtzzentrum für Schwerionenforschung, 64291, Darmstadt, Germany
[4]Paul Scherrer Institut, 5232, Villigen, Switzerland

Abstract

Machine Learning (ML) techniques are widely used in science and industry to discover relevant information and make predictions from data. The application ranges from face recognition to High Energy Physics experiments. Recently, the application of ML has grown also in accelerator physics and in particular in the domain of diagnostics and control. The target of this paper is to provide an overview of ML techniques and to indicate beam diagnostics tasks where ML based solutions can be efficiently applied to complement or potentially surpass existing methods. Besides, a short summary of recent works will be given demonstrating the great interest for use of ML concepts in beam diagnostics and latest results of incorporating these concepts into accelerator problems, with the focus on beam optics related applications.

MOTIVATION

Traditional optimization tools demonstrate successful performance in applications on linear optics corrections and problems with limited amount of optimization targets [1–6]. Bigger challenges emerge when diagnostics of complex non-linear behavior is required and several variables have to be taken into account as final objective. The amount of time and computational power required by traditional methods might become unacceptable for future accelerator facilities.

ML is well known for surpassing human performance in some specific tasks such fraud detection, forecasting of market trends and risks, online recommendations, recognition of voice and images and in general in discovering correlations in large scale data sets. Most of these tasks can find analogies in beam control and diagnostics. For example, anomaly detection methods applied for fraud detection can be used to detect defects in the instrumentation and forecasting techniques can be transferred to predict beam behavior during operation.

Free Electron Lasers (FEL) problems for optimization and diagnostics have to deal with non-linear, multi-objective functions which depend on thousands of time-varying machine components and settings. These properties meet the limitations of traditional optimization methods and make this problem a perfect candidate for application of ML-based techniques. The main limitation of traditional optimization methods is that the objective function or specific rules and thresholds have to be known. ML methods can learn from given examples without requiring explicit rules.

* elena.fol@cern.ch

RELEVANT MACHINE LEARNING CONCEPTS

ML techniques aim to build computer programs and algorithms that automatically improve with experience by learning from examples with respect to some class of task and performance measure, without being explicitly programmed [7]. Depending on the problem and existence of learning examples, different approaches are preferred. If pairs of input and desired output are available, an algorithm can generalize the problem from the given examples and produce prediction for unknown input. ML algorithms that learn from input/output pairs are called *supervised learning* algorithms. Opposite to supervised learning, *unsupervised learning* algorithms solve the tasks where only input data is available. Unsupervised learning is suitable for the problems such anomaly detection, signal denoising, pattern recognition, dimensionality reduction and feature extraction. In the following a brief overview on significant machine learning concepts that can be used as supervised as well as unsupervised approaches is presented. We also give a short introduction to Reinforcement Learning - ML technique which recently became of great interest especially for control tasks.

Artificial Neural Network

Artificial Neural Networks (ANNs) are well suited for learning tasks, where data is represented by noisy, complex signals and the target output function may consist of several parameters. A basic ANN consists of a single processing unit (*neuron*), that takes the *weighted* inputs and an additional activation function to introduce the nonlinearity in the output. For more complex practical problems, ANNs are composed of several interconnected *hidden layers* with multiple neurons stacked. ANNs can be used for both regression and classification problems. In case of classification the output can be either a class label or a probability of an item belonging to a class. The learning of ANN is performed using *backpropagation* algorithm [8] on a set of examples. For each example the training algorithm computes the derivatives of the output function of the network. The obtained gradients with respect to all weights are then used to adjust the weights in order to achieve a better fit to the target output. In backpropagation *stochastic gradient descent* or one of its improved extensions [9,10] is applied as optimization method in order to minimize the loss between the network output values and the target values for these outputs by updating the connection weights. ANNs with many hidden layers called *deep neural networks* are able to use fewer neurons per layer and have a better generalization

Content from this work may be used under the terms of the CC BY 3.0 licence (© 2019). Any distribution of this work must maintain attribution to the author(s), title of the work, publisher, and DOI

ISBN: 978-3-95450-210-3 doi:10.18429/JACoW-FEL2019-WEB04

Content from this work may be used under the terms of the CC BY 3.0 licence (© 2019). Any distribution of this work must maintain attribution to the author(s), title of the work, publisher, and DOI

FEW-FEMTOSECOND FACILITY-WIDE SYNCHRONIZATION OF THE EUROPEAN XFEL

S. Schulz*, M. K. Czwalinna, M. Felber, M. Fenner, Ch. Gerth, T. Kozak, T. Lamb, B. Lautenschlager, F. Ludwig, U. Mavric, J. Müller†, S. Pfeiffer, H. Schlarb‡, C. Schmidt, M. Titberidze, F. Zummack, Deutsches Elektronen-Synchrotron (DESY), Hamburg, Germany
C. Sydlo§, Paul Scherrer Institut (PSI), Villigen, Switzerland

Abstract

In this paper, we report on the first facility-wide evaluation of the optical synchronization system at the European XFEL, resulting in excellent arrival time stability of the electron bunches at the end of the 2 km long linac of the machine. It has been measured using two adjacent, individual single-shot femtosecond-resolution bunch arrival time monitors. While each of the monitors is independently connected by a stabilized optical fiber link to a master laser oscillator, with one being installed in the injector building and one in the experimental hall, these two reference lasers are tightly synchronized through another few-km long fiber link and by balanced optical cross-correlation. Thus, our results are not only benchmarking the accelerator performance, but at the same time the optical synchronization infrastructure itself. Femtosecond arrival time stability can only be achieved by also locking the RF reference for cavity field control to the stabilized optical reference and requires an unprecedented synchronization of the master laser oscillator to the accelerator's master RF oscillator, enabled by a novel laser-to-RF phase detection scheme. Finally, with the seed oscillators of the experiment's optical lasers tightly synchronized to the master laser oscillator, first pump-probe experiments at two independent scientific instruments proved a relative X-ray/optical timing jitter in the low tens of femtoseconds.

OVERVIEW

In 2017 the European XFEL officially started operation with early user experiments and has meanwhile been fully commissioned with all three SASE beamlines and six scientific instruments. The machine is capable delivering up to 27,000 hard and soft X-ray pulses per second with a few tens of femtoseconds duration in flexible patterns to the three beamlines, such that three user experiments can be carried out simultaneously. At each beamline, a distinct laser system is available with matching pulse patterns, providing ultrashort optical pulses for exciting samples in pump-probe geometries, and usage in local timing tools. In addition, every scientific instrument is equipped with another optical laser system fulfilling specific requirements of the instrument. One key component for such time-resolved experiments at the instruments and crucial for accelerator stability is the optical synchronization infrastructure, which had been under commissioning since early 2016 [1–5]. Founded on an ultra-low noise laser oscillator (master laser oscillator, MLO) locked to the facility's master RF oscillator, the synchronization signals are distributed over actively-stabilized optical fiber links, and are used to re-synchronize the reference signal of the accelerator's low-level RF (LLRF) system, the synchronization of the various laser systems, and to provide a reference for longitudinal electron bunch diagnostics. The system evolved from the implementation at the soft X-ray free-electron laser FLASH [6], which showed already 28 fs rms X-ray/optical relative pulse arrival time jitter [7] based on earlier work on electron bunch arrival time stabilization [8]. Since then, significant improvement in all core systems, computing and controls [9, 10] had been made, additional components were developed, and a robust implementation is realized.

TOPOLOGY AND CORE SYSTEMS

At the European XFEL, shown schematically in Fig. 1, the main synchronization laboratory provides precisely controlled environmental conditions with < 0.1 K temperature and < 3% RH (relative humidity) for the core systems of the synchronization infrastructure. The optical timing reference is a commercial, SESAM-based passively mode-locked oscillator at telecom wavelength emitting 200 fs FWHM pulses at a repetition rate of 216.667 MHz. For redundancy, a second identical laser oscillator is operated as hot-spare, such that the system can be switched from one to the other within minutes, with an automated failure detection and switching process under development.

Both laser oscillators are synchronized to the 1.3 GHz main RF oscillator [11] of the facility, which had been realized by a standard heterodyne scheme based on RF generation in a fast photodetector [12] in the first two years of operation. Recently, a Mach-Zehnder-Modulator (MZM)-based laser-to-RF phase detection scheme has been commissioned, resulting in a significant improvement of the timing jitter from 7.2 fs rms (bandwidth 10 Hz to 100 kHz) of the old scheme down to 3.0 fs rms, while also nearly eliminating long-term drifts. This performance is permanently monitored by a second, identical MZM-based laser-to-RF phase detector providing a true out-of-loop measurement (see Fig. 2).

The pulse train of the MLO is then distributed and split by means of polarizing beamsplitters and half-wave plates on a SuperInvar optical table to up to 24 so-called fiber link stabilization units, with presently 18 units in operation.

* corresponding author: seb.schulz@desy.de
† corresponding author: jost.mueller@desy.de
‡ corresponding author: holger.schlarb@desy.de
§ formerly also affiliated with DESY

ISBN: 978-3-95450-210-3 doi:10.18429/JACoW-FEL2019-WEP003

BALANCED OPTICAL-MICROWAVE PHASE DETECTOR FOR 800-nm PULSED LASERS WITH SUB-FEMTOSECOND RESOLUTION

K. Şafak†, H. P. H. Cheng, A. Dai, P. Schiepel, E. Cano, J. Derksen, A. Berlin, M. Neuhaus
Cycle GmbH, Hamburg, Germany
F. X. Kärtner, Deutsches Elektronen Synchrotron and Center for Free Electron Science, Hamburg, Germany

Abstract

We report a novel optical-to-microwave phase detector designed for 800-nm pulsed laser operation. The detector is based on electro-optic sampling between the microwave and the optical pulse train which is incorporated into a fiber-based Sagnac interferometer containing a phase modulator. The detector has a timing resolution of 0.01 fs RMS for offset frequencies above 100 Hz and a total noise floor of less than 10 fs RMS integrated from 1 Hz to 1 MHz.

INTRODUCTION

Modern light-matter interaction experiments conducted in free-electron lasers, ultrafast electron diffraction instruments and extreme light infrastructures require synchronous operation of microwave sources with femtosecond pulsed lasers [1,2]. In particular, Titanium-sapphire (Ti:Sa) lasers have become the most common near-infrared light source used in these facilities due to their wide gain spectrum, translating into wavelength tunability and ultrashort pulses at around 800-nm optical wavelength [3]. Therefore, a highly sensitive optical-to-microwave phase detector operating at 800 nm is an indispensable tool to synchronize these ubiquitous lasers to the microwave clocks of photon science facilities. Electro-optic sampling is one approach that has proven to be the most precise in extracting the relative phase noise between microwaves and optical pulse trains [4-7]. However, their implementation at 800-nm wavelength has been so far limited to a few specialized laser laboratories [3,8].

Here, we show a novel optical-microwave phase detector designed for 800-nm operation promising 10-fs level synchronization precision from 1 Hz up to 1 MHz offset frequency.

OPERATION PRINCIPLE

Operation principle of the detector is based on a differentially-biased, fiber-based Sagnac interferometer (SGI) and synchronous detection at half the repetition rate of the optical pulse source. This scheme adopted from the balanced optical–microwave phase detectors (BOMPD) previously demonstrated for 1550-nm operation by our former group members [6,9]. Figure 1 shows the schematic of our 800-nm BOMPD. As inputs, the detector takes an 800-nm pulsed laser (e.g., a Ti:Sa laser) and a microwave signal whose frequency is a higher harmonic of the laser's pulse repetition rate. The optical signal is split into two arms. The first arm (i.e., bias arm) is tapped off by a photodiode to generate a high-frequency (multi GHz) microwave signal which is adjusted in amplitude and phase to achieve quadrature bias. The second arm is sent into a fiber-based SGI containing an optical phase modulator. When both the bias and the microwave signals are applied to the modulator, any phase error between the laser and the microwave source induces an amplitude modulation in the pulse train.

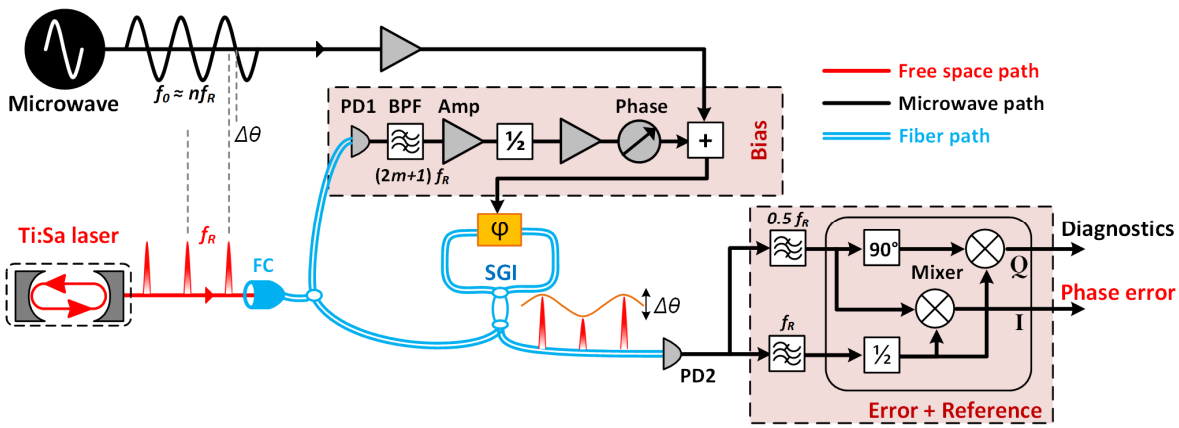


Figure 1: Schematic of the 800-nm BOMPD. Δθ: Phase error between the microwave and optical pulse train; PD: photodetector; BPF: bandpass filter; Amp: electronic amplifier; ½: frequency divider; Phase: RF phase shifter; +: microwave diplexer; φ: electro-optic phase modulator; SGI: Sagnac-interferometer; FC: fiber collimator, I: in-phase output, Q: in-quadrature output.

† kemal.shafak@cyclelasers.com

Content from this work may be used under the terms of the CC BY 3.0 licence (© 2019). Any distribution of this work must maintain attribution to the author(s), title of the work, publisher, and DOI

ISBN: 978-3-95450-210-3 doi:10.18429/JACoW-FEL2019-WEP004

TIMING STABILITY COMPARISON STUDY OF RF SYNTHESIS TECHNIQUES

E. Cano Vargas †, F. X. Kärtner, Deutsches Elektronen Synchrotron (DESY)
and Center for Free Electron Science (CFEL), Hamburg, Germany
A. Berlin, H. P. H. Cheng, A. Dai, J. Derksen, P. Schiepel, K. Shafak
Cycle GmbH, Hamburg, Germany

Abstract

In this paper, we implement and compare two of the most common techniques used for laser-to-RF synthesis in FEL facilities: (i) microwave signal extraction from the optical pulse train using photodiodes (i.e. direct photodetection), and (ii) voltage-controlled oscillator (VCO)-to-laser synchronization. Test setups are built to measure both the absolute phase noise of the generated RF signal and the relative timing jitter with respect to the mode-locked laser. Short-term timing jitter values varying between 10s and 100s of femtoseconds are achieved for different test setups, while long term timing drift ranging to some hundreds of femtoseconds due to environmental influence are observed.

INTRODUCTION

High-precision and low-noise timing transfer from a master oscillator to different end stations of a free-electron laser (FEL) is a critical requirement. Timing precisions ranging from a few femtoseconds, to sub-femtosecond are required for seeded FELs and attosecond science centers for the generation of shorter x-ray pulses with unmatched brightness [1], which ultimately enables subatomic and attosecond spatiotemporal resolution.

Mode-locked lasers referenced to RF standards are commonly used as master oscillators, due to their superior stability and timing precision, depicting timing jitter in the attosecond range [2]. In this matter, one of the biggest challenges is to transfer the timing stability of mode-locked lasers to RF sources.

Recently, timing distribution systems (TDS) have been demonstrated and implemented, taking advantage of the timing stability of pulsed-optical sources to perform timing distribution along different links, creating a link between different remotely located lasers, through balanced optical cross-correlators (BOCs) and laser-to-microwave synthesis and synchronization based on balanced optical-microwave phase detectors (BOMPDs). These devices can deliver sub-femtosecond precision between remotely synchronized lasers and microwave sources [3,4]. Figure 1 depicts a general overview of the TDS as deployed in [5]. Despite many achievements in these techniques over the last years, laser to microwave synchronization is still one of the bottlenecks of the system by being affected by so many noise sources and perturbations.

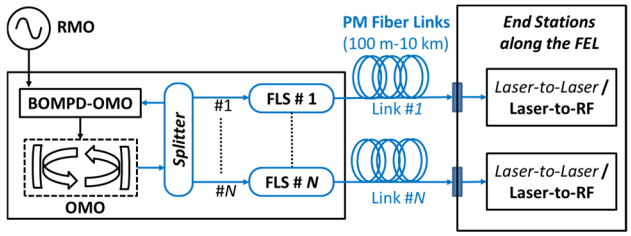


Figure 1: Layout of timing distribution system as deployed in [5]. RMO: RF master oscillator; OMO: optical master oscillator; FLS: fiber link stabilization; BOMPD: balanced optical-microwave phase detector.

Here, we focus on two of the most common techniques used for laser-to-RF synthesis in FEL facilities: (i) RF signal extraction from the optical pulse train using photodiodes, and (ii) VCO-to-laser synchronization. First, we describe the implementation and the test setups. Then, we present measurements of both the absolute phase noise of the generated microwave signal and its relative timing jitter with respect to the mode-locked laser, together with the relative timing drift.

DIRECT PHOTODETECTION

The simplest approach to synthesize microwave signals from an optical source coming from mode-locked lasers is by using a fast response photodiode. Here the optical pulse train envelope is detected by the photodiode and then transduced into an electrical current pulse train, which is limited by the photodiodes response (i.e. bandwidth). A further limitation is the so-called AM-PM conversion which translates amplitude noise, i.e. power fluctuations, from the optical pulse train, into phase noise in the electrical signal [6,7]. Figure 2 illustrates the optical pulse train and the electrical current pulse train after photodetection in time and frequency domain.

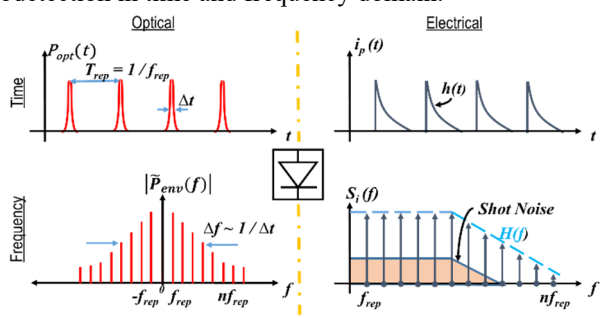


Figure 2: Optical pulse train transduced by fast photodetector in the time and frequency domain.

† erwin.cano.vargas@cfel.de

Content from this work may be used under the terms of the CC BY 3.0 licence (© 2019). Any distribution of this work must maintain attribution to the author(s), title of the work, publisher, and DOI

ISBN: 978-3-95450-210-3 doi:10.18429/JACoW-FEL2019-WEP006

A PolariX TDS FOR THE FLASH2 BEAMLINE

F. Christie[†,*], J. Rönsch-Schulenburg, M. Vogt
Deutsches Elektronen-Synchrotron, Hamburg, Germany
[†]also at Universität Hamburg, Hamburg, Germany

Abstract

Transverse Deflecting RF-Structures (TDS) are successfully used for longitudinal diagnostic purposes at many Free-Electron Lasers (FEL) (LCLS, FLASH, EU-XFEL, FERMI). Moreover, by installing a TDS downstream of the FEL undulators and placing the measurement screen in a dispersive section, the temporal photon pulse structure can be estimated, as was demonstrated at LCLS and sFLASH. Here we describe the installation of a variable polarization X-band structure (PolariX TDS) downstream of the FLASH2 undulators. The installation of such a TDS enables longitudinal phase space measurements and photon pulse reconstructions, as well as slice emittance measurements in both planes using the same cavity due to the unique variable polarization of the PolariX TDS.[1]

INTRODUCTION

The lasing process in a free-electron laser (FEL) is dominated by the longitudinal parameters of the electron bunches. Hence, the measurement of their longitudinal properties is of utmost importance to control the lasing process. This can, for example, be achieved by means of a Transverse Deflecting Structure (TDS). With this device it is possible to relate the longitudinal coordinate of an electron beam to a transverse one, which then can be imaged using a screen. Additionally, an energy spectrometer, such as a dipole magnet, can be used to relate the beam energy to the other transverse coordinate by deflecting the beam in the plane transverse to the streaking plane of the TDS. By combining both methods, the longitudinal phase space density of the electron bunches can be mapped onto a screen [2]. Additionally, the slice emittance can be measured using a TDS [3, 4]. Such a measurement station is planned as an essential part of the Free-Electron Laser in Hamburg (FLASH) midterm refurbishment and the FLASH2020+ upgrade plans [5]. It will be installed downstream of the FLASH2 undulators to ensure high beam-qualities at FLASH2 as well as brilliant and high-quality photon pulses. The measurement station comprises a novel TDS with a variable polarization feature (PolariX TDS[2]) [6–8] and will be used as an indispensable diagnostic tool for short electron bunches and photon pulses at FLASH2.

In the following, we will describe the optics for longitudinal phase space density measurements and slice emittance measurements in both planes. In addition, tracking simulations for longitudinal phase space measurements as well as photon pulse reconstructions and slice emittance measurements are presented.

LAYOUT OF THE TDS DIAGNOSTIC SECTION AT FLASH2

The TDS diagnostic section will be situated directly downstream of the FLASH2 undulators. It will feature two PolariX TDSs [8], which are X-band transverse deflecting structures ($f_{RF} \approx 12$ GHz) with variable polarization yielding arbitrary streaking directions. A technical drawing of the two cavity supports is displayed in Fig. 1. Additionally, a kicker to deflect the beam onto an off-axis screen station will be installed.

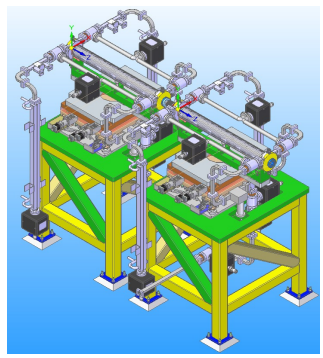


Figure 1: Technical drawing of the supports for the two PolariX TDSs at FLASH2. Courtesy of M. Föse.

The new TDSs at FLASH2 will share their radio frequency (RF) station with the FLASH Forward [9] TDS as both experiments require longitudinal beam diagnostics [7]. The waveguide distribution and RF components can be seen in Fig. 2. The RF source is connected via an RF switch to both experiments. This installation scheme prohibits simultaneous operation, but requires only a single RF station and therefore reduces costs and saves space. The RF source comprises a 6 MW Toshiba E37113A klystron with an Ampegon Type μ, S-Class modulator [8] and is similar to the CERN Xbox3 design [10]. To minimize the attenuation in the waveguides and achieve high deflecting powers, the klystron will be placed as close to the FLASH2 TDSs as possible. Therefore, the klystron will be installed inside the tunnel while the radiation sensitive modulator and low-level RF-rack are placed outside. The klystron and the modulator are connected by pulse cables of 15 m length. The total waveguide length from the klystron to the cavities is about 5 m. In the final stage, an X-band version of the PSI C-band barrel open cavity (BOC) [11] compressor will be installed between the TDSs and the klystron, approximately raising

* florian.christie@desy.de
[1] This article contains excerpts from [1].
[2] Polarizable X-band TDS

Content from this work may be used under the terms of the CC BY 3.0 licence (© 2019). Any distribution of this work must maintain attribution to the author(s), title of the work, publisher, and DOI

ISBN: 978-3-95450-210-3 doi:10.18429/JACoW-FEL2019-WEP007

USAGE OF THE MicroTCA.4 ELECTRONICS PLATFORM FOR FEMTOSECOND SYNCHRONIZATION SYSTEMS

M. Felber#, E. P. Felber, M. Fenner, T. Kozak, T. Lamb, J. Mueller, K. Przygoda, H. Schlarb, S. Schulz, C. Sydlo, M. Titberidze, F. Zummack, DESY, Hamburg, Germany

Abstract

At the European XFEL and FLASH at DESY optical synchronization systems are installed providing sub-10 femtosecond electron bunch arrival time stability and laser oscillator synchronization to carry out time-resolved pump-probe experiments with high precision. The synchronization system supplies critical RF stations with short- and long-term phase-stable reference signals for precise RF field detection and control while bunch arrival times are processed in beam-based feedbacks to further time-stabilize the FEL pulses. Experimental lasers are tightly locked to the optical reference using balanced optical cross-correlation. In this paper, we describe the electronic hardware for supervision and real-time control of the optical synchronization system. It comprises various MicroTCA.4 modules including fast digitizers, FPGA processor boards, and drivers for piezos and stepper-motors. Advantages of the system are the high-level of integration, state-of-the-art performance, flexibility, and remote maintainability.

INTRODUCING MicroTCA.4

MicroTCA is an electronic framework for signal processing derived from the Advanced Telecommunication Computing Architecture (ATCA). MicroTCA.4 was released as an official standard by the PCI Industrial Manufacturers Group (PICMG) in 2011 and is supported by the xTCA for physics group, a network of physics research institutes and electronics manufacturers. Opposed to other xTCA standards it is also designed for analog processing of low-noise signals. Its main improvements are enhanced rear I/O connectivity and provisions for precision timing. MicroTCA.4 has inherited many of the advantages of ATCA including capabilities for remote monitoring, remote maintenance, hot-swap of components, and the option to duplicate critical components, making the standard highly modular, reliable and flexible. It also made the outstanding digital signal processing performance of ATCA systems more affordable and less demanding in terms of space requirements and energy consumption.

MicroTCA.4 System Architecture

Fundamental components are the chassis which is available in different form factors and sizes, the optionally redundant power supply, an optionally redundant crate management controller (MCH), and CPU with hard drive [1].

For user applications specific analog and digital processing cards are used. From the front, Advanced Mezzanine Cards (AMC) which can also be used on ATCA carrier cards are inserted to the crate. There are various connections on the backplane which provide e.g. Gigabit Ethernet and PCI Express links between the slots and the MCH, dedicated clock and trigger distribution lines, and point to point links between the slots for fast real time communication between the cards. Additionally, there is the possibility to insert cards from the rear of the crate, so-called Rear Transition Modules (RTM) which connect to the according AMC board via the Zone 3 connector. This connection provides 60 differential pairs for analog or digital signals, which are defined in the standard [1]. Some cards incorporate connectors for additional industrial standard piggy back boards like FPGA Mezzanine Cards (FMC) or IndustryPack (IP) modules.

MicroTCA.4 AT DESY

Meanwhile, for basically all accelerators at DESY the technical groups decided to use the MicroTCA.4 standard. For example at the European XFEL and FLASH this involves the LLRF field control [2], the timing and machine protection systems, standard diagnostics like beam position monitors [3] and camera readouts, and the optical synchronization system [4]. In the course of the developments required for fulfilling the demanding tasks, the standard was further adapted and improved.

In order to facilitate the development of new boards for extending the portfolio of applications and to ensure the availability of spare parts, DESY took the initiative for a better establishment of the MicroTCA.4 standard in industry. With financial support from the Helmholtz Association and industry partners the Helmholtz Validation Fund (HVF) was established in 2012.

Therefore, most board designs are licensed to various industry partners who offer those components as 'commercial of the shelf' products. This way it is easy for other institutes and companies to make use of the sophisticated designs (e.g. high speed digital or low noise analog cards) without the need for own developments or additional agreements.

As successor of the HVF the MicroTCA Technology Lab [1] was founded at DESY to help external partners with their MicroTCA related projects. A competent team of engineers offers support for all aspects like hardware and firmware development, or the implementation and commissioning of MicroTCA systems at the facility.

#matthias.felber@desy.de

Content from this work may be used under the terms of the CC BY 3.0 licence (© 2019). Any distribution of this work must maintain attribution to the author(s), title of the work, publisher, and DOI

ISBN: 978-3-95450-210-3 doi:10.18429/JACoW-FEL2019-WEP008

MULTI-BEAMLINE OPERATION AT THE EUROPEAN XFEL

L. Fröhlich*, A. Aghababyan, V. Balandin, B. Beutner, F. Brinker, W. Decking, N. Golubeva, O. Hensler, Y. Janik, R. Kammering, H. Kay, T. Limberg, S. Liu, D. Nölle, F. Obier, M. Omet, M. Scholz, T. Wamsat, T. Wilksen, J. Wortmann, DESY, Hamburg, Germany

Abstract

The European XFEL uses a unique beam distribution scheme to direct electron bunches to its three undulator lines. The accelerator delivers up to 600 microsecond long bunch trains, out of which parts or individual bunches can be selected for photon production in any of the FELs. This contribution gives a brief overview of the kicker-septum scheme facilitating this and highlights how even complex bunch patterns can easily be configured via the timing system.

INTRODUCTION

The European X-ray Free-Electron Laser (XFEL) [1–3] delivers bursts of hard and soft X-ray laser pulses with an unprecedented average power to its experimental end stations. The facility is driven by a superconducting 17.5 GeV pulsed linear accelerator operating at a repetition rate of 10 Hz. Each pulse provides stable accelerating conditions for ~600 µs, which allows the transport of up to 2700 electron bunches at the maximum rate of 4.5 MHz. Distributing these bunches to the three undulator lines in a reliable and easily configurable way is challenging and requires the interoperation of multiple hard- and software systems. In this paper, we first give an overview of the involved systems before we focus on the high-level software for configuring the bunch distribution.

BEAM DISTRIBUTION SCHEME

The accelerator uses a unique beam distribution scheme to guide the electron bunches to its three undulator lines. This scheme is illustrated in Fig. 1: After the linac, a system of up to 10 in-vacuum stripline kickers [4] can generate pulses of ~30 ns width, which is short enough to selectively kick individual bunches to the left. A Lambertson septum [5] then deflects these bunches upwards into the transfer line to the linac dump (*TLD*).

The unkicked electrons continue straight to the next system of kickers, which consists of 6 air coils that are mounted on the outside of a ceramic vacuum chamber [6] and deflect upwards. With rise and fall times on the order of 10 µs, these *beam distribution* kickers are significantly slower than the previous set. This means that they provide better bunch-to-bunch stability, but they can only be used to influence an entire portion of the train, not individual bunches. Again, the kicked bunches are picked up by a Lambertson septum and deflected to the left and into the SASE2 undulator line which ends in the *T5D* dump.

Electrons that are influenced by neither kicker system take the straight path to SASE1 and SASE3 and finally end up

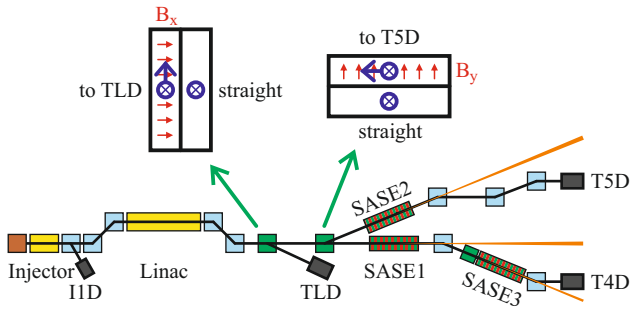


Figure 1: Schematic overview of the European XFEL. Accelerating structures are shown in orange and yellow, major bending magnets in blue, fast kicker systems in green, and beam dumps in dark gray. SASE1–3 are the undulator lines. The drawings above the beamline illustrate the operating direction of the magnetic Lambertson septa.

in the *T4D* dump. A summary of the optics design for the beam distribution system can be found in [7].

The photoinjector is driven by a single laser [8] that can produce a continuous train of pulses at 4.5 MHz, 1.1 MHz, or different rates. While the generated bunch train can be changed in length, it is currently not possible to leave gaps in it. Together with the characteristics of the two main kicker systems, this defines the boundary conditions for bunch distribution:

- From the gun up to the first *TLD* kicker, the beam forms a train of 0–2700 equidistant bunches.
- The *TLD* kickers can send an arbitrary number of the incoming bunches to the linac dump so that they never arrive in any undulator line. This can be decided individually for each bunch.
- Typically once per train the *distribution* kickers can change their state from on to off or vice versa so that a part of the remaining bunches is directed to SASE2 and the other part to SASE1/3. While these kickers are ramping, the incoming bunches must be sent to the linac dump by the *TLD* kickers.
- All of the settings above can be changed from pulse to pulse (i.e. at 10 Hz).

The common electron beamline shared by the SASE1 and SASE3 undulators adds another complication.

SASE1 and SASE3: Fresh Bunch Technique

Bunches destined for the hard X-ray undulator line SASE1 inevitably traverse the soft X-ray undulator line SASE3 and vice versa. This poses a serious problem for the concurrent

* lars.froehlich@desy.de

Content from this work may be used under the terms of the CC BY 3.0 licence (© 2019). Any distribution of this work must maintain attribution to the author(s), title of the work, publisher, and DOI

ISBN: 978-3-95450-210-3 doi:10.18429/JACoW-FEL2019-WEP009

LONG TERM STABILITY AND SLOW FEEDBACK PERFORMANCE AT THE EUROPEAN XFEL

R. Kammering†, Deutsches Elektronen-Synchrotron DESY, Hamburg, Germany

Abstract

The European XFEL is now routinely running in user operation since more than two years. Up to 8 longitudinal and 9 transversal slow feedback loops are routinely used to keep the accelerators chosen operation conditions. First tests of comparing the machine 'free-floating' state versus fully fixing all relevant monitoring signals have been carried out and show interesting results.

Here we will review the feedback systems in terms of software architecture and conceptual layout but also in respect to feedback and FEL performance.

SOME HISTORY: SLOW FEEDBACKS AT FLASH

Both the transversal and longitudinal feedbacks (FBs) used at the European XFEL have first been introduced at the Free Electron Laser in Hamburg FLASH [1]. The first implementations of a transversal feedback as it is used at the European XFEL [2], date back to 2011. While prior implementations at FLASH where Matlab graphical user interface (GUI) based 'stand-alone' applications, the nowadays used implementation is a DOOCS [3] server based centrally managed application.

While round trip time and also interfacing to monitors and actuators for the stand-alone implementations where acceptable, these architectures hold risk of having multiple instances running at the same time, to name just one of the drawbacks of such an implementation.

THE SLOW TRANSVERSAL FEEDBACK

The server based slow transversal feedback (also called 'orbit feedback') [4] is running on a central server machine hosting the data acquisition system (DAQ) [5]. This system synchronizes all incoming data streams on the level of macro-pulses (this is the repetition rate the machine is triggered with – typically 10 Hz. For details on the structure of beam delivery at the European XFEL see [6]). This ensures that all beam position data served to upstream clients is originating from the same macro-pulse. The general architecture in terms of involved infrastructure and dataflow is shown in Figure 1.

The orbit feedback is using a simple PI controller to correct orbit deviations at the currently active beam position monitors (BPMs). The needed amount of correction is calculated using the theoretically calculated orbit response matrix which is read from the online optics model [7] and doing a singular-value-decomposition (SVD).

All parameters like active actuators (up till now we just use corrector magnets), active monitors (BPMs) as well as SVD parameters etc. can be re-configured on-the-fly. Thereby the orbit feedback offers a lot of flexibility, while the underlying control algorithm is kept very simple and thereby robust! This has proven to be exactly the combination which was needed to allow for a fast and reliable commissioning of the European XFEL accelerator.

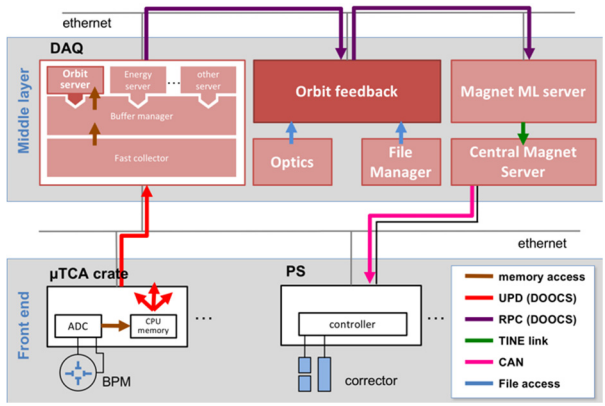


Figure 1: Implementation of the slow transversal feedback within the overall control software architecture.

Layout of Orbit Feedback Along the Linac

First idea has been to run the orbit stabilization as a global feedback. While the software architecture and overall concepts behind the feedback also allow for this, it has shown to be much more practical to use several decoupled instances of the feedback. One global feedback would impose a much more complex architecture in terms of sensitivity and exception handling. Further allows the operation of decoupled feedbacks for more flexibility in terms of the various operation modes of the facility (e.g. only injector operation versus full beam transport to main dumps).

The nowadays used distribution of all orbit feedback instances along the accelerator is shown in Figure 2.

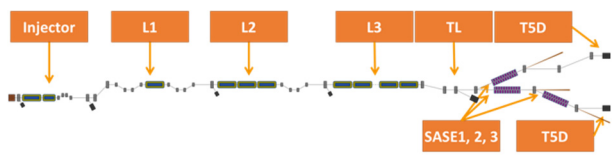


Figure 2: Distribution of orbit feedback instances along the accelerator.

While the single feedback instances are all derived from the same software (and just get configured differently), the demands and targets for the individual instances differ a lot. One can roughly divide the feedbacks into three classes:

- Orbit keeper
  - Here the feedback is aiming for maintaining the orbit over larger sections. Examples are: L2, L3
- Launch stabilization

† raimund.kammering@desy.de

Content from this work may be used under the terms of the CC BY 3.0 licence (© 2019). Any distribution of this work must maintain attribution to the author(s), title of the work, publisher, and DOI

ISBN: 978-3-95450-210-3 doi:10.18429/JACoW-FEL2019-WEP010

FEMTOSECOND LASER-TO-RF SYNCHRONIZATION AND RF REFERENCE DISTRIBUTION AT THE EUROPEAN XFEL

T. Lamb*, M. Felber, T. Kozak, J. Müller, H. Schlarb, S. Schulz, C. Sydlo,
M. Titberidze, F. Zummack, Deutsches Elektronen-Synchrotron (DESY), Hamburg, Germany

Abstract

At the European XFEL, optical pulses from a mode-locked laser are distributed in an optical fiber network providing femtosecond stability throughout the accelerator facility. Due to the large number of RF reference clients and because of the expected higher reliability, the 1.3 GHz RF reference signals are distributed by a conventional coaxial RF distribution system. However, the provided ultra-low phase noise 1.3 GHz RF reference signals may drift over time. To remove these drifts, an optical reference module (REFM-OPT) has been developed to detect and correct environmentally induced phase errors of the RF reference. It uses a femtosecond long-term stable laser-to-RF phase detector, based on an integrated Mach-Zehnder amplitude modulator (MZM), to measure and resynchronize the RF phase with respect to the laser pulses from the optical synchronization system with high accuracy. Currently nine REFM-OPTs are permanently operated at the European XFEL, delivering femtosecond stable RF reference signals for critical accelerating field control stations. The operation experience will be reported together with a detailed evaluation of the REFM-OPT performance.

INTRODUCTION

The European X-ray Free-Electron Laser (XFEL) uses a 1.7 km long superconducting linear accelerator (linac) to drive the FEL. A pulsed optical synchronization system has been built and is operated 24/7 at the European XFEL in order to meet various synchronization requirements [1]. For example the synchronization between the FEL and the pump-probe laser systems needs to be in the femtosecond range in order to make time-resolved, ultra-fast pump-probe experiments possible. This synchronization system also allows to provide RF reference signals with femtosecond stability throughout the linac [2] in order to meet the stability requirement for the accelerating field stability of 0.01° at 1.3 GHz (≈ 20 fs) [3]. See Fig. 1 for a schematic overview of the complete system.

* Thorsten.Lamb@desy.de

OPTICAL SYNCHRONIZATION SYSTEM

The master laser oscillator (MLO) of the optical synchronization system is a redundant, low jitter, commercial laser system with a repetition rate of 216.66 MHz at a wavelength of 1553 nm. The MLO is precisely phase-locked to the 1.3 GHz RF master oscillator (RF-MO) of the accelerator facility. The laser pulse train from the MLO is split up and distributed in polarization maintaining optical fibers to numerous end stations throughout the accelerator facility. Optical length changes of these fibers are permanently measured and actively corrected. Three different types of end stations are currently supplied by the optical synchronization system and all end stations are synchronized with femtosecond precision [4]. The system is used to precisely synchronize laser systems like the photoinjector laser [5] or the pump-probe laser systems, to operate the bunch arrival time monitors (BAMs) [6, 7], and to provide femtosecond stable RF reference signals to dedicated end stations along the linac via the optical reference module (REFM-OPT).

RF REFERENCE DISTRIBUTION

The conventional RF reference distribution system installed at the European XFEL is a highly reliable system. It is however susceptible to temperature and humidity variations. The RF cables installed along the accelerator tunnel

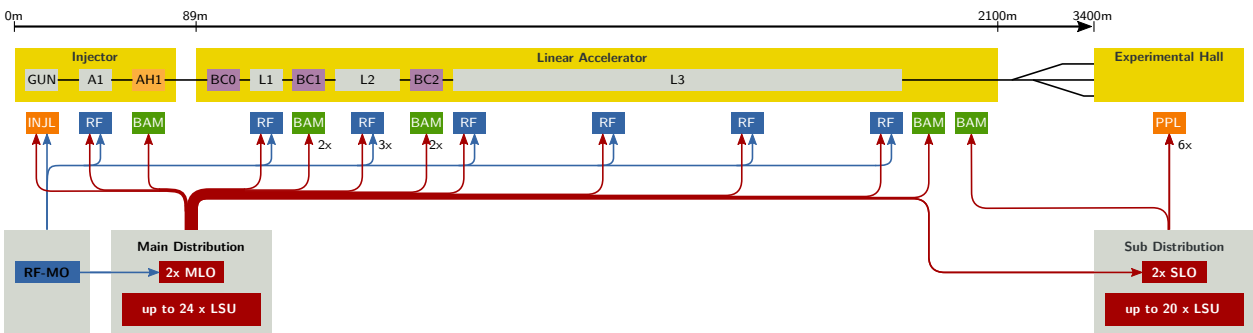


Figure 1: Layout of the RF reference distribution and the pulsed optical synchronization systems of the European XFEL. The RF reference distribution system including the RF-MO and the REFM-OPTs is shown in blue. Stabilized fiber links, MLO/SLO and FSD are presented in red. BAMs are illustrated in green and external laser systems in orange.

Content from this work may be used under the terms of the CC BY 3.0 licence (© 2019). Any distribution of this work must maintain attribution to the author(s), title of the work, publisher, and DOI

ISBN: 978-3-95450-210-3 doi:10.18429/JACoW-FEL2019-WEP011

LONGITUDINAL INTRA-TRAIN BEAM-BASED FEEDBACK AT FLASH

S. Pfeiffer*, L. Butkowski, M. K. Czwalinna, B. Dursun, Ch. Gerth, B. Lautenschlager, H. Schlarb, C. Schmidt, Deutsches Elektronen-Synchrotron DESY, Hamburg, Germany

Abstract

The longitudinal intra-train beam-based feedback has been recommissioned after major upgrades on the synchronization system of the FLASH facility. Those upgrades include: new bunch arrival time monitors (BAMs), the optical synchronization system accommodating the latest European XFEL design based on PM fibers, and installation of a small broadband normal conducting RF cavity. The cavity is located prior to the first bunch compressor at FLASH and allows energy modulation bunch-by-bunch (1 μs spacing) on the per mille range. Through the energy dependent path length of the succeeding magnetic chicane the cavity is used for ultimate bunch arrival time corrections. Recently the RF cavity operated 1 kW pulsed solid-state amplifier was successfully commissioned. First tests have been carried out incorporating the fast cavity as actuator together with SRF stations for larger corrections in our intra-train beam-based feedback pushing now arrival time stabilities towards 5 fs (rms). The latest results and observed residual instabilities are presented.

INTRODUCTION

The free-electron laser in Hamburg (FLASH) at DESY is a research facility which provides laser radiation in the soft X-ray range with tunable wavelengths down to 4.2 nm. The accelerator operates in pulsed mode with a repetition rate of 10 Hz. The laser radiation is generated by the self-amplified spontaneous emission (SASE) process. The electron bunch trains with a variable length and repetition rate are accelerated by superconducting radio frequency (SRF) cavities up to the electron beam energy of 1.25 GeV, with a maximum number of 800 bunches per pulse and a bunch repetition rate of 1 MHz [1].

A high precision synchronization in the range of femtoseconds between an external laser and the free-electron laser (FEL) pulses is required, e.g., for pump-probe experiments. An intra-train beam-based feedback is used to correct arrival time fluctuations of the electron bunches in the magnetic bunch compression chicane in order to improve the bunch arrival time stability, which contributes to the photon beam quality delivered to the experiments. The important signal for the beam-based feedback is provided by the bunch arrival time monitors (BAMs) [2].

The low level radio frequency (LLRF) controller, regulating the 1.3 GHz RF field in amplitude A and phase Φ of the SRF cavities, includes different control strategies like a learning feedforward controller to minimize repetitive amplitude and phase errors from pulse to pulse and a second order multiple-input multiple-output (MIMO) controller to react within a pulse. The LLRF control system is based on the MicoroTCA.4 standard. The RF field regulation typically reaches an amplitude stability of $\Delta A/A \approx 0.008$ % and a phase stability of $\Delta\Phi \approx 0.007$ deg for the SRF cavities [3]. In addition, the superposition of the RF field information with beam-based measurements, e.g. the arrival time measured by the BAMs, is included in the control strategy of the RF field [4, 5].

The control strategy with the superposition of the RF-field and the beam-based information is called longitudinal intra-train beam-based feedback. This beam-based feedback control strategy and the controller design is already introduced in [5, 6].

In addition to the recent upgrades of the BAMs [4, 7, 8] and optical synchronization system [9], now using the latest European XFEL design based on PM fibers, a normal conducting cavity has been integrated into the beamline as a fast energy corrector cavity to further improve the arrival time stability to reach the goal of an arrival time stability of about 5 fs (rms). This cavity is called "Bunch Arrival Corrector CAvity" (BACCA). The latest measurement results will be presented in this paper.

SYSTEM DESCRIPTION

Figure 1 shows a scheme of FLASH with the above mentioned diagnostic units and beam-based feedback loops marked with the colored areas. The measured arrival time data of the second BAM (BAM2) after the first bunch compressor (BC2) is transmitted via a high-speed optical link to the LLRF controller and used for the arrival time regulation by adjusting the RF field at the SRF module ACC1. The same arrival time signal is used for the regulation of the fast feedback cavity BACCA. The first BAM (BAM1) is not affected by the beam-based feedbacks and measures the incoming arrival time jitter. After the second bunch compressor the accelerator modules ACC4 to ACC7 increase the beam energy but do not influence the bunch arrival time. Marked in grey and dashed lines are the bunch compression monitors (BCMs) and the additional feedback loop for the regulation of the SRF modules ACC2 and ACC3 by using the arrival time measurements of the third BAM (BAM3). These parts are planned as add-ons in the future for the beam-based control strategy.

Bunch Arrival Time Monitors

The intra-train beam-based control strategy uses the arrival time of every single bunch for the regulation. The bunch arrival time monitors consist of three main parts, the RF unit, the electro-optical unit and the data acquisition (DAQ) unit. The readout electronics according to the MicroTCA.4 standard are in operation since 2013 [10].

* sven.pfeiffer@desy.de

Content from this work may be used under the terms of the CC BY 3.0 licence (© 2019). Any distribution of this work must maintain attribution to the author(s), title of the work, publisher, and DOI

ISBN: 978-3-95450-210-3 doi:10.18429/JACoW-FEL2019-WEP012

THz SPECTROSCOPY WITH MHz REPETITION RATES FOR BUNCH PROFILE RECONSTRUCTIONS AT EUROPEAN XFEL

N. M. Lockmann*, Ch. Gerth, B. Schmidt, S. Wesch
Deutsches Elektronen-Synchrotron DESY, Hamburg, Germany, EU

Abstract

The European X-ray Free-Electron Laser generates most powerful and brilliant X-ray laser pulses. Exact knowledge about the longitudinal electron bunch profile is crucial for the operation of the linear accelerator as well as for photon science experiments. The only longitudinal diagnostic downstream of the main linac is based on spectroscopy of diffraction radiation (DR). The spectral intensity of the DR in the THz and infrared regime is monitored by a four-staged grating spectrometer and allows non-invasive bunch length characterization based on form factor measurements in the range 0.7 – 60 THz. As the readout and signal shaping electronics of the spectrometer allow MHz readout rates, the longitudinal bunch profile of all bunches inside the bunch train can be characterized non-invasively and simultaneously to FEL operation. In this paper, form factor measurements along the bunch train will be described and presented as well as the resulting reconstructed current profiles.

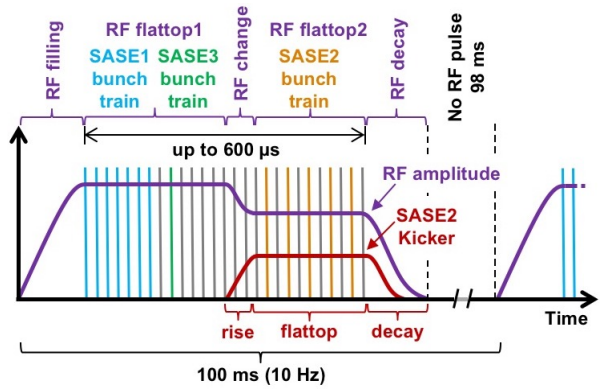


Figure 1: Simplified diagram of the EuXFEL bunch pattern. The RF accelerating pulses (purple line) can be split into two flattops to optimize independently the bunch compression for SASE1/SASE3 and SASE2.

INTRODUCTION

The European XFEL (EuXFEL) generates femtosecond X-ray laser pulses in the wavelength range 0.05 – 6 nm based on Self-Amplified Spontaneous Emission (SASE) at MHz repetition rates [1]. The super-conducting linear accelerator of EuXFEL [2] has recently been operated at a beam energy of 14 GeV, a bunch charge of 250 nC, and with 600 µs-long trains of up to 675 bunches at a rate of 10 Hz. The femtosecond electron bunches can be distributed into three different SASE undulator beamlines and serve three experimental stations in parallel for which a flexible bunch pattern can be adjusted independently as depicted schematically in Fig. 1.

For a stable operation of the accelerator, e.g. to suppress beam-loading in the accelerator modules, the full bunch train is filled with bunches. Bunches requested by the user experiments, marked as blue, green, and orange bars in Fig. 1, are distributed to the individual undulator beamlines SASE1, SASE2, and SASE3, whereas all other bunches are kicked out by a fast kicker-septum arrangement into a local dump upstream of the SASE undulators (grey bars in Fig. 1). The hard X-ray undulator SASE1 is located in a straight section and followed by the soft X-ray undulator SASE3 downstream of a bending magnet which separates the hard X-rays from the electron beam. A flattop kicker, indicated as a red line in Fig. 1, is used to deflect electron bunches into a septum which deflects the bunches into the undulator beamline SASE2. The radio-frequency (RF) accelerating pulses (solid purple line in Fig. 1) can be split into two flattop regions for which the RF accelerating voltage, i.e. amplitude and phase, can be adjusted within certain limits for independent optimization of the bunch compression and FEL power of SASE2. The SASE2 bunch train can also be swapped with the SASE1/SASE3 bunch trains to have the SASE2 bunch train in the RF flattop1. The bunches that are accelerated during the time between the RF flattops, required both for adjustment of the accelerating voltage and rise or decay time of the SASE2 flattop kicker, are taken out by the fast kicker-septum arrangement. A layout of the undulator beamlines is shown in Fig. 2.

The exact knowledge of the longitudinal current profile of the individual electron bunches is of high interest for the photon experiments as well as for accelerator operation. At EuXFEL the current profile at final compression is monitored by terahertz (THz) and infrared (IR) spectroscopy of coherent diffraction radiation (DR) just upstream of the undulator beamlines, see also Fig. 2. The spectral content of this coherently emitted radiation is determined by the modulus of the longitudinal form factor, the Fourier transform of the current profile. Therefore, the modulus of the longitudinal form factor $|F_l|$, which is accessible by measurements of the coherently emitted DR [3], yields information about the time structure of the electron bunch.

As the emission of DR does not influence the electron beam quality, it allows for non-invasive bunch length characterization. A four-staged single-shot grating spectrometer [4] has been utilized to measure the spectral intensity of the DR with single bunch resolution. Consequently, the longitudinal form factor of all bunches inside the bunch train can be measured simultaneously during FEL operation.

* nils.maris.lockmann@desy.de

Content from this work may be used under the terms of the CC BY 3.0 licence (© 2019). Any distribution of this work must maintain attribution to the author(s), title of the work, publisher, and DOI

ISBN: 978-3-95450-210-3 doi:10.18429/JACoW-FEL2019-WEP013

FAST KICKER SYSTEM FOR EUROPEAN XFEL BEAM DISTRIBUTION

F. Obier, W. Decking, M. Hüning, J. Wortmann, DESY, Hamburg, Germany

Abstract

A special feature of the European XFEL [1] X-ray laser is the possibility to distribute the electron bunches of one RF pulse to different free-electron laser (FEL) beamlines. This is achieved through a combination of kickers and a Lambertson DC septum. The integration of a beam abort dump allows a flexible selection of the bunch pattern at the FEL experiment, while the superconducting linear accelerator operates with constant beam loading. The driver linac of the FEL can deliver up to 600 µs long bunch trains with a repetition rate of 10 Hz and a maximum energy of 17.5 GeV. The FEL process poses very strict requirements on the stability of the beam position and hence on all upstream magnets. It was therefore decided to split the beam distribution system into two kicker systems, long pulse kickers (KL) with very stable amplitude (10^{-4}) and a long flat-top (~300 µs) with relatively slow rise/fall times (~20 µs) and fast stripline kickers (KS) with moderate stability but very fast pulses (~5 0ns).

OVERVIEW

Figure 1 shows a schematic overview of the European XFEL fill pattern and beam distribution system. The six KL flat-top kickers are operated with a rectangular pulse with variable pulse length and switch the beam between the two main FEL beamlines. To create the flexible bunch pattern, a kicker-septum combination including ten KS stripline kickers is installed, with which it is possible to extract individual bunches into the dump beamline (TLD) with the maximum bunch frequency of 4.5 MHz. Pilot bunches for the intra-bunch feedback that is needed to stabilise the beam, bunches during the still-needed gap for rise time of the KL beam distribution kickers and all bunches not needed for lasing are extracted to the dump. Bunches for the SASE3 undulator can be stimulated with a KS kicker so that they do not lase in the SASE1 undulator. All of this requires a sophisticated bunch pattern generator and timing system [2].

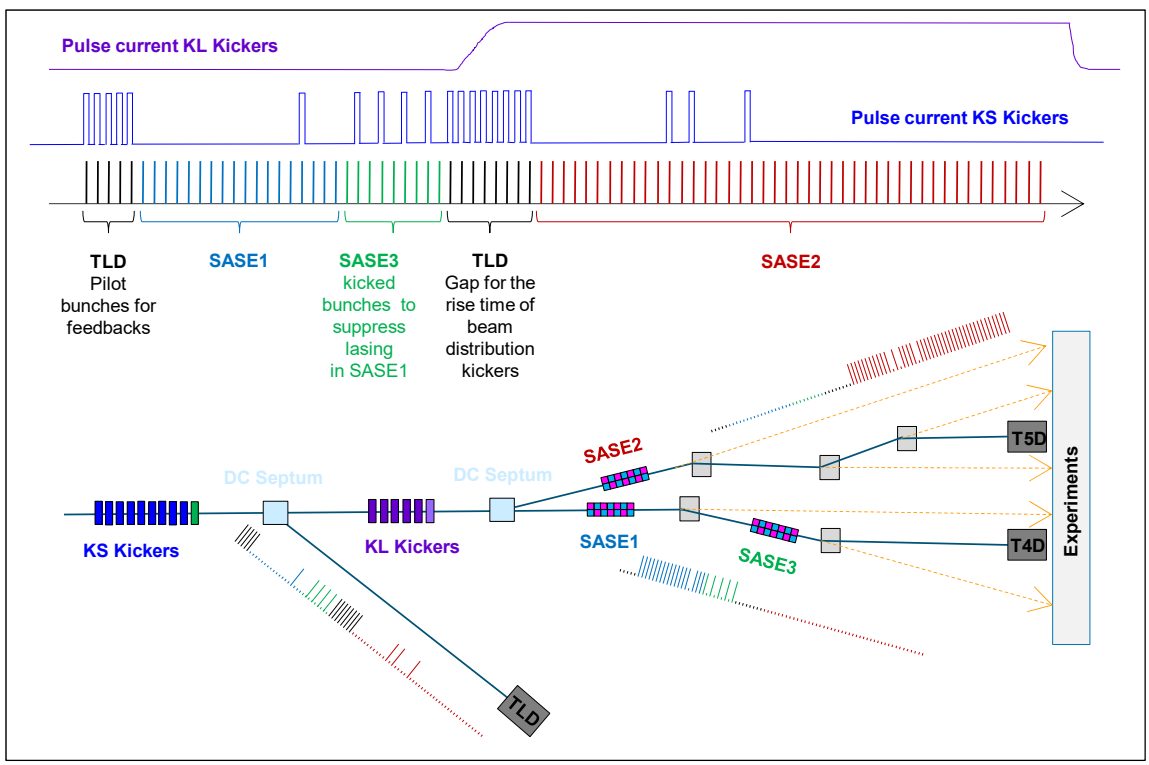


Figure 1: European XFEL fill pattern scheme: The flexible bunch pattern for the FEL lines is created by kicking all bunches that are not used for lasing into the main dump line (TLD) by means of the KS kickers. The bunch train parts for the FEL lines are distributed by the KL kickers. SASE2 bunches are kicked, SASE1/3 bunches are not.

Content from this work may be used under the terms of the CC BY 3.0 licence (© 2019). Any distribution of this work must maintain attribution to the author(s), title of the work, publisher, and DOI

ISBN: 978-3-95450-210-3 doi:10.18429/JACoW-FEL2019-WEP014

LONG PULSE KICKER FOR EUROPEAN XFEL BEAM DISTRIBUTION

F. Obier, W. Decking, M. Hüning, J.Wortmann, DESY, Hamburg, Germany

Abstract

A special feature of the European XFEL [1] X-ray laser is the possibility to distribute the electron bunches of one RF pulse to different free-electron laser (FEL) beamlines. This is achieved through a combination of kickers and a Lambertson DC septum. The integration of a beam abort dump allows a flexible selection of the bunch pattern at the FEL experiment, while the superconducting linear accelerator operates with constant beam loading. The driver linac of the FEL can deliver up to 600µs long bunch trains with a repetition rate of 10Hz and a maximum energy of 17.5GeV. The FEL process poses very strict requirements on the stability of the beam position and hence on all upstream magnets. It was therefore decided to split the beam distribution system into two kicker systems, long pulse kickers (KL) with very stable amplitude (10^{-4}, flat-top) and relatively slow pulses (~300µs) and fast stripline kickers (KS) with moderate stability but very fast pulses (~50ns).

OVERVIEW

Figure 1 shows a schematic overview of the European XFEL fill pattern and beam distribution system. The six so-called KL flat-top kickers are operated with a rectangular current pulse with variable pulse length and switch the beam between the two main FEL beamlines. To create the flexible bunch pattern, a kicker-septum combination including ten so-called KS stripline kickers is installed, with which it is possible to extract individual bunches into the dump beamline (TLD) with the maximum bunch repetition frequency of 4.5MHz. Pilot bunches for the intra-bunch feedback that is needed to stabilise the beam, bunches during the still-needed gap for rise time of the KL beam distribution kickers and all bunches not needed for lasing are extracted to the dump. Bunches for the SASE3 undulator can be stimulated with a KS kicker so that they do not lase in the SASE1 undulator. All of this requires a sophisticated bunch pattern generator and timing system [2].

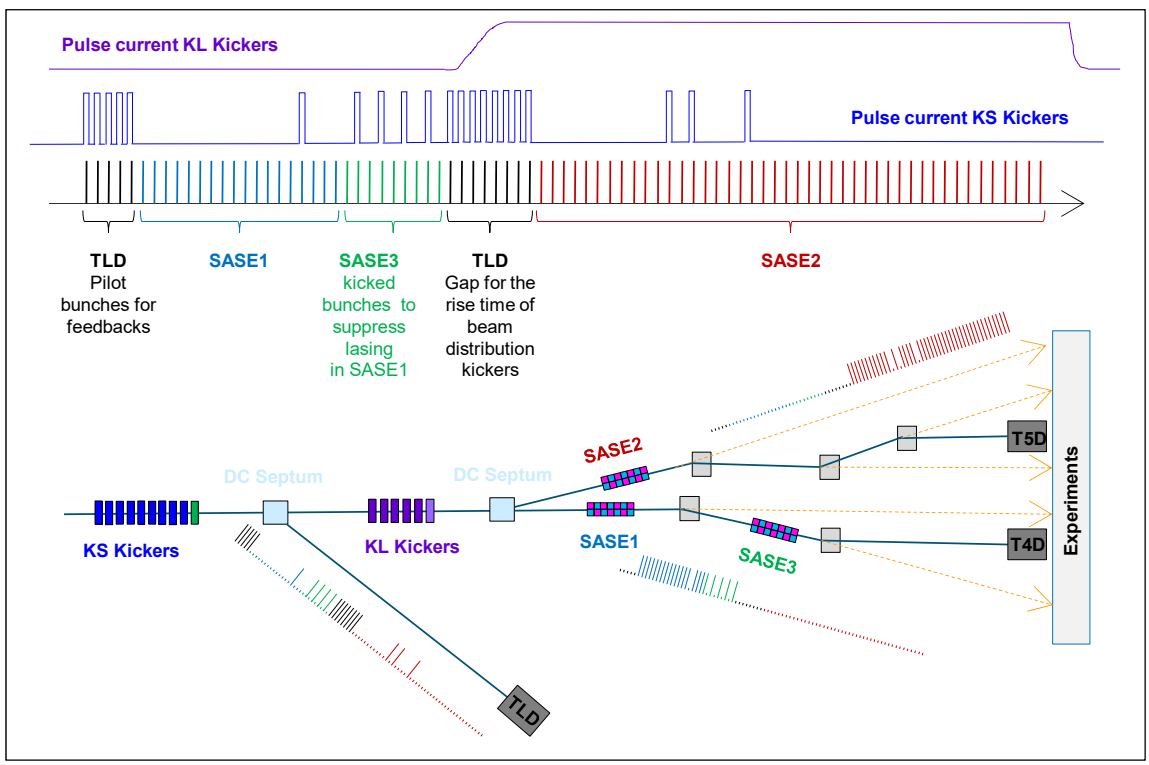


Figure 1: European XFEL fill pattern scheme: The flexible bunch pattern for the FEL lines is created by kicking all bunches that are not used for lasing into the main dump line (TLD) by means of the KS kickers. The bunch train parts for the FEL lines are distributed by the KL kickers. SASE2 bunches are kicked, SASE1/3 bunches are not.

Content from this work may be used under the terms of the CC BY 3.0 licence (© 2019). Any distribution of this work must maintain attribution to the author(s), title of the work, publisher, and DOI

ISBN: 978-3-95450-210-3 doi:10.18429/JACoW-FEL2019-WEP015

ELECTRO-OPTICAL BUNCH LENGTH DETECTION AT THE EUROPEAN XFEL

Bernd Steffen*, Marie Kristin Czwalinna, Christopher Gerth
Deutsches Elektronen-Synchrotron DESY, Hamburg, Germany
Eléonore Roussel, Serge Bielawski, Clement Evain, Christophe Szwaj
Univ. Lille, CNRS, UMR 8523 - PhLAM - Physique des Lasers, Atomes et Molécules,
Centre d'Étude Recherches et Applications (CERLA), Lille, France

Abstract

The electro-optical bunch length detection system based on electro-optic spectral decoding has been installed and is being commissioned at the European XFEL. The system is capable of recording individual longitudinal bunch profiles with sub-picosecond resolution at a bunch repetition rate of 1.13 MHz. Bunch lengths and arrival times of entire bunch trains with single-bunch resolution have been measured as well as jitter and drifts for consecutive bunch trains. In addition, we are testing a second electro-optical detection strategy, the so-called photonic time-stretching, which consists of imprinting the electric field of the bunch onto a chirped laser pulse, and then "stretching" the output pulse by optical means. As a result, we obtain is a slowed down "optical replica" of the bunch shape, which can be recorded using a photodiode and GHz-range acquisition. These tests are performed in parallel with the existing spectral decoding technique based on a spectrometer in order to allow a comparative study.

In this paper, we present first results for both detection strategies from electron bunches after the second bunch compressor of the European XFEL.

INTRODUCTION

The accelerator for the European X-ray Free-Electron Laser (EuXFEL) delivers femtosecond electron bunches at an energy of up to 17 GeV at a repetition rate of up to 4.5 MHz in bursts of up to 2700 bunches every 100 ms. The electron bunches can be distributed between three undulator beamlines, and the generated femtosecond X-ray laser pulses at wavelengths between 0.05 nm and 6 nm can serve up to three user experiments in parallel [1].

Short electron bunches with a high peak current are needed to drive the SASE process in the magnetic undulators. To reach these short bunches, the initially long electron bunches created at the photocathode gun are compressed in three magnetic bunch compressor chicanes at electron bunch energies of 130 MeV,700 MeV, and 2.4 GeV, respectively, in between the four accelerating sections.

Electro-optical bunch length detection (EOD) [2] offers the possibility of measuring the longitudinal bunch profile and arrival time in a non-destructive manner with single bunch resolution for every bunch in the bunch train. The measurements presented in this paper were performed at the EOD system downstream of the second bunch compressor at a beam energy of 700 MeV and with an expected bunch length of around 250 ps.

ELECTRO-OPTICAL BUNCH LENGTH DETECTION AT THE EUROPEAN XFEL

Electro-optically active crystals like gallium phosphide (GaP) become birefringent in the presence of an electric field. The electro-optical detection techniques use this effect to transfer the temporal profile of fast changing electric fields by sampling the change in birefringence with laser pulses. Afterwards, the modulated temporal profile of the laser pulse can be analyzed with classical laser techniques.

For the EOD system at the EuXFEL the spectrally resolved electro-optical detection technique (EOSD) was chosen. It uses a chirped laser pulse, where the frequency components of a broadband laser pulse are sorted in time. The temporal profile of the modulation can be retrieved from its modulated spectrum using the known relationship between wavelength and longitudinal (temporal) position in laser pulse [3]. It has been shown that sub-ps electron bunches of about 100 pC charge can be measured with about 200 fs resolution using EOSD [2, 4].

Temporally [5] and spatially [6] resolved detection offer a higher time resolution as good as 60 fs, but they have higher demands on the imaging system for the laser and need higher laser pulse energies compared to EOSD. For a more comprehensive description of electro-optical detection techniques and theory see [4, 7]. The maximum rate of all techniques is limited by both the repetition rates of the laser system and (line) detector.

To measure single shot laser spectra as needed for EOSD with a high repetition rate, currently two different techniques are available. One can use a spectrometer with a high-speed line camera like the KALYPSO detector [8]. The KALYPSO detector can measure spectra with an repetition rate up to 2.7 MHz and was used previously to measure bunch length in the EOSD systems at the European XFEL [9]. Alternatively one can stretch the picosecond short laser pulse in a fiber of known dispersion to a length of several nanoseconds and measure the temporal profile of the laser pulse with a fast photodiode and gigahertz bandwidth oscilloscope, known as photonic time-stretch [10]. Photonic time-stretch has first be proposed for recording GHz-range RF signals [11]. The principle has been then applied to electro-optic sampling of free-propagating CSR THz pulses at SOLEIL [12], and more

* bernd.steffen@desy.de

Content from this work may be used under the terms of the CC BY 3.0 licence (© 2019). Any distribution of this work must maintain attribution to the author(s), title of the work, publisher, and DOI

ISBN: 978-3-95450-210-3 doi:10.18429/JACoW-FEL2019-WEP016

Content from this work may be used under the terms of the CC BY 3.0 licence (© 2019). Any distribution of this work must maintain attribution to the author(s), title of the work, publisher, and DOI

PRECISE LASER-TO-RF SYNCHRONIZATION OF PHOTOCATHODE LASERS

M. Titberidze*, M. Felber, T. Kozak, T. Lamb, J. Müller, H. Schlarb, S. Schulz, F. Zummack
Deutsches Elektronen-Synchrotron, DESY, Hamburg, Germany
C. Sydlo, Paul Scherrer Institut, PSI, Villigen, Switzerland

Abstract

RF photo-injectors are used in various large, mid and small-scale accelerator facilities such as X-ray Free Electron Lasers (XFELs), external injection-based laser-driven plasma accelerators (LPAs) and ultrafast electron diffraction (UED) sources. Many of these facilities require a high precision synchronization of the photo-injector laser system, either because of beam dynamics reasons or the photo-injector directly impacting pump-probe experiments carried out to study physical processes on femtosecond timescales. It is thus crucial to achieve synchronization in the order of 10 fs rms or below between the photocathode laser and the RF source driving the RF gun. In this paper, we present the laser-to-RF synchronization setup employed to lock a commercial near-infrared (NIR) photocathode laser oscillator to a 2.998 GHz RF source. Together with the first results achieving ~ 10 fs rms timing jitter in the measurement bandwidth from 10 Hz up to 1 MHz, we describe an advanced synchronization setup as a future upgrade, promising even lower timing jitter and most importantly long-term timing drift stability.

INTRODUCTION

The (short and innovative bunches and accelerators at DESY) SINBAD facility will host several accelerator research and development experiments like ARES [1] and AXSIS [2]. These experiments will mainly focus on the production of ultra-short electron bunches (0.2 fs to 10 fs) and testing novel high gradient acceleration techniques. The (accelerator research experiment at sinbad) ARES is a conventional S-band linear RF accelerator (linac) which is currently in the construction and commissioning phase [3]. It consists of S-band (f_{RF} = 2.998 GHz) normal conducting accelerating structures: 1.5 cell RF gun [4] and two travelling wave structures (TWS1, TWS2) [5]. The electron bunches are produced by impinging ultrashort laser pulses on a photocathode inside the RF gun.The ARES linac is schematically shown in Fig. 1. The final electron beam parameters at ARES are defined in [3] and require an arrival time jitter of < 10 fs rms. In order to meet this requirement it is crucial to achieve a precise laser-to-RF synchronization between the pulsed injector laser and the 2.998 GHz RF reference signal from the RF master oscillator (MO). The injector laser is a commercial system from Light Conversion[1] with a fundamental wavelength of 1030 nm and variable pulse duration of 0.16 ps to 10 ps. The laser oscillator of this system is designed such that the repetition rate of the optical pulses f_{rep} = 83.28 MHz is the 36th sub-harmonic of the RF reference frequency f_{RF} = 2.998 GHz.

DIRECT CONVERSION BASED LASER-TO-RF SYNCHRONIZATION

General Concept

One of the most common techniques to synchronize a mode-locked laser to an RF signal is using a fast photodetector [6–9]. The pulsed optical signals are converted to electrical pulses which are composed of high spectral purity harmonics of the laser repetition rate. The cutoff frequency of the RF comb is given by the bandwidth of the photodetector. The desired frequency component of the RF comb can be filtered out using an RF band-pass filter (BPF) and amplified until the signal level is sufficient for downconvertion. The downconverted signal is digitized using an analog-to-digital converter (ADC) employing so called non-IQ sampling [6, 10, 11]. The amplitude and phase information is extracted in the digital domain. The obtained phase error information is fed back to the piezo actuator of the laser oscillator using a piezo driver to establish the phase locked loop (PLL).

There are several advantages of downconverting the photodetected signal to an intermediate frequency (IF) instead of baseband. Baseband signals are often degraded by undesired DC offsets due to imperfections of the electronics and they are highly susceptible to electromagnetic interference (EMI). Both effects limit the overall PLL performance potentially leading to a poor synchronization performance. These problems are mitigated by direct sampling the IF signal and using digital phase detection.

However, there are still fundamental limitations related to the photodetection process, such as the AM-PM effect, where optical power fluctuations are converted to phase fluctuations of each frequency component of the generated frequency comb [12, 13] while low signal levels from the photodetector together with the intrinsic thermal and shot noise sources lead to a limited signal-to-noise ratio (SNR).

One can estimate the thermal noise limited timing jitter for a 50 Ω terminated photodetector using the following expression [14]:

$$T_{\mathrm{rms}} = \frac{1}{2\pi f_{\mathrm{c}}} \sqrt{\frac{P_{\mathrm{th}}}{P_{\mathrm{c}}} \Delta f}. \quad (1)$$

Here, $P_{\mathrm{th}} = -174\,\mathrm{dBm/Hz}$ is the thermal noise power at room temperature in a 1 Hz bandwidth. P_{c} and f_{c} are the

* mikheil.titberidze@desy.de
[1] Pharos SP-06-200-PP

ISBN: 978-3-95450-210-3 doi:10.18429/JACoW-FEL2019-WEP019

Content from this work may be used under the terms of the CC BY 3.0 licence (© 2019). Any distribution of this work must maintain attribution to the author(s), title of the work, publisher, and DOI

CONCEPT OF A NOVEL HIGH-BANDWIDTH ARRIVAL TIME MONITOR FOR VERY LOW CHARGES AS A PART OF THE ALL-OPTICAL SYNCHRONIZATION SYSTEMS AT XFEL AND FLASH*

Andreas Penirschke†, Technische Hochschule Mittelhessen (THM), Friedberg, Germany
Marie Kristin Czwalinna, Holger Schlarb
Deutsches Elektronen-Synchrotron (DESY), Hamburg, Germany
Wolfgang Ackermann, Technische Universität Darmstadt, Darmstadt, Germany

Abstract

Numerous advanced applications of X-ray free-electron lasers require pulse durations and time resolutions in the order of only a few femtoseconds or better. The generation of these pulses to be used in time-resolved experiments require synchronization techniques that can simultaneously lock all necessary components to a precision in the range of 1fs only. To improve the experimental conditions at existing facilities and enable future development of seeded FELs, a new all-optical synchronization system at FLASH and XFEL was implemented, which is based on pulsed optical signals rather than electronic RF signals. In collaboration with DESY, Hamburg the all-optical synchronization system is used to ensure a timing stability on the 10-fs scale at XFEL.

For a future ultra-low charge operation mode, down to 1 pC at XFEL an overall synchronization of 5+1 fs rms. or better is necessary.

This contribution presents a new concept of an ultra-wideband pickup structure for beampipe-diameters down to 10mm for frequencies up to 80 GHz or higher and at the same time providing sufficient output signal for the attached EOMs.

INTRODUCTION

In order to investigate dynamical processes down to the femtosecond (fs) time scale, free electron lasers (FELs) are conducted to deliver ultrashort x-ray pulse for pump-probe experiments [1,2]. These time-resolved measurements require synchronization between an external pumping laser and the FEL pulse for probing lower than the pulse duration, i.e., a few femtoseconds. The FEL pulse timing can be determined by high-resolution arrival-time measurements of electron bunches at the undulators [3].

In recent years, the interest for ultrashort x-ray pulses is continuously rising which requires for the accelerator an ultra-low bunch charge operation down to a few pC only [4,5]. Different schemes for bunch arrival time measurements have been implemented so far allowing. for single-shot detection with a resolution of a few fs and below. [6-10].

At the free-electron lasers European XFEL and FLASH in Hamburg, pickup-based arrival-time monitors with electro-optical detection schemes have been implemented.

* This work is supported by the German Federal Ministry of Education and Research (BMBF) under contract no. 05K19RO1.

† andreas.penirschke@iem.thm.de

As part of a laser-based synchronization system, bunch arrival-time monitors (BAMs) measure the arrival time with a sub-10 fs time resolution for bunch charges higher than 500 pC [11]. A beam-induced signal modulates the amplitude of an external laser pulse in a Mach-Zehnder type electro-optic modulator (EOM). This laser pulse is delivered through a stabilized optical fiber link with a drift stability of around 10 fs=day. Thus, as a direct client of this highly stable optical reference, the BAM based on standard telecom EOMs at 1550 nm has an intrinsic low drift feature, in addition to the high resolution. The reference timing is the zero crossing of the pickup signal, where the sampling laser pulse has no modulation. The EOM DC bias is such that without an external rf modulation the amplitude of the sampling laser pulses is halved. Any deviation from the zero crossing of the pickup transient, i.e., bunch arrival-time jitter, results in an amplitude modulation of the reference laser pulse. With a proper calibration with a precession delay line, this amplitude modulation is directly converted to arrival-time information with a dynamic range corresponding to the linear part of the pickup slope. More details are given in [11-12]. The slope steepness at the zero crossing defines the modulation voltage which the laser pulse experiences in the presence of an arrival-time jitter. This determines the time resolution as well as the sensitivity of the BAMs. The slope steepness reduces proportionally with the bunch charge leading to a BAM performance degradation for charges lower than 200 pC [3,13]. In order to achieve sub-10 fs time resolution for a low charge operation mode down to a few pC, the bandwidth of the current BAMs needs to be increased from 40 GHz up to 80 GHz or higher. As a part of the high bandwidth BAM, cone-shaped pickups were introduced in [14]. The cone shaped pickups are part of the synchronization systems at XFEL, FLASH and ELBE (Helmholtz-Zentrum Dresden- Rossendorf) [14-16].

This paper presents a new concept of an ultra-wideband pickup structure for beampipe-diameters down to 10mm for frequencies up to 80 GHz or higher with sufficient output signal for driving the attached EOMs.

CONE SHAPED PICKUP DESIGN

The rf properties of the pickup is defined by its shape, the material, the used connectors, and the cables connected to the pickup. However, the pickup shape has the largest influence on the performance of the system.

In [14] a tapered coaxial structure was proposed, which comprises a cone-shaped pickup electrode with the

ISBN: 978-3-95450-210-3 doi:10.18429/JACoW-FEL2019-WEP024

1.3 GHz SOLID STATE POWER AMPLIFIER FOR THE BUNCHER IN CTFEL FACILITY*

T. H. He†, C. L. Lao, P. Li, X. Luo, L. J. Shan, K. Zhou
Institute of Applied Electronics, China Academy of Engineering Physics, Mianyang, China

Abstract

The THz Free Electron Laser facility (CAEP THz FEL, CTFEL) of the China Academy of Engineering Physics uses high-quality electron beams to generate high average power terahertz radiations. A 1.3 GHz RF buncher is used in front of the superconducting linear accelerator of the CTFEL facility to improve the electron beams quality. The RF buncher is driven by a solid state power amplifier (SSPA), and the SSPA is feedback controlled by a low level RF (LLRF) control system to ensure the high stability of the amplitude and phase of the bunching field in the buncher cavity. The SSPA operates at 1.3 GHz and outputs 0 to 5 kW of continuous wave power. This paper mainly introduces the principle and composition of the SSPA, and presents some experiments on the RF buncher driven by the SSPA.

INTRODUCTION

In recent years, with the development of science and technology, high-power terahertz sources have become more and more important in the world. A high average power terahertz radiation facility (CAEP THz FEL, CTFEL) has been developed by the China Academy of Engineering Physics. This is the first THz user facility based on free electron lasers in China [1]. The CTFEL facility is designed to produce 1-3 THz radiation with an average output power beyond 10 W.

The CTFEL facility mainly includes a photocathode high voltage direct current (HV-DC) electron gun [2], an RF buncher, an RF superconducting linear accelerator [3], a high performance undulator [4] and so on. Its general layout is shown in Figure. 1. High quality electron beams are generated by the photocathode HV-DC electron gun. When the electron beams come through the RF buncher cavity, the bunch length of the electron beams will be compressed to 4-8 ps. Then, the electron beams come into the RF superconducting linear accelerator, and will be accelerated to 6-8 MeV, passing through an achromatic section, coming into an undulator with the periodical magnetic field and generate spontaneous THz radiation. The THz radiation oscillates back and forth in the optical cavity. Under resonant conditions, the power of the THz radiation increases rapidly until reaching saturated output state.

The RF buncher is an indispensable component of the CTFEL facility, which provides a longitudinal manipulation of the electron beams and ensures that the bunch length of the electron beams to be compressed to 4-8 ps when coming into the superconducting cavity. In the CTFEL facility, the electron beams are quasi-continuously operated, so the RF buncher needs to be driven by continuous wave. The designed output power of the microwave source is about 2.7 kW. Considering the improvements and upgrades in the future, the CTFEL facility uses an L-band 5 kW continuous wave solid state power amplifier (SSPA). The bunch length and energy spread of the electron beams are directly related to the amplitude and phase of the buncher cavity. In order to ensure that the amplitude and phase stability of the buncher cavity field are less than 0.3% and 0.3°, respectively, the SSPA is cooled by a high precision water cooler and controlled by a low-level RF (LLRF) control system for real-time feedback. This paper mainly introduces the principle and composition of the SSPA, and presents some experiments on the buncher driven by the SSPA.

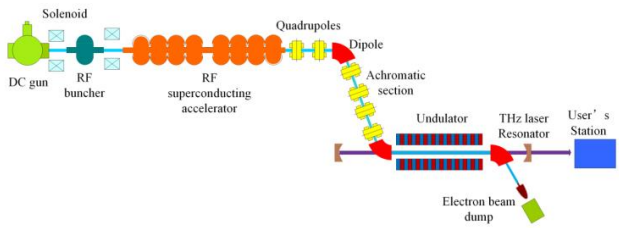


Figure 1: Layout of the CTFEL facility.

SOLID STATE POWER AMPLIFIER

The SSPA is used to drive the RF buncher, its main function is to amplify the input signal and output a continuous wave of high power. And the output power of the SSPA can be adjusted with the change of the input signal.

The SSPA consists of a preamplifier (with one-two splitter, two 3 kW final stage power amplifier arrays, two 3 kW coaxial directional couplers, two waveguide coaxial converters, a two in one waveguide power combiner, a 5 kW waveguide directional coupler, a controller and an embedded computer. The 3 kW final stage power amplifier array consists of a pre-stage power amplifier, ten final stage power amplifier modules, eleven power supply modules, a one-tenth power splitter, a ten in one power combiner and a water cooled board. Board composition. The MCU acquisition unit is integrated in the power supply modules, and the parameters such as voltage, current and temperature are uploaded to the industrial computer through the RS-485 serial ports.

The block diagram of the SSPA is shown in Figure. 2. When a 0 dBm signal is input to the SSPA, it can output a 5 kW continuous wave. The SSPA design targets and test

* Work supported by China National Key Scientific Instrument and Equipment Development Project (2011YQ130018)
† htth111@163.com

Content from this work may be used under the terms of the CC BY 3.0 licence (© 2019). Any distribution of this work must maintain attribution to the author(s), title of the work, publisher, and DOI

ISBN: 978-3-95450-210-3 doi:10.18429/JACoW-FEL2019-WEP026

Content from this work may be used under the terms of the CC BY 3.0 licence (© 2019). Any distribution of this work must maintain attribution to the author(s), title of the work, publisher, and DOI

PRELIMINARY GEOMETRY OPTIMIZATION OF A 3.5-CELL SRF GUN CAVITY AT ELBE BASED ON BEAM DYNAMICS *

K. Zhou, Institute of Applied Electronics, CAEP, Mianyang, China
Institute of Radiation Physics, HZDR, Dresden, Germany
P. Li, Institute of Applied Electronics, CAEP, Mianyang, China
A. Arnold, J. Schaber, J. Teichert†, R. Xiang, S. Ma
Institute of Radiation Physics, HZDR, Dresden, Germany

Abstract

At present, ELBE radiation source at HZDR is optimizing the SRF cavity for the next generation ELBE SRF GUN. This paper presents a preliminary study on the geometry optimization of a 3.5-cell SRF gun cavity based on beam dynamics. By changing the lengths of the half cell and the first TESLA like cell, two new cavity models with higher electric field in the half cell are built and their RF fields are compared with SRF GUN I and SRF GUN II. Through the scanning of the RF phases and the electric fields, the simulation results indicate that new models have smaller transverse emittance at relatively lower electric field gradients and better performance on longitudinal emittance than SRF GUN I and SRF GUN II.

INTRODUCTION

Developing electron sources delivering high quality electron beams is always an active research field for high intensity particle accelerators, such as free electron laser (FEL), energy recovery linacs (ERLs) and electron linear colliders. Superconducting radio-frequency electron gun (SRF gun) is a superior alternative, which is capable to generate high-brightness and low-emittance electron beams when operating in continuous wave (CW) mode. The concept of SRF gun was firstly proposed in 1988 [1], and the first experiments were carried out at the University of Wuppertal four years later [2]. In 2002, world's first electron beams were obtained by the Drossel SRF gun at FZD (now HZDR) [3]. Inspired by this success, SRF gun projects based on different approaches were launched worldwide [4].

In 2004, a SRF photoelectron injector (SRF GUN I) was developed at HZDR in collaboration with DESY, HZB and MBI [5], as shown in Fig. 1. SRF GUN I was the world's first SRF gun with a 3.5-cell niobium cavity operating for a linac and was used to demonstare the first lasing with the far-infrared FEL at ELBE [6].

After the proof-of-principle demonstration of SRF GUN I, an improved SRF gun (SRF GUN II) was developed as shown in Fig. 2 and has been in operation up to now. Comparing to SRF GUN I, the electric field strength in the first half cell was improved, and a superconducting solenoid was installed in the cryomodule [7]. The influences of RF focus, cathode position and superconducting solenoid on emittance compensation have been investigated in detail [8].

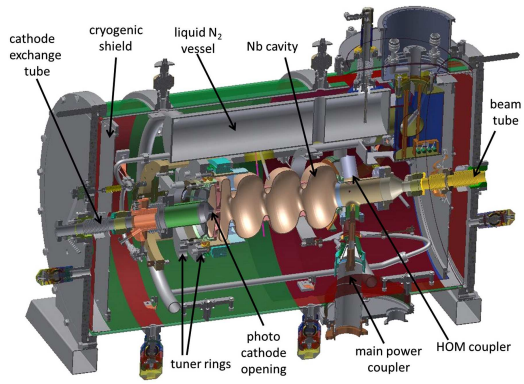


Figure 1: ELBE SRF GUN I.

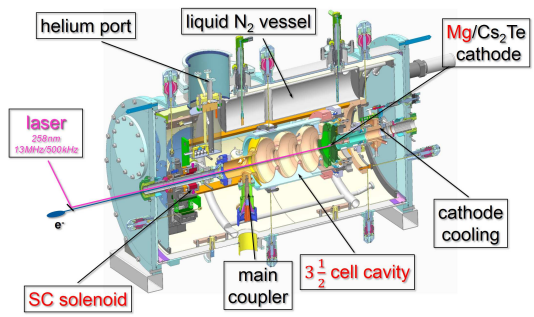


Figure 2: ELBE SRF GUN II.

Due to a degradation of available maximum field gradient of SRF GUN II, the construction of the third version, SRF GUN III, was initiated with the same niobium cavity of SRF GUN I refurbished at DESY and a newly built cryomodule with a superconducting solenoid [9].

At present, HZDR is also optimizing the SRF cavity for the next generation ELBE SRF GUN. To optimize the geometry of the 3.5-cell SRF gun cavity, the distributions of the electromagnetic fields and output beam qualities with different geometric models have been investigated and compared [10]. This paper mainly presents an analysis of the output beam parameters of two new models comparing to SRF GUN I and SRF GUN II.

* Work supported by National Natural Science Foundation of China with Grant [11605190 and 11805192].
† Email address: j.teichert@hzdr.de

ISBN: 978-3-95450-210-3 doi:10.18429/JACoW-FEL2019-WEP027

A FAST AND ACCURATE METHOD TO SHIM UNDULATOR USING MULTI-OBJECTIVE GA*

Yan Longgang, Chen Lijun, Deng Derong, Li Peng†
Institute of Applied Electronic, China Academy of Engineering and Physics, Mianyang, China

Abstract

GA (Genetic Algorithm) is one of the most excellent methods to search the optimal solution for a problem, which has been applied to solve various problems. It is hard to estimate shim applied on raw undulator precisely. There are many methods have been developed to solve the problem. In this proceeding, we proposed a fast and accurate method to conclude the shim using multi-objective GA. A multi-objective objective function was set, and multi-objective optimization was also implemented. The evolution time is reduced by setting optimal evolution parameters. To demonstrate the method, we also finished some test on a prototype undulator U38. As a result, it can be achieved only by shimming three times that all the parameters of trajectory center deviation, peak-to-peak error and phase error satisfied the requirements.

INTRODUCTION

Light sources based on accelerator, including Synchrotron Radiation (SR) and Free Electron Laser (FEL), use extensively undulators creating a periodic magnetic field for the production of intense of radiation for users [1, 2]. The common-used permanent magnet undulator was invented by K. Halbach in 1980's and contains two magnet and pole arrays [3]. Imperfections and errors are inevitable during design and manufacture of undulators, such as positioning errors of the magnets and poles, small differences of magnetization value and direction from one magnet block to the next, the inhomogeneities of the magnetization inside a volume of a single block. These will introduce magnetic field errors [4, 5]. Uncontrolled magnetic field errors of undulators, including electron trajectory center deviation, peak-to-peak error and phase error, will degrade light sources [6]. There are various shimming methods for correcting them in order to optimize undulator performance. The shimming methods are based on the fact that either moving a magnet or a pole (mechanical shim) or by placing some thin piece of iron at the surface of the magnet (magnetic shim) can make a small local correction of the magnetic field [7]. To shim undulator, it must be concluded that how much to move or how thin piece to place first. Many methods have been developed to solve the problem. In this proceeding, a method based on multi-objective GA to conclude shim fast and accurately was proposed, and in order to demonstrate the method prototype undulator U38 was also shimmed.

* Work supported by National Natural Science Foundation of China under grant of 11505174, 11505173 and 11605190.
† burnlife@sina.com

METHOD

Multi-Objective GA

GA was first put forward by professor J. Holland in 1975 and had a prosperous development era in the 90's. Now, GA has been applied in various areas and especially shows many advantages in combination optimization problem.

In an optimization problem based on GA, there is a population consisting of candidate solutions of the problem (individuals). Every candidate solution in population has a set of properties (chromosomes) which can mutate and crossover. An initial population usually contains individuals generated randomly or as required, which is evolved toward better populations. The evolution is an iterative process, and the population in every iteration is a generation. In every generation, the fitness of every individual is evaluated. Portion of individuals is selected from the current population, where fitter individuals decided by fitness are more likely to be selected. Then, chromosome of every individual being selected is modified (crossover and mutation) to form a new generation. The new generation of candidate solutions is then used in the next iteration of the algorithm. Commonly, the algorithm terminates when either a maximum number of generations has been produced, or a satisfactory fitness level has been reached for the population.

In practical optimization problem, there are usually many objectives, and in most cases the objectives are conflicting each other. The weight coefficient transformation method gives the jth sub-objective function $t(p_1,\ldots\ (p_l)$ weight coefficient w_j, and all k sub-objective functions are weighted linearly to form a new objective function T (Eq.1). By this method, the multi-objective optimization problem is transformed into a single-objective optimization problem.

$$T = \sum_{j=1}^{k} w_j t_j(p_1, \ldots, p_l) \tag{1}$$

Model Setup

Model setup includes the following steps:

- *S(z)*, the relation between correction of local magnetic field distribution and minimal shim is built either by calculation or by measurement.
- For undulator with $2N_u$ modules, the correction of local magnetic field distribution for other shim can be concluded by multiplying a coefficient C_n (n is module's number) with *S(z)*. Now, the problem was changed to find optimal C_n for every module.

Content from this work may be used under the terms of the CC BY 3.0 licence (© 2019). Any distribution of this work must maintain attribution to the author(s), title of the work, publisher, and DOI

ISBN: 978-3-95450-210-3 doi:10.18429/JACoW-FEL2019-WEP030

Content from this work may be used under the terms of the CC BY 3.0 licence (© 2019). Any distribution of this work must maintain attribution to the author(s), title of the work, publisher, and DOI

ALL-FIBER PHOTONIC, ULTRALOW-NOISE, ROBUST OPTICAL AND MICROWAVE SIGNAL GENERATORS FOR FELs AND UED

D. Kwon, D. Kim, I. Jeon, and J. Kim,
Korea Advanced Institute of Science and Technology, Daejeon, South Korea

Abstract

Optical timing and synchronization is becoming a more important and essential element for future ultrafast X-ray and electron science [1, 2]. As a result, compact, ultralow-noise, mechanically robust and long-term stable optical/microwave signal generators are highly desirable for future XFELs and UEDs. Here we show that the combination of mode-locked fiber laser and fiber delay-based stabilization method enables the generation of ultralow-noise optical and microwave signals. We show that all-PM fiber lasers can provide excellent mechanical robustness: stable laser operation over >1 hour is maintained even in continuous 1.5g vibrations [3]. Using a compactly packaged fiber delay as the timing reference, we could stabilize the repetition-rate phase noise of mode-locked lasers [4, 5] down to -100 dBc/Hz and -160 dBc/Hz at 1-Hz and 10-kHz offset frequency, respectively, at 1-GHz carrier, which corresponds to only 1.4 fs rms absolute timing jitter [1 Hz - 100 kHz]. With DDS-based electronics, low-noise and agile microwave frequency synthesizer was also realized [6]. This new class of photonic signal generator will be suitable for master oscillators in various accelerator-based light sources.

INTRODUCTION

Robust operation of mode-locked lasers is highly desirable for optical timing and synchronization of free electron lasers (FELs) and ultrafast electron diffraction (UED). In accelerator facilities, the environment is often harsher than well controlled optics laboratories due to vibrations, radiation and high voltage and current pulsed signals. Although nonlinear polarization evolution-based mode-locked lasers have been widely used to generate low-noise timing signals, the mode-locking state is sensitive to environment-induced perturbations. In order to operate the mode-locked lasers in a long-term stable way in these facilities, mechanical robustness is important. As a solution, polarization-maintaining fiber-based mode-locked lasers have been investigated because strong birefringence relieves the environment sensitivity.

In addition, for effective optical timing and synchronization, low timing jitter is very important. Mode-locked lasers have shown great short-term timing jitter. Typically, timing jitter (i.e., repetition-rate phase noise) of free-running laser oscillator is fs-level within ~ms time scale. However, it starts diverging over time due to lack of restoring force. Therefore, locking laser oscillator to more longer-term stable reference is highly desirable to maintain great short-term timing jitter over longer time scale. Many microwave reference oscillators and optical references have been used to lock the mode-locked lasers. Among them, an ultra-stable Fabry-Perot cavity-based locking system has been an effective way to suppress timing jitter over ~10 s time scale. However, it is a high-cost instrument and technically difficult to implement outside of well-controlled laboratories. As an alternative way of timing stabilization, fiber delay line-based technique was developed [4].

In this paper, a simple structured polarization-maintaining fiber-based mode-locked laser is discussed. We examined the mechanical robustness of an all-PM 3 x 3 coupler-based nonlinear amplifying loop mirror (NALM) mode-locked laser under > 1 hour of $1.5g_{rms}$ vibration condition. Also, a continuous operation of graphene saturable absorber (SA) based mode-locked laser under gamma ray radiation is also discussed [7]. To reduce short-term timing jitter, a compact, robust and all-fiber delay line-based timing jitter suppression technique is introduced. By combining the robust laser with the fiber-based timing jitter stabilization technique and DDS-based electronics, ultralow-noise optical/microwave synthesizer, which can be effectively used for FELs and UED facilities, is demonstrated.

RESULTS

We demonstrated a simple structured, mechanically robust 3 x 3 coupler-based all-PM fiber laser [Schematic shown in Fig. 1(a)]. A 3 x 3 coupler has intrinsic 120 deg phase bias between each port so that it does not require any additional phase shifter to initiate mode-locking in NALM laser. Moreover, mode-locking threshold is reduced compared to 2 x 2 coupler-based PM-NALM laser.

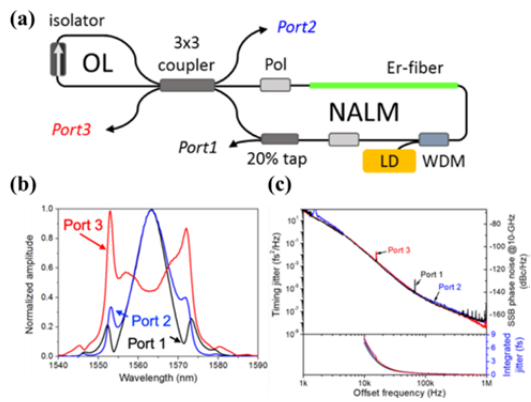


Figure 1: (a) Schematic of an all-PM-fiberized 3 x 3 coupler based NALM laser (b) optical spectra and (c) timing jitter spectra from each port. The data and figures are based on [3].

We can use three fiberized outputs from the 3 x 3 coupler -based PM-NALM laser. Figure 1(b) shows normalized optical spectra of each port, which respectively has

ISBN: 978-3-95450-210-3 doi:10.18429/JACoW-FEL2019-WEP031

TIMING SYNCHRONIZATION ACTIVITIES FOR DRIFT-FREE OPERATION OF ULTRAFAST ELECTRON DIFFRACTION SYSTEM AT KAERI

J. Shin, J. Kim†, Korea Advanced Institute of Science and Technology, Daejeon, Republic of Korea,
I. H. Baek, H. W. Kim, K. Y. Oang, S. Park, Y. U. Jeong, Korea Atomic Energy Research Institute, Daejeon, Republic of Korea

Abstract

Precise timing synchronization of an ultrafast electron diffraction facility is essential requirement for femtosecond resolution structure analysis. Recent studies of THz-based electron deflectors have enabled the timing drift measurement between ultrafast electrons and an optical pump beam with few femtosecond resolution. In this work, we will introduce timing synchronization activities to suppress the drift of an electron beam. As timing drift of the electron beam originates from every sub-element, each timing drift contribution from RF transfer, RF-to-optical synchronization, and optical amplification is measured. Timing drift of RF transfer through coaxial cable, which exposed to temperature fluctuation, is actively stabilized from 2 ps to 50 fs by active feedback loop. Further additive drift from RF-to-optical synchronization is maintained below 100 fs. Also optical drift due to the regenerative amplifier, measured by optical correlator, is maintained below 20 fs over an hour. This work allows ultrafast electron diffraction system to operate with less drift correction procedure and increased user availability.

INTRODUCTION

Ultrafast electron diffraction allows time-resolved structure analysis at atomic scale [1,2], which enables many potential applications on material science. Note that ultrafast electron offers unique opportunities as a matter, and it takes complementary role with light-based method such as free electron lasers. To further pave the way for ultrafast electron diffraction, it is of importance to optimize the temporal stability of electron sources. High temporal stability of electron sources will flourish not only ultrafast electron diffraction, but also ultrafast electron microscopy [3], and free electron lasers [4]. To generate low noise ultrafast electrons with MeV energy, DC photoguns and RF photoguns could be utilized. DC photogun itself is inherently synchronized with optical gating pulses, while further accelerating stages should be managed properly [5]. RF photogun could provide MeV energy electrons without further acceleration stages due to its intrinsically high electric field strength. Unfortunately, synchronizing RF field with injected optical pulses train could be a challenge [6]. With the recent advancement of THz-driven streak camera [7], jitter-free operation of RF photogun is enabled by optimizing laser injection phase. To fully exploit the jitter-free ultrafast electron sources, suppressing timing drift and maintaining performance over long time are essential. In this paper, we optimize the timing drift of the ultrafast electron diffraction facility in KAERI, which already achieved jitter-free condition with a RF photogun. To stabilize the timing drift of entire system, all timing contribution from subsystems are investigated. Subsystems are classified into RF distribution, RF-to-optical synchronization, and optical amplification as depicted in Fig. 1. Optimization of each subsystem is described in following sections.

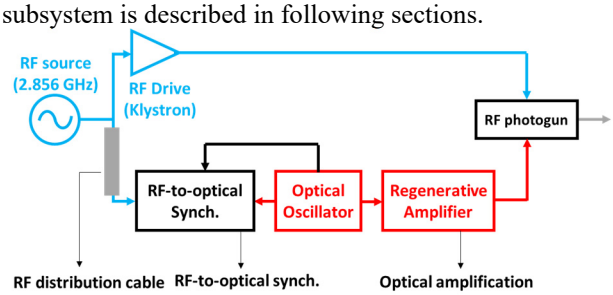


Figure 1: Subsystems contributing timing drift of electron pulses.

RF DISTRIBUTION

To distribute RF carrier from RF oscillator to laser, coaxial cable is installed across the facility. Due to the distance between two locations, cable length of 30 m is required. Note that longer length of coaxial cable is more vulnerable to thermal fluctuation. To mitigate the impact of thermal fluctuation, many previous researches such as stabilizing the cable temperature and measuring thermal sensitivity of cable are reported [4]. In our system, SUCOFLEX404 (H&S) cable is installed for high stability against temperature. Furthermore, active drift compensation system is introduced as shown in Fig. 2. The proposed scheme compares phase between original RF signal and round-trip signal, which reflected from the end of coaxial cable. Detected phase error is feedback controlled by voltage-controlled phase shifter.

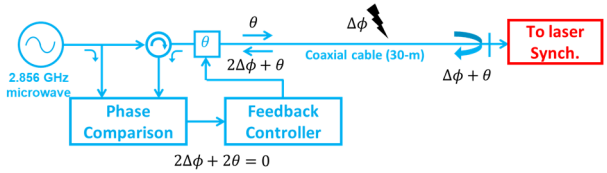


Figure 2: Active drift compensation scheme for the 30-m coaxial cable.

Timing drift of the coaxial cable is stabilized for 60,000 s and recorded with 10 s sampling time. All of stabilization performance, compensated drift amount, and temperature change of cable are recorded and plotted in Fig. 3. Note

†jungwon.kim@kaist.ac.kr

Content from this work may be used under the terms of the CC BY 3.0 licence (© 2019). Any distribution of this work must maintain attribution to the author(s), title of the work, publisher, and DOI

ISBN: 978-3-95450-210-3 doi:10.18429/JACoW-FEL2019-WEP034

CHARACTERIZATION OF FEL SPECTRA USING SPECIFIC FIGURES OF MERIT

Mihai Pop*, Francesca Curbis, MAX-IV, Lund University, Lund, Sweden
Enrico Allaria, Elettra Sincrotrone Trieste, Basovizza, Italy

ABSTRACT

There is an increasing demand from the user community for high quality FEL radiation. The spectrum of this radiation can prove to be a useful tool in characterizing the FEL process. Starting from a tool initially developed at FERMI we extend its capabilities to be able to analyze the modal components of the FEL spectrum. In this paper we will describe and compare two different figures of merit and offer initial bench-marking with respect to classic figure of merit for spectra such as FWHM and RMS.

INTRODUCTION

It is a common practice to optimize the setup of the FEL by looking at the spectrum of the radiation. However in order to have any type of automation procedure feeding back on this measurement, a simple figure of merit is needed. This can help not only in automation of the optimization procedure but also in removing biases that a human inevitably has while looking at a spectrum. Important work regarding FEL optimization procedure has been carried out at FERMI FEL as presented in [1].

With this in mind we sought out to create such a figure of merit. The real time acquisition system used at FERMI FEL, REALTA , is capable of using real time scans of numerous hardware components. Along with an offline data analysis software, PyDart, provides a strong tool in characterizing the machine, both software tools are described in [2]. The initial goal of the project was to create a few figures of merit (from here on out referred to as *fom*) that can better characterize the "*goodness*" of a spectrum. The main addition to the capabilities of PyDart was the decomposition into spectral components by identifying the different peaks in the spectra.

PEAK DETECTION WORK-FLOW AND CAPABILITIES

The peak detection algorithm is a more complex version of scipy's find peaks routine [3] with the added ability to not only detect peaks but also valleys and even find peaks that do not have a prominence but manifest as a shoulder, see Figure 1.

The work-flow is structured as follows:

1. Subtracting a linear background from the Spectrum
2. Evaluate the background in terms of height periodicity and prominence

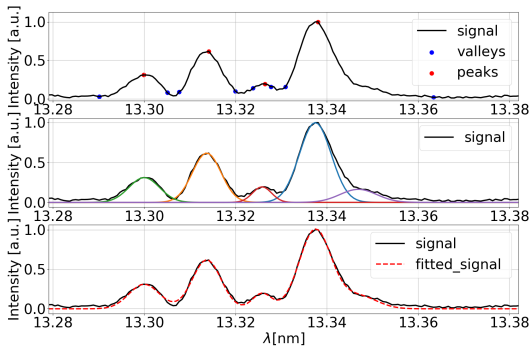


Figure 1: Illustration of work-flow : finding peaks and valleys (top) fitting (mid and bottom). Spectra supplied by Fermi.

3. Find all peaks that Are several times higher that the background, Have a prominence much higher that the background,Are separated from other peaks by n times the peak separation in the background Figure 1 (top).
4. Find the corresponding valleys to the peaks 1 (top).
5. Fit Gaussian functions to the region of interest defined by the peaks and valleys.
6. Calculate goodness of fit Figure 1 (bottom).

For a more comprehensive explanation of the working of the algorithm refer to [4].

FIGURES OF MERIT

In this section we will go through the *fom* to be able to understand their individual strengths and weaknesses. For the present analysis we have chosen a total of 6 *fom* but the list is by no means exhaustive with more work still remaining to be done.

- **Intensity** : the total intensity contained in a spectrum
- **FWHM** : width of the spectrum at half of the maximum intensity
- **Sigma 0** : the weighted RMS of the spectrum with respect to the weighted mean position
- **W of 80 %** : the minimum continuous width over which 80% of the intensity is located
- **A ratio** : the ratio between the area of the highest peak found by gaussian fitting to the total Intensity
- **Multi G sig** : the sigma of the highest peak fond by gaussian fit

* mihai.pop@maxiv.lu.se

Content from this work may be used under the terms of the CC BY 3.0 licence (© 2019). Any distribution of this work must maintain attribution to the author(s), title of the work, publisher, and DOI

ISBN: 978-3-95450-210-3 doi:10.18429/JACoW-FEL2019-WEP035

Content from this work may be used under the terms of the CC BY 3.0 licence (© 2019). Any distribution of this work must maintain attribution to the author(s), title of the work, publisher, and DOI

NIR SPECTROMETER FOR BUNCH-RESOLVED, NON-DESTRUCTIVE STUDIES OF MICROBUNCHING AT EUROPEAN XFEL

S. Fahlström, M. Hamberg, Uppsala University, Uppsala, Sweden
Ch. Gerth*, N. M. Lockmann, B. Steffen, DESY, Hamburg, Germany

Abstract

At the European X-ray Free Electron Laser high brilliance femtosecond FEL radiation pulses are generated for user experiments. For this to be achieved, electron bunches must be reliably produced within very tight tolerances. In order to investigate the presence of microbunching, i.e. charge density variation along the electron bunch with features in the micron range, a prism-based NIR spectrometer with an InGaAs sensor, sensitive in the wavelength range 900 nm to 1700 nm was installed. The spectrometer utilizes diffraction radiation (DR) generated at electron beam energies of up to 17.5 GeV. The MHz repetition rate needed for bunch resolved measurements is made possible by the KALYPSO line detector system, providing a read-out rate of up to 2.7 MHz. We present the first findings from commissioning of the NIR spectrometer, and measurements on the impact of the Laser Heater system for various bunch compression settings, in terms of amplitude and bunch-to-bunch variance of the NIR spectra as well as FEL pulse energy.

INTRODUCTION

The European XFEL

In the linear accelerator of the European X-ray Free-Electron Laser (EuXFEL) electron bunches are accelerated to energies of up to 17.5 GeV. The bunches are accelerated in bunch trains of up to 2700 bunches, with an intra-train repetition rate of up to 4.5 MHz (currently 1.1 MHz operation is most common). Trains are generated at 10 Hz, for a total of up to 27 000 bunches per second.[1] After acceleration, the electron bunches are distributed to three undulator sections (designated SASE1, SASE2, and SASE3) where via Self-Amplified Spontaneous Emission (SASE) laser-like X-rays are produced. This enables parallel Free-Electron Laser (FEL) operation of three experimental stations.

Bunch Compression

The peak currents needed for the SASE process demand that the bunches are longitudinally compressed during acceleration. To compress the bunches a longitudinal energy-position correlation called *chirp* is imparted by accelerating them off crest and then leading them through a chicane where energy dependent path length allows the higher energy tail to catch up to the head. At the EuXFEL this is done in 3 stages, for a total compression factor of ~100, and final peak current ~5 kA. [2]

* christopher.gerth@desy.de

Microbunching and Laser Heater

Collective effects during bunch compression can lead to so called *microbunches* developing [3, 4], where random periodic features on the longitudinal charge density from shot noise from the electron-gun can be amplified many orders of magnitude. These features lead to growth of slice emittance, detrimental to the FEL process. Previously similar facilities have implemented Laser Heaters (LH) to inhibit microbunching, with clear improvements to FEL performance.[5–7] In the LH, part of the laser pulse for the photo-cathode electron gun is coupled out and overlapped with the electron bunches in an undulator inside a chicane. This imparts a non-correlated energy spread, which dampens microbunching in the bunch compressor chicanes. A LH was also installed at the EuXFEL.[8–12]

Longitudinal Diagnostics of Short Bunches

For the study of microbunching effects at the EuXFEL a prism based Near Infra-red (NIR) spectrometer was installed.

For longitudinal diagnostics of sub picosecond electron bunches, frequency domain methods using coherent radiation can provide a non-invasive option, important for user facilities. The spectral density of coherent radiation is dependent on the magnitude of the longitudinal form factor, F_l, which is the Fourier transform of the longitudinal charge density of the electron bunch. Coherent Diffraction Radiation (CDR) spanning mm-waves to visible light is generated when the relativistic electron bunches pass through a hole in an aluminum screen. At EuXFEL this CDR is used to non-invasively monitor bunch compression and longitudinal profiles at several stations along the accelerator. [13] Bunch Compression Monitors (BCM) use simple and robust broadband sensors to monitor the overall bunch length. Spectroscopic investigation offer a more complete bunch profile, and at the last CDR station, after full acceleration, a THz spectrometer [14, 15] was previously installed.[16] That spectrometer works in the mid infrared (MIR) to THz spectral range, 5 µm to 450 µm, and can provide complete bunch profiles. However, the smallest features it can resolve is limited by its detection range. Since microbunching is suspected with features in the single µm range, the spectrometer that this paper concerns was installed alongside it, sensitive in the NIR range. Due to the stochastic origins of microbunching great variance from bunch to bunch is expected, which requires bunch-resolved measurements. The development of the KALYPSO detector unit [17–20] has made this possible, with read-out rates up to 2.7 MHz.

ISBN: 978-3-95450-210-3 doi:10.18429/JACoW-FEL2019-WEP036

THE PolariX-TDS PROJECT: BEAD-PULL MEASUREMENTS AND HIGH-POWER TEST ON THE PROTOTYPE

P. Craievich*, M. Bopp, H.-H. Braun, A. Citterio, R. Ganter, F. Marcellini, T. Kleeb, M. Pedrozzi, E. Prat, S. Reiche, PSI, 5232 Villigen, Switzerland
A. Grudiev, W. Lee Millar[1], N. Catalan-Lasheras, G. McMonagle, S. Pitman, V. del Pozo Romano, K. T. Szypula, W. Wuensch, CERN, 1211 Geneva 23, Switzerland
B. Marchetti, R. W. Assmann, F. Christie, R. D'Arcy, U. Dorda, M. Foese, P. Gonzalez Caminal, M. Hoffmann, M. Huening, R. Jonas, O. Krebs, S. Lederer, V. Libov, D. Marx, J. Osterhoff, M. Reukauff, H. Schlarb, S. Schreiber, G. Tews, M. Vogt, A. de Z. Wagner, DESY, 22607 Hamburg, Germany
[1]also at Cockcroft Institute, Warrington, Cheshire

Abstract

A collaboration between DESY, PSI and CERN has been established to develop and build an advanced modular X-band transverse deflection structure (TDS) system with the new feature of providing variable polarization of the deflecting force. The prototype of the novel X-band TDS, the Polarizable X-band (PolariX) TDS, was fabricated at PSI following the high-precision tuning-free production process developed for the C-band Linac of the SwissFEL project. Bead-pull RF measurements were also performed at PSI to verify, in particular, that the polarization of the dipole fields does not have any rotation along the structure. The high-power test was performed at CERN and now the TDS is at DESY and has been installed in FLASHForward, where the first streaking experience with beam will be accomplished. We summarize in this paper the status of the project, the results of the bead-pull measurements and the high power test.

INTRODUCTION

Several experiments at DESY (FLASH2, FLASHForward, SINBAD) and PSI (ATHOS at SwissFEL) are interested in the utilization of high gradient X-band TDS systems for high resolution longitudinal diagnostics [1]. In this context, a collaboration between DESY, PSI and CERN has been established to develop and build an advanced modular X-Band TDS system with the new feature of providing variable polarization of the deflecting force [2]. The prototype of the novel X-band TDS, the Polarizable X-band (PolariX) TDS, has been fabricated at PSI following the high-precision tuning-free production process developed for the C-band Linac of the SwissFEL project and already used for the fabrication of the tuning-free X-band structure prototypes for CLIC [3–5]. Bead-pull RF measurements has been performed at PSI between December 2018 and January 2019 in order to verify that the polarization of the dipole fields does not have any rotation along the structure. Figure 1 shows the detail of the input and output couplers (left), the whole TDS prototype (middle) and the basic disk geometry (right). The main RF parameters of the TDS and RF pulse compressor are summarized in Table 1. High power test on the prototype has been performed at CERN between March and April 2019. In this paper we summarize the status of the collaboration focusing on the results of the bead-pull measurements and the high power tests.

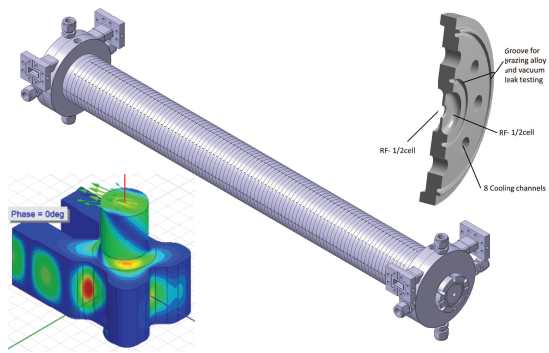


Figure 1: Left: detail of the input/output coupler. Middle: whole TDS prototype. Right: basic disk.

BEAD-PULL MEASUREMENTS

The dipole field flatness and polarization were measured with the bead-pull method. The structure was allocated in a vertical frame and a stepper motor was used to drive along the structure a 2 mm diameter dielectric sphere fixed to a dielectric wire with diameter of 0.16 mm. The bead pulling has been repeated for different offsets, both in the XZ and YZ planes, in ± 2 mm range. The measurements were performed with a 4-port VNA and the reflection coefficient resulted to be less than -35 dB with an insertion loss of -5.5 dB. Figure 2 (upper plot) shows results of the bead-pull measurement with offset 0 mm both in X and Y and phase difference between ports of 0 deg. Cell-to-cell phase advance (lower plot) resulted to be $2\pi/3$ with a dispersion of 0.8° rms at the working frequency of 11995.2 MHz with a temperature of 33.9°C. It is worthwhile noting that same results for the phase ad-vance was obtained varying the relative phase between ports, namely for different polarizations. A spherical and dielectric bead perturbs only the electric field, but cannot distinguish between longitudinal and transverse components. However, since the longitudinal component has the largest

* paolo.craievich@psi.ch

Content from this work may be used under the terms of the CC BY 3.0 licence (© 2019). Any distribution of this work must maintain attribution to the author(s), title of the work, publisher, and DOI

ISBN: 978-3-95450-210-3 doi:10.18429/JACoW-FEL2019-WEP037

RF JITTER AND ELECTRON BEAM STABILITY IN THE SwissFEL LINAC

Z. Geng#, P. Craievich, R. Kalt, J. Alex, C. H. Gough, T. Lippuner, M. Pedrozzi, F. Löhl, V. R. Arsov, S. Reiche, E. Prat, Paul Scherrer Institut, Villigen PSI, Switzerland

Abstract

The X-ray FEL machine SwissFEL at the Paul Scherrer Institut in Switzerland is commissioned and transiting to user operation smoothly. FEL operation requires stringent requirements for the beam stability at the linac output, such as the electron bunch arrival time, peak current and energy. Among other things, a highly stable RF system is required to guarantee the beam stability. The SwissFEL RF system is designed based on the state-of-the-art technologies that have allowed achieving excellent RF stability. The propagation of RF amplitude and phase jitter to the electron beam are analyzed theoretically and compared with the measurements performed at SwissFEL.

INTRODUCTION

The layout of SwissFEL is depicted in Figure 1 [1,2]. The accelerator consists of an S-band (2998.8 MHz) RF Gun, two S-band Booster sections, an X-band (11995.2 MHz) RF station and 3 C-band (5712 MHz) Linacs. SwissFEL requires highly stable electron beams for FEL generation. The stability goals reported in [3] require at the exit of Linac 3 the beam energy jitter to be < 0.05% rms, the peak current fluctuation < 5% rms and the bunch arrival time jitter < 20 fs rms. In order to meet the stability goals, the RF system must satisfy tight requirements on amplitude and phase stability down to 0.018% RMS in amplitude jitter and 0.018°, 0.036° and 0.072° RMS in phase jitter for S-band, C-band and X-band stations respectively [4].

SwissFEL works in pulsed mode with a repetition rate up to 100 Hz. The pulse-to-pulse jitter of the SwissFEL RF system is dominated by the stability of the klystron driver amplifiers and the high-voltage klystron modulators. The RF pulse width (from 100 ns to 3 μs) is too short to implement efficient and reliable intra-pulse feedbacks. Pulse-to-pulse feedbacks were implemented in the low-level radio frequency (LLRF) system [5] to compensate for the RF fluctuations at frequencies below 1 Hz. For longer time intervals, the drifts of the LLRF detection chain must be corrected by the beam based feedbacks.

In this paper, the measured RF and beam stability for the operation mode with 200 pC will be presented. In order to crosscheck the measurements, a beam dynamics model will be used to predict the beam jitter from the measured RF jitter and compare with the direct beam measurements.

RF STABILITY

The pulse-to-pulse phase and amplitude jitter of the RF field used for beam acceleration is measured with the RF detectors. For each pulse, the RF waveforms are averaged within a time window determined by the time constant of the standing wave cavities (e.g. RF Gun) or within the filling time of the traveling wave structures (1000 ns for S-band, 322 ns for C-band, and 105 ns for X-band). This limits the measurements to the RF-beam interaction bandwidth of the cavities or structures: RF Gun 330.8 kHz, S-band structure 475.8 kHz, C-band structure 1346.5 kHz and X-band structure 4219.0 kHz. Because the drifts slower than 1 Hz are suppressed by the RF feedbacks, the jitter given in this section contains the noise power from 1 Hz to the RF-beam interaction bandwidth of the cavities or structures.

The lab tests of the RF detectors promise a phase resolution of 0.0036° rms and an amplitude resolution of 2.6e-5 rms within the noise band. Compared to the overall RF field jitter, the RF detector added jitter can be neglected.

The pulse-to-pulse RF phase and amplitude jitter measured during this campaign at different RF stations is shown in Figure 2. The red lines show the jitter specification mentioned in the last section.

During the test, the beam based feedbacks were switched off, the phase and amplitude feedbacks of the Gun, S-band and X-band stations were on, while for C-band stations, only the phase feedbacks were on but the amplitude feedbacks were off because the C-band klystrons worked in saturation. Some RF stations did not satisfy the stability requirements and the reasons are summarized below:

- The average window of the RF Gun probe signals was much smaller than the cavity time constant, therefore, the measurement contains high frequency noises including the π/2-mode signal. Furthermore, the RF Gun modulator was not in good condition during the test resulting in higher amplitude and phase jitter.
- The X-band amplitude jitter was slightly above the specified threshold due mainly to the contribution of

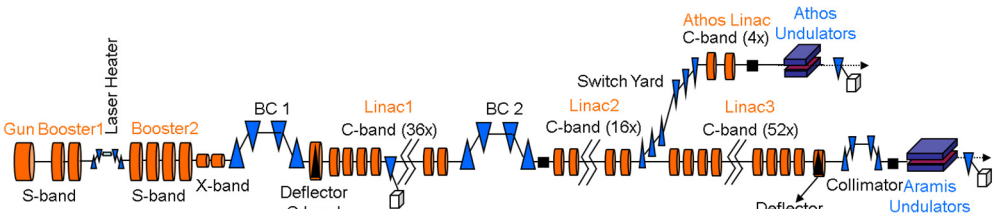


Figure 1: Layout of SwissFEL

#zheqiao.geng@psi.ch

Content from this work may be used under the terms of the CC BY 3.0 licence (© 2019). Any distribution of this work must maintain attribution to the author(s), title of the work, publisher, and DOI

ISBN: 978-3-95450-210-3 doi:10.18429/JACoW-FEL2019-WEP038

COMMISSIONING AND STABILITY STUDIES OF THE SwissFEL BUNCH-SEPARATION SYSTEM

M. Paraliev†, S. Dordevic, R. Ganter, C. Gough, N. Hiller, R. Krempaska, D. Voulot
Paul Scherrer Institute, Villigen PSI, Switzerland

Abstract

SwissFEL is a linear electron accelerator based, X-ray Free Electron Laser at the Paul Scherrer Institute, Switzerland. It is a user oriented facility capable of producing short, high brightness X-ray pulses covering the spectral range from 1 to 50 Å. SwissFEL is designed to run in two electron bunch mode in order to serve simultaneously two experimental beamline stations (hard and soft X-ray one) at its full repetition rate. Two closely spaced (28 ns) electron bunches are accelerated in one RF macro pulse up to 3 GeV. A high stability resonant kicker system and a Lambertson septum magnet are used to separate the bunches and to send them to their respective beamlines. With the advancement of the construction of the second beamline (Athos) the bunch-separation system was successfully commissioned. In order to confirm that the beam separation process is fully transparent a stability study of the electron beam and the free electron laser in the main beamline (Aramis) was done.

INTRODUCTION

The first undulator line of Swiss X-ray Free Electron Laser (SwissFEL) [1], Aramis, was inaugurated in 2016 and the first pilot experiment was conducted in 2017. In 2018 the nominal electron beam energy was achieved and the free electron laser reached its shortest designed X-ray wavelength of 1 Å. The two experimental stations of Aramis (Alvira and Bernina) were commissioned and in the beginning of 2019 Aramis SwissFEL line started regular user operation. In parallel, the second undulator line (Athos) is being constructed [2]. First electron beam to Athos was sent in September 2018 and in December the bunch-separation system was commissioned and the separation of the two bunches was successfully demonstrated. Starting two bunch operation in the early stages of Athos commissioning is very beneficial because it can be done in parallel with regular Aramis user operation.

In order to separate the two electron bunches they both are deflected by a fast resonant kicker system [3] – one up and one down. Compensating dipoles counteract the deflection of the down-kicked bunch and send it straight through the zero-field region of the Lambertson septum to the Aramis beamline. The up-kicked bunch is deflected by the Lambertson field sideways and it is sent to Athos beamline. Since the two bunches are deflected the stability of the kicker system is crucial for the proper operation of both beamlines. To confirm that the bunch-separation is fully transparent and does not affect operation of Aramis beamline several tests were conducted. The results of these tests are discussed below.

† martin.paraliev@psi.ch

RESONANT KICKER COMMISSIONING

The two Resonant Kicker (RK) magnets are a key component of SwissFEL electron bunch-separation system. They deflect the two consecutive electron bunches in opposing directions vertically before they are finally separated by a Lambertson septum about 8 m downstream. To work properly RKs need adequate electrical excitation and tight synchronization to the electron beam. To ensure that the deflection amplitude stability down to the ppm level is not dominated by the phase error the RK should be synchronised to a 10s of ps level. A dedicated synchronization module was developed to combine the trigger from the generic accelerator timing system (providing 7 ns resolution) and high stability RF clock in order to generate proper timing with 10 ps programmable delay resolution. High stability RF driver (17.8 MHz) excites the resonant structure to reach the required current, respectively the deflecting magnetic field.

Envelope Synchronization

The RKs were first commissioned in the straight accelerator beamline (Aramis). Using a small deflection amplitude (within the machine acceptance) and detecting the kick with beam position monitors (BPMs) downstream the resonance envelope was located. Figure 1 shows an envelope scan of the RKs excitation. The excitation curve appears backwards because the RKs' delay with respect to the beam arrival time in the scan is increased.

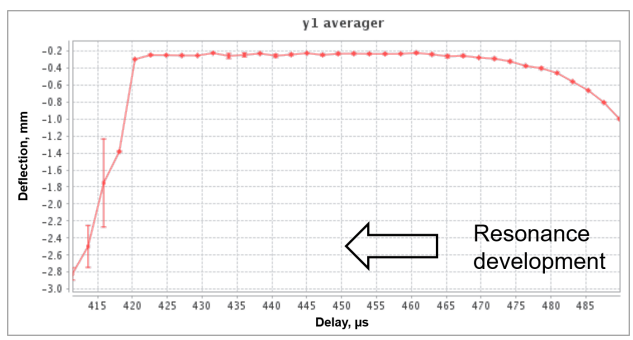


Figure 1: RKs' excitation envelope scan of vertical deflection downstream the kickers.

Phase Synchronization

Once the rough position of the resonance envelope is located the correct phase has to be found. A much finer scan (Fig. 2) was used to probe RKs' deflection and later was used to position the electron bunch at the sine wave crest, where the deflection is maximum and is least sensitive to phase error.

Content from this work may be used under the terms of the CC BY 3.0 licence (© 2019). Any distribution of this work must maintain attribution to the author(s), title of the work, publisher, and DOI

ISBN: 978-3-95450-210-3 doi:10.18429/JACoW-FEL2019-WEP041

FEASIBILITY OF SINGLE-SHOT MICROBUNCHING DIAGNOSTICS FOR A PRE-BUNCHED BEAM AT 266 nm*

A. H. Lumpkin#[1] and D.W. Rule[2]
[1]Argonne Associate, Argonne National Laboratory, Lemont, IL, USA
[2]Silver Spring, MD, USA

Abstract

We describe potential characterization of microbunched electron beams obtained after a modulator and chicane by using coherent optical transition radiation (COTR) imaging techniques. Beam transverse size (~50 microns), divergence (sub-mrad), trajectory angle (within ~0.1 mrad), spectrum (to a few nm), and pulse length (sub-ps) can be measured. The transverse spatial alignment is provided with near-field imaging, and the angular alignment is done with far-field imaging and two-foil COTR interferometry (COTRI). Analytical model results for a 266-nm wavelength COTRI case with a 10% microbunching fraction will be presented. COTR gains of $7x10^6$ were calculated for an initial charge of 300 pC, and this enables splitting the optical signal for single-shot measurements of all the cited parameters.

INTRODUCTION

Co-propagating a relativistic electron beam and a high-power laser pulse through a short undulator (modulator) provides an energy modulation which can be converted to a periodic longitudinal density modulation (or microbunching) via the R56 term of a chicane [1]. Such pre-bunching of a beam at the resonant wavelength and the harmonics of a subsequent free-electron laser (FEL) amplifier seeds the process and results in improved gain. We describe potential characterizations of the resulting microbunched electron beams after the modulator using coherent optical transition radiation (COTR) imaging techniques for transverse size (50 micron), divergence (sub-mrad), trajectory angle (0.1 mrad), spectrum (few nm), and pulse length (sub-ps). The transverse spatial alignment is provided with near-field imaging and the angular alignment is done with far-field imaging and two-foil COTR interferometry (COTRI). Analytical model results for a 266-nm wavelength COTRI case with a 10% microbunching fraction will be presented. COTR gains of 7 million were calculated for an initial charge of 300 pC which enables splitting the optical signal for single-shot measurements of all the cited parameters. Since the beam and laser position jitters may cause some fluctuations in the microbunching spatial distribution, single-shot diagnostics will be beneficial.

*Work supported under Contract No. DE-AC02-07CH11359 with the United States Department of Energy, Basic Energy Sciences.
#lumpkin@anl.gov

EXPERIMENTAL ASPECTS

The APS Linac

The APS linac is based on an S-band rf photocathode (PC) gun which injects beam into an S-band linear accelerator with acceleration capability up to 450 MeV [2]. Beam diagnostics include imaging screens, rf BPMs, and coherent transition radiation (CTR) autocorrelators located before and after the chicane at the 100 MeV point.

The Microbunching Diagnostics

The diagnostics for the microbunching experiments would be located in the linac extension area (LEA) [2]. A schematic of a potential setup is shown in Fig. 1. A seed laser at 266 nm would be injected onto the beamline axis at a chicane to co-propagate with a 375-MeV electron beam micropulse through a modulator section. Immediately after the modulator, a set of 4 magnets would provide a small dispersive, R56 term to convert the energy modulation to the longitudinal density modulation. Such an electron beam would be transported to the COTR diagnostics. As will be shown later, the COTR gain will be significant at 6 orders of magnitude over incoherent OTR so the signal can be split over multiple optical paths for near field (NF) imaging, far-field (FF) imaging, spectral measurements, gain measurements, and a bunch length measurement with a streak camera. A thin laser blocking foil will be inserted before a mirror at 45 degrees to the beam direction as indicated in Fig. 1. A microscope objective will be focused on the back surface of the foil for the forward COTR beam size to provide a NF image in one UV camera. The combination of this source and the backward COTR from the mirror will result in interference fringes when viewed in the far field by a second UV camera. The enhanced light may also be split to provide signals to a UV-visible spectrometer (also readout by a UV camera) and a UV-visible streak camera. We may utilize a C5680 Hamamatsu streak camera with S20 PC operating with the M5675 synchroscan vertical deflection unit phase locked to 119.0 MHz, the 24th subharmonic of the linac S-Band at 2856 MHz. As will be noted in a subsequent section, a unique beam-based alignment technique will be employed using the COTR and COTRI images. The shape and intensity of the images at 266 nm will provide immediate online information on the overlap of the seed laser and e-beam, both spatially and temporally.

Content from this work may be used under the terms of the CC BY 3.0 licence (© 2019). Any distribution of this work must maintain attribution to the author(s), title of the work, publisher, and DOI

ISBN: 978-3-95450-210-3 doi:10.18429/JACoW-FEL2019-WEP042

OBSERVATIONS OF SHORT-RANGE WAKEFIELD EFFECTS IN TESLA-TYPE SUPERCONDUCTING RF CAVITIES*

A.H. Lumpkin#, R. Thurman-Keup, D. Edstrom Jr., J. Ruan
Fermi National Accelerator Laboratory, Batavia, IL 60510 USA

Abstract

The Fermilab Accelerator Science and Technology (FAST) facility has a unique configuration of a photocathode rf gun beam injecting two TESLA-type single cavities (CC1 and CC2) in series prior to the cryomodule. To investigate short-range wakefield effects, we have steered the beam to minimize the signals in the higher-order mode (HOM) detectors of CC1 and CC2 for a baseline, and then used a vertical corrector between the two cavities to steer the beam off axis at an angle into CC2. A Hamamatsu synchroscan streak camera viewing a downstream OTR screen provided an image of y-t effects within the micropulses with ~10-micron spatial resolution and 2-ps temporal resolution. At 500 pC/b, 50 b, and 4 mrad off-axis steering into CC2, we observed an ~ 100-micron head-tail centroid shift in the streak camera image y(t)-profiles. This centroid shift value is 5 times larger than the observed HOM-driven centroid oscillation within the macropulse and is consistent with a calculated short-range wakefield effect. Additional results for kick-angle compensations will be presented.

INTRODUCTION

The accelerators for high-power x-ray free-electron laser (FEL) facilities such as the European XFEL [1] and planned LCLS-II x-ray FEL [2] are employing TESLA-type SCRF cavities. Beam propagation off axis in these cavities can result in both short-range and long-range transverse wakefields which can lead to emittance dilution within the micropulses and macropulses, respectively. There are limited beam-effects data available, although we recently reported the clear observations of submacropulse beam centroid oscillation effects due to the long-range effects of HOMs [3].

We report here sub-micropulse effects on beam transverse position centroids and sizes correlated with off-axis beam steering in TESLA-type cavities at the Fermilab Accelerator Science and Technology (FAST) Facility [4]. We used a 3-MHz micropulse repetition rate, a unique two separated-single-cavity configuration, and targeted diagnostics for these tests. Our initial data from an optical transition radiation (OTR) imaging source indicated our streak camera can provide ~10-micron spatial resolution with 1-2 ps (σ) temporal resolution depending on the bandpass filter employed. Since the observed bunch lengths were 10-15 ps (σ), we had sufficient resolution for up to 20 time slices in the 4σ profile. In this sense we also obtained slice-emittance information. We used the HOM detectors and rf BPMs to assess our off-axis steering to generate and then evaluate the short-range wakefield effects on the beam dynamics.

EXPERIMENTAL ASPECTS

The FAST Injector Linac

The FAST linac is based on the L-band rf photocathode (PC) gun which injects beam into two superconducting rf (SCRF) capture cavities denoted CC1 and CC2, followed by transport to a low-energy electron spectrometer. A Cs_2Te photocathode is irradiated by the UV component of the drive laser system described elsewhere [5]. The basic diagnostics for the studies include the rf BPMs located before, between, and after the two cavities as shown in Fig. 1. These are supplemented by the imaging screens at X107, X108, X121, and X124. The HOM couplers are located at the upstream and downstream ends of each SCRF cavity, and these signals are processed by the HOM detector circuits with the output provided online though ACNET, the Fermilab accelerator controls network. The HOM detectors' bandpass filters were optimized for two dipole passbands from 1.6 to 1.9 GHz, and the 1.3 GHz fundamental was reduced with a notch filter. The rf BPMs electronics were configured for bunch-by-bunch capability with reduced noise. At 2 nC per micropulse, the rms noise was found to be 25 μm in the horizontal axis (x) and 15 μm in the vertical axis (y) in B101 in the test with 4.5-MeV beam from the gun. However, for these experiments on short-range transverse wakefields, we relied on a streak camera to provide the sub-micropulse spatial information.

The Streak Camera System

We utilized a C5680 Hamamatsu streak camera with S20 PC operating with the M5675 synchroscan vertical deflection unit that was phase locked to 81.25 MHz. In addition, we used a phase-locked-loop C6878 delay box that stabilizes the streak image positions to about 1 ps temporal jitter over 10s of minutes. These steps enabled the synchronous summing of 50-150 micropulses or bunches (b) generated at 3 MHz by the photoinjector or the offline summing of 10-100 images to improve statistics in the sum images. We applied the principle to optical transition radiation (OTR) generated from an Al-coated Si substrate at the X121 screen location (see Fig.1) with subsequent transport to the beamline streak camera. Commissioning of the streak camera system was facilitated through a suite of

*This manuscript has been authored by Fermi Research Alliance, LLC under Contract No. DE-AC02-07CH11359 with the U.S. Department of Energy, Office of Science, Office of High Energy Physics.

#lumpkin@fnal.gov

Content from this work may be used under the terms of the CC BY 3.0 licence (© 2019). Any distribution of this work must maintain attribution to the author(s), title of the work, publisher, and DOI

ISBN: 978-3-95450-210-3 doi:10.18429/JACoW-FEL2019-WEP043

MULTI-ENERGY OPERATION ANALYSIS IN A SUPERCONDUCTING LINAC BASED ON OFF-FREQUENCY DETUNE METHOD*

Z. Zhang†, Y. Ding, C. Adolphsen, and T. Raubenheimer
SLAC National Accelerator Laboratory, Menlo Park, CA 94025, USA

Abstract

The free-electron laser facilities driven by a superconducting radio-frequency (SRF) linac provide high-repetition-rate electron beam, which makes it feasible to feed multiple undulator lines at the same time. In this paper, we study a method of controlling the beam energy of multiple electron bunches by off-frequency detuning of the SRF linac. Based on the theoretical analysis, we present the optimal solutions of the method and the strategy to allocate linac energy for each possible off-frequency detune. The initial acceleration phases before detuning of the SRF linac can be optimized to reduce the necessary SRF linac energy overhead. We adopt the LCLS-II-HE configuration as an example to discuss possible schemes for two undulator lines.

INTRODUCTION

The successful operation of several hard x-ray free-electron laser (XFEL) facilities [1–4] over the world represents a revolution in the development of light source. Most of the present-day XFELs are driven by copper linac with a repetition rate around 100 Hz. This low repetition rate determines only a modest average brightness, similar to that of the third generation storage ring based sources. Another drawback of these facilities is that they typically only serve one user end-station at a given time.

XFELs driven by a superconducting radio-frequency (SRF) linac are capable to deliver Mega-Hertz (MHz) electron beams, which greatly enhances the photon average brightness and supports multiple beamlines in parallel and/or cascading configurations [5–8]. In this case, the photon energy from different beamlines can be varied by adjusting the undulator gap for a given electron beam energy. To further extend the photon energy range, schemes to control the electron beam energy of every undulator line independently are highly desired.

To provide different beam energies for multiple undulator lines from a SRF linac, different schemes can be applied. For example, one can extract electron beams with a fast kicker at the desired energy point and then send them to the undulator line through a bypass line, as shown in Fig. 1 (*a*). This scheme is adopted as the baseline design of the present SRF XFEL facilities [6–8]. In this scheme, we can make full use of the energy capability of the SRF linac. However, since the kicker positions are fixed, the beam energy for each undulator line is almost constant. Besides, adding the extraction regions to the SRF linac is lengthy and costly. Recently, another scheme using achromatic electron delay system is proposed to produce multi-energy beams for the SRF linac-driven XFELs [9].

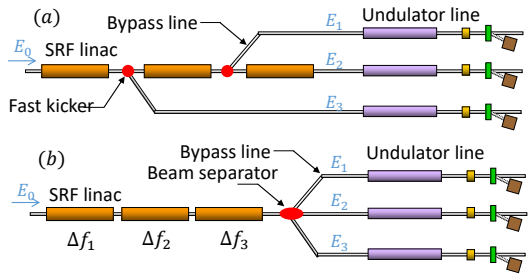


Figure 1: Two schemes of multi-energy operation of a SRF XFEL: (a) kick the beam to bypass line at desired energy point (b) control the beam energy independently by off-frequency detune of SRF cavities.

In this paper, we study a new scheme for multiple-energy operation of a SRF linac based on the off-frequency detune method [10,11]. The SRF cavities are very sensitive to small mechanical perturbations due to their narrow bandwidth. The resonant frequency can be varied by compressing the cavity. With enough detune range, we can produce periodic energy pattern in CW electron beams. The main advantage is the possibility to control the beam energy independently and extend the XFEL parameter space. In addition, we can adopt the dispersive energy separator, rather than the fast kicker/septum system, to separate beams to different undulator lines.

THEORETICAL ANALYSIS

For CW electron beams, we assume the beam repetition rate f_r and the time separation $T = 1/f_r$. At the nominal resonant frequency of the cavity f_c, all electron beams are accelerated at the same phase ψ_c, as shown in Fig. 2. When the frequency is detuned by Δf and the acceleration phase of the first beam is kept at ψ_c, the acceleration phase of the j-th electron beams is $\psi_c + (j-1)\Delta\phi$ with phase difference of two neighbouring beams (or we can call it as phase shift)

$$\Delta\phi = 2\pi T \Delta f \,. \tag{1}$$

In order to reduce the off-frequency detune range, we limit the range of the phase shift to be $\Delta\phi \in [-\pi, \pi]$.

To support M undulator lines, the acceleration phase of the $(M+1)$-th beam has to be the same with the first one, which can be named as the periodic condition

$$\psi_c + M\Delta\phi = \psi_c + 2\pi k \,, \tag{2}$$

* Work supported by U.S. Department of Energy Contracts No. DE-AC02-76SF00515 and submitted to *Phys. Rev. Accelerator and Beams*.
† zzhang@slac.stanford.edu

Content from this work may be used under the terms of the CC BY 3.0 licence (© 2019). Any distribution of this work must maintain attribution to the author(s), title of the work, publisher, and DOI

ISBN: 978-3-95450-210-3 doi:10.18429/JACoW-FEL2019-WEP045

STATUS OF THE KLYSTRONS FOR THE EUROPEAN XFEL AFTER COMMISSIONING AND FIRST USER OPERATION PHASE

V. Vogel, M. Bousonville, A. Cherepenko, S. Choroba, H.-J. Eckoldt, T. Grevsmuehl, V. Katalev, K. Machau, P. Morozov, B. Yildirim, DESY, Hamburg, Germany

Abstract

At present 26 RF stations for the European XFEL are in operation. Each of the RF stations consists of a HV modulator located on the DESY campus, up to 1600 m long 10 kV HV cables that connect the modulators and the HV pulse transformers located in the underground tunnel, the horizontal multi-beam klystron (MBK), and an air filled waveguide distribution system (WG) between the klystron and the cavities input couplers. The klystrons can produce RF power up to 10 MW, 1.5 ms RF pulse length and 10 Hz repetition rate. Two RF stations of the injector have already achieved about 30,000 hours of operation, RF stations of the XFEL bunch compressor area have operated up to 20,000 hours and the klystrons in the XFEL main linac already have about 18,000 hours of operation. To increase the lifetime of the klystrons we are using a fast protection system (KLM) that is in routine operation since 2018 in addition to the common interlock system. In this article we will give a summary of the present klystrons operation status including the number of HV and RF arcs in the klystrons and in the WG system and operation statistics for the high power RF part of machine.

INTRODUCTION

The European X-ray Free-Electron Laser (XFEL) [1] can be operated up to energy of 17.5 GeV (July 2018). Currently up to 300 coherent laser pulses per second with duration of less than 100 fs and with photon energy up to 19.1keV are delivered to the experiments. In future the number of pulses will increase to the design value of 27000 per second. For the production of these laser pulses, electrons have to be accelerated using a 2 km long accelerator based on superconducting radio frequency (RF) technology. For the XFEL project for a source of RF power of 26 RF stations were chosen the series horizontal MBKs made by two companies: MBK TH1802 from “Thales” [2, 3] and MBK E3736H from “Toshiba” [4, 5]. Both types of MBKs were equipped with CMs [6, 7] and 3 m long HV cables, and then they were tested on DESY MBK test stands [8]. The test was done with full RF power of 10 MW, full RF pulse length of 1.5 mS and with repetition rate of 10 Hz. Big advantages of using CM and HV cable connection between MBK and HV transformer are that we don’t have to work with the oil during MBK installation in the tunnel and that MBK and WGS can be easy connected together. CM has monitors for the measurement of klystron voltage and cathode current. Figure 1 shows the one of 24 RF stations in the XFEL tunnel.



Figure 1: XFEL tunnel view.

Since 2013 the commissioning of the first RF station for XFEL injector has been started. In 2015 the second RF station started operation for the first cold AC module and since 2016 the commissioning of the main part of linac has been started.

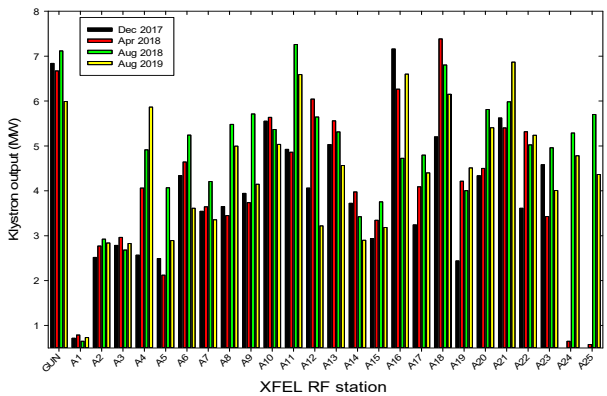


Figure 2: Output power for each of MBK.

In beginning of 2018 the commissioning of last two RF stations was done and in July 2018 the XFEL reached the design energy of 17.5 GeV. Figure 2 shows the output RF power for each of RF station. The average power from one MBK is 4.87 MW, but for several of RF stations the level of output power are more than 7 MW. Figure 3 shows the high voltage level for each of RF stations. In average the high voltage is 104.5 kV. For the moment we don’t have any limitation for XFEL operation from RF stations, the level of RF power from each of RF stations are determinates by XFEL longitudinal beam dynamics and bunch compression system.

Content from this work may be used under the terms of the CC BY 3.0 licence (© 2019). Any distribution of this work must maintain attribution to the author(s), title of the work, publisher, and DOI

ISBN: 978-3-95450-210-3 doi:10.18429/JACoW-FEL2019-WEP046

THE EUROPEAN XFEL PHOTOCATHODE LASER

L. Winkelmann, A. Choudhuri†, H. Chu, I.Hartl, C. Li, C. Mohr, J. Mueller, F. Peters,
S. Pfeiffer, S. Salman, U. Grosse-Wortmann, ,
Deutsches Elektronen-Synchrotron (DESY), Hamburg, Germany

Abstract

We present the design, performance and long-term stability of the hybrid Yb:fiber, Nd:YVO_4 laser system used to drive the RF photocathode gun and laser heater at the European XFEL facility. The laser system provides deep UV output pulses in 600 µs long bursts of laser pulses with variable intra-burst repetition rates ranging from 500 kHz to 4.5 MHz. Due to its robust laser architecture, comprised of a mode-locked and synchronized Yb:fiber oscillator, Yb:fiber pre-amplifiers and Nd:YVO_4 power amplifiers, the laser has operated with >99% uptime since January 2017. Using this laser system, the European XFEL reported landmark electron beam energies of 17.5 GeV in July 2018, and simultaneous multi-mJ lasing in its three SASE beamlines. The photocathode laser system offers two parallel outputs, each providing pulses of >100 µJ energy and 11 ps FWHM duration at 1064 nm center wavelength. One output is converted to the deep UV (266 nm) with conversion efficiencies > 25%. The second beam is sent to a laser heater to reduce microbunching instabilities, increasing the SASE efficiency. For efficient XFEL operation several state-of-art laser controls were implemented, such as: feed-forward algorithm to flatten electron charge along the bunch, active beam stabilization with < +/-10 µm beam pointing jitter at the photocathode, state machines for hands-off operation, temporal pulse synchronization and drift compensation. The latter reduces the timing jitter of the electron bunches to less than 45 fs rms.

INTRODUCTION

The high availability requirements of the photocathode injector laser (>8000 hours of 24/7 operation) [1] for the European XFEL merited the installation of a second laser system, based on high-gain Nd:YVO_4 material to act as a "hot swap" backup in case of failure or temporary downtime of the already existing complex chirped pulse amplifier (CPA) Yb:YAG laser system in 2017. This simpler non-CPA Nd:YVO_4 system was designed for producing all required laser parameters for European XFEL operation with exception of an experimental 3 ps "short pulse" mode with high availability and low jitter. After the integration of the Nd:YVO_4 laser into the XFEL injector, its demonstrated robust performance (>99% uptime for 2018) made the Nd:YVO_4 system the primary driving laser for the XFEL. This paper focuses on key technology developments for the injector laser beamline that enable delivery of laser light to the cathode with high reliability and stability.

THE SYSTEM

Both European XFEL photocathode laser systems offer two outputs, for electron gun (UV) and laser heater (NIR), respectively. Relevant laser parameters are provided in Table 1. The UV and NIR outputs from both lasers are multiplexed; with one laser blocked during normal operation. We also can produce complex bunch trains by simultaneously using both sources. A schematic system overview is provided in Figure 1.

Table 1: Summary of Laser Parameters.

Parameter	**Nd:YVO_4 Laser**	**Yb:YAG Laser**
Oscillator Type	Yb:fiber	Yb:YAG
Amplifier Type	Nd:YVO_4	Yb:YAG
IR Wavelength	1064 nm	1032 nm
UV Wavelength	266 nm	257 nm
Pulse Width (UV)	8 ps	Short pulse: 3 ps Long pulse: 12 ps
Intra burst repetition rate	500 kHz, 1.13 MHz, 2.25 MHz, 4.5 MHz	
Energy (UV)	>5 µJ / pulse	>3 µJ / pulse
Energy (IR)	50 µJ / pulse	

The Nd:YVO_4 system consist of three modules (see Figure 1): a frontend oscillator module, a pulse picking and amplification module, and a frequency conversion module [2].

The oscillator is a saturable absorber-modelocked polarization maintaining (pm) Yb:fiber linear cavity design, dispersion managed and wavelength stabilized by a chirped fiber Bragg grating centered at 1064 nm. The cavity is synchronized to the main RF timing of the European XFEL using slow and fast PZT actuators. Control circuits monitor the oscillator's mode-locking state, carrier power and noise levels. A fiber-coupled acousto optic modulator (AOM) after the oscillator is used to pick pulses at the user-selected intra burst repetition rate (see Table 1) out of the 54 MHz repetition rate oscillator signal. The picked pulses are then amplified to ~1.2µJ/pulse in cascaded pm-Yb:fiber and Nd:YVO_4 amplifiers.

The picked pulses enter the amplification module, where a second AOM is used to cut out 10 Hz bursts from the pulse train (to generate electron bunches with 10Hz burst repetition rate), to further amplify the pulses in the first Nd:YVO_4 power amplifier to ~8.5µJ.

† ara.choudhuri@desy.de

Content from this work may be used under the terms of the CC BY 3.0 licence (© 2019). Any distribution of this work must maintain attribution to the author(s), title of the work, publisher, and DOI

ISBN: 978-3-95450-210-3 doi:10.18429/JACoW-FEL2019-WEP047

UPDATE ON THE PHOTOCATHODE LIFETIME AT FLASH AND EUROPEAN XFEL

S. Lederer*, F. Brinker, S. Schreiber,
Deutsches Elektronen-Synchrotron, Hamburg, Germany
L. Monaco, D. Sertore,
INFN Milano - LASA, Segrate, Italy

Abstract

The photoinjectors of FLASH and the European XFEL at DESY (Hamburg, Germany) are operated by laser driven RF-guns. In both facilities Cs_2Te photocathodes are successfully used. In this paper we give an update on the lifetime, quantum efficiency (QE), and dark current of the photocathodes used over the last years. At FLASH cathode #73.3 was operated for a record lifetime of 1413 days and was replaced December 2018 by cathode #105.2. At the European XFEL cathode #680.1 is in operation since December 2015, for 1356 days up to now.

INTRODUCTION

At DESY (Hamburg, Germany) two free-electron laser user facilities are operated. Since 2005 FLASH [1–4] delivers successfully high brilliance femtosecond short XUV and soft X-ray SASE to photon experiments. Based on TESLA type superconducting linac technology, FLASH is able to accelerate in burst mode several thousand electron bunches per second. The macro-pulse repetition rate is 10 Hz with a useable length of the RF pulses of maximal 800 µs. With a micro-bunch frequency of 1 MHz up to 8000 bunches per second can be accelerated at FLASH, limited by the present laser systems. The bunch charge depends on the requirements on the FEL-light and is usually within a span of 20 pC to 1 nC. After acceleration to 1.25 GeV, the electron bunches are distributed into two different undulator beamlines. While the FLASH1 beamline utilizes fixed gap undulators, the FLASH2 beamline is equipped with variable gap undulators.

The second FEL user facility operated at DESY is the European XFEL [5]. It aims for the delivery of high brilliance femtosecond short X-ray pulses in the energy range of 0.25 to 25 keV. As FLASH, the European XFEL uses TESLA type superconducting linac technology with 10 Hz macro-pulse repetition rate. With a micro-bunch frequency of up to 4.5 MHz and an RF-pulse length of 600 µs, the European XFEL can deliver 27000 bunches per second. Downstream the accelerator the beam can be distributed to three variable gap undulator sections generating the desired SASE light. After the successful commissioning of the accelerator in 2016 [6] and first lasing in May 2017 [7], the first user periods have been successfully accomplished [8].

* sven.lederer@desy.de

THE ELECTRON SOURCES

The photoinjectors of FLASH and the European XFEL are very similar. They are both driven by a normal conducting 1.5 cell 1.3 GHz L-band RF-gun, based on the design by [9]. Currently the accelerating field at the photocathode during standard operation at FLASH is 52 MV/m and 54 MV/m for the European XFEL respectively. The complete gun set-ups are dedicated to be interchangeable between both facilities.

Since August 2013 Gun3.1 is operated at FLASH [10]. The first RF-gun operated at the European XFEL was Gun4.3. It was installed in 2013 and operated during the commissioning phase and the first user runs. In December 2017 it was exchanged with Gun4.6 and serves now as hot spare.

In both facilities the electron bunches are generated inside the RF-gun by means of photoemission. The drive lasers at FLASH operate at a wavelength of 262 nm and 257 nm [11], the two lasers at the European XFEL at 257 nm and 266 nm. The vacuum pressure in the RF-guns during operation is in the lower 10^{-9} mbar regime or better. The good vacuum condition allows for the operation of Cs_2Te as photocathode emitting material. The high quantum efficiency (QE) of this material in the UV keeps the required average laser power in a reasonable regime.

The photocathodes are either prepared at INFN-LASA in Milano, Italy, [12] or at DESY. Transfer to the accelerators is done with UHV transport boxes, maintaining a pressure in the low 10^{-10} mbar range. The transport boxes can be equipped with up to four cathodes.

In both facilities a very similar load-lock transfer system is used to insert the Cs_2Te photocathodes under the required UHV conditions into the RF guns [12].

QE AND LIFETIME

QE measurement procedure

To monitor the photocathode performance we perform QE measurements on a regularly bases, if the operational schedules allow. For monitoring purposes the QE is measured always under comparable conditions. The on-crest accelerating field during the measurements is in the order of 52 MV/m. The launch phase is set to 38° w.r.t. zero crossing. This phase was chosen years ago and kept as reference for the QE measurements. It is neither the on-crest phase nor the launch phase during standard operation of the accelerators. On-crest, about 30% more charge is extracted than at 38°.

To determine the QE we measure the charge as function of the laser energy. The charge is measured by means of a toroid

Content from this work may be used under the terms of the CC BY 3.0 licence (© 2019). Any distribution of this work must maintain attribution to the author(s), title of the work, publisher, and DOI

ISBN: 978-3-95450-210-3 doi:10.18429/JACoW-FEL2019-WEP048

FLASH PHOTOINJECTOR LASER SYSTEMS

S. Schreiber*, K. Klose, C. Grün, J. Rönsch-Schulenburg, B. Steffen, DESY, Hamburg, Germany

Abstract

The free-electron laser facility FLASH at DESY (Hamburg, Germany) operates two undulator beamlines simultaneously for FEL operation and a third for plasma acceleration experiments (FLASHForward). The L-band superconducting technology allows accelerating fields of up to 0.8 ms in length at a repetition rate of 10 Hz (burst mode). A fast kicker-septum system picks one part of the electron bunch train and kicks it to the second beamline such that two beamlines are operated simultaneously with the full repetition rate of 10 Hz. The photoinjector operates three laser systems. They have different pulse duration and transverse shapes and are chosen to serve best for the given user experiment in terms of electron bunch charge, bunch compression, and bunch pattern. It is also possible to operate the laser systems on the same beamline to provide specific double pulses for certain type of experiments.

INTRODUCTION

FLASH, the free-electron laser (FEL) user facility at DESY (Hamburg) [1–3] simultaneously operates two undulator beamlines [4,5]. It delivers high brilliance XUV and soft X-ray SASE radiation to photon experiments. FLASH is a user facility since 2005. [6]

A unique feature of FLASH is its superconducting accelerating technology. It allows to accelerate several thousand electron bunches per second. The bunches come in bursts with a duration of 0.8 ms and a repetition rate of 10 Hz. The laser systems of the photoinjector have to produce as many bunches within the burst as possible. For FLASH, the intra-burst repetition rate delivered to user experiments is 1 MHz and lower. Some experiments ask for 100 kHz, photon hungry experiments are able to take higher repetition rates.

An important feature of FLASH is, that one part of the burst is delivered to users at the FLASH1 beamline, the second part to users at the FLASH2 beamline. In order to serve different kind of experiments, the properties of the electron bunches usually differ between the two parts of the burst in charge, duration, and pulse pattern. [7] Therefore, FLASH has three photoinjector lasers running simultaneously on operator chosen beamlines. [8] Two lasers provide bursts of laser pulses with high single pulse energy but fixed single pulse duration. A third system has the feature of short and variable pulse duration optimized for high compression for ultra-short single spike SASE photon pulses, as an example.

THE ELECTRON SOURCE

The electron source of FLASH is a photoinjector based on a normal conducting L-band 1.5 cell RF-gun. The gun is operated with an RF power of 5 MW at 1.3 GHz, with an RF pulse duration of 650 µs at a repetition rate of 10 Hz.

Since FLASH can accelerate many thousands of electron bunches per second with a charge of up to 2 nC, the quantum efficiency of the photocathode must be in the order of a few percent in order to keep the average laser power at an acceptable limit. Cesium telluride has been proven to be a reliable and stable cathode material with a quantum efficiency (QE) well above 5 % for a wavelength in the UV (around 260 nm). The lifetime is much longer than 1000 days of continuous operation. [9] To give an idea of the required laser single pulse energy, as an example, for a bunch charge of 1 nC and a QE of 1 % a single pulse energy of 0.5 µJ is required. For 10,000 bunches per second this corresponds to a reasonable intra-train power of 0.5 W (1 ms burst) and an average power of 5 mW in the UV.

The actual challenge for the laser systems is its burst mode structure with 1 ms long flat bursts of laser pulses. Flat in terms of single pulse energy and arrival time at the RF-gun. A feature is implemented to apply a linear slope over the laser pulse train using the phase of the 1.3 GHz synchronization RF. This is used to compensate possible arrival time slopes in respect the the accelerator due to heating of the BBO crystal along the burst (green to UV conversion). The pulse duration of the laser pulses must be in the order of a few degrees in 1.3 GHz RF phase. An optimum duration for longitudinal Gaussian shaped pulses is σ = 5 to 10 ps and 1 ps for ultra-short pulse operation.

Since FLASH delivers SASE pulses below 100 fs in duration, the required arrival time stability must be better than 50 fs (rms). This is achieved by synchronizing the laser oscillator with an external ultra-stable 1.3 GHz RF-source. The lasers are cross-correlated with the master laser oscillator of the FLASH synchronization system [10, 11] to measure the stability and to realize a slow feedback to compensate slow drifts.

THE LASER SYSTEMS

Laser 1 and Laser 2

The two laser systems [12] described in this section have been installed in 2010 [13] and 2012, and are a substantial upgrade compared to the previous lasers in operation at FLASH and the former TESLA Test facility (TTF) [14, 15]. The lasers have been developed in the Max Born Institute, Germany partially tested at DESY (Zeuthen, PITZ) and finally installed at FLASH.

The layout of both Laser 1 and Laser 2 are very similar. Both systems consist of a pulsed laser oscillator with subsequent amplification stages. A recent description of the laser systems can be found in [8, 16]. The laser material is Nd:YLF lasing at a wavelength of 1047 nm. Nd:YLF has a high gain and a long upper-state lifetime of 480 µs, and

* siegfried.schreiber@desy.de

Content from this work may be used under the terms of the CC BY 3.0 licence (© 2019). Any distribution of this work must maintain attribution to the author(s), title of the work, publisher, and DOI

ISBN: 978-3-95450-210-3 doi:10.18429/JACoW-FEL2019-WEP049

RF POWER WAVEGUIDE DISTRIBUTION FOR THE RF GUN OF THE EUROPEAN XFEL AT DESY

B. Yildirim, S. Choroba, V. Katalev, P. Morozov, Y. Nachtigal
DESY, Hamburg, Germany
E. Apostolov, Technical University of Sofia, Bulgaria

Abstract

The first section of the European XFEL provides the 43 m long injector. The injector consists of a 1.3 GHz RF gun, a 1.3 GHz cryomodule, a 3.9 GHz cryomodule and an extensive diagnostic section. The RF gun operates with a maximum RF peak power up to 6.5 MW, 10 Hz repetition rate and up to 650 µs pulse length. The starting point in the 1.5 cell normal conducting L-Band cavity of the RF gun is a Cs2Te photocathode, which produces electron bunches, which are injected into the superconducting accelerating section of the European XFEL. The RF power is generated by a 10 MW multi beam klystron and distributed to the RF gun through a RF power waveguide distribution system. In order to enhance the reliability of the distribution system, the peak power is minimized in every section of the system by splitting the power in different branches. The RF power reaches its maximum just in front of the RF gun after combination of all branches. An additional air pressure system decreases the break down level in the waveguides of the distribution.

We present the layout of the waveguide distribution system for the XFEL RF gun at Desy and report on first operation experiences.

REQUIREMENTS FOR THE WAVEGUIDE DISTRIBUTION FOR THE RF GUN

The main requirement is to feed the gun at the 7th underground floor in the XFEL tunnel with a klystron located at the 3rd underground floor with high reliability [1]. Therefore the connecting waveguide distribution has been designed and installed in a narrow shaft with high precision and high accuracy. The connecting waveguide distribution, as shown in Fig. 1, compensates the mechanical misaligment, the thermal expansion and the weight of the waveguide distribution due to flexible waveguides and a customized support system, which consists of several hanging units to stabilize the waveguide system from upper, lateral and lower sides.

To create a system as reliable as possible the two klystron outputs are splitted into four branches, which lead the RF power to unique developed isolators each at the end of the shaft. Through power combiners those branches are connected and the RF power is transferred to the RF gun window.

The Figure 1 shows the Connecting Waveguide Distribution with all four branches, which extend from the 3rd to the 7th underground floor.

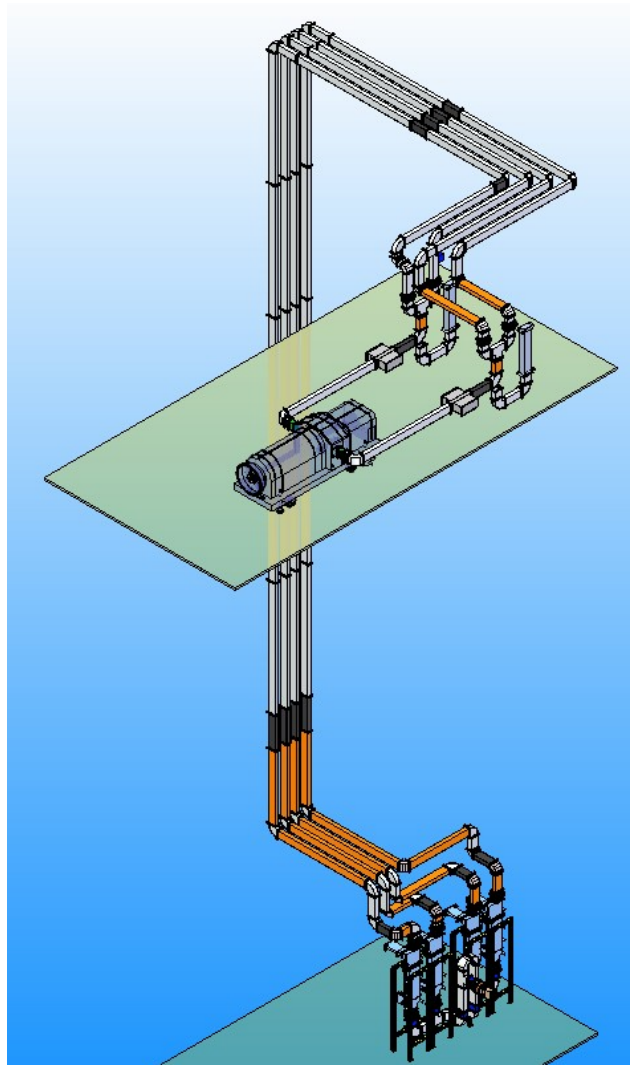


Figure 1: Connecting waveguide distribution for the RF gun.

WAVEGUIDE DISTRIBUTION FOR THE RF GUN

The complex waveguide distribution system for the RF gun consists of 236 parts both standard type WR650 and specific waveguide components [2]. To manage the distance in the injector shaft of approximately 25 m between the 10 MW klystron and the individual gun waveguide distribution, straight waveguides, H – bends as well as flexible waveguides are used and assembled with a support system only developed for this purpose. Several special bearings with springs compensate the waveguide weight over the entire length between the 3rd and 7th

Content from this work may be used under the terms of the CC BY 3.0 licence (© 2019). Any distribution of this work must maintain attribution to the author(s), title of the work, publisher, and DOI

ISBN: 978-3-95450-210-3 doi:10.18429/JACoW-FEL2019-WEP050

STATUS OF CHIRPED PULSE LASER SHAPING FOR THE PITZ PHOTOINJECTOR

C. Koschitzki*, J. Good, M. Gross, Y. Chen, G. Loisch,
M. Krasilnikov, R. Niemczyk, F. Stephan, DESY Zeuthen, Germany
L. Winkelmann, T. Lang, DESY Hamburg, Germany
S. Mironov, E. Khazanov, IAP RAS Nischni Nowgorod, Russia

Abstract

In this publication we show the current status on spectral-spatial shaping of laser pulses at the Photo Injector Test facility at DESY-Zeuthen (PITZ) for providing temporally and spatially variable laser pulse intensities at a photo injector cathode. The temporal and spatial distribution of these laser pulses will determine the properties of the emitted electron bunch, which will influence the properties of Free-Electron Laser (FEL) radiation, after these electron bunches are further accelerated in the linac. The presented pulse shaper modulates the spectral amplitude of a chirped pulse with the additional capability to transversely vary the pulse shape, thus allowing a three dimensional pulse shaping. However, these pulses are particularly difficult to convert to shorter wavelength in nonlinear crystals preserving their shape. Shaping components like the spatial light modulator are not available for the required UV radiation and thus a specialized conversion setup had to be built, utilizing angular chirp matching and imaging to achieve shape preservation. In this work we present preliminary results of laser pulses shaped in the infrared and the similarity to their converted ultraviolet counterparts.

INTRODUCTION

Free-Electron Lasers (FEL) are currently the most powerful source for coherent x-rays. They are typically driven by a linear electron accelerator, which as opposed to ring type accelerators, preserves electron bunch properties from its injector source. Thus the performance of photo injectors is studied at PITZ. The initial temporal and spatial distribution of the electron bunch is determined by the shape of the laser pulse used to emit electrons from the photo cathode via the photo electric effect. As laser amplifiers for short-pulse amplification with high average power output are only available for infrared (IR) wavelength, it is necessary to use harmonic generation processes in nonlinear crystals to convert the laser pulses to the ultraviolet (UV) in order to overcome the work function of the photo cathode material. In this case this is a dicaesium telluride (Cs_2Te) with a vacuum threshold energy of 3.5 eV or 354 nm. Two consecutive second harmonic generation (SHG) processes are applied to get to the fourth harmonic of a 1030 nm IR laser and thus 257 nm or 4.8 eV. UV optical components needed for the shaper are either not available, very expensive or inefficient at these wavelength ranges. Thus laser pulse shaping is done in IR and special care has to be taken to preserve pulse shapes through the conversion process. In particular the conversion from visible (VIS) to UV light is challenging. A laser pulse shaper capable of shaping in three dimensions, i.e. spatially and temporarily, has been developed at PITZ, based on a prior system by Mironov et al. [1]. Preserving such pulses in all three dimensions through the conversion process is a key challenge in order to use the pulse shaper system for the photo injector application. Mironov et al. have proposed and simulated a method for shape preserving conversion [2], using an angular chirp matching with type I phase matching. In this work preliminary experimental results will be shown.

SLM PULSE SHAPER

The most prominent scheme to alter the laser pulses temporal distribution from its typical Gaussian shape is the coherent pulse stacking technique, in which copies of short laser pulses are delayed, attenuated and recombined. The precision depends on the amount of copies produced. Such a system is also operated at PITZ [3]. Spatial shaping is added by masking the transverse distribution typically by a round aperture after the laser pulses have longitudinally been shaped in IR and converted to UV. The dispersive pulse shaper, as proposed and demonstrated by Mironov et al. [1], uses a principle very similar to a spectrograph. The beam is focused into a line onto a spatial light modulator (SLM)by a cylindrical lens, where the spread out spatial dimension can be modulated. Perpendicular to the line focus the beam is dispersed by an optical grating, allowing for a simultaneous modulation of one spatial dimension and the spectrum. The beam path is then reversed to undo the cylindrical focusing and the dispersion (see Figure 1). SLMs can shift the laser phase on each of its pixels between 0 and 2π. The phase shifting of the SLM is polarization dependent, so one can apply quarter $\frac{1}{4}\lambda$ plates and a polarizer in order to turn the phase shift into a spatial-spectral attenuation. Without the $\frac{1}{4}\lambda$ plates the shaper can be operated as variable prism as shown in section . As a single shaper allows only access to one spatial dimension, the beam is rotated by 90 degrees and the shaping process is repeated. Thus the 3D spectral-spatial attenuation function $f_a(x, y, \lambda)$ is not fully arbitrary, but must fulfill the condition

$$f_a(x, y, \lambda) = f_1(x, \lambda) * f_2(y, \lambda). \quad (1)$$

This condition results in 3D shaped pulses consisting of rectangular spatial profiles along the wavelength axis. In order to achieve a targeted attenuation of the laser pulse

* christian.koschitzki@desy.de

Content from this work may be used under the terms of the CC BY 3.0 licence (© 2019). Any distribution of this work must maintain attribution to the author(s), title of the work, publisher, and DOI

ISBN: 978-3-95450-210-3 doi:10.18429/JACoW-FEL2019-WEP051

PITZ EXPERIMENTAL OPTIMIZATION FOR THE AIMED CATHODE GRADIENT OF A SUPERCONDUCTING CW RF GUN

M. Krasilnikov*, P. Boonpornprasert, Y. Chen, G. Georgiev, J. Good, M. Gross, P. Huang, I. Isaev, C. Koschitzki, S. Lal, X.-K. Li, O. Lishilin, G. Loisch, D. Melkumyan, R. Niemczyk, A. Oppelt, H. Qian, H. Shaker, G. Shu, F. Stephan, G. Vashchenko, DESY, Zeuthen, Germany
M. Dohlus, E. Vogel, DESY, Hamburg, Germany

Abstract

A continuous wave (CW) mode operation of the European X-ray Free-Electron Laser (XFEL) is under considerations for a future upgrade. Therefore, a superconducting radio frequency (SRF) CW gun is under experimental development at DESY in Hamburg. Beam dynamics simulations for this setup have been done assuming 100 pC bunch charge and a maximum electric field at the photocathode of 40 MV/m. Experimental studies for these parameters using a normal conducting RF photogun have been performed at the Photo Injector Test facility at DESY in Zeuthen (PITZ). The beam transverse emittance was minimized by optimizing the main photo injector parameters in order to demonstrate the feasibility of generating electron beams with a beam quality required for successful CW operation of the European XFEL for conditions similar to the SRF gun setup.

INTRODUCTION

For successful CW operation of modern XFEL facilities the electron source should combine high average power and peak beam brightness sufficiently high for proper lasing. A high cathode gradient in the gun is one of the important factors to achieve high phase space density of the generated electron beams. However due to the CW requirements (high average power) on the electron source the peak RF power (gradient) in the RF gun is limited and is typically lower than in the case of pulsed guns. An SRF CW L-band gun is under experimental development at DESY in Hamburg [1]. A maximum electric field at the photocathode of 40 MV/m is considered for the operation of this gun in the CW mode of the European XFEL. Beam dynamics simulations for the SRF photo injector (CW SRF PI) setup have been done for 100 pC bunch charge generated with Gaussian photocathode laser pulses. Optimization of the projected normalized emittance yielded 0.45 mm mrad. In order to demonstrate this brightness the normal conducting PITZ photo injector has been tuned to the proposed conditions, namely 40 MV/m maximum electric field at the cathode and bunch charge of 100 pC. Results of experimental studies at PITZ supplied with corresponding beam dynamics simulations are compared with the optimized SRF CW photo injector setup.

LAYOUTS OF PHOTO INJECTORS

One essential difference between PITZ and the SRF gun setup is the location of the main solenoid. Due to the superconducting environment a focusing solenoid has to be separated from the SRF gun cavity and located downstream. For the normal conducting PITZ RF gun cavity the main solenoid is located closer to the cathode plane and its field overlaps with RF fields of the L-band PITZ gun cavity. Axial distributions of RF and solenoid fields are shown in Fig. 1 for both setups.

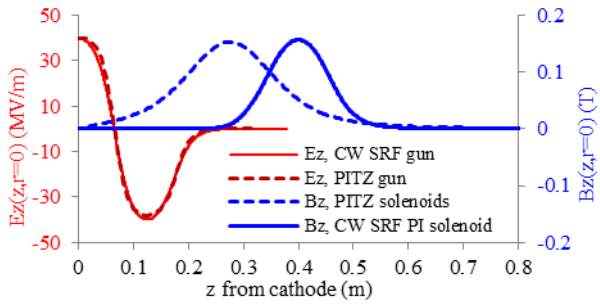


Figure 1: Axial distributions of RF electric fields (amplitudes $E_z\,(z, r = 0)$) and longitudinal magnetic field of solenoids ($B_z\,(z, r = 0)$) for SRF and PITZ guns.

BEAM DYNAMICS SIMULATIONS

Beam dynamics optimization for the CW SRF PI setup were performed using ASTRA [2] for 100 pC bunches applying photocathode laser pulses with a Gaussian temporal profile of 4 ps RMS duration. A module with 8 TESLA cavities (with 14.5 MeV energy gain per cavity) was applied to accelerate the beam up to 120 MeV. RF phase of the gun, strength of the solenoid (corresponding field profiles shown in Fig. 1) and laser transverse spot size were optimized to minimize a transverse emittance at the injector exit. Beam dynamics simulations for the PITZ setup were performed for parameters compromising between assumed CW SRF PI simulations and currently available parameters in experiment. Photocathode pulses with Gaussian temporal profile with 2.6 ps RMS duration (35% shorter than in the CW SRF PI simulations) were applied. The gun with maximum RF field of 40 MV/m at the photocathode and launch phase at the maximum mean momentum gain (MMMG) was used. The CDS booster [3] accelerates the beam up to ~17 MeV which is comparable with 1st cavity in cryomodule acceleration in the CW SRF PI case. The photocathode laser spot size and the main solenoid peak field were tuned in order to minimize projected normalized RMS emittance at z=5.27 m, the standard location of emittance measurements at PITZ.

Optimized simulated transverse RMS beam size and

* mikhail.krasilnikov@desy.de

Content from this work may be used under the terms of the CC BY 3.0 licence (© 2019). Any distribution of this work must maintain attribution to the author(s), title of the work, publisher, and DOI

ISBN: 978-3-95450-210-3 doi:10.18429/JACoW-FEL2019-WEP052

SIMULATION STUDIES ON THE SATURATED EMISSION AT PITZ

X.-K. Li*, P. Boonpornprasert, Y. Chen, J. Good, M. Gross, I. Isaev, C. Koschitzki, M. Krasilnikov, S. Lal, O. Lishilin, G. Loisch, D. Melkumyan, R. Niemczyk, A. Oppelt, H. Qian, H. Shaker, G. Shu, F. Stephan, G. Vashchenko, DESY, Zeuthen, Germany

Abstract

In this paper we report our consideration and simulation on the space charge dominated emission in the L-band photocathode RF gun at the Photo Injector Test facility at DESY in Zeuthen (PITZ). It has been found that the emission curve, which relates the extracted and accelerated bunch charge after the gun to the laser energy, doesn't agree very well with Astra simulations when the emission is nearly or fully saturated. Previous studies with a core-halo model for a better fit of the experimentally measured laser transverse profile as well as with an improved transient emission model have resulted in a better agreement between experimental data and simulation. A 3D FFT space charge solver including mirror charge and binned energy/momentum has been built, which also allows more emission mechanisms to be included in the future. In this paper, the energy spread during emission was preliminarily analyzed. Experimentally measured emission curves were compared with simulation, showing the effect of the inhomogeneity of the laser on the emission and beam parameters.

INTRODUCTION

The space charge effect during photo emission in an RF photocathode gun is one of the key factors determining the quality of the accelerated electron beam. For a given bunch charge, it can be optimized, for instance, by tuning gun gradient, injection phase or by cathode laser pulse shaping. According to the magnitude of space charge, the photo emission can be either source dominated or space charge dominated. For the former, the emitted charge depends on the laser energy and the quantum efficiency (QE) of the cathode. For the latter, the space charge is comparable to the accelerating gradient, therefore suppressing the emission. At PITZ [1], the measurement of the emission curve, which gives the relation between the incoming laser energy and the outgoing bunch charge, is a routine task. The modeling of the emission using a particle tracking code such as Astra [2] does not always give satisfying agreement, especially for the space charge dominated emission or saturated emission. Along with the investigation of cathode physics such as Schottky effect [3], a 3D space charge solver has been developed for considerations of effects such as the inhomogeneity of the laser transverse profile and the quantum efficiency over the cathode and the large energy spread of the electron bunch during the emission. Further development will also take into account the physics behind the emission process. In this paper, we report about our 3D space charge solver based on fast Fourier transformation (FFT) [4] and the application of the solver to study the energy spread effect and to simulate the emission under experimental conditions. The measured laser profile was used to modify a homogeneous distribution generated by Astra for the 3D solver. The simulation results are compared and discussed.

* xiangkun.li@desy.de

3D SPACE CHARGE SOLVER

In order to calculate the space charge forces, the whole electron bunch of a given distribution is transformed into its rest frame, which turns the problem of space charge into solving the Poisson's equation. The method of solving it in 3D using FFT has been described in detail in Ref. [4]. In this method, the solution of Poisson's equation (or the static potential ϕ) is given by

$$\phi(\vec{r}) = \frac{1}{4\pi\epsilon_0} \times \int G(\vec{r}, \vec{r'})\,\rho(\vec{r'})\,d\vec{r'}, \tag{1}$$

where $\vec{r} = (x, y, z)$, ρ is the charge density and G is Green's function defined as

$$G(\vec{r}, \vec{r'}) = \frac{1}{|\vec{r} - \vec{r'}|}. \tag{2}$$

In Eq. (1) the static potential is written as the convolution of Green's function and the charge density and therefore can be solved efficiently using FFT [5]. After knowing the static potential, the electric fields in the rest frame can be derived by $\vec{E} = -\nabla\phi$ and the fields in the laboratory frame can be obtained by Lorentz transformation.

The mirror charge effect during emission is not negligible and is solved in a similar way by using the shifted Green's function method [4]. In the above, it has been assumed that the bunch has a very small energy spread which makes the bunch static in the Lorentz transformed rest frame. In the case of large energy spread, the bunch should be treated specially, for example, by binning the bunch according to the kinetic energies or momenta of individual electrons or by slicing them longitudinally, if a strong correlation between the kinetic energy and position exists. The fields solved from each bin or slice are then summed together.

EFFECTS OF ENERGY SPREAD ON SPACE CHARGE CALCULATION

As mentioned above, the transformation of the bunch into its rest frame for calculating the static potential is valid when the beam has a small energy spread. In fact, the energy spread during emission is large. For instance, the longitudinal phase space shown in Fig. 1 (left) gives an RMS energy spread ($\Delta E/E$) as high as 140%, when half of the bunch was emitted.

Content from this work may be used under the terms of the CC BY 3.0 licence (© 2019). Any distribution of this work must maintain attribution to the author(s), title of the work, publisher, and DOI

ISBN: 978-3-95450-210-3 doi:10.18429/JACoW-FEL2019-WEP053

DEVELOPMENT OF A MULTIALKALI ANTIMONIDE PHOTOCATHODE AT INFN LASA

S. K. Mohanty †[1], DESY Zeuthen, Zeuthen, Germany
P. Michelato, L. Monaco, D. Sertore, INFN - LASA, Segrate, Italy
C. Pagani, G. Guerini Rocco, Università degli Studi di Milano & INFN, Segrate, Italy
[1]also at INFN-LASA, Segrate, Italy

Abstract

Owing to their excellent properties including high quantum efficiency (QE), low emittance, good lifetime and fast response, alkali antimonides Photocathodes has been considered as one of the eminent candidates for the electron source such as in energy recovery linacs (ERL) and free electron laser (FEL). Along with this fact, our recent projects are aiming for CW operation, where these kinds of material are more suitable for the laser specification. So, by considering this fact and stimulating from former successful development of Cesium Telluride photocathodes, our R&D activity has been started to develop specifically the K-Cs-Sb based multi-alkali photocathodes which are sensitive to the green light at INFN LASA. The primary goal is to develop a stable reproducible alkali antimonide film on INFN plug and test them in the photo injector test facility at DESY in Zeuthen (PITZ). In this report, we present and discuss the different growth procedure and results so far obtained for KCsSb material.

INTRODUCTION

Semiconductor materials belonging to the alkali antimonides family have been widely used for many decades in photon detection application because of their high efficiency in the visible range of the spectrum [1]. But, the reliable growth process for these materials is largely based on recipes obtained by trial and error [2]. So, in order to get highly efficient cathode, a series of different growth procedure and characterization techniques is currently being followed in our R&D activity. Currently our major interest on to develop a reliable and reproducible recipe of K-CS-Sb material, in which we have implemented our past gathered data related on these types of photocathode material [3]. Also, we have included some surface science techniques to investigate the material growth [4].

Information about the film thickness, substrate temperature, thermal treatment and their possible effects on properties of photocathode are discussed in this paper together with a comparison of the performances of the photocathode produced so far.

EXPERIMENTAL LAYOUT

In order to get a stable and reproducible recipe, the current R&D activity has been developed in a dedicated UHV (Ultra High Vacuum) system [5] that consists of two interconnected chambers which are used for cathode growing and storage of samples. The cathode growing chamber is maintained with based pressure in the 10^{-11} mbar range provided by eight SAES Getters NEG St707® modules and a 400 ls^{-1} ion pump. It is also connected with a μ-metal chamber which hosts a Time Of Flight spectrometer used for thermal emittance measurements [6].

A LDLS (Laser Drive Light Sources) system accompanied by a certain dedicated optical filter (in a range of 239 nm to 436 nm) is used to measure the spectral response of the photocathode. An Ar^{+} and three He-Ne lasers are also used to cover the range from 457 nm to 633 nm.

Photocathode Preparation

To get a better handling, the photo emissive materials are currently being developed on a simplified Mo sample instead of INFN real plug, used in RF guns. These samples are prepared from a thin slab of high purity molybdenum (99.95 %) through machining. Afterwards, these samples are polished to a mirror like finishing (reflectivity > 54 % @ 543 nm w.r.t. 57 % theoretical) to allow reflectivity measurements during and after the photocathode growth. All samples are ultrasonically cleaned before loading then into the UHV system. Afterwards, each sample is heat up to 450 °C for at least one hour to remove the eventual residual on the surface before starting the deposition process.

A custom-made source for Sb and SAES Getters dispensers for Cs and K is used in the operation. Each source is carefully degassed before each deposition and calibrated to have the proper evaporation rate during the cathode growth. The calibration is repeated before each growth process. The usual rate during deposition is 1 nm/min.

FABRICATION RECIPES

Up to now, six photocathodes have been grown and four of them have already been reported in previous papers [5, 7] and summarized in Table 1. The main outcome of this experience was the need for a better temperature control and a diversification of the temperatures for K and Cs. We explored also photocathodes with different Sb thickness to evaluate its influence on the photocathode properties. The details of growth of two successive cathodes including the influence of both temperature and thickness on photo-cathode's properties has been reported in this report.

KCsSb-5

Since, we recorded a low Quantum Efficiency (QE) for KCsSb-4 (Table 1) where we used 5 nm of Sb, we assumed this was mainly related to the thickness of photocathode material. So, we decided to grow a thicker photocathode. We have grown 10 nm Sb followed by K and Cs at 90 °C

† sandeep.mohanty@desy.de.

Content from this work may be used under the terms of the CC BY 3.0 licence (© 2019). Any distribution of this work must maintain attribution to the author(s), title of the work, publisher, and DOI

ISBN: 978-3-95450-210-3 doi:10.18429/JACoW-FEL2019-WEP054

Content from this work may be used under the terms of the CC BY 3.0 licence (© 2019). Any distribution of this work must maintain attribution to the author(s), title of the work, publisher, and DOI

BEAM DYNAMICS OPTIMIZATION OF A NORMAL-CONDUCTING GUN BASED CW INJECTOR FOR THE EUROPEAN XFEL*

H. Shaker†, H. Qian, S. Lal, G. Shu, F. Stephan, DESY, Zeuthen, Germany

Abstract

The European XFEL is operating up to 17.5 GeV electron energy with maximum 0.65% duty cycle. There is a prospect for continuous wave and long pulse mode (CW/LP) operation of the European XFEL, which enables more flexible bunch pattern time structure for experiments, higher average brightness and better stability. Due to engineering limitations, the maximum electron beam energy in the CW/LP mode is about 8.6/12.8 GeV [1], which puts more pressure on the injector beam quality for lasing at the shortest wavelength. This paper optimizes the beam dynamics of an injector based on a normal-conducting VHF gun.

INTRODUCTION

The European XFEL operates in the pulsed mode at the moment. The duration of each RF pulse is max. 650 µs and the repetition rate is 10 Hz. The time interval between bunches inside a pulse is 220 ns. This result to 27000 bunches per second and 0.65% duty cycle. For future development, the CW/LP mode operation is considered. Recent study shows a maximum 25 µA average current capability of SRF cavities in the European XFEL [1]. Based on this, the optimal value for the CW mode is selected to be 100 pC bunch charge with 4us bunch time interval. The maximum achievable energy is about 8.6 GeV for the CW mode. For the LP mode the energy can be increased to about 12.8 GeV [1]. More pressure on the beam quality is at the lower energy of the CW mode for lasing at short wavelengths. This requires better beam quality in comparison to the pulsed mode. The pulsed mode injector is based on a normal-conducting photocathode RF gun which is located in the XTIN1 tunnel [2]. To have the ability to work in dual modes, a new injector is required which will be placed in the XTIN2 tunnel on top of the XTIN1 tunnel. The second injector should have more or less the same energy as the first injector which is above 120 MeV [2,3]. To have a complete superconducting machine, the first choice is a super-conducting gun. This kind of injector is under study and test [4]. As a backup solution a normal-conducting gun based CW injector is studied at PITZ [5,6]. CW Normal conducting photo-cathode RF guns were developed at LBNL in last decade based on mature room temperature RF technology [7], and the main limitation is the high average heat loss which limits both the achievable cathode gradient and the gap voltage. From DC to gigahertz frequency range, VHF band frequencies give us a reasonable cathode gradient, gap voltage and surface heat power. The successful CW APEX gun operates at 187 MHz, 20MV/m cathode gradient and 750KV gap voltage [7]. This gun is used as the electron source for LCLS-II at SLAC [8].

Based on the APEX experience, a 216.6 MHZ gun is under physics design at PITZ, and the cathode gradient and gun voltage are increased to 28 MV/m and 830 kV respectively[5, 6]. Besides, a 400 kV normal-conducting 1.3GHz buncher was developed [9]. To validate the gun and buncher design, a new injector dynamics optimization is presented in this paper. A multi-objective optimizer parallel processing code[10] based on the NSGA-II [11] algorithm is used to drive ASTRA [12] simulations for optimizing the injector.

MAIN BEAMLINE ELEMENTS

Figure 1 shows the conceptual beamline layout. To find the right amount of input parameters for the optimization algorithm we will talk about each component in the beamline. The initial laser beam has a flat-top longitudinal distribution with 2ps rise/fall time. The transverse distribution is Gaussian truncated at 1σ. The laser duration and radius are variable in the optimizer. Two cathode thermal emittances are assumed for injector optimizations: 1mm.mrad/mm for conservative case and 0.5mm.mrad/mm for optimistic case. The first case is close to the Cs_2Te cathode [13], and the second case is close to the multi-alkali cathode, such as K_2CsSb and NaKSb [14].

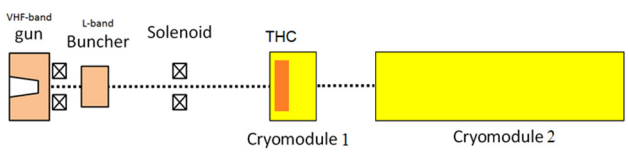


Figure 1: Beamline Layout

Gun and Main Solenoid

To minimize the emittance growth due to space charge, the electrons should be accelerated into the relativistic regime after photoemission as fast as possible. Then the maximum cathode gradient and gap voltage is desirable, but the average heat loss and the peak electric field on cavity surface limits the cathode gradient. Based on APEX gun experience, a maximum 100 kW heat loss and 30 MV/m peak surface field are considered as the baseline parameters. Due to these limitations a gun with 28 MV/m cathode gradient, 832 kV gap voltage and 3cm gap length was designed [5, 6]. Only the gun phase is variable during the beam dynamics optimization. The cathode position is assumed to be zero (z=0). The gun solenoid

* Work supported by the European XFEL
† hamed.shaker@desy.de

ISBN: 978-3-95450-210-3 doi:10.18429/JACoW-FEL2019-WEP055

MULTIPHYSICS ANALYSIS OF A CW VHF GUN FOR EUROPEAN XFEL

G. Shu*, H. Qian, S. Lal, H. Shaker, Y. Chen, F. Stephan, DESY, Zeuthen, Germany
*on leave from IHEP/CAS, Beijing, China

Abstract

R&D for a future CW operation mode of the European XFEL (E-XFEL) started after the successful commissioning of the pulsed mode. For the electron source upgrade, a fully superconducting CW gun is under experimental development at DESY in Hamburg, and a normal conducting (NC) CW gun is under physics design at the Photo Injector Test facility at DESY in Zeuthen (PITZ) as a backup option. Based on the experience of the LBNL 185.7 MHz gun, PITZ designed a 216.6 MHz gun with increased the cathode gradient and RF power of 28 MV/m and 100 kW, respectively, to further improve the beam brightness. In this paper, the multiphysics analysis investigating the RF, thermal and mechanical properties of the NC CW gun are presented.

INTRODUCTION

Driven by the user experimental requirements, a future upgrade of the E-XFEL towards to CW operation has been proposed [1-2]. For the electron source upgrade, one option is a superconducting RF gun, which is under experimental verification at DESY Hamburg [3]. The other option is a VHF band NC CW RF gun which has demonstrated high brightness, high repetition rate (MHz-class) beam at LBNL in the APEX project [4]. Based on the APEX gun experience, a VHF band NC CW RF gun resonating at 216.6 MHz is under physical design stage at PITZ as a backup solution for the SRF gun. To further improve the beam brightness the cathode gradient and cavity voltage were pushed to 28 MV/m and 830 kV, respectively, yielding an average power loss of 100 kW.

The aim of this paper is to evaluate the cooling scheme for the PITZ CW gun to avoid excessive structural temperature, stress, and deformation. In addition, the predicted frequency shift due to heat expansion and air pressure can give a hint for the coarse tuning in the machining phase.

METHODOLOGY

The CST Microwave Studio (MWS) [5] in combination with the CST Mphysics Studio (MPS) were used to perform the coupled electromagnetic-thermal-structural finite element analysis to characterize the cooling capability of the water channels. The methodology of multiphysics simulations is described in Fig. 1. We start from the eigenmode solver in the MWS to obtain the RF induced surface heating distribution. Then, the field map is transferred into the MPS thermal module to evaluate the steady-state temperature distribution. Afterwards, the thermal simulation results are imported into the MPS structure module to simulate the heat induced expansion, i.e. the structure deformations and the von Mises stresses. In the last step, the resonant frequency is calculated again with the deformed shape in the MWS to estimate frequency detuning due to thermal load and vacuum pressure.

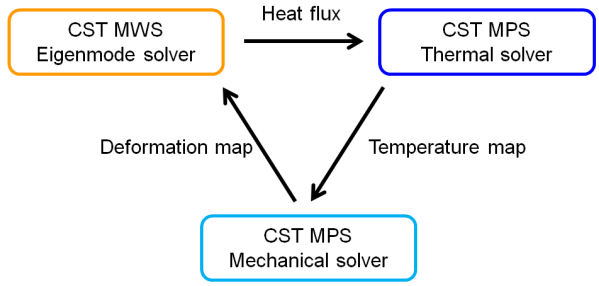


Figure 1: Schematic of the multiphysics simulations.

RF SIMULATION

The 6th sub-harmonic of 1.3 GHz (216.6 MHz), which is higher than the resonant frequency of the APEX gun (185.7 MHz), was selected as resonant frequency for better compatibility with the existing E-XFEL timing system. To improve the beam quality, the cathode gradient and the cavity voltage were enhanced to 28 MV/m and 830 kV, respectively. The cavity shunt impendence was optimized to minimize the heating load to ~100 kW in the gun. By adopting the Rogowski profile, the surface peak electric field was restricted to 2.0 Kilpatrick limit under the consideration of breakdown risk. More details about the RF design can be found in Ref. [6].

Figure 2 shows the RF model in the multiphysics simulations. The vacuum model consists of a re-entrant cavity, 90 vacuum conduction slots and a pump chamber. Figure 2 also indicates the heating distribution on the inner surface and the power dissipation on the sub-assemblies. The total power loss on the cathode nose cone is 36.2 kW with a peak surface loss density of 36.6 W/cm^2, which can be further reduced by elongating the nose cone. The RF heating on the rear plate, cylinder wall and the anode plate are 25.2 kW, 14.7 kW and 23.9 kW, respectively.

* guan.shu@desy.de

Content from this work may be used under the terms of the CC BY 3.0 licence (© 2019). Any distribution of this work must maintain attribution to the author(s), title of the work, publisher, and DOI

ISBN: 978-3-95450-210-3 doi:10.18429/JACoW-FEL2019-WEP056

ENGINEERING DESIGN OF LOW-EMITTANCE DC-SRF PHOTOCATHODE INJECTOR

Y. Q. Liu†, M. Chen, S. Huang, L. Lin, K. X. Liu, S. W. Quan, F. Wang, S. Zhao
Institute of Heavy Ion Physics, School of Physics, Peking University, Beijing, China

Abstract

An upgraded version of DC-SRF photocathode injector (DC-SRF-II) is under development at Peking University. The goal is to achieve an emittance below 0.5 mm-mrad at the bunch charge of 100 pC and repetition rate of 1 MHz. The engineering design of the DC-SRF-II photoinjector was accomplished in this May and the fabrication is ongoing now. This paper presents some details of the engineering design.

INTRODUCTION

Superconducting RF (SRF) photocathode injector has the advantage in principle to generate high average current, high-brightness electron beams and has been developed by several laboratories around the world [1-5]. To prevent the contamination of SRF cavity by the semiconductor photocathode materials, at Peking University, we have been developing a DC and SRF combined photocathode injector, known as the DC-SRF injector [6-8]. To meet the requirements of continuous-wave (CW) X-ray FELs, we are developing an upgraded DC-SRF photocathode injector (referred to as DC-SRF-II for short) with the goal to achieve an emittance below 0.5 mm-mrad at the bunch charge of 100 pC and repetition rate of 1 MHz. Recently, the engineering design of the new injector (which is shown in Fig. 1) has been finished and the fabrication is under way. In this paper, we present some results of the engineering design, including the redesign of the DC structure, the evaluation of thermal load for cryomodule, the design of magnetic shielding, and the evaluation of the mechanical property.

NEW DESIGN OF DC STRUCTURE

The DC structure of the injector has been redesigned according to our operation experience with the first-generation DC-SRF injector. The new design reduces the number of ceramics to two and provides a detachable protective electrode for the brazed position of ceramic and metal. Figure 2 shows the new DC structure. An inverted-geometry ceramic insulator approach was adopt. This insulator extends into the vacuum chamber serving as the cathode support structure. The advantage of this design is that it is compact and it helps to reduce field emission [9]. In addition, the shape of the high-voltage electrode was optimized, and the highest surface field has been controlled below 10 MV/m.

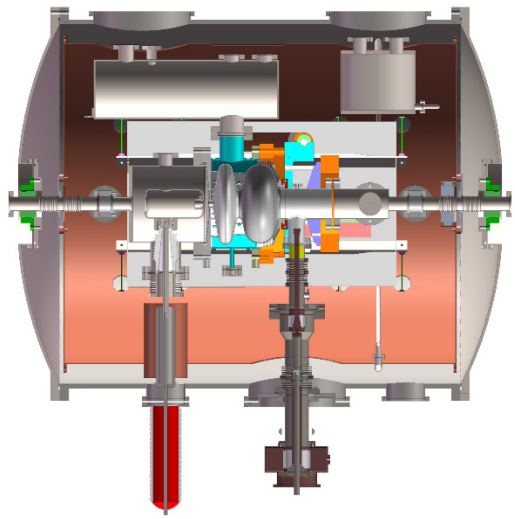


Figure 1: An overview of DC-SRF photocathode injector.

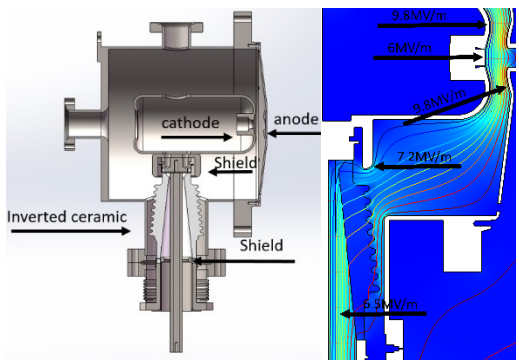


Figure 2: The new design of the DC structure (left) and electric field (right).

THERMAL EVALUATION OF THE CRYOMODULE

The heat load of the cryomodule has been calculated via COMSOL Multiphysics [10]. Static heat load and dynamic heat load are shown in Table 1 and Table 2. The superconducting cavity surface loss can be estimated from the RF parameters in Table 3. The total heat load of cryomodule is about 12 W at 2 K and about 36 W at 77 K.

In addition, the flow direction of the liquid nitrogen pipe has been redesigned to obtain an optimized temperature distribution on the copper screen. Figure 3 shows that the highest temperature is about 87.5 K.

* Work supported by National Key Research and Development Program of China (Grant No. 2016YFA0401904).
† yqliu17@pku.edu.cn

Content from this work may be used under the terms of the CC BY 3.0 licence (© 2019). Any distribution of this work must maintain attribution to the author(s), title of the work, publisher, and DOI

ISBN: 978-3-95450-210-3 doi:10.18429/JACoW-FEL2019-WEP057

PERFORMANCE OPTIMIZATION OF LOW-EMITTANCE DC-SRF INJECTOR USING Cs_2Te PHOTOCATHODE*

Sheng Zhao, Dongming Ouyang, Yunqi Liu, Senlin Huang†, Kexin Liu
Institute of Heavy Ion Physics & State Key Laboratory of Nuclear Physics and Technology Physics and Technology, Peking University, Beijing 100871, China

Abstract

A low-emittance DC-SRF injector (DC-SRF-II) is under construction at Peking University, in the earlier design of which K_2CsTe photocathode was chosen. Recently we changed the cathode to Cs_2Te which is more widely used nowadays, and carried out a detailed performance optimization. In this paper, we present our latest simulation results, which show that an emittance under 0.5 mm−mrad can be achieved at the bunch charge of 100 pC.

INTRODUCTION

DC-SRF photocathode injector, which combines a DC gun and a superconducting radio-frequency (SRF) cavity [1, 2], is capable of generating CW electron beams. It was brought into stable operation in 2014 [3] at Peking University. In order to accommodate the requirement of electron beam with higher bunch charge (100 pC) and lower emittance (< 1 μm), an upgraded version of DC-SRF injector (referred to as "DC-SRF-II" herein) adopting K_2CsTe cathode has been designed and the fabrication is under way now.

In this paper, we present the simulation study of the DC-SRF-II injector with the extensively used Cs_2Te cathode. To investigate its performance as an electron source for CW XFEL, the injector beamline was designed for optimized projected emittance, bunch length, and higher-order energy spread. The multi-objective optimization algorithm was implemented to obtain the global optimal solution.

INJECTOR LAYOUT

A sketch of the DC-SRF-II injector beamline is shown in Fig.1. The photocathode (Cs_2Te) is located at the entrance of the DC gap, soon after which a 1.3 GHz, 1.5-cell SRF cavity boosts the electron beam to a few MeV. Two solenoids downstream the DC-SRF-II injector confine the beam size and compress/compensate the transverse emittance. Following the solenoids is an electron buncher, which is composed of a 1.3 GHz, 2-cell cavity operated around zero crossing phase and a third-harmonic cavity introduced to improve the bunching performance. A standard cryomodule comprising eight 1.3 GHz, 9-cell cavities (referred to as "injection linac" later on) finally accelerates the average energy up to above 100 MeV, followed by a third-harmonic linearizer (four 3.9 GHz, 9-cell cavities) to remove the lower-order energy spread.

* Work supported by National Key Research and Development Program of China (Grant No. 2016YFA0401904).
† huangsl@pku.edu.cn

The fields of the DC structure, the SRF cavity, and the solenoids are cylindrically symmetric in first order. Our study indicates that the higher-order effects that break the symmetry only have insignificant impact on the emittance, bunch length, and higher-order energy spread herein. Therefore, this paper focuses on the cylindrically symmetric issues. The higher order effects, such as those due to the dipole filed of RF coupler and off-axis drive laser, will be discussed elsewhere.

OPTIMIZER DESCRIPTION

Optimization Goals

XFEL operation requires electron beam with low emittance and high peak current. At the exit of injector beamline, the electron beam should have a low emittance and a moderate bunch length ~ 10 picoseconds. The electron beam from the injector beamline will be further accelerated by main linacs and compressed by magnetic compressors to achieve the required energy and peak current. The energy distribution of electrons within a bunch [$E(z) \sim E_0 + c_1 z + c_2 z^2 + O(z^3)$, where z is the position within the bunch] has significant impact on the performance of compression. Its linear and quadratic correlation terms (c_1 and c_2) can be largely eliminated with properly set rf phases and amplitudes of the linac and linearizer (harmonic cavity). The higher-order energy spread $O(z^3)$, however, needs to be suppressed in the injector beamline.

Boundary Conditions

In the optimization, the thermal emittance coefficient of Cs_2Te cathode was assumed to be 1.0 mm−mrad/mm. The drive laser pulse has a plateau distribution with the length of 24 ps and rise time of 2 ps, which can be achieved via coherent pulse stacking [4]. The transverse distribution of the laser is a 2D-Gaussian function truncated at 1 sigma. The initial bunch charge is 100 pC.

The first solenoid downstream the DC-SRF-II injector (see Fig. 1) will be fixed at 1 m, mainly limited by the length of the cryomodule. The position of the second solenoid and the strength of both solenoids need to be optimized. Other knobs used in the optimization, including the amplitude and phase of 1.5-cell cavity field, are given in Table 1. The DC voltage was fixed at 100 kV.

Optimization Process

For the optimization, the MOGA-II algorithm [5] was chosen to drive ASTRA [6] simulations. Since more than one objectives need to be optimized, the result is not a single

Content from this work may be used under the terms of the CC BY 3.0 licence (© 2019). Any distribution of this work must maintain attribution to the author(s), title of the work, publisher, and DOI

ISBN: 978-3-95450-210-3 doi:10.18429/JACoW-FEL2019-WEP058

DRIVE LASER TEMPORAL SHAPING TECHNIQUES FOR SHANGHAI SOFT X-RAY FREE ELECTRON LASER*

Chunlei Li[1], Xingtao Wang†, Wenyan Zhang, Lie Feng, Taihe Lan, Meng Zhang, Bo Liu[1]
Shanghai Advanced Research Institute, Chinese Academy of Science, Shanghai, China
[1]also at Shanghai Institue of Applied Physics, Chinese Academy of Science, Shanghai, China

Abstract

The design of Shanghai soft X-ray free electron laser (SXFEL) is based on laser driven photocathode, which can provide normalized emittance <2.5 mm·mrad with 500 pC charge. The temporal shape of drive laser has significant influence on the electron beam brightness. This paper presents the transport line of drive laser system and the temporal shaping techniques for SXFEL. This drive laser produces 8 picosecond 266nm ultraviolet pulses with repetition rate 10Hz. A transverse deflecting cavity was used for indirectly characterizing the laser pulse temporal structure. Here we present the drive laser system with its temporal shaping method, and measurement results.

INTRODUCTION

Drive laser is a crucial component for photo injector producing high density, high brightness electron bunches. The pulse parameters of drive laser determine the properties of electron bunches, such as bunch length, bunch charge, the stability of the produced charge, and its synchronization accuracy to the RF of the photo injector, as well as the emittance of the electron bunches [1-3]. Simulation and experiment indicate that flattop pulse can help photoinjector generate uniform temporal and spatial electron distribution with lower transverse emittance [4-6]. Therefore, effective temporal pulse shaping methods are important to photoinjector laser system. The pulse length required for excitation photocathode are around 260nm, 5~10ps with flattop distribution. Several methods have been explored with their pros and cons, such as α-BBO crystal stacking [7-8], double prism or grating pair stretcher [5]. Presently, Simulation also indicates that quasi ellipsoidal laser pulse can help producing electron bunches with minimized emittance [9].

Table 1 shows the laser parameter requirement of Shanghai soft X ray free electron laser (SXFEL). Currently, no commercial laser system can provide all the requirements. Therefore, an integrated laser system based on α-BBO crystal stacking was developed for producing 8ps ultraviolet (UV) pulse. The temporal structure was characterized by cross correlation method with difference frequency generation (DFG) crystal. By illuminating the UV pulse to copper photocathode RF gun, 10 Hz repetition rate ultrashort electron bunch was produced with emittance less than <2.0 mm·mrad with 500 pC charge.

Table 1: Drive Laser System Requirements

Name	Parameters
Wavelength	260 nm~270 nm
Repetition rate	1~10 Hz
Pulse energy on the photocathode	150 μJ
Energy stability in UV	<2.0%rms
Spatial profile	Flat top
Laser spot radius on photocathode	0.5~1.5 mm hard edge radius
Laser spot diameter jitter at photocathode	2% rms radius
Pointing jitter	<2% rms radius
Pulse shape	Flat-top
Pulse duration	Flat-top 10ps edge to edge
Timing stability	< 0.25 ps rms

DRIVER LASER SYSTEM

Figure 1 shows the schematic of driver laser system which consists 4 main stages, 1) Oscillator, 2) Amplifier, 3) Frequency tripled modulator, 4) α-BBO crystal stacking. An oscillator (Vitara-T, Coherent Inc.) pumped by 4.88 W Verdi (Coherent Inc.) deliver 800 nm, 0.7 W pulse (79.33 MHz, horizontal polarization) to Ti:sapphire amplifier (Spitfire Ace PA, Spectrum Physics Inc.). The pre-amplified pulses (8.8 nJ) are firstly stretched to 200 ps using grating pair, then amplified to 5 mJ by regenerative amplifier, and further amplified to 10mJ by single pass amplifier. Finally the amplified pulse are compressed to 1ps (10 mJ) and delivered to third harmonic generation (THG).

The compressed pulses was converted from 800 nm to 400nm by second harmonic generation in a β-BBO crystal (type I, o + o = e, 0.5 mm, θ =29.2°), and subsequently sum-frequency generated in a second β -BBO crystal (type I, 0.5 mm, θ=44.4°). The conversion efficiency from 800 nm to 266 nm was about 2%. As shown in Fig. 1, temporal pulse shaping at 266 nm was conducted by 3 pieces of α-BBO crystals.

The transverse homogenisation shown in Fig. 2 was achieved by selecting the centre part of intensity profile using iris, which was then relay imaging to the photocathode shown in Fig. 1.

* Work supported by Shanghai Sailing Program (18YF1428700)
† email address wangxingtao@zjlab.org.cn

Content from this work may be used under the terms of the CC BY 3.0 licence (© 2019). Any distribution of this work must maintain attribution to the author(s), title of the work, publisher, and DOI

ISBN: 978-3-95450-210-3 doi:10.18429/JACoW-FEL2019-WEP059

CHARACTERIZING A COHERENT ELECTRON SOURCE EXTRACTED FROM A COLD ATOM TRAP*

Hang Luo, Yanxia Xu, Jie Guo, Peixin Chu, Xi Zhao, Qinghong Zhou, Xiaohong Li, Tao Liu, Kelin Wang, Dept. of Physics, Southwest University of Science and Technology, Mianyang, China

Abstract

In order to generate a fully coherent free electron laser (FEL) within a compact system, one potential approach is to interact a coherent electron bunch with a high power laser operating in the quantum FEL regime. The coherent electron source can be obtained by ionizing the Rydberg atoms in a magneto-optical trap (MOT). The qualities of the electron source will have direct effects on the brightness, coherence, and line width of the free electron laser. A high quality ultra-cold electron source can be obtained by carefully optimizing the extraction electrode structure, the acceleration and focusing system as well as the MOT. Through parameter optimization, a coherent electron source with a temperature lower than 10K is predicted. Details of the optimization and the characteristics of the coherent electron source are reported in this paper.

INTRODUCTION

The planar cathode photoemissive source is simple and stable in performance, and is the most commonly used electron source for time-resolved electron diffraction (TRED) [1], however, the electron source size, effective temperature, the space charge effect, and energy spread [2] factors limit the achievable lateral coherence length [3]; the cutting-edge optoelectronic emission source can be controlled at the sub-femto second time scale [4], which can achieve ultra-short electronic pulse width. It has extremely high coherence and brightness, but the non-uniformity of its initial trajectory and near-field acceleration and the energy spread of electrons lead to the rapid divergence and elongation of the electron beam during propagation [5]. Femtosecond photoemissive sources based on solid cathodes operate well, but lack of coherence [6]. The typical effective field temperature of a conventional field emission or photoemission source is about 5000 K, and the lateral coherence length of an electron pulse has a strong relation with the effective temperature: $L_{\perp} \propto 1/\sqrt{T}$. The lower the temperature, the greater the lateral coherence length. Based on this, we used laser cooling technology to obtain an electron source from a cold atom trap. The electron beam quality will directly affect the brightness, coherence and linewidth of the free electron laser. The electron source transverse temperature obtained by this technology can be as small as 10K or lower, and the atom is very easy to handle, so that coherent electron source can be extracted from the cold atom. The coherent electron beam can form a very low emittance, coherence temperature. The low emittance of a coherent electron beam results from a high phase space density and a small volume of the coherent electron beam at low temperatures, which is several orders of magnitude lower than conventional electron beam. In addition, the cold electron source can also reach sub-picosecond ultrashort pulse lengths [7]. Thanks to the high coherence and high energy resolution, the cold electron source thus obtained has great applications to various frontier researches.

In order to construct a high-quality ultra-low temperature coherent electron source, a special electrode structure is needed to extract electrons, accelerate and focus. Therefore, we have carried out an optimized design of the electrode structure in the cold atomic trap, and simulated and analyzed the evolution of the three electrode geometries, the position and the influence of the electrode voltage on the electron beam quality.

DEFINITION OF THE QUALITY OF COHERENT ELECTRON

Therefore, our main focus on the coherent electron beam quality factor includes five aspects: energy spread, emittance, electron beam length, beam spot size, and coherent electron beam temperature. Below we give definitions of quality factors:

Energy spread $\frac{\delta}{E}$

Electron beam energy spread has an important impact on the performance of accelerator-based ultrafast scientific devices. The energy spread is closely related to the temperature of the electron, defined as:

$$\frac{\delta}{E} = \frac{\sqrt{\frac{1}{N}\sum_i^N (Ek_i - < Ek >)^2}}{< Ek >} \times 100\% \quad (1)$$

Emittance

Emittance is the product of the beam size and the opening angle, which is interpreted statistically, that is, using the average of all particles to describe the emittance of the electron beam:

* Work supported by the National Natural Science Foundation of China

Content from this work may be used under the terms of the CC BY 3.0 licence (© 2019). Any distribution of this work must maintain attribution to the author(s), title of the work, publisher, and DOI

ISBN: 978-3-95450-210-3 doi:10.18429/JACoW-FEL2019-WEP062

TEST OF Cs_2Te THICKNESS ON CATHODE PERFORMANCE AT PITZ

P. Huang*, H. Qian†, Y. Chen, A. Grigoryan, M. Gross, I. Isaev, P. Kitisri, C. Koschitzki, M. Krasilnikov, S. Lal, X. Li, O. Lishilin, D. Melkumyan, R. Niemczyk, A. Oppelt, H. Shaker, G. Shu, F. Stephan, G. Vashchenko, T. Weilbach, DESY, Platanenallee 6, 15738 Zeuthen, Germany
S. Lederer, DESY, Notkestrasse 85, 22607, Hamburg, Germany
L. Monaco, P. Michelato, D. Sertore, INFN Milano - LASA, Segrate, I-20090, Italy

Abstract

Cesium telluride is a widely used cathode in photo injectors, and its performance is one of the keys for not only emittance but also reliable operation. Over the years lots of experiences with Cs_2Te photocathodes produced with the same recipe and thickness were gained at the DESY photo injectors, but cathode performance dependence on the cathode layer thickness were not investigated. In this paper, we test fresh Cs_2Te cathodes with different thickness at the Photo Injector Test Facility at DESY in Zeuthen (PITZ). The dark current, quantum efficiency (QE) and thermal emittance of these cathodes inside the high gradient RF gun will be compared.

INTRODUCTION

The photocathode is one of the key components of photoinjectors. The performances of the photocathode, including quantum efficiency (QE), thermal emittance, response time, dark current and life time, are closely related to the photoinjector performance and its subsystems, such as the photocathode laser, gun gradient, vacuum, and injector emittance [1]. Even for the same cathode material, different cathode recipes may lead to different cathode performances [2]. Several studies have shown that the thickness of cathodes is one of the parameters to optimize the cathode performance. For transmission mode photocathodes, which are illuminated by laser from the back side, greater thickness would increase electrons possibility to scatter with phonons and reduce thermal emittance [3]. Besides, a fine control of cathode film thickness and substrate can optimize the photon absorption and lead to a higher QE [4]. For K_2CsSb cathodes, a thicker Sb layer has shown improvement in both QE and life time [5]. Among all these studies, a performance dependence test of cathode film thickness in high gradient RF guns is missing.

Cs_2Te cathodes are one of the most widely used cathodes in photoinjectors, especially for applications requiring an average current from 1 μA to 1 mA. It has a typical high QE of around 10 % in UV and a long life time (months to years [6]), compatible with a gun vacuum of 10^{-9} mbar. DESY has been collaborating with INFN-LASA, Milano, on testing and optimizing Cs_2Te cathodes for decades, and Cs_2Te cathodes are reliably used for the user facilities, FLASH and European XFEL, and the Photo Injector Test Facility at DESY in Zeuthen (PITZ). In 2010, INFN-LASA reported the Tellurium thickness effects for Cs_2Te measured in a cathode preparation system [7]. The cathode thickness is specified with the tellurium thickness. They are 5 nm, 10 nm and 15 nm, respectively. The corresponding cesium thickness is determined during the deposition process, where the QE is optimized and the final peak of the QE determines the Cs thickness [7]. At this stage, the cathode is believed to be a complete Cs_2Te film [8]. The three cathodes were maintained in a UHV cathode box after fabrication at Milano and sent to PITZ for testing in the high gradient RF gun [9]. The three fresh Cs_2Te cathodes were tested continuously at PITZ for two weeks in the sequence of 5 nm, 15 nm and 10 nm Te thickness. The testing items include dark current, QE and thermal emittance against electric field, QE and thermal emittance maps. The testing results are reported in this paper.

EXPERIMENTAL SETUP

The experiments were carried out on the PITZ beam line. The simplified layout for the measurements in this paper is shown in Fig. 1. Currently Gun4.2 is installed at PITZ, a 1.5 cell L-band RF-gun operated at high gradient and long pulse train [10]. There are two solenoids around the gun. The main solenoid locates at the gun exit. The other one is the bucking solenoid and it is for compensating the residual magnetic field at the cathode. The dark current is measured with a Faraday cup located at the exit of the gun and the solenoid current is tuned to achieve the strongest signal. The QE is measured by the same Faraday cup and a laser energy meter. For thermal emittance measurement, we use the cathode transverse momentum imaging and the details of this method can be found in [11]. The wavelength of the cathode driving laser is 257 nm. The laser profile is transversely uniform and longitudinally gaussian (6 ~ 7 ps FWHM).

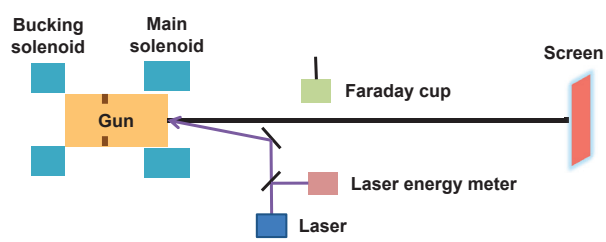


Figure 1: The beam line layout for the experiments. Only the elements related to the experiments are shown.

* hpw17@mails.tsinghua.edu.cn; on leave from Tsinghua University, Beijing 100084, China
† houjun.qian@desy.de

Content from this work may be used under the terms of the CC BY 3.0 licence (© 2019). Any distribution of this work must maintain attribution to the author(s), title of the work, publisher, and DOI

ISBN: 978-3-95450-210-3 doi:10.18429/JACoW-FEL2019-WEP063

THE PRELIMINARY STUDY OF A PRE-BUNCHED TERAHERTZ FREE ELECTRON LASER BY A VELOCITY BUNCHING SCHEME*

Ruixuan Huang†, Zhouyu Zhao, Heting Li, Qika Jia
NSRL, University of Science and Technology of China, Hefei, Anhui, 230029, China

Abstract

Terahertz (THz) radiation has broad applications in biological sciences, materials imaging and radar communications and so on. High-power, frequency tunable THz radiation sources are desired. An electron beam, generated in a photoinjector and bunched at THz frequency, can excite a coherent THz radiation in an undulator. The radiation power mainly depends on the particle number and the bunching factor of the electron beam, which is limited by the space charge effect among the microbunches and the total rf phase width the macrobunch occupied. Previously we have designed a pre-bunched THz free electron laser (FEL) with the radiation frequency covering 0.5-5 THz. While the radiation intensity for the lower frequency (below 1 THz) is not very high because of the large energy spread and the low bunching factor. We will report a THz FEL by a velocity bunching scheme, which could realize more highly bunched beam especially in the low THz frequency region. The physical design of the electron source is described in detail.

INTRODUCTION

The undulator-based terahertz (THz) source is a promising way to generate an intense narrow-band THz radiation with a broad frequency tuning range. For instance, a single-pass free electron laser (FEL) driven by a THz-pulse-train photoinjector, in which the electron beam is pre-bunched before entering the undulator and will excite coherent emission during the whole radiation process. The fundamental radiation frequency can be easily tuned by varing the time interval between the electron microbunches (laser micropulses). With the harmonic generation technique, the radiation could be further extended to higher frequency.

Previously, we have introduced a pre-bunched THz FEL by a linear accelerator which is composed of a photocathode rf gun and a short travelling wave (TW) tube [1]. The electron source can launch 16 microbunches with 15 pC charge for each bunch. This project is designed to have a tunable frequency range of 0.5-5 THz. One of the issues is their limited bunching factor at the frequency below 1 THz, since the large pulse width of the whole electron beam. The bunching factor is critical to determine the total radiation power, which will be discussed later. The most straight forward method to achieve a higher bunching factor at a shorter macropulse width is to reduce the microbunch number and increase its charge at the same time.

* Work supported by the National Natural Science Foundation of China Grant Number 11805200
† rxhuang@ustc.edu.cn

BUNCH TRAIN GENERATION BASED ON VELOCITY BUNCHING

It is possible to produce electron pulse trains with several hundreds pC charge within the same accelerating bucket [2]. When each pulse is linearly chirped in energy, it can be longitudinally compressed either by a velocity bunching (VB) scheme, or by a magnetic compression scheme [3, 4]. In the VB procedure, the electron beam performs a rectilinear motion, which is free from the emittance degradation in a magenetic compressor. Moreover, the VB scheme is associated with the emittance compensation by focusing solenoids surrounding the accelerating section and as well as an energy increase. In short, the VB technique may be more suitable to maintain a high-brightness electron pulse train in the low-energy situation. In this section, we investigate the possible VB scheme for the pre-bunched THz FEL.

The scheme is illustrated in Fig. 1, which utilizes a typical setup for an S-band photoinjector. A 51-cell TW accelerator (TWA) is placed about 0.7 meters after a 1.6-cell BNL-type photocathode gun. A femtosecond laser followed by a proper optical system provides the required laser pulse train on the cathode. The TW tube operates at a brake-applied VB mode [5] which is also known as the over-compression regime. The whole compression is served by the TW tube together with a downstream drift segment. Three solenoids and four quadrupoles are used to focus the beam into the undulator. Three solenoids are 0.2 m, 0.5 m and 0.5 m long, respectively. And the quadrupoles are 0.05 m long with a maximum strength of 30 m^{-2}. A short undulator is located approximately 4.5 meters downstream of the TW tube. It should be indicate that the parameter setup is not the optimization result, but just a typical example instead. The designed parameters of this instance are shown in Table 1.

Table 1: Main Parameters of the Beam Line

Parameter	Value
Gradient of the rf gun	115 MV/m
Phase of the rf gun	20°
Gradient of the TWA	~ 12 MV/m
Phase of the TWA	~ -150°
Solenoid strength	~ 0.2 T (in the gun) 0.03~0.07 T (in the TWA)
Quadrupole strength	~ 30 m^{-2}
Undulator length	0.432 m for 8 periods
Drift segment length downstream the TWA	4.5 m

Content from this work may be used under the terms of the CC BY 3.0 licence (© 2019). Any distribution of this work must maintain attribution to the author(s), title of the work, publisher, and DOI

ISBN: 978-3-95450-210-3 doi:10.18429/JACoW-FEL2019-WEP064

PERFORMANCE OF S-BAND PHOTOCATHODE RF GUN WITH COAXIAL COUPLER

J. Hong*, C.-K. Min, J.-H. Han, PAL, Pohang, Kyungbuk 790-784, Korea

Abstract

To improve the characteristics of electron beams, new S-band photocathode RF gun with a coaxial coupler has been developed and fabricated at the Pohang Accelerator Laboratory (PAL). This new RF gun is improved the field symmetry inside the cavity cell by applying the coaxial coupler, and the cooling performance by improving the cooling lines. The RF gun is installed in the injector test facility (ITF) for high power RF test. This paper reports the recent results on the RF conditioning process and the beam tests of the RF gun with high power RF at ITF. We present and discuss the measurement results of the basic beam parameters.

INTRODUCTION

The Pohang Accelerator Laboratory (PAL) has developed two types of S-band photocathode RF guns to generate electron beams for the X-ray free electron laser (PAL-XFEL) [1–3]. The first gun is the four ports side coupled RF gun (GUN-I) and the second one is the coaxial coupled RF gun (GUN-II). Currently we are using GUN-I as an electronic source for PAL-XFEL [4,5]. In the case of GUN-II, an electron gun with a replaceable Cu plug has been fabricated in 2013. In 2015, an electron gun with fixed Cu cathode has been fabricated. Until we were interested again in 2018, GUN2 was out of our memory.

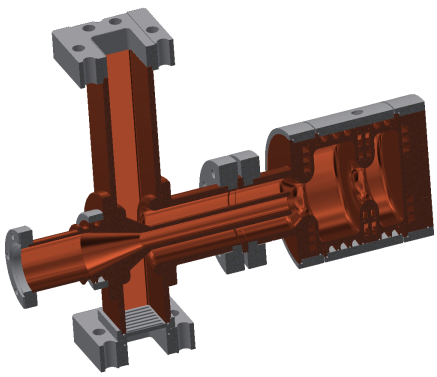


Figure 1: Cutaway view of GUN-II.

The electron gun used in this experiment is an electron gun with fixed Cu cathode. The 3-dimensional cutaway view of GUN-II is shown in Fig. 1. The features of GUN-II are as follows:

- Coaxial coupler is applied for axisymmetric E-field.
- Modified cooling channels to be uniform the RF heating.
- Fixed Cu cathode is applied for easy fabrication and operation.
- Has a narrow (diameter = 14 mm) beam tube. (difficult laser transmission)
- Does not have an gun probe. (can not measure the gun power directly)

The RF parameters of GUN-II are listed in Table 1.

Table 1: RF Parameters

Property	GUN-II	Unit
Operating Frequency	2856	MHz
Mode Separation	20	MHz
Quality Factor	14400	
Coupling coefficient	1.1	
Field Belance	1.02	

TEST SETUP

From August 2015, the important devices in the injector test facility (ITF) were moved to PAL-XFEL. Moved devices are an electron gun, two accelerator columns, a gun energy spectrometer, and a deflector, etc. Until the end of 2018, ITF was shutdown. In April 2019, ITF was restructured to perform the high power beam test for GUN-II. The schematic diagram of the new ITF beam-line for GUN-II is shown in Fig. 2. Electron beams are generated from the new GUN-II.

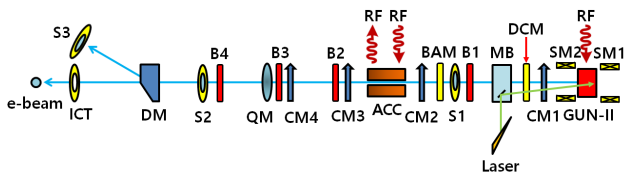


Figure 2: Schematic diagram of the ITF beam-line. Letter abbreviations in the figure are as follows: ACC for accelerating column, SM for solenoid magnet, CM for corrector magnet, DM for dipole magnet, QM for quadrupole magnet, BCM for beam current monitor, MB for laser mirror box, S for screen Monitor, B for beam position monitor, DCM for dark current monitor, BAM for bunch arrival-time monitor.

The main solenoid (SM2 in Fig. 2) and the bucking solenoid (SM1 in Fig. 2) was installed before and after GUN-II to focus the generated electron beams. Downstream of the main solenoid, the dark current monitor (DCM) was installed to measure the dark current. Downstream of the DCM, the laser mirror box for GUN-I (not GUN-II) which permits an UV laser beam to strike the gun cathode was installed. Now we do not have a laser mirror box for GUN-II. If we want laser cleaning and emittance optimization, we need a laser mirror box for GUN-II. The electron beam is accelerated by the new 3-meter dual-feed racetrack-type S-band

* npwinner@postech.ac.kr

Content from this work may be used under the terms of the CC BY 3.0 licence (© 2019). Any distribution of this work must maintain attribution to the author(s), title of the work, publisher, and DOI

ISBN: 978-3-95450-210-3 doi:10.18429/JACoW-FEL2019-WEP067

Content from this work may be used under the terms of the CC BY 3.0 licence (© 2019). Any distribution of this work must maintain attribution to the author(s), title of the work, publisher, and DOI

DEVELOPMENT AND COMMISSIONING OF A FLIP COIL SYSTEM FOR MEASURING FIELD INTEGRALS*

J. E. Baader†, University of Campinas, Campinas, Brazil

Abstract

Many techniques for measuring magnetic fields are available for accelerator magnets. In general, methods based upon moving wires are suitable for characterizing field harmonics, and first and second field integrals. The flip coil moving wire technique stands out due to simplicity, speed, precision, and accuracy. We aimed to develop a reliable, fast and precise flip coil system capable of characterizing field integrals in the two transverse axes. The coil was a single turn loop made of insulated beryllium copper wire. The width of the loop was 5 mm. The approach of measuring second field integrals by changing the coil's width at one of the ends was analyzed and included in the system. High-performance motorized stages performed angular and transverse positioning of the coil, while manual stages were used to stretch the wire, execute fine adjustments in its transverse position, and change coil's geometry. Initial tests with the Earth's field and also with a reference magnet of 126 Gauss-centimeter (G cm) demonstrated that the system achieves repeatability of 0.2 G cm for a 60-cm long coil. This work was carried out for the LCLS-II project at SLAC.

INTRODUCTION AND FLIP COIL SYSTEM OVERVIEW

Various methods are available for the measurement of the magnetic field. The choice of a method depends on many requirements, such as precision, accuracy, speed, geometric constraints, field measurements range, etc [1]. A complete magnetic measurements laboratory would have most of the main available techniques, given that each method offers distinct advantages and the ability to cross-check the results.

The available techniques for characterizing magnetic field at the SLAC Magnetic Measurement Facility (MMF) includes a rotating coil for measuring magnetic center in quadrupoles, a vibrating wire used to fiducialize the quadrupoles, a moving wire for measuring field integrals and Hall probes used to map magnetic fields [2–6]. This paper describes the development of a new flip coil moving wire system to measure field integrals at the SLAC MMF for the LCLS-II project.

In the flip coil technique a long coil is rotated within the magnet by 180° during the measurement, and the induced voltage V is recorded. The flux change $\Delta\phi$ during the measurement is equal to twice the flux ϕ_0 linked with the coil in the initial angular position θ_0, so $\int V dt = -2N\phi_0$ (N is the number of turns). If the loop of the coil forms two parallel wires with a small distance of W along the magnet's length, $\phi_0 = WI_1$, where I_1 is the first field integral of the field component perpendicular to the plane θ_0 constant. Therefore, $|I_1| = \int V dt/(2NW)$. If the coil's width is set to zero at one of the ends, it is possible to proof that $\phi_0 = WI_2/L$, where L is the coil's length and I_2 is the second field integral of the field component perpendicular to the plane θ_0 constant. Therefore, $|I_2| = L\int V dt/(2NW)$. For both cases, we assume that the field does not depend on the radial axis of the coil.

* This study was financed in part by the Coordenação de Aperfeiçoamento de Pessoal de NÍvel Superior - Brasil (CAPES) - Finance Code 001. This work was also supported by FAEPEX-UNICAMP and by DOE contract DE-AC02-76SF00515 in support of the LCLS-II project at SLAC.

† jebaader@gmail.com

SYSTEM DEVELOPMENT

Mechanical Design and Motion

The flip coil is mounted in two towers, each composed of two motorized Newport stages model MTMPP.1 with 250 mm of travel attached at right angles for y (vertical) and x (horizontal) movements. Each tower has one motorized Newport rotation stage model RGV100BL that holds two manual Edmund linear stages with 13 mm of travel for fine adjustments in x-axis and y-axis. All motorized stages are controlled by the Newport Motion Control XPS-Q8. Each end has also one linear stage that moves towards z-axis and is used to stretch the coil. Figure 1 shows the system. A zoomed picture of each end of the system (called End A and End B in Fig. 1) is presented in Fig. 2.

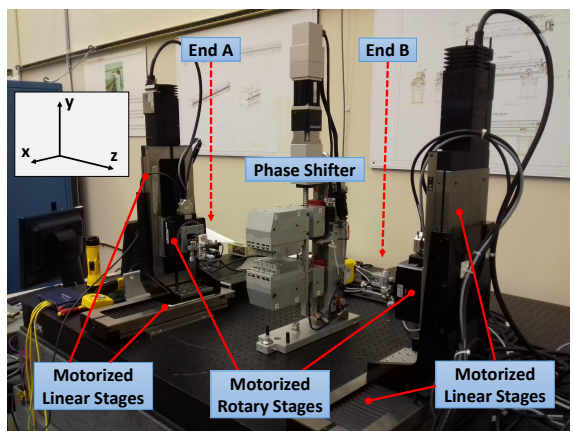


Figure 1: Flip coil system set up at the SLAC MMF.

The coil is a single turn of a 100 µm diameter insulated beryllium copper wire looped between two spools placed on each end, which forms one continuous loop of 5 mm of width (the minimum LCLS-II undulators' gap is 7.2 mm). The coil's length is approximately 60 cm. The End A has one manual Edmund rotary stage with 30 mm of diameter that allows changing the coil's width to measure second field integrals (see details 7 and 8 in Fig. 2). A low noise

ISBN: 978-3-95450-210-3 doi:10.18429/JACoW-FEL2019-WEP070

INFLUENCE OF RADIATION EXPOSURE ON THE FEL PERFORMANCE AT FLASH

B. Faatz*, M. Tischer, P. Vagin, DESY, Hamburg, Germany

Abstract

FLASH has been operated as user facility for about 14 years. In this time, the total charge accelerated and transported through the FLASH1 undulator is around 35 Coulomb. Based on detailed monitoring of the radiation loss and reference measurements on degradation of the magnetic field of the undulator, we have performed simulations to study the change in FEL performance and compare the simulations with the changes we observe during operation.

INTRODUCTION

FLASH is the first FEL user facility in the XUV and has been running since 2005 [1]. Continuous upgrades have increased the beam energy from initially about 700 MeV to the present 1.25 GeV, resulting in a wavelength from 13 nm in 2005 to the present 4.2 nm. It is also the only XUV-FEL based on superconducting technology, which produces up to 5000 bunches per second as compared to the typical 50 to 100 for normal conducting machines [2]. And finally, since 4 years FLASH runs two FELs simultaneously from the same accelerator, thus increasing the available beamtime for users [3].

In the foreseeable future, several new facilities will be built with the same superconducting technology, but in this case running in CW mode [4, 5]. Where beam loss in the undulator plays only a minor role for most facilities, for a facility like FLASH or the European XFEL [6], this has resulted in more elaborate systems to detect beam loss and in interlock and machine safety systems that switch off the beam as fast as possible to avoid deterioration of the undulator magnetic field due to radiation damage.

Even after running for 14 years, the accumulated charge produced by FLASH is around 35 C. Had FLASH been running continuously at the highest repetition rate at around 0.3 nC bunch charge, the accumulated charge would have been around 660 C. However, since experiments want different properties and bunch spacing, the machine has been occasionally running 100 kHz or even single bunch and regularly at much lower charge to produce ultra-short pulses with single spikes [7]. Machines running in CW mode at 1 MHz with a charge of 100 pC will produce a similar charge within weeks.

In order to be prepared for this increase in charge and possible damage to the undulators, we have studied the effect of radiation loss on the undulator over the past years [8] and have also gained experience in the magnetic behaviour of radiation-damaged undulators [9, 10]. For this purpose, a one-period, sacrificial undulator is installed in front of the FLASH main undulators. This device is periodically removed from the beamline and the field re-measured on a magnetic bench. At the same time, both in this undulator and in the main undulator, TLDs are regularly exchanged and the accumulated dose is evaluated. This way, a correlation between integrated dose and magnetic field is determined.

In this paper, we will show the dose which has been accumulated over the years in FLASH1.

ACCUMULATED DOSE IN THE FLASH1 UNDULATOR

A dose is accumulated inside the undulator because of Continuous loss of dark current, continuous loss of beam or because of single events due to operation errors.

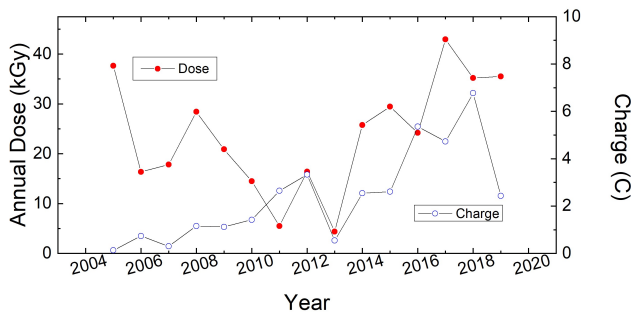


Figure 1: Accumulated annual dose in the sacrificial undulator at two locations since the commissioning of FLASH in 2005 (left scale). Also shown is the charge transmitted through the undulator during the same period (right scale).

As was mentioned, in front of the main undulator a one-period sacrificial undulator is installed. This undulator at FLASH1 has accumulated over the years the largest dose, namely around 350 kGy. As can be seen in Fig. 1, the initial losses are, normalized to the charge, much higher during the first few years. In recent years, the dose is similar to the one in the early years. The transmitted charge has grown by at least an order of magnitude because more users request longer bunch trains. Nevertheless, the increased loss in 2017 can also be observed in the main undulator, as we will see. For 2019, the charge has gone down significantly, but the losses have not. This has not been understood yet.

Losses during the first year of operation (2005) have been exceptionally high. As can be seen in Fig. 2 (top), the loss during the first year has been about half of the total loss, assuming we exclude specific events, that will be discussed below. It becomes even more clear when the data are normalized to the charge, shown in Fig. 2 (bottom). Normalized to the charge the loss in 2005 is up to an order of magnitude more than all of the following years.

Losses during 2006 occurred at the end of the undulator, as can be seen in Fig. 3. The reason was that the beam

* bart.faatz@desy.de

Content from this work may be used under the terms of the CC BY 3.0 licence (© 2019). Any distribution of this work must maintain attribution to the author(s), title of the work, publisher, and DOI

ISBN: 978-3-95450-210-3 doi:10.18429/JACoW-FEL2019-WEP072

EXPECTED RADIATION PROPERTIES OF THE HARMONIC AFTERBURNER AT FLASH2

M. Mehrjoo*, B. Faatz, G. Paraskaki, M. Tischer, P. Vagin, DESY, Hamburg, Germay

Abstract

We discuss the afterburner option to upgrade the FLASH2 undulator line, at the FLASH facility at DESY in the Hamburg area, for delivering short wavelengths down to approximately 1.5 nm with variable polarization. This relatively straightforward upgrade enables us to study scientific cases involving the absorption L-edges of 3d metals. The proposed afterburner setting with an energy upgrade to 1.35 GeV will cover many of the community's requests for the short wavelength radiation and circular polarization. We also study the influence of reverse tapering on the radiation output. This contribution presents a series of simulations for the afterburner scheme and some of the technical choices made for implementation.

INTRODUCTION

FLASH delivers radiation in the fundamental wavelength down to 4 nm with the linear polarization [1]. Typical pulse energies that can be delivered are in the order of 100 µJ, depending on the exact parameters required. Many users, however, are interested in much shorter wavelength, and with variable polarization. A typical example are those users aiming at the L-edges of 3d metal metals between 1.3 and 1.6 nm. This clearly beyond the 1st harmonic wavelength range of FLASH. However, because many of these experiments do not require much pulse energy, in many cases less than a microjoule, one could offer to produce this in a harmonic at FLASH. Because the FEL produces bunching at all harmonics, one could use either 2nd or 3rd harmonic radiation. Since the 2nd harmonic is still not in the desired wavelength range, only 3rd and higher harmonics can be used. As the main undulator only delivers linearly polarized light, an afterburner with circular polarization tuned to the 3rd harmonic of the main undulator will be placed behind it.

In the afterburner, the produced circularly polarized radiation is superimposed to the linearly polarized radiation of the main undulator. Because the bunching in the afterburner does not change significantly, the pulse energy of the linear and circular contributions will be of similar magnitude. Because this is not desirable, one can either place the afterburner under an angle, thus separating linear from circular light [2], or use reverse tapering to suppress the radiation from the main undulator while keeping the bunching [3].

In this contribution, we will show results of simulations with the code GENESIS 1.3, version2 [4]. We will study at different beam parameters the wavelength range between 1.3 and 1.6 nm and check the influence of the reverse taper on pulse energy and contrast, defined as the ration between circular radiation from the afterburner and the linearly polarized light from the main undulator [5].

SIMULATION OF STANDARD CONFIGURATION

The parameters chosen for the simulations are listed in Table 1. It assumes the energy upgrade from the present 1.25 GeV to 1.35 GeV planned in the next years and an additional bunch compressor at final energy, which should enable us to improve the electron beam quality significantly [6]. Therefore, simulations are performed for both a pessimistic set of beam parameters and the expected beam quality after the upgrade.

Table 1: FLASH2 Parameters Used for the Simulations

Electron beam	
Beam energy	1.35 GeV
Peak current	2.5 kA
Emittance, norm. (x,y)	0.7–1.4 mm mrad
Energy spread	0.2–0.5 MeV
Bunch length	15 µm
Main Undulator	**planar**
Period	31.4 mm
K_{rms}	0.87–1.05
Segment length	2.5 m
Number of segments	12
Afterburner	**APPLE III, circ.**
Period	16 mm
K	0.385–0.61
Segment length	2.5 m
Number of segments	1

The main undulator is the one already installed in FLASH2. For the afterburner undulator, we consider an APPLE III device with a K-value that has been obtained from Radia-simulations for the helical mode (see Table 1 and Fig. 1). The minimum undulator gap for the afterburner is 8 mm. This gives us the required tunability from about 1.3 to 1.6 nm as maximum wavelength, where for 1.3 nm, we still have $K = 0.38$.

The first set of simulation has been performed with all 12 undulators set to the same gap and the APPLE undulator to a gap corresponding to the third harmonic. The wavelength in the afterburner undulator is 1.3, 1.45 and 1.6 nm. As can be seen from Fig. 2, the pulse energy that we get from the APPLE undulator increases with increasing K of the undulator, as expected. Furthermore, the dependence on the beam quality is not dramatic, as the pulse energy varies

* masoud.mehrjoo@desy.de

Content from this work may be used under the terms of the CC BY 3.0 licence (© 2019). Any distribution of this work must maintain attribution to the author(s), title of the work, publisher, and DOI

ISBN: 978-3-95450-210-3 doi:10.18429/JACoW-FEL2019-WEP073

EXPERIENCE WITH MCP-BASED PHOTON DETECTOR AT FLASH2

S. Grunewald, E. Mueller, E. A. Schneidmiller, K. Tiedtke, M. V. Yurkov, DESY, Hamburg, Germany
O. I. Brovko, A. Grebentsov, E. M. Syresin, JNR, Dubna, Russia

Abstract

We present recent experimental results on statistical measurements of amplification process in FLASH2 SASE FEL. Micro-channel plate (MCP) detector is used for precise measurements of the radiation pulse energy. DAQ based software is used for cross-correlation of the SASE FEL performance and electron beam jitters. Analysis of machine jitters essential for SASE FEL operation has been performed. Application of gating strategy with measured machine parameters allows us to isolate machine jitters from fundamental SASE fluctuations. Subsequent application of statistical techniques for characterization of SASE FEL radiation allows to derive such important quantities as gain length, saturation length, radiation pulse duration, coherence time, and degree of transverse coherence.

INTRODUCTION

VUV and soft x-ray free electron laser FLASH is in operation at DESY since the year 2000 [1–3]. Several upgrades of the facility have been performed, and currently FLASH covers a wavelength range from 3.5 nm to 100 nm in the fundamental. Two beamlines operate in parallel, FLASH1 with fixed gap undulator (period length λ_w = 2.73 cm), and FLASH2 with variable gap undulator (period length λ_w = 3.14 cm). FLASH is equipped with a set of detectors for measurements of the energy in the radiation pulse: gas monitor detectors (GMD), micro channel plate (MCP) based detectors, photodiodes, and thermopiles [4, 5]. MCP detectors are installed in front of all other detectors and are used for precise measurements of the radiation pulse energy of single pulses. The MCP detector measures the radiation scattered by a metallic mesh placed behind an aperture. The electronics of MCP-detector has low noise, about 1 mV at the level of signal of 100 mV which provides a 1% relative accuracy of the radiation pulse energy measurement.

Measurements have been performed in the framework of the experimental program at FLASH2 aiming at development of statistical techniques for characterization of SASE FEL process. In February, 2019 we recorded status of FLASH2 operation corresponding to typical conditions of user run during last months. One of the features during user run was sporadic appearance of machine jitters affecting stability of the SASE FEL output. There were several goals of our studies. Main goal was to include MCP detector into the DAQ system recording essential machine parameters. The next step was to measure FEL gain curve and derive essential parameters of the radiation from these measurements . Final step was to analyze correlation data of SASE output and essential parameters of the electron beam (jitters of orbit and beam formation system) and localize origin of the jitters. It turned out that frequency of sporadic machine jitters during our shift was pretty big, which moved the last planned goal (jitter correlation studies) to the first priority.

Analysis of experimental results shows that the main jitter problem is sporadic orbit jitter which develops from the very beginning of the accelerator. An important feature of this jitter are correlated x-y orbit kicks. Bunch compression system also contributes to the SASE FEL output, but at a smaller level. We also applied gating strategy for cleaning experimental results with subsequent application of statistical techniques for determination of essential parameters of the SASE FEL: gain length, saturation length, coherence time, radiation pulse duration, number of radiation modes in the pulse (longitudinal and transverse), degree of transverse coherence [6–8].

RAW DATA AND MACHINE JITTERS

Measurement of the radiation pulse energy (average and dispersion) provides reliable way for determination of key parameters of the SASE FEL process. In practical situation there are always machine jitters (orbit, beam formation system, sporadic failures of subsystems, etc) which contribute additionally to fluctuations of the SASE FEL output, so relevant technique for gating of the experimental results with measured parameters of the machine has been developed [2, 6–8]. FLASH is modern facility with global computer control of machine operation, electron and photon

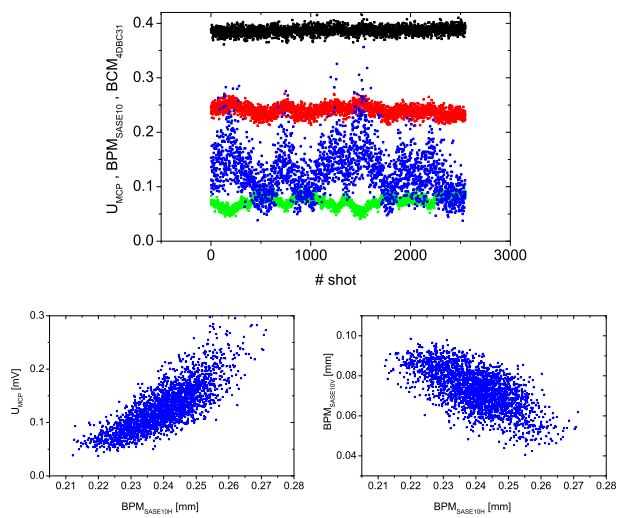


Figure 1: Top: raw signal of MCP detector (blue), BPM 3FL2SASE10 (x - red, y - green), and BCM 4DBC31 (black). Bottom: correlation plots of MCP signal versus BPM 3FL2SASE10H (left), and x and y positions of BPM 3FL2SASE10 (right). Measurements are performed after 7 undulator modules. Radiation wavelength is 10 nm.

Content from this work may be used under the terms of the CC BY 3.0 licence (© 2019). Any distribution of this work must maintain attribution to the author(s), title of the work, publisher, and DOI

ISBN: 978-3-95450-210-3 doi:10.18429/JACoW-FEL2019-WEP076

A SUPERCONDUCTING UNDULATOR WITH VARIABLE POLARIZATION DIRECTION FOR THE EUROPEAN FEL

Y. Li, European XFEL GmbH, Schenefeld, Germany
R. Rossmanith, DESY, Hamburg, Germany

Abstract

In the SASE3 beam line at the European XFEL a planar undulator produces linearly polarized radiation. In order to obtain a circularly polarized radiation an afterburner will be installed to produce coherent radiation with variable polarization. Recently Argonne National Lab developed a super conductive undulator (called SCAPE) for a storage ring which allows to change polarization direction and field strength without moving mechanically the undulator parts. In this paper it is investigated if a similar device could be useful for an FEL. Such device is also a possible choice for the future undulator beam lines where circular and variable polarization are required.

INTRODUCTION

The magnetic field for undulators is in general produced by permanent magnets at room temperature. During the last years experiments were performed to increase the magnetic field either by cooling the permanent magnets to cryogenic temperatures [1] or by replacing the permanent magnets by superconducting wires.

The magnetic field of cryogenically cooled permanent magnets (CPMUs: cryogenic permanent magnet undulator) is in general higher by only about 15 % but the magnets are less sensitive to radiation. The disadvantage is that the frequency and the polarization of the emitted radiation have to be changed by moving mechanically the undulators gap.

Undulators with superconducting wires (SCU) can produce up to a factor of two higher undulator fields compared with cryogenic undulators and are also almost insensitive to radiation. The SCU technology has in addition the advantage that it is possible to tune the output frequency and the polarization direction electrically without mechanically moving the magnet coils. The disadvantage is that liquid Helium is needed to cool the coils. This problem was recently reduced by using cryocooler. The cryocooler, mechanically attached to the undulator, has a closed helium system. Undulator and cooler together comprise a standalone unit and require therefore not a conventional cryoplant. The cooling time for such a system is about 70 hours. APS and KIT both used such undulators successfully. The advantage is the tunability of the frequency of the produced radiation.

Recently a NbTi undulator was proposed by the Argonne group (SCAPE: Super Conducting Arbitrary Polarization Emitter) [2] was proposed to build an undulator with electrically adjustable photon wavelength and polarization.

The winding technics with NbTi superconducting wires lead to low phase errors (less than 3 degree) and therefore shimming is not required. NbTi wires are at the moment the used for SCUs. Nb_3Sn wires can produce in general higher fields but are at the moment still difficult to handle. The use of high temperature superconductors are investigated at various institutes.

In this paper first ideas on a program on the development and tests SCUs with the parameters for the European XFEL are presented.

PLANAR SCU

A SCU with the period of 18mm can serve for an ultra-high photon energy SASE beam line up to 100keV at the European XFEL. It also applies the factor of 1.5 to the tenability of the photon energy [3]. Therefore in this section we focus on the field simulations for an 18mm period planar SCU, U18.

Both of the successful examples of planar SCU from APS and KIT take use of so called the vertical winding technique for the magnet coils. It is winding the superconducting coil continuously on a block of iron core with grooves. In this paper we follow it for the undulator design and simulations.

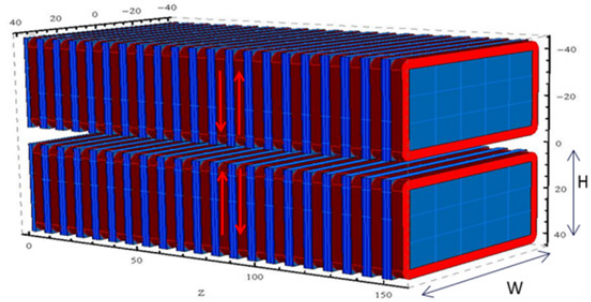


Figure 1: The radia model for the planar SCU.

Figure 1 shows the Radia [4] model for the planar SCU U18. The red coil indicates the NbTi wire and the blue part is the iron core for the wire winding and poles assembling. The arrows indicate the current direction. The wire material is supposed to be NbTi and the iron core is supposed to be normal low carbon steel.

In order to simulate the maximum undulator field it is firstly needed to evaluate the critical current density. It is well known that the superconducting condition is maintained by the nonlinear relations of the temperature, the magnetic field and the current density. We assume the undulator wire is constant in the temperature of the liquid helium which is 4.2K. Following the suggestion of Ref. [5] the critical current density is assumed linearly relates to the magnet field:

$$j_c = j_a\left(1 - \frac{B_m}{B_{c2}}\right), \quad (1)$$

Content from this work may be used under the terms of the CC BY 3.0 licence (© 2019). Any distribution of this work must maintain attribution to the author(s), title of the work, publisher, and DOI

ISBN: 978-3-95450-210-3 doi:10.18429/JACoW-FEL2019-WEP079

EFFECT OF HEAT LOAD ON CRYO-COOLED MONOCHROMATORS AT THE EUROPEAN X-RAY FREE-ELECTRON LASER: SIMULATIONS AND FIRST EXPERIMENTAL OBSERVATIONS

I. Petrov†, U. Boesenberg, M. Dommach, J. Eidam, J. Hallmann, K. Kazarian, C. Kim, W. Lu, A. Madsen, J. Moeller, M. Reiser, L. Samoylova, M. Scholz, R. Shayduk, H. Sinn, V. Sleziona, A. Zozulya, European XFEL GmbH, Schenefeld, Germany
X. Dong[1], Shanghai Institute of Applied Physics, Shanghai, China
J. Anton, S. Kearney, D. Shu, ANL, Argonne, Illinois, United States
[1]also at Shanghai Advanced Research Institute, Shanghai, China

Abstract

Due to the high intensity of photon pulses generated at the European X-ray Free-Electron Laser facility, the heat load on silicon crystal monochromators becomes an issue. Here, first experimental data of heat load effects on the performance of a cryogenically cooled monochromator are presented. The measurements are compared with a model of X-ray diffraction taking beam absorption and heat deformation into account.

INTRODUCTION

A number of experimental techniques at hard XFELs require monochromators. Such devices reduce the spectral bandwidth, thus improving the temporal coherence of photon pulses. For instance, X-ray Photon Correlation Spectroscopy (XPCS) in wide-angle scattering benefits from increased speckle contrast enabled by a larger coherence time [1,2]. At European X-ray Free-Electron Laser (EuXFEL), several mJ of pulse energy can be reached in every femtosecond-long X-ray pulse. These pulses are arranged into trains containing from one to several hundreds of pulses. Within a train the pulses arrive at MHz repetition rate and ten trains are delivered per second. Currently, the facility operates at 1.1 MHz repetition rate. The planned 4.5 MHz repetition rate has recently been achieved [3]. Such intense radiation renders stable monochromator operation a challenge. Due to absorption and energy deposition in the crystals, the crystal lattice is deformed, which in turn affects the diffraction of X-rays. Here, we experimentally study the performance of cryogenically cooled Si(111) monochromator [4] for various numbers of pulses per train using first experimental data obtained at the Materials Imaging and Dynamics (MID) instrument of EuXFEL. Theoretical simulation results are also shown to estimate the heat load effect on XFEL pulse diffraction in crystals.

ROCKING CURVE MEASUREMENTS

Due to the stochastic nature of Self-Amplified Spontaneous Emission (SASE), the energy spectrum and temporal structure of XFEL pulses are irregular [5]. For example, a characteristic ~40 eV width of the energy spectrum results in ~0.2 fs coherence time.

† ilia.petrov@xfel.eu

At the MID instrument of EuXFEL a two-bounce artificial channel cut Si(111) monochromator in vertical scattering geometry has recently been commissioned and is available for user experiments in the range from about 6 to 18 keV. After two consecutive reflections, the spectral bandwidth is reduced from ~$5{\cdot}10^{-3}$ to ~10^{-4}, which significantly increases the temporal coherence of pulses. The optical layout of the MID beamline (Fig. 1) includes offset mirrors, Si(111) and Si(220) monochromators and split-and-delay line (SDL) optics. For instance, the SDL (currently under production) will be used for the generation of pulses with the variable delay time. For the measurements presented in this paper, the Si(111) monochromator has been used.

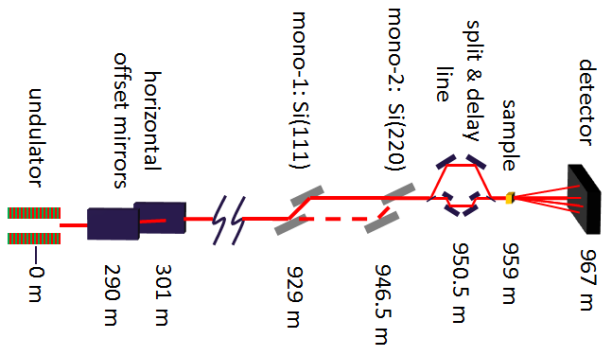


Figure 1: Sketch of MID beamline optical components. Relative positions of each component are shown under elements.

In order to analyse diffraction properties of the monochromator crystals, rocking curves have been measured for various numbers of pulses in the train, while the monochromator crystals have been cryo-cooled to 100 K. The energy of the hard X-rays in a pulse was ~0.25 mJ; the photon energy was 9 keV, the repetition rate 1 MHz, the beam size ~0.5 mm. The bunch charge was 250 pC, the electron energy 14 GeV. Rocking curve measurements were done with the pitch scan of the second crystal of the monochromator.

Content from this work may be used under the terms of the CC BY 3.0 licence (© 2019). Any distribution of this work must maintain attribution to the author(s), title of the work, publisher, and DOI

ISBN: 978-3-95450-210-3 doi:10.18429/JACoW-FEL2019-WEP080

Content from this work may be used under the terms of the CC BY 3.0 licence (© 2019). Any distribution of this work must maintain attribution to the author(s), title of the work, publisher, and DOI

ROSA: RECONSTRUCTION OF SPECTROGRAM AUTOCORRELATION FOR SELF-AMPLIFIED SPONTANEOUS EMISSION FREE-ELECTRON LASERS

Svitozar Serkez*, Natalia Gerasimova, Gianluca Geloni, European XFEL, Schenefeld, Germany
Bohdana Sobko, Lviv National University, Lviv, Ukraine
Oleg Gorobtsov†, DESY, Hamburg, Germany

Abstract

X-ray Free Electron Lasers (FELs) have opened new avenues in photon science, providing coherent x-ray radiation pulses orders of magnitude brighter and shorter than previously possible. The emerging concept of "beam by design" in FEL accelerator physics aims for accurate manipulation of the electron beam to tailor spectral and temporal properties of radiation for specific experimental purposes, such as x-ray pump/x-ray probe and multiple wavelength experiments. A cost-efficient method to extract information on longitudinal Wigner distribution function of emitted FEL pulses is proposed. It requires only an ensemble of measured FEL spectra.

INTRODUCTION

There has been a rapid growth both in the number of scientific users and in the diversity of new science enabled by Free-Electron laser sources. This growth is possible due to the continuously improving capabilities of FEL facilities. One promising avenue which opens the way to new experiments is is the tuning of spectral and temporal properties of radiation for specific experimental purposes, e.g., generating wide bandwidth [1–3], narrow-bandwidth [4] or extremely short [5, 6] radiation pulses. Some information about duration of the typical radiation pulse, hence the length of an electron beam lasing window, can be extracted from radiation spectra of FEL operating in Self-Amplified Spontaneous Emission (SASE) mode. Taking advantage of the radiation statistical properties [7] and assuming a particular temporal profile, spectral correlation analysis gives an estimate of the average duration of the SASE FEL pulse [8, 9]. The close relation between electron phase space and radiation characteristics must be taken into account while trying to performing radiation pulse diagnostics. For example, a chirp in the electron beam energy yields a chirp in radiation frequency [10], it affects the range of spectral coherence [11], and hence the spectrum-based estimation of the SASE pulse duration. We present a fast and efficient method to provide feedback on the temporal and spectral properties of FEL radiation: measurement of the autocorrelation of an ensemble-averaged pulse Wigner distribution. We study an ensemble-averaged Wigner distribution of SASE FEL pulses and its temporal autocorrelation. We discuss how to calculate it based on measured SASE spectra and what information such reconstruction reveals. We also present results of numerical simulations performed with the code GENESIS [12] and compare calculated Wigner distribution with evaluated reconstructions. It relies entirely on spectrometry of the generated pulses and does not require additional equipment.

THEORY

Consider a scalar field $E(t)$ in the time domain and slowly varying field amplitude $\widetilde{E}(\omega) = \bar{E}(\omega)\exp(-i\omega_c z/c)$ of its Fourier transform $\bar{E}(\omega)$, where ω_c is a carrier frequency and z is the direction of propagation.

Measurable single-shot radiation spectra are proportional to the square-modulus of the single-shot scalar field[1]

$$\widetilde{I}(\omega) \equiv \widetilde{E}(\omega)\widetilde{E}^*(\omega)\,. \tag{1}$$

The statistical autocorrelation function of the field $E(t)$ in the time and frequency domains can then be defined as

$$\begin{aligned}\Gamma(t,\Delta t) &= \left\langle E\left(t-\frac{\Delta t}{2}\right)E^*\left(t+\frac{\Delta t}{2}\right)\right\rangle,\\ \widetilde{\Gamma}(\omega,\Delta\omega) &= \left\langle \widetilde{E}\left(\omega-\frac{\Delta\omega}{2}\right)\widetilde{E}^*\left(\omega+\frac{\Delta\omega}{2}\right)\right\rangle,\end{aligned} \tag{2}$$

where angle brackets $\langle\rangle$ denote ensemble average. Note that the autocorrelation function depends on both time t and time separation Δt, allowing to describe non-stationary radiation fields. The intensity autocorrelation function is, instead

$$\begin{aligned}\Gamma_I(t,\Delta t) &= \left\langle I\left(t-\frac{\Delta t}{2}\right)I\left(t+\frac{\Delta t}{2}\right)\right\rangle,\\ \widetilde{\Gamma}_I(\omega,\Delta\omega) &= \left\langle \widetilde{I}\left(\omega-\frac{\Delta\omega}{2}\right)\widetilde{I}\left(\omega+\frac{\Delta\omega}{2}\right)\right\rangle.\end{aligned} \tag{3}$$

The Wigner distribution

$$\begin{aligned}\mathcal{W}(t,\omega) &= \frac{1}{2\pi}\int_{-\infty}^{\infty} d(\Delta t)\Gamma(t,\Delta t)\exp(i\omega\Delta t)\\ &= \int_{-\infty}^{\infty} d(\Delta\omega)\widetilde{\Gamma}(\omega,\Delta\omega)\exp(-i\Delta\omega t)\end{aligned} \tag{4}$$

is commonly used to describe properties of FEL radiation [13–17].

Spectrogram of a signal is a two-dimensional convolution of Wigner distribution of that signal with Wigner distribution of the spectrogram window function:

* svitozar.serkez@xfel.eu
† current address: Cornell University, Ithaca, New York, USA

[1] considering cross section perpendicular to the direction of propagation

ISBN: 978-3-95450-210-3 doi:10.18429/JACoW-FEL2019-WEP081

Content from this work may be used under the terms of the CC BY 3.0 licence (© 2019). Any distribution of this work must maintain attribution to the author(s), title of the work, publisher, and DOI

DESIGN AND DEVELOPMENT OF HIGH-SPEED DATA ACQUISITION SYSTEM AND ONLINE DATA PROCESSING WITH A HETEROGENEOUS FPGA/GPU ARCHITECTURE

M. Bawatna†, J. Deinert, O. Knodel, S. Kovalev
Helmholtz-Zentrum Dresden-Rossendorf (HZDR), Dresden, Germany
R. Spallek, Institut für Technische Informatik, Technische Universität, Dresden, Germany.

Abstract

The superradiant THz sources at TELBE facility is based on the new class of accelerator-driven terahertz (THz) radiation sources that provide high repetition rates up to 13 MHz, and flexibility of tuning the THz pulse form. The THz pulses are used for the excitation of materials of interest, about two orders of magnitude higher than state-of-the-art tabletop sources. Time-resolved experiments can be performed with a time resolution down to 30 femtoseconds (fs) using the novel pulse-resolved Data Acquisition (DAQ) system. However, the increasing demands in improving the flexibility, data throughput, and speed of the DAQ systems motivate the integration of reconfigurable processing units close to the new detectors to accelerate the processing of tens of GigaBytes of data per second. In this paper, we introduce our online ultrafast DAQ system that uses a GPU platform for real-time image processing, and a custom high-performance FPGA board for interfacing the image sensors and provide a continuous data transfer.

INTRODUCTION

TELBE THz facility is performing ultra-fast pump-probe experiments by providing a unique combination of high pulse energies and high repetition rates. In this type of experiment, the electric or magnetic field in the THz pump pulse acts as the excitation of dynamics in the matter. This dynamic in turn is then probed by ultra-short (light) pulses, typically with the sub THz cycle resolution as in [1]. A pulse resolved DAQ system has been developed at TELBE user facility as in [1] to allow the performance of time-resolved THz spectroscopy measurements with sub 30 fs Full-Width Half Maximum (FHWM) time resolution with excellent dynamic range up to 120 dB as in [2]. However, the high-speed commercial cameras used at TELBE user facility have several drawbacks in terms of data transfer, recording time, and data processing. Currently, most of the operating time is spent on the data transfer, rather than the data acquisition. Images are stored in the camera's internal buffer before being sent further. New data acquisition is only possible when all data is transferred. Therefore the commercial cameras are usually not able to provide online data processing.

The dominant technology used in the visible light detectors is the Charge Coupled Device (CCD) as in [3] due to its sensitivity and low noise performance. However, the high frame rate of the current imaging detectors is limited by the pixel access time. Therefore, commercially available imaging detectors decrease the number of pixels while increasing the frame rate.

Another drawback is that the firmware that interfaces the visible light detectors is not available to the developers, with a few parameters available for optimization. Therefore optimization of the camera's functionality to the application requirements is not possible.

Recently, there is an increased performance in large-scale real-time data processing using massively parallel architectures such as Graphics Processing Units (GPU) and Field Programmable Gate Arrays (FPGAs).

Accelerating the image processing using FPGAs or GPUs is not a new concept. Although GPUs can provide better performance than the FPGAs for applications where the data processing can be implemented with no inter-dependency in the data flow, the FPGAs are more suitable for applications that require many control operations and parallel processing. FPGAs not only provides flexibility in developing the desired algorithms, but also the ability for parallel data processing.

In this paper, we will present an online DAQ system for applications capable of providing both high data throughput and real-time data processing.

The paper is organized as follows: the first section introduces the requirements for the pulse-resolved DAQ system at TELBE. The second section presents the online pulse-resolved DAQ system, the implemented signal processing techniques, and the implemented firmware. The third section presents the arrival time information measurements. After summarizing the results, foreseeable future development and upgrades are discussed.

REQUIREMENTS FOR THE PULSE RESOLVED DAQ SYSTEM AT TELBE

Femtosecond level diagnostic and control of sub-picosecond electron bunches is an essential topic in modern accelerator research. At the ELBE user facility, there are two available electron injectors in use [4] as in Fig. 1. The thermionic injector, which supports repetition rates up to 13 MHz and bunch charges up to 100 pC, and the Super Radio Frequency (SRF) photo-cathode injector, which is used for experiments that may require lower emittance or higher bunch charges of up to 1 nC as in [4]. Moreover, the SRF injector at ELBE also has a maximum repetition rate of 13 MHz with different macro pulse modes of operation.

† m.bawatna@hzdr.de

ISBN: 978-3-95450-210-3 doi:10.18429/JACoW-FEL2019-WEP085

FIELD INTEGRAL MEASUREMENTS OF DAVV UNDULATORS AND FUTURE MEASUREMENT PLAN

M. Gehlot, S. M. Khan, G. Mishra, R. Khullar
IddA Laboratory, Devi Ahilya University, Indore, India
H. Jeevakhan, Department of Applied Science, NITTTR, Bhopal, India
F. Trillaud, Instituto de Ingeniería, National Autonomous University of Mexico, México

Abstract

The Insertion device development and Application (IddA) laboratory of Devi Ahilya University, Indore, India has ongoing activities on undulator design and development[1-3]. In this paper, we analyze the field integral properties of the two DAVV undulator. The first is the IddA U20 prototype NdFeB-cobalt steel hybrid in house designed device of 20 mm period length with twenty five periods. The uniform gap variable hybrid undulator provides magnetic flux density (in rms) from 2400 G to 500 G in the 10 mm-20 mm gap range. The second is the NdFeB based U50II undulator of 50 mm period length with 20 number of periods. Hall probe results are described. A short description of the measurement plan of the undulator on the pulsed wire bench and stretched wire bench is described.

INTRODUCTION

In the case of an undulator, the magnetic flux density.on axis is given by,

$$B_y = \hat{y} B_{peak} \sin(k_u z)$$

Where B_{peak} is the peak magnetic flux density. In case of hybrid undulator, it is given by

$$B_{peak}(T) = a \exp\left[b(g/\lambda_u) + c(g/\lambda_u)^2 \right] \quad (1)$$

where the a, b, c are the empirical coefficients of Eq. (1) and depend on the magnet–pole dimensions, material properties of the NdFeB or $SmCo_5$ magnets and the poles of the undulator. g, λ_u are the undulator gap and period length respectively. In the case of PPM undulator $c = 0, b = \pi$ Eq. (1) describes the field integral as,

$$I_1 = \int B_y dz \quad I_2 = \int (\int B_y dz) dz \quad (2)$$

Eq. (2) when multiplied by $(e/\gamma mc)$ gives the calculated angular deviation and trajectory offset of the electron respectively. A typical requirement for a good quality undulator is that the value of the measured field integral values should be less than the tolerance limit. A standard procedure to determine the field integrals is the Hall probe measurement. In this method, the field is mapped by the Hall probe point by point along the length of the undulator and the field is integrated by a numerical code over the length of the undulator.

HALL PROBE MEASUREMENT

The undulators specifications are described in Table.1 Fitting the Hall probe data for U20 hybrid undulator to Eq.(1) reads the field coefficients reads a =3.06, b = -5.59, c =1.123 (Fig. 1). The uniform gap variable hybrid undulator provides a magnetic flux density (in rms) from 2400 G to 500 G in the 10 mm-20 mm gap range. Fig. 2 describes the Hall probe data for the PPM undulator. A linear fit of the Hall probe data for reads a=1.62 and b=-3.24. The magnetic flux density for U50II undulator with variation in the gap range from 10 mm to 35 mm is 1 T to 0.1612 T. Fig. 3 and Fig. 4 are the Hall probe data field mapping for U20 and U50II undulator for the gap of 10 mm. Fig. 5 represents the magnetic field deviation(rms) for the both the undulators. In the operating gap of 10 to 20 mm, the deviation is in 60-140 G range for U50II undulator and 20-50 G for the U20 udulator.

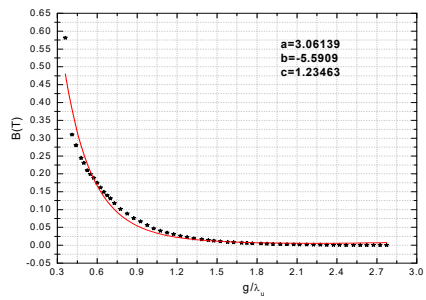


Figure 1: Linear fit to Hall probe data of U20 undulator.

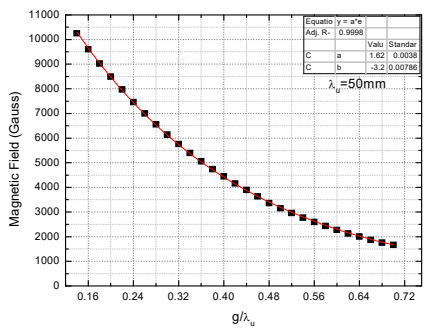


Figure 2: Linear fit to Hall probe data of U50II undulator.

Content from this work may be used under the terms of the CC BY 3.0 licence (© 2019). Any distribution of this work must maintain attribution to the author(s), title of the work, publisher, and DOI

ISBN: 978-3-95450-210-3 doi:10.18429/JACoW-FEL2019-WEP086

CAPABILITIES OF TERAHERTZ SUPER-RADIANCE FROM ELECTRON BUNCHES MOVING IN MICRO-UNDULATORS

N. Balal†, V.L. Bratman[1], Yu. Lurie, and A. Friedman
Ariel University, Ariel, Israel
[1] also at Institute of Applied Physics, Russian Academy of Sciences, Nizhny Novgorod, Russia

Abstract

An available frequency range of powerful coherent radiation from sub-picosecond and picosecond bunches with high charge and comparatively moderate particle energy of 3 - 6 MeV that are formed in laser-driven linacs significantly extends if one uses a micro-undulator. Such an undulator with a helical symmetry and a high transverse field can be implemented by redistributing a strong uniform magnetic field by a helical ferromagnetic or copper insertion. According to simulations and experiments with prototypes, a steel helix with a period of (8-10) mm and an inner diameter of (2-2.5) mm inserted in the 3T-field of a solenoid can provide a helical undulator field with the same periodicity and an amplitude of about of 0.6 T. Using a more complex hybrid system with a permanently magnetized helical structure can increase this value up to 1.1 T. The necessary helices can be manufactured on the machine, assembled from steel wires, formed from powder placed into a hollow helical shell or 3D - printed. Simulations based on the WB3D code demonstrate that using such undulators with the length of (30-40) cm enable single-mode super-radiance from bunches with charge of 1 nC and duration of 2 ps moving in an over-sized waveguide in frequency range of 3-5 THz. The calculated efficiency of such process many times exceeds efficiency that can be obtained with short bunches of the same initial density.

INTRODUCTION

Advanced laser-driven photo-injectors make possible formation of very dense picosecond and sub-picosecond electron bunches with charge of the order of 1 nC and larger at moderate relativistic energy [1–4]. Such bunches can be attractive for simple production of powerful THz electromagnetic pulses using various mechanisms of the so-called coherent spontaneous radiation and super-radiance [5-16]. In particular, it is planned to use a coherent spontaneous Doppler-upshifted undulator radiation of bunches whose longitudinal size or period of preliminary density modulation is smaller than the wavelength of radiation in first experiments at the Israeli THz source [13]. The modulation can also arise self-consistently in extended bunches during their interaction with the radiated electromagnetic pulses in process of super-radiance (see, e.g., [10-12] and literature cited therein).

At the fixed electron energy, the radiation frequency of the Israeli source can be obviously increased by decreasing of the undulator period. Simple and efficient ways for creation of helical undulators with small periods and strong amplitudes of a transverse magnetic field were independently proposed in [15-18] and [19-22]. They present modifications of old ideas and based on redistribution of a uniform magnetic field by ferromagnetic [23-25] or conducting bodies placed inside a solenoid.

When using a small-period undulator for implementation of coherent spontaneous radiation it is necessary to provide a very short initial bunch duration. Because of very strong mutual Coulomb repulsion of the particles in the dense bunch this can be only fulfilled at a very limited length of bunch propagation. Other opportunities are opened when one uses radiation of pre-modulated bunches or super-radiance of extended bunches; in the latter case a self-modulation of density and particle bunching in the field of the radiated wave occur [10-12].

HELICAL MICRO-UNDULATORS BASED ON REDISTRIBUTION OF UNIFORM MAGNETIC FIELD

The undulator field with a small period and a large transverse amplitude can be created by redistributing the strong uniform field on a periodic ferromagnetic insertion [15-18, 20-22]. This method was successfully demonstrated many years ago in planar systems with periodic planar ferromagnetic insertions [23-25]. In papers [20-22] and [15-18], it has been proposed to use a helical insertion for creation of a helical undulator field. Experiments with helixes including ones with small periods (Fig. 1a) have demonstrated a satisfactory coincidence with calculations [17]. A steel helixes with the period of 8-10 mm and inner diameter of 2-2.5 mm placed into a strong uniform field of 3 T can provide a helical undulator field with the amplitude of 0.6 T (Fig. 1). The larger amplitude can be obtained using a hybrid system (Fig. 2). [15] consisting of a steel helix (“bolt”) placed inside a permanently magnetized helical block. To avoid changing the direction and value of the magnetic field of the permanent magnet we performed the calculations for the latter system with a low solenoid field of 1.2 T; the rest parameters (Fig. 1a) are as follows: a=4 mm, R_1=0.75 mm, R_2=4 mm, and d=8 mm. According to simulations this system can provide the helical undulator field with the amplitude of 1.1 T at the axis.

† nezahb@ariel.ac.il

Content from this work may be used under the terms of the CC BY 3.0 licence (© 2019). Any distribution of this work must maintain attribution to the author(s), title of the work, publisher, and DOI

ISBN: 978-3-95450-210-3 doi:10.18429/JACoW-FEL2019-WEP089

PULSE ENERGY MEASUREMENT AT THE SXFEL

Zipeng Liu [1,2],Luyang Yu [1],Chao Feng [1],Haixiao Deng [*1],Bo Liu [*1],Dong Wang [1]
[1]Shanghai Institute of Applied Physics, Chinese Academy of Sciences, ShangHai, China
[2] Chinese Academy of Sciences, Beijing, China

Abstract

The test facility will generate 8.8 nm FEL radiation by using an 840 MeV electron linac passing through the two-stage cascaded HGHG-HGHG or EEHG-HGHG (high-gain harmonic generation, echo-enabled harmonic generation) scheme. Several methods have been developed to measure the power of pulse. The responsivity of silicon photodiode having no loss in the entrance window. Silicon photodiode reach saturates at the SXFEL. In this work, we simulated the attenuator transmittance for different thicknesses. We also show the preparations of the experiment results at the SXFEL.

INTRODUCTION

The Shanghai soft X-ray Free-Electron Laser Facility (SXFEL) is a phased project, including the SXFEL test facility (SXFEL-TF), and the SXFEL user facility (SXFEL-UF). SXFEL-TF is mainly used for the study of the external seeding FEL operation mode, including High-gain Harmonic Generation (HGHG) and Echo-enabled Harmonic Generation (EEHG) schemes. And various cascade combinations of HGHG and EEHG. The upgrading of the test facility to the water window user facility, SXFEL-UF, has been undertaken by the collaboration between the Shanghai Institute of Applied Physics (SINAP) and Shanghai-Tech University. Shanghai-Tech University is in charge of developing science cases and experimental end-stations, and SINAP is responsible for the remaining parts of facility development, including upgrading the linac energy to 1.5 GeV, building a second undulator line, facility integration, and constructing the utility and SXFEL-UF buildings. The civil construction was started in November 2016.

The SXFEL-TF

The SXFEL-TF is composed of an 840 MeV electron linac and a two-stage cascaded seeding scheme-based undulator system. The initial proposal of the SXFEL-TF project in 2016 was to test the cascaded HGHG scheme [1]. In the following years, it was gradually optimized and more contents of the EEHG were added to the project when the construction started in 2014. A new cascaded EEHG-HGHG operation scheme was incorporated into the SXFEL-TF to further improve the ultra-high harmonic up-conversion efficiency.

The main parameters of SXFEL-TF are shown in Table 1. The first stage uses a seeded laser with a wavelength of 265 nm. The first stage output radiation wavelength is about 44nm. An 8.8 nm radiation pulse is generated in the second stage based on the HGHG scheme.

Table 1: The Main Parameters of SXFEL-TF [2]

Undulator	Stage 1	Stage 2
Seed laser wavelength	265 nm	*
FEL output wavelength	44 nm	8.8 nm
Modulator undulator period	80 mm	40 mm
Modulator undulator K value	5.81	2.22
Radiator undulator period	40 mm	22.5 mm
Radiator undulator K value	2.22	1.43

Pin Photodiode

The principle of a silicon diode is similar to that of an ionization chamber, absorption of a photon in a silicon crystal creates separations of charge, which are called electron–hole pairs and require an average energy, ", of 3.66±0.03 eV [3,4] Silicon photodiodes (AXUV series) are being used as absolute devices for 50 eV to 1500 eV photons because of their wellknown device parameters, mainly the Internal Quantum Efficiency (IQE). The IQE is 100% from 270 to 800 nm and higher at shorter wavelengths due to the creation of multiple electron-hole pairs by a single high energy photon [5]. IQE is defined as the percentage of internal charge generated in the diode per incident photon. Figure 1 shows the cross-section of the photodiode investigated. The diode is not suitable for high pulse energy measurement at the SXFEL.

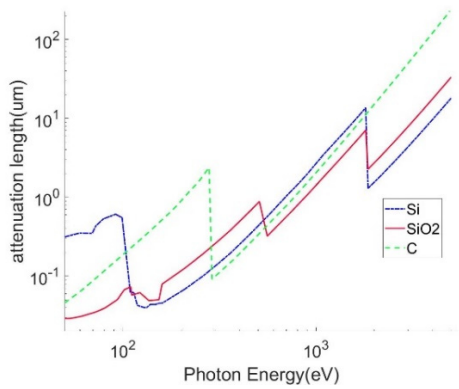


Figure 1: Photodiode absorption attenuation lengths used to calculate soft x-ray responsivity from the model and parameters described in the text. The sources of the data are references [6-8].

Attenuators

A solution to this problem would be to place an absorber in the beam to reduce the flux to a manageable value. Using

Content from this work may be used under the terms of the CC BY 3.0 licence (© 2019). Any distribution of this work must maintain attribution to the author(s), title of the work, publisher, and DOI

ISBN: 978-3-95450-210-3 doi:10.18429/JACoW-FEL2019-WEP092

SPARE UNDULATOR PRODUCTION FOR PAL-XFEL HX1 BEAMLINE

Jang-Hui Han*, Sojeong Lee, Young Gyu Jung, Dong-Eon Kim,
Pohang Accelerator Laboratory, Pohang, Korea

Abstract

In the PAL-XFEL hard X-ray beamline, 20 undulator segments with a 26 mm period and a 5 m length are installed and operated for XFEL user service. One spare undulator was manufactured in December 2018. The magnetic measurements and tuning was carried out recently. We report the magnet block sorting, the magnetic measurements and the tuning results.

INTRODUCTION

Pohang Accelerator Laboratory X-ray Free Electron Laser (PAL-XFEL) is operational for users since 2017 [1, 2]. PAL-XFEL has two undulator beamlines, one hard X-ray and one soft X-ray. The hard X-ray undulator line is placed at the end of the main linac, where an electron beam is accelerated up to 10 Gev. The soft X-ray line is branched at the 3 GeV point of the main linac and further accelerated up to 3.15 GeV.

The hard X-ray beamline has twenty undulator segments. The undulator is a hybrid type with NdFeB magnets and Vanadium Permendur poles. The period is 26 mm and the segment length is 5 m. The magnet gap is 8.3 mm. At the minimum gap, the effective flux density is 0.812 T and the deflecting parameter K is 1.973. The undulators for the soft X-ray line are similar the hard X-ray ones except for the period, 35 mm [3].

In 2018, a new hard X-ray undulator was built by refurbishing the mechanical frame and control system of a prototype undulator. The prototype undulator was originally constructed in the very early stage of the PAL-XFEL project. The undulator period was different from the present hard or soft X-ray undulators. Even though the magnet structure could not be re-used, the frame was reused for this spare one. During 2020 summer maintenance, this new undulator will be installed upstream of the first undulator segment of the hard X-ray beamline.

MAGNET BLOCK SORTING

The magnetic field through an undulator segment should be as uniform as a tens thousandth to make the phase error within a few degrees. Field errors of the magnet blocks for this undulator production are in one percent range (Fig. 1).

The permanent magnet block has a “hot and cold side effect”. This effect is caused by the magnet block manufacturing process. The magnetization vector of a magnet block has not only M_z component, but also minor M_x and M_y components [4]. Due to the imperfection of magnetization, there is a difference in the B_z field strength between top and bottom sides. The information of the measured magnetic field and moment of the magnet blocks were supplied by the vendor. The field of the blocks was measured at a few centimeters from the face.

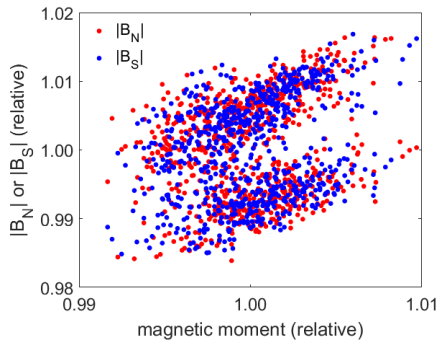


Figure 1: Magnetic field distribution of magnet blocks to magnetic moments.

Figure 2 shows the possible pole field when magnet blocks are distributed randomly. The dotted lines at the middle show the median values of $|B_N|$ and $|B_S|$. The pole fields are placed within about 1%, however a significant pole tuning should be carried out to satisfy the phase error requirement.

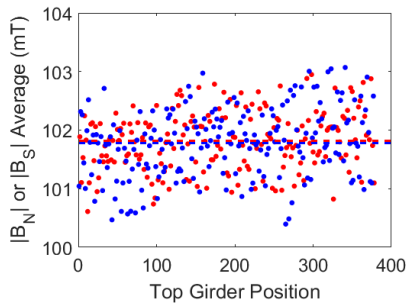


Figure 2: Pole field distribution for randomly installed magnet blocks. The horizontal axis is the pole number in the top magnet structure.

To achieve a field uniformity through an undulator segment, the magnet blocks were sorted and arranged to minimize the field difference among poles as shown in Fig. 3. First, all the magnet blocks were ordered by the $|B_N|$ and $|B_S|$. Then, the magnet block with the median value of $|B_N|$ (or $|B_S|$) is selected to be placed at the first place where an end of the top or bottom magnet structure. In Fig. 3, the block is M1 and the field is B_{1Z}(s). Even though the magnetic field to the end direction (left direction here) is close to the median value, the field of the other side (right direction) of the magnet block (B_{1z}(N) in Fig. 3) can be far from the median value. After placing a pole (P1), a pair magnet block (M3) is chosen so that the field at the pole is averaged by the

* janghui_han@postech.ac.kr

Content from this work may be used under the terms of the CC BY 3.0 licence (© 2019). Any distribution of this work must maintain attribution to the author(s), title of the work, publisher, and DOI

ISBN: 978-3-95450-210-3 doi:10.18429/JACoW-FEL2019-WEP093

RADIATION DAMAGE MONITORING AT PAL-XFEL

Sojeong Lee*, Jang-Hui Han, YoungGyu Jung, Dong Eon Kim and Geonyeong Mun
Pohang Accelerator Laboratory, Pohang, Korea

Abstract

Pohang Accelerator Laboratory X-ray Free Electron Laser (PAL-XFEL) has two undulator beamlines, one hard and one soft X-ray beamlines. These two undulator beamlines are in operation since 2017. To maintain the FEL radiation property, the B-field properties of the PAL-XFEL undulators need to be kept at certain level. Under the beam operation condition up to 10 GeV, the accumulated radiation can affect the permanent magnet properties of the undulators. However, the radiation damage of permanent magnet can be different by the operation environment and the geometry of the undulator. Accumulated radiation sensors and a miniature undulator with a few periods are installed in the PAL-XFEL hard X-ray undulator line to monitor the undulator radiation damage. In this proceeding, the radiation monitoring activities and the recent measurement results are introduced.

PAL-XFEL UNDULATOR SYSTEM

Pohang Accelerator Laboratory X-ray Free Electron Laser (PAL-XFEL) has run user beamtime since 2017. Two undulator beamlines, one hard X-ray and other soft X-ray beamlines provide FEL by using up to 10 GeV for hard X-ray, and 3.15 GeV electron beam for soft X-ray beamline. The maximum repetition rate of electron beams is 60 Hz [1, 2]. The undulators are under radiation environment for about 250 days per year except for shutdown.

The hard X-ray beamline consists of twenty undulator segments, and one additional undulator segment. One additional undulator segment will be installed in the summer maintenance of the next year. For the soft X-ray, beamline consists of the seven undaultor segments. The hard and soft X-ray undulator segment have the same magnetic length, 5 m. The undulator period is 26 mm for hard X-ray and 35 mm for soft X-ray beamline undulator. The undulator is hybrid type based on NdFeB magnets and vanadium permendur poles [3]. The Vaccumschmelze VAVODYM 776AP, which has $H_{cJ,min}$ = 1670 kA/m, was chosen as NdFeB magnets [4].

To maintain the magnetic field strength and the quality of the XFEL facility, the radiation accumulation of undulator needs to be monitored and controlled. The demagnetization of NdFeB base magnets occurs for a kGy level of accumulated radiation dose. The demagnetization of the magnets can lead a undulator kick and K-value change [5, 6].

UNDULATOR RADIATION MONITORING

PAL-XFEL has two different types of radiation damage monitor for the undualtor system: on-line dosimeter systems based on the radFET sensor and a miniature hard X-ray undulator.

RADFET Sensors

As an on-line dosimeter system, the DOSFET-L02 systems from Elettra-Sincrotron Trieste were adopted (Fig. 1). DOSFET-L02 system can monitor the accumulated radiation dose by using the radFET sensors. This system measures the output voltage of the radFET sensors, and accumulated dose level can be estimated using the voltage difference of sensors [7].



Figure 1: DOSFET-L02 controller and sensor mount module from Elettra-Sincrotron Trieste.

After the commissioning of PAL-XFEL, the twelve radFET sensors were installed into the six undaultor segments in November 2017, as shown in Fig. 2. Before the radFET sensor installation, the OSLD sensors were installed for every undaultor segments from March 2017 to July 2017. Based on the OSLD reading result, the radFET sensor installation points were selected, where the measured dose is high. For the hard X-ray undulator beamline, the first two (HXU105 and HXU106) 11th (HXU116), and 12th (HXU117) undulator segments were selected. For the soft X-ray beamline, the 2nd and 3rd undulator segments (SXU407 and SXU408) were selected. The two radFET sensors were installed into each undulator's upstream and downstream upper manget structure. The TY1003 radFET sensors from Tyndall were installed for these six undulators segments [8].

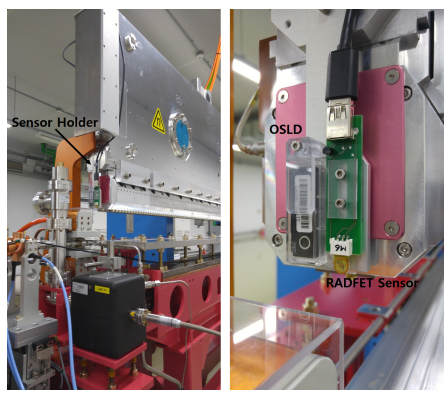


Figure 2: Installation of radFET sensors into undulator. The two sensors were installed into upstream and downstream face of undulator magnet structure [8].

* sojung8681@postech.ac.kr

Content from this work may be used under the terms of the CC BY 3.0 licence (© 2019). Any distribution of this work must maintain attribution to the author(s), title of the work, publisher, and DOI

ISBN: 978-3-95450-210-3 doi:10.18429/JACoW-FEL2019-WEP094

VARIABLE-PERIOD VARIABLE-POLE NUMBER HYBRID UNDULATOR DESIGN FOR NOVOSIBIRSK THz FEL

I. V. Davidyuk†, O. A. Shevchenko, V. G. Tcheskidov, N. A. Vinokurov
Budker INP SB RAS, Novosibirsk, Russia

Abstract

The undulator developed for the first FEL of Novosibirsk FEL facility employs variable-period structure based on the hybrid undulator scheme with poles splinted into halves. The design was adapted to deliver optimal performance, estimations were made based on results of three-dimensional field simulations. According to the modeling results, the undulator will not only widen significantly the first FEL tuning range moving the long-wavelength border of the first harmonic from 200 μm to 450 μm but also provide wider aperture and increase efficiency at shorter wavelengths.

INTRODUCTION

Undulators are magnetic devices designed to provide intensive interaction of a monochromatic electromagnetic wave with a relativistic electron beam (see [1]). They are used in both spontaneous and stimulated emission modes. FELs are based on the second one but in both cases, it needs to provide the ability to tune the wavelength of the radiation. The undulator radiation properties depend on the parameters of an electron beam and field distribution in an undulator, but mainly first radiation harmonic properties are determined by following three parameters: electron energy, undulator period, and undulator field amplitude. One way to tune the wavelength is to vary the electron energy. This approach was implemented successfully [2,3] in the first hard x-ray FEL LCLS. Field amplitude variation is the most common way of wavelength tuning. In permanent magnet undulators, it is frequently realized due to change in the gap between the upper and lower halves of undulator [4]. Alternatively, an undulator period may be varied to shift radiation wavelength, some advantages of this approach in comparison with other techniques of radiation tuning are described in [5], where a bellows-like scheme was proposed. A design of electromagnetic variable-period undulators for storage rings was developed in [6]. Recently, a Halbach structure based on an arrangement of rotating cylindrical permanent magnets was proposed, the period of such an undulator may be varied by tuning magnetization rotation angle between adjacent cylinders[7].

A concept of hybrid undulator with freely moving poles was proposed in [8], and a similar helical device was constructed and commissioned at KAERI [9]. Following this concept, a planar undulator with a variable period and a variable pole number was designed for the second FEL of the Novosibirsk FEL facility [10–13]. Results of modeling in [14] show that the new undulator will widen the radiation wavelength tuning range and the gain variation will be smaller within this range in comparison with existing electromagnetic (EM) undulator and hypothetical optimal variable gap undulator. A prototype of this device has been manufactured; details of tests of its properties can be found in [15].

In this paper authors describe a new permanent magnet variable-period undulator (VPU) that was designed to upgrade the first (terahertz) FEL of the Novosibirsk FEL facility. In order to shift the long-wave limit of the tuning range from 200 μm to 400 μm and beyond, the aperture of the vacuum chamber in the new undulator will be increased, which will reduce the diffraction losses at the ends of the insertion device section. The enlarged gap undulator will be installed on the first track of the energy recovery linac. It will replace the existing two 4-meter long undulators and phase shifter between them. Both old undulators are planar electromagnetic devices with a period of 12 cm, a gap of 8 cm, and the undulator deflecting parameter K varying from zero to 1.1, see Table 1.

Table 1: Basic Undulator Parameters

Parameter	Former EM undulators	VPU
Period, cm	12	10 – 16
Gap (Inner Diameter), cm	8	14
Number of Periods	2 * 32	50 – 80
Radiation Wavelength, μm	90 – 240	82 – 450
Deflection Parameter	0 – 1.1	0.45 – 1.9
Full Length, cm	800	860

DESIGN

Focusing of electron beam due to the undulator field is strong at low electron beam energies (10.5 to 13.3 MeV for the first stage FEL). A concave pole is a common solution to redistribute focusing between the transverse directions. Moreover, it weakens the field dependence on the distance from the undulator axis, which is useful in the case of large aperture. Both the magnet and pole profiles will be segments enveloping the vacuum pipe with different outer diameters; the dimensions are shown in Figure 1.

† i.v.davidyuk@inp.nsk.su

Content from this work may be used under the terms of the CC BY 3.0 licence (© 2019). Any distribution of this work must maintain attribution to the author(s), title of the work, publisher, and DOI

ISBN: 978-3-95450-210-3 doi:10.18429/JACoW-FEL2019-WEP095

THE ATHOS SOFT X-RAY BEAMLINES AT SwissFEL

R. Follath*, U. Flechsig, U. H. Wagner, and L. Patthey
Paul Scherrer Institut, 5232 Villigen PSI, Switzerland

Abstract

SwissFEL is a free electron laser facility for hard and soft X-rays at the Paul Scherrer Institut in Switzerland. The hard X-ray FEL Aramis started 2016 with the first experiments and now the soft X-ray FEL named Athos is close to completion with the first light being expected in 2019. Athos will cover the photon energy range from 250 eV to 1900 eV with pulse energies up to 8 mJ. It will operate with three end stations. Two stations are already defined and are currently in the design and construction phase. Maloja, the first station, is dedicated to Atomic and Molecular physics as well as nonlinear spectroscopy. It will get first light in mid 2020. The second station, Furka, is for condensed matter physics and will go online in 2021.

The performance of the beamline was already presented in an earlier paper [1], here we report on the various operation modes and the latest changes in the optical design.

ATHOS SOURCE

In standard operation mode SwissFEL generates double eletron bunches with a separation of 28 ns at a repetition rate of 100 Hz and accelerates them in the first part of the main LINAC. Afterwards one of the double bunches stays in the main LINAC and is further accelerated up to 5.9 GeV before entering the Aramis undulator. The other bunch is extracted from the main LINAC at beam energies between 2.9 GeV and 3.15 GeV and send to the Athos LINAC where the electron energy is modified between 2.65 GeV and 3.4 GeV before it enters the Athos undulator. By this, both FELs can operate independently and at a repetition rate of 100 Hz. The Athos undulator consist of 2 m long APPLE-X [2] modules in a FODO lattice with 2.8 m period length. Each APPLE-X module is composed of 50 magnet periods with a period length of 38 mm. By tuning the electron beam trajectory it is possible to lase with the tail part of the electron bunch in the first section and with the head part in the second undulator section. The time delay between both pulses can be tuned between -50 fs to +950 fs. The photon wavelength of each undulator section can vary within the tuning range of the undulators (K = 1 …3.5) while the working point is determined by the electron beam energy.

The FEL was optimized with the help of Genesis [3] and foresees several operation modes e.g. high power, low bandwidth or two color modes. The pulse length is about 30 fs (rms), with the ability to reduce it below 1 femtosecond in the attosecond mode.

For the beamline design the high power and two color mode are the most relevant. In the high power mode a maximum pulse energy together with the least photon beam divergence result in the highest fluence values. This must be considered in the optical layout to avoid single shot damage of the optical elements. In the two color mode the undulator is divided into two sections, each 25.2 m long, with individual k-values where both sections can lase at different wavelengths. The larger photon beam divergence together with the long distance from the first undulator section to the optical elements produce the widest beam cross section at the optical elements and determines the geometrical dimensions of the optical elements. Table 1 summarizes the beam parameters for the largest divergence and the highest fluence.

Table 1: Beam Parameters for the Athos Undulator UE38

Photon energy	**(eV)**	**250**	**250**
Mode		power	2 color
Source size*	(μm)	39.6	30.4
Source divergence*	(μrad)	19.8	25.8
Pulse energy	(mJ)	8.1	2.35
Spectr. bandw.*	(%)	0.9	0.57
Source position	(m)	−15.6	−3.9/ − 29.1
Beam size* in 73 m	(mm)	1.8	1.9/2.6

*rms-values

BEAMLINE

The Athos beamline is based on a common grating monochromator and distributes the beam afterwards by means of horizontally steering mirrors to three branches. Its overall scheme is shown in Figure 1. The first, horizontally deflecting mirror separates the FEL-radiation from the Bremsstrahlung that is absorbed in the subsequent radiation shielding. The mirror itself is bendable with a surface profile between flat and a meridional radius of 5000 m. It can either produce an intermediate horizontal focus nearby the exit slit for the Maloja-branch or set to flat for an undisturbed beam divergence. An intermediate focus allows for a gas based diagnostic unit with small apertures after the monochromator to derive an intensity signal of the monochromatized beam.

The monochromator uses variable line-space gratings on spherical substrates with a variable included angle in a SX-700 geometry [4] and operates without an entrance slit. By mounting the optics in a SX-700 mechanics a vertical beam offset of 9 mm between the incoming and outgoing beam is introduced. The setup of mirror and gratings is reverted with respect to the original setup [5] and the plane mirror is now facing downwards whereas the gratings are oriented face upwards. By this the deflection angle on the plane mirror can be reduced while maintaining a larger deflection angle at the gratings. This results in an slightly upward pointing

* rolf.follath@psi.ch

Content from this work may be used under the terms of the CC BY 3.0 licence (© 2019). Any distribution of this work must maintain attribution to the author(s), title of the work, publisher, and DOI

ISBN: 978-3-95450-210-3 doi:10.18429/JACoW-FEL2019-WEP097

OPERATIONAL MODEL OF THE ATHOS UNDULATOR BEAMLINE

C. Kittel*[1,2], M. Calvi[1], X. Liang[1,3], T. Schmidt[1], N. J. Sammut[2]
[1]Paul Scherrer Institut, Villigen PSI, Switzerland
[2]University of Malta, Msida, Malta
[3]Paris-Sud University, Orsay, France

Abstract

Athos, the new Soft X-ray beamline of SwissFEL, operates 16 Apple X undulators and 15 compact chicanes to implement novel lasing schemes. With the data available after the end of the magnetic measurement campaign (middle 2020), a self-consistent set of equations will be used to summarize all the relevant properties of those devices to start their commissioning. The analytic approach planned will be discussed in great detail and tested with the preliminary experimental data available. Finally, the accuracy of this approach will be evaluated and critically compared to the requirements of the new FEL beamline.

INTRODUCTION

In Apple X undulators [1] synchrotron radiation can be produced with any polarization. Also the deflection parameter K can be changed by radially moving the arrays in and out, defining the gap (pole tip to central axis) of the undulator, also called radius (r). We differentiate between the standard cases: Linear Horizontal (LH), Linear Vertical (LV), Circular plus/minus ($Circ$+/-) and plus/minus 45 degrees (+/-45°). Moreover, elliptical polarization angles are possible, but not specifically detailed in this article.

All previous mentioned polarizations but +/-45° can be produced by shifting two opposite magnetic arrays (e.g. No. 1 and No. 3) parallel against their neighboring arrays (e.g. No. 2 and No. 4) [1]. Linear polarization of any angle however can be produced by shifting two opposite magnetic arrays anti-parallel to each other, against their neighboring arrays.

In the following sections we are deducing models from measurement data, in order to predict the undulator positions for any given K and polarization angle α. We are not looking into the Energy mode [1] nor the transverse gradient undulator (TGU) mode in this paper,

In order to allow for a proper set up of the different operational modes, the models should predict K with an error of a few $\frac{\Delta K}{K} = 10^{-4}$.

PARALLEL MODES

Assuming the magnetic field is equal in strength in x and y dimension the parallel modes should be easy to predict. In this case the effective K does not depend on the phase shift of the two moving arrays. However, in the case of a real undulator we have to correct for the slight variation between the magnetic field for the transverse dimensions, B_x and B_y. When moving the arrays in a parallel way, the K-value varies on a 1% level (see blue points in Fig. 1), which had to be taken into account in order to achieve the requested prediction error. Thus to predict the dependencies of the overall gap and the parallel shift needed for a given K-value a universal model based on the magnetic model was developed.With the magnetic model of sinusoidal form, a variation of K_{eff} (background) can be described by a difference between B_x and B_y, see red line in Fig. 1. For a single gap it can be expressed by Eq. (1), which is discussed in more detail in [2].

$$K(\phi) = 2\sqrt{2}\kappa\sqrt{B_x^2 + B_y^2 - \cos(\phi_p)(B_x^2 - B_y^2)} \quad (1)$$

Here ϕ_p is the shift defined as a relative phase difference of two neighboring arrays and $\kappa = \frac{e\lambda_U}{2\pi m_e c}$. A result can be seen in Fig. 1, where it is fitted for a single gap (red line).

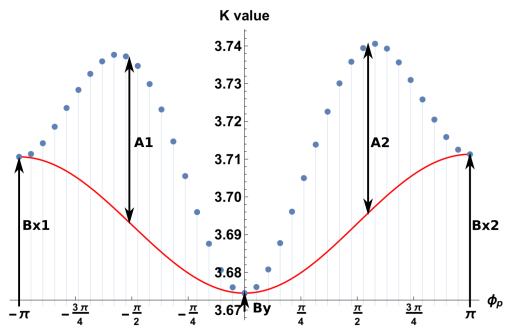


Figure 1: Measured points for a single gap (blue points), background (red line) and model coefficients (black).

Furthermore a second correction has to be added on top to describe the variation probably caused by mechanical deformation due to strong magnetic forces, especially at small gap sizes. It can be described empirically by Eq. (2).

$$K(\phi_p) = A\sin^2(\phi_p) \quad (2)$$

For the data of the same gap as shown in Fig. 1, but with the background removed, the K-correction can now be fitted depending also on the parallel shift ϕ_p (see Fig. 2).

An asymmetry was observed when shifting the arrays in one direction with respect to the opposite direction. Therefore the model coefficients need to be calculated separately for each direction. This helped to minimize the errors at the five points of the dedicated modes ($LH, LV_1, LV_2, Circ+, Circ-$) to below $\frac{\Delta K}{K} = 2 * 10^{-4}$. For all measured gaps the fitting errors can be seen in Fig. 3.

With the above mentioned corrections five coefficients are needed to fit K for each gap (B_{x1}, A_1, B_y, A_2, B_{x2}). Doing

* email: christoph.kittel [at] psi.ch

Content from this work may be used under the terms of the CC BY 3.0 licence (© 2019). Any distribution of this work must maintain attribution to the author(s), title of the work, publisher, and DOI

ISBN: 978-3-95450-210-3 doi:10.18429/JACoW-FEL2019-WEP098

ADVANCED OPERATIONAL MODELS OF THE APPLE X UNDULATOR

X. Liang*[1,2], M. Calvi[1], C. Kittel[1,3], T. Schmidt[1] and N. J. Sammut[3]
[1]Paul Scherrer Institut, 5232 Villigen PSI, Switzerland
[2]Paris-Sud University, 91400 Orsay, France
[3]University of Malta, Msida, Malta

Abstract

Athos is a new soft X-ray beamline at SwissFEL, where the Apple X type undulators will be equipped. These devices are flexible to produce light in different polarization modes. An adequate magnetic field model is required for the operation of undulator. The undulator deflection parameter K and its gradient are calculated starting from the Fourier series of the magnetic field. In the classical parallel and anti-parallel operational modes - respectively elliptical and linear modes, the variation of the magnetic field as well as its parameters are evaluated by computer modeling. The results are compared to the magnetic measurements of the first Apple X prototype.

INTRODUCTION

16 Apple X undulators will be installed on Athos Beamline. Each one contains 800 magnets distributed in a Halbach configuration in 4 arrays (see Fig. 1 top right). Motors are equipped to move the arrays longitudinally and radially. The different operational modes of the undulator are defined by the way of longitudinal shifting of the arrays.

In parallel mode, the opposite arrays are shifted in same direction. The polarization of light changes its elliptical form. While in anti-parallel mode, we move the opposite arrays in different direction, which turns the polarization axes of the photon beam. Moreover, by changing the radial gap between the arrays, we are able to adjust the magnetic strength.

During the parallel mode, the K value variation (see Fig. 2) in the measurement results is not able to be explained with the previous magnetic (single harmonic) model. An updated and adapted physical model with higher harmonics of the Fourier series was proposed. The correction was applied for the non-sinusoidal magnetic field. The analysis of the influence of the high harmonic coefficients are mainly discussed in this contribution. The calculation result indicates that the updated model is not enough to describe the phenomenon. Further discussion about the K value variation will be carried out in the last part.

UPDATED MAGNETIC FIELD MODEL

The convention of the coordinate system of the magnetic field composes a transverse plane (x,y) along with its longitudinal position z. The horizontal and vertical components of the magnetic field are named as B_x and B_y respec-

* xiaoyang.liang@psi.ch, xiaoyang.liang@u-psud.fr

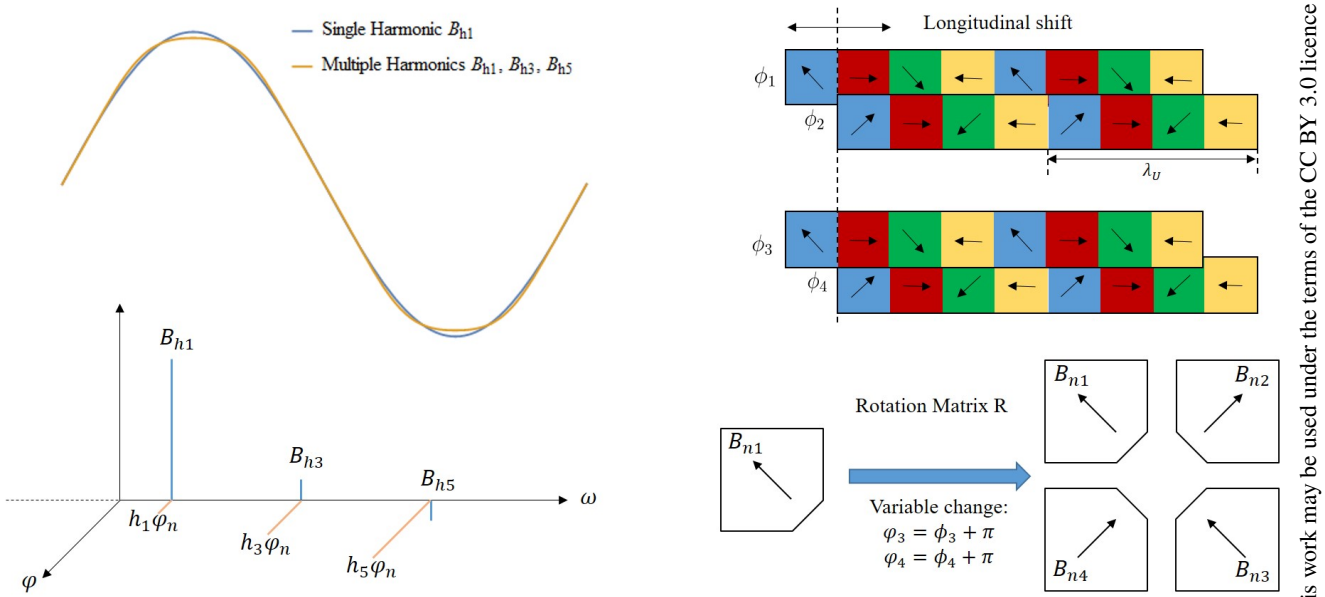


Figure 1: Top left: Example of a non-sinusoidal field correction with multiple harmonics. Top right: Scheme of the longitudinal shift of 4 arrays (Circular mode as an example). Bottom left: Scheme of simplified expression of the magnetic field in Fourier domain. Bottom right: Using the mathematical tools to express 4 arrays as a function of the first array.

Content from this work may be used under the terms of the CC BY 3.0 licence (© 2019). Any distribution of this work must maintain attribution to the author(s), title of the work, publisher, and DOI

ISBN: 978-3-95450-210-3 doi:10.18429/JACoW-FEL2019-WEP100

CONCEPTUAL DESIGN OF A PERMANENT MAGNET UNDULATOR FOR FAST PULSE-TO-PULSE POLARIZATION SWITCHING IN AN FEL*

Ting-Yi Chung† and Ching-Shiang Hwang
National Synchrotron Radiation Research Center, Hsinchu, Taiwan

Abstract

In this paper, we propose the design of an undulator to alter polarization at a fast frequency and the energy spectrum pulse-to-pulse in free-electron lasers (FELs). A fast time varying magnetic field generated in an undulator can alter characteristic light features. An electromagnetic (EM) and permanent magnet (PM) type undulator provides typically a magnetic field switching frequency below 100 Hz. Inductance and heating issues from coils limit the performance for the EM type and favor small magnetic fields and longer periods and for the PM type, strong magnetic forces between magnet arrays create undesired relative motion. In this paper, we discuss these issues and propose an undulator made of Halbach cylinders with rotating magnet arrays to switch the magnetic fields. Concept, magnet structure and performance are discussed in this note.

INTRODUCTION

Polarization control in synchrotron light sources and FELs has many applications in the study of structural, electronic and magnetic properties of materials. Many experiments demand particularly circularly polarized light to probe electronic spin in materials. Several schemes have been implemented at X-ray FELs to fulfil these requirements. There are two important schemes. One is to convert linearly polarized lights to circular polarization based on interference effects [1-3]. The other is to control the motion of the electron beams in helical undulators [4-6].

Polarization switching is another approach to polarization control. The possibility of fast switching would benefit the signal-to-noise ratio for experiments, for instance, for X-ray magnetic circular dichroism (XMCD) [7]. A straightforward method is to switch the helicity using an EM helical undulator by a flip of excitation currents [8,9]. However, the magnetic field strength and the switching frequency of the device is significantly limited by the capacity of power supplies and heating limits generated in coils. A PM helical undulator is compact, promises a shorter period length and is usually arranged linearly according to a Halbach structure [10], as seen in Fig. 1(a). A helical undulator consists of four arrays with a narrow gap between them and can creates a helical field by relative linear motion of the arrays to switch the helicity [11,12]. Because of the narrow gap between the arrays, the motion must overpower extremely large magnetic forces, resulting typically in a low switching frequency of around 1 Hz. Some remedies, such as dedicated force compensation [13] or a driving system [14] have been used to increase the switching frequency.

Except for a superconducting linac, an FEL is normally driven in a pulsed mode by an electron beam from a room temperature linac at a repetition rate of the order of 100 Hz. An undulator with a compatible and tuneable switching frequency would allow multi-polarization and pulse-to-pulse energy changes. This study proposes an undulator consisting of PM cylinders to change the magnetic fields by rotation of magnets, as seen in Fig. 1(b). The switching frequency is tuneable and can exceed 100 Hz.

PM cylinders are useful in many applications, such as particle accelerators [15], motors [16] and for nuclear magnetic resonance (NMR) [17]. A rotatable cylinder structure has been shown to change magnetic fields of focusing quadrupole magnets in Laser Plasma acceleration [18] and the field of steering magnets for modulating the phase between two undulators in a storage ring [19]. A delicate linear configuration of rotatable rods has been developed to modulate the period length of an undulator [20]. These pioneering works inspired us to create a PM cylinder undulator with the ability to switch the polarization quickly. This paper is organized as follows. In Section 2, we discuss operations of polarization changes using a relative rotation of PM cylinders. In Section 3, we study the torque for a practical construction and discuss construction feasibilities. To increase the switching frequency, two types of PM cylinders are studied in Section 4. A discussion for an application in an FEL is given in Section 5.

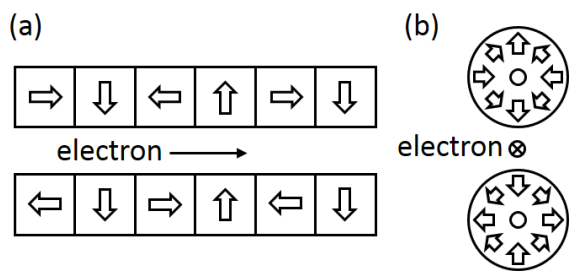


Figure 1: (a) A PM undulator consisting of Halbach arrays. (b) Rotatable Halbach cylinders. The magnetization of the PM is indicated by arrows.

MAGNETIC FIELD CHANGES AND POLARIZATION CONTROL

The magnetic field in our proposed structure is produced by a pair of PM cylinders. Several magnetization configurations in a cylinder are feasible.

* This work was supported in part by the Ministry of Science and Technology under Contract MOST 108-2112-M-213-011
†chung.albert@nsrrc.org.tw

Content from this work may be used under the terms of the CC BY 3.0 licence (© 2019). Any distribution of this work must maintain attribution to the author(s), title of the work, publisher, and DOI

ISBN: 978-3-95450-210-3 doi:10.18429/JACoW-FEL2019-WEP101

LINEAR POLARISATION VIA A DELTA AFTERBURNER FOR THE COMPACTLIGHT FACILITY*

H. M. Castañeda Cortés†, N. R. Thompson, D. J. Dunning
ASTeC and Cockcroft Institute, STFC Daresbury Laboratory, Warrington, United Kingdom

Abstract

We studied the degree of polarisation of the FEL radiation from the diverted-beam scheme [1, 2] using the layout of the CompactLight facility [3], which is in the process of being designed. To satisfy the polarisation requirements defined by the users [4] without compromising the aim of the facility to be compact, we studied a configuration comprising a helical Super Conductive Undulator (SCU) followed by a Delta afterburner (configured to generate linearly polarised light). The trade-offs between the SCU length, afterburner length, degree of polarisation and pulse energy are presented and discussed.

INTRODUCTION

The CompactLight project aims to design next generation light sources which provide competitive FEL performance whilst aiming for a compact design and lower maintenance costs [3]. A study is carried out to characterise a scheme with an afterburner to generate linearly polarised radiation for the CompactLight project. The FEL performance of the undulator line with the afterburner is compared to the case where a variable polarising undulator is considered as stand-alone (set up to generate linearly polarised coherent radiation). The afterburner in the undulator line constrains the beam energy, radiation wavelength and degree of polarisation of the facility. The design choices on the undulator and the afterburner will provide an optimization of the pulse energy without losing sight of the objective of being compact.

AFTERBURNER AND FEL PERFORMANCE (SIMULATION)

A comparison of FEL performance is done for two scenarios:

I. An undulator line with a stand-alone undulator delta undulator configured to generate linearly polarised light.

II. Helical SCU as main undulator and delta undulator to generate linearly polarised radiation as afterburner (see Fig. 1).

Both options are tuned up to the same resonant wavelength, corresponding to 16 keV photon energy (list of design parameters for both undulators displayed in Table 1). An electron beam traversing the undulator line with beam parameters listed in Table 2 is simulated in Genesis1.3 [5] to assess the FEL performance of the proposed scenarios. Preliminary estimations of the FEL saturation length and saturation power for the SCU and delta undulators (in stand-alone mode) are calculated and shown in Table 3.

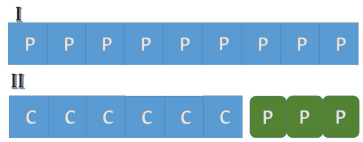


Figure 1: Options to generate linearly polarised radiation.

Table 1: Undulator Parameters Defined for SCU and Delta Undulator

Undulator type	a_w	λ_u (mm)	$l_{section}$ (m)
SCU	0.907	9.85	2.27
Delta (AB)	0.546	13.83	2.28

Table 2: Electron Beam Parameters

Electron beam parameter	Value
Beam Energy	5.5 GeV
Peak Current	5 kA
Normalised $\epsilon_{x,y}$	0.2 mm–mrad
RMS slice energy spread	0.01%
Average β function	9 m

Table 3: FEL Figures of Merits for Both SCU and Delta Undulator in its Configuration to Generate Linearly Polarised Radiation

Undulator type	$L_{sat.}$ (m)	$P_{sat.}$ (GW)	$E_{sat.}$ (μJ)
SCU	15.61	9.53	52.11
Delta	29.13	7.53	41.19

Given that the normal saturation length for the SCU is 15.61 m and the saturation length for the delta undulator is 29.13 m, option II is more compact than option I as long as the length of the afterburner is less than 13 m. Table 4 shows the amount of space saved by different afterburner lengths (with ΔL being the difference between the lengths of both options).

Figure 2 shows the ratio of pulse energies obtained for option II compared to option I. The green dotted line in Fig. 2 corresponds to the maximum pulse energy obtained per number of afterburner sections (from 1 to 5). As shown, the maximum pulse energies for option II take values between 17% up to 68.4% of the pulse energy of the radiation

* This work has received funding from the H2020 CompactLight Project via the European Union's Horizon 2020 research and innovation programme under grant agreement No 777431.
† hector.castaneda@stfc.ac.uk

Content from this work may be used under the terms of the CC BY 3.0 licence (© 2019). Any distribution of this work must maintain attribution to the author(s), title of the work, publisher, and DOI

ISBN: 978-3-95450-210-3 doi:10.18429/JACoW-FEL2019-WEP103

A PLASMA ATTENUATOR FOR SOFT X-RAYS IN LCLS-II*

Alan S. Fisher†, Andrew L. Benwell, Bryce T. Jacobson, and Yiping Feng
SLAC National Accelerator Laboratory, Menlo Park, California, USA

Abstract

LCLS used a gas column to attenuate soft x-ray pulses by factors of up to 10^5. In LCLS-II, thermal effects from x-ray absorption at high repetition rates will lead to unpredictable attenuation that depends on the spacing and energy of prior pulses. An argon plasma in an RF cavity is presented as an alternative. X-ray absorption then becomes a perturbation compared to the energy deposited from RF excitation. An LCLS-II solid-state RF amplifier, generating up to 5 kW at 1.3 GHz, can provide the drive, and the FPGA-based low-level RF controller can be programmed to track tuning with plasma density. Several diagnostics are planned to monitor plasma properties over a fill-pressure range of 10 to 1000 Pa.

INTRODUCTION

Temporary reduction of the pulse energy of an x-ray FEL beam is often required to prevent damage to critical components, such as highly specialized x-ray detectors, for alignment, or to study x-ray nonlinear effects. An x-ray attenuator allows the user to vary the incident pulse energy in a well-controlled manner without altering other FEL characteristics, unlike other methods such as operating at different points of the FEL gain curve or lowering the electron bunch charge. For soft x-rays, a fully saturated FEL pulse at a typical operating bunch charge of 100 pC would completely damage any solid attenuator located sufficiently close to the FEL source point. Consequently, attenuation in gas has been considered the only viable solution; gas attenuators have been implemented at many facilities around the world, including the Linac Coherent Light Source (LCLS) [1] at SLAC.

At a sufficiently low repetition rate, such as 120 Hz at LCLS, a gas attenuator at room temperature provides an effective attenuation that is simply governed by the Beer-Lambert law [2-4] (relating the gas pressure at a constant temperature to the attenuation length), and is deterministic and independent of the FEL beam parameters. However, LCLS-II will operate at repetition rates up to 1 MHz. With increasing rate, a gas attenuator will begin to exhibit nonlinearities that depend on the FEL pulse rate and energy, along with the thermal diffusivity and absorption cross section of the gas. Even more troubling is the onset of hysteresis: the attenuation of trailing pulses depends on the intensities and arrival times of earlier ones. Such previously unsuspected behavior arises because the energy deposited by an FEL pulse requires a finite time to dissipate, on the order of 1 ms. The original gas density distribution is perturbed, modifying the effective attenuation of the pulses that come during this recovery time.

* SLAC is supported by the U.S. Department of Energy, Office of Science, under contract DE-AC02-76SF00515.
† email address afisher@slac.stanford.edu

Here we present the concept of a column of partially ionized plasma in place of the gas, in order to stabilize the attenuation at high repetition rates. The plasma is hotter, and its thermal relaxation is much faster. The energy deposited by a few-mJ FEL pulse would then present only a small perturbation, and the densities of electrons, neutrals, and ions will recover between LCLS-II pulses. The plasma would provide a stable, controllable, and deterministic x-ray attenuator.

ATTENUATION IN A GAS COLUMN

A typical gas-based attenuator for x-ray FEL pulses consists of a few-meter-long gas column, bookended by differential pumping sections to maintain ultra-high vacuum elsewhere along the beamline. Nitrogen and argon are common, inexpensive choices, operating at pressures between 10 and 1000 Pa. Soft x-rays below 1.5 keV can be attenuated by a factor of up to 10^5.

Early in the planning for LCLS-II, concerns about the effect of its high repetition rate led to thermodynamic and hydrodynamic simulations [5,6] of a gas attenuator. It was found that the x-ray energy deposited by photoabsorption would eventually thermalize into the kinetic degrees of freedom of the gas molecules, raising the temperature on axis and reducing the local density to create a “hole” that lasts for a few ms, during which the attenuation of subsequent pulses is reduced.

When the FEL runs at a high but steady rate and pulse energy, a gas attenuator may stabilize, although at a level different from that prescribed by the Beer-Lambert law. However, the pulse energy fluctuations of a SASE FEL cause each pulse to encounter a different gas density distribution. Instead of a true steady state, the distribution depends on the deposited energy and arrival time of earlier pulses, causing hysteresis in the effective attenuation.

Experimental evidence of the density “hole” induced by an FEL pulse was first demonstrated at LCLS using a two electron bunches separated by 123 ns. Each bunch generated a hard x-ray pulse that passed through a test gas cell. The transmission of the second pulse relative to the first increased by approximately 20% [7].

ATTENUATION IN A PLASMA COLUMN

Concept

The fundamental deficiency of a room-temperature gas attenuator operating at high repetition rate stems from its relatively low energy scale of 25 meV/atom, corresponding to a temperature of 300 K. Thermal equilibrium is destroyed when the gas absorbs a mJ x-ray pulse and recovers after a thermal relaxation time of a few ms, 1000 times too slow for MHz pulse spacing. In contrast, the plasma electron temperature would be 5 eV, or 60 000 K.

Content from this work may be used under the terms of the CC BY 3.0 licence (© 2019). Any distribution of this work must maintain attribution to the author(s), title of the work, publisher, and DOI

ISBN: 978-3-95450-210-3 doi:10.18429/JACoW-FEL2019-WEP104

A HIGH-POWER, HIGH-REPETITION RATE THz SOURCE FOR LCLS-II PUMP-PROBE EXPERIMENTS*

Z. Zhang, A. S. Fisher, M. C. Hoffmann, Z. Huang†, B. Jacobson,
P. S. Kirchmann, W.-S. Lee, A. Lindenberg, E. Nanni, R. Schoenlein
SLAC National Accelerator Laboratory, Menlo Park, CA, USA
S. Sasaki, J. Xu, Argonne National Laboratory, Lemont, IL, USA

Abstract

Experiments using a THz pump and an x-ray probe at an x-ray free-electron laser (XFEL) facility like LCLS-II require frequency-tunable (3 to 20 THz), narrow bandwidth (~10%), carrier-envelope-phase-stable THz pulses that produce high fields (> 1MV/cm) at the repetition rate of the x rays and well synchronized with them. In this paper, we study a two-bunch scheme to generate THz radiation at LCLS-II. We describe the two-bunch beam dynamics, the THz wiggler and radiation, as well as the transport system bringing the THz pulses from the wiggler to the experimental hall.

INTRODUCTION

The effective coupling of advanced THz sources with XFEL capabilities will open many new science opportunities. THz oriented workshops at SLAC [1], FERMI, Eu-XFEL [2] and elsewhere in the past eight years have highlighted the demand for the ability to carry out these types of experiments.

The new science opportunities presented by a high-repetition rate FEL such as the LCLS-II create new opportunities, demands, and challenges for THz sources that go beyond what has been considered in previous workshops. Some critical capability gaps can already be identified that appear to be beyond the projected achievable properties of table-top sources. Among them are the intense sources in the well-known THz gap between 3-15 THz. For field driven effects, a broadband, single-cycle THz pulse with a peak electric field strength of 10 MV/cm can approach the atomic bonding strength in matters. For resonant excitation, a tunable, narrow bandwidth (~ 10%) source with at least 10 μJ pulse energies are desired. These required THz characteristics are summarized in Table 1.

Table 1: Required THz Characteristics

Waveform	Single cycle		10 cycles	
E-field	10 MV/m		1 MV/m	
Frequency	5 THz	15 THz	5 THz	15 THz
Spot Size	200 μm	100 μm	200 μm	100 μm
Pulse Duration	100 fs	33 fs	1000 fs	330 fs

Although a dedicated accelerator with tens of MeV beam energy can achieve some of these capabilities [3, 4], it becomes increasingly difficult to reach 10 THz and higher frequencies with significant pulse energies. In addition, a high-repetition rate stand-alone accelerator with the technical issues of synchronization and the associated machine protections becomes rather complex. Inspired by the pioneering work of the FLASH THz beamline [5], we propose to install a permanent-magnet or electromagnet wiggler after the LCLS-II undulators and to use a two-bunch scheme to produce intense THz pulses for high-rep rate pump-probe experiments. We note that an earlier study of a THz source for Eu-XFEL has a similar two-bunch scheme while employing a high-field superconducting wiggler [6].

TWO-BUNCH SCHEME

Figure 1 shows a schematic of the two-bunch concept at LCLS-II to produce intense THz radiation. Both bunches are generated by the LCLS-II injector with suitable time separation (~110 ns). Because the THz pump must arrive before the X-ray probe, a first bunch is used to produce THz in the wiggler and a second bunch is for FEL lasing. In our design, the THz bunch will be accelerated to 4 GeV and then kicked out to the bypass line. For THz generation, a higher bunch charge and a shorter bunch length are always desirable. The beam parameters of the THz bunch will be optimized to cover the frequency range from 3 to 20 THz. Moreover, stronger compression of the THz bunch results in poorer beam quality and hence suppress its FEL lasing in the SXR undulator.

The accelerator settings of the LCLS-II are optimized to deliver electron bunches for FEL lasing. The control of the THz bunch cannot be allowed to alter the beam dynamics of the FEL bunch. The compression of the THz bunch can be adjusted by the laser injection time, which changes the acceleration phase in the SRF linac (L1) before the first magnetic chicane (BC1). Figure 2 shows that offsetting the laser injection time changes the beam arrival time of 200-pC bunch at the start of L1. The simulations were performed with ASTRA [7]. The change of arrival time at the start of the L1 varies the beam energy chirp and beam compression downstream. An earlier laser pulse shortens the first bunch for better THz generation. Figure 3 shows the final RMS bunch length at the undulator entrance for the 200-pC THz bunch at different offsets of the relative laser injection time.

Figure 4 shows the bunching factors of the THz beam (100 pC and 200 pC) at different frequencies. The bunching factor of the 200-pC bunch damps quickly with increasing frequency. In practice, we can optimize the bunch charge

* Work supported by U.S. Department of Energy Contracts No. DE-AC02-76SF00515.
† zrh@slac.stanford.edu

Content from this work may be used under the terms of the CC BY 3.0 licence (© 2019). Any distribution of this work must maintain attribution to the author(s), title of the work, publisher, and DOI

ISBN: 978-3-95450-210-3 doi:10.18429/JACoW-FEL2019-WEP107

POLARIZING AFTERBURNER FOR THE LCLS-II UNDULATOR LINE*

H.-D. Nuhn†, SLAC National Accelerator Laboratory, Stanford, USA

Abstract

A fixed-gap polarizing undulator (Delta) has been successfully operated in afterburner mode in the LCLS FEL beamline at the SLAC National Accelerator Laboratory (SLAC) from August 2014 to the end of operations of the LCLS facility in December 2018. The LCLS undulator line is currently being replaced by two new undulator lines (as part of the LCLS-II project) to operate in the hard and soft x-ray wavelength ranges. Polarizing afterburners are planned for the end of the soft x-ray (SXR) line. A new polarizing undulator (Delta-II) is being developed for two reasons: (1) increased maximum K value to be resonant over the entire operational range of the SXR beamline (2) variable gap for K value control. It has been shown that using row phase control to reduce the K value while operating in circular polarizing mode severely degrades the performance of a polarizing undulator in afterburner mode. The device is currently scheduled for installation 2020-2021. The paper will explain the need for the variable gap design backed up by beam based measurements done with the LCLS Delta undulator.

INTRODUCTION

The LCLS Delta polarizing afterburner has been successfully operated [1] with the LCLS FEL for user experiments [2–4] until the shutdown of the facility in December 2018. The SLAC National Accelerator Laboratory (SLAC) is now getting ready to commission a new FEL facility with two undulator lines to produce soft x-ray (SXR) and hard x-ray radiation (HXR). It is planned to install up to three polarizing afterburners at the end of the SXR undulator beamline. It was clear that the 32-mm-period LCLS Delta, which is based on a concept developed by Alexander Temnykh [5], could not be made resonant with the SXR undulators over the high K regime of the operating range because the undulator period of the SXR undulator is 39 mm compared to the 30 mm period length of the LCLS undulators. A new Delta undulator with longer period was required. As work on designing the new device started, the team became aware of a PSI paper by Thomas Schmidt et. al [6]. The PSI group had found that line-width broadening occurred to the undulator radiation under certain operating conditions, when operating a fixed gap APPLE-II undulator, which uses 4 independently movable rows of magnets similar to the Delta undulator and has similar properties. The source of the line-width broadening was found to be a transverse gradient of the undulator parameter, K, that appears when operating the undulator in circular polarizing and at reduced strength. This effect is described in the next section.

* Work was supported by U.S. Department of Energy, Office of Basic Energy Sciences, under Contract DE-AC02-76SF00515.
† nuhn@slac.stanford.edu

TRANSVERSE K GRADIENT

It turns out that polarizing undulators such as the Apple [7] and Delta devices that are basically constructed from 4 rows of permanent magnets, where the longitudinal row positions can be changed during operation to adjust the polarization mode and the undulator parameter, K, will generate a transverse gradient of K for certain combinations of row positions. Such an undulator can be conceptualized as made from two crossed planar pure permanent magnet undulators, each having two rows of permanent magnets in Halbach array [8] configuration mounted on opposite sites of the beam axis. The on-axis field is strongest when north poles at the permanent magnet block end closest the beam axis on one row exactly oppose south poles at the permanent magnet block ends closest to the beam axis on the other row. When the two rows are moved longitudinally with respect to each other by a distance Δz, the on-axis field changes with the cosine of that distance

$$K = K_0 \cos\left(2\pi \frac{\Delta z}{\lambda_u}\right) \tag{1}$$

at constant gap. Here, K_0 is the maximum K value that occurs at $\Delta z = 0$. Such a device is called an Adjustable Phase Undulator [9]. The relative longitudinal position of the two adjustable phase undulators determines the polarization mode, i.e., they will produce planar polarized light when they are aligned and various forms of elliptical, circular or planar light when they are displaced with respect to each other. It turns out that a transverse K gradient occurs in the device when operated in circular mode while $K < K_0$. After the initial observation, this fact was theoretically derived by Zachary Wolf [10] and by Marco Calvi et al. [11]. According to [10], the K gradient can be expressed to first order as

$$\left.\frac{\partial K}{\partial x}\right|_{x=y=0} = \frac{\pm K_{max} k_s^2}{\sqrt{2k_s^2 + 2k_u^2}} \sin\left(\cos^{-1}\left(\frac{K|_{x=y=0}}{K_{max}}\right)\right) \sin\delta,$$
$$\left.\frac{\partial K}{\partial y}\right|_{x=y=0} = 0,$$

where the "+" sign applies when $z_{A,up} > z_{A,dn}$ and $z_{B,up} > z_{B,dn}$ and the "−" sign applies when $z_{A,up} < z_{A,dn}$ and $z_{B,up} < z_{B,dn}$, or

$$\left.\frac{\partial K}{\partial x}\right|_{x=y=0} = 0,$$
$$\left.\frac{\partial K}{\partial y}\right|_{x=y=0} = \frac{\pm K_{max} k_s^2}{\sqrt{2k_s^2 + 2k_u^2}} \sin\left(\cos^{-1}\left(\frac{K|_{x=y=0}}{K_{max}}\right)\right) \sin\delta,$$

where the "+" sign applies when $z_{A,up} > z_{A,dn}$ and $z_{B,up} < z_{B,dn}$ and the "−" sign applies when $z_{A,up} < z_{A,dn}$ and $z_{B,up} > z_{B,dn}$.

Content from this work may be used under the terms of the CC BY 3.0 licence (© 2019). Any distribution of this work must maintain attribution to the author(s), title of the work, publisher, and DOI

ISBN: 978-3-95450-210-3 doi:10.18429/JACoW-FEL2019-WED01

EXPERIENCE WITH SHORT-PERIOD, SMALL GAP UNDULATORS AT THE SwissFEL ARAMIS BEAMLINE

T. Schmidt*, M. Calvi, C. Kittel, D. Voulot, N. Hiller, T. Schietinger
E. Prat-Costa, S. Bettoni, S. Reiche, E. Ferrari, M. Aiba, R. Ganter, F. Löhl, A. Alarcon,
U. Wagner, R. Follath, P. Juranic, C. Arrell, , Paul Scherrer Institut, 5232 Villigen, Switzerland
A. Cassar, N.J. Sammut, Univerity of Malta, MSD2080 Msida, Malta

Abstract

The SwissFEL Aramis beamline provides hard X-ray FEL radiation down to 1 Angström with 5.8 GeV and short period, 15mm, in-vacuum undulators (U15). To reach the maximum designed K-value of 1.8 the U15s have to be operated with vacuum gaps down to 3.0 mm. The thirteen-undulator modules are 4m long and each of them is equipped with a pair of permanent magnet quadrupoles at the two ends, aligned magnetically to the undulator axis. Optical systems and dedicated photon diagnostics are used to check the alignment and improve the K-value calibration. In this talk the main steps of the undulator commissioning will be recalled and a systematic comparison between the magnetic results and the electron and photon based measurements will be reported to highlight achievements and open issues.

INTRODUCTION

The hard x-ray Aramis beamline of SwissFEL started operation with first lasing end of 2016, but only in the soft x-ray at 400 eV. This was caused by a delay with the newly developed solid state rf modulators. During 2018, the energy could be successively increased until the full energy with 6 GeV has been reached end of 2018. In March 2018, the working range of the monochromator has been reached, so that a first photon based alignment campaign could be done. Because of the short period length of 15 mm, only 13 undulator modules with 265 periods in 4 m length each are needed for lasing down to 1 Å, as shown in Fig. 1. The gain length is typically between 2 and 3 m, so that every undulator causes a significant increase in power. The undulators are placed on remotely controlled 5-axis cam-shaft mover which allow horizontal and vertical positioning and all 3 angles with µm precision. The mover have a range of up to 3 mm, but are limited by the bellow transverse motion of only 0.5 mm. For the planar U15, height and pitch alignment are the most relevant, but the original design strategy was to use the same support units also for the soft x-ray undulators of APPLE type where in addition horizontal position and yaw angle are of equal importance.

The main issue of the Aramis beamline, like for all the others, is to get the orbit straight at the tolerances of an hard X-ray FEL, align the undulators to this orbit and set the correct K - values and phase matching between two successive undulators. For this reason, the first step in setting up the Aramis beamline is the beam based alignment (BBA). While



Figure 1: SwissFEL hard x-ray Undulator Aramis.

not needed for the commissioning of the fixed gap LCLS, the photon based undulator alignment was essential for the commissioning of SACLA [1]. The strategies for photon based alignment and optimisation have been adapted for SwissFEL, which, however, could start lasing with lower electron energies at longer wavelengths and could successively improve the alignment.

The magnetic field data taken during the magnetic optimisation and characterisation of the undulators in the undulator laboratory are prepared with a bundle of models including the gaps, the corrector settings and the correct phase shifter settings which has been named SUBLIME (aramiS Undulator BeamLIne ModEl) [2], see Fig. 2.

In the following, the setup for the alignment of the undulators is discussed with a focus on the photon based diagnostic

* thomas.schmidt@psi.ch

Content from this work may be used under the terms of the CC BY 3.0 licence (© 2019). Any distribution of this work must maintain attribution to the author(s), title of the work, publisher, and DOI

ISBN: 978-3-95450-210-3 doi:10.18429/JACoW-FEL2019-WED02

ABSORBED RADIATION DOSES ON THE EUROPEAN XFEL UNDULATOR SYSTEMS DURING EARLY USER EXPERIMENTS

F. Wolff-Fabris†, H. Sinn, J. Pflüger, European XFEL GmbH, Schenefeld, Germany
F. Hellberg, A. Hedqvist, Stockholm University, Stockholm, Sweden
F. Schmidt-Foehre, D. Noelle, W. Decking, DESY, Hamburg, Germany

Abstract

The European XFEL GmbH (EuXFEL) is a FEL user facility based on a superconducting accelerator with high duty cycle. Three movable gap SASE Undulator Systems using hybrid NdFeB permanent magnet segments are in operation. We observed in a dedicated diagnostic undulator for radiation damage doses up to 4 kGy and 3% demagnetization effect during the commissioning phase. In this work we present characteristics of the absorbed radiation doses in undulators during photon beam delivery for users. Lower absorbed doses are measured since the start of user operation. While ramping up electron beam parameters and repetition rates, individual segments located at the downstream end of the SASE systems show persistent absorbed doses which are proportional to the transmitted charge. In addition, the dose per charge ratio shows photon energy dependence. Portable magnetic flux measurement systems allow in-situ tunnel assessment of undulator magnetic properties in order to estimate radiation dose limits for future user operation.

INTRODUCTION

The European XFEL GmbH is a free-electron laser user facility which started operation in 2017. Its superconducting accelerator is designed to operate at energies up to 17.5 GeV and has the highest duty cycle machine currently in operation with a repetition rate of up to 27000 bunches per second and at 1nC [1]. The EuXFEL operates three separate undulator systems named SASE1, SASE2 and SASE3 to produce FEL radiation with tunable wavelengths from 0.05 to 5.2 nm and pulse lengths of less than 100 fs [2]. These Undulator Systems are built with 91 5-m long undulator segments based on hybrid NdFeB (VACODYM 776AP) permanent magnets, which are tuned to to optimize the SASE effect [3].

De-magnetization effects of the permanent magnets due to radiation damage have been reported [4-8] in several facilities through the years and have been also observed at EuXFEL [9]. Dedicated passive and active machine protection systems have been designed to minimize such effects and the EuXFEL operates a collimation system [10], an array of on-line readable dosimeters [11], and diagnostic undulators (DU) installed at the upstream extremity of each SASE system. These permit to investigate, reduce and/or minimize the demagnetization effects on the undulator systems.

Table 1 summarizes the starting date of accelerator commissioning, first lasing and start of user program in each SASE system. The EuXFEL has adopted a ramping up schedule for the beam parameters and the currently used electron and photon parameters available for users are also indicated in Table 1. In this work we consider the commissioning phase for each SASE system stretching from the first beam transmission through the undulators until the start of the early user operation and therefore it also includes the beam delivery for the beamlines commissioning phase. It is important to note that the electron beam transmitted through SASE1 necessarily travels through SASE3 before reaching the nearest dump.

Table 1: Main Event Dates for SASE1-3 and Typical Beam Parameters for User Experiments

System	SASE1	SASE2	SASE3
1st beam transm.	27.04.2017	13.03.2018	27.04.2017
1st lasing	02.05.2017	01.05.2018	02.08.2017
1st Early user exp.	14.09.2017	20.03.2019	28.11.2018
Typical e-beam user par.	14 GeV 250 pC 2000 bps	14 GeV 250 pC 2000 bps	14 GeV 250 pC 2000 bps
Typical photon user par.	6-12keV	6-14keV	0.7-1.6keV

In this manuscript we report on the evolution and characteristics of the absorbed doses during the initial phase of photon beam delivery for users. In particular we discuss time, charge, and photon energy dependences of the absorbed doses. Additionally, we present further enhancement on magnetic measurement capabilities allowed by in-situ tunnel measurements.

ABSORBED DOSES DURING COMMISIONING AND USER OPERATION

The importance of on-line dosimetry system and diagnostic undulators in the EuXFEL Undulator Systems was demonstrated in the commissioning phase. We have measured de-magnetization effects associated to magnetic field degradation in the diagnostic undulators [9] and to a change in the vertical entrance kick of a 5-m undulator

† f.wolff-fabris@xfel.eu

Content from this work may be used under the terms of the CC BY 3.0 licence (© 2019). Any distribution of this work must maintain attribution to the author(s), title of the work, publisher, and DOI

ISBN: 978-3-95450-210-3 doi:10.18429/JACoW-FEL2019-THA04

Content from this work may be used under the terms of the CC BY 3.0 licence (© 2019). Any distribution of this work must maintain attribution to the author(s), title of the work, publisher, and DOI

ULTRAFAST MAGNETISATION DYNAMICS AT THE LOW-FLUENCE LIMIT SUPPORTED BY EXTERNAL MAGNETIC FIELDS

M. Riepp†, L. Müller[1], A. Philippi-Kobs, W. Roseker, R. Rysov, K. Bagschik, M. Walther, T. Golz, N. Stojanovic, G. Grübel[1], DESY, Hamburg, Germany
R. Frömter, H. P. Oepen,
Universität Hamburg, Center for Hybrid Nanostructures, Hamburg, Germany
D. Naumenko, E. Pedersoli, F. Capotondi, M. Kiskinova,
Elettra-Sincrotrone Trieste S.C.p.A., Trieste, Italy
[1]also at Universität Hamburg, Department of Physics, Hamburg, Germany

Abstract

We report on ultrafast magnetisation dynamics in ferromagnetic cobalt/platinum multilayers upon pumping by near and mid to far infrared radiation, utilizing sub-100 femtosecond free-electron laser pulses. The evolution of the excited magnetic state is studied on femtosecond timescales with nanometre spatial resolution and element selectivity, employing time-resolved magnetic small-angle X-ray scattering. The obtained results contribute to the ongoing discussion to what extent either coupling of the electromagnetic field or rather quasi-instantaneous heating of the electron-system is the driving force for phenomena like ultrafast demagnetization or all-optical helicity-dependent switching.

INTRODUCTION

Ultrafast demagnetisation on sub-100 femtosecond to picosecond time scales [1] and the related phenomenon of all-optical helicity-dependent switching (AO-HDS) of magnetisation [2] are fascinating effects in fundamental physics with potential for, e.g., energy-efficient future data-storage devices [3,4]. First discovered in amorphous ferrimagnets like GdFeCo [2,5], AO-HDS has also been found recently in various ferromagnets including Co/Pt multilayers [6]. In the latter case, the impact of the laser pulse is controversially debated. Reports on deterministic single-pulse switching in micron-sized magnetic domains [7] contrast with the stochastic nature of a multi-pulse switching mechanism found in different experiments, see, e.g., Ref. [8]. Modelling the deterministic process by means of the magnetic two-temperature model resulted in thresholds for the pump fluence and the duration of the inverse Faraday effect (IFE)-induced magnetic field, set by the length of the pump pulse [9,10]. In that interpretation, the impact of the laser pulse is assumed to be twofold. First, quasi-instantaneous heating of the electron-system above the Curie temperature mediates a transient paramagnetic state (demagnetisation). Second, opto-magnetic coupling of the laser-induced effective magnetic field ($\mathbf{H}_{\mathrm{IFE}}$) to the spin system during subsequent cooling down to the paramagnetic phase can result in nucleation and consecutive growth of reversed magnetic domains, depending on the helicity of the laser light. As the spatial resolution in commonly used Kerr microscopy experiments is limited to the micron range, information on changes in nanoscopic domain systems during demagnetisation is scarce. In this respect, free-electron lasers (FELs), like FERMI and FLASH, providing sub-100 femtosecond extreme ultraviolet (XUV) pulses, allow to explore femtosecond dynamics also in nanometre-sized magnetic domains [11-15]. Tuning the photon energy to resonance with one of the dichroic transitions in the magnetic element, here the $M_{2,3}$-absorption edge of Co at 59.6 eV, adds element selectivity to studies of magnetisation dynamics [16].

This paper reports on a near-infrared (NIR)-pump–FEL-probe experiment (pump wavelength of 800 nm), in which the pump helicity-dependent response of a magnetic multi-domain state was studied in the presence of an external magnetic field, $\mathbf{H}_{\mathrm{ext}}$, following observations in Ref. [17]. The evolution of the domain system was monitored by time resolved resonant magnetic small-angle X-ray scattering (tr-mSAXS). Complementarily, we show the feasibility to study the laser beam's **H**-field influence on demagnetisation by using polychromatic mid to far-IR pump radiation (wavelength of 30– 150 µm) for simplicity denoted in the following as THz-radiation (frequency of 2– 10 THz). Since the oscillation periods of the electromagnetic field are slower than for NIR radiation, a direct field-induced response of the magnetic system can be expected [18-20].

EXPERIMENTAL

Cobalt/platinum multilayers with perpendicular magnetic anisotropy were deposited by sputtering techniques on freestanding 50 nm-thin Si_3N_4 membranes [21]. The experiment using NIR-pump wavelength was conducted in tr-mSAXS geometry (Fig. 1) at the DiProI beamline of FERMI at ELETTRA [22]. A multilayer with 6 bilayer repetitions of Co/Pt was used, which is fully remanent with a coercive field of $\mu_0 H_c \approx 15$ mT. The global energy minimum, obtained after out-of-plane demagnetization, is a multi-domain state with a characteristic periodicity of 460 nm. A perpendicular magnetic field increases the characteristic length scale as predominantly small domains, oriented oppositely to the field, are erased. The characteristic periodicity at a field of 15 mT is 532 nm.

† Matthias.Riepp@desy.de

ISBN: 978-3-95450-210-3 doi:10.18429/JACoW-FEL2019-THB02

Content from this work may be used under the terms of the CC BY 3.0 licence (© 2019). Any distribution of this work must maintain attribution to the author(s), title of the work, publisher, and DOI

UNDERSTANDING 1D TO 3D COHERENT SYNCHROTRON RADIATION EFFECTS

A. D. Brynes*
STFC Daresbury Laboratory & Cockcroft Institute, Warrington, UK

Abstract

Collective effects such as coherent synchrotron radiation (CSR) can have a strong influence of the properties of an electron bunch with respect to the quality of the FEL light that it produces. In particular, CSR experienced by a bunch on a curved trajectory can increase the transverse emittance of a beam. In this contribution, we present an extension to the well-established 1D theory of CSR by accounting fully for the forces experienced in the entrance and exit transients of a bending magnet. A new module of the General Particle Tracer (GPT) tracking code was developed for this study, showing good agreement with theory. In addition to this analysis, we present experimental measurements of the emittance growth experienced in the FERMI bunch compressor chicane as a function of bunch length. When the bunch undergoes extreme compression, the 1D theory breaks down and is no longer valid. A comparison between the 1D theory, experimental measurements and a number of codes which simulate CSR differently are presented, showing better agreement when the transverse properties of the bunch are taken into account.

INTRODUCTION

Synchrotron radiation – the emission of radiation by a charged particle when travelling on a curved trajectory – can become coherent when the length of a particle bunch is shorter than the wavelength of the radiation emitted. This coherent synchrotron radiation (CSR) can degrade the quality of an electron bunch, causing an increase in projected and slice emittance, and energy spread [1–5]. The theoretical explanation of CSR has made significant progress since its initial formulation [6–11], and some experimental studies have demonstrated good agreement between experimental measurements and simulation results [3, 4].

Much of the existing literature on CSR, however, neglects to account for the transverse extent of the electron bunch, however, and this may become increasingly important for future free-electron laser (FEL) facilities and schemes which place increasingly stringent demands on high-brightness, high quality electron bunches. We present some new insights on the theory of the 1D CSR transient field at the edges of dipole magnets, based on the interactions between the velocity and acceleration components of the Liénard-Wiechert field. This work suggests novel compressor designs for the minimization of this instability. A new CSR feature of the General Particle Tracer (GPT) [12] tracking code was developed specifically for this study, which does not use the small-angle or ultrarelativistic approximations.

* alexander.brynes@stfc.ac.uk

A number of other codes exist which are capable of simulating the effects of CSR [13, 14], some of which utilise a 1D approximation, based on Refs. [15, 16], and others which extend the model to incorporate 2D and 3D effects [17–19]. While previous studies have shown good agreement between results from some of these simulation codes and experimental data [3, 4], there is a point at which the 1D approximation is no longer valid, as shown in [20], which suggests that projecting the bunch distribution onto a line may overestimate the level of coherent emission, particularly when the bunch has a large transverse-to-longitudinal aspect ratio. There are a number of effects that must be included for a simulation code to fully take account of 3D CSR effects, including (but perhaps not limited to):

1. Taking the transverse extent of the bunch into account for all particles, rather than assuming that all electrons emit and receive on-axis.

2. Self-consistently solving for the trajectory during emission rather than neglecting deviations from the nominal trajectory.

3. Taking the full Liénard-Wiechert field into account rather than only the term which arises during acceleration.

4. Including stochastic effects due to the long-range interaction between a discrete number of radiation cones.

One of the aims of this study is to determine if, during strong bunch compression, or for bunches with a large transverse-to-longitudinal aspect ratio, the limits of the 1D approximation could be found. This is achieved through comparing analytic results with simulation codes that incorporate the transverse bunch distribution, and with experimental data. The projected emittance of the electron beam was measured in parameter scans at the exit of the first bunch length compressor of the FERMI FEL [21, 22].

NUMERICAL VALIDATION

An extension to the 1D theory of CSR was presented in [23], which demonstrated the importance of the so-called 'velocity' term of the Liénard-Wiechert field in cases when an electron bunch enters and exits a bending magnet. It was demonstrated that, while the radiation cone from a particle is reduced in volume as the particle becomes ultrarelativistic, there is a small spike in the field experienced by a receiving particle as it enters or exits the curved trajectory which is due to this term. For a full derivation of this effect, see [23]. In order to validate these analytic results, we have

ISBN: 978-3-95450-210-3 doi:10.18429/JACoW-FEL2019-THB04

LONGITUDINAL PHASE SPACE STUDY ON INJECTOR BEAM OF HIGH REPETITION RATE X-RAY FEL*

Qiang Gu†, Zhen Wang, Shanghai Advanced Research Institute, Shanghai, China

Abstract

The longitudinal phase space of electron beam from the high repetition rate injector usually twisted and deteriorated by the space charge force. It causes the high order correlated energy spread and the local chirp within the beam, which could not be compensated by the harmonic correction before the compression in the linac. As a consequence of this problem, one could not get ideal beam with a peak current more than kiloamperes. In this paper several approaches have been studied to relieve this effect and get the well compressed beam for the lasing.

INTRODUCTION

Two high repetition rate X-ray free electron laser facilities based on the continuous wave linac are under construction [1-2]. In the early stage of the LCLS-II injector design, people have compared the beam dynamics optimization, as well as the beam performance between the VHF gun and DC gun based injectors. Both of the injectors shown the good transverse emittance, but the longitudinal phase space of the electron beam at the exit of the DC gun based injector had larger high order correlated energy spread which could not be compensated before compression system in main linac. Finally, the VHF gun has been adopted by LCLS-II.

Table 1: Main Parameters of the Electron Beam

Parameter	Value	Unit
Beam energy	8	GeV
Slice emittance, nor.	0.2-0.7	μmrad
Bunch charge	10-300	pC
Repetition rate, max.	1	MHz
Peak current	0.5-1.5	kA

SHINE is a hard X-ray free electron laser facility with a shortest FEL wavelength of 15keV. The main parameters of the electron beam are listed in Table 1. To obtain the FEL with higher energy, LCLS-II HE chose the lower emittance [3], while SHINE chose higher peak current and even higher peak current is preferred for the higher photon energy up to 25keV. LCLS-II and SHINE now has adopted a photo-injector consisting of a VHF gun followed by a velocity bunching and accelerating system to generate the qualified beam. It has shown that even with the VHF gun, the high order correlated energy spread is too large to get a beam current larger than kA. The solution for SHINE is to linearize the global or local high order correlated energy spread before compression and it is better to complete the correction locally in the injector.

The high repetition rate photo injector usually consists of a photo cathode gun which generates the electron beam, followed by a velocity bunching system to reduce the bunch length which could be accepted by the further acceleration and compression in the linac, and an emittance compensation system with solenoids, drifts and acceleration. Here we show the layout of SHINE injector in Figure 1 for example.

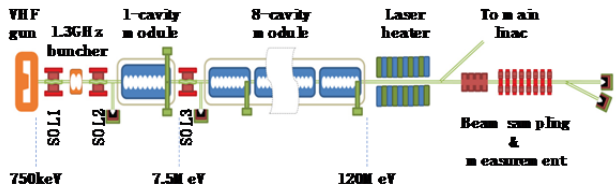


Figure 1: Layout of SHINE injector.

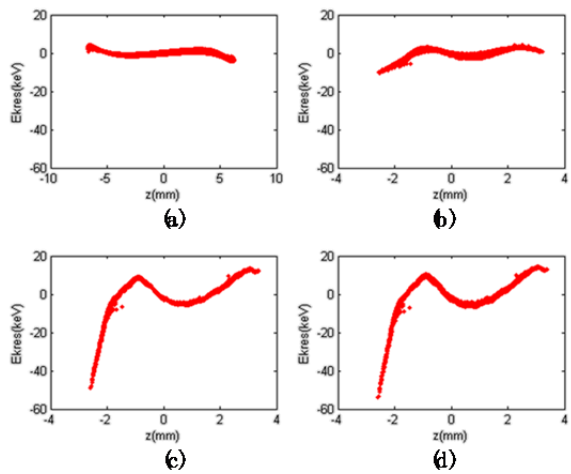


Figure 2: High order energy spread along the injector,
(a) at the middle of the buncher;
(b) at the entrance of the 1-cavity module;
(c) at the entrance of the 8-cavity module;
(d) at the end of the injector.

In the injector, the high order correlated energy spread is driven by the space charge force and velocity bunching process. The initial energy modulation is generated from the cathode to the buncher, which contributes the nonlinear chirp during the bunching process. Together with the nonlinear velocity modulation from the buncher, the nonuniform longitudinal density distribution of the bunched beam is produced. After bunching, this distribution enhances the energy modulation when the electron beam goes through the accelerating and drifting. Growth of the energy modulation almost stops at the end of the injector,

* Work supported by SHINE project
† guqiang@sinap.ac.cn

Content from this work may be used under the terms of the CC BY 3.0 licence (© 2019). Any distribution of this work must maintain attribution to the author(s), title of the work, publisher, and DOI

ISBN: 978-3-95450-210-3 doi:10.18429/JACoW-FEL2019-THP001

STEFFEN HARD-EDGE MODEL FOR QUADRUPOLES WITH EXTENDED FRINGE-FIELDS AT THE EUROPEAN XFEL

N. Golubeva*, V. Balandin, W. Decking, L. Fröhlich, M. Scholz,
DESY, Hamburg, Germany

Abstract

For modeling of linear focusing properties of quadrupole magnets the conventional rectangular model is commonly used for the design and calculations of the linear beam optics for accelerators. At the European XFEL the quadrupole magnets are described using a more accurate Steffen hard-edge model. In this paper we discuss the application of the Steffen approach for the European XFEL quadrupoles and present the examination of the model with the orbit response matrix technique.

INTRODUCTION

The 3.4 km long European XFEL facility is in operation since 2017 and currently serves three FEL beamlines simultaneously for user experiments [1, 2]. The facility is based on superconducting accelerator technology. After the injector which contains one standard superconducting accelerating module and a 3rd harmonic module, the beam is accelerated in the superconducting linear accelerator. To achieve a high peak current, the bunches are longitudinally compressed in three magnetic chicanes which are located in the injector and after the first (Linac 1) and second (Linac 2) parts of the accelerator. Diagnostic sections are placed in the injector and after the second and third compression stages. After the final acceleration in Linac 3 the beam passes a collimation section, and then the bunches of one bunch train are distributed between two electron beamlines leading to the SASE1 and SASE3 undulators and to the SASE2 undulator. Individual bunches can be selectively directed to the linac dump.

In such complicated machine the design linear optics incorporates many constraints on the behaviour of optical functions. For example, in the bunch compressors a special choice of Twiss function reduces the emittance growth due to coherent synchrotron radiation, diagnostic sections have to provide the special conditions for measurements of beam parameters, the optical functions in the collimation section have to be suitable for collimation purposes, the distribution system based on the kicker-septum scheme presents challenges for the dispersion suppression in both planes.

To provide a good performance of such sophisticated design optics, a good knowledge of optical properties of all magnetic elements is required. Before the commissioning, on the stage of the manufacturing of magnets we have arranged the comprehensive set of magnetic measurements. The accurate measurements of longitudinal field and field-gradient profiles have been made for all types of the European XFEL magnets. But an analysis of measured data for quadrupole magnets has shown that for all quadrupoles the conventional hard-edge model does not provide a sufficient accuracy. For example, for the QI quadrupole type the conventional model can not provide more than two correct decimal digits in the transfer matrix elements (see Figure 1), that does not seem to be very satisfactory. This motivated us to consider other models for quadrupole magnets.

In general, having the field gradient profiles one may develop a special code calculating the focusing of quadrupoles with extended fringe-fields, but for practical purposes and especially for online optics calculations it is desirable to employ more practicable model. We have considered a Steffen approach [3] to quadrupole modeling. As it has been shown in the paper [4], for the European XFEL quadrupoles the Steffen parameters exist, and with sufficient for our purposes accuracy can be approximated using low order polynomials in the variable k_0 (mth-order Steffen model). And, for our luck, already the zeroth-order Steffen model can essentially improve the accuracy in comparison with the conventional hard-edge model (see Figure 1). In this paper we discuss the application of the zeroth-order Steffen model for the European XFEL quadrupoles. One should note that although the Steffen approach is not yet widely known, the interest seems to grow during last time (for example, see references in [4]).

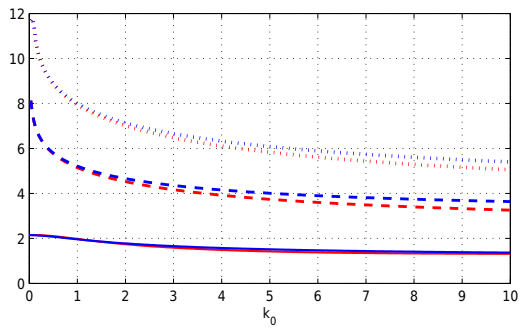


Figure 1: Quadrupole QI. The number of correct decimal digits in the approximation of the transport matrices $M^{\pm}(k_0)$ by conventional rectangular model (solid curves), and by zeroth (dashed curves) and first (dotted curves) order Steffen models. Red and blue colors refer to the focusing and defocusing matrices, respectively.

CONVENTIONAL AND STEFFEN HARD-EDGE MODELS

Optical linear properties of quadrupoles are determined by the quadrupole focusing strength k_0 and by the field gradient shape function $k(s)$ (the longitudinal field gradient profile). Figure 2 shows an example of the function $k(s)$

* nina.golubeva@desy.de

Content from this work may be used under the terms of the CC BY 3.0 licence (© 2019). Any distribution of this work must maintain attribution to the author(s), title of the work, publisher, and DOI

ISBN: 978-3-95450-210-3 doi:10.18429/JACoW-FEL2019-THP002

BEAM BASED ALIGNMENT IN ALL UNDULATOR BEAMLINES AT EUROPEAN XFEL

M. Scholz*, W. Decking, DESY, Hamburg, Germany
Y. Li, European XFEL, Hamburg, Germany

Abstract

The Free Electron Laser European XFEL aims at delivering X-rays from 0.25 keV up to 25 keV out of three SASE undulators. A good overlap of photon and electron beams is indispensable to obtain good lasing performance, especially for the higher photon energies. Thus the quadrupole magnets in the undulators must be aligned as good as possible on a straight line. This can only be realized with a beam based alignment procedure. In this paper we will report on the method that was performed at the European XFEL. We will also discuss our results.

INTRODUCTION

The European XFEL aims at delivering X-rays from 0.25 to up to 25 keV out of 3 SASE undulators [1,2]. The radiators are driven by a superconducting linear accelerator based on TESLA technology [3]. A schematic layout of the European XFEL is shown in Fig. 1. The linac operates in 10 Hz pulsed mode and can deliver up to 2700 bunches per pulse. The electron beam can be distributed to three different undulator beamlines within a pulse [4,5]. The European XFEL is being realized as a joint effort by 12 European countries. European XFEL's accelerator and major parts of the infrastructure are contributed by the accelerator construction consortium, coordinated by DESY.

The alignment of the magnets in FELs, especially in the undulator beamlines is crucial for top performance in the sense of maximum SASE pulse energy. This is especially the case with hard X-ray beamlines, which are extraordinarily sensitive to misalignments. In order to provide an efficient overlap between the electron and photon beams inside the undulator, the electron beam has to go through the undulators on a straight line with displacements below 10 μm. This alignment precision cannot be achieved by traditional optical alignment procedures thus beam based alignment (BBA) becomes necessary. The BBA procedure has been regularly carried out for all undulator beamlines at European XFEL. The method is well tested at other facilities [6, 7] and it was also studied theoretically for European XFEL [8] before the start of the commissioning. We will report on the BBA activities at European XFEL as well as on some results we have achieved so far.

UNDULATOR SECTIONS

The two hard X-ray undulator beamlines SASE1 and SASE2 (see Fig. 1) are build up with 35 undulator cells. SASE3, the soft X-ray undulator consists of 21 undulator cells [9]. Each cell is 6.1 meters long and is composed of the 5 m long undulator itself and a 1.1 m long intersection. The elements of the intersections are, inter alia, a beam position monitor (BPM) as well as a quadrupole magnet. The magnet is mounted on a mover that allow adjusting its position in both transverse directions. The undulator period length is 40 mm for the hard X-ray undulators and 68 mm for the soft X-ray undulator. Figure 2 shows a technical drawing of an undulator cell including the intersection. The beam position monitors in the intersections are cavity BPMs with a sub μm resolution [10]. This is crucial because the alignment has to be accomplished in the μm range.

BEAM BASED ALIGNMENT METHOD

The BBA method has been described in previously published papers and reports e.g. [6–8]. We will refrain from a further description in detail in order to leave room for the presentation of the BBA results. In summary: The goal is to find the offsets of all BPMs as well as of all quadrupole magnets. The concept is to measure the electrons' trajectory for different beam energies while the magnetic field of the quadrupoles is kept constant. This allows to distinguish between BPM offsets, which are not depending on the beam energy, and the quadrupole offsets which lead to an energy depending kick when the they are aligned off axis. The greater the energy difference between the measurement steps, the better the distinction between BPM and magnet offsets. The alignment procedure has to be carried out in several iterations until the final precision can be reached. BBA at European XFEL is carried out with four different electron beam energies, namely 10, 12, 14 and 17 GeV. 5-10 iteration are typically necessary to accomplish the BBA's goal. The whole procedure takes about 4-8 hours depending on the initial beamline setup. A significant part of the time is used to prepare all three undulator beamlines for beam transport with all four electron energies. The electron beam's energy is precisely determined for each energy step. This can be done most efficiently using the highly chromatic beam optics in the collimation section. Comparisons of measured and design trajectory responses to a horizontal kick upstream the collimations section allows to determine the beam energy to a precision in the per mille level. This ensures that the transfer matrices in the undulator, which are necessary to calculate the BPM and magnet offsets, are as precise as possible. For each energy, a machine setup is saved to a dedicated file, which can then be loaded during the BBA iterations within minutes. The fast kicker distribution system of European XFEL [4, 5] allows to do BBA for all three beamlines at the same time. The BBA iterations are always carried out from low to high beam energies.

* matthias.scholz@desy.de

Content from this work may be used under the terms of the CC BY 3.0 licence (© 2019). Any distribution of this work must maintain attribution to the author(s), title of the work, publisher, and DOI

ISBN: 978-3-95450-210-3 doi:10.18429/JACoW-FEL2019-THP003

ARBITRARY ORDER PERTURBATION THEORY FOR A TIME-DISCRETE MODEL OF MICRO-BUNCHING DRIVEN BY LONGITUDINAL SPACE CHARGE

Ph. Amstutz*, Lawrence Berkeley National Lab, Berkeley, USA
M. Vogt, Deutsches Elektronen-Synchrotron DESY, Hamburg, Germany

Abstract

A well established model for studying the micro-bunching instability driven by longitudinal space charge in ultra-relativistic bunches in FEL-like beamlines can be identified as a time-discrete Vlasov system with general drift maps and Poisson type collective kick maps. Here we present an arbitrary order perturbative approach for the general system and the complete all-orders solution for a special example. For this example we benchmark our theory against our Perron-Frobenius tree-code.

INTRODUCTION

Longitudnial dynamics in the magnetic bunch-compressors of free-electron laser injectors can drive a micro-bunching instability, deteriorating the electron bunch quality [1, 2]. As established in References [3, 4] the space-charge driven micro-bunching effect – in the ultra-relativistic limit – be investigated by means of an time-discrete model. In this model the longitudinal dynamics of the system are exactly captured by a combination of drift maps $D[\lambda]\colon \mathbb{R}^2 \to \mathbb{R}^2$

$$D[\lambda]\colon z = (q,p) \mapsto (q + \lambda(p), p)$$

with a dispersion function $\lambda \in C^1(\mathbb{R},\mathbb{R})$ and kick maps $K[k]\colon \mathbb{R}^2 \to \mathbb{R}^2$

$$K[k]\colon (q,p) \mapsto (q, p + k(q))$$

with a kick function $k \in C^1(\mathbb{R},\mathbb{R})$. The collective nature of the micro-bunching is accounted for by adopting the Vlasov-picture, where the electron bunch is described by its probability density in phase space $\Psi\colon \mathbb{R}^2 \to \mathbb{R}$. A remarkable property of the model is the fact that it remains exactly solvable in terms of time-discrete maps, even in presence of *collective* kick functions $k[\Psi]$. It can be shown that a phase-space density (PSD) evolves as

$$\Psi(x) \mapsto \Psi(M^{-1}(x))$$

where M is the solution of the equations of motion of the system. A PSD is therefore propagated by objects defined by

$$\mathcal{M}\Psi := \Psi \circ M^{-1}$$

called Perron-Frobenius operators (PFO). The overall effect of a single bunch-compressor stage is then given by

$$\mathcal{M}[\Psi] = \mathcal{D}_{\text{Chic}}\,\mathcal{K}_{\text{Cav}}\mathcal{K}[\Psi]_{\text{SC}}$$

where $\mathcal{D}_{\text{Chic}}$ is the PFO associated to the drift map describing the dispersive magnetic chicane. $\mathcal{K}_{\text{Cav}}$ and $\mathcal{K}_{\text{SC}}$ are the PFOs of the kick maps describing the impact of the accelerating cavity and the collective self-interaction of the bunch in the field-free region upstream of the chicane, respectively. Thus the complete time-discrete Vlasov system is defined by

$$\Psi \mapsto \mathcal{M}[\Psi]\,\Psi\,.$$

PERTURBATION THEORY

The effect that initially small perturbations $\varepsilon\phi$ of an otherwise homogeneous charge distribution Ψ amplify themselves by virtue of a collective self-interaction

$$\mathcal{M}[\Psi + \varepsilon\phi](\Psi + \varepsilon\phi) \tag{1}$$

is generally referred to as *Micro-bunching*. While PFOs are linear operators in the sense that $\mathcal{M}(c_1\Psi_1 + c_2\Psi_2) = c_1\mathcal{M}\Psi_1 + c_2\mathcal{M}\Psi_2$, collective PFOs are generally not linear in their *internal* dependence on the PSD $\mathcal{M}[c_1\Psi_1 + c_2\Psi_2] \neq c_1\mathcal{M}[\Psi_1] + c_2\mathcal{M}[\Psi_2]$. This drives the need for a perturbation theory to investigate Equation (1), as derived in [4, 5]. It has been shown that Equation (1) for a general collective PFO $\mathcal{M}[\Psi]$ can be expanded in ε

$$\begin{aligned}\mathcal{M}[\Psi_0 + \varepsilon\phi_0](\Psi + \varepsilon\phi_0) &= \mathcal{M}[\Psi_0]\Psi_0 + o(\varepsilon^{N+1}) \\ &+ \sum_{n=1}^{N} \varepsilon^n \left(\mathcal{M}^{(n)}[\Psi_0]\phi_0^n\Psi_0 + \mathcal{M}^{(n-1)}[\Psi_0]\phi_0^n\right) \\ &\equiv \Psi_1 + \sum_{n=1}^{N} \varepsilon^n \phi_{1,n} + o(\varepsilon^{N+1}),\end{aligned} \tag{2}$$

where $\mathcal{M}^{(n)}$ is the n-th Frechet derivative of $\mathcal{M}$. $\Psi_1 \equiv \mathcal{M}[\Psi_0]\Psi_0$ is the solution of the unperturbed system.

For a collective PFO of the form

$$\mathcal{M}[\Psi] = \mathcal{L}\mathcal{K}[k[\Psi]] \tag{3}$$

with an arbitrary non-collective PFO $\mathcal{L}$ it can be shown that the n-th order propagated perturbations take the form

$$\begin{aligned}\phi_{1,n} = (-1)^n\mathcal{M}[\Psi_0]\Big(&\frac{k[\phi_0]^n \circ Q}{n!}\partial_p^n\Psi_0 \\ &-\frac{k[\phi_0]^{n-1} \circ Q}{(n-1)!}\partial_p^{n-1}\phi_0\Big),\end{aligned} \tag{4}$$

where the projection operator $Q\colon \mathbb{R}^2 \to \mathbb{R}$

$$Q\colon (q.p) \mapsto q$$

has been introduced. For a detailed derivation see References [4, 5].

* amstutz@lbl.gov

Content from this work may be used under the terms of the CC BY 3.0 licence (© 2019). Any distribution of this work must maintain attribution to the author(s), title of the work, publisher, and DOI

ISBN: 978-3-95450-210-3 doi:10.18429/JACoW-FEL2019-THP007

FREQUENCY-DETUNING DEPENDENT TRANSIENT COAXIAL RF COUPLER KICK

Y. Chen*[1,2], H. Qian[1], M. Krasilnikov[1], F. Brinker[2], W. Decking[2], J. Good[1], M. Gross[1], P. Huang[1], I. Isaev[1], C. Koschitzki[1], S. Lal[1], X. Li[1], O. Lishilin[1], G. Loisch[1], D. Melkumyan[1], R. Niemczyk[1], A. Oppelt[1], H. Shaker[1], G. Shu[1], F. Stephan[1], G. Vashchenko[1]
[1]DESY, 15738 Zeuthen, Germany; [2]DESY, 22603 Hamburg, Germany

Abstract

A transverse kick which results from the coaxial RF coupler in the L-band RF gun at the Photo Injector Test facility at DESY in Zeuthen (PITZ) has been modeled and characterized. The used RF pulse is typically 600 μs long and used to produce a train of up to 2700 electron bunches. The kick is transient and found to be dependent on the detuning of the resonance frequency of the gun cavity. The frequency-detuning within the RF macro-pulse results in a variation in the kick strength along the pulse. This leads to a downstream orbit and size change of individual bunches within the train. Using 3D RF field distributions, calculated at detuned frequencies of the cavity, particle tracking simulations are performed to simulate the behavior of the transient kick onto the electron bunch. The temperature of the cooling water for the gun is tuned, allowing detailed characterization of the frequency-detuning within the RF pulse and thereby measurements of the kick which are of practical interest. Systematic measurements of the kick along the bunch train have meanwhile been carried out. The results will be presented and discussed.

INTRODUCTION

The European X-ray Free-Electron Laser (XFEL) provides excellent opportunities in pursuing excellence in physics and advanced applications of coherent x-ray radiation [1]. The photoelectron source in use at the European XFEL is a photocathode RF gun developed at the Photo Injector Test facility at DESY in Zeuthen (PITZ) [2, 3]. The key component of the PITZ gun is a 1.6-cell 1.3 GHz copper resonator. The gun can be operated with a high electric field gradient of about 60 MV/m on the cathode surface with long RF pulses of up to 650 μs at a repetition rate of 10 Hz. This allows the production of a maximum number of 27000 bunches per second at the XFEL and results in a high peak RF power of about 6.5 MW in the cavity while a high average RF power of about 42 kW dissipates in a rather short cavity length of about 20 cm and a cavity radius of about 9 cm. The RF power in the gun is supplied by a 10 MW multi-beam klystron. The power is coupled from the input waveguide via a door-knob transition into the rotationally symmetric coaxial coupler and the gun cavity.

A transient transverse kick, due to the disturbed RF fields of rotational symmetry by the transition from the input rectangular waveguide to the coaxial power coupler of the PITZ gun, has been simulated and quantified in [4]. In this paper, we present the dependency of the kick on the detuning of the resonance frequency of the gun cavity within the RF pulse. The effect is then demonstrated in both simulation and experiment. Consequently, measurements of the resulting downstream orbit and size change of individual bunches along the train are reported.

KICK VS. FREQUENCY-DETUNING

The reflection coefficient (S_{11}) is defined as the ratio of the reflected power over the forward power for a resonant cavity with a resonance frequency f_0 (~1.3 GHz for the PITZ case) fed by the RF with a frequency f. In order to protect the microwave source (klystron), the reflected power from the cavity must be low (typically $\ll$ 2 MW). This requires a resonant frequency kept close to the RF frequency. The frequency-detuning, $\Delta f = f - f_0$ is then used to describe how much the cavity is detuned from its resonance.

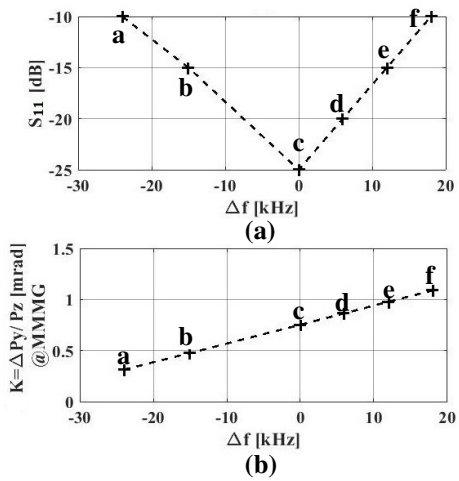


Figure 1: Simulated reflection coefficient and kick dependency on frequency-detuning.

Simulation

To simulate the kick behavior in response to the frequency-detuning, a simplification is made in the simulations: the RF frequency is varied at the port position of the input waveguide (see Fig. 1 in Ref. [4]) for defining the detuned frequency w.r.t. the cavity resonance. This allows computing 3D RF field distributions of the gun cavity at the detuned frequencies in frequency domain calculation. Using the obtained field distributions, particle tracking simulations using CST Particle Studio [5] are enabled and the kick strength

* ye.lining.chen@desy.de

Content from this work may be used under the terms of the CC BY 3.0 licence (© 2019). Any distribution of this work must maintain attribution to the author(s), title of the work, publisher, and DOI

ISBN: 978-3-95450-210-3 doi:10.18429/JACoW-FEL2019-THP008

DESIGN OF A MULTI-CELL SRF REDUCED-BETA CAVITY FOR THE ACCELERATION OF LOW ENERGY ELECTRON BEAMS

D. Bazyl, H. De Gersem, W.F.O. Müller, TEMF, TU Darmstadt, Darmstadt, Germany
J. Enders, S. Weih, Institut für Kernphysik, TU Darmstadt, Darmstadt, Germany

Abstract

A recent upgrade of the superconducting Darmstadt linear accelerator (S-DALINAC) allowed the operation in the energy recovery linac (ERL) regime. The ERL mode provides significant benefits for free electron laser (FEL) experiments. At the same time, it imposes strict requirements for the quality of the accelerated beams. Presently, an increased longitudinal energy spread is observed at the S-DALINAC due to the mismatch in phase in the first accelerating structure, which is a superconducting radio-frequency (SRF) 5-cell $\beta = 1$ cavity. In this work we discuss an alternative design for accelerating low-energy electron beams using an SRF multi-cell cavity with a constant geometric β.

INTRODUCTION

Historically, the S-DALINAC is the third superconducting particle accelerator in the world [1]. Recently, the accelerator has been commissioned for ERL operation [2]. High currents available at ERLs prove beneficial for driving FELs or other radiation sources, and, hence, investigating ERL beam dynamics at the S-DALINAC is expected to provide insight into FEL operation in multiturn ERLs. Historically, the S-DALINAC has been the driver of the first German FEL [3].

There are several projects aimed at improving the performance of the S-DALINAC. This work deals with finding a solution for the problem of the significantly increased energy spread of the beam that has been observed at the S-DALINAC. The increased energy spread originates from the capture section which is a part of the injector linac.

Two electron guns are available at the S-DALINAC: a spin polarised gun (SPG) and a thermionic gun (TG), which produce electron beams with initial energies of 200 keV (after upgrade [4]) and 250 keV, respectively. The purpose of the injector linac is to accelerate these low-energy electron beams. Presently, it consists of a 3 GHz 5-cell SRF $\beta = 1$ cavity and two 3 GHz 20-cell SRF $\beta = 1$ cavities. Initially, in addition to the 5-cell structure a 2-cell cavity with a reduced value of geometric β has been implemented in order to preaccelerate the beam. Figure 1 shows the cooling cryostat (red) which hosts the 2-cell and the 5-cell cavity and the RF power input system (green). Nowadays, the 2-cell cavity is permanently out of operation and cannot be replaced without a new cryostat. This situation necessitates to accelerate electron beams with relative velocities β of 0.69 in the 5-cell $\beta = 1$ cavity. A significant mismatch in phase results in an inefficient acceleration (see Fig. 2) and an increased energy spread of 27 keV for the output beam.

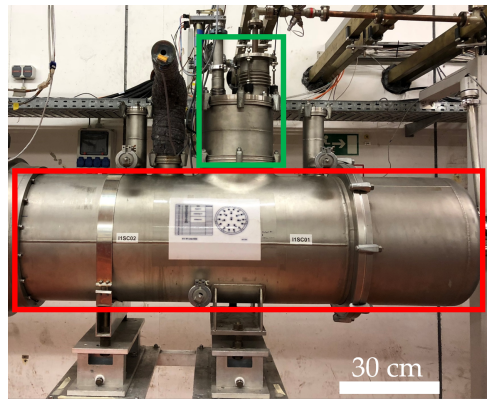


Figure 1: Cryostat.

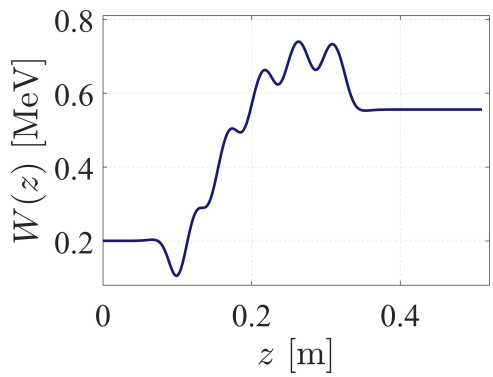


Figure 2: Energy gain of the beam in the 5-cell cavity.

UPGRADE OF THE CAPTURE SECTION

In order to reduce the energy spread of the beam at the S-DALINAC, the 5-cell cavity must be replaced with a new cavity. The new cavity must be capable of accelerating the electron beam up to an energy of at least 1 MeV while keeping the energy spread minimal. Other important requirements for the new structure are mechanical reliability and minimal investment costs.

The most commonly used methods for the acceleration of low energy electron beams are normal conducting β-graded cavities and SRF 1-cell or 2-cell independently driven structures. At the S-DALINAC spatial restrictions exclude a possibility of implementation of a normal conducting cavity for the injector linac. The implementation of independently driven SRF cavities would require a new cryostat, thereby failing to satisfy the minimal investment-cost requirement.

Hence, a cavity that can be operated with the existing cooling cryostat and the existing RF input power system was developed. As result of a quantitative and qualitative analysis, a 6-cell reduced-β cavity has been designed and will replace the 5-cell cavity [5]. The 6-cell cavity is now

Content from this work may be used under the terms of the CC BY 3.0 licence (© 2019). Any distribution of this work must maintain attribution to the author(s), title of the work, publisher, and DOI

ISBN: 978-3-95450-210-3 doi:10.18429/JACoW-FEL2019-THP009

SPACE CHARGE FIELD BEAM DYNAMICS SIMULATIONS FOR THE THz SASE FEL AT PITZ*

S. A. Schmid†, E. Gjonaj, and H. De Gersem, TU Darmstadt, TEMF, Darmstadt, Germany
M. Krasilnikov, DESY, Zeuthen, Germany
M. Dohlus, DESY, Hamburg, Germany

Abstract

A proof-of-principle experiment on a THz SASE FEL is under consideration at the Photo Injector Test facility at DESY in Zeuthen (PITZ). One of its options assumes utilization of 4.0 nC bunches at 16.7 MeV [1]. In this operation mode, space charge interaction strongly influences the dynamics of the electron beam inside the undulator. In this contribution, we investigate the beam dynamics in the THz undulator of PITZ using a particle-particle interaction model based on a Liénard-Wiechert approach. We analyze the influence of retardation and radiation fields on the beam dynamics resulting in the microbunching effect. Furthermore, we compute the radiation field and estimate the radiation power at the exit of the undulator. The validity of the underlying numerical models is discussed.

INTRODUCTION

The photoinjector test facility at DESY in Zeuthen (PITZ) is currently developing a high power, tunable THz radiation source for pump and probe experiments at the European XFEL [1]. The source design uses SASE-FEL to generate THz pulses with 100 µm center wavelength and up to ~ 40 MW peak power [1]. Reaching the design specifications requires a 16.7 MeV electron beam with up to 4.0 nC bunch charge. Due to the moderate energy, space charge induced beam divergence along the 3.4 m long FEL undulator is extremely critical. In the following, we use a 3D, fully relativistic Liénard-Wiechert simulation code [2] to analyze the beam dynamics inside the undulator. Furthermore, we evaluate the particle fields at the exit of the undulator and investigate the generation of THz radiation.

MODELING APPROACH

The undulator field is modeled as,

$$\vec{B}(\vec{r}) = -B_0 \cdot \vec{\nabla}\phi(y,z), \tag{1}$$

$$\phi(y,z) = \sinh(k_u y)\sin(k_u z)/k_u \tag{2}$$

using a periodic 2D potential of an idealized planar undulator [3]. In addition to the oscillatory motion of the particles in the x-direction, this model allows to reproduce the undulator focusing effect in the y-direction. The parameter values for the field amplitude $B_0 = 1.28$ T and the undulator wavelength $\lambda_u = 2\pi/k_u = 3.0$ cm reflect the experimental setup described in [1]. Figure 1 shows the magnetic field map for a 3.6 m long undulator with 120 periods as used in the simulations. We use a linearly increasing or decreasing amplitude, $B_0 = B_0(z)$, towards the entrance or exit of the undulator, respectively, to guarantee a smooth transition of the particle beam at both undulator ends.

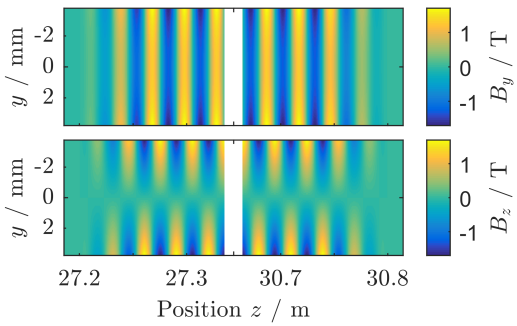


Figure 1: Magnetic field map used in the simulations. Only a small section including the entrance and exit of the 3.6 m long undulator model is shown.

A complete electromagnetic field model for relativistic particles undergoing oscillatory motion has to take retardation and radiation effects into account. Our simulation code [2] models the space charge interaction based on the Liénard-Wiechert (LW) fields of a charged particle moving along a trajectory $r_s = r_s(t)$:

$$\vec{E}(\vec{r},t) = \frac{q_s \left\{ \underbrace{\frac{\left(\vec{n}_s - \vec{\beta}_s\right)}{\gamma_s^2 \, |\vec{r} - \vec{r}_s|^2}}_{\text{static}} + \underbrace{\frac{\vec{n}_s \times \left[\left(\vec{n}_s - \vec{\beta}_s\right) \times \dot{\vec{\beta}}_s\right]}{c_0 \, |\vec{r} - \vec{r}_s|}}_{\text{radiation}} \right\}}{\left(1 - \vec{n}_s \vec{\beta}_s\right)^3}, \tag{3}$$

$$\vec{B}(\vec{r},t) = \frac{\vec{n}_s \times \vec{E}(\vec{r},t)}{c_0}, \tag{4}$$

where q_s is the charge of the particle, c_0 the speed of light, γ_s the Lorentz factor, $\beta_s = \dot{r}_s/c$, and $\vec{n}_s \equiv (\vec{r} - \vec{r}_s)/|\vec{r} - \vec{r}_s|$. All s-indexed expressions in (3) have to be evaluated at the retarded time t_s such that

$$c_0(t - t_s) = |\vec{r} - \vec{r}_s| \tag{5}$$

holds. Equations (3) and (4) need to be evaluated for every particle pair. This implies, first, that the calculation of space charge forces in this simulation model scales with N^2, where N is the number of particles. Second, the full history of

* This work is supported by the DFG in the framework of GRK 2128.
† schmid@temf.tu-darmstadt.de

Content from this work may be used under the terms of the CC BY 3.0 licence (© 2019). Any distribution of this work must maintain attribution to the author(s), title of the work, publisher, and DOI

ISBN: 978-3-95450-210-3 doi:10.18429/JACoW-FEL2019-THP010

SIMPLE AND ROBUST FREE ELECTRON LASER DOUBLER*

S. Di Mitri †, G. De Ninno[1], R. Fabris, S. Spampinati, Elettra Sincrotrone Trieste, 34149, Italy
N. R. Thompson[2], ASTeC, STFC Daresbury Laboratory, Warrington,WA44AD Cheshire, UK
[1]also at Laboratory of Quantum Optics, University of Nova Gorica, Nova Gorica 5001, Slovenia
[2]also at Cockcroft Institute, Sci-Tech Daresbury, Warrington, WA44AD, UK

Abstract

We present the design of a Free-Electron Laser (FEL) doubler suitable for the simultaneous operation of two FEL lines. The doubler relies on the physical selection of two longitudinal portions of an electron bunch at low energy, and on their spatial separation at high energy. Since the two electron beamlets are naturally synchronized, FEL pump-FEL probe experiments are enabled when the two photon pulses are sent to the same experimental station. The proposed solution offers improved flexibility of operation w.r.t. existing two-pulse, two-color FEL schemes, and allows for independent control of the color, timing, intensity and angle of incidence of the radiation pulses at the user end station. Detailed numerical simulations demonstrate its feasibility at the FERMI FEL facility.

INTRODUCTION

We propose a scheme in which two longitudinal portions of the electron bunch (beamlets) are physically selected with a thick mask at low energy in the linac (beam scraping), and spatially separated with a septum magnet at high energy. Each beamlet is then sent to a distinct undulator line. Unlike any of the preceding schemes, ours allows the simultaneous operation of two FEL lines, naturally synchronized at (sub-)fs level, with continuously tuneable relative delay from few fs to ps. Since two undulator lines are used, full and independent control of color, timing, intensity and angle of incidence of the individual radiation pulses on the sample is ensured. If the two FEL pulses are directed to the same user end station, FEL-pump FEL-probe experiments can be done with unprecedented flexibility, either in self-amplified spontaneous emission (SASE) [1,2] or in seeded configurations [3,4].

ELECTRON BEAM MANIPULATION

The scheme is sketched in Fig. 1, and typical parameters at FERMI [5,6] are considered in the following as a case study. A high brightness electron bunch is generated in a photo-injector (gun) and time-compressed in a magnetic chicane (BC1). The bunch length compression factor is $C \equiv \frac{\sigma_{t,i}}{\sigma_{t,f}} \cong \left(1 - \frac{R_{56}\sigma_\delta}{c\sigma_{t,i}}\right)^{-1}$, with $\sigma_\delta = 2\%$ the relative energy spread linearly correlated to the initial bunch duration $\sigma_{t,i} = 2.8$ ps. A mask with two apertures is installed in the middle of BC1, where the particles horizontal position w.r.t. the reference trajectory is $x(s) \cong \eta_x(s)\delta$, and betatron oscillations can be neglected. The mask, made of ~10 mm thick copper, physically selects two transversally displaced beamlets, the rest of the bunch being scattered at large angles and absorbed in the chamber. Since the chicane is achromatic, the two beamlets exit BC1 separated both in energy and in time, but spatially aligned. With V-shape geometry, the vertical position of the mask determines both the width of the two apertures and their transverse separation. The beamlets duration at the exit of BC1, as well as their time separation, is estimated by [7] $\Delta t_{FWHM} \approx \frac{2\Delta x}{\eta_x}\frac{\sigma_{t,i}}{C\sigma_\delta}$, with Δx either the apertures width or the width of the central slit, respectively. For example, with C = 10 and Δx = 3 mm, $\Delta t_{FWHM} \approx 320$ fs.

Downstream of BC1, the linac RF phases are adjusted to ensure both a large relative energy offset of the beamlets (δ_f), which is suitable for their spatial separation in the switchyard, and a small energy spread in each beamlet ($\sigma_{\delta,f}$), as required for efficient lasing. The RF phasing takes into account the effect of the longitudinal wakefields excited by the leading beamlet on the trailing one. For example, we obtain in simulation δ_f = 0.9% and $\sigma_{\delta,f}$ = 0.04%. Doing so, the final mean energy is lowered from 1.40 GeV for the standard whole bunch preparation, to 1.25 GeV (see Fig. 2).

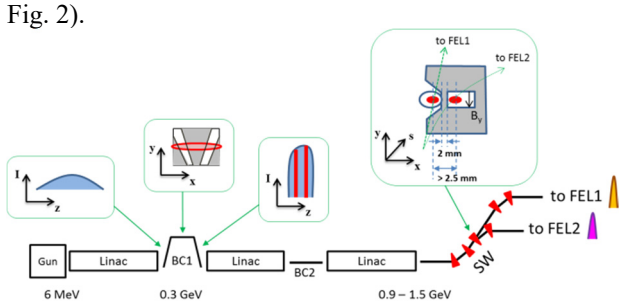


Figure 1: FEL doubler applied to FERMI (not to scale): selection of electron beamlets in BC1 with a mask (red slices), and separation in the switchyard (SW) with a septum magnet.

The FERMI switchyard (SW in Fig. 1) is a ~40 m long line working in the energy range 0.9-1.5 GeV. It comprises two branches, each including two modified double bend achromatic cells. The first cell is in common, and the dipoles bending angle is 3 deg. The two branches lead to the FEL1 and FEL 2 undulator lines; these are parallel and separated by 1 m. Depending on the electron beam energy and on the resonant harmonic jump set by the variable gap undulators, FERMI covers the fundamental wavelength range 20–100 nm with FEL1, and 4–20 nm with FEL2, in high gain harmonic generation (HGHG) mode of operation [3].

For the purpose of separating the beamlets in the bending plane, the SW optics was modified. A dispersion function

* Work supported by European Union's Horizon2020 research and innovation programme under Grant Agreement No. 777431
† simone.dimitri@elettra.eu

Content from this work may be used under the terms of the CC BY 3.0 licence (© 2019). Any distribution of this work must maintain attribution to the author(s), title of the work, publisher, and DOI

ISBN: 978-3-95450-210-3 doi:10.18429/JACoW-FEL2019-THP011

EXPERIMENTAL BENCHMARKING OF WAKEFIELDS AT THE FERMI FEL LINAC AND UNDULATOR LINE

S. Di Mitri †,1,2, L. Sturari[1], Elettra Sincrotrone Trieste, Trieste, Italy
C. Venier, R. Vescovo, University of Trieste, Dept. of Engineering, Trieste, Italy
[2]also at University of Trieste, Dept. of Physics, Trieste, Italy

Abstract

Collective effects such as wakefields affect the dynamics of high brightness electron beams in linear accelerators (linacs), and can degrade the performance of short wavelength free-electron lasers (FELs). If a reliable model of wakefields is made available, the accelerator can be designed and configured with parameters that minimize their disrupting effect. In this work, the simulated effect of geometric (diffractive) wakefields and of coherent synchrotron radiation on the electron beam energy distribution at the FERMI FEL is benchmarked with measurements, so quantifying the accuracy of the model. Wakefields modelling is then extended to the undulator line, where particle tracking confirms the limited impact of the resistive wall wakefield on the lasing process. The study reveals an overall good understanding of collective effects in the facility.

INTRODUCTION

At the FERMI FEL [1,2], a systematic study of collective effects has been carried out since the early stage of machine design [3–7]. In the last decade, numerical predictions were benchmarked with experimental results to demonstrate the interplay of longitudinal geometric wakefields and beam current profile [8,9], to quantify the effect of transverse wakefields on the beam projected emittance [10,11], and to compare 1- vs. 3-dimensional CSR effects on the beam emittance [12–14]. They all confirm, on top of the routine operation of the facility, that the electron beam dynamics is strongly affected by geometric (diffractive) wakefields in the linac sections (L0–L4 in Fig.1), and by CSR emission in the magnetic chicane devoted to bunch length compression (BC1). In addition to this, a semi-analytical formulation of the resistive wall wakefield in the undulator elliptical vacuum chamber was provided [15]. Still, a systematic characterization of the longitudinal wakefields acting in the linac, as well as a start-to-end particle tracking run in the presence of resistive wall wakefield in the undulator line, is lacking. The present work targets these two points.

After a theoretical introduction to wakefields, we complement the aforementioned studies by investigating the effect of linac geometric wakefields and of CSR on the beam energy distribution. The effect is quantified by measuring the beam mean energy and energy spread in a spectrometer line installed at the linac end, as function of bunch length and bunch charge. The final bunch length is determined by magnetic compression, and it was varied by scanning the RF phase of the upstream linac. The bunch charge was varied by changing the intensity of the laser pulse that drives the photoelectron emission at the Gun cathode. The study is extended to the computation and simulation of resistive wall wakefields in the FERMI FEL-2 undulator vacuum chamber. This is the second and longer undulator line of the two currently installed at FERMI. It is devoted to the emission of the shortest FEL wavelengths, in the range 4–20 nm, and it is expected to be more sensitive to the degradation of electron beam brightness.

The FERMI layout is sketched in Fig.1. The electron beam is generated in the RF Gun by photoelectron emission from a Copper cathode illuminated by a UV laser. Electrons are accelerated up to 1.5 GeV in the L0–L4 S-band linac sections. It is time-compressed, nominally by a factor ~10, in the BC1 bunch compressor, at the energy of 0.3 GeV (BC2 is not used routinely). Each linac section includes different travelling wave accelerating structures, which are grouped by length and inner geometry. They are of type “INJ” (3.2 m-long each; 9 mm average radius), “LIL” (4.5 m-long each; 10 mm average radius), “BTW” (6.1 m-long each; 5 mm average radius), and “X-band” (0.75 m-long; 5 mm average radius). “LH” stays for laser heater. The whole linac is 175 m long. The Spreader transfer line is ~30 m long. The FEL-1 and FEL-2 undulator lines are, respectively, 30 m and 44 m long.

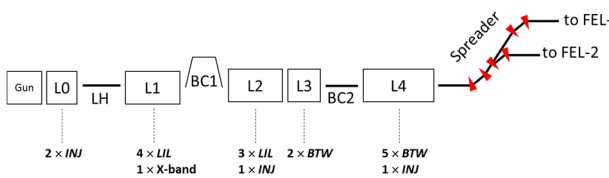


Figure 1: Sketch (not to scale) of the FERMI electron beam delivery system. Published in [16].

WAKEFIELDS MODEL

Geometric Wakefield in RF Cavities

The analytical expressions of the FERMI linac wake functions, in unit of V/(pC m), are given in Eq.1, and are plotted in Fig.2. They well represent the e.m. field pattern established along the whole multi-cell accelerating structure, and apply to bunch lengths shorter than 5 mm [3,5]. The upper-case label of each wake function refers to the structures naming in Fig.1. Please note that the numerical coefficients are consistent with the s-coordinate expressed in units of meter.

$$w_l^{INJ}(s) = 380 \cdot e^{-\sqrt{\frac{s}{1.28 \cdot 10^{-3}}}}$$
$$w_l^{LIL}(s) = 311 \cdot e^{-\sqrt{\frac{s}{1.38 \cdot 10^{-3}}}} \quad (1)$$

† simone.dimitri@elettra.eu

Content from this work may be used under the terms of the CC BY 3.0 licence (© 2019). Any distribution of this work must maintain attribution to the author(s), title of the work, publisher, and DOI

ISBN: 978-3-95450-210-3 doi:10.18429/JACoW-FEL2019-THP012

COMPACT FEL-DRIVEN INVERSE COMPTON SCATTERING GAMMA-RAY SOURCE

M. Placidi[1], G. Penn, Lawrence Berkeley National Laboratory, Berkeley, CA 94720, USA
S. Di Mitri†, Elettra - Sincrotrone Trieste S.C.p.A., 34149 Basovizza, Trieste, Italy
C. Pellegrini[2], Stanford Linear Accelerator Center, Menlo Park, CA 94025, USA
[1]on leave
[2]also at University of California, Los Angeles, CA 90095, USA

Abstract

We explore the feasibility of a compact source of quasi-monochromatic, multi-MeV gamma-rays based on Inverse Compton Scattering (ICS) from a high intensity ultra-violet (UV) beam generated in a free-electron laser by the electron beam itself [1]. This scheme introduces a stronger relationship between the energy of the scattered photons and that of the electron beam, resulting in a device much more compact than a classic ICS for a given scattered energy. The same electron beam is used to produce gamma-rays in the 10-20 MeV range and UV radiation in the 10-15 eV range, in a ~4x22 m^2 footprint system.

INTRODUCTION

We discuss the feasibility and the performance of an Inverse Compaton Scattering (ICS)-based scheme where the electron beam interacts with its own radiation emitted in a Free Electron Laser (FEL). The energy of the outgoing radiation has a steeper dependence on the electron energy than a classical ICS scheme, thus providing a relatively compact layout.

Methods of X-ray production presently include ICS facilities and synchrotron radiation sources from insertion devices in electron storage rings. Contrast imaging of massive sculptures would profit [2] from radiation sources more powerful than the X-ray CT industrial instruments operating in the 450 keV range. Specific case studies can be identified, for example, on the basis of the energy content of the scattered light. At low photon energy (up to few MeV), contrast imaging of massive objects in Geo-archeology [2] would greatly benefit from such an intense and compact source, and this was actually the driving case of this work. At photon energies in the 1–10 MeV range, photons propagating though dense materials prompt nuclear reactions, generating *e.g.* alpha particles and neutrons, which can be easily identified and used for isotope separation [3]. At photon energies higher than 10 MeV, the proposed scheme would approach the specifications for an elastic photon-photon scattering source for frontier experiments in QED [4]. As a by-product of the proposed scheme, a naturally synchronized UV beam with large fraction of coherent photons at 100 fs duration level, ideal for pump-probe experiments, would be provided by the FEL. High-flux multi-MeV gamma-ray beams and UV radiation can be simultaneously available for applications in Nuclear Physics, Security Inspections, Cultural Heritage and UV Science.

FEL-ICS CONCEPT

In a classical ICS process a relativistic electron transfers a fraction of its energy to an incoming laser photon which is scattered in the electron direction of flight with a Doppler-upshifted frequency. The scattered radiation energy

$$E_s = \frac{a_C}{1+X}\,\gamma^2 \hbar\omega_{ph} \qquad (1)$$

exhibits a quadratic energy dependence on the electron energy as the incoming photon energy is constant. The kinematic factor

$$a_c \approx \frac{2\,(1+cos\varphi)}{1+(\gamma\theta)^2} \leq 4 \qquad (2)$$

modulates the scattered energy via the collision angle φ within the semi-aperture θ of the emission cone, while the term

$$X = 4\gamma\frac{\hbar\omega_{ph}}{m_e} \qquad (3)$$

accounts for the recoil of the electron [5].

The FEL-ICS scheme introduces a stronger γ-dependence by making the relativistic electron beam interact with its own UV radiation produced in an FEL [6]. The on-axis FEL radiation wavelength is related to the axial electron velocity β_z and the undulator period λ_u as [7]:

$$\lambda_r = \lambda_u\frac{1-\beta_z}{\beta_z} \approx \frac{\lambda_u}{2\gamma^2}(1+a_u^2) \qquad (4)$$

Here $a_u = K_u = eB_0\lambda_u/2\pi m_e c = 93.4\,B_0[T]\,\lambda_u[m]$is the helical undulator parameter, B_0 the undulator central magnetic field, e the electron charge. The energy of the FEL photons in terms of the electron energy reads:

$$E_r \equiv \frac{hc}{\lambda_r} = a_{FEL}hc\frac{\gamma^2}{\lambda_u} \qquad (5)$$

where we define $a_{FEL} = 2/(1+a_u^2)$ for on axis undulator radiation. When the FEL photon energy (5) replaces that from the laser in (1), the scattered photon energy can be written as:

$$E_s = a_C E_r\gamma^2 = a_C\,a_{FEL}\,hc\frac{\gamma^4}{\lambda_u}. \qquad (1')$$

The term (3), of the order of 10^{-2}, has been neglected in this kinematic scaling. Introducing the Compton wavelength $\lambda_c=hc/m_ec^2$=2.426x10^{-3} nm, the scattering efficiency, *i.e.* the fraction of the electron energy transferred to the scattered photons, reads

† simone.dimitri@elettra.eu

Content from this work may be used under the terms of the CC BY 3.0 licence (© 2019). Any distribution of this work must maintain attribution to the author(s), title of the work, publisher, and DOI

ISBN: 978-3-95450-210-3 doi:10.18429/JACoW-FEL2019-THP013

USER OPERATION OF SUB-PICOSECOND THz COHERENT TRANSITION RADIATION PARASITIC TO A VUV FEL

S. Di Mitri †,1, N. Adhlakha, E. Allaria, L. Badano, G. De Ninno[2], P. Di Pietro, G. Gaio, L. Giannessi[3], G. Penco, A. Perucchi, P. Rebernik Ribic, S. Spampinati, C. Spezzani, M. Trovo', M. Veronese, Elettra - Sincrotrone Trieste S.C.p.A., Basovizza, Trieste, Italy
S. Lupi, Sapienza University of Rome, Italy
E. Roussel, PhLAM/CERCLA, Villeneuve d'Ascq Cedex, France
Federica Piccirilli, IOM-CNR, Trieste, Italy
[2]also at University of Nova Gorica, Slovenia
[3]also at ENEA C.R. Frascati, Rome, Italy

Abstract

Coherent transition radiation is enhanced in intensity and extended in frequency spectral range by the electron beam manipulation in the beam dump beam line of the FERMI FEL, by exploiting the interplay of coherent synchrotron radiation instability and electron beam optics [1]. Experimental observations at the TeraFERMI beamline [2] confirm intensity peaks at around 1 THz and extending up to 8.5 THz, for up to 80 µJ pulse energy integrated over the full bandwidth. By virtue of its implementation in an FEL beam dump line, this work might stimulate the development of user-oriented multi-THz beamlines parasitic and self-synchronized to VUV and X-ray FELs.

INTRODUCTION

This study demonstrates that coherent transition radiation (CTR) with sub-picosecond duration, up to nearly 80-µJ pulse energy in the THz gap, was produced by exploiting the electrons' interaction with coherent synchrotron radiation (CSR) emitted in the post-undulator dispersive region of the VUV FERMI free electron laser (FEL) [3,4]. THz radiation with those characteristics finds application in experiments involving, for example, resonantly exciting collective modes as phonons, polarons, charge/spin-density-wave gaps, superconducting gaps in high-temperature superconductors and plasmons.

A sketch of the FERMI electron beam delivery system is shown in Fig.1. Only the first magnetic bunch length compressor (BC1) is routinely active for lasing. Start-to-end simulations of the electron beam dynamics were carried out, for diverse linac settings, from the Gun (G) through the linac sections (L0–L4) until the Main Beam Dump (MBD), where the Al target for CTR emission is installed. The bottom plot is a 3-D rendering of the MBD, from the FEL post-undulator region to the dump. The active dipole magnets, named "Dipole 1" and "Dipole 2" in the figure, are long 1.12 m and 2.44 m, with bending angles of 15.7 deg and 31.4 deg respectively. Three quadrupoles between "Dipole 1" and "Dipole 2" tune the momentum compaction (R_{56}) of the beam line. CTR is emitted at the 1 µm-thick Al target. Four quadrupoles installed upstream of the first dipole control the beam envelope along the line without affecting the R_{56} value. The transverse RMS beam sizes at the CTR target are kept smaller than 0.5 mm. Steering magnets and beam position monitors (not shown) allow control of beam trajectory. While electrons are bent and eventually dumped, FEL propagates straight to the downstream experimental hall (EH).

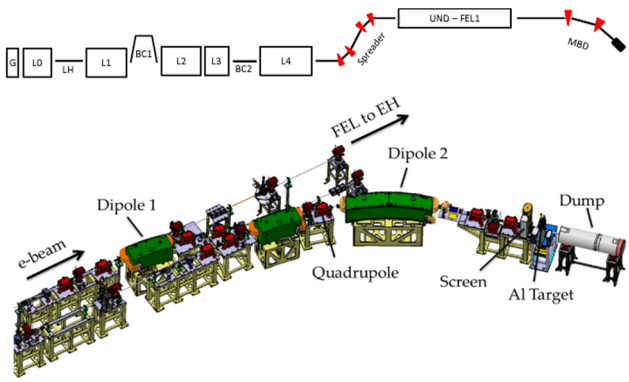


Figure 1: Sketch (not to scale) of the FERMI electron beam delivery system (top) and MBD line. Published in [1].

CSR-DRIVEN BUNCH COMPRESSION

The full width duration of the electron bunch prepared for lasing, thus entering the MBD line, is approximately 1 picosecond full width. In order to maximize transition radiation intensity at frequencies of 1 THz and above, a sub-picosecond charge density structure, *i.e.*, a kA-level current spike has to be generated in the bunch passing through the MBD, before reaching the Al target. Doing so, radiation can be emitted coherently in the multi-THz range at several tens of µJ-energy per pulse.

The FERMI dump line was designed to enhance the CSR wakefield by adopting relatively long and large angle dipole magnets, and for producing a tuneable but yet relatively large and positive R_{56}. This term couples with the CSR-induced negative energy chirp [5,6] and, as shown in the following, generates a ~100 fs-long leading current spike that radiates coherently in the THz range. The CSR-induced single particle energy deviation is actually correlated with z and, in particular, a negative linear chirp $h_1 < 0$ is produced at the bunch head, *i.e.*, leading particles are moved to higher energy with respect to trailing ones.

At the linac exit, the linear energy chirp in the head of the bunch was approximately –2 MeV/ps (see Fig.2). The

Content from this work may be used under the terms of the CC BY 3.0 licence (© 2019). Any distribution of this work must maintain attribution to the author(s), title of the work, publisher, and DOI

ISBN: 978-3-95450-210-3 doi:10.18429/JACoW-FEL2019-THP015

THE X-BAND LINEAR COMPRESSION SYSTEM IN DALIAN COHERENT LIGHT SOURCE

Yong Yu, Qinming Li, Jiayue Yang, Hongli Ding, Kai Tao, Lei Shi, Zongbin Li, Long Huang, Guanglei Wang, Gongkui Cheng, Jitao Sun, Zequn Wang, Zhigang He, Yuhuan Tian, Zhichao Chen, Guorong Wu, Dongxu Dai, Weiqing Zhang†, Xueming Yang†

State Key Laboratory of Molecular Reaction Dynamics, Dalian Institute of Chemical Physics, Chinese Academy of Sciences, Dalian, P. R. China

Abstract

Dalian Coherent Light Source (DCLS) is a free-electron laser (FEL) user facility working in the extreme ultraviolet (EUV) wavelength region from 50 to 150 nm. It mainly operates on the High Gain Harmonic Generation (HGHG) mode with the seed laser, although it can also run in the Self Amplified Spontaneous Emission (SASE) mode. The brightness and bandwidth of FEL radiation strongly depends on electron bunch quality, such as normalized transverse emittance, electron bunch energy, energy spread, peak current, etc. The high peak current with uniform longitudinal distribution is especially helpful for high peak power and narrow bandwidth of FEL, although it is not easy to achieve, due to the nonlinearity of sinusoidal accelerating radio frequency (RF) field and the 2nd-order momentum compaction coefficient T_{566} of bunch compressor. An X-band linearizer will be installed before the bunch compressor in order to correct this nonlinearity properly. In this paper, the beam dynamics design of the X-band linear compression system in DCLS is focused, and the simulation results with Elegant are presented and discussed.

INTRODUCTION

As shown in Fig. 1, DCLS is composed of linear accelerator (LINAC) and FEL Amplifier, and its main parameters are listed in Table 1 [1]. The high-quality electron bunch is produced, accelerated and compressed in the LINAC, and then delivered into the FEL Amplifier to generate the desired FEL radiation. In this process, bunch compression plays a vital role in the generation of intense FEL radiation, because the brightness of the radiation is closely related to the peak current and longitudinal distribution of electron bunch. In order to achieve high peak current, the longitudinal phase space of electron bunch is compressed in the bunch compressor. For DCLS, the compression ratio is 3-5 indicating the peak current up to 300 Amperes. Furthermore, the flat longitudinal current distribution is critical to increase the pulse energy of FEL radiation, and the flat longitudinal energy distribution is essential to improve the bandwidth of FEL spectrum when the FEL facility operates on HGHG mode [2]. Hence, the linear compression system is usually a standard configuration for the HGHG-mode FEL facility with narrow bandwidth and high brightness.

Table 1: Main Parameters of DCLS

Parameter	Nominal Value
Electron Bunch	
Energy	300 MeV
Slice Energy Spread	<20 keV
Normalized Emittance	1-2 mm·mrad
Charge	500 pC
Peak Current	≥300 Amp
Repetition Rate	50 Hz
FEL Radiation	
Wavelength	50-150 nm
Pulse Energy@1ps	≥100 μJ
Pulse Duration (FWHM)	130fs / 1ps

The configuration of X-band linear compression system is shown in Fig. 1. L1 provides a positive chirp for the electron bunch, and then the chirped bunch can be compressed in the chicane with negative (1st-order) momentum compaction coefficient R_{56}. In order to eliminate the nonlinear longitudinal part imposed by sinusoidal curve of L1 and 2nd-order momentum compaction coefficient T_{566} of Chicane, an X-band RF structure is employed following L1. The theoretical description of X-band linear compression system has been illustrated in detail by P. Emma [3]. According to the theory, the X-band RF structure works on the maximal decelerating RF phase π, and the linear compression can be achieved when the following condition is satisfied

$$eV_x = \frac{E_0\left\{1+\frac{1}{2\pi^2}\frac{\lambda_S^2 T_{566}}{|R_{56}|^3}(1-\sigma_z/\sigma_{z0})^2\right\}-E_i}{(\lambda_s/\lambda_x)^2-1}, \quad (1)$$

where e is elementary charge, V_x is the desired decelerating voltage of X-band, E_i and E_0 are the electron bunch energy at the exit of L0 and at the exit of Chicane, σ_z and σ_{z0} denote the rms bunch length at the entrance of L1 and at the exit of Chicane, λ_s and λ_x represent the wavelength of S-band and X-band RF field, and $\lambda_s = 4\lambda_x$. For the Chicane of DCLS, the approximate relation $T_{566} = -\frac{3}{2}R_{56}$ can be used.

† weiqingzhang@dicp.ac.cn, xmyang@dicp.ac.cn

Content from this work may be used under the terms of the CC BY 3.0 licence (© 2019). Any distribution of this work must maintain attribution to the author(s), title of the work, publisher, and DOI

ISBN: 978-3-95450-210-3 doi:10.18429/JACoW-FEL2019-THP016

STUDY OF MICROBUNCHING INSTABILITY IN SHINE LINAC*

Dazhang Huang†, Duan Gu, Meng Zhang, Shanghai Advanced Research Institute, Shanghai, China

Abstract

Microbunching instability usually exists in the linear accelerator (linac) of a free electron laser (FEL) facility. If it is not controlled effectively, the beam quality will be damaged seriously and the machine will not operate properly. As a typical example, the microbunching instability in the linac of the proposed Shanghai high repetition rate XFEL and extreme light facility (SHINE) is investigated in detail by means of both analytical formulae and simulation tools.

INTRODUCTION

As the beam passes through a bunch compressor, for example, a magnetic chicane, the energy modulation introduced by those effects is transformed into density modulation and may thus introduce the so-called microbunching effects. In certain situations, the microbunching effects can be so large that the microbunching instability can also take effects, and the final gain of the instability can become significant. On the other hand, the FEL process has a high demand for electron beam quality in terms of peak current, emittance, energy spread, etc. Therefore to preserve the beam quality, the microbunching effects must be studied in the design stage of the machine. In this paper, the study of microbunching instability in the linear accelerator (linac) of Shanghai high repetition rate XFEL and extreme light facility (SHINE) is reported, the comparison between numerical and analytical results shows very good consistency, given the gain curve of the instability. Meanwhile, the preliminary study of the laser heater to suppress the instability is also illustrated. The paper is organized as the following: first the basic methods to study the microbunching instability is introduced and the results are shown, followed by the study of the laser heater including its effect on the instability and the transverse matching. The conclusion is drawn as the last part.

METHODS

The recently approved SHINE project is a high repetition rate hard X-ray free electron laser (XFEL) facility based on the superconducting radio-frequency (SCRF) technology. In order to fulfil the goal of the project, a high energy, high peak current and low emittance electron beam is required as an output of linac. The main design parameters are illustrated in Table 1, and the schematic layout of the whole facility is shown in Figure 1 as well.

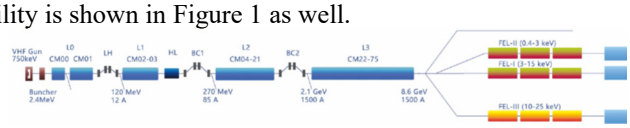


Figure 1: Layout of SHINE facility.

Table 1: Main Design Parameters of SHINE Linac

Parameter	Value
Beam energy (GeV)	4 - 8.6
Bunch charge (pC)	10 - 300
Peak current (kA)	1.5 – 3
Repetition rate (MHz)	Up to 1
Pulse length (fs)	5 - 200

The microbunching instability starts from the initial beam current/density modulation, turned into the energy modulation by a variety of impedances such as linac wake, longitudinal space charge (LSC), coherent synchrotron radiation (CSR), and gets amplified by the dispersion in a bunch compressor (chicane). As usual, the SHINE linac includes multiple stage of bunch compression. In the physical design, two bunch compressors are employed and the third one is reserved as a spare to compress the bunch current up to 3 kA. The main parameters of the bunch compressors are listed in Table 2.

Table 2: Main Parameters of Bunch Compressors in SHINE Linac

Parameter	BC1	BC2
Beam energy (MeV)	269	2156
Compression ratio	7	15
R_{56} (mm)	-60.8	-34.6
Total length (m)	12.2	24

The microbunching is modelled with the simulation code ELEGANT [1], which is commonly considered as a high-fidelity code in accelerator and beam physics. Due to the computing power, 20 million macro-particles are used to simulate 100 pC charge in the simulation. However, referring to [2], this number of macro-particle are nearly enough for this amount of charge.

To study the microbunching effects, equation (1) [3] is used to estimate the wavelength of the microbunching at the peak. Or in other words, the smearing of microbunching from the uncorrelated energy spread across the chicane is not effective until

$$\lambda_0 \leq \left|\frac{2\pi R_{56}}{1+hR_{56}}\right| \sigma_\delta \equiv \lambda_c, \quad (1)$$

Where h is the energy chirp, R_{56} is the momentum compaction of the chicane, and σ_δ is the uncorrelated energy spread of the beam before compression. With the magnetic chicane parameters in Table 1 and the corresponding beam parameters, we have $\lambda_c = 70.9$ μm for BC1, and $\lambda_c = 15.1$ μm for BC2 which corresponds to the initial density modulation of $\lambda_c \approx 106$ μm before BC1. Therefore, one

* Work supported by National Natural Science Foundation of China, Grant No. 1675248
† email address: huangdazhang@zjlab.org.cn

Content from this work may be used under the terms of the CC BY 3.0 licence (© 2019). Any distribution of this work must maintain attribution to the author(s), title of the work, publisher, and DOI

ISBN: 978-3-95450-210-3 doi:10.18429/JACoW-FEL2019-THP018

TRANSVERSE DEFLECTING STRUCTURE DYNAMICS FOR TIME-RESOLVED MACHINE STUDIES OF SHINE

J. W. Yan[1,2], H. X. Deng[1,3*], B. Liu[1,3], D. Wang[1,3]
[1]Shanghai Institute of Applied Physics, Chinese Academy of Sciences, Shanghai, China
[2]University of Chinese Academy of Sciences, Beijing, China
[3]Shanghai Advanced Research Institute, Chinese Academy of Sciences, Shanghai, China

Abstract

The transverse deflecting structure (TDS) has been widely used in modern free electron laser facilities for the longitudinal phase space diagnostics of electron beams. As the first hard x-ray free electron laser in China, the SHINE is designed to deliver photons with a repetition rate up to 1 MHz. In this paper, we present the beam dynamics study of the X-band TDS behind the undulator of SHINE. In order to prevent the screen from being damaged by electron bunches with a high repetition rate, the phase of the transverse deflecting cavity is designed to deviate from zero, and only those electron bunches that are kicked by the transverse deflecting cavity are sent to the screen. In addition, the evolutionary algorithm is introduced to optimize the lattice of the TDS line to reach the highest possible resolution.

INTRODUCTION

Due to characteristics of high peak brightness, short pulse duration, and coherence, X-ray free electron lasers (XFELs) play an important role in many research fields. In recent years, the high-repetition-rate XFEL based on superconducting linac attracts increasing attention because of its ability to produce radiation with higher average brightness. SHINE [1] is designed to be a continuous-wave x-ray free electron laser generating photons between 0.5 keV and 30 keV with a repetition rate up to 1 MHz. The high resolution measurement of the longitudinal phase space of the electron bunch is critical for the XFEL operation.

In recent years, the transverse deflecting structure (TDS) has been widely used in the measurement of the length of electron bunch [2,3]. The transverse kick induced by the cavity translates the time coordinate into a transverse coordinate of the downstream screen. Therefore, the longitudinal properties of the electron beam can be probed. Combined with dipoles, the TDS can be used to reconstruct the longitudinal phase space of the electron beam. Moreover, the x-ray FEL temporal shape can be reconstructed through measuring the difference in the electron beam longitudinal phase space between FEL-on and FEL-off [4]. The TDS will be equipped after each undulator line of SHINE. However, the electron bunches with high-repetition-rate will easily damage the screen used for measurement.

In this paper, to separate the kicked electron bunches from the electron bunches that are not kicked by the TDS, we propose to provide an additional transverse kick to the electron beam by letting the phase of the TDS deviate from zero. In addition, the lattice of the TDS line are optimized to achieve the highest possible resolution.

LAYOUT OF THE TDS LINE

Since the design of TDS lines behind the undulator lines of SHINE is similar, the TDS line after FEL-III will be taken as an example in this paper. The schematic layout of the TDS line behind FEL-III is shown in Fig. 1. There are six quadrupoles before the transverse deflecting cavity to match the electron beams coming from the undulator to achieve a high temporal resolution of the TDS. Two X-band transverse deflecting cavities with a length of 2 m and a voltage of 20 MV are used to kick the electron bunch in the horizontal direction. Behind the transverse deflecting cavities, there are a bend that gently deflects the beams without generating significant synchrotron radiation in the forward direction and three strong bending magnets that deflect the beams to the screen or beam dump.

In general, the phase of the TDS is set to 0°to obtain the maximum deflection force. However, in this case, those electron bunches that are not kicked by the TDS are also sent to the screen. This causes the screen to be easily damaged when the machine is operated at a high repetition rate. In order to separate the kicked and un-kicked electron bunches, we set the phase of the TDS to -3°. Due to the extra transverse kicking force, those electron beams that are kicked by the TDS will be horizontally offset. As shown in Fig. 2, those electron bunches that have been kicked by the TDS can be offset in the horizontal direction by about 10 mm from the un-kicked electron bunches. Therefore, those two kinds of electron beams can be sent to the screen and dump, respectively. According to the basic theory of TDS [2], the temporal resolution can be calculated as:

$$\Delta_s = \frac{c(E/e)}{\omega V_0} \frac{\sqrt{\varepsilon_x}}{\sqrt{\beta_d \sin\Delta\psi \cdot \gamma}}, \quad (1)$$

where β_d is β functions at the centre of the TDS, $\sin\Delta\psi$ is the phase advance between the TDS and screen. According to the Eq. (1), a high temporal resolution of the TDS can be achieved with high voltage of the deflecting cavity, large beta function at the deflecting cavity, and appropriate phase advance between the deflecting cavity and monitor. The optimal beta function and phase advance can be obtained by optimizing the lattice of the TDS line. Therefore, the strength of the twelve quadrupoles of the TDS line are

* denghaixiao@zjlab.org.cn

Content from this work may be used under the terms of the CC BY 3.0 licence (© 2019). Any distribution of this work must maintain attribution to the author(s), title of the work, publisher, and DOI

ISBN: 978-3-95450-210-3 doi:10.18429/JACoW-FEL2019-THP020

MICROBUNCHING ENHANCEMENT BY ADIABATIC TRAPPING

Xiujie Deng*, Alex Chao[1], Wenhui Huang, Chuanxiang Tang,
Tsinghua University, Beijing, China
[1] also at SLAC, Menlo Park, USA

Abstract

Storage ring based concept called steady-state microbunching (SSMB) was proposed years ago for generating high average power narrowband coherent radiation. There are now active efforts on-going by the SSMB collaboration established among Tsinghua University and several other institutes. In this paper we study the particle trap and filamentation process of beam in RF or Micro Bucket which is useful for understanding the injection beam dynamics of SSMB. One remarkable result is the steady-state current distribution after full filamentation has little dependence on the bucket height as long as it is several times larger than the energy spread. A discrete increase of bucket height after filamentation can boost the bunching, with the sacrifice of emittance growth. An adiabatic change of bucket height from a smaller value to the final desired value is then proposed to boost the bunching while preserving the longitudinal emittance.

INTRODUCTION

Microbunching is and will continue to be in the coming years one of the accelerator physics research focus. Storage ring based concept called steady-state microbunching (SSMB) [1] was proposed years ago for high average power narrowband coherent radiation generation, digging the potential of longitudinal coherence of beam which is parallel to the efforts on diffraction limited rings emphasizing on the transverse dimension. The idea of SSMB is using laser modulator to play the role of RF focusing in traditional rings as shown in Fig. 1 and 2. By precise longitudinal phase space manipulations (laser modulator cooperated with dedicated lattice), microbunching is formed and maintained turn-by-turn each time passing through the radiator. The high peak power coherent radiation from microbunches and high repetition rate from storage ring combined lead to a high average power facility.

There are now active research efforts on-going for different issues of SSMB by a collaboration established among Tsinghua University and several other institutes [2–5]. In this paper we investigate the particle trap and filamentation process of beams in RF or Micro Bucket which is useful for understanding the dynamics of SSMB beam injection.

PARTICLE TRAP AND FILAMENTATION IN RF OR MICRO BUCKET

To simplify the analysis, we restrict ourselves to longitudinal dimension only and ignore the various noises from laser and lattice. Quantum excitation and radiation damping

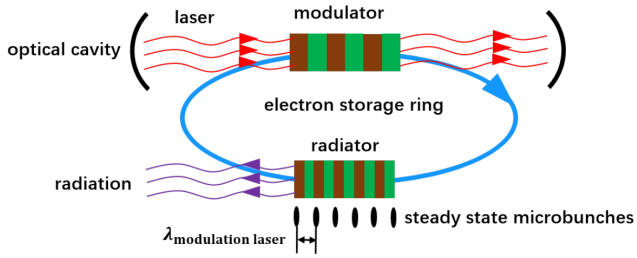


Figure 1: Schematic layout of SSMB.

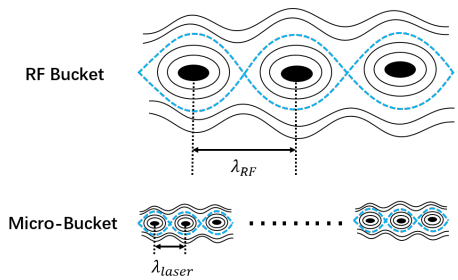


Figure 2: From RF Bucket to Micro-Bucket.

is also neglected as this paper focus on the first stage after the beam injection. The symplectic longitudinal dynamics of a particle in a storage ring with a single RF cavity (laser modulator) can be modeled by the well-known "standard map" [6]

$$\begin{aligned} I_1 &= I_0 + K\sin\theta_0, \\ \theta_1 &= \theta_0 + I_1, \end{aligned} \tag{1}$$

in which

$$\theta = kz,\ I = R_{56}k\delta,\ K = VR_{56}k. \tag{2}$$

Equation 1 can be described with the pendulum Hamiltonian driven by a periodic perturbation

$$H(I,\theta,t) = \frac{1}{2}I^2 + K\cos\theta\sum_{n=-\infty}^{\infty}\cos(2\pi nt). \tag{3}$$

For small K and I, which is the case for usual storage rings, the differences in Eq. 1 can be replaced approximately by derivatives and the Hamiltonian by a pendulum Hamiltonain

$$H = \frac{1}{2}I^2 + K\cos\theta. \tag{4}$$

The separatrix is $H = K$ with a bucket half-height of $2\sqrt{K}$. Chaos is beyond the discussion of this paper.

The longitudinal phase space evolution of a mono-energetic beam after injection into RF bucket described by Eq. 1 is shown in Fig 3. As can bee seen in Fig. 4, there is

* dxj11@tsinghua.org.cn

Content from this work may be used under the terms of the CC BY 3.0 licence (© 2019). Any distribution of this work must maintain attribution to the author(s), title of the work, publisher, and DOI

ISBN: 978-3-95450-210-3 doi:10.18429/JACoW-FEL2019-THP022

Content from this work may be used under the terms of the CC BY 3.0 licence (© 2019). Any distribution of this work must maintain attribution to the author(s), title of the work, publisher, and DOI

A GENERAL OPTIMIZATION METHOD FOR HIGH HARMONIC GENERATION BEAMLINE

Yao Zhang*, Xiujie Deng, Zhilong Pan, Wenhui Huang, Chuanxiang Tang
Tsinghua University, Beijing 100084, China

Abstract

Shorter bunches produce a more coherent radiation and contain higher harmonic components. Here, based on transverse and longitudinal phase space coupling, a general method for analyzing the production of very short beam and searching for compression beamline is presented. With this method, several beamlines are found and optimized. The electron beam can be compressed to tens of nanometers, generating coherent high harmonic radiation.

INTRODUCTION

The coherence of synchrotron radiation depends strongly on beam length and has been enormously demanded by many applications. Generally, a beam will radiate coherently while its length is comparable to the radiation wavelength [1]. For this reason, shortening bunch length in storage ring has been studied widely, but the length is still on the order of tens femtoseconds [1–4]. On the other hand, free electron laser (FEL), benefiting from the natural microbunching process, holds the shortest length achieved. Combining these short bunches with storage rings, and uniting the high brightness of FEL with the high repetition rate of synchrotron radiation will create a new light source with excellent properties. However, this combination requires to compress the beam to a very short length before injecting it into the undulator. Several compression methods and beamlines have been proposed [5–12]. But the optimization methods vary. In this paper, we present a general method for analyzing the production of very short beam and searching for compression beamlines. Based on this method, several beamlinems are found and optimized. The electron beam can be compressed to tens of nanometers, and very coherent high harmonic radiation can be generated.

GENERAL METHOD

Transfer matrix is used to analyze the compression problem. For simplicity, the electron six-dimensional phase space is shortened to four, $(x,\ x',\ z,\ \delta)^T$. Here, the symbol x can be either horizontal or vertical direction. Under this simplification, a general matrix form for both dipole and quadrupole magnets is

$$a = \begin{pmatrix} a_{11} & a_{12} & 0 & a_{14} \\ a_{21} & a_{22} & 0 & a_{24} \\ a_{31} & a_{32} & 1 & a_{34} \\ 0 & 0 & 0 & 1 \end{pmatrix}. \quad (1)$$

The symplectic condition tells that only six elements in the matrix are free. Besides, it can be proved that the product of any number of matrix in this type has the same form. Hence, this matrix is actually a general expression for an arbitrary beamline consisting of only dipoles and/or quadrupoles. Now, we use symbols A (with elements A_{ij}), B (with elements B_{ij}) to express two such beamlines.

Another critical component is the modulator, where an undulator and a laser cooperate to act like a radio frequency (RF) cavity. Considering the case that laser incidents with a small angle t, the beam energy modulation can be expressed as

$$\delta = \delta_0 + \tilde{\delta}\sin(kz + tkx), \quad (2)$$

with $\tilde{\delta} = \frac{\Delta\gamma}{\gamma_c}$ the maximum absorbed energy, and γ_c the beam central energy. k is laser wave number. Panofsky-Wentzel theorem [13] indicates that this energy modulation will be accompanied by an angular modulation

$$x' = x'_0 + t\tilde{\delta}\sin(kz + tkx). \quad (3)$$

Thus, the linearized transfer matrix for a modulator is

$$M = \begin{pmatrix} 1 & 0 & 0 & 0 \\ ht^2 & 1 & ht & 0 \\ 0 & 0 & 1 & 0 \\ ht & 0 & h & 1 \end{pmatrix}. \quad (4)$$

Here, $h = k\tilde{\delta}$, is a parameter representing modulation strength. With $t = 0$, M degenerates into a standard modulator, which changes electron energy only.

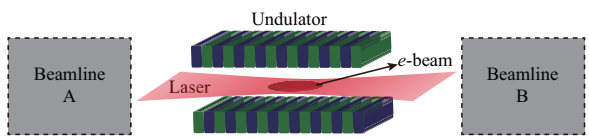


Figure 1: Structure of a compression beamline.

Generally, a full compression cell is a modulator sandwiched by two beamlines, assuming the upstream one A and downstream one B, shown as Fig. 1. The complete transfer matrix can be written into

$$T = BMA \quad (5)$$

Hence, the final longitudinal position of an electron is

$$z = T_{31}x_0 + T_{32}x'_0 + T_{33}z_0 + T_{34}\delta_0, \quad (6)$$

with

$$\begin{aligned} T_{31} &= A_{21}B_{32} + A_{31}(1 + B_{34}h + B_{32}ht) \\ &\quad + A_{11}[B_{31} + ht(B_{34} + B_{32}t)] \\ T_{32} &= A_{22}B_{32} + A_{32}(1 + B_{34}h + B_{32}ht) \\ &\quad + A_{12}[B_{31} + ht(B_{34} + B_{32}t)] \\ T_{33} &= 1 + B_{34}h + B_{32}ht \\ T_{34} &= A_{24}B_{32} + B_{34} + A_{34}(1 + B_{34}h + B_{32}ht) \\ &\quad + A_{14}[B_{31} + ht(B_{34} + B_{32}t)]. \end{aligned}$$

* zhangyao18@mails.tsinghua.edu.cn

ISBN: 978-3-95450-210-3 doi:10.18429/JACoW-FEL2019-THP024

SPONTANEOUS COHERENT RADIATION OF STABILIZED DENSE ELECTRON BUNCHES*

Yu. S. Oparina†, A. V. Savilov, Institute of Applied Physics, Nizhny Novgorod, Russia
V. L. Bratman, Yu. Lurie, N. Balal, Ariel University, Ariel, Israel

Abstract

Modern electron sources allow formation of dense bunches with energies of 3–6 MeV, ps pulse durations, and charges of up to 1 nC. Such bunches can be used for the realization of relatively simple terahertz sources based on spontaneous coherent radiation. This regime is realized when the effective bunch phase size doesn't exceed 2π. Power and duration of the process of such type of emission are limited due to an increase in the bunch length under the Coulomb repulsion. This complicates the effective implementation of the regime of spontaneous coherent radiation for dense bunches. Therefore, special methods for stabilization of the length of the bunch should be used. We describe several methods of the stabilization used in different systems (cyclotron radiation, emission in the traditional undulator system, and emission in the "negative-mass" undulator system).

CYCLOTRON RADIATION

We consider particles motion in a waveguide immersed in a uniform longitudinal magnetic field (Fig. 1a).There are two characteristic regimes of radiation for electrons moving in a waveguide depending on the value of the magnetic field (Fig. 1b): group synchronism, regime of the "grazing" of dispersion characteristics (G), at which the group velocity of the wave is close to the initial longitudinal velocity of particles, and intersection of the dispersion characteristics, at which high-frequency (H) and low-frequency (L) waves are simultaneously excited. In the case of grazing of dispersion characteristics, the total compensation of Coulomb repulsion takes place [1]. In the case of two waves excitation low-frequency spontaneous radiation provides the bunch forming respect to high-frequency wave [2-4].

The change in electron energy is the sum of the changes in energy due to the Coulomb interaction and the wave effect: $\Delta\gamma = \Delta\gamma_c + \Delta\gamma_w$. Evolution of the cyclotron electron phase is described as follows

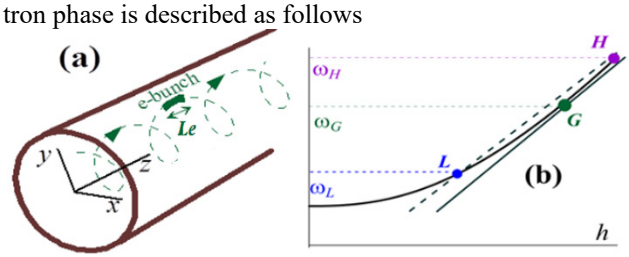


Figure 1. (a) Electron bunch moving along a helical undulator. (b) Dispersion diagram of the operating mode.

* Work supported by Russian Foundation for Fundamental Research, projects 18-32-00351 and 18-02-00765, as well as by the IAP RAS Project 0035-2019-0001.
†oparina@appl.sci-nnov.ru

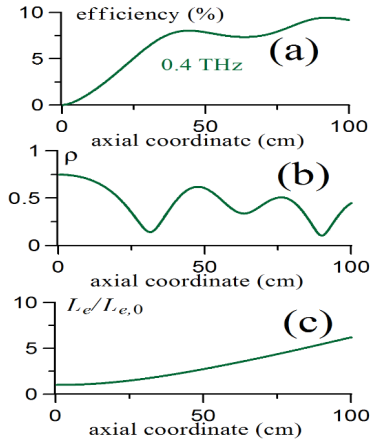


Figure 2: (a) Efficiency of the electron-wave interaction $\langle\gamma_0 - \gamma\rangle/(\gamma_0 - 1)$. (b) Electron bunching efficiency $\rho =$ cy $\rho = \langle exp(-i\vartheta)\rangle$. (c) Effective normalized bunch length $L_e/L_{e,0}$(c) versus the axial coordinate.

$$\frac{d\vartheta}{d(\omega t)} = \frac{\Delta\gamma_c}{\gamma_0}\left(\beta_{z,0} - \beta_{gr}\right)\left(\beta_{z,0} + \frac{1}{\gamma_{z,0}^2}\right) + \frac{\Delta\gamma_w}{\gamma_0}\left(1 - \beta_{gr}{}^2\right). \quad (1)$$

here $\vartheta = \omega t - k_z z - \int \omega_c dt$ is the electron resonance phase change, ω is the frequency of the radiated wave, which described by the Doppler up-conversion of non-relativistic cyclotron frequency

$$\omega = \frac{\Omega_c}{\gamma\left(1 - \beta_{gr}\beta_z\right)}, \quad (2)$$

$\gamma = \sqrt{1-\beta^2}$ is the relativistic gamma-factor, $\beta = V/c$ is the normalized electron velocity, β_z is the normalized longitudinal velocity, β_{gr} is the normalized wave group velocity; $\Delta = 1 - \beta_{gr}\beta_{z,0} - b/\gamma_0$ is the mismatch of the electron-cyclotron resonance (here, $b = \Omega_c/\omega$).

Approximate equation (1) makes it obvious, that the Coulomb interaction of the particles does not change the phase of the electron relative to the wave in the regime of group synchronism, $\beta_{z,0} = \beta_{gr}$, despite change in bunch length. This is due to the electron bunch spreads along the helix of the constant phase [1].

We consider the spontaneous radiation of a cylindrical bunch with a diameter of 1 mm, a charge of 0.2 nC, a duration of 0.5 ps, a particle energy of 6 MeV, and initial transverse velocities $\beta_{\perp 0} = 1/\gamma_0$ in a waveguide with a diameter of 4 mm. The particles are in group synchronism with the TE_{11} mode at the field H_0 = 2.2 T. The frequency of radiation is 0.4 THz, and efficiency of about 8% (Fig. 2a). In the process of motion of the bunch along the operating waveguide, the bunch length increases (Fig. 2c). However, such an increase in the bunch length doesn't lead to a significant increase in the bunch phase size, described by the bunching efficiency $\rho = \langle exp(-i\vartheta)\rangle$, which remains at a level ρ~0.5 (Fig. 2b).

Content from this work may be used under the terms of the CC BY 3.0 licence (© 2019). Any distribution of this work must maintain attribution to the author(s), title of the work, publisher, and DOI

ISBN: 978-3-95450-210-3 doi:10.18429/JACoW-FEL2019-THP027

SIMULATION AND OPTIMIZATION OF THE TRANSPORT BEAMLINE FOR THE NOVOFEL RF GUN

A. S. Matveev[1†], I. V. Davidyuk[1], O. A. Shevchenko, V. G. Tcheskidov, N. A. Vinokurov[1], V. N. Volkov, BINP, Novosibirsk, Russia
[1]also at Novosibirsk State University, Russia

Abstract

A new low-frequency CW RF gun was developed and tested at Budker Institute of Nuclear Physics recently. We plan to use it to upgrade the ERL of the Novosibirsk FEL facility. It will allow increasing the average beam current (due to higher beam repetition rate) and thus increasing the average radiation power. The transport beamline for the RF gun uses the ninety-degree achromatic bend. It is designed in a way that keeps an option to operate with the old electrostatic gun as well. Due to the low beam energy (290 keV) the beam dynamics is strongly influenced by space-charge forces. The paper describes results of simulation and optimization of the RF gun transport beamline. Space-charge forces were taken into account with the code ASTRA. Main sources of emittance degradation were considered in order to decrease their influence during the optimization. In addition, the RF gun output beam parameters were measured for various RF gun emission phases. These experiments were simulated, and the results were compared. The resulting beam parameters meets requirements of the Novosibirsk FEL facility ERL.

INTRODUCTION

Injector of the Novosibirsk FEL [1] now uses static electron gun. In near future it is planned to be supplemented with new low-frequency CW RF gun [2]. It will allow increasing the maximum of the average beam current from 30 mA to 100 mA and more due to higher beam repetition rate. The cathode grid assembly of the RF gun is the same as the static gun one. Basic RF gun parameters are listed in Table 1.

Increasing of the average beam current should lead to increasing of the average radiation power. It requires accurate simulation and optimization of beamline magnetic optics in order to reduce losses of high current beam, and consequently to prevent vacuum chamber heating and vacuum breakdown.

Table 1: Basic RF Gun Parameters

Parameter	Value	Unit
Average Current	≤ 100	mA
Electron Energy	240-300	keV
Bunch Charge	≤ 2.0	nC
Bunch Length (FWHM)	1.0	ns
Peak Current	15	A
Beam repetition rate	0.002 – 90.2	MHz

† matveev.a.s@yandex.ru

TRANSPORT BEAMLINE FOR THE RF GUN

Beamline Scheme

The scheme of the Novosibirsk FEL injector is illustrated in Fig. 1. A 300 kV static electron gun, a bunching RF resonator and two RF cavities are in operation now. A beam is generated in the static electron gun. Then it is bunched and accelerated up to an electron energy of 1.8 MeV. At the injector output the beam normalized emittance is 30 mm·mrad.

The RF gun will be connected to the injector by the ninety-degree achromatic bend (as shown in Fig. 1) in order to keep an option to operate it with the static gun. The working regime of the RF gun is around 40° from the phase of the maximum beam acceleration. So, the bunching resonator is not required for the RF gun beamline.

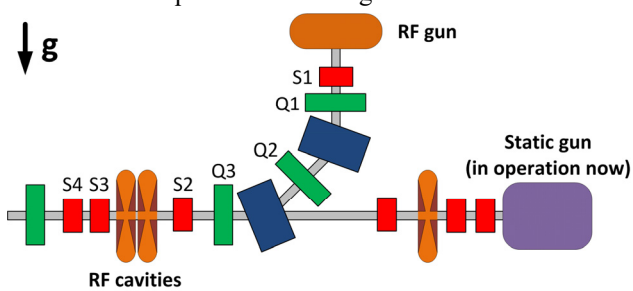


Figure 1: A scheme of the NovoFEL injector with the new RF gun: red – solenoids, green – quadrupoles.

Simulation

Simulations of beam dynamics in the injector are performed with the code ASTRA [3] by the following reasons: taking into account space-charge forces and a possibility of defining 1D and 3D electromagnetic field distribution of magnet and accelerator elements.

The simulation starts from the cathode. The cathode grid assembly and anode focusing is considered.

Optimization

The program package ASTRA has a lack of optimization features, except scanning or optimizing by one parameter in predefined value range. Thus, it has been decided to write a script for automatic calculations of beamline regimes with ASTRA that would be easily used with external optimization modules. The program language Python was chosen due to powerful open-source mathematical libraries.

Two Python scripts AstraTools.py and AstraProc.py were written that make the simulation as a calculation of

Content from this work may be used under the terms of the CC BY 3.0 licence (© 2019). Any distribution of this work must maintain attribution to the author(s), title of the work, publisher, and DOI

ISBN: 978-3-95450-210-3 doi:10.18429/JACoW-FEL2019-THP030

AN UPDATED DESIGN OF THE NSRRC SEEDED VUV FREE ELECTRON LASER TEST FACILITY

W.K. Lau[1], C.K. Chan[1], C.C. Chang[1], C.H. Chang[1], L.H. Chang[1], C.H. Chen[1], M.C. Chou[1], P.J. Chou[1], F.Z. Hsiao[1], H.P. Hsueh[1], K.T. Hsu[1], K.H. Hu[1], C.S. Hwang[1], J.Y. Hwang[1], J.C. Jan[1], C.K. Kuan[1], A.P. Lee[1], M.C. Lin[1], G.H. Luo[1], S.Y. Teng[2], K.L. Tsai[1], J. Wu[3], A.W. Chao[3]
[1] NSRRC, Hsinchu, Taiwan
[2] Department of Physics, NTHU, Hsinchu, Taiwan
[3] SLAC National Accelerator Laboratory, Menlo Park, USA

Abstract

In this report, we present an updated design of the facility which is a 200 nm seeded, HGHG FEL driven by a 250 MeV high brightness electron linac system with dogleg bunch compressor for generation of ultrashort intense coherent radiation in the vacuum ultraviolet region. It employs a 10-periods helical undulator for enhancement of beam energy modulation and a helical undulator of 20 mm period length as the radiator (i.e. THU20) to produce hundreds of megawatts radiation with wavelength as short as 66.7 nm. An optional planar undulator can be added to generate odd harmonics (e.g. 22.2 nm, 13.3 nm etc.) of the fundamental. The facility layout and expected FEL output performance is reported.

INTRODUCTION

The Baseline design of the test facility is a VUV high-gain harmonic generation (HGHG) FEL seeded by a 200 nm laser. The seed laser is injected to a 10-periods helical undulator of 24 mm period length (i.e. THU24) for beam energy modulation. A small chicane located at downstream of THU24 provides the required dispersion for microbunching. In the first phase of the project, a THU20 undulator of length at about twice of gain length will be used as the radiator which allows generation of MW-level coherent radiation at 66.7 nm wavelength (i.e. the third harmonic of the seed). If the more segmented THU20 undulators are used, the radiation grows and saturates in ~6 m. In the initial stage, the facility has to be fitted into the existing 38 m × 5 m tunnel in the Accelerator Test Area (ATA). Since the total length of the accelerator system from the gun to beam modulator entrance is about 25.5 m, the length of the FEL section and its output diagnostics station is limited to 12.5 m. Future extension of the laboratory building will be necessary if more THU20 undulators are installed for FEL operation at saturation. Extra space will also be needed for photon beamlines and experimental stations if a practical user facility is under consideration. Nevertheless, a 1.5 m long THU20 undulator prototype will be used to demonstrate the concepts in the initial stage. A schematic of the overall layout is shown in Fig. 1.

Broad tunability of radiation wavelength of the VUV FEL can be achieved by using tunable seed laser. The klystron systems operate at 10 Hz pulse-prepetition-rate rate, and can be increased up to 50 Hz if demand arises.

ACCELERATOR SYSTEM

The facility is based on a recently built 2998 MHz laser driven photoinjector which delivers low emittance electron beam for the 250 MeV drive linac system. Since the beam brightness required for the seeded VUV FEL system located at downstream of the linac system is as high as $5x10^{13}$ A/m^2, bunch compressor with capability to linearize electron distribution in longitudinal phase space is therefore essential. Conventional four-dipole chicanes are usually equipped with harmonic rf linearizers to compensate the nonlinearities introduced into beam distribution by the rf curvature of chirper linac. However, harmonic rf linac as well as the corresponding pulsed klystron system do not fit into our budget plan, we therefore consider to exploit the concept of dogleg bunch compressor with linearization optics. After bunch compression, the sub-100 fs beam is then accelerated to designed beam energy by two rf linac sections that are powered by a single klystron with standard SLED cavity for rf pulse compression. A linear achromatic beam transport system delivers the beam to the FEL system and allows coupling seed laser collinearly with the beam in the beam energy modulator unit. Beam parameters are listed in Table 1.

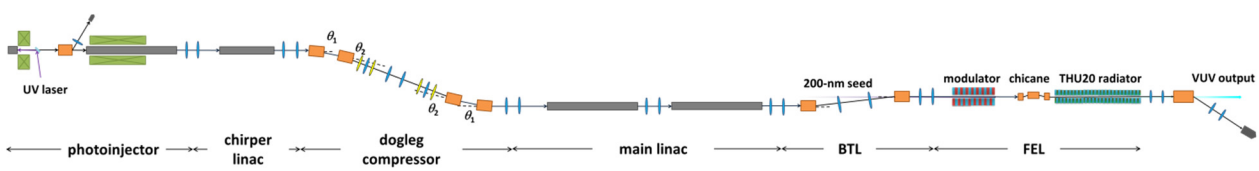


Figure 1: Layout of the NSRRC VUV FEL test facility.

Content from this work may be used under the terms of the CC BY 3.0 licence (© 2019). Any distribution of this work must maintain attribution to the author(s), title of the work, publisher, and DOI

ISBN: 978-3-95450-210-3 doi:10.18429/JACoW-FEL2019-THP031

Content from this work may be used under the terms of the CC BY 3.0 licence (© 2019). Any distribution of this work must maintain attribution to the author(s), title of the work, publisher, and DOI

SIMULATION AND OPTIMIZATION OF INJECTOR SYSTEM FOR THE PRE-BUNCHED THz FEL

N. Chaisueb[a,b,†], S. Rimjaem[a,c,††]
[a]Plasma and Beam Physics Research Facility (PBP), Department of Physics and Materials Science, Faculty of Science, Chiang Mai University, Chiang Mai, Thailand
[b]Doctor of Philosophy Program in Physics (International Program), Department of Physics and Materials Science, Faculty of Science, Chiang Mai University, Chiang Mai, Thailand
[c]Thailand Center of Excellence in Physics, CHE, Bangkok, Thailand

Abstract

A linac-based light source for generation of infrared free-electron laser is under the development at the Plasma and Beam Physics (PBP) Research Facility, Chiang Mai University, Thailand. The injector system of the facility consists mainly of an S-band thermionic cathode RF electron gun, a pre-bunch compressor in a form of an alpha magnet and a travelling-wave linac structure. Two 180-degree magnetic bunch compressors, which each system has 4 dipole magnets, quadrupoles and steering magnets, are installed downstream the injector system. Two separate radiation beamlines for mid-infrared (MIR) and terahertz (THz) free-electron laser (FEL) are located following the bunch compressor systems. In this contribution, we focus only on the coherent and high-power pre-bunch THz FEL that is generated from electron bunches with a femtosecond length. Electron beam dynamic simulations with program ASTRA were performed to obtain optimal electron beam properties. Optimization of the injector system for the THz FEL is thus presented. The simulated results show that the beam at the linac exit has a bunch length of 282 fs with a charge of 200 pC when the linac RF phase is 90° and the alpha gradient is 300 G/cm. This optimal condition will be used as an input for simulation in the 180-degree bunch compressor system and in the THz undulator magnet.

INTRODUCTION

Nowadays, the THz radiation has been used in many applications due to its unique features. Since the THz wave can pass through non-metallic materials, reflected by metal and absorbed by liquid, it is suitably used in THz imaging for non-destructive analysis of different density materials e.g. investigation of chemical structures of pharmaceutical materials or imperfection observation of integrated circuits, semiconductor devices or electronic cards [1].

The frequency ranges of the THz radiation also correspond well with rotational and vibration modes of many bio-molecules. Therefore, it can be used to study the characteristics of intermolecular bonds such as hydrogen bonding, Van der Waals forces, and molecule-ion attractions by using the THz spectroscopy technique. Various applications of THz radiation lead to broad studies on development of THz light sources, detectors, and experimental techniques. An accelerator-based light source is one of the most powerful sources for producing the THz radiation. Many accelerator centers and laboratories develop the THz light sources worldwide including free-electron lasers.

In typical FELs, the radiation emits when an electron bunch moving through magnetic field of an undulator magnet interacts with the radiation, which is produced in the first section of a long undulator or inserted from external seed laser. The co-propagating radiation modulates the longitudinal velocity of electrons and eventually the electrons are bunched, which is called the micro bunching process. Contradictory, in case of pre-bunched FELs, ultrashort and high-charged electron bunches are produced before injecting the beam into the undulator. When the electron bunches with a length of equal or shorter than the radiation wavelength travelling in the undulator magnetic field, the radiation will be coherently emitted. In this case, the radiation emitted from different undulator poles along the beam trajectory overlaps and interferes constructively. This leads to properly add up of the radiation in the forward direction and results in the enhancement of the radiation intensity that is proportional to the electron number squared.

The construction of the pre-bunched THz FELs from femtosecond electron bunches and the typical MIR FEL oscillator (as shown in Fig. 1) are underway at our laboratory. The accelerator system includes the injector part, the 180-degree bunch compressors, and radiation stations. However, this paper focuses only on optimization of the injector system for generation of the femtosecond electron bunches at the entrance of the THz undulator magnet. This system consists of a thermionic cathode RF electron gun, an alpha magnet and a travelling-wave linac structure. The optimization was divided into three parts; in the RF-gun, from the gun exit to the alpha magnet and from the alpha magnet to the linac. The optimal electron beam with small emittance, low energy spread, short bunch length, and high beam current is expected to achieve downstream the linac.

METHOD

Properties of the radiation from charged particle beam depend significantly on the beam qualities. Numerical optimization of electron beam properties has to be done before installation of the accelerator components. Electron beam dynamic simulations throughout the injector system by using program ASTRA [2] were performed to determine the appropriate operational parameters of the

†natthawut_chai@cmu.ac.th, ††sakhorn.rimjaem@cmu.ac.th

ISBN: 978-3-95450-210-3 doi:10.18429/JACoW-FEL2019-THP033

XFEL ISOCHRONOUS CHICANES: FEASIBILITY STUDY

N. R. Thompson*
ASTeC and Cockcroft Institute, STFC Daresbury Laboratory, Warrington, United Kingdom

Abstract

FEL schemes such as High-Brightness SASE [1] and Mode-Locking [2] require electron beam delays inserted between undulator sections. These schemes have been shown in simulations to perform most effectively when the electron beam delays are very close to isochronous, i.e. the first order longitudinal dispersion is very small. To minimise the disruption to the FEL process in the inter-undulator gaps, these delays must also be as compact as possible. In this paper we study the maximum longitudinal space that a delay chicane could occupy in an XFEL operating at 6 GeV before the peak power drops below a defined threshold, and we present a limit for the maximum longitudinal dispersion of the delay chicanes. We then present the optical designs of two chicanes that satisfy the requirements of length and isochronicity and show how these designs could be realised practically using small-aperture high-field quadrupoles.

ISOCHRONOUS CHICANES

A number of related schemes have been proposed in which electron beam delay chicanes are used to manipulate the electron/radiation interaction within the FEL, for example Mode-Locking [2], the Mode-Locked Afterburner [3] and High-Brightness SASE (HB-SASE) [1]. For all of these schemes, the performance has been shown to be better if the delays are isochronous [4], meaning that the first order dispersion $R_{56} = 0$. For HB-SASE, simulation studies have been done in 1D and 3D codes, and in two different wavelength regimes, to assess the performance as a function of the level of isochronicity. These studies showed that for performance very close to that obtained with purely isochronous chicanes, the normalised chicane dispersion D, defined here as the ratio of the R_{56} to that of a standard 3 dipole chicane imparting the same delay, must satisfy $D \leq 0.01$.

SPACE CONSTRAINTS FOR AN XFEL

In any FEL it is normal practice to make the inter-undulator gaps as compact as possible to minimise the total length of the FEL and to mitigate the degradation to the FEL performance caused by debunching and radiation diffraction. Some initial chicane design work indicated that the minimum length would be several meters. To investigate the impact of a chicane length of this order, two FEL lattices were set up using typical XFEL parameters, with $E = 6$ GeV, $Q = 50$ pC, $\varepsilon_n = 0.5$ mm-mrad, $\sigma_\gamma/\gamma_0 = 10^{-4}$, $I_{pk} = 2$ kA, $\lambda_r = 0.124$ nm and $\lambda_w = 25$ mm. The nominal SASE lattice comprised 4 m undulator modules within a FODO focussing structure with half period 5 m. This meant the gap between undulators was 1m. An alternative lattice was set up in which every other undulator was removed to allow delay chicanes up to several metres long to be inserted. In this lattice the gap between undulator modules is therefore 6 m.

In SASE mode, for the nominal lattice with 1m gaps, the saturation power of 5 GW was reached after 17 undulator modules. For the alternative lattice, with the gap length increased to 6m, the saturation power of 2.2 GW was reached after 18 undulator modules. For the 6m gaps the rms radiation size stabilises at a level about double that of the case with 1m gaps. These results indicate that a 5 m chicane is acceptable in terms of FEL performance, assuming a 50% reduction in output power and 100% increase in floor length are viable.

DELAY CHICANE DESIGNS

The first consideration is the magnitude of the required electron beam delay. For the generic XFEL parameters of a gaussian electron bunch of peak current $I_{pk} = 2$ kA and charge $Q = 50$ pC, the bunch duration is 3 µm. For HB-SASE it is assumed the largest delay ever required would be $\delta = 2.5$ µm. In fact the required delay turns out not to be the limiting factor in making the chicanes as compact as possible. For a three-dipole chicane the beam delay, found from simple geometry, is given by $\delta = (L_m^3/2 + 2L_dL_m^2)(Bc/E[\text{eV}])^2$ where L_m is the dipole length, L_d is the drift length between dipoles and B is the dipole field. For $L_m = L_d$, $\delta = 2.5$ µm, $B = 1$ T and $E = 6$ GeV the mininimum total chicane length of a dipole-only chicane is $L_c \simeq 0.4$ m. However, to obtain an isochronous solution, space must be left for quadrupoles to control dispersion. It is assumed that the aperture is $d = 10$ mm, and the minimum dipole length is $L_m = 3d = 30$ mm. The bend angle is then $\theta = BL_mc/E = 1.5$ mrad and the drift length $L_d = 0.5$ m.

To obtain an isochronous chicane the R_{56} of the chicane transfer matrix must be set to zero. The R_{56} is defined as the integral of the dispersion over the bend radius, i.e. $R_{56} = \int \eta(s)/\rho(s)\mathrm{d}s$ so can be minimised by balancing positive and negative dispersion within the dipoles using quadrupoles. Two chicane options are considered. Option 1 is a three-dipole chicane with four quads which are inserted 1/4 and 3/4 of the way along the drifts between the dipoles. Option 2 is a four dipole chicane with three quads inserted midway between the dipoles. Both options are shown in Fig. 1 with properties summarised in Table 1.

Option 1

Option 1 is shown in Fig. 1 (top). The quadrupoles set the dispersion to zero at the midpoints between the dipoles and at the dipoles themselves. This means the effect of the quadrupole is to invert the sign of the dispersion gradient

* neil.thompson@stfc.ac.uk

Content from this work may be used under the terms of the CC BY 3.0 licence (© 2019). Any distribution of this work must maintain attribution to the author(s), title of the work, publisher, and DOI

ISBN: 978-3-95450-210-3 doi:10.18429/JACoW-FEL2019-THP035

BEAM SHAPING FOR HIGH-REPETITION-RATE X-RAY FELS*

Y. Ding†, K. Bane, Y. Nosochkov, SLAC National Accelerator Laboratory, Menlo Park, USA

Abstract

Beam shaping at normal-conducting, accelerator-based FELs, such as LCLS, plays an important role for improving lasing performance and for supporting special operating modes, such as the self-seeding scheme. Beam shaping methods include horn-collimation and dechirper manipulation. Applying the beam shaping concept to high-repetition-rate FELs driven by a superconducting linac, such as LCLS-II, beam invasive methods are not preferred due to concerns about high power deposition. We have recently studied a few shaping options for LCLS-II, such as manipulating the beam chirp before compression using corrugated devices, and modifying higher order optics terms in a chicane using octupoles. In this report we will discuss the results.

INTRODUCTION

In LCLS-II x-ray FEL pulses will be generated that have high average brightness at a megahertz-level repetition rate, opening up remarkable, new capabilities for various scientific research fields. The electron beam quality is the most important factor affecting the FEL performance; typically what is required is an electron beam with low emittance and high current. While the (slice) emittance is determined at the gun, high peak current can be achieved by longitudinal compression of the bunch.

For the LCLS-II driven by superconducting linacs, the electron bunch, coming from a very-high-frequency (VHF) gun, has a lower peak current and a lower energy than what is achieved at the present (normal conducting) S-band RF gun of LCLS. To achieve a final peak current at the kA-level, stronger compression is required. However, the achievable peak current is limited by strong nonlinearities in single particle and collective effects in the linacs and bunch compressors. For example, according to the present LCLS-II design, at 100 pC bunch charge, the peak current is about 800 A [1]. For some operating scheme such as the self-seeding mode, electron beam longitudinal phase space distribution is also critical for seeded FEL lasing performance.

Beam shaping schemes typically include electron beam phase space manipulation for achieving higher beam current, lower transverse emittance, and uniform longitudinal phase space. This type of beam phase space manipulation can be realized by direct interaction on the electron beam phase space, or by machine configuration optimization. For example, at the LCLS, beam shaping methods such as horn collimation [2] and emittance spoiling by foil [3, 4] have greatly improved the FEL performance and operating flexibility. Unfortunately, such beam invasive methods are not preferred for high-repetition rate FELs and new schemes have to be developed. We summarize two beam shaping methods for the high-repetition rate FELs in this paper. The LCLS-II machine layout is shown in Fig. 1.

MANIPULATION OF BEAM CHIRP BEFORE FINAL COMPRESSION

In a technical note [5], manipulation of electron beam high-order time-energy chirp has been studied. The idea is to add a dechirper-like corrugated structure in the low energy region of the LCLS-II linac, where it can function as a passive phase space linearizer and help customize the beam energy chirp before it enters the second bunch compressor. After optimizing the parameters of the system, it is possible to enhance the compression factor in the final bunch compressor and thus to achieve a higher final peak current. Note also that, with this method, the current profile can be shaped to avoid large spikes at the head and tail of the distribution. Details of this scheme can be found in [5], and in Fig. 2 we show one result of the final beam before the undulator with using a 0.25-m long corrugated structure (diameter of the structure is 1 mm). Comparing to standard LCLS-II simulation results, we found that the current horn at the bunch head is suppressed, and the core beam current is improved to above 1 kA.

MANIPULATION OF HIGH ORDER OPTICS TERMS IN COMPRESSOR CHICANE

To shape the beam current profile after compression, besides manipulation of the electron beam chirp as discussed above, one can also modify the high-order (nonlinear) terms of the compressor optics. We investigated a scheme recently reported in [6], where an octupole magnet has been adopted in the chicane for U5666 control. Following the methods in [6], we studied the requirement of the U5666 for a given electron beam at the LCLS-II before final compression, developed an optimization procedure using LiTrack code [7], derived formulas to calculate the corresponding octupole strength from U5666, and verified the solutions by Elegant [8] tracking simulations. We discuss these results in the following subsections.

Required U5666 for Current Horn Suppression

With a known beam longitudinal chirp before compression and the chicane R56, to avoid current spikes, one can solve the required high-order term U5666 following the method developed in [6]. But for the overall machine setup, the system should be optimized with also including the machine parameters such as linac phase and amplitude, harmonic linearizer amplitude and phase, BC1 chicane R56, BC2 chicane R56, etc. LiTrack tracking is fast and can be

* Work supported by US Department of Energy under Contract DE-AC02-76SF00515.
† email: ding@slac.stanford.edu

Content from this work may be used under the terms of the CC BY 3.0 licence (© 2019). Any distribution of this work must maintain attribution to the author(s), title of the work, publisher, and DOI

ISBN: 978-3-95450-210-3 doi:10.18429/JACoW-FEL2019-THP036

MICROBUNCH ROTATION FOR HARD X-RAY BEAM MULTIPLEXING*

R. A. Margraf†[1], Z. Huang[1], J. MacArthur, G. Marcus, SLAC National Laboratory, 94025 Menlo Park, USA
X. Deng, Tsinghua University, Beijing, China
[1]also at Stanford University, Stanford, USA

Abstract

Electron bunches in an undulator develop periodic density modulations, or microbunches, which enable the exponential gain of X-ray power in a SASE FEL. Many FEL applications could from the ability to preserve microbunching through a dipole kick. For example, X-ray beam multiplexing can be achieved if electron bunches are kicked into separate beamlines and allowed to lase in a undulator. The microbunches developed in upstream undulators, if properly rotated, will lase axis, producing radiation at an angle from the initial beam axis. Microbunch rotation with soft X-rays was previously published and demonstrated experimentally [1], multiplexing LCLS into three X-ray beams. Additional 2018 data demonstrated multiplexing of hard X-rays. Here we describe ts to reproduce these hard X-ray experiments using an analytical model and Genesis simulations. Our goal is to apply microbunch rotation to outcoupling from a cavity-based XFEL, (RAFEL/XFELO) [2].

ANALYTICAL MODEL

Microbunch rotation can be accomplished by providing a dipole kick to a bunch as it travels through a defocusing quadrupole. This dipole kick can be provided by either a dipole magnet or a transversely quadrupole. An analytical model for microbunch rotation within a defocusing quadrupole was developed previously by MacArthur et al. [1]. Here, we introduce a new analytical method for describing microbunch rotation using matrices, which is more intuitive to use with multiple quadrupoles.

Microbunch Rotation by Offset Thin Quadrupole

We begin by a thin quadrupole in 4D phase space (y, y', z, δ). The quadrupole has focal length f, and is in y by a distance o_1, producing a kick $\theta = -\frac{1}{f}(y_0 + o_1)$, where y_0 is the transverse beam position before the quadrupole. We treat an quadrupole as an on-axis quadrupole which also rotates the coordinate system in the y-z plane by θ to follow the beam trajectory. We assume a small kick angle ($sin(\theta) \approx \theta$, $cos(\theta) \approx 1$), and neglect order terms, ($\theta z \approx 0$, $-\theta y' \approx 0$) to simplify the rotation matrix.

$$M_\theta \approx \begin{bmatrix} 1 & 0 & 0 & 0 \\ 0 & 1 & 0 & \theta \\ -\theta & 0 & 1 & 0 \\ 0 & 0 & 0 & 1 \end{bmatrix} \tag{1}$$

our initial microbunch size and divergence in the center of the quadrupole, we an quadrupole matrix with double the focal length of our full quadrupole

$$M_{Q\theta} = M_Q + M_\theta = \begin{bmatrix} 1 & 0 & 0 & 0 \\ \frac{-1}{2f} & 1 & 0 & \theta \\ -\theta & 0 & 1 & 0 \\ 0 & 0 & 0 & 1 \end{bmatrix}. \tag{2}$$

Note that we still rotate the coordinate system by the full kick, θ, produced by the quadrupole. This is because the y-z plane (which we must rotate) is initially at the angle of the beam entering the quadrupole, $y_0' = 0$, but our microbunch rotation analysis begins with particles at the center of the quadrupole, $(y_1, y_1', z_1, \delta_1)$.

We apply a drift of length L to get our transfer matrix,

$$M = M_L M_{Q\theta} = \begin{bmatrix} 1 - \frac{L}{2f} & L & 0 & L\theta \\ \frac{-1}{2f} & 1 & 0 & \theta \\ -\theta & 0 & 1 & 0 \\ 0 & 0 & 0 & 1 \end{bmatrix}. \tag{3}$$

We assume a single Gaussian microbunch, with a sigma matrix that is uncorrelated in the center of the quadrupole,

$$\Sigma_1 = \begin{bmatrix} \sigma_{y_1}^2 & 0 & 0 & 0 \\ 0 & \sigma_{y_1'}^2 & 0 & 0 \\ 0 & 0 & \sigma_{z_1}^2 & 0 \\ 0 & 0 & 0 & \sigma_{\delta_1}^2 \end{bmatrix}. \tag{4}$$

We then evolve the microbunch envelope using the transfer matrix, and obtain the second moments.

$$\Sigma = M \Sigma_1 M^T \tag{5}$$

$$\begin{aligned} \langle y^2 \rangle &= \left(1 - \frac{L}{2f}\right)^2 \sigma_{y_1}^2 + L^2 \sigma_{y_1'}^2 + L^2 \theta^2 \sigma_{\delta_1}^2 \\ \langle z^2 \rangle &= \sigma_{z_1}^2 + \theta^2 \sigma_{y_1}^2 \\ \langle yz \rangle &= -\left(1 - \frac{L}{2f}\right) \theta \sigma_{y_1}^2 \end{aligned} \tag{6}$$

The tilt in the rotated coordinate system, t_{yz}, can then be geometrically found from,

$$tan(2t_{yz}) = \frac{2\langle yz \rangle}{\langle y^2 \rangle - \langle z^2 \rangle}, \tag{7}$$

$$t_{yz} \approx \frac{\langle yz \rangle}{\langle y^2 \rangle - \langle z^2 \rangle}. \tag{8}$$

In the limit of pancake microbunches, $\langle z^2 \rangle << \langle y^2 \rangle$ and if $\theta^2 \approx 0$, we write the tilt in terms of the Beta function, β_1.

$$t_{yz} \approx \frac{\langle yz \rangle}{\langle y^2 \rangle} = \frac{-\left(1 - \frac{L}{2f}\right)\theta}{\left(1 - \frac{L}{2f}\right)^2 + \frac{L^2}{\beta_1^2}} \tag{9}$$

* This work was supported by the Department of Energy, Laboratory Directed Research and Development program at SLAC National Accelerator Laboratory, under contract DE-AC02-76SF00515.
† rmargraf@stanford.edu

Content from this work may be used under the terms of the CC BY 3.0 licence (© 2019). Any distribution of this work must maintain attribution to the author(s), title of the work, publisher, and DOI

ISBN: 978-3-95450-210-3 doi:10.18429/JACoW-FEL2019-THP037

A NOVEL ONE-DIMENSIONAL MODEL FOR CSR WAKEFIELDS*

Gennady Stupakov†, SLAC National Accelerator Laboratory, Menlo Park, CA, USA

Abstract

The existing 1D models of the coherent synchrotron radiation (CSR) wakefield in free space assume that the longitudinal bunch distribution remains constant when the beam propagates through a magnetic lattice. In this paper, we derive a formula for a 1D CSR wake that takes into account variation of the bunch length along the orbit. The formula is valid for arbitrary curvilinear beam trajectory. We analyze the validity of the 1D model in a typical implementation of an FEL bunch compressor.

INTRODUCTION

When the trajectory of a relativistic beam is bent by magnetic field, the beam radiates electromagnetic field and experiences a radiation reaction force. A popular 1D model for this force in the case of a circular motion, often called the coherent synchrotron radiation (CSR) wake, was first developed in Refs. [1–3]. A generalization of this model for the case of a bending magnet of finite length is described in Refs. [4, 5] and is implemented in several computer codes[1]. These models assume a constant bunch length, σ_z, along the orbit. Their applicability becomes questionable in a bunch compressor where $\sigma_z(s)$ is a function of the beam position s. In practice, one usually substitutes a local bunch length $\sigma_z(s)$ into the formulas derived with the assumption $\sigma_z = \text{const}$. Such a substitution, strictly speaking, is not justified because it ignores the fact that the wake is formed by the beam radiation emitted at previous times, when the bunch length is different from the value of σ_z at the moment when the wake interacts with the beam. More recently, in Ref. [6], a 1D CSR model was derived from Jefimenko's form for the electric field of a relativistic beam with an attempt to include a time dependent bunch length by heuristically introducing $\sigma_z(t)$ into equations derived with the assumption of constant bunch length.

In this paper, we derive a 1D CSR wake that takes into account the variation of the bunch length along the orbit. Our derivation is based on the 3D formulas from Ref. [7].

We use the CGS system of units throughout this paper.

FORMULA FOR THE LONGITUDINAL WAKE IN 3D

We begin from the formulation of general 3D wake from Ref. [7]. In 3D, the beam is represented by its charge density $\rho(\boldsymbol{r},t)$ that depends on time t and the position vector $\boldsymbol{r}$, and its velocity $\boldsymbol{v}(\boldsymbol{r},t)$, with the beam current density $\boldsymbol{j}$ given by the product $\boldsymbol{j} = \rho\boldsymbol{v}$. Note that in this model assigning a particular value of $\boldsymbol{v}$ at each point we neglect the uncorrelated velocity spread in the beam due the the angular and energy spread — an approximation that is typically well satisfied for relativistic beams. For given functions $\rho(\boldsymbol{r},t)$ and $\boldsymbol{j}(\boldsymbol{r},t)$, one can derive an equation for the electric field in the beam, $\boldsymbol{E}(\boldsymbol{r},t)$, and calculate the instantaneous energy change per unit time and *per unit charge*, $\mathcal{P}$,

$$\mathcal{P}(\boldsymbol{r},t) = \boldsymbol{v}(\boldsymbol{r},t)\cdot\boldsymbol{E}(\boldsymbol{r},t). \tag{1}$$

We will loosely call $\mathcal{P}$ the *longitudinal wake*, although the classical wake fields are typically associated with the energy loss integrated over the beam path and the transverse cross section of the beam.

A general expression for the quantity $\mathcal{P}$ is given in Ref. [7]. It consists of three terms two of which in many cases are much smaller that the third one. We neglect these terms in our analysis leaving only the dominant one:

$$\mathcal{P}(\boldsymbol{r},t) = -c\int\frac{d^3r'}{|\boldsymbol{r}'-\boldsymbol{r}|}\,[\boldsymbol{\beta}(\boldsymbol{r},t) - (\boldsymbol{\beta}(\boldsymbol{r},t)\cdot\boldsymbol{\beta}(\boldsymbol{r}',t_{\rm ret}))\boldsymbol{\beta}(\boldsymbol{r}',t_{\rm ret})]\cdot\partial_{\boldsymbol{r}'}\rho(\boldsymbol{r}',t_{\rm ret}), \tag{2}$$

where $\boldsymbol{\beta} = \boldsymbol{v}/c$, $t_{\rm ret}(\boldsymbol{r},\boldsymbol{r}',t) = t - |\boldsymbol{r}'-\boldsymbol{r}|/c$, and we use the notation $\partial_{\boldsymbol{r}'}\rho(\boldsymbol{r}',t_{\rm ret})$ to indicate differentiation with respect to the space coordinates in function $\rho(\boldsymbol{r}',t_{\rm ret})$ with a fixed $t_{\rm ret}$ (in other words, the operator $\partial_{\boldsymbol{r}'}$ ignores the fact that $t_{\rm ret}$ also depends on $\boldsymbol{r}'$). Note that due to the factor $|\boldsymbol{r}'-\boldsymbol{r}|^{-1}$ the integrand has a singularity at $\boldsymbol{r}'\to\boldsymbol{r}$, however, this singularity is integrable[2]. The singularity disappears in the ultra-relativistic limit $|\boldsymbol{\beta}| = 1$ because the factor in square brackets vanishes when $\boldsymbol{r}\to\boldsymbol{r}'$. As one can see, the integral (2) is taken over the volume around the beam trajectory at preceding times $t_{\rm ret} < t$.

1D MODEL

It is known that the transverse size of the beam, $\sigma_\perp$, does not affect the CSR wake if $\sigma_\perp \lesssim (\sigma_z^2 R)^{1/3}$, where R is the bending radius [3] (see, however, discussion below). Assuming that this is the case, we can simplify integral (2) and derive a 1D model for the wake $\mathcal{P}$. In 1D all particles in the beam move along a curve given by the radius-vector $\boldsymbol{r}_0(s)$, where s is the path length measured along the orbit. Positions in the vicinity of this orbit are represented in a Frenet–Serret coordinate system as $\boldsymbol{r}_0(s) + \hat{\boldsymbol{x}}(s)x + \hat{\boldsymbol{y}}(s)y$, where $\hat{\boldsymbol{x}}(s)$ and $\hat{\boldsymbol{y}}(s)$ are the unit vectors perpendicular to the tangential vector, $\boldsymbol{\tau}(s) \equiv d\boldsymbol{r}_0/ds$, and each other so that x, y and s constitute a local orthogonal coordinate system. In what follows we will assume an ultra-relativistic beam

* Work supported by the Department of Energy, contract DE-AC03-76SF00515

† stupakov@slac.stanford.edu

[1] Here, we only deal with the longitudinal part of the forces in the bunch that changes particles' energy in the beam; for the effect of the transverse force, see a recent study [8].

[2] It is also integrable in a 2D model when the three dimensional integration $\int d^3r'$ is replaced by $\int d^2r'$. It is not integrable in 1D.

Content from this work may be used under the terms of the CC BY 3.0 licence (© 2019). Any distribution of this work must maintain attribution to the author(s), title of the work, publisher, and DOI

ISBN: 978-3-95450-210-3 doi:10.18429/JACoW-FEL2019-THP041

INTERACTION OF POWERFUL ELECTRO-MAGNETIC FIELDS WITH BRAGG REFLECTORS*

I. Bahns†, W.Hillert, P. Rauer, J. Rossbach, Universität Hamburg, Hamburg, Germany
H. Sinn, European XFEL GmbH, Schenefeld, Germany

Abstract

The interaction of an X-ray free electron laser (XFEL) with a Bragg Reflector can cause a change of the lattice constant, which has a direct influence on the stability of the reflection conditions [1] and can also excite modes of vibration [2]. The dynamical thermoelastic effects of the photon-matter-interaction are simulated with a finite-element-method (FEM) using the assumptions of continuums mechanics. To compare the simulation results with measured signals, a Michelson interferometer with ultrafast photodiodes (risetime < 175 ps bandwith > 2 GHz) has been built up. To test the experimental setup in an in-house environment a pulsed UV laser is used to introduce a temporal displacement field in a silicon crystal created by about 0.26 µJ of absorbed energy. The measured signal is in agreement with the FEM simulation and has shown that if averaging over thousands of pulses is applied a resolution < 0.5 pm is feasible. This makes this experimental setup useful to investigate the X-ray-matter-interaction of Bragg reflectors at modern X-ray facilities.

INTRODUCTION

When electro-magnetic fields are interacting with an X-ray Bragg reflector, the absorbed part of the energy will cause a change of the local thermal energy of the crystal. Due to thermal expansion this also affects the value of the local lattice parameter, and due to Bragg's law this has a direct influence on the reflection conditions. To investigate such effects one method is to directly observe the temporal change of the lattice by using X-ray radiation [1]. However, for this experimental method a modern X-ray facility is needed where the beam time for experiments is mostly limited. An alternative method could be to use optical methods like thermoreflectance [3], the knife-edge method or interferometry [4]. In the present work a Michelson interferometer is tested in terms of the requirements for such a measurement. For the first test measurement, a pulsed UV laser introduced temporal change of the displacement on the backside of a silicon crystal was detected (Fig. 1). The temporal development of the displacement can be simulated with numerical methods like the finite-element-methode (FEM), which can solve the coupled partial differential equations of thermoelasticity using the assumption of continuum mechanics. These results can be compared with measured displacements such as presented in the present paper. This is useful to investigate the stability of an X-ray free electron laser oscillator [5].

* Work supported by BMBF (FKZ 05K16GU4)
† immo.bahns@desy.de

EXPERIMENTAL SETUP

To built up a Michelson interferometer a linear polarized continuous wave laser operating at a wavelength of 532 nm is used. As illustrated in Fig. 1 polarizing beamsplitters (PBS) in combination with rotatable wave plates ($\lambda/2$ and $\lambda/4$) give control over the intensity, which is transmitted or reflected by the PBS. Film polarizers (FP) reduce the amount of intensity, which reaches the photo detector areas to the desired value. A PID controller stabilizes the working point of the interferometer by controlling the position of the mirror in the reference arm of the interferometer. Spherical lenses are used to collimate and focus the beam in a way that the focal plane lies on the surface of the silicon crystal and at the detector areas. Also the focal spot at the detector area is reduced to a size which is smaller than the area of the detector. The $\lambda/4$ wave plates are adjusted such that the total amount of the reflected beam of both interferometer arms goes into the direction of PBS3. The setup is adjusted in a way that the beam waists coming from each interferometer are equal. The beam size at the focal spot lying on the surface of the crystal and the reference mirror is ω_0=25 µm.

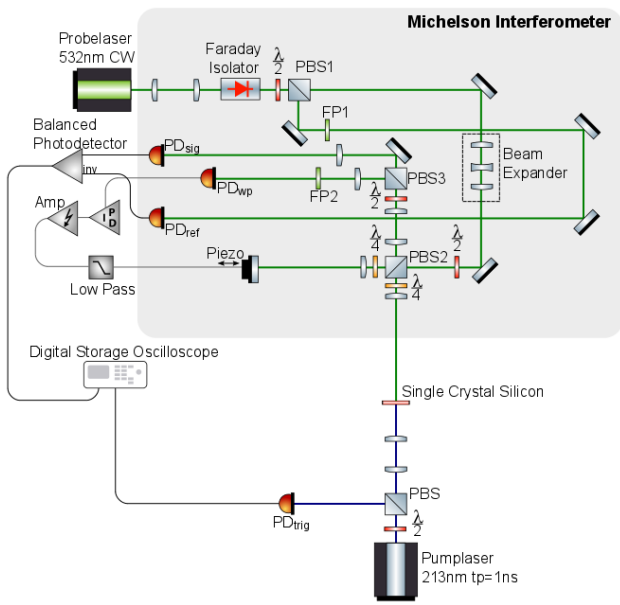


Figure 1: Pump-probe setup with Michelson interferometer. For a detailed description see the text.

The electric field amplitude and phase of the probe laser is described by using the Jones calculus:

$$\vec{J} = \begin{pmatrix} E_{0x}e^{i\varphi_x} \\ E_{0y}e^{i\varphi_y} \end{pmatrix} . \quad (1)$$

Content from this work may be used under the terms of the CC BY 3.0 licence (© 2019). Any distribution of this work must maintain attribution to the author(s), title of the work, publisher, and DOI

ISBN: 978-3-95450-210-3 doi:10.18429/JACoW-FEL2019-THP044

THE SIMULATION STUDY FOR SINGLE AND MULTI TURN ERL BASED EUV FEL

K. M. Nam and G. S. Yun, Department of Advanced Nuclear Engineering, POSTECH, Pohang, Korea
Y. W. Parc†, Pohang Accelerator Laboratory, Pohang, Korea

Abstract

Photolithography technology is the core part of the semiconductor manufacturing process. It has required that the power of EUV light should be higher about ~ kW for higher throughput. ERL based EUV FEL is emerging as a next generation EUV source which can produce over 10 kW EUV power. In this simulation study, EUV-FEL design with single turn is presented. An electron beam with 40 pC beam charge is accelerated to 600 MeV and produces EUV light with 37 kW power. Secondly, multi-turn based design is also presented. Multi-turn design improved compactness for industrial application. Simulation study shows that the multi-turn design can also generate about 15.5 kW average power. This study is expected to increase the practical industrialization potential of ERL-based photolithography.

INTRODUCTION

Photolithography process means microfabrication to pattern certain circuit into wafer. It is the core part of semiconductor manufacturing process and has been evolved from I-line, Krypton Fluoride Lasers (248 nm), Argon Fluoride Lasers to Laser-Produced Plasma (LPP, 13.5 nm). However, semiconductor industries have demanded new light source with high average power over 1 kW and high repetition rate in order to produce much-integrated semiconductor [1-5]. Thus, new EUV source has been studied and Energy Recovery Linac (ERL) based Free Electron Laser (FEL) has been received attention, which is believed that can replace the LPP source. ERL is a new type of accelerator, which can reuse kinetic energy of accelerated electron beams in order to accelerate other electron beam. ERL-based FEL can supply high current over 500 A to generate high power over 10 kW per second. This field faced many beam dynamics issues such as longitudinal phase space manipulation, bunch compressing, high order effect control, energy recovery [6], and space charge effect [7]. Therefore, it is vital to consider many collective effects and beam dynamics to produce high quality EUV.

In this paper, single and multi-turn ERL simulation study was performed by using ASTRA [8], ELEGANT [9] and GENESIS simulation [10]. It includes generation of electron from dc gun, bending, compression, acceleration, bending, compression and EUV generation. Most of simulations were performed through ELEGANT code, but we used ASTRA code to optimize injector part and GENESIS 1.3 code for simulation of FEL.

* Work supported by Max Planck POSTECH/KOREA Research Initiative Program [Grant No 2016K1A4A4A01922028] through the National Research Foundation of Korea (NRF) funded by Ministry of Science, ICT & Future Planning.
† young1@postech.ac.kr

OVERVIEW

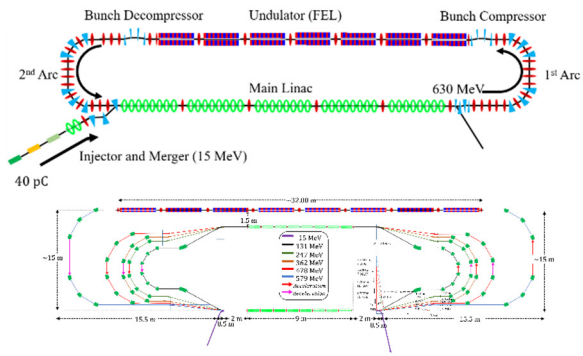


Figure 1: Layout of Single turrn(Upper part) and multi-turn design(Lower part) used in the simulation study.

In Fig.1, two designs of the EUV-FEL used in the simulation are shown. For the both designs, an electron beam with 40 pC beam charge is generated from the injector, accelerated to 15 MeV at superconducting RF cavity and transmitted to a merger. The merger compresses the beam, and transports it to linac simultaneously for both designs. However, they have different structural concept. At single turn design, electron beam circulates only one time. Thus, it requires multiple number of rf modules in the linac part as it cannot pass same linac before deceleration. Thus, the single turn design (upper part of Fig. 1) has larger size than multi turn case. Multi-turn design concept, suggested in 2011 [11], means circulating the electron beams to improve the compactness of facility. In multi-turn design (lower part of Fig. 1), electron beam circulates several times and it passes the same linac two or three times during acceleration process. This point can improve the compactness of a EUV facility.

SINGLE TURN SIMULATION RESULT

Injector in Fig. 2 consists of high average current DC photocathode gun, two solenoids, buncher cavity, superconducting RF cavities and merger that transfers the beam to main linac. DC photocathode gun produces 40 pC bunch charge and accelerates it to 960 kV with 1.3 GHz repetition rates.

In single turn design, superconducting RF cavities In Fig. 3 accelerate the beam from 15 MeV to 638 MeV while it makes chirp of electron beam linearly. It also recovers the kinetic energy of the used beam down to 15 MeV. Dump magnets separate high and low energy electron beam to dump the low energy beam. After the electron beam passes matching section that consists of 4

Content from this work may be used under the terms of the CC BY 3.0 licence (© 2019). Any distribution of this work must maintain attribution to the author(s), title of the work, publisher, and DOI

ISBN: 978-3-95450-210-3 doi:10.18429/JACoW-FEL2019-THP047

Content from this work may be used under the terms of the CC BY 3.0 licence (© 2019). Any distribution of this work must maintain attribution to the author(s), title of the work, publisher, and DOI

LASER-DRIVEN COMPACT FREE ELECTRON LASER DEVELOPMENT AT ELI-BEAMLINES

A.Molodozhentsev*, G.Korn, K.Kruchinin, J.Hawke, D.Kocon, T.Green, M.Kaur
ELI-BL, Institute of Physics of CAS, Prague, Czech Republic
A. R. Maier, University of Hamburg and CFEL, Hamburg, Germany

Abstract

ELI-Beamlines Centre, located near Prague (Czech Republic) is an international user facility for fundamental and applied research using ultra-intense lasers and ultra-short high-energy electron beams. Using the optical parametric chirped-pulse amplification (OPCPA) technique, the ELI-Beamlines laser system will provide the laser pulse energy up to 10 Joules with the repetition rate up to 25 Hz. Combination of new laser development with constant improvement of the LWFA electron beam parameters has great potential in future development of a next generation of the compact high repetition rate Free Electron Laser, which is extremely demanded by the X-ray community.

The LWFA-driven FEL project, called 'LUIS', is currently under preparation at ELI-Beamlines in collaboration with University of Hamburg. The goal of the project is improvement of the electron beam parameters in order to demonstrate the amplification and saturation of the SASE-FEL photon power in a single unit of a FEL undulator.

An overview of the LUIS project including design features and a description of all instrumentations used to characterize the laser, plasma, electron beam, photon generation is presented in frame of this report.

INTRODUCTION

Extreme Light Infrastructure (ELI) [1] was heralded by the European Community to develop in Europe a new type of large-scale laser infrastructure specifically designed to provide high peak power and focused intensity ultrashort pulses. ELI should be the world's first international laser research infrastructure implemented as a distributed research infrastructure based on 3 specialized and complementary facilities located in the Czech Republic, Hungary and Romania. ELI-Beamlines (located in Dolni Brezany, near Prague, the Czech Republic) will be the high-energy beam facility responsible for development and use of ultrashort pulses of high-energy particles and radiation stemming from the ultra-relativistic interaction. In particular, using laser systems in ELI-Beamlines it will be possible to accelerate electrons up to a few GeV.

The principle of the 'laser-wake-field-acceleration' (LWFA) [2] is based on an ultra-high longitudinal electric gradient, created by the high-intensity laser pulse focused in underdense plasma (in a gas-jet, gas-cell or capillary discharge targets). A travelling longitudinal electric field can reach several hundreds of GV/m, which is much larger than the accelerating field achievable in conventional accelerators, making LWFA extremely attractive as a compact accelerator to provide high-energy beams for different applications. During last decades, a remarkable progress has been made in the field of electron acceleration based on the LWFA concept. Electron beams with peak energies of multi-GeV in a short plasma channel (a few cm) have been obtained experimentally [3].

Using these achievements [4] one can define the parameters of the LWFA electron beam at the exit of the plasma channel as following: the electron beam energy is in the range of 300÷1000 MeV; the RMS transverse beam size in the horizontal and vertical plane is less than 1μm; the RMS transverse beam divergence in the horizontal and vertical planes is less than 1 mrad; the RMS bunch length is about 1μm; the RMS relative (total) energy spread is less than 1 %; the normalized RMS transverse beam emittance in the horizontal and vertical planes is 0.2 π mm.mrad and the bunch charge is about 50 pC.

The novel acceleration methods open a new way to develop a compact "laser-based" SASE [5] free electron laser (FEL) with the 'fsec' photon pulse length. We present the laser-driven 'demo'-FEL setup, which is under development at ELI-Beamlines. After commissioning this setup will deliver to users a photon peak brightness up to 10^{30} photons/pulse/mm^2/mrad^2/0.1%BW using a single undulator. The 'laser-driven' FEL at ELI-Beamlines can operate with high repetition rate (up to 50Hz), which is limited by the current 'state-of-art' of the laser technology. Successful realization of the 'demo'-FEL research program at ELI-Beamlines will open a new perspective in development of compact soft and hard X-ray FELs with few or even sub-femtosecond photon bunches for a very wide user community.

LASER-DRIVEN 'DEMO'-FEL

The goal of the 'demo'-FEL setup at ELI-Beamlines is experimental demonstration of the laser-driven FEL in a single unit FEL undulator. For this purpose, a commercial-available 'in-vacuum' planar undulator, based on the hybrid permanent magnets [6], can be used. Such undulator has the undulator period of 15 mm with the variable gap (3 ÷ 6 mm).. The undulator parameter (K_0) is in the range of 0.8÷1.6 depending on the gap size. In order to simplify the 'matching' condition the total length of such undulator should be 2.5 m. The average beta-function is 1.6 m. The saturation length ($L_{sat} \sim 20L_{g,3D}$), estimated by using the Xie parametrization of the gain length [7] and checked by using the fitting formula for free-electron lasers with strong space charge effects [8], does not exceed such undulator length for the electron beam summarized in Table 1.

*Alexander.Molodozhentsev@eli-beams.eu

ISBN: 978-3-95450-210-3 doi:10.18429/JACoW-FEL2019-THP048

Content from this work may be used under the terms of the CC BY 3.0 licence (© 2019). Any distribution of this work must maintain attribution to the author(s), title of the work, publisher, and DOI

PROGRESS TOWARDS LASER PLASMA ELECTRON BASED FREE ELECTRON LASER ON COXINEL

M. E. Couprie *, T. André, F. Blache, F. Bouvet, F. Briquez, Y. Dietrich, J. P. Duval, M. El-Ajjouri, A. Ghaith, C. Herbeaux, M. Khojoyan, N. Hubert, C. Kitégi, M. Labat, N. Leclercq, A. Lestrade, A. Loulergue, O. Marcouillé, F. Marteau, D. Oumbarek Espinos, P. Rommeluère, M. Sebdaoui, K. Tavakoli, M. Valléau, Synchrotron SOLEIL, GIF-sur-YVETTE, France
C. Benabderrahmane, ESRF, Grenoble, France
S. Corde, J. Gautier, J. P. Goddet, O. Kononenko, G. Lambert, A. Tafzi, K. Ta Phuoc, C. Thaury, Laboratoire d'Optique Appliquée, Palaiseau, France
S. Bielawski, C. Evain, E. Roussel, C. Szwaj, Laboratoire PhLAM, Villeneuve d'Ascq, France
I. Andriyash, V. Malka, S. Smartzev, Weizmann Institute, Rehovot, Israel

Abstract

Laser plasma acceleration (LPA) [1] with up to several GeV beam in very short distance appears very promising. The Free Electron Laser (FEL), though very challenging, can be viewed as a qualifying application of these new emerging LPAs. The energy spread and divergence, larger than from conventional accelerators used for FEL, have to be manipulated to answer the FEL requirements. On the test COXINEL experiment [2–4] line, "QUAPEVA" permanent magnet quadrupoles of variable strength [5, 6] handle the emittance growth and a decompression chicane reduces the slice energy spread, enabling FEL amplification for baseline reference parameters [2]. A beam pointing alignment compensation method enables to properly transport the electrons along the line, with independent adjustments of position and dispersion [7]. The measured undulator spontaneous emission radiated exhibits the typical undulator radiation pattern, and usual features (gap tunability, small linewidth...).

INTRODUCTION

Accelerator based light sources presently know a very wide development [8], with the FEL [9] advent in the X-ray domain [10] coming along with an increase of the peak brightness by several orders of magnitude, enabling fifty years after the laser invention [11] to decipher the matter structure in unexplored areas and dynamics on ultra-fast time scales unraveling the processes involved various domains [12]... Following the laser invention, alternately of developing FELs relying on non bounded relativistic electrons in an undulator periodic permanent magnetic field as a gain medium [9], laser have been considered to generate and accelerate electrons in plasmas [1]. An intense laser focused onto a gas target ionizes the gas and creates a plasma. As the laser pulse propagates, the ponderomotive force expels electrons from the optical axis, forming a cavity free of electrons in the laser wake with large amplitude electric fields where electrons can be trapped and accelerated. With the growth of ultra high power laser making advantage of Chirped Pulse Amplification techniques [13], electrons can be accelerated with plasma up to several GeV within ultra-short distances [14–16] with kA peak current, ultra-short bunches, 1π mm.mrad normalized emittance beams, enabling to consider LPA to drive an FEL [3, 17]. Even though some LPA features such as peak current and emittance seem to be quite suitable for the FEL application, energy spread and divergence do not meet conventional accelerator µrad divergence and per mille of energy spread beams. They should be handled to mitigate chromatic effects [18, 19], that can lead to a dramatic emittance growth and afferent beam quality degradation in the transfer lines. Large divergence requires strong focusing right after the electron source, with for instance high gradient permanent magnet quadrupoles [20]. Large energy spread can be managed by a decompression chicane [3, 21] or a transverse gradient undulator [22, 23]. The energy-position correlation introduced by the chicane [2] can be turned into an advantage. There are still very few experiments with LPA electron beam transport towards an undulator [24] and preliminary observation of undulator radiation [25–28]. The COXINEL program [29] aiming at demonstrating FEL amplification using a dedicated manipulation line is developed in the frame of the LUNEX5 project of advanced compact free electron laser demonstrator [30, 31]. We report here the progress on the COXINEL experimental program.

THE COXINEL LINE DESIGN

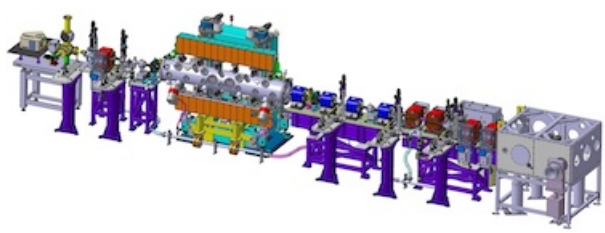


Figure 1: COXINEL line CATIA sketch.

The COXINEL line (see Fig. 1) has been designed and built at Synchrotron SOLEIL [4, 32] (ERC Advanced COXINEL 340015) using the baseline reference parameters given in Table 1 for the 180 MeV case, for being installed at Labora-

* couprie@synchrotron-soleil.fr

ISBN: 978-3-95450-210-3 doi:10.18429/JACoW-FEL2019-THP049

A VERSATILE THz SOURCE FOR HIGH-REPTITION RATE XFELS

F. Lemery [1*], K. Floettmann [1], M. Dohlus [1], M. Marx [1], M. Ivanyan [2], V. Tsakanov [2]
[1] DESY, Hamburg, Germany
[2] Center for the Advancement of Natural Discoveries using Light Emission, Yerevan, Armenia

Abstract

The development of high-repetition rate XFELs brings an exciting time for novel fundamental science exploration via pump-probe interactions. Laser-based pump sources can provide a wide range of wavelengths (200-10000 nm) via various gain media. These sources can also be extended with optical parametric amplifiers to cover a largely versatile spectral and bandwidth range. However beyond 10 μm, toward the THz regime, there exists no suitable gain media, and optical-to-THz efficiencies are limited below 1%. In this paper we discuss the use of Cherenkov-based radiators with conventional electron bunches to generate high-power THz radiation over a wide range of parameters for existing and future XFEL facilities.

INTRODUCTION

The last decades of accelerator physics flourished, the development of superconducting radio frequency (SRF) machines has provided a surge toward unparalleled efficiencies, leading to incredible beam powers $O(1\ MW)$ at MHz repetition rates for a plethora of applications. These machines are very suitable candidates for colliders as in the proposal of the International Linear Collider (ILC), but the limited (but increasing) accelerating gradients of SRF cavities has limited such TeV-frontier facilities to 10s of kilometers.

Other fundamental sciences desire X-rays to explore life sciences, chemistry and more, which require more modest beam energies $O(10\ GeV)$ to provide X-ray energies $O(10\ keV)$ using conventional undulators. While a large portion of users are interested in direct-imaging of their samples, pump-probe spectroscopy has gained significant interest, where generally a pump-laser of specific wavelength and bandwidth is shone onto the sample to e.g. excite it, subsequently an X-ray pulse then measures the developing effects. This technique provides a way to diagnose electromagnetic responses of samples of interest.

Unfortunately the limited optical-to-THz conversion efficiencies below 1% has left an electromagnetic hole of research opportunities in various sciences [1]. Alternatively electron beam based THz sources can in principle cope with the high power, repetition rate, and frequency requirements. The freely available spent beam after a SASE undulator is an attractive option for this purpose, as it still has a high beam power. Moreover it is naturally synchronized to the X-ray pulses and can fulfill all repetition rate requirements. (For a detailed discussion on the compensation of path length differences between THz and X-ray pulses see [2])

* francois.lemery@desy.de

At the XUV FEL FLASH, for example, a 9 period electromagnetic undulator with 40 cm period length is installed behind the SASE undulator [3, 4]. The generated THz radiation in the range of 1.5 – 30 THz is transported through a 65 m long evacuated beam line to the experimental chamber where it meets the XUV pulse on the sample [5, 6]. Six refocusing mirrors in combination with planar mirrors keep the beam size under control and direct the beam to the experiment. A variable delay line allows for adjusting the relative timing of pump and probe beam.

Following the design ideas of FLASH the installation of a special undulator for the generation of THz radiation behind a SASE undulator at XFEL-facilities is discussed in [7]. However, the high beam energy of XFEL facilities (>10 GeV) requires a total undulator length of 10 m with peak fields of up to 7.3 T and a period length of 1 m to comply with the requested THz parameters. While such an undulator appears to be technically feasibly with state-of-the-art superconducting technology the cost and complexity of such a device is unattractive. Another conceivable option is the installation of a separate accelerator near the experimental hutch, because THz radiation can be generated with conventional undulator parameters already at modest ~10 MeV beam energies. While the SASE process in the THz range is possible at these low electron beam energies [8, 9], this option is complex and expensive. Finally, compact accelerators based on advanced concepts like e.g. plasma acceleration are not yet able to deal with the beam quality, charge and repetition rate requirements.

In this paper we consider an alternative method which has not yet been proposed in the context of pump-probe sources at XFEL user facilities: the usage of Cherenkov-type waveguides to produce high-power, superradiant THz radiation in a wide range of desired parameters [10–13]. There are various types of radiating structures which include dielectric-lined waveguides (DLW), corrugated structures, and bimetallic waveguides [14, 15]. We provide a brief introduction to various suitable radiation waveguides before discussing the wakefield generation process in arbitrary waveguides. This is followed by a section on radiation extraction and finally, a case for the European XFEL is presented.

SUITABLE RADIATORS

There are many existing candidate structures which have come forward for e.g. beam-driven acceleration and radiation generation with phase velocites of the speed of light. Of these there exists the dielectric-lined waveguide (DLW), the corrugated waveguide, a bimetallic waveguide, and others e.g. photonic bandgap structures, see Fig 1. We give a

Content from this work may be used under the terms of the CC BY 3.0 licence (© 2019). Any distribution of this work must maintain attribution to the author(s), title of the work, publisher, and DOI

ISBN: 978-3-95450-210-3 doi:10.18429/JACoW-FEL2019-THP051

GENERATING TRAINS OF ATTOSECOND PULSES WITH A FREE-ELECTRON LASER

Svitozar Serkez*, Gianluca Geloni, European XFEL, Schenefeld, Germany
MyungHoon Cho, Inhyuk Nam, Heung-Sik Kang, Gyujin Kim,
Chang-Ki Min, Jun Ho Ko, Chi Hyun Shim, PAL, Pohang, Korea
Franz-Josef Decker, SLAC, Menlo Park, California, USA
Yuri Shvyd'ko, ANL, Argonne, Illinois, USA

Abstract

Recently, a Hard X-ray Self-Seeding setup was commissioned at PAL XFEL. Its main purpose is to actively increase the temporal coherence of FEL radiation. We report another application of this setup, namely - to generate trains of short sub-femtosecond pulses with linked phases. We discuss the preliminary results of both experiment and corresponding simulations as well as indirect diagnostics of the radiation properties.

INTRODUCTION

Hard X-ray Self-Seeding (HXRSS) based on a single chrystal monochromator [1–4] allows for an increased spectral density and longitudinal coherence at hard X-ray SASE FELs through active spectral filtering. It was originally proposed to use a single Bragg or Laue reflection from a thin diamond to generate a series of trailing maxima following SASE pulse. The electron beam is delayed to temporally overlap with one of these maxima, which is then amplified in a downstream undulator up to saturation and beyond. Later it was proposed to use two crystals [5], or several reflections of a single crystal simultaneously [6, 7], to generate a seed that contains more than one frequency within the FEL amplification bandwidth. Then, the final FEL section amplifies such multi-frequency seed radiation and due to non-linear intermodulation yields satellites – "beat waves" – observable at saturation [8].

One easy way to understand the emergence of satellite frequencies is to consider the amplification process of two spectral lines in the time domain. Combination of two overlapped seed beams with frequencies different by $\Delta\omega$ yields sinusoidal "beating" of the resulting seed power in the time domain at that difference frequency. Upon amplification of this seed to saturation, the now-increased radiation slippage distorts the shape of that sinusoidal modulation. Such distortion manifests itself in the frequency domain via the emergence of the additional equidistant "satellites". The resulting train of short pulses will allow studies of ultrafast phenomena [9–11].

SELF-SEEDING WITH "PHANTOM LINES"

PAL-XFEL at Pohang accelerator laboratory is the world's third hard X-ray free-electron laser facility starting its user

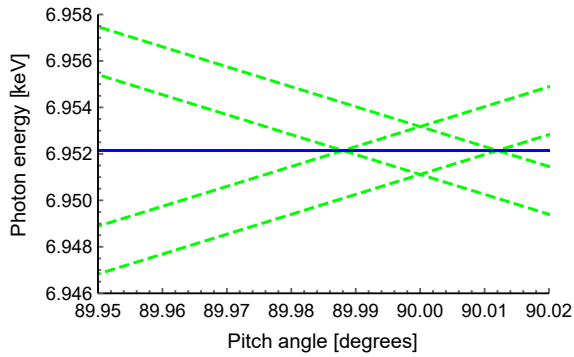


Figure 1: Seeding lines for Bragg reflections from diamond with photon energy versus crystal pitch angle for [004] reflection and four reflections from the [022] family assuming 0.012° yaw angle.

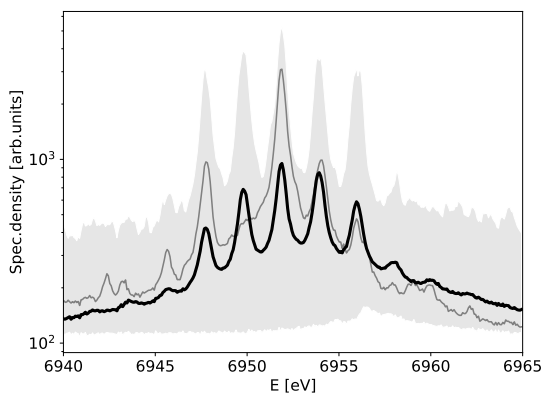


Figure 2: Radiation power spectrum as a function of photon energy for the case of seeding with 5 equidistant reflections. Also we can already see non-linear effects as additional maxima on both sides. Black line depicts the ensemble average over the ensemble of 10000 events, dark grey line shows a single-shot spectrum, light grey band represents the range of maximum and minimum values in the ensemble.

* svitozar.serkez@xfel.eu

Content from this work may be used under the terms of the CC BY 3.0 licence (© 2019). Any distribution of this work must maintain attribution to the author(s), title of the work, publisher, and DOI

ISBN: 978-3-95450-210-3 doi:10.18429/JACoW-FEL2019-THP054

NANOSECOND PULSE ENHANCEMENT IN NARROW LINEWIDTH CAVITY FOR STEADY-STATE MICROBUNCHING

Qinghong Zhou†, Science School, Southwest University of Science and Technology, Mianyang, China

Abstract

In steady-state microbunching (SSMB), nanosecond laser pulse with megawatt average power is required. We build up a theoretic model to simulate the enhancement process of such pulse in narrow linewidth (e.g. kHz level) cavity for this demand, which shows that a mode-locked mechanism in frequency domain should be considered. Simulations indicate that such pulse can be enhanced sufficiently under this condition. And we also propose some experimental schematics to realize it.

INTRODUCTION

In SSMB, nanosecond pulse laser field with megawatt average power is required [1]. To our knowledge, such power level is difficult and expensive to achieve with direct generation methods. In another hand, power enhancement by an optical cavity has been studied intensively in both cw and ultrashort pulse case last few decades, and 7.5kW [2] and 670kW [3] intracavity average power has been realized respectively. Also, enhancement of nanosecond laser pulse [4] has been studied theoretically and experimentally, which illustrate that such pulse can be sufficiently enhanced with the condition that the pulse linewidth is narrower than or comparable to that of the cavity. However, the linewidth of the cavity used for SSMB is narrower than ordinary one under same finesse because of its larger round trip length, which indicate that a nanosecond pulse hardly can be enhanced by such cavity.

In this paper, we propose a kind of nanosecond pulse with comb structure in frequency domain, which can be sufficiently enhanced in such narrow linewidth cavity. Using the model of pulsed multi-beam interference we numerically analyze the enhancement process of a nanosecond pulse in a travelling wave narrow linewidth cavity, which indicate that the pulse with any time duration can be sufficiently enhanced by this method. We also propose some schemes to generate such pulse.

MODEL OF NANOSECOND PULSE ENHANCEMENT FOR SSMB

Figure 1 shows the schematic of the enhancement cavity for SSMB. Here, a standard bowtie travelling wave ring cavity is chosen, whose advantages have been discussed already in detail [5].

To quantify the enhancement process, pulsed multi-beam interference model should be considered. However, two differents should be noticed here. Frist, the transmissions occur at every mirror. Second, the reflectivity and transmission of input coupler should be different from other mirrors because of the requirement for impedance matching.

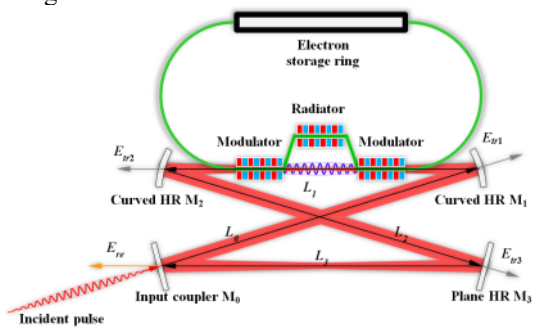


Figure 1: Schematic of SSMB with standard bowtie ring cavity.

To quantify the enhancement process, pulsed multi-beam interference model should be considered. However, two differents should be noticed here. Frist, the transmissions occur at M_1, M_2 and M_3. Second, the reflectivity and transmission of input coupler M_0 should be different from M_1-M_3 because of the requirement for impedance matching. Then, the model is modified as follow,

$$E_{re} = \left[\sqrt{R_0}\cdot E(t) + T_0\sum_{n=1}^{\infty}\left(-\sqrt{R_0}\right)^{n-1}\left(-\sqrt{R}\right)^{3n}E\left(t-\frac{nL}{c}\right)e^{in\delta}\right]e^{i(\omega t-kz)} \quad (1)$$

$$E_{tr1} = \left[\sqrt{T_0T}\sum_{n=0}^{\infty}\left(-\sqrt{R_0}\right)^{n}\left(-\sqrt{R}\right)^{3n}E\left(t-\frac{nL+L_0}{c}\right)e^{in\delta}\right]e^{i(\omega t-kz)} \quad (2)$$

$$E_{tr2} = \left[\sqrt{T_0T}\sum_{n=0}^{\infty}\left(-\sqrt{R_0}\right)^{n}\left(-\sqrt{R}\right)^{3n+1}E\left(t-\frac{(2n+1)L}{2c}\right)e^{in\delta}\right]e^{i(\omega t-kz)} \quad (3)$$

$$E_{tr3} = \left[\sqrt{T_0T}\sum_{n=0}^{\infty}\left(-\sqrt{R_0}\right)^{n}\left(-\sqrt{R}\right)^{3n+2}E\left(t-\frac{(n+1)L-L_3}{c}\right)e^{in\delta}\right]e^{i(\omega t-kz)} \quad (4)$$

$$E_{in} = \sqrt{T_0}\sum_{n=0}^{\infty}\left(-\sqrt{R_0}\right)^{n}\left(-\sqrt{R}\right)^{3n}E\left(t-\frac{z}{c}-\frac{nL}{c}\right)e^{i\left(\omega\left(t-\frac{z}{c}-\frac{nL}{c}\right)-kz-n\delta\right)} \quad (5)$$

Where, E_{re}, E_{in} represent reflection and intracavity field. E_{tr1}, E_{tr2} and E_{tr3} are the transmission fields from M_1 to M_3. c and z is the speed of light and the position in the cavity along the direction of the beam propagation, and the origin of z is set at M_0. L_0 -L_3 is the distance between two mirrors. $L=L_0+L_1+L_2+L_3$, is the round trip length of the cavity and δ is the corresponding phase shift. R_0, T_0 is the reflectivity and transmittance of M_0, and R, T is that of

† email address: nanguaa51@163.com

Content from this work may be used under the terms of the CC BY 3.0 licence (© 2019). Any distribution of this work must maintain attribution to the author(s), title of the work, publisher, and DOI

ISBN: 978-3-95450-210-3 doi:10.18429/JACoW-FEL2019-THP055

A STORAGE RING DESIGN FOR STEADY-STATE MICROBUNCHING TO GENERATE COHERENT EUV LIGHT SOURCE

Zhilong Pan*[1], Tenghui Rui[1], Weishi Wan[2], Alex Chao[3],
Xiujie Deng[1], Yao Zhang[1], Wenhui Huang[1], Chuanxiang Tang[1]
[1]Department of Engineering Physics, Tsinghua University, Beijing, China
[2]School of Physical Science and Technology, Shanghai Tech University, Shanghai, China
[3]SLAC, Menlo Park, CA, USA

Abstract

The proposal of Steady State Microbunching (SSMB) makes it available to generate high average power coherent radiation, especially has the potential to generate kW level of EUV source for lithography. In order to achieve and maintain SSMB, we propose several concepts. One is that a very short electron bunch below 100 nm is stored in the ring, inserting a strong focusing part to compress the bunch to ~3 nm, then radiating coherently, which is called longitudinal strong focusing (LSF) scheme. We have optimized the candidate lattice to achieve the very short electron bunch storage and microbunching for electron beam. The tracking results show the equilibrium length of the electron bunch is about 400 nm and no particles lose after 4.3 damping time while only single-particle effect is considered. More optimization and some new design based on the simulation results are still implementing.

INTRODUCTION

Because of the limitation of electron beam size in the traditional storage ring based synchrotron facilities, the average power of the incoherent radiation from this kind of facility will still be low although with extremely high repetition rate. On the other hand, the linac based FEL facilities can't generate high average power radiation due to the low repetition rate. The SSMB makes it achievable to radiate coherently in storage ring with high repetition rate, in other words, high average power radiation is available.

To achieve SSMB, several schemes have been proposed and pushed by our collaboration team in recent time, including longitudinal strong focusing (LSF) [1], reversible seeding[2], and hybrid scheme. Among those schemes, the LSF scheme requires that the storage ring can stably store the electron beam with a bunch length under 100 nm.

Based on the conventional formula by Sands[3], the length of electron bunch is determined by momentum compaction factor of the storage ring and RF parameters.

$$\sigma_s = \sigma_\delta L \frac{\alpha_c}{2\pi\nu_s}, \tag{1}$$

where α_c is momentum compaction factor, L is the circumference of the storage ring, σ_δ is equilibrium rms energy spread, ν_s is synchrotron tune.

According to eq.1, a storage ring with low momentum compaction factor on the magnitude of 1×10^{-6} or lower is needed to match our requirements. On the other hand, the second order momentum compaction factor may dominate the longitudinal dynamics and reduce the RF bucket area if not been optimized properly in the low momentum compaction factor storage ring [4].

The bunch length formula from Sands neglects the part of path length fluctuation from photon emission, which associates with local momentum compaction factor, or partial alpha [1]. The bunch length formula by taking account this effect in is [5]

$$\sigma_s = \sigma_\delta L \sqrt{(\frac{\alpha_c}{2\pi\nu_s})^2 + I_{\tilde{a}}}, \tag{2}$$

where $I_{\tilde{a}}$ is the variance of partial alpha. So the partial alpha of the storage ring should also be minimized to prevent the bunch length increasing.

The isochronous cell scheme has been proposed by our team to design the SSMB lattice [6]. We adopt that lattice in this paper and make some improvement in terms of slight adjustment of momentum compaction factor, minimizing second order momentum compaction factor, and dynamic aperture optimization. Then we do some single-particle simulation based on this lattice. The simulation results will show some direction for further lattice optimization.

LATTICE PARAMETERS

The lattice layout can refer to [6]. There are two dispersion free straight sections and two arc sections, and 6 isochronous cells in per arc section. The twiss function of one isochronous cell is shown in Fig.1. The integration of $\int_0^{L_b} \frac{\eta_x(s)}{\rho} ds$ will be 0 through the dipole in the isochronous cell, where L_b is the dipole length. So the momentum compaction factor of the whole ring could be very small. Three families of sextupoles named S1, S2, S3 are introduced to minimize the chromaticity and second order momentum compaction factor. The ring parameters are listed in Table.1.

The second order compaction factor has been optimized and the relation $\alpha_c > 10\alpha_{c2}\sigma_\delta$ is satisfied by referring to Table.1, so the longitudinal dynamics is still dominant by α_c. The bunch length induced by partial alpha is related with $\sqrt{I_{\tilde{a}}}$, the value will be ~ 300 *nm*. The equilibrium bunch length of this lattice will not be shorter than 300 *nm*, we will do some single-particle simulation based on this lattice later to check the partial alpha theory and get some guideline on the next step optimizaion.

* pzl15@mails.tsinghua.edu.cn

Content from this work may be used under the terms of the CC BY 3.0 licence (© 2019). Any distribution of this work must maintain attribution to the author(s), title of the work, publisher, and DOI

ISBN: 978-3-95450-210-3 doi:10.18429/JACoW-FEL2019-THP060

Content from this work may be used under the terms of the CC BY 3.0 licence (© 2019). Any distribution of this work must maintain attribution to the author(s), title of the work, publisher, and DOI

DEVELOPMENT OF RF-UNDULATORS AND POWERING SOURCES FOR COMPACT EFFICIENT COMPTON FEL-SCATTRONS*

A.V. Savilov†, E.B. Abubakirov, N. S. Ginzburg, S.V. Kuzikov, N. Yu. Peskov, A.A. Vikharev, V. Yu. Zaslavsky, Institute of Applied Physics, Nizhny Novgorod, Russian Federation

Abstract

Conception of Compton-type FELs operating up to X-ray band is under development currently at IAP RAS. This concept is aimed at reducing energy of a driving relativistic electron beam and thereby increasing efficiency of the electron-wave interaction in FEL, as well as achieving relative compactness of the generator. The basis of this concept is RF-undulators of a new type - the so-called 'flying' undulators. Results of current research of these RF-undulators, their simulations and 'cold' tests in the Ka-band are presented. For powering RF-undulators spatially-extended narrow-band Cerenkov masers are developed in the specified frequency range. In order to achieve the required sub-gigawatt power level of the pumping wave in a strongly oversized oscillator, we exploit the original idea of using two-dimensional distributed feedback implemented in the 2D doubly-periodical slow-wave structures. The design parameters of Ka-band surface-wave oscillator intended for powering RF-undulators, results of its simulation and initial experimental studies are discussed.

INTRODUCTION

Free electron lasers (FELs) are the most powerful sources of coherent radiation in the ranges up to X-rays and are being actively developed around the world. However, the main challenge of these projects are related currently with the gigantic size of the facilities, low efficiency of the electron-wave interaction and strong requirements to the quality of driving beams. As a way to solve these problems, development of Compton FELs can be considered. The use of the counter-propagating pumping wave (so-called RF-undulator) of the mm- wavelength band (instead of "traditional" magnetostatic undulators, the period of which is limited to several centimeters) makes it possible significantly reduce the energy of driving electron beam required for operation in the X-ray range, resulting in a decrease in the length of both the accelerator and the FEL interaction region (by increasing the FEL electron-wave interaction parameter), and enhance the efficiency of radiation generation.

The conception of Compton FEL-scattron has been developing in recent years at IAP RAS. The basis of this concept is a novel scheme of RF-undulator - the so-called "flying" undulator [1]. Simulations of various schemes of such undulators, including the ones with profiled parameters were conducted currently. It is shown that the use of these undulators allows realization of a non-resonant multi-pulse trapping regime [2], which leads to a decrease in sensitivity to the quality (i.e. energy and velocity spread) of the driving beam and, thus, to a further increase in the efficiency of this type FEL [3].

Experimental studies of the prototype of pumping system (including RF-undulators and RF-power sources) for FEL-scattron were started at IAP RAS in the Ka-band. The required high power level in powering pulsed relativistic masers is planned to be achieved by extending their transverse size and exploiting novel two-dimensional (2D) distributed feedback mechanism to maintain narrow-band operation in strongly oversized systems. Operation principles, design parameters and results of simulation of Ka-band Surface-Wave Oscillator (SWO) intended for the experiments on powering "flying" rf undulator are discussed in this work.

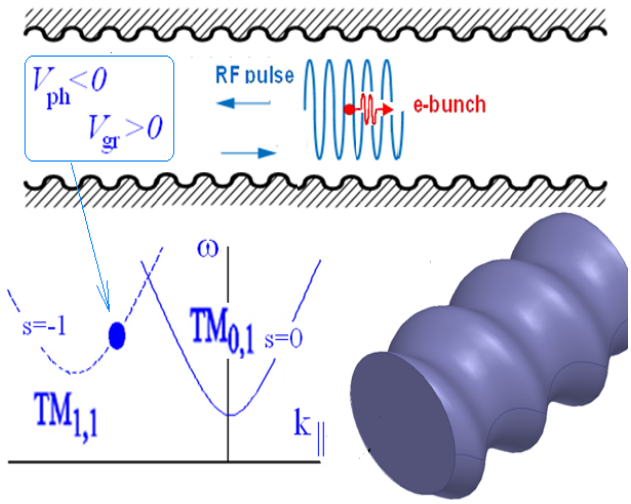


Figure 1: Flying RF-undulator. Microwave system and dispersion diagram of the operating undulator wave.

FLYING RF UNDULATOR

The "flying" RF-undulator [1] represents a powerful short pulse of coherent microwave radiation propagating synchronously with the electron bunch (Fig. 1). The microwave system of this RF-undulator consists of a cylindrical waveguide section with helical corrugation, which ensures the presence in the microwave pulse of a wave component with a backward (with respect to the direction of the electron bunch propagation) phase velocity but, simultaneously, with a group velocity close to the speed of light. Thus, the proximity of the group velocity of the microwave pulse wave and the electron bunch velocity realizes a long-time electron-wave interaction, while the

* Work is partially supported by the Russian Foundation for Basic Research (grant # 18-02-40009). Experimental facilities are developed and exploited in the frame of the Russian State Task Program (project #0035-2019-0001) and the RAS Presidium Project no.10 (#0035-2018-0022).
† savilov@appl.sci-nnov.ru

ISBN: 978-3-95450-210-3 doi:10.18429/JACoW-FEL2019-THP061

BAYESIAN OPTIMISATION FOR FAST AND SAFE PARAMETER TUNING OF SWISSFEL

J. Kirschner, M. Nonnenmacher, M. Mutný, A. Krause, Dept. of Computer Science, ETH Zurich
N. Hiller, R. Ischebeck, A. Adelmann, Paul Scherrer Institute

Abstract

Parameter tuning is a notoriously time-consuming task in accelerator facilities. As tool for global optimization with noisy evaluations, Bayesian optimization was recently shown to outperform alternative methods. By learning a model of the underlying function using all available data, the next evaluation can be chosen carefully to find the optimum with as few steps as possible and without violating any safety constraints. However, the per-step computation time increases significantly with the number of parameters and the generality of the approach can lead to slow convergence on functions that are easier to optimize. To overcome these limitations, we divide the global problem into sequential subproblems that can be solved efficiently using safe Bayesian optimization. This allows us to trade off local and global convergence and to adapt to additional structure in the objective function. Further, we provide slice-plots of the function as user feedback during the optimization. We showcase how we use our algorithm to tune up the FEL output of SwissFEL with up to 40 parameters simultaneously, and reach convergence within reasonable tuning times in the order of 30 minutes (< 2000 steps).

INTRODUCTION

Empirical parameter tuning is an important and reoccurring task of the FEL setup. Common tuning objectives include the pulse energy or spectrum of the FEL signal and loss minimization, or a combination of multiple criteria. A recent effort started to use optimization methods to automate the tuning process [1–6], and significant speedups compared to manual operator tuning have been obtained. As only point evaluations of the objective function are available, one has to rely on *zero-order or blackbox optimization methods*. Due to their simplicity, the Nelder-Mead (Simplex) [7] algorithm and random walk optimizers have become popular choices to assist operator tuning in some facilities. As an alternative, Bayesian optimization (BO) [8, 9] has recently gained interest also in the accelerator community [1, 2]. Bayesian optimization deals with observation noise in a principled way, allows to leverage prior data and comes with theoretical convergence guarantees in some cases [10]. A variant (SafeOPT) has been proposed [11], that takes additional safety constraints into account. This is of importance for tuning FEL parameters, for instance to avoid electron losses or to maintain a minimum level of the FEL signal during optimization. However, these benefits come at the expense of increased computational requirements as well as additional complexity in the choice and sensitivity of BO hyperparameters. We believe that these issues constitute the main reasons that prevent a more wide-spread use of Bayesian optimization in this context beyond an academic setup. Moving forward with this, we present the following contributions.

- We implement the LineBO [12] algorithm at SwissFEL. The algorithm is designed to be computationally efficient when used with a large number of parameters and allows to take safety critical constraints into account.
- On SwissFEL we compare our methods to a simple parameter scan and the Nelder-Mead method, and obtain promising results when tuning up to 40 parameters.

Mathematical Setting

Let d denote the number of tuning parameters. The parameter space is $\mathcal{X} = [a_1; b_1] \times \cdots \times [a_d; b_d] \subset \mathbb{R}^d$, where $a_i \leq x_i \leq b_i$ defines the allowed range for each parameter $i = 1, \ldots, d$. The objective function (e.g. the FEL pulse energy) is an unknown function $f : \mathcal{X} \to \mathbb{R}$. The constraints are modelled by some unknown $g : \mathcal{X} \to \mathbb{R}$. A parameter $x \in \mathcal{X}$ is said to satisfy the safety constraint if $g(x) \leq \tau$ for a user-specified threshold level $\tau \in \mathbb{R}$. For simplicity, we use the formulation with a single constraint but multiple constraints are possible by choosing g vector valued. The only way to access f and g is to measure at any $x \in \mathcal{X}$, which yields noisy point observations of the objective and the constraint, $y = f(x) + \epsilon$ and $s = g(x) + \eta$. We refer to this process as *evaluating at x*, which in our case includes averaging the FEL signal over multiple shots. Formally, the tuning objective is

$$x^* = \underset{x \in \mathcal{X}; g(x) \leq \tau}{\arg\max} f(x) \,. \tag{1}$$

An optimization algorithm iteratively chooses a sequence of parameters $x_1, \ldots, x_T$ and obtains evaluations of f and g for each point. After T steps (when the user stops the optimization), a final solution x_T is returned. A tuning method is called *safe* if all the iterates $(x_t)_{t=1}^T$ satisfy $g(x_t) \leq \tau$. In the unconstrained case the requirement $g(x) \leq \tau$ is dropped.

BAYESIAN OPTIMIZATION

Bayesian optimization is a method for global optimization. The idea is to learn a model of the objective function based on the data collected during the optimization (and possibly any available prior data). The decision where to place the next evaluation is then based on the model's predictions of plausible locations of the optimum x^* and also takes the model uncertainty into account. More formally, in the unconstrained case, Bayesian optimization uses the following steps.

Content from this work may be used under the terms of the CC BY 3.0 licence (© 2019). Any distribution of this work must maintain attribution to the author(s), title of the work, publisher, and DOI

ISBN: 978-3-95450-210-3 doi:10.18429/JACoW-FEL2019-THP065

MULTI-OBJECTIVE FEL DESIGN OPTIMISATION USING GENETIC ALGORITHMS

D. J. Dunning*, J. K. Jones, H. M. Castañeda Cortés, N. R. Thompson
STFC Daresbury Laboratory and Cockcroft Institute, Daresbury, UK

Abstract

Simulation studies were carried out to optimise the performance of various FEL designs, with examples including longitudinal current profile shaping for a seeded FEL, and selection of the chicane delays for the High-Brightness SASE technique. In these examples multi-objective genetic algorithms were applied to a single section of the overall facility simulation, i.e. the undulator, as is the common approach. Further studies are also reported in which a full start-to-end simulation chain was optimised, with the aim of delivering a more holistic facility design optimisation.

INTRODUCTION

Simulations are a key component in the design and operation of modern FEL facilities. The full machine is often modelled with a 'start-to-end' (S2E) chain of different simulation codes, each developed for specific sections of the facility (e.g. gun, accelerator, FEL, photon beamline), shown schematically in Fig. 1 (a). Optimisation within this simulation chain is often segmented in the same way, e.g. the accelerator section is often optimised to meet a set of target electron beam properties, which themselves are specified to allow the FEL section to deliver the target photon output, see Fig. 1 (b).

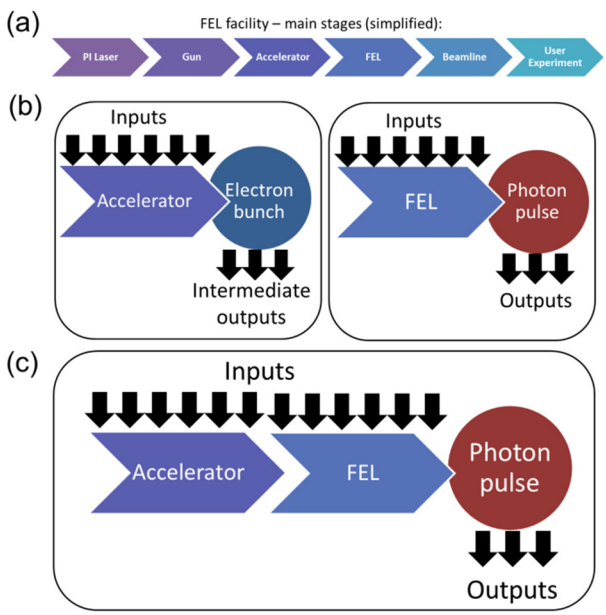


Figure 1: (a) Example of the main stages in a FEL facility, (b) a segmented optimisation approach requires specification of intermediate parameters, (c) joining up stages allows optimisation on the final outputs.

* david.dunning@stfc.ac.uk

A problem with this method is that mapping from electron bunch properties to photon output is a complex non-linear process. Intermediate parameters such as emittance and bunch length are often overly reductive as a predictor of FEL performance when applied to realistic – sometimes highly non-Gaussian – distributions. One solution is to develop more prescriptive specifications of the intermediate parameters; however this can become increasingly elaborate, as illustrated in the first section of this paper.

An alternative approach, considered in the second section, is to combine multiple stages of the simulation chain into a single optimisation problem, Fig. 1 (c). This allows, e.g. the accelerator parameters to be directly optimised on the FEL output, without the need to specify intermediate targets. Previous studies have combined accelerator simulation codes with FEL analytical models, however not all effects are included [1]. Here we present a combined accelerator + FEL simulation framework with examples.

In the final section a more advanced FEL scheme is considered. In each case multi-objective genetic algorithms (MOGA) are used as the optimisation technique.

SINGLE-STAGE OPTIMISATION

This section considers an example of optimising a single stage of the S2E chain, as shown in Fig 1 (b).

At the interface between the accelerator and FEL sections a common starting point is to specify the longitudinal profile in terms of peak current and electron bunch length. For non-Gaussian distributions these measures can be poor predictors of FEL performance, such that more refined targets (e.g. bunch shape) are required. A simple case was set up to optimise the current profile for a seeded FEL, using parameters of the CLARA project [2,3]. 3D FEL simulations were carried out using the Genesis 1.3 FEL code [4] (version 2, utilising the OCELOT framework [5]), in which the current profile was described by a 36-element array, entered via the 'beamfile' method (with all other properties kept constant). Optimisation was carried out using the NSGA-II [6] MOGA method, inside DEAP [7] and FEL performance was optimised on peak power and bandwidth at the end of the undulator (further refinement is discussed later).

In the first instance the system started from random current distributions. The mutation effect was to randomly modify a randomly selected subset of the current array elements. The crossover effect was to interleave elements from two existing current profiles. In both cases a further step to maintain constant charge was applied. Figure 2 shows the results of the optimisation. Some effects were expected – concentrating charge into a high current region in order to increase pulse energy: indeed surpassing the pulse energy of a Gaussian but with larger bandwidth.

Content from this work may be used under the terms of the CC BY 3.0 licence (© 2019). Any distribution of this work must maintain attribution to the author(s), title of the work, publisher, and DOI

ISBN: 978-3-95450-210-3 doi:10.18429/JACoW-FEL2019-THP066

XARA: X-BAND ACCELERATOR FOR RESEARCH AND APPLICATIONS

D. J. Dunning*, L. S. Cowie[1], J. K. Jones
STFC Daresbury Laboratory and Cockcroft Institute, Daresbury, UK,
[1]also at University of Lancaster, Lancaster, UK

Abstract

XARA (X-band Accelerator for Research and Applications) is a proposal for a compact ~1 GeV/c accelerator to produce attosecond light pulses in the EUV to soft X-ray region. It is under consideration as a potential future upgrade to the CLARA facility at Daresbury Laboratory, utilising high-performance X-band RF technology to increase the electron beam momentum from 250 MeV/c. Emerging techniques for generating single-cycle undulator light would give access to attosecond timescales, enabling studies of ultra-fast dynamics, while also being very compact. XARA would also enhance the existing capabilities for accelerator science R&D by incorporating X-band development and increasing the electron beam momentum for novel acceleration studies.

INTRODUCTION

We propose a high-energy upgrade of the CLARA facility [1], utilising high-gradient X-band RF technology to achieve a maximum beam momentum of around 1 GeV/c, with FEL light output in the extreme-ultra-violet (EUV) to soft X-ray (SX) regime, including the 'water window' wavelength region between 2.3-4.4 nm. In addition to its inherent scientific interest due to the presence of important K-edges and transparency of water, this wavelength region coincides with state-of-the art technological developments in temporally coherent FEL output [2] and attosecond pulse generation [3, 4].

The aim of the proposal is therefore to deliver a photon source that is attractive to both FEL and HHG users, and to do so through developing advanced accelerator technologies. XARA represents an opportunity to implement the developments in X-band technology and innovative short-period undulators coming from the Horizon 2020-funded project 'CompactLight' [5], of which STFC is a member. STFC is also involved with EuPRAXIA [6] and XARA would be synergistic with EuPRAXIA@SPARC_LAB [7]. Another key feature is the potential to utilise emerging techniques for single-cycle undulator light, as developed by the LUSIA consortium [8]

CLARA is presently supported to phase 2 (250 MeV/c plus full energy beam extraction (FEBE) line and user station). The UK is developing a science case for its XFEL project, due to report in May 2020, which will inform thinking regarding CLARA phase 3 (the FEL line – to demonstrate novel FEL schemes for use in an XFEL [9]). XARA is therefore considered as an alternative or future upgrade option for the straight-ahead line, which would utilise the existing CLARA front-end and building. XARA is currently aiming to fit inside the existing CLARA building footprint, however extension of the building by several tens of meters is feasible, if required.

* david.dunning@stfc.ac.uk

SCIENCE CASE

The science case for XARA comprises photon science, particle accelerator R&D and electron beam exploitation.

Photon Science

The science case for XARA is centred on the opportunity to study ultra-fast dynamics [10] in e.g. photosynthesis, photo-induced catalysis and light-wave electronics, and to influence such effects e.g. through coherent control [11]. To do so requires pulse durations on the scale of tens to hundreds of attoseconds. Figure 1 shows the parameter space for relevant existing sources in this area. HHG provides the shortest pulses but with relatively low number of photons per pulse compared to FELs, particularly at higher photon energy. The target for XARA (also shown in Fig. 1) would extend EUV-SX FELs to shorter pulse duration, aiming for higher pulse energies than HHG.

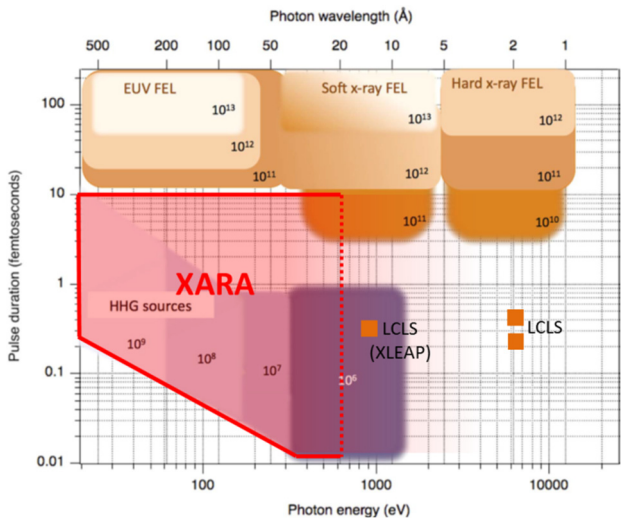


Figure 1: XARA target parameter space relative to the ultrafast science landscape, adapted from [10].

Accelerator R&D/Electron Beam Exploitation

XARA would enhance CLARA's existing function as a centre for accelerator R&D and electron beam exploitation. At present the beam from the CLARA front-end (~35 MeV/c) is used for topics that include novel acceleration, medical applications and basic accelerator R&D [12]. Novel acceleration is a particular focus of the Cockcroft Institute, which is co-located at Daresbury Laboratory (dielectric WFA, PWFA). Medical studies on CLARA include VHEE dose and damage studies, and there are strong links with nearby universities and hospitals. Accelerator R&D includes commissioning of the 400 Hz 1.5

Content from this work may be used under the terms of the CC BY 3.0 licence (© 2019). Any distribution of this work must maintain attribution to the author(s), title of the work, publisher, and DOI

ISBN: 978-3-95450-210-3 doi:10.18429/JACoW-FEL2019-THP068

LCLS-II EXTRUDED ALUMINUM UNDULATOR VACUUM CHAMBERS—NEW APPROACHES TO AN IMPROVED APERTURE SURFACE FINISH*

Greg Wiemerslage†, Patric Den Hartog, Jun Qian, Marion M. White
Argonne National Laboratory, 9700 South Cass Ave., Lemont, IL 60439, USA

Abstract

The Linac Coherent Light Source (LCLS), the world's first x-ray free-electron laser (FEL), became operational in 2009. The Advanced Photon Source (APS) contributed to the original project by designing and building the undulator line. Two slightly different variations of these chambers were required for LCLS-II: one for a soft x-ray (SXR) undulator line and one for a hard x-ray (HXR) undulator line. Because of the extremely short electron bunch length, a key physics requirement was to achieve the best possible surface finish within the chamber aperture. Improvements to our earlier fabrication methods allowed us to meet the critical surface roughness finish defined by rf impedance requirements. We were able to improve the surface finish from an average of 812 nm rms to 238 nm rms. The average longitudinal surface roughness slope of all chambers was to be less than 20 mrad. We achieved an average longitudinal surface roughness slope of 8.5 mrad with no chamber exceeding 20 mrad. In the end, sixty-four undulator vacuum chambers and alignment systems were delivered to SLAC National Accelerator Laboratory for the LCLS-II Upgrade project. Here we will report on the process improvements for the fabrication of these chambers.

NEW APPROACHES TO AN IMPROVED APERTURE SURFACE FINISH

The Linac Coherent Light Source (LCLS) at the SLAC National Accelerator Laboratory was the world's first x-ray free-electron laser (FEL) when it became operational in 2009 [1]. The Advanced Photon Source (APS) contributed to the project by designing and building the undulator line, including 41 undulator vacuum chambers [2]. The chamber's thin wall, small aperture, and aperture surface finish presented new production challenges. Although the aperture surface finish met requirements, schedule constraints at that time prevented us from further improving the polishing method beyond what was needed for the project. When presented with the opportunity to produce new undulator vacuum chambers for the new undulator lines of the LCLS-II upgrade, we were eager to improve the process and meet the technical requirements of the LCLS-II FEL.

Because of the extremely short electron bunch length, one of the key requirements from the LCLS-II physics specification was to achieve the best possible surface finish within the chamber aperture. The highly-polished aperture was achieved through a renewed collaboration with Engineered Finishing Corporation [2], the abrasive-flow machining vendor that polished the original LCLS vacuum chambers. Normally, the maximum aspect ratio for this process is 8/1, length/aperture. In this case, the process was modified to enable polishing of a small oval aperture extrusion (5 vertical mm × 11 horizontal mm × 4000 mm deep) with an aspect ratio ~700/1. The improved process permitted simultaneous polishing of two 4-m-long extrusions to meet the critical surface roughness finish defined by the radio-frequency impedance requirements—and with more consistent polishing results than before. The surface finish was improved from an average of 812-nm rms for an unpolished extrusion to an average surface finish of 238-nm rms after polishing. More importantly for the success of the project, the average longitudinal rms surface roughness slope (dh/dz, where h is the height of the peak) rms of all chambers was to be less than 20 mrad [3]; in fact, an average longitudinal surface roughness slope of 8.50 mrad was achieved, with no chamber exceeding 20 mrad. An example of the effects of polishing are best seen in comparing the unpolished samples and the after polishing samples of the same extrusion (shown in Fig. 1).

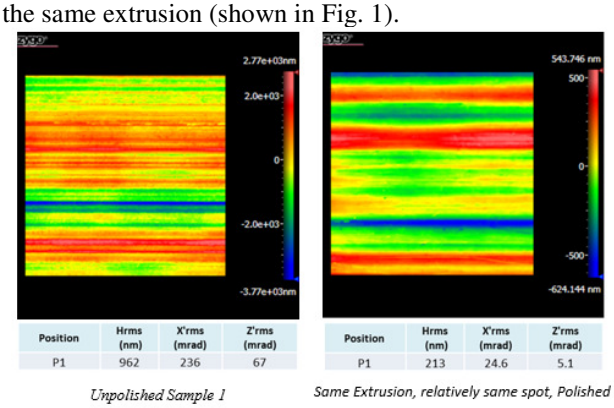


Figure 1: A comparison of unpolished (left) vs. polished surface roughness profiles (right).

To achieve these surface finish requirements, we modified our previously invented ninety-degree diverter. Our original polishing process only utilized one of the pistons of the abrasive flow machining equipment to push the polishing paste through the right angle diverter, through the extrusion aperture from one end, and allowed it to flow into a bucket at the other end. The paste was reloaded periodically as needed, which required constant attention from the operator, and the pressure of the paste on the aperture walls decreased down the length of the aperture [2]. The new diverter was built so that it now serves both the upper and lower pistons at the same time (see Fig. 2.) Second, we

* Work supported by the U.S. Department of Energy, Office of Science under Contract No. DE-AC02-06CH11357.
† wiemer@anl.gov

Content from this work may be used under the terms of the CC BY 3.0 licence (© 2019). Any distribution of this work must maintain attribution to the author(s), title of the work, publisher, and DOI

ISBN: 978-3-95450-210-3 doi:10.18429/JACoW-FEL2019-THP069

Content from this work may be used under the terms of the CC BY 3.0 licence (© 2019). Any distribution of this work must maintain attribution to the author(s), title of the work, publisher, and DOI

OBSERVATIONS ON MICROBUNCHING OF ELECTRONS IN LASER-DRIVEN PLASMA ACCELERATORS AND FREE-ELECTRON LASERS*

A.H. Lumpkin#[1], D.W. Rule[2], M. LaBerge[3], and M.C. Downer[3]
[1]Fermi National Accelerator Laboratory, Batavia, IL 60510 USA
[2]Silver Spring, MD 20904 USA
[3]Physics Department, University of Texas at Austin, Austin, TX 78712 USA

Abstract

We provide observations on the visible-wavelength microbunching of relativistic electrons at beam energies >200 MeV in both laser-driven plasma accelerators (LPAs) and a self-amplified spontaneous emission (SASE) free-electron laser (FEL). An analytical model for coherent optical transition radiation interferometry (COTRI) addresses both cases. It is noted that the COTR/OTR gain observed in the LPA rivals that of the SASE FEL at saturation, although the few micron transverse sizes of the microbunched beamlets are much smaller than in the FEL. The broadband microbunching observed in the LPA case could act as a seed for a SASE FEL experiment with tunability over the visible regime, in principle.

INTRODUCTION

The periodic longitudinal density modulation of relativistic electrons at the resonant wavelength (microbunching) is a well-known, fundamental aspect of free-electron lasers (FELs) [1]. In one classic case, microbunching fractions reached 20% at saturation of a self-amplified spontaneous emission (SASE) FEL resulting in gains of 10^6 at 530 nm [2]. In that experiment the concomitant z-dependent gain of coherent optical transition radiation (COTR) was also measured at the $>10^5$ level. Microbunching at visible wavelengths in laser-driven plasma accelerators (LPAs) had been reported previously [3,4], but it has only recently been measured in near-field and far-field images on a single shot for the first time with significant COTR enhancements involved [5-7].

We reintroduce an analytical model for COTR interferometry (COTRI) first developed for the SASE-FEL-induced microbunching case [8] to evaluate the LPA case. The coherence function was treated in this analytical model that addresses both cases and the expected fringe patterns. In the FEL, one identified microbunched transverse cores of 25-100 microns in extent while in the LPA the recently reported transverse sizes at the exit of the LPA were a few microns [5-7]. In the latter case, signal enhancements $>10^5$ and extensive fringes out to 30 mrad in angle space were recorded. We suggest the broadband microbunching observed in the LPA case could act as a seed for a SASE FEL experiment with tunability in principle over the visible regime.

* This manuscript has been authored by Fermi Research Alliance, LLC under Contract No. DE-AC02-07CH11359 with the U.S. Department of Energy, Office of Science, Office of High Energy Physics.

EXPERIMENTAL ASPECTS

The APS Linac and Previous SASE FEL Setup

The APS linac is based on an S-band rf photocathode (PC) gun which injects beam into an S-band linear accelerator with acceleration capability currently up to 450 MeV as shown in Fig. 1 [9]. The drive laser is a Nd:Glass-based chirped pulse amplifier (CPA) operating at an IR wavelength of 1053 nm, twice frequency doubled to obtain UV output at 100 μJ per pulse which irradiated the Cu photocathode of the gun [10]. Beam diagnostics in the linac include imaging screens, rf BPMs, and coherent transition radiation (CTR) autocorrelators located before and after the chicane at the 150-MeV point.

The previous SASE FEL configuration is also seen in Fig. 1 and included up to 9 undulators (~21 m of magnetic structure) with a period of 3.3 cm and appropriate undulator parameter, *K*, of value 3.1 resulting in lasing at 530-540 nm at a beam energy of 217 MeV The FEL gain saturated at about z=15 m, or ~20 gain lengths. Diagnostic imaging stations were located before the first undulator and after each undulator to provide assessment of both the optical gain and uniquely the COTR gain. These are described in more detail in Ref. [11]. This experiment motivated the development of the COTRI model which is now being applied to the recent LPA results.

The LPA at HZDR

The LPA is based on the DRACO laser with a peak power of 150 TW at a central wavelength 800 nm interacting with a He gas jet (with 3% Nitrogen) at the Helmholtz-Zentrum Dresden-Rossendorf (HZDR) facility [12]. The LPA was operated with a plasma electron density ne ~3 x 1018 cm-3 in the self-truncated ionization-injection mode. Beam energies of ~215 MeV in a quasi-monoenergetic peak were observed in a downstream spectrometer. After the LPA, a 75-μm thin Al foil blocked the laser pulse and was followed by an Al-coated Kapton foil as shown in Fig. 2. The latter's back surface provided the source point of the near field (NF) COTR imaging, and a polished Si mirror at 45° to the beam direction redirected this light to the microscope objective. The configuration provided a magnification factor of 42 at the camera and a calibration factor of 0.09 μm/pixel. This mirror was located 18.5 mm downstream of the Al-coated Kapton and also generated backward COTR that combined with the first source to provide COTRI in the far-field (FF) imaging

ISBN: 978-3-95450-210-3 doi:10.18429/JACoW-FEL2019-THP071

PROGRESS IN HIGH POWER HIGH BRIGHTNESS DOUBLE BUNCH SELF-SEEDING AT LCLS-II

A. Halavanau, F.-J. Decker, C. Emma, A. Krasnykh, G. Marcus, A.A. Lutman, Z. Huang, Y. Ding, D. Zhu, J. Krzywinski, A. Ratti, A. Marinelli, C. Pellegrini[1]
[1] SLAC National Accelerator Laboratory, Stanford University, Menlo Park CA 94025, USA

Abstract

We have previosuly shown that we can generate near TW, 15 fs duration, near transform limited X-ray pulses in the 4 to 8 keV photon energy range using the LCLS-II copper linac, two electron bunches, a 4-crystal monochromator/delay line and a fast transverse bunch kicker. The first bunch generates a strong seeding X-ray signal, and the second bunch, initially propagating off-axis, interacts with the seed in a tapered amplifier undulator, where it propagates on axis. In this paper, we investigate the design of the 4-crystal monochromator, acting also as an X-ray delay system, and of the fast kicker, in preparation of the implementation of the system in LCLS-II.

INTRODUCTION

The Double-Bunch FEL (DBFEL) is a method to generate high power and brightness in an X-ray FEL. In this scheme, shown in Fig. 1, the first bunch generates a high power SASE signal, near to saturation value, in the first undulator section and is not used in the second undulator section. The second bunch is seeded at the entrance of the second tapered undulator section by the high power SASE signal, filtered by a four crystals monochromator, also acting as a delay line. A transverse kicker is used to put the second bunch in oscillations around the undulator axis in the first section to avoid lasing. The kick is compensated to propagate the second bunch on axis in the second tapered section.

This concept was first considered to improve the performance of European XFEL and LCLS in Refs [1–3]. The overall design of the DBFEL at LCLS-II has been outlined in [4, 5]. A similar configuration using the second bunch as a fresh bunch with an ultra-fast kicker has been analyzed in the context of self-seeding and harmonic lasing in Ref. [6]. The experimental demonstration of fresh bunch self-seeding in a single bunch was also reported in Ref. [7].

Over the years of LCLS operations, electron beams containing multiple bunches separated by a few RF-buckets have been routinely created in LCLS CuRF linac [8–11]. It was previously demonstrated the DBFEL configuration of LCLS-II HXR undulator gives high peak power and high brightness X-rays in the photon range of 4 to 8 keV [4]. In this proceeding, we provide an update on DBFEL four crystal monochromator design, ultra-fast kicker and XFEL performance.

DBFEL NUMERICAL SIMULATIONS

The LCLS CuRF beamline is simulated using the code elegant [12], to evaluate the effects of the wakefields in the linac and bunch compressors. The particle distribution is then converted and passed to the FEL code genesis [13] running in time-dependent mode. For tapering studies, we utilize the technique described in [4]. In our simulations, the two bunches are considered to be identical, with 4 kA peak current and 15 fs quasi-flat top profile. We note that optimizing start-to-end beam and optimum taper profile for the amplifier section is a subject of an ongoing study.

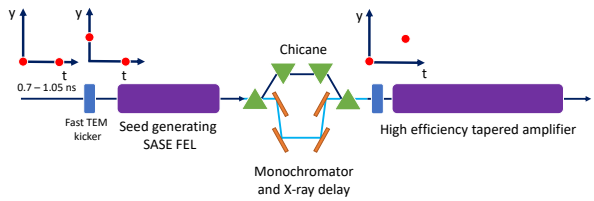


Figure 1: DBFEL schematics: two bunches with 0.7 - 1.05 ns separation are used to generate a high power seed on the second cold bunch at the entrance of the tapered amplifier.

FOUR CRYSTAL MONOCHROMATOR

An important part of the DBFEL system is the four crystal monochromator, presented in Fig. 2, that provides narrow bandwidth for double bunch seeding, and matches the delay $\Delta\tau$ between the two bunches. Currently, the monochromator is planned to be installed in the same chicane with the proposed LCLS-II RAFEL project, limiting its horizontal size to $L = 0.67$ cm.

In order to proceed with the design of the four bounce monochromator, let us discuss a few salient parameters of this device. We first start with the location of the monochromator in the undulator beamline. LCLS-II HXR undulator is built with 33 sections, each 3.6 m long, separated by a 0.4 m of free space. Two empty slots at U8 and U 15 are available for self-seeding chicane installation.

LCLS-II HXR undulator currently has two empty slots at U8 and U15 locations available for self-seeding chicanes installation. Figure 3 displays gain curves of different photon energies in the SASE section. 4 keV case saturates after 8 undulators, while 8 keV case continues to grow exponentially until U12 location. At the next empty slot at U15 both 4 keV and 8 keV photon energies are saturated. Thus, we conclude that a SASE section of 8 undulators provides more seeding power for DBFEL. We note, that ultimately, experimental electron beam parameters and HXR gain length should be the key factors that determine the location of the DBFEL four crystal monochromator. These measurements are planned shortly after LCLS-II HXR undulator commissioning.

Content from this work may be used under the terms of the CC BY 3.0 licence (© 2019). Any distribution of this work must maintain attribution to the author(s), title of the work, publisher, and DOI

ISBN: 978-3-95450-210-3 doi:10.18429/JACoW-FEL2019-THP073

Content from this work may be used under the terms of the CC BY 3.0 licence (© 2019). Any distribution of this work must maintain attribution to the author(s), title of the work, publisher, and DOI

STATUS UPDATE FOR THE HIGH GAIN HIGH EFFICIENCY TESSA-266 EXPERIMENT

Youna Park, Pietro Musumeci, Paul Denham, David Dang, Nick Sudar, UCLA, Los Angeles, USA
Alexander Zholents, Yine Sun, ANL, Argonne, USA
Tara Campese, Ivan Gadjev, Ronald Agustsson, Alex Murokh, RadiaBeam, Los Angeles, USA
Stephen Webb, Chris Hall, RadiaSoft, Boulder, USA

Abstract

This paper will provide a status report on the high gain high efficiency TESSA-266 experiment planned at the Linac Extension Area (LEA) facility at Argonne Photon Source (APS). The goal of this project which is carried forward by a multi-institutional collaboration between university (UCLA), national laboratory (ANL) and small industries (Radiabeam and Radiasoft) is to demonstrate very high efficiency electron beam energy extraction in a 4-meter long strongly tapered helical undulator seeded by an ultraviolet 1 GW peak power laser seed pulse, and to study the spatial and spectral properties of the amplified radiation. We focus here on the discussion of the break-section area in between the undulators which has been designed to maximize the efficiency, and show the results of the numerical simulations for the system.

INTRODUCTION

Free-Electron-Lasers enjoy many unique properties as radiation sources, including high power, coherence and tunability and have been at the forefront of scientific research for decades. Especially in the short wavelength region of the electromagnetic spectrum, FELs have enabled a novel generation of radiation sources opening new frontiers in scientific research. On the other hand a characteristic drawback for conventional Free-Electron-Lasers amplifiers is that the energy efficiency is actually relatively poor, limited by the Pierce parameter [1] which at short wavelength (ultraviolet and below) is typically below 1 percent and often below 0.1 percent.

Following up earlier work on Inverse Free Electron Laser acceleration [2], few years ago a novel regime of operation has been proposed to greatly increase the FEL efficiency using prebunched electron beams, intense seed laser, and strongly tapered undulators (so called TESSA scheme) [3]. An experimental demonstration of the TESSA concept in the mid-infrared was carried out at BNL [4] where using a 200 GW seed laser at 10 μm wavelength, an energy extraction efficiency as high as 30 % was demonstrated. The intense seed laser pulse used for this experiment hindered measurements of the spatial and spectral properties of the newly generated radiation (i.e. the experiment was carried out in the low-gain TESSA regime).

The current TESSA-266 project aims at pushing the performances of the proof-of-principle BNL experiment and explore this interaction in the high gain regime (using a less intense seed laser pulse) and extending the scheme to shorter wavelengths where high efficiency radiation sources would be extremely attractive (EUVL). The experimental design is based on a tapered gap-tunable helical Halbach [5] undulator which will be installed in the Linac Extension Area (LEA) at the end of the Argonne Photon Source injection linac. The APS linac will provide 375 MeV and up to 1 kA e-beam at 1-10 Hz pulse repetition rate in the interleaving mode that makes the beam available for this experiment 75 % of time. A seed laser of 1 GW and pulse length 0.6 ps will then be used first to bunch, extract energy and quickly decelerate the electron beam, yielding high gain TESSA amplification and an extraction efficiency which in the ideal simulation case reaches values as high as 10 percent (see Table 1 for a summary of the experiment parameters).

EXPERIMENT DESIGN

The tapered helical undulator for TESSA-266 is designed to maintain the resonant condition as the electrons lose their energy to the radiation along the interaction varying the undulator K factor while keeping the undulator period constant [6]:

$$\gamma_r^2 = \frac{\lambda_u}{2\lambda}(1 + K^2) \tag{1}$$

where λ_u is the undulator period, λ is the laser wavelength, and K the normalized undulator vector potential.

The undulator period is chosen to be at 3.2 cm in order to satisfy the resonance condition with e-beam energy of 375 MeV and wavelength of 266 nm with a gap of sufficient size to hose the vacuum pipe (> 5.5 mm).

Table 1: TESSA266 Nominal Parameters

Element	
Beam Energy	375 MeV
Peak Current	1 kA
Emittance	2 um
Energy Spread	0.1 %
RMS Mean Spot Size	47 um
Undulator Period	32 mm
Undulator K Parameters	2.8 - 2.4
Radiation wavelength	266 nm
Seed Power	1 GW

A number of considerations entered the final choice on the length of the undulator sections in the design of the experiment. There is enough space in the LEA tunnel to house

ISBN: 978-3-95450-210-3 doi:10.18429/JACoW-FEL2019-THP074

Content from this work may be used under the terms of the CC BY 3.0 licence (© 2019). Any distribution of this work must maintain attribution to the author(s), title of the work, publisher, and DOI

FLASH: THE PIONEERING XUV AND SOFT X-RAY FEL USER FACILITY

K. Honkavaara*, S. Schreiber, DESY, Hamburg, Germany†

Abstract

FLASH, the free-electron laser (FEL) at DESY (Hamburg), started user operation in summer 2005. It delivers high peak and average brilliance XUV and soft X-ray FEL radiation to photon experiments. Nowadays, FLASH has a 1.25 GeV superconducting linac, and two undulator beamlines, which are operated simultaneously. This paper provides an overview of its evolution from a test facility for superconducting accelerator technology to a full-scale FEL user facility.

INTRODUCTION

FLASH [1–6] at DESY (Hamburg, Germany) is an FEL user facility. It started user operation in summer 2005, and it was the first user facility worldwide delivering FEL radiation in XUV wavelengths to photon experiments.

Presently, FLASH consists of a photoinjector, a superconducting linac, two undulator beamlines (FLASH1 and FLASH2), and two experimental halls. The schematic layout is shown in Fig. 1. In addition, FLASH hosts a seeding experiment sFLASH [7], and a plasma wakefield acceleration experiment FLASHForward [8].

Electron bunches are generated by a photoinjector consisting of a normal conducting RF-gun with an exchangeable Cs_2Te photocathode, and three injector lasers. The linac has seven TESLA type 1.3 GHz superconducting accelerator modules, and two magnetic chicane bunch compressors. The maximum electron beam energy is 1.25 GeV. The use of superconducting RF cavities allows operation with long RF-pulses (800 µs), and thus with long electron bunch trains. FLASH1 and FLASH2 beamlines are operated simultaneously with a bunch train repetition rate of 10 Hz [9]. The separation of the bunch trains is realized by a kicker-septum system downstream of the last accelerator module.

The production of FEL radiation is based on the SASE (Self Amplified Spontaneous Emission) process. The FLASH1 undulator beamline consists of six 4.5 m long fixed gap (12 mm) undulator modules, which are the original ones and in use since 2004. FLASH2 has twelve 2.5 m long variable gap undulators. A planar electromagnetic undulator, installed downstream of the FLASH1 SASE undulators, provides, on request, THz radiation for user experiments.

The photon wavelength of FLASH1, due to fixed gap undulators, is defined by the electron beam energy. The minimum wavelength (fundamental), which FLASH1 can provide for user experiments is 4.2 nm, the maximum one slightly above 50 nm. FLASH2 with variable gap undulators provides FEL radiation at wavelengths between 4 nm and 90 nm.

* katja.honkavaara@desy.de
† for the FLASH team

Part of the material presented here has been discussed also in previous conferences, for example in [10–14].

TESLA TEST FACILITY (TTF) LINAC

The origin of FLASH is the TESLA Test Facility (TTF) Linac [15], constructed at DESY in mid 1990's. TTF was originally dedicated to test the feasibility of high gradient superconducting accelerator technology in the framework of the TESLA linear collider project [16].

The TTF injector I [17], operated in 1996-1998, consisted of a thermionic gun, a subharmonic buncher, a capture cavity (one superconducting TESLA type 9-cell cavity), and a diagnostics section. The first electron beam was produced in April 1996. The first complete TESLA type accelerator module with eight 9-cell superconducting niobium cavities was installed into the TTF Linac in spring 1997. Successful beam tests were carried out in 1997-1998 [18].

In autumn 1998, the injector was replaced by a photoinjector (Injector II) consisting of a laser-driven RF-gun with a Cs_2Te photocathode, a capture cavity (the same one as used in Injector I), a bunch compressor, and a diagnostic section [19]. In addition, a second bunch compressor [20] and a second accelerator module [21] were installed. The bunch compressor was located between the two accelerator modules.

Moreover, the TTF Linac was used to drive the SASE free-electron laser pilot facility TTF-FEL [22]. Three fixed gap undulator modules, similar to those still in use at FLASH1, were installed in 1999. In addition, the first accelerator module was replaced by a new one. The first SASE lasing in VUV worldwide (109 nm) was achieved in February 2000 [23]. TTF-FEL was successfully operated at photon wavelengths from 80 nm to 120 nm [24, 25] to demonstrate the feasibility of SASE FELs in the VUV range for photon experiments. The operation of the TTF Linac finished in November 2002.

FEL USER FACILITY FLASH

FLASH – originally called VUV-FEL at TTF2 – was constructed in 2003-2004. The first stage consisted of a photoinjector, a superconducting linac of five TESLA type accelerator modules, two bunch compressors, and an undulator beamline of six fixed gap undulator modules. The injector and the first part of the linac were located in the former place of TTF-FEL. An extension tunnel was built to host the undulator beamline, and a new experimental hall was constructed for the photon beamlines and user experiments.

The first lasing (32 nm) was achieved in January 2005 [26]. The user operation started in summer 2005, opening new possibilities for photon science, for example diffractive imaging [27]. During 2005-2007, FLASH delivered FEL radiation in wavelengths from 13 nm to 47 nm (fundamental),

ISBN: 978-3-95450-210-3 doi:10.18429/JACoW-FEL2019-THP078

Content from this work may be used under the terms of the CC BY 3.0 licence (© 2019). Any distribution of this work must maintain attribution to the author(s), title of the work, publisher, and DOI

STATUS OF THE COMPACTLIGHT DESIGN STUDY*

G. D'Auria†, S. Di Mitri, R. Rochow, Elettra Sincrotrone Trieste, 34149 Basovizza, Italy
A. Latina, X. Liu, C. Rossi, D. Schulte, S. Stapnes, X. Wu, W. Wuensch, CERN, 1211 Geneva, CH
H. M. Castañeda Cortes, J. Clarke, D. Dunning, N. Thompson, STFC Daresbury Lab., Warrington, UK
W. Fang, Shanghai Institute of Applied Physics, Shanghai 201800, P. R. China
E. Gazis, N. Gazis‡, E. Tanke‡, E. Trachnas‡, IASA, Athens, Greece
V. Goryashko, M. Jacewicz, R. Ruber, Uppsala University, Uppsala, Sweden
G. Taylor, Melbourne University, Melbourne, Australia
R. Dowd, D. Zhu, Australian Synchrotron, ANSTO, Australia
A. Aksoy, Z. Nergiz, Ankara University, Ankara, Turkey
R. Apsimon, G. Burt, A. Castilla, Lancaster University, Lancaster, UK
H. Priem, X. Janssen, VDL Enabling Technology Group, Eindhoven, Netherlands
J. Luiten, P. Mutsaers, X. Stragier, Tech. University of Eindhoven, Netherlands
D. Alesini, M. Bellaveglia, B. Buonomo, F. Cardelli§, M. Croia, M. Diomede, M. Ferrario,
A. Gallo, A. Giribono§, L. Piersanti§, J. Scifo, B. Spataro, C. Vaccarezza, INFN-LNF, Frascati, Italy
R. Geometrante, M. Kokole, Kyma S.r.l., Trieste, Italy
J. Arnesano, F. Bosco, L. Ficcadenti, A. Mostacci, L. Palumbo, Sapienza University, Rome, Italy
G. Dattoli, F. Nguyen, A. Petralia, ENEA, Frascati, Italy
J. Marcos, E. Marin, R. Munoz Horta, F. Perez, ALBA Synchrotron, Barcelona, Spain
A. Faus-Golfe, Y. Han, CNRS, Paris, France
A. Bernhard, J. Gethmann, Karlsruher Institut für Technologie, Karlsruhe, Germany
M. Calvi, T. Schmidt, K. Zhang, Paul Scherrer Institut, 5232 Villigen, Switzerland
D. Esperante, J. Fuster, B. Gimeno, D. Gonzalez-Iglesias, IFIC (CSIC-University of Valencia), Spain
M. Aicheler, Helsinki University, Helsinki, Finland
R. Hoekstra, ARCNL, Amsterdam, Netherlands
A. W. Cross, L. Nix, L. Zhang, Strathclyde University, Glasgow, UK

Abstract

CompactLight (XLS) is an International Collaboration of 24 partners and 5 third parties, funded by the European Union through the Horizon 2020 Research and Innovation Programme. The main goal of the project, which started in January 2018 with a duration of 36 months, is the design of an hard X-ray FEL facility beyond today's state of the art, using the latest concepts for bright electron photo-injectors, high-gradient accelerating structures, and innovative short-period undulators. The specifications of the facility and the parameters of the future FEL are driven by the demands of potential users and the associated science cases. In this paper we will give an overview on the ongoing activities and the major results achieved until now.

INTRODUCTION

The CompactLight project aims to design a hard X-ray FEL facility beyond today's state of the art, combining the latest and most innovative technologies for the major components of the FEL system, very high gradient accelerating structures at X-band (12 GHz), the most advanced concepts for high brightness electron photo injectors, and innovative compact short-period undulators. Compared to existing facilities, the proposed facility will have a smaller footprint due to the high gradient and will require a lower electron beam energy, owing to the enhanced undulator performance. The whole infrastructure will have lower electrical power demand, construction and operation costs. The user requirements have been identified by existing and potential FEL users via discussions at several workshops, meetings, and surveys. They are summarised in Table 1 and in [1].

Table 1: Baseline Parameters of the CompactLight FEL

Parameter	Unit	SXR	HXR
Photon Energy	keV	0.25-2.0	2.0-16.0
Repetition rate	Hz	250	100
Pulse duration	fs	0.1-50	1-50
Polarization		Variable, selectable	
Two-pulse delay	fs	± 100	± 100
Two-colour separation	%	20	10
Synchronization	fs	< 10	< 10

* This project has received funding from the European Union's Horizon2020 research and innovation programme under grant agreement No 777431.
† gerardo.dauria@elettra.eu
‡ Now at ESS-ERIC, Lund, Sweden
§ Now at ENEA, Frascati, Italy

ISBN: 978-3-95450-210-3 doi:10.18429/JACoW-FEL2019-THP079

Content from this work may be used under the terms of the CC BY 3.0 licence (© 2019). Any distribution of this work must maintain attribution to the author(s), title of the work, publisher, and DOI

STATUS AND PERSPECTIVES OF THE FERMI FEL FACILITY (2019)

L. Giannessi†, E. Allaria, L. Badano, S. Bassanese, F. Bencivenga, C. Callegari, F. Capotondi, D. Castronovo, F. Cilento, P. Cinquegrana, M. Coreno, I. Cudin, M. B. Danailov, G. D'Auria, R. De Monte, G. De Ninno, P. Delgiusto, A. Demidovich, M. Di Fraia, S. Di Mitri, B. Diviacco, A. Fabris, R. Fabris, W. M. Fawley, L. Foglia, M. Ferianis, P. Furlan Radivo, G. Gaio, F. Gelmetti, F. Iazzourene, S. Krecic, M. Lonza, G. Kurdi, N. Mahne, M. Malvestuto, M. Manfredda, C. Masciovecchio, M. Milloch, R. Mincigrucci, N. Mirian, I. Nikolov, F. H. Oshea, G. Penco, A. Perucchi, O. Plekan, M. Predonzani, K. C. Prince, E. Principi, L. Raimondi, P. Rebernik Ribič, F. Rossi, L. Rumiz, C. Scafuri, C. Serpico, N. Shafqat, P. Sigalotti, A. Simoncig, S. Spampinati, C. Spezzani, M. Svandrlik, M. Trovò, A. Vascotto, M. Veronese, R. Visintini, D. Zangrando, M. Zangrando
Elettra Sincrotrone Trieste S.C.p.A., Basovizza, Italy

Abstract

FERMI is the seeded Free Electron Laser (FEL) user facility at the Elettra laboratory in Trieste, operating in the VUV to EUV and soft X-rays spectral range; the radiation produced by the seeded FEL is characterized by wavelength stability, low temporal jitter and longitudinal coherence in the range 100-4 nm. During 2018 a dedicated experiment has shown the potential of an Echo Enabled Harmonic Generation (EEHG) scheme to cover most of this spectral range with a single stage cascade [1]. Such a scheme, combined with an increment of the beam energy and of the accelerator performances, could extend the FERMI operating range up to the oxygen K-edge. With this future perspective, we present the development plans under consideration for the next 3 to 5 years. These include an upgrade of the linac and of the existing FEL lines, consisting in the conversion of FEL-1 first, and FEL-2 in a second moment, into EEHG seeded FELs.

INTRODUCTION

FERMI is located at the Elettra laboratory in Trieste. The FEL facility covers the VUV to soft X-ray photon energy range with two seeded FELs, FEL-1 [2] and FEL-2 [3], both based on the High Gain Harmonic Generation seeded mode (HGHG) [4-6] to operate in the range 100-4 nm, producing radiation characterized by wavelength stability, low temporal jitter and longitudinal coherence [7-10].

The FELs are in operation with users since 2010. During the commissioning phase "with users", concluded in December 2018, seven calls for experiments (see Fig.1) contributed to establish and consolidate the various modes of operation. In January 2019 the facility entered into standard operation mode, with two calls for experiments every year and more than 4k hours per year of user operation regularly scheduled.

Strategic development goals for FERMI are the reduction of the pulse duration, which is typically in the range 30-100 fs depending on the duration of the seed and on the harmonic order [11], and the extension of the photon energy range of operation; there is indeed significant interest and there are important science opportunities in extending the photon energy range to include the K-edges of nitrogen (410 eV) and oxygen (543 eV) [12-14].

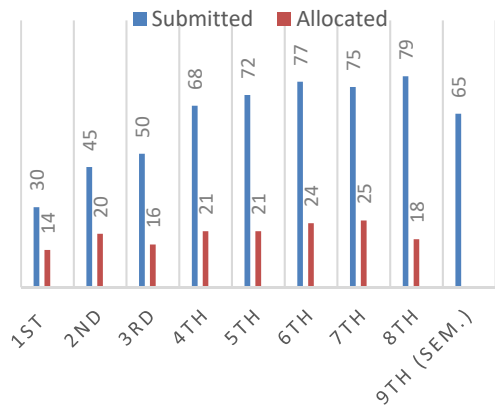


Figure 1: User proposal statistics at FERMI

As to the reduction of the pulse duration, an upgrade of the laser system to start with a shorter seed is under development. This, combined with nonlinear dynamics in the FEL amplifier [15] has shown the potential to reduce to sub 10-fs the FEL pulse duration. As to the extension of the photon energy range, the amplitude of the energy modulation necessary to initiate the HGHG process grows with the order of the harmonic conversion, and the induced energy dispersion has a detrimental effect on the high gain amplification in the final radiator. This fact limits the harmonic multiplication factor of FERMI FEL-1 to 13-15. Substantially higher orders can be reached with FEL-2 with the double stage HGHG cascade, where the harmonic conversion is performed with the fresh bunch injection technique [6]. This scheme was implemented for the first time on FERMI FEL-2 [3] and was used to demonstrate the seeded FEL coherent emission in the soft-X rays, up to harmonic orders of 65, and higher [7].

An alternative method to increase the order of the harmonic conversion in a single stage is the Echo Enabled Harmonic Generation (EEHG) scheme proposed in [16-17]. During 2018 a dedicated experiment has shown the potential of EEHG to cover at FERMI most of this spectral

ISBN: 978-3-95450-210-3 doi:10.18429/JACoW-FEL2019-THP081

PolFEL - NEW FACILITY IN POLAND*

K. Szamota-Leandersson†, R. Nietubyć, P. Czuma, P. Krawczyk, J. Krzywiński, J. Sekutowicz[1], M. Staszczak, J. Szewiński, National Centre for Nuclear Research, Otwock-Świerk, Poland
W. Bal, J. Poznański, Institute of Biochemistry and Biophysics, PAS, Warsaw, Poland
A. Bartnik, H. Fiedorowicz, K. Janulewicz, N. Pałka
Institute of Optoelectronics, Military University of Technology, Warsaw, Poland
[1]DESY, Hamburg Germany

Abstract

PolFEL will be first free electron laser in the part of eastern Europe, Poland. The source of low energy linac will be superconducting photocathode. PolFel will operate in CW and long pulse (lp) mode. PolFEL will generate THz, IR and VIS-VUV radiation. PolFEL is going to prepare number of end-stations for user activities. The most unique end-station base on Inverse Compton Scattering phenomena will allow to perform measurements with X-ray photons with time resolution in fs range.

PolFEL DESCRIPTION

In this short document the main parameters of PolFEL are mentioned. In last three decades Polish scientists and engineers participated in and contributed to many projects related to Free Electron Laser- and High Energy Physics facilities worldwide, not having any of these facilities in the country. Therefore, group of Polish scientific institutes interested in the modern research with coherent radiation was very pleased receiving in 2018 funds for the free electron laser PolFEL project from the Smart Growth Operational Programme, Measure 4.2: Development of modern research infrastructure of the science sector.

A PolFEL consortium was established with NCBJ as project leader and eight Polish research institutes and universities as members. PolFEL will be driven by cw operating superconducting linac with SRF electron source developed in collaboration with DESY and 8 superconducting TESLA cavities housed in 4 Rossendorf type cryomodules. Moreover, accebility of new superconducting technology enabled us to designed state-of –art linear accelerator operating both in the continuous wave (cw) mode and long pulse (lp) mode. The cw mode allows for full flexibility of electron beam time structure and hence photon beams. Time structure (max repetition rate 50 KHz) is defined by laser beam irradiating the cathode in a superconducting injector (SRF injector). The injector cryomodule for PolFEL contains one 1.3 GHz SRF 1.5-cell cavity made of nobium. Designing of this cryomodule base on the conceptual design from DESY is a part of project and cryomodule will be made at NCBJ. Cavity is housed in a titanium helium vessel in temperature range 1,8 – 2,0 K. Thermal shielding is the most crucial system, will include two lines of the helium (2 K, 5 K) and Liquid Nitrogen. The PolFEL project has received already significant hardware support from the STFC Daresbury Laboratory, e.g. components of a 120 W@2K cryogenic plant, many beam optics components and RF-components. The cryogenic system design is in charge of specialist from Wroclaw University of Science and Technology. PolFEL will generate THz, IR radiation and VIS-VUV radiation in two beam lines, respectively. In the first one, with electron beam below 80 MeV, the THz/IR radiation source will be generated in permanent magnet supper-radiant undulator, delivering THz radiation in 0.5–3 THz range. IR undulators will be positioned upstream THz undulators. In the second beam line with up to 180 MeV electrons, the VIS/VUV radiation will be generated in the SASE undulator delivering coherent radiation down to 55 nm in the third harmonic. Both undulators will be based on the modified Bazin design shared by the STFC Daresbury Lab and assisting the NCBJ team in the modification effort. Both undulators are going to be made in NCBJ.

PolFEL parameters are written in Table 1 and Table 2.

Table 1: PolFEL Electron Beam Parameters

	Unit	Gun	VUV /electron line	THz line
Bunch charge	pC	20-250	max 100	250
Bunch repetition rate	kHz	50	50	50
Transvers normalized 80% slice emittance	µm·rad	0.1-0.4	< 0.5	<0.75
Bunch duration at the electron line exit	ps	2-10	0.4	up to 10
Beam energy at the line exit: cw mode lp mode @ duty factor of 40%	MeV	4	90-154 up to 187	up to 65
Maximal beam current	µA	12.5	5	12.5
Beam power at dump: cw lp @ duty factor of 40%	W	-	650 374	813

* Work supported by Smart Growth Operational Programme, Measure 4.2: Development of modern research infrastructure of the science sector.
† Karolina.Szamota-Leandersson@ncbj.gov.pl

Content from this work may be used under the terms of the CC BY 3.0 licence (© 2019). Any distribution of this work must maintain attribution to the author(s), title of the work, publisher, and DOI

ISBN: 978-3-95450-210-3 doi:10.18429/JACoW-FEL2019-THP084

STATUS OF THE SOFT X-RAY LASER (SXL) PROJECT AT THE MAX IV LABORATORY*

F. Curbis†, J.Andersson, F. Lindau, L. Isaksson, M. Kotur, E. Mansten, M. Pop, W. Qin, H. Tarawneh, P. Tavares, S. Thorin, S. Werin‡, MAX IV laboratory, Lund, Sweden
A. Nilsson, M. Larsson, P. Salen, S. Bonetti, Stockholm University, Stockholm, Sweden
J. A. Sellberg, KTH Royal Institute of Technology, Stockholm, Sweden
V. Goryashko, Uppsala University, Uppsala, Sweden
P. Johnsson, Lund University, Lund, Sweden

Abstract

A Soft X-ray Laser project (the SXL) aiming to produce FEL radiation in the range of 1 to 5 nm is currently in a conceptual design phase and a report on the design is expected to be delivered by March 2021. The FEL will be driven by the existing 3 GeV linac at MAX IV laboratory, which also serves as injector for the two storage rings. The science case has been pushed by a large group of mainly Swedish users and consists of experiments ranging from AMO physics to condensed matter, chemistry and imaging in life science. In this contribution, we will present the current conceptual design of the accelerator and the FEL operation modes together with a general overview of the beamline and experimental station. In particular design options for the FEL will be discussed in conjunction with the features of the electron beam from the MAX IV linac and the connection with the proposed experiments.

INTRODUCTION

The linear accelerator, which serves as injector for the two storage rings and the Short Pulse Facility (SPF) at the MAX IV laboratory in Sweden, can also drive a soft X-ray FEL with minor modifications. The SXL project has been proposed by Swedish users interested in exploiting FEL radiation in the range between 1 and 5 nm.

The linac will for the SXL project run at its maximum energy of 3 GeV with 100 Hz repetition rate and an upgraded photo cathode gun [1].

Several Swedish universities are engaged in this project: Stockholm university, Royal Institute of technology (KTH), Uppsala University and Lund University.

The project timeline sees now a three years period to work on a Conceptual Design Report (CDR) with final delivery in March 2021. The CDR work is divided in six work packages; Science Case, Accelerator, FEL, Insertion Devices, Beamline and Experimental Station.

GENERAL LAYOUT

A schematic layout of the SXL is shown in Fig. 1. The 3 GeV linac is followed by the undulator modules (currently 3 m long, with 4.0 cm period). A long drift space, where photon diagnostics will be placed and the power density allowed to drop until reaching the first mirror, will be followed by the monochromator. The experimental station will also include a laser for pump-probe experiments. Different options for the timing/synchronization system are now under discussion to make sure the best stability can be achieved with very short pulses. The data handling and collection will prove a challenge and is envisaged to be integrated into the existing capabilities and future capacity upgrades of MAX IV laboratory.

THE SCIENCE CASE

Following a successful workshop in March 2016 where more than 100 Swedish (mostly but not only) users gathered in Stockholm to contribute to the science case [2] for the SXL, a set of representative experiments has been selected in the following categories: AMO, Condensed matter, chemistry and imaging in life science. The AMO experiments will explore processes from charge migration to charge transfer thanks to ultrashort pulses and the possibility to have two pulses with different colors in order to implement pump-probe schemes. For the chemistry applications the main focus is in understanding the dynamics of heterogeneous catalysis and probing transition states in surface reactions, and for these variable polarization is desired. In condensed matter the goal is to create new phases in quantum materials (like strontium titanate) with THz radiation and probe the emergent order with the SXL beam. Also experiments on coherence control in the attosecond frontier are foreseen, and they will require sub-fs pulses, besides the full control of the FEL polarization. Pumping with an HHG (High Harmonic Generation) source will also be beneficial. In Life Science the combination of THz or other pump lasers with the FEL radiation will allow to probe conformational changes in solution for the scattering experiments. Relatively long (50 fs) pulses with two colors will be required together with a split-and-delay line for dynamics between 100 fs and 10 ms.

LINAC

The SXL will use the 3 GeV S-band linac currently serving the MAX IV 1.5 and 3 GeV storage rings and Short Pulse Facility (SPF). As of today a photo cathode gun and two bunch compressors provide 100 fs long pulses for the

* Work supported by KAW foundation.
† francesca.curbis@maxiv.lu.se
‡ sverker.werin@maxiv.lu.se

Content from this work may be used under the terms of the CC BY 3.0 licence (© 2019). Any distribution of this work must maintain attribution to the author(s), title of the work, publisher, and DOI

ISBN: 978-3-95450-210-3 doi:10.18429/JACoW-FEL2019-THP085

STATUS OF Athos, THE SOFT X-RAY FEL LINE OF SwissFEL

R. Ganter†, G. Aeppli, J. Alex, A. Al Haddad, C. Arrell, V. Arsov, C. Bostedt, S. Bettoni, H.H. Braun, M. Calvi, T. Celcer, P. Craievich, R. Follath, F. Frei, N. Gaiffi, Z. Geng, C. Gough, M. Huppert, R. Ischebeck, H. Jöhri, P. Juranic, B. Keil, F. Loehl, F. Marcellini, G. Marinkovic, G. L. Orlandi, C. Ozkan Loch, M. Paraliev, L. Patthey, M. Pedrozzi, C. Pradervand, E. Prat, S. Reiche, T. Schietinger T. Schmidt, K. Schnorr, C. Svetina, A. Trisorio, C. Vicario, D. Voulot, U. Wagner, A. Zandonella, PSI, Villigen, Switzerland

Abstract

The Athos line will cover the photon energy range from 250 to 1900 eV and will operate in parallel to the hard X-ray line Aramis of SwissFEL. The Athos FEL line starts with a fast kicker magnet followed by a dogleg transfer line, a small linac and 16 APPLE undulators. From there the photon beam passes through the photonics front end and the beamline optics before reaching the experimental stations Maloja and Furka. This contribution summarizes the two-bunch operation commissioning (two bunches in the same RF macropulse), which started in 2018, and the characterization of key components like the APPLE X undulator UE38. The Athos installation inside the tunnel is alternating with Aramis FEL user operation, and the first lasing is planned for winter 2019 / 2020.

Athos FEL LAYOUT

Athos [1] is the soft X-ray FEL line of SwissFEL (Fig. 1). Athos is currently under assembly and will deliver first FEL beam to the Maloja experimental station in 2020. This second branch of SwissFEL (Aramis being the hard X-ray FEL) starts at meter 270 (distance to the photocathode) with a resonant kicker [2,3]. This fast kicker separates the two bunches: one going to Aramis and the second one going to the Athos FEL line. The electron beamline portion between the resonant kicker (z=265 m) and the beam stopper (z= 383m) just upstream the 1st undulator is already installed and currently under beam commissioning. The undulator line consists of 16 APPLE X undulator [4] segments of 2 m length (Fig. 2). The inter-undulator section will have the usual quadrupole / BPM combination and also a small magnetic chicane made of permanent magnets. This chicane can be operated as an intra-undulator phase shifter or used to delay (5 fs max.) or shift transversally the bunch (250 µm max.). This chicane is the essential tool to provide a large variety of operation schemes [5]. In addition, a delay line chicane (500 fs max. delay) with four electro magnets splits the FEL line in two halves (Fig. 2). Each half can be tuned to a different K value to produce two different colors. The main diagnostic of the Athos FEL line will be an X band RF Transverse Deflecting Structure (PolariX –TDS [6, 7]) positioned downstream the last undulator to allow on line monitoring of the lasing portion of the electron bunch. The variable polarization of the deflecting force will allow measurements of the bunch length, energy and of the transverse slice emittances (vertical and horizontal). Downstream the beam dump, starts the X-ray front end which will include a gas monitor to measure the FEL pulse energy and position. The mirrors to deflect the FEL beam to the different end stations are located in a separate room outside the tunnel [8]. Athos will have three experimental stations, where two (Maloja and Furka) are already under construction. Maloja will start commissioning tests in 2020 and will focus on very short FEL pulses (few fs and below). After first SASE lasing, the next goal will be to operate Athos in the optical klystron regime using the inter-undulator chicane. This scheme will speed up the SASE process so that lasing with only half of the undulator line becomes possible. This will then allow the test of the two color mode of operation.

TWO BUNCH OPERATION

Two distinct lasers are illuminating the photocathode to produce two electron bunches separated by 28 ns. The repetition rate and also the machine protection system logic can be set independently for bunch 1 and bunch 2. This independence of both timing event systems is important for parallel operation of Aramis and Athos FEL lines. Both bunches are accelerated simultaneously up to 3.15 GeV. The radio-frequency macropulses of the injector S band and X band modulator have an extra step of about 28ns length in order to control the phase and amplitude of the bunch 2 independently of bunch 1.

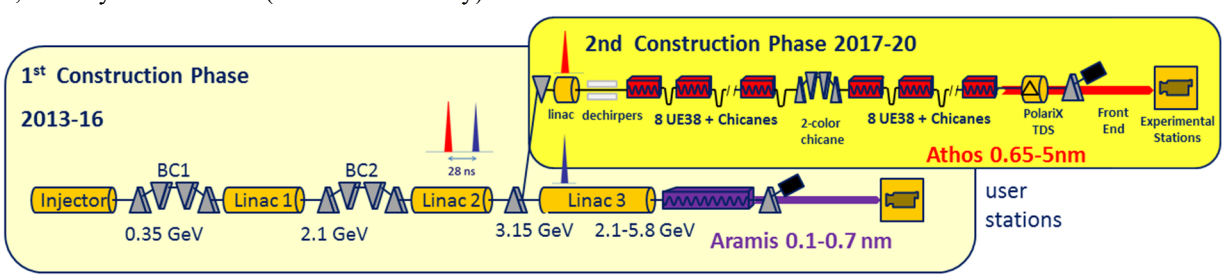


Figure 1: Layout of SwissFEL showing the extraction of second bunch at 3.15 GeV which is then transported along the Athos branch of SwissFEL.

Content from this work may be used under the terms of the CC BY 3.0 licence (© 2019). Any distribution of this work must maintain attribution to the author(s), title of the work, publisher, and DOI

ISBN: 978-3-95450-210-3 doi:10.18429/JACoW-FEL2019-THP086

OPERATION MODES OF THE SwissFEL SOFT X-RAY BEAMLINE ATHOS

S. Reiche*, E. Ferrari, E. Prat, T. Schietinger, Paul Scherrer Institut, Villigen PSI, Switzerland

Abstract

The SwissFEL linac drives the two FEL beamlines Aramis and Athos, a hard and soft X-ray FEL, respectively. The layout of Athos extends from a simple SASE FEL beamline with the addition of delaying chicanes, external seeding and beam manipulation with wakefield sources (dechirper). It also reserves space for a possible upgrade to self-seeding. This presentation gives an overview on the detailed layout enabling the unique operation modes of the Athos facility.

INTRODUCTION

Since the first demonstration of Free-electron Lasers (FEL) [1], based on SASE [2] – the amplification of the spontaneous undulator radiation – several user facilities became operational worldwide [3–7] to extend the wavelength down to the hard X-rays. While there has been significant progress to overcome the limited longitudinal coherence of the SASE pulse or to control the pulse length and peak power, only FERMI [8] can be considered a user facility, which deviates significantly from basic SASE operation by providing a fully seeded signal with an external seed laser.

The soft X-ray beamline Athos of SwissFEL [9], which is currently realized as a second step after the commissioning of the hard X-ray beamline Aramis, features a layout optimized away from basic SASE operation at the cost of shorter undulator modules, more focusing quadrupoles and delaying chicanes about 1000 times stronger than phase shifters. It has also sufficient space to host additional hardware such as external seeding.

So far simulations have shown better performances than SASE in terms of saturation length or brilliance but also a more direct control on the FEL output pulse characteristics. This leads to a catalog of various operation modes, depending on the specific needs of user experiments. In the following we give a very brief description of the capabilities of the Athos soft X-ray FEL beamline.

DESIGN AND LAYOUT CONSIDERATIONS

The aim to operate the soft X-ray beamline Athos at SwissFEL independently of the hard X-ray beamline Aramis, whose wavelength is mostly tuned by the electron beam energy between 2.1 GeV and 5.8 GeV, resulted in an optimum solution to extract a second bunch at the intermediate energy of 3 GeV to drive Athos. Up to that point the machine is fixed in its energy profile and only the succeeding linac changes the beam energy for Aramis. The two FEL beamlines share the same infrastructure, they are installed parallel to each other with a shift of 50 m to accommodate the layout of the end stations, see Fig. 1. Also the experimental stations are in the same building. The Athos undulator modules are 2 m long and interlined with dispersive chicanes, thereby offering new modes of operation, as explained in more detail in the next section. A re-optimization of the undulator length resulted in a reduction from 4 m to 2 m [10]. This change did not compromise the baseline SASE operation of Athos, but it allowed for a reduction of the total undulator length since the optical klystron (OK) effect [11] reduces the saturation length. Currently there are 16 modules of 2 m each in the baseline layout with a chicane of 2 m length and a delay of 500 fs in the middle, splitting the undulator beamline in two halves for two-color operation based on tilted beams [12].

An additional grant now allows financing the interaction of the electron beam with a laser. This will be realized in two stages. The first is an energy modulation and conversion into a current modulation (ESASE) [13] by means of a chicane identical to that of the two-color operation. The second phase adds another modulator and a larger chicane for an Echo-Enabled Harmonic Generation (EEHG) [14] set-up to provide seeded pulses to the users at least for the low photon energy range of Athos. The required infrastructure is placed directly in front of the main undulator with the exception of the first modulator, which is located all the way upstream at the end of the out-coupling switchyard to eliminate the need for an additional chicane. The modulator is resonant in the wavelength range between 250 to 1500 nm.

Self-seeding [15] was considered a possible upgrade option for Athos but the decision for shorter undulator modules makes a simple implementation difficult, since the filtering of the FEL signal by a monochromator does not fit into the 2.8 m periodicity of the Athos lattice, much shorter than the implementation at LCLS [16]. Also, self-seeding requires a rather uneven split of the 16 undulator modules for best performance, which is not compatible with two-color operation. Therefore, self-seeding is no longer part of the baseline design. However, the large chicane in the first stage of EEHG is upgradable to include a spectrometer, and the available space before can host up to 5 undulator modules, providing the SASE signal for self-seeding.

Figure 1 shows the final layout with a total length of about 80 m for the FEL beamline, split into 50 m for the main undulator line, 15 m for the EEHG chicanes and modulator and another 15 m for the first stage in a possible self-seeding upgrade. In addition to the standard SASE operation, this arrangement allows control of the bandwidth via either external seeding, self-seeding or HB-SASE [17], as well as the possibility to achieve extremely short pulses. A summary of the Athos parameters are given in Table 1.

* sven.reiche@psi.ch

Content from this work may be used under the terms of the CC BY 3.0 licence (© 2019). Any distribution of this work must maintain attribution to the author(s), title of the work, publisher, and DOI

ISBN: 978-3-95450-210-3 doi:10.18429/JACoW-FEL2019-THD03

FEL OPTIMIZATION: FROM MODEL-FREE TO MODEL-DEPENDENT APPROACHES AND ML PROSPECTS

S. Tomin†, G. Geloni, The European XFEL, Schenefeld, Germany
M. Scholz, DESY, Hamburg, Germany

Abstract

Users beam-time at modern FEL sources is an extremely valuable commodity. Moreover, maximization of FEL up-time must always be performed accounting for stringent requirements on the photon pulse characteristics. These may vary widely depending on the Users requests, which poses challenges to parallel operation of high-repetition rate facilities like the European XFEL. Therefore, both model free or model-dependent optimization schemes, where the model might be given, or provided by machine-learning approaches, are of high importance for the overall efficiency of FEL facilities. In this contribution we review our previous activities and we report on current efforts and progress in FEL optimization schemes at the European XFEL. Finally, we provide an outlook of future developments.

INTRODUCTION

Automatic optimization of accelerator performance is part of the daily operation procedures at the European XFEL [1,2] and other FEL facilities, e.g. [3-5]. The dedicated tools help to tune machines performance faster and more efficient (multidimensional optimization) in comparison to manual tuning. However, the tuning of the large-scale facilities as the European XFEL remains a time-consuming procedure. Moreover, the best machine performance is usually achieved for the most explored operation modes, see Fig. 1, which also points to the importance of optimization procedures. Figure 1 shows dependence of the photon energy against the photon pulse energy for the hard X-Ray undulator SASE1. The colour shows number of machine files – a snapshot of the machine in a stable state. As it can be seen, one of the most frequently used photon energy is around 9–9.3 keV, where the maximum photon pulse energy was around 2.7 mJ. At longer wavelengths, for example 8 keV the maximum photon pulse energy was half as much.

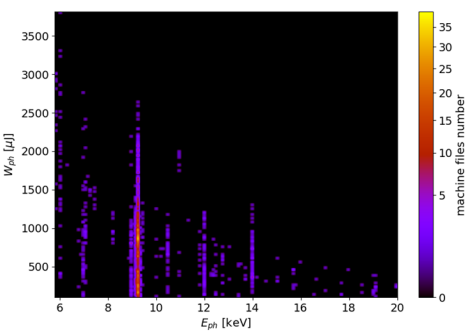


Figure 1: EuXFEL SASE1 performance statistics.

† sergey.tomin@xfel.eu

Taking into account high pressure on the machine availability for parallel multi-user operation, the European XFEL is looking for more automation of optimization procedures and new effective approaches to speed up the machine performance tuning.

The analysis of the collected optimization logs performed by OCELOT Optimizer [6] shows that one of the problems is the high dimensionality of parameter space that needs to be explored in the optimization process. For example, 446 unique devices have been used in optimizations at the European XFEL to maximize the SASE pulse energy within the last 2.5 years [2]. Although the frequency of use of a particular set of devices varies. It can still give an indication of how complex the tuning is. Another obstacle to fast and efficient machine tuning is that hyperparameters of optimization algorithms and set of devices which need to tune specific physical parameters, e.g. beam matching, are not always optimally selected, which also affect efficiency. In this paper we will consider the current state of optimization methods used in the European XFEL, and possible ways to overcome the problems discussed.

MODEL-FREE OPTIMIZATION

The main tool for a model-free SASE optimization in the European XFEL is the OCELOT Optimizer. It is the next generation of the SASE optimizer developed for FLASH [6] but with the possibility of creating/modifying an objective function by the operator. Each optimization is logged including an objective function and actuator changes during optimization and can be analyzed afterwards. The tool was deployed in the EuXFEL control room at the beginning of 2017. Since then we collected experience of more than 6000 optimizations (Fig. 2). More details of OCELOT optimizer statistics analysis can be found in [2].

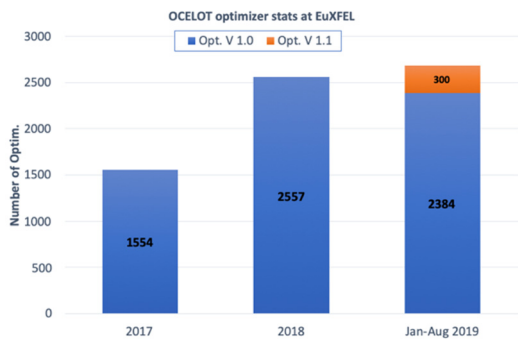


Figure 2: OCELOT optimizer statistics.

As it was mentioned above high dimensionality of the parameter space is one of the problems for fast FEL ma-

Content from this work may be used under the terms of the CC BY 3.0 licence (© 2019). Any distribution of this work must maintain attribution to the author(s), title of the work, publisher, and DOI

ISBN: 978-3-95450-210-3 doi:10.18429/JACoW-FEL2019-FRA01

FEL OPERATION AT THE EUROPEAN XFEL FACILITY*

D. Nölle†, Deutsches Elektronen-Synchrotron DESY, Hamburg, Germany
on behalf of the European XFEL Operation Team

Abstract

The European XFEL is a SASE FEL based user facility in the metropole region of Hamburg providing hard and soft X-ray photons with extremely high brilliance. The three FEL lines are operated simultaneously and are powered by a superconducting LINAC based on TESLA technology. Average power levels of up to several W have been demonstrated as well for soft and hard X-rays and can be requested by user experiments on day by day basis. This paper will report on the operation within the last two years. Typical operation conditions for parallel operation of 3 SASE lines will be discussed. The perspective for the operation with an extended photon energy range, as well as for full power operation with up to 27000 pulses per second will be presented.

Content from this work may be used under the terms of the CC BY 3.0 licence (© 2019). Any distribution of this work must maintain attribution to the author(s), title of the work, publisher, and DOI

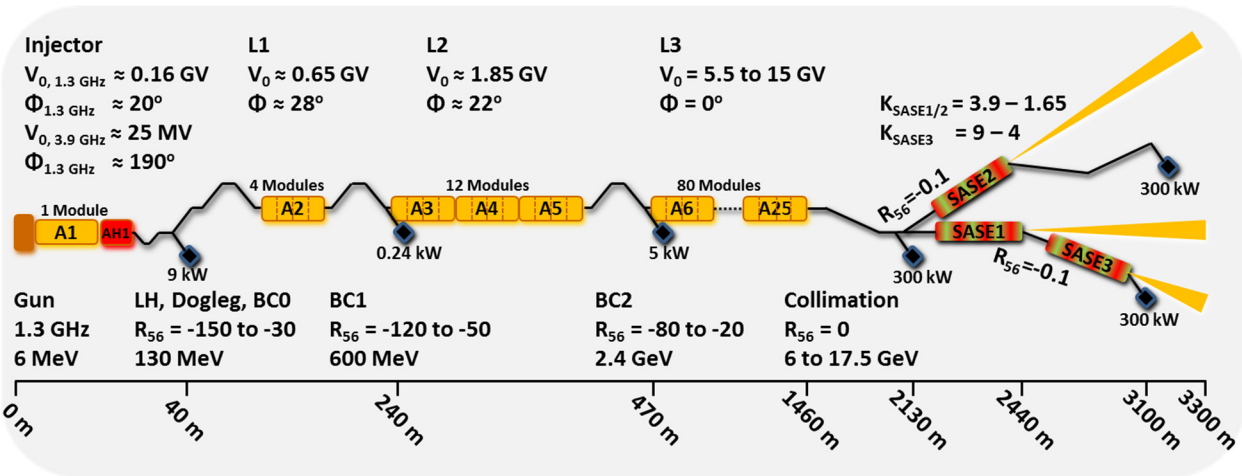


Figure 1: Schematic overview of the European XFEL accelerator. Single RF stations are named An and feed either one module (A1) or 4 accelerating modules (A2-A25). R56 ranges for the bunch compressors are given in mm, and the phases of the different linac sections refer to typical compression set-ups. The maximum allowed beam power of the three commissioning dumps after the injector and the 2nd and 3rd bunch compressor (BC1 and BC2) as well as of the main dumps after the linac and each beam distribution line is given.

INTRODUCTION

The European XFEL aims at delivering X-rays from 0.25 to up to 25 keV out of three SASE FEL lines [1, 2]. The FELs are driven by a superconducting linear accelerator based on TESLA technology [3]. The accelerator operates in 10 Hz pulsed mode and can deliver up to 2,700 bunches per RF-pulse. Electron beams can be distributed to three different beamlines: the two FEL branches and a dump line. The switching is done within the RF-pulse allowing for simultaneous operation of three FELs.

Construction of the European XFEL started in early 2009. Commissioning of the facility began end of 2015 with a ½ year long injector run [4]. End of 2016 the commissioning of the superconducting accelerator started. 9 month later in Sept. 2017 the instruments at SASE1 started with photon energies of 9.3 keV. In spring 2018 within one year from the first lasing of SASE1 parallel lasing in all 3 FELs was established [5, 6]. Distribution of the electron beam to the different sources with almost arbitrary bunch pattern is done by the flexible beam switchyard [7]. While SASE1 is in operation since fall 2017 SASE3 and SASE2 served first users at the end of 2018 and beginning of 2019. All experiments are far advanced on their way from first to standard user operation.

FACILITY LAYOUT

The complete facility is constructed in an underground tunnel up to 30 m below surface level. Access to the tunnels is possible in the injector area as well as through shaft buildings at the bifurcation points, where one tunnel splits up into two. The longest tunnel is the main accelerator tunnel with about 2 km length. Total length of the entire tunnel system is about 6 km. The distance of injector to experimental hall is 3.3 km. Besides of the three already installed FEL lines, the tunnels provide space for two more FEL sources [8]. The schematic layout of the accelerator is shown in Fig. 1.

The injector consists of the normal conducting gun, one TESLA type accelerating module and a 3.9 GHz module

* Work supported by the respective funding agencies of the contributing institutes; for details please see http:\\www.xfel.eu
† dirk.noelle@desy.de

ISBN: 978-3-95450-210-3 doi:10.18429/JACoW-FEL2019-FRA02

Content from this work may be used under the terms of the CC BY 3.0 licence (© 2019). Any distribution of this work must maintain attribution to the author(s), title of the work, publisher, and DOI

LCLS-II – STATUS AND UPGRADES*

Brachmann†, B. Dunham, J. Schmerge for the LCLS-II Collaboration,
SLAC National Accelerator Laboratory, Menlo Park, CA, USA

Abstract

LCLS-II is a major project to build and operate a 1 MHz, continuous-wave Free Electron Laser covering a wide photon energy range from ~ 200eV up to 25 keV. A superconducting accelerator, providing beams up to 4 GeV, drives two variable gap undulator systems, one providing soft energy X-rays (SXR) up to ~ 2keV, the other hard energy X-rays (HXR) up to 25 keV. In addition, the normal conducting accelerator used for LCLS-I will remain in operation, primarily driving the hard X-ray undulator beam line delivering photon energies up to 25 keV. We will summarize the project goals, current status of construction of the main sub-systems and future plans. The focus of this contribution will be the FEL itself. We will mention the X-ray instrumentation for context.

LCLS-II PROJECT OVERVIEW

A detailed overview of the LCLS-II facility is given in the Technical Design Report [1]. A schematic layout of the facility is shown in Figure 1. The project is supported by the United States Department of Energy and is a collaboration of several National Laboratories and Cornell University. The cryomodules are built by the Thomas Jefferson National Accelerator Facility (JLab) and Fermilab (FNAL). The undulator systems for the hard and soft X-ray energy ranges are provided by Argonne National Laboratory (ANL) and Keller Technology Corporation, New York, USA (KTC), respectively. The electron gun is a contribution of the Lawrence Berkeley National Laboratory (LBNL). This system is already fully installed, and commissioning activities are in progress. A key system is the cryo-plant. It is based on the 2K plant in operation at JLAB. The entire cryogenic system was designed and constructed collaboratively by SLAC, JLab, FNAL and several industrial partners. A 'dual' plant is installed to provide headroom for capacity and future extension of the cryogenic linac.

The goal of the project is to construct and operate an FEL user facility for advanced X-ray science that will be available to the international user community. Scientific motivation and opportunities have been summarized in [2]. The existing normal conducting (NC) accelerator will continue to operate and primarily provide beams in the HXR energy range but will also be used to assist commissioning of the new SXR beamlines and instrumentation.

The main construction activities will be completed in 2021. User operation based on the NC accelerator will commence in the spring of 2020. 'First light', generated by SC accelerator beams is anticipated in 2021, followed by a ramp-up period to full performance, over 3-4 years. A set of Design Parameters is given in table 1. Figure 2 shows the X-ray energy range and average beam brightness.

Table 1: Design Parameters

KPP	SC linac	NC linac
Linac Energy	4 GeV	15 GeV
Repetition Rate	1 MHz	120 Hz
Nominal Bunch Charge	0.1 nC	0.125 nC
Photon Energy Range	0.2-5 keV	0.2 - 25 keV
Photon Pulse Energy	0.5 mJ	~ 2 mJ

Approximately half of the cryomodules are now installed in the first kilometre of SLAC's linac tunnel. The undulators both for SXR and HXR systems are in the process of magnetic measurement and calibration. Installation is imminent and we expect completion of commissioning in the early part of 2020, enabling the restart of the facility and user operation based on the NC linac. Many other systems are currently installed, for example the RF systems, cryogenic plant and cryogenic distribution system, beam transport and switching systems, beam dumps, controls and safety systems. In parallel, a major upgrade of the X-ray instrumentation is taking place: 3 new end stations will be added, high repetition rate capabilities will be implemented, and appropriate data processing technology is being developed and installed. A comprehensive description of photon and experimental system development is summarized in a strategic development plan [3].

LCLS-II Injector

The LCLS-II Injector uses a normal conducting VHF electron gun. The gun has been developed at LBNL and a prototype has been in operation for several years, also known as the 'APEX gun.' The injector design and gun are described in references [4, 5]. Beam is generated by a Cs_2Te cathode driven by a 257 nm laser system. The LCLS-II electron gun is installed in its final location. We succeeded to generate first beam, including a measurement of the electron beam energy, confirming specified performance (Figures 3 and 4).

* Work supported by the U.S. Department of Energy, Office of Basic Energy Sciences, Contract No. DE-AC02-76SF00515.
†brachman@slac.stanford.edu

ISBN: 978-3-95450-210-3 doi:10.18429/JACoW-FEL2019-FRA03

FLASH - STATUS AND UPGRADES

J. Rönsch-Schulenburg*, K. Honkavaara, S. Schreiber, R. Treusch, M. Vogt,
DESY, Hamburg, Germany

Abstract

FLASH, the Free-Electron Laser at DESY in Hamburg was the first FEL user facility in the XUV and soft X-ray range [1–5]. The superconducting RF technology allows to produce several thousand SASE pulses per second with a high peak and average brilliance. It developed to a user facility with a 1.25 GeV linear accelerator, two undulator beamlines running in parallel, and a third electron beamline containing the FLASHForward plasma wakefield experiment. Actual user operation and FEL research are discussed. New concepts and a redesign of the facility are developed to ensure that also in future FLASH will allow cutting-edge research. Upgrade plans are discussed in the contribution.

FLASH FACILITY

FLASH, the Free-Electron Laser at DESY in Hamburg is a user facility which delivers FEL pulses based on the self-amplified spontaneous emission (SASE) in the wavelength range from 4 to 90 nm for user experiments. The extension of the FLASH facility by a second undulator beamline allows multi-user operation [6, 7]. Both FLASH undulator-beamlines are driven by a common linear accelerator consisting of a laser driven radio-frequency (RF) gun with a photocathode, seven superconducting accelerating modules, a third-harmonic accelerating module, and two bunch compressors. The superconducting technology allows the acceleration of electron bunch trains of several hundred bunches with a spacing of a microsecond or more and a repetition rate of 10 Hz for both beamlines. An electron beam energy of up to 1.25 GeV can be reached. A fast kicker system and a Lambertson septum are used to extract one part to FLASH1 and the other part of the bunch train into the FLASH2 beamline.

The FLASH1 beamline has six fixed-gap undulators, with a length of 4.5 m each. The SASE wavelength of FLASH1 is determined by the electron beam energy. Additionally a planar electromagnetic undulator is installed downstream of the FLASH1 SASE undulators providing THz radiation. The FLASH1 beamline also contains a seeding experiment called sFLASH [8–10].

In the FLASH2 beamline a third bunch compressor was installed in June 2019 to increase the compression flexibility, reduce the effects of space charge and of coherent synchrotron radiation (CSR). The new bunch compressor in the FLASH2 beamline has been commissioned and is now a part of the standard operation. FLASH2 contains twelve variable-gap undulators with a length of 2.5 m each, which allow choosing the wavelength to a certain extend independently from FLASH1 by varying the gap width of the undulators. In order to operate FLASH2 almost independently of FLASH1, a second injector laser and a flexible low level RF system are used. First lasing of FLASH2 was achieved in August 2014 simultaneous to FLASH1 SASE operation. In April 2016, two user experiments, one at FLASH1 and the other at FLASH2, were running in parallel for the first time. Two experiments, requiring different beam parameters, can run simultaneously, since the bunch pattern and compression scheme can be chosen almost independently for FLASH1 and FLASH2 beamlines, allowing to tune the SASE properties specifically for each of the experiments [11].

Figure 1 shows a schematic layout of the FLASH facility with its common accelerator and the two undulator beamlines with their own experimental halls. In addition, a third electron beamline, FLASH3, hosts a pioneering beam driven plasma-wakefield acceleration experiment, FLASH-Forward [12, 13].

An overview of the photon science at FLASH and the evolution of the FLASH facility over the years can be found in [4,5,14]. For more details of the facility and its parameters we refer to [6, 7, 15, 16].

FLASH OPERATION

FLASH has two user periods per year. In 2018, FLASH1 was operated a total of 7103 hours, of which 59% (4189 h) was devoted to FEL user operation, 30% for studies and user preparation, and 11% for general accelerator R&D. FLASH2 was operated 6831 hours, of which 33% (2269 h) was FEL user operation. In 2018 FLASH served beam time for 38 experiments; many wavelengths in the XUV and soft X-ray range from 52 down to 4.4 nm have been realized. In 2018, two photon beamlines have been completed in the FLASH2 Kai Siegbahn experimental hall. This led to an increase of scheduled user experiments in FLASH2, a plus of 50% compared to 2017.

FLASH2 Pump-Probe Laser

The new FLASH2 pump-probe laser system [17] was commissioned in September 2018 with a successful pilot experiment, and is now in routine use. Since most experiments at FLASH1 are indeed pump-probe experiments with optical lasers, for example 58% in the first half of 2018, and 71% in the second half of 2018, the availability of the new pump-probe laser system at FLASH2 significantly increases the number of possible experiments.

New Photon Diagnostics

Another new improvement is a fast line detector for intra-train spectrum measurements named KALYPSO [18] which has been installed in the FLASH1 photon beamline. It offers an online single shot measurement of the SASE wavelength spectrum along the whole bunch train for several hundreds of

* juliane.roensch@desy.de

Content from this work may be used under the terms of the CC BY 3.0 licence (© 2019). Any distribution of this work must maintain attribution to the author(s), title of the work, publisher, and DOI